ABSTRACT BOOK

Advances in Functional Materials

University of Calefornia, LA, USA

Aug 14 - Aug 17, 2017

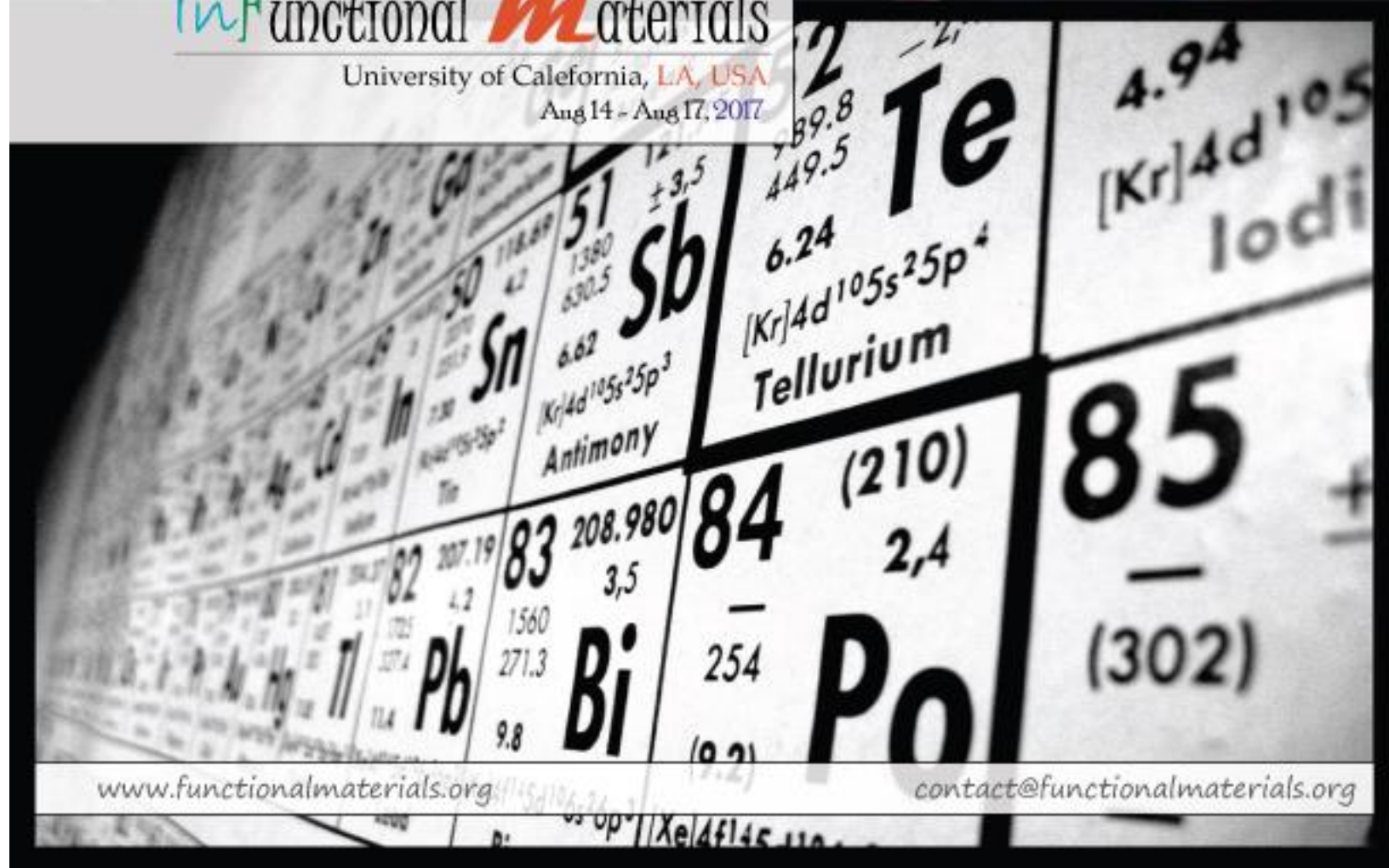

www.functionalmaterials.org

contact@functionalmaterials.org

WELCOME TO THE CONFERENCE ON ADVANCES IN FUNCTIONAL MATERIALS 2017

Overview

After the grand success of the 1st and the 2nd edition of Advances in functional Materials (AFM) Conference, we, the Conference Co-chairs and the organizing committee welcome you again to the 3rd International Conference on Advances in Functional Materials (AFM 2017) that is going to be held at University of California, Los Angeles Campus (UCLA) from August 14-17, 2017 in the sprawling Southern California city and the center of the international film and television industry.

The objective of this international event is to present and share up to date researches and findings in the field of functional materials science. The conference will provide a platform for the researchers to find global partners for future collaboration. More than 1300 abstracts have been received from all over the world. A large number of participants including scientists, engineers, educators and students from all over the world will attend this event.

In order to maintain the quality of the presented work, all the abstracts have been reviewed by international researchers carefully. Conference participants will benefit from opportunity to submit full original articles for consideration at Materials & Design, a multi-disciplinary journal (impact factor 3.997) published by Elsevier.

In addition, the participants of the conference will also be able to attend the talks from our highly-reputed Keynote Speakers from all over the world.

The venue of the conference is always carefully chosen for you to spend quality and enjoyable time on and off the conference. Los Angeles is an ideal location for leisure and recreational activities. Magnificent nature, abundant tourist assets, convenient access and lodgings, warm and friendly people.

We are warm-heartedly extending our welcome to you and hope that you will join us in UCLA for a stimulating Conference, a friendly gathering amongst friends and simply a good time.

Table of Contents

Co-Chairs

PROF. XIANGFENG DUAN
University of California, LA USA

PROF. YU HUANG
University of California, LA, USA

PROF. DAE JOON KANG
Sungkyunkwan University, Korea

PROF. TAE JIN KIM
Stony Brook University, USA

PROF. IMRAN SHAKIR
King Saud University, KSA

Advisory Committee

Co-Chairs

Prof. Xiangfeng Duan, University of California, LA, USA
Prof. Yu Huang, University of California, LA, USA
Prof. Dae Joon Kang (Sungkyunkwan University, Jangan-gu Suwon, Korea)
Prof. Tae Jin Kim (Stony Brook University, Stony Brook, USA)
Prof. Imran Shakir (King Saud University, Saudi Arabia)

International Advisory Committee

1. Graphene/2D materials, Synthesis :
Prof. Manish Chowalla, (The State University of New Jersey, USA)
Prof. Huiming Cheng, (Shenyang National Laboratory for Materials Science, China)
Prof. Zhonfan Liu, (Peking University, China)
Prof. Dapeng Yu, (Peking University, China)
Prof. Hua Zhang, (Nanyang Technological University, Singapore)
Prof. Anliang Pan, (Purdue University, USA)
Prof. Hailin Peng, (Peking University, China)
Prof. Rodney Ruoff, (Institute of Basic Sciences, Korea)
Prof. Jing Kong, (Massachusetts Institute of Technology, USA)
Prof. Pulickel Ajayan, (Rice University, USA)
Prof. Yunqi Liu, (Peking University School of Advanced Materials, China)
Prof. Xiangfeng Duan, (University California Los Angles, USA)
Dr. Abbas Amini (Western Sydney University, Sydney, Australia)
2. 2D Physics and Device :
Prof. Philip Kim (Harvard University, USA)
Prof. Kang Wang (University California Los Angles, USA)
Prof. Shoucheng Zhang (Stanford University, USA)
Prof. Jeanie Lau (University of California, Riverside, USA)
Prof. Toney Heinz, (Columbia University, USA)
Prof. Xiaodong Xu, (University of Washington, USA)
Prof. Andras Kis (École Polytechnique Fédérale De Lausanne, Switzerland)
Prof. Lianmao Peng (Peking University School of Advanced Materials, China)
Prof. Han Wang, (Nanyang Technological University, Singapore)
Prof. Fengnian Xia, (Yale University, USA)
Prof. Tomas Palacios (Massachusetts Institute of Technology, USA)
Prof. James Hone (Columbia University, USA)
Prof. Feng Wang (University of California Berkeley, USA)
Prof. Yoshihiro Iwasa (The University of Tokyo, Japan)
Prof. Kian Ping Loh, (National University Singapore, Singapore)
Prof. Peide Ye (Purdue University, USA)
Prof. Ali Javey, (University of California at Berkeley)
Prof. Kaustav Banerjee, (University of California at Santa Barbara)

3. Energy Solar:
Prof. Yang Yang, (University of California Los Angeles)
Prof. Aditya Mohite, (Los Alamos National Laboratory)
4. Battery/Supercapacitor:
Prof. Bruce Dunn, (University of California Los Angeles)
Prof. Sarah Tolbert, (University of California Los Angeles)
Prof. Richard Kaner, (University of California Los Angeles)
Prof. Xiangfeng Duan (University of California Los Angeles)
5. Fuel Cell:
Dr. Nenad M. Markovic (Argonne National Laboratory, Lemont)
Prof. Allen Bard, (University of Texas at Austin)
Dr. Rod Borup (Los Alamos National Laboratory),
Dr. Yu Seung Kim (Los Alamos National Laboratory chemistry)
Dr. Deborah Myers (Argonne National Laboratory),
Prof. Shao-Horn Yang (Massachusetts Institute of Technology),
Dr. Vojislav R. Stamenkovic (Argonne National Laboratories),
Prof. Liming Dai (Case Western Reserve University),
Prof. Yu huang (University of California Los Angeles)
6. Catalysis/Photocatalysis:
Prof. Xinhe Bao, (Chinese Academy of Sciences, China)
Prof. Nanfeng Zheng (Xiamen University, China)
Prof. Hong Yang (University of Illinois, USA)
Prof. Yat Li (University California, SANTA, USA)
Prof. Yadong Li (Tsing Hua University, China)
Prof. Peidong Yang (University California Berkerley, USA)
Prof. Fuat Celik (Rutgers University, New Jersey, USA)
Prof. Jean-Marie Basset (Director, KAUST Catalysis Research Center)
Prof. Tae Jin Kim (Stony Brook University, Stony Brook, USA)
7. Flexible/Wearable electronics:
Prof. John Rogers (University of Illinois, USA)
Prof. Zhenan Bao (Stanford University, USA)
Prof. Younghee Lee (Sungkyunkwan University, Korea)
Prof. Marc Hersam (Northwestern University, USA)
Prof. Takao Someya, (University of Tokyo, Japan)
Prof. Dae-hyeong kim (Seoul National University, Korea)
Prof. Zhong Lin Wang (Georgia Tech, USA)
8. Nanobio:
Prof. Charles Lieber (Harvard University, USA)
Prof. Hongjie Dai (Stanford University, USA)
Prof. Chunhua Yan (Peking University, China)
Prof. Weihong Tan (University of Florida, USA)
Dr. Tan Sui (University of Oxford UK)
9. Porous materials:
Prof.Omar Yaghi (University of California, Berkeley, USA)
Prof. Dongyuan Zhao (Fudan University, China)
Prof. Pingyuan Feng (University of California, Santa Barbara, USA)

10. Nanocrystals synthesis/assembly:
Prof. Chad Mirkin (Northwestern University, USA)
Prof. Chris Murray (University of Pennsylvania, USA)
Prof. Younan Xia (Geogia Tech. USA)
Prof. Yadong Yin (UC Riverside)
Prof. Kwanghee Lee (Gwangju Institute of Science & Technology (GIST), Korea),
Dr. Michael De Volder (University of Cambridge, UK)
Prof. Li Zhang (The Chinese University of Hong Kong)
Prof. Hui-Ming Cheng (Chinese Academy of Sciences, China)
11. Imaging and 3D image:
Prof. James De Yoreo (University of Washington, USA)
Prof. John Miao (University California, Los Angles, USA)
Prof. Haimei Zheng (Lawrence Berkeley National Laboratory, USA)
Prof. Angus Kirkland (University of Oxford, UK)
Prof. Xiaoqing Pan (University of California,USA)
Prof. Alexander Korsunsky (University of Oxford UK)
12. Nanophotonics:
Prof. Harry Atwater (California Institute of Technology, USA)
Prof. Qihua Xiong (Nanyang Technological University, Singapore)
Prof. Teri Odom (Northwestern University, USA)
Prof. Xiaoyang Zhu (Columbia Chemistry, USA)
13. Theory:
Prof. William A. Goddard (California Institute of Technology, USA)
Prof. Philip Sautet, (Prof. Philip Sautet, France)
Prof. Anastassia N. Alexandrova (University of California, Los Angeles, USA)

Keynote Speakers

1.	Prof. Catherine J. Murphy	University of Illinois Urbana-Champaign, USA
2.	Prof. Hua Zhang	Nanyang Technology University, Singapore
3.	Prof. Jian Bin Xu	University of Hong Kong
4.	Prof. John A. Rogers	Northwestern University, USA
5.	Prof. Lain-Jong li	KAUST, KSA
6.	Porf. Liming Dai	Case Western Reserve University, USA
7.	Prof. Michael S. Strano	Cambridge University, USA
8.	Prof. Oamr M. Yaghi	University of California, Berkeley, USA
9.	Prof. Paul S. Weiss	University of California, Los Angeles, USA
10.	Prof. Sarah H. Tolbert	University of California, Los Angeles, USA
11.	Prof. Yang Yang	University of California, Los Angeles, USA
12.	Prof. Yur Gogotsi	Drexel Univeristy, USA
13.	Prof. Qihua Xiong	Nanyang Technology University, Singapore

CATHERINE J. MURPHY

Peter C. and Gretchen Miller Markunas Professor of Chemistry
Affiliate, Materials Science and Engineering
Affiliate, Micro and Nanotechnology Laboratory
Associate Director, Materials Research Laboratory

Going for the Gold

Gold nanoparticles have fascinating optical and photothermal properties that are tunable with nanoparticle size and shape. Upon illumination into their plasmon bands, gold nanoparticles generate scattered light, electric fields, and heat, all of which can be used for numerous applications in chemical sensing, biological imaging, and photothermal therapy. Biological applications especially require understanding of the surface chemistry of these nanomaterials. In this talk I will describe some of our latest results in growing, modifying, and using gold nanoparticles for understanding the nano-bio interface.

HUA ZHANG

Center for Programmable Materials, School of Materials Science and Engineering, Nanyang Technological University, Singapore

Crystal Phase-Controlled Synthesis of Novel Noble Metal Nanomaterials

In this talk, I will summarize the recent research on the crystal phase-controlled synthesis of novel noble metal nanomaterials in my group. It includes the first-time synthesis of hexagonal-close packed (*hcp*) Au nanosheets (AuSSs) on graphene oxide, surface-induced phase transformation of AuSSs from *hcp* to face-centered cubic (*fcc*) structures, alternating *hcp*/*fcc* Au square-like plates from AuSSs, ultrathin Au nanowires containing *hcp* phase, synthesis of ultrathin *fcc* Au@Pt and Au@Pd rhombic nanoplates through the epitaxial growth of Pt and Pd on the *hcp* AuSSs, respectively, the first-time synthesis of 4H hexagonal phase Au nanoribbons (NRBs) and their phase transformation to *fcc* Au RNBs, the epitaxial growth of Ag, Pt, Pd, PtAg, PdAg, PtPdAg, Rh, Ir, Ru, Os and Cu on 4H Au NRBs to form the 4H/*fcc* Au@metal core–shell NRBs, and the synthesis of 4H/*fcc*-Au@metal sulfide core-shell NRB heterostructures. Currently, my group focuses on the crystal phase-based properties and applications in catalysis, surface enhanced Raman scattering, waveguide, photothermal therapy, chemical and biosensing, etc., which we believe are unique and critically important not only fundamentally, but also practically. Importantly, the concepts of crystal phase noble metal heterostructures is proposed.

Keywords: Crystal Phase; Noble Metal Nanomaterials; Hexagonal-Close Packed; Face-Centered Cubic; Gold; Ultrathin Nanosheets

Jian Bin XU

Vice-Chancellor's Outstanding Fellow of the Faculty of Engineering, Chinese University of Hong Kong

Exploration of Inorganic and Organic Electronic Materials in the Flatland

In this presentation, we will report on our recent progress in preparation and characterization of high–quality two-dimensional (2D) layered materials in two categories. The first category is inorganic materials, namely graphene, MoS_2, WS_2, WTe_2, and $MoTe_2$. The second one is organic materials, namely, pentacene and C_8-BTBT small molecules.

We will present in detail the unique formation mechanisms of graphene, MoS_2, WS_2 WTe_2, $MoTe_2$, and pentacene sheets with various vapor deposition techniques. Afterwards we will discuss their heterostructures and applications in optoelectronic devices. By leveraging on strong photonic interactions via hybrid layered material/photonic waveguide and heterostructure architectures, we are able to devise the high performance photodetectors/modulators from visible to the infrared spectral regions, and even in the terahertz region.

Finally we deliberate the scattering mechanisms responsible for the electronic transport properties on the supported 2D layered sheets on SiO_2/Si substrate. We will discuss an interface engineering strategy based on highly-ordered self-assembled monolayer (SAM) passivated SiO_2/Si substrate. Thanks to the passivation, we have successfully constructed the high-performance transistors by significantly reducing the electrically deleterious species in the active channels. We envision that both atomically-flat SAM platform and photonic-active structures will be generically applicable to realizing high performance devices.

JOHN A. ROGERS

Swanlund Chair | Professor of Material Science & Engineering

Materials and Device Concepts for Biodegradable Electronics

A remarkable feature of modern integrated circuit technology is its ability to operate, almost indefinitely, in a stable, reliable fashion, without physical or chemical change. Recently developed classes of electronic materials create an opportunity to engineer the opposite outcome, in the form of devices that dissolve, in a controlled fashion, completely and harmlessly in water. Enabled applications include zero-impact environmental monitors, 'green' consumer electronics and temporary bioelectronic implants. This presentation describes foundational concepts in chemistry, materials science and assembly processes for these types of technologies. Wireless sensors of intracranial temperature, pressure and electrophysiology designed to monitor recovery from traumatic brain injury provide some application examples.

LAIN-JONG LI

Professor of Materials Science and Engineering
Physical Sciences and Engineering Division, King Abdullah University of Science and Technology, Thuwal, Kingdom of Saudi Arabia

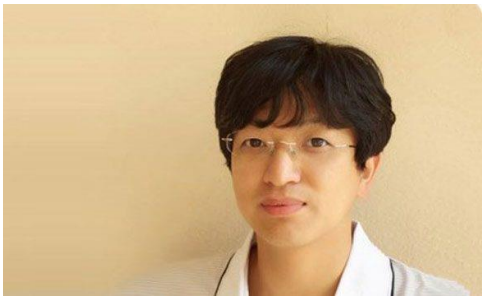

Advanced Growth of 2D Transition Metal Dichalcogenide Monolayers and Their Heterostructures

Our recent demonstration in vapor phase growth of TMD monolayers such as MoS_2 and WSe_2 has stimulated the research in growth and applications (1). The growth mechanism and the orientation control of the 2D flakes will be first discussed. These 2D monolayer building blocks can be used to form *p-n* junctions. For example, the heterostructures of 2D materials formed by vertical stacking have been realized via transfer of their exfoliated flakes, where their electronic structures are dominated by the stacking orientation and strength of interlayer coupling(2). Another very attractive structure is the lateral heterojunction, where we have demonstrated that the atomically sharp p-n junction exhibits diode properties and a large strain exhibits at the junction region which offers tunability in electronic structures (3).

In addition to the symmetry 2D materials, we have also developed a method that can precisely manipulate arrangement of chalcogenide atoms (S and Se) along the vertical direction of TMD. This new strategy allows us to fabricate a MoSSe Janus structure, where the transition metals are sandwiched by selenium at upmost and sulfur at bottom. Such a Janus 2D monolayer exhibits piezoelectric responses and optical dipole along out-of-plane direction (4).

LIMING DAI

Center of Advanced Science and Engineering for Carbon
Departments of Macromolecular Science and Engineering,
Case Western Reserve University, Cleveland, Ohio, USA

Multifunctional carbon-based metal-free catalysts for efficient energy conversion and storage

Green and renewable energy technologies, such as fuel cells, batteries, and water-splitting systems, hold great promise to solve current energy and environmental challenges. However, noble metal catalysts (*e.g.*, Pt, Pd, RuO_2, IrO_2) are generally needed to promote the *hydrogen evolution reaction* (HER) for hydrogen fuel generation from photo-electrochemical water-splitting, *oxygen reduction reaction* (ORR) in fuel cells for energy conversion, and *oxygen evolution reaction* (OER) in metal-air batteries for energy storage. The high cost of precious metal-based catalysts and their l*imited reserve* have precluded *these renewable energy technologies from* large-scale applications.

Along with the recent intensive research efforts in reducing/replacing noble metal based catalysts (*i.e.*, Pt) for ORR in fuel cells, we have previously demonstrated that vertically aligned nitrogen-doped carbon nanotubes (VA-NCNTs) could actively catalyze ORR *via* a four-electron process free from the methanol crossover and CO poisoning effects with a 3-time higher electrocatalytic activity and better long-term durability than that of commercial Pt/C catalysts. The improved catalytic performance was attributed to the doping-induced charge transfer from carbon atoms adjacent to the nitrogen atoms to change the chemisorption mode of O_2 and to readily attract electrons from the anode for facilitating the ORR (*cf.* figure).

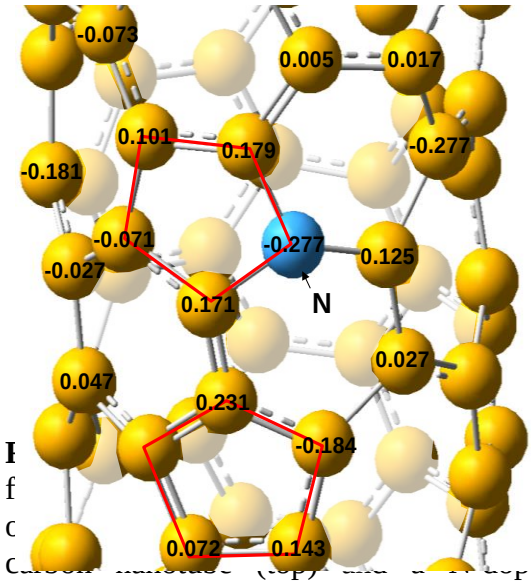

(bottom). [Figure Source: Gong; Du; Xia; Durstock; Dai *Science* **2009**. *323*. 760.]

Subsequently, it was demonstrated that various carbon nanomaterials, doped with heteroatoms of different electronegativities from that of carbon atom, physically adsorbed with certain polyelectrolytes, and even without any apparent dopant or physically adsorbed polyelectrolyte, could also exhibit good ORR performance. More recent studies have further demonstrated that certain heteroatom-doped *carbon nanomaterials* could act as metal-free bifunctional catalysts for ORR/OER in metal-air batteries for energy storage, and even ORR/OER/HER trifunctional catalysts for self-powered water-splitting to generate hydrogen fuel and oxygen gas from water as well as integrated energy systems.

In this talk, we will summarize some of our work on the metal-free catalysts based on carbon nanomaterials for various energy-related reactions, along with an overview on the recent advances and perspectives in this exciting field.

MICHAEL S. STRANO

Professor | Department of Chemical Engineering,
Massachusetts Institute of Technology, Cambridge, USA

New Functional Materials Enabled by 1D and 2D Nanomaterials

Our laboratory has been interested in how 1D and 2D electronic materials such as carbon nanotubes, graphene and transition metal dichalogenides, can manipulate electrons, phonons and photons in unique ways. This presentation will focus on recent advances from our laboratory at MIT to create materials with new combinations of functions and properties. Two-dimensional (2D) materials can uniquely span the physical dimensions of a surrounding composite matrix in the limit of maximum reinforcement. However, the alignment and assembly of continuous 2D components at high volume fraction remain challenging. We use a stacking and folding method to generate aligned graphene/polycarbonate composites with as many as 320 parallel layers spanning 0.032 to 0.11millimeters in thickness that significantly increases the effective elastic modulus and strength at exceptionally low volume fractions of only 0.082%. An analogous transverse shear scrolling method generates Archimedean spiral fibers that demonstrate exotic, telescoping elongation at break of 110%, or 30 times greater than Kevlar. Both composites retain anisotropic electrical conduction along the graphene planar axis and transparency. These composites promise substantial mechanical reinforcement, electrical, and optical properties at highly reduced volume fraction. Additionally, we present a theory, experimentally validated, of how fluid phase equilibria is significantly altered when confined to nanometer scale dimensions, creating the potential to embed tunable phase change materials, as well as unique liquid or solid properties encapsulated within new matricies. Our theory, based on the Turbull number, can predict the solid/liquid coexistence for any fluid and any Nanoconfined system down to approximately 4 nm. Below this limit, we show remarkable departures experimentally. Fluid phase transitions inside isolated nanotubes deviate substantially from classical thermodynamics and also allow the study of ice nanotube (ice-NT) properties. Herein, we measure, using two different techniques, the diameter dependent phase boundaries of ice-NTs within isolated CNTs 1.05, 1.06, 1.15, 1.24, and 1.52nm in diameter using Raman spectroscopy. The results reveal both an exquisite sensitivity to diameter and substantially larger temperature elevations of the melting transition than theoretically predicted by as much as 100°C. Dynamic water filling and reversible freezing transitions were marked by 2 to 5cm-1 shifts in the radial breathing mode (RBM) frequency, revealing reversible melting at 138°C and 102°C for 1.05 and 1.06nm single and double-walled CNTs, respectively. A near-ambient phase change at 15°C was observed for 1.52nm CNT, whereas freezing inside 1.24nm tube was suppressed at -30°C. These extreme phase transitions enable the study of ice-NT at high temperatures and their potential utilization as novel phase change materials. These new fabrication and thermodynamic concepts promise fundamentally new materials with unique combinations of properties.

OMAR M. YAGHI

James and Neeltje Tretter Chair Professor of Chemistry, UC Berkeley | Senior Staff Scientist, Lawrence Berkeley National Laboratory | Ph.D., University of Illinois-Urbana

Reticular Chemistry and the design of new materials for clean energy

Reticular Chemistry - the chemistry of linking molecular building blocks by strong bonds into crystalline extended structures, such as metal–organic frameworks (MOFs) and covalent organic frameworks (COFs), has significantly

expanded the scope of chemical compounds and useful materials. These materials have the highest surface areas known to date, making them useful in many applications including the (1) storage and separation of hydrogen, methane, and carbon dioxide, (2) conversion of carbon dioxide to fuels and high value chemicals, (3) capture of water from air for fresh water production, (4) highly selective cleavage of peptides using enzyme-inspired catalysis, and (5) storage of ions in supercapacitor devices, and transport of protons and electrons in conductive frameworks.

Paul S. Weiss

Distinguished Professor of Materials Science & Engineering, University of California, Los Angeles

Precise Chemical, Physical, and Electronic Nanoscale Contacts

The physical, electronic, mechanical, and chemical connections that materials make to one another and to the outside world are critical. Just as the properties and applications of conventional semiconductor devices depend on these contacts, so do nanomaterials, many nanoscale measurements, and devices of the future. We discuss the important roles that these contacts can play in preserving key transport and other properties. Initial nanoscale connections and measurements guide the path to future opportunities and challenges ahead. Band alignment and minimally disruptive connections are both targets and can be characterized in both experiment and theory. I discuss our initial forays into this area in a number of materials systems.

SARAH H. TOLBERT

Professor, Department of Chemistry and Biochemistry, UCLA
Member, NanoElectronics, Photonics, Architectonics, NanoMechanical and Nanofluidic Systems, California NanoSystems Institute
Researcher, Inorganic, Nanoscience and Materials, Physical

Nanostructured Materials for Next Generation Electrochemical Energy Storage

In this talk, we examine ways that solution processed nanostructured materials can be used to address both fundamental and practical issues relevant to next generation electrochemical energy storage. We begin with nanoporous materials for application in fast charging battery-like applications. Materials with appropriate porous architectures can be synthesized using a range of solution phase methods, including polymer templating, nanoparticle assembly, and selective solution phase dealloying of mixed metal solid-state precursors. The resulting nanoporous materials can form the basis for high power electrochemical energy storage materials known as pseudocapacitors. In such materials, the nanoscale porosity can produce a very desirable combination of electrical connectivity, electrolyte access to the interior of the material, ample surface redox sites, and very short solid-state diffusion lengths for lithium ions. With idealized architectures and bonding geometries, a unique combination of high energy density and high power density can be achieved, in some case combined with reactivity toward ions other than Li^+. Similar architectures can also be used to increase stability and cycle life in high capacity electrode materials that normal show significant strain related degradation. Finally, related systems show promise for chemical energy storage in the form of electro-catalytic water splitting. Taken together, these results emphasize the key role played by nanoscale structure in energy storage materials.

YANG YANG

Department of Materials Science and Engineering and California NanoSystems Institute, University of California, Los Angeles, California, United States

Engineering of Interfaces and Intermediate Phases for Efficient Perovskite Solar Cells

Certified power conversion efficiencies (PCE) of perovskite solar cells have risen to reach an impressive 22.1%. However, despite such high device efficiencies, it has been reported that microscopic inhomogeneity of PCE still exists that reduces cell performance. Recent studies have uncovered the origins of the inhomogeneity to be related to structural disorders (defects). The defects at grain boundaries and interfaces induce shallow trap states, localizing charge carriers that are ultimately lost through non-radiative recombination, while the defect density across the grain interior is found to be dependent on the crystal facet, resulting in facet-dependent photovoltaic performance within a single grain. Therefore, to achieve a higher performance, careful engineering of grain growth and passivation of resulting boundaries is essential.

In this presentation, I will report our recent developments on methods for controlling of crystallization and passivation of the defects. Careful engineering of intermediate phases enabled management of crystallization kinetics of the perovskite layer, which resulted in significantly enhanced crystallinity with reduced defects. The remaining surface and interfacial defects were passivated by a self-assembly monolayer or Lewis base additive. As a consequence of the reduced defect states and enhanced carrier lifetime, PCE exceeding 19% (steady-state PCE >18%) was achieved with planar heterojunction perovskite solar cells.

In addition, I will also report our works on the perovskite tandem solar cell progresses. The engineering of the tunneling junction is one of the keys in our high performance tandem devices.

Yury Gogotsi

Trustee Chair Professor, Department of Materials Science and Engineering

2D ordered double transition metal carbides (MXenes)

Two-dimensional (2D) transition metal carbides and nitrides (MXenes) are an emerging family of 2D materials that have been expanding rapidly. About 30 different MXenes have been synthesized to date, such as Ti_2C, Ti_3C_2, Nb_2C, V_2C, Mo_2C, and Nb_4C_3, and several more theoretically predicted.[1] The MXenes reported to date have surface functionalities, such as hydroxyl, fluorine, and oxygen, which add hydrophilicity to their surfaces. The family was expanded in 2015,[2] by the discovery of ordered double transition metal MXenes, such as Mo_2TiC_2 and $Mo_2Ti_2C_3$, in which one or two layers of a transition metal (*e.g.*, Ti) are sandwiched between the layers of another transition metal (*e.g.*, Mo) in a 2D carbide structure. This tailoring of atomic ordering, where one atomic plane in a MXene can be replaced by another type of transition metal, gives unique control over properties in 2D.[3,4] MXenes' versatile chemistry renders their properties tunable for different applications, such as energy storage, electromagnetic interference shielding, reinforcement for composites, water purification, chemical, photo- and electro-catalysis, bio- and gas-sensors, lubrication, etc. Attractive electronic, optical, plasmonic and thermoelectric properties have also been predicted.[1] The structure, properties and applications of these MXenes followed by an outlook for the future research will be presented.

Qihua Xiong

Professor, Nanyang Technological University, Singapore

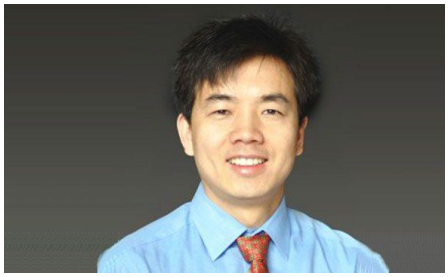

Interlayer Coupling and Charge Transfer in 2D Semiconductors and Heterostructures

2D semiconductors, such as transitional metal chalcogenides and black phosphorus, have attracted considerable attention due to fascinating physical properties a wide range of applications in valleytronics, optoelectronics and superconductivity. The interlayer interaction is particularly important in both homogenous few-layer systems and heterogeneous structures formed by "lego" fashion, which underpins the foundation for rational engineering towards unprecedented functionality. In this talk, I will introduce our work on interlayer coupling and charge transfer in 2D atomically thin semiconductors and their heterostructures. The unique charge transfer mechanism in 2D semiconductor heterostructures leads to an interesting blinking phenomenon, whereby a bright state emission occurs in one monolayer while a dark state emission occurs in the other, and vice versa. Such correlated blinking can be probed in detail by steady-state and transient spectroscopy measurements, providing new platform to study the long-standing puzzling blinking phenomenon in nanomaterials. In homogenous system, I will present how the charge transfer by a gate modulation breaks the symmetry in a bilayer sample such that a charge-induced second harmonic generation is produced, due to a confined charging in W-atomic plane and a screening effect.

Session Chairs

14 AUGUST, 2017

Session 1A-HER Chair
PROF Philip Bradford

Session 1B-HER Chair
PROF Mingzhu Li

Session 1C-HER Chair PROF. IMRAN SHAKIR

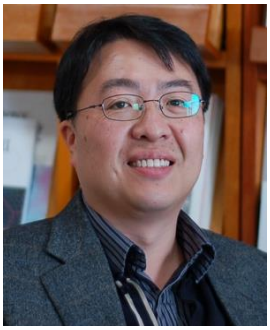

Session 1B Aud Chair
Prof. Dae Joon Kang

Session 1A/1C Aud Chair
Prof. Yail Jimmy Kim

Session 1A PALD Chair
Prof. KEYOU YAN

Session 1B PALD Chair
Prof. Moshe Averbukh

Session 1C PALD Chair
Prof. Mahmoud M Khader

Session 1A PALE Chair
Prof.MALING GUO

Session 1B PALE Chair
Prof. YA DING

Session 1C PALE Chair
Prof. AMIR SYAHIR

Session 1A VEN Chair
Prof. Önder Metin

Session 1B VEN Chair
Prof. Yuksel Ufuktepe

Session 1C VEN Chair
Prof. JOZEF HURAN

15 AUGUST, 2017

SESSION 2A HER CHAIR
PROF. SUTAPA ROY RAMANAN

SESSION 2A AUD CHAIR
PROF. YOUNG-SEOK

SESSION 2A PALD CHAIR
PROF. LIOIANG MAI

SESSION 2A PALE CHAIR
PROF. MEENAL

SESSION 2A VEN CHAIR
PROF. MING-SHOW WONG

16 AUGUST, 2017

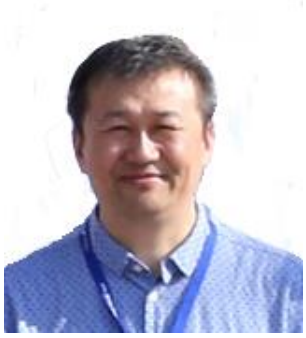

SESSION 3A AUD CHAIR
PROF. DONG CHEN

SESSION 3B AUD CHAIR
PROF. YOUNG-SEOK SHON

SESSION 3C AUD CHAIR
PROF. *Xuexi Zhang*

SESSION 3A PALD CHAIR
PROF. NAGENDRA PRASAD PATHAK

SESSION 3B PALD CHAIR
PROF. DANMIN LIU

SESSION 3C PALD CHAIR
PROF. VUK USKOVIC

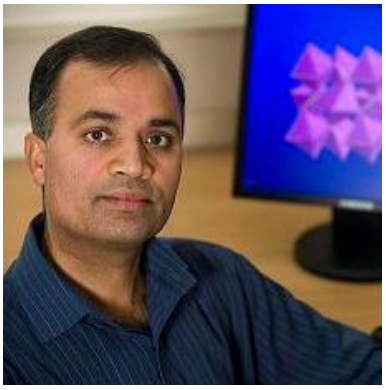

SESSION 3A PALE CHAIR
PROF. VARGHESE

SESSION 3B PALE CHAIR
PROF. JELENA

SESSION 3C PALE CHAIR
PROF. CHUNLEI

17 AUGUST, 2017

SESSION 4A CHAIR
PROF. WILLY W. CHU

SYMPOSIUM 1: Advances in Multifunctional Composite Materials

Nanomaterials for dental applications: from academic innovation to commercialisation

*G. C. Cotton,[1] D. R. Schwass,[2] W. J. Duncan[3] and C. J. Meledandri[1]**

[1]Department of Chemistry and MacDiarmid Institute of Advanced Materials and Nanotechnology, University of Otago, PO Box 56, Dunedin 9054, New Zealand.
[2]Department of Oral Rehabilitation, Faculty of Dentistry, University of Otago, PO Box 56, Dunedin 9054, New Zealand.
[3]Department of Oral Sciences, Faculty of Dentistry, University of Otago, PO Box 56, Dunedin 9054, New Zealand.

Email address of presenting author: cmeledandri@chemistry.otago.ac.nz

In recent years, our team has developed an interdisciplinary research programme dedicated to the development of new silver nanoparticle-based materials for application in dentistry. This work aims to solve a series of dental problems, ranging from tooth decay to periodontal disease, by providing persistent antibacterial action to manage disease and prevent recurring infections. Our approach involves the preparation of a range of selectively-functionalised, antibacterial silver nanoparticles through the use of microemulsion techniques for incorporation into a variety of materials, from hydrogels to glass ionomer cements. Our materials demonstrate significant antimicrobial activity against a range both planktonic cells and biofilm species, and offer significant advantages over currently-used treatment strategies to combat disease.

Our team have been committed to pursuing both beneficial health and commercial outcomes for our work, and in this talk, our journey from the lab bench, through animal trials and onto successful commercialisation of a range of technologies, including spin-out company formation, will be highlighted.

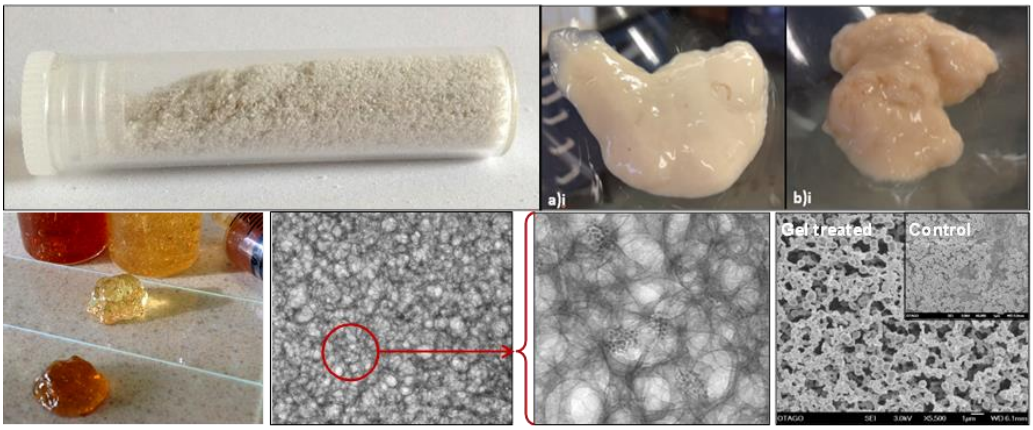

In-situ X-ray diffraction on sol-gel doped-PZT ferroelectric thin film

B. Allouche[1], I. Gueye[1, 2], G. Le Rhun[1, 2], P. Gergaud[1, 2] and N. Vaxelaire[1, 2]

[1]CEA/LETI, MINATEC Campus, Grenoble F-38054, France.
[2]Université Grenoble Alpes, Grenoble F-38000, France.
E-Mail: billal.allouche@cea.fr

In this work we present in-operando measurements performed on functional polycristalline thin films using conventional X-ray diffraction [1, 2]. Nb and La doped lead zirconate titanate films have been prepared by the chemical sol-gel deposition technique at the morphotropic phase boundary composition (i.e. $PbZr_{0.52}Ti_{0.48}O_3$). Films have been studied in the capacitance shape using Pt and Ru electrodes (i.e. Ru/PZT/Pt). Without applying electrical field, PZT films show (001) fiber texture with three types of domains (i.e. tetragonal-a, tetragonal-c and rhombohedral). Via the open access Python programming software an algorithm has been developed to fit the obtained X-ray data by using LmFit package [3] and taking into a count some constraints as that related to the used wavelengths (Cu ka1 and Cu ka2) and Scherrer peak broadening. The ferroelectric switching current has been measured simultaneously when applying bipolar triangular electric field and recording the corresponding X-ray diffraction data. Thus, the observed structural changes can be related to the macroscopic polarization and therefore to ferroelectric domain switching. From the relative lattice electro-strain and phase change (between tetragonal-a, tetragonal-c and rhombohedral) the intrinsic and extrinsic contributions to PZT properties have been quantified. It was found that the domain wall motion has an important role compared to that of domain extension (Fig. 1). One can consider these helpful results to design future piezoelectric materials with high performances.

Keywords: In-situ X-ray diffraction, polycrystalline PZT thin film, MPB, ferroelectric domain.

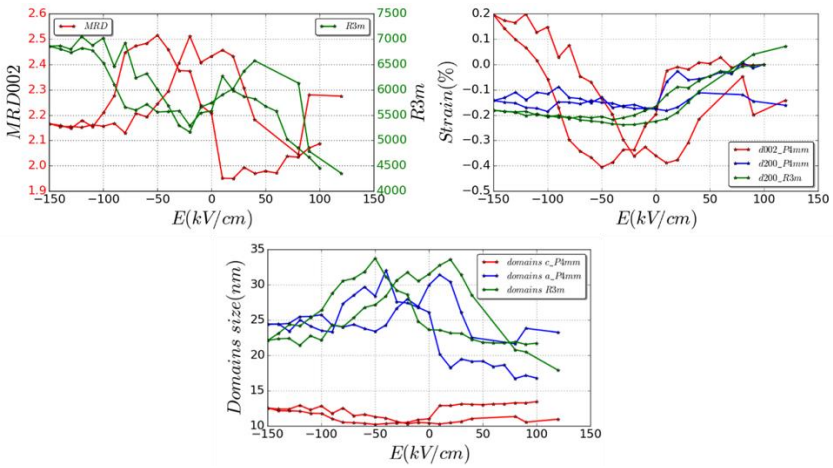

Fig.1: Electrical field effect on domain fraction, relative strain and domain size as revealed by X-ray diffraction.

References:

[1] VAXELAIRE, V., KOVACOVA, N. BERNASCONI, A., LE RHUN, G, ALVAREZ-MURGA, M, VAUGHAN, G. B. M., DEFAY, E. & GERGAUD P. 2016. Effect of structural in-depth heterogeneities on electrical properties of $Pb(Zr_{0.52}Ti_{0.48})O_3$ thin films as revealed by nano-beam X-ray diffraction. *Journal of Applied Physics* 120, 104101.

[2] KOVACOVA, V., VAXELAIRE, N., LE RHUN, G., GERGAUD, P., SCHMITZ-KEMPEN, T., & DEFAY, E. 2014 Correlation between electric-field-induced phase transition and piezoelectricity in lead zirconate titanate films. *Phys. Rev. B* **90**, 140101(R).

[3] NEWVILLE, M.; STENSITZKI, T.; ALLEN, D. B. & INGARGIOLA, A. 2014. LMFIT: Non-Linear Least-Square Minimization and Curve-Fitting for Python. *Zenodo.10.5281/zenodo.11813*.

Self-healing Properties of Thermoplastic Poly(azomethine-co-urethanes) Containing Reversible Covalent Bonds

Dae Woo Lee, Hanna Kim, and Dai Soo Lee

Department of Semiconductor and Chemical Engineering, Chonbuk National University, 567 Baekje-daero, Deokjin-gu, Jeonju-si, Chonbuk, 54896, Republic of Korea
dslee@jbnu.ac.kr / 82-63-270-2310

Polyurethane is one of versatile polymers for foams, coatings, adhesives, and elastomers. Such thermoplastic polyurethane (TPU) elastomers consisted of soft and hard segment. It show the microphase separation into the soft and hard domains. The hydrogen bonds between the urethane groups of TPU as well as the miscibility of soft and hard domain affect the microphase separation. The microphase separation of TPU determines the mechanical properties as well as thermal properties. Strong hydrogen bonds of TPU play the role of physical crosslinks and impart excellent elastomeric mechanical properties to TPU. However, due to the strong hydrogen bonds of TPU, TPU melts shows high viscosity. Moreover TPU will be exposed to the risk of degradation when heating of TPU for melt process. Recently, we found that TPU showed the self-healing properties by reversible nature of urethane groups which are formed by the reactions between phenolic hydroxyl groups and aromatic isocyanate [1]. In this paper, azomethine diol was synthesized by condensation reaction between vanillin and aliphatic diamine to introduce phenolic hydroxyl group in polyols. As the urethane groups show reversible nature above the glass T_g of poly(azomethine-co-urethane) (PAU), it was observed that PAU become self-healable. Furthermore, viscosities of PAU in melts can be lowered very much by the decrease of molecular weights due to the reversible nature of the specific urethane groups and the processing of PAU becomes very easy in the melts. We have investigated relaxation behaviors of PAUs with reversible covalent bonds employing Dynamic Mechanical Analyzer [2]. With increasing the temperatures, more decrease of relaxation time was observed in the PAU with reversible covalent bonds in comparison with the TPU without reversible covalent bonds in the range of temperatures. From the relaxation times measured with DMA, activation energies were obtained following Arrhenius plot. The calculated activation energies show decrease with increasing the content of azomethine diol. It is postulated that the tertiary amine in azomethine units play the role of catalyst for the reversible nature of the urethanes in the PAU investigated.

Keywords: relaxation time, reversible covalent bond, polyurethane, self-healing, azomethine

[1] LEE, D., KIM H., & LEE D., 2015. Characteristics of Polyurethane Elastomers Having Reversible Urethane Linkages. *Proceeding of Annual Conference of Korea Polymer Society in Fall, 10,* 104.

[2] DENISSEN W , RIVERO G , R. NICOLAY R, LEIBLER L , WINNE JM, & Du Prez FE, 2015. Vinylogous Urethane Vitrimers. *Adv. Funct. Mater. 25*, 2451–2457

LIGHT-EMITTING MATERIALS FOR TEXTILE APPLICATIONS

Pravin C. Patel, Hireni R. Mankodi, Anuradha Ajmera

Textile Engineering Department, Faculty of Technology and Engineering,
The M.S. University of Baroda, Vadodara:390001

Advance functional materials have attracted much attention as a next generation of textile fibres. The fibres functionality depends on end-use and covers wide range of applications. Luminous material is one of the functional materials in which rare earth minerals with luminescent properties are added in proper proportion to get desired luminescence. This type of material can be used to produce novel functional fibres also known as Luminescent Fibres. It is a fibre/filament which can emit its own light. Luminescent fibres have wide range of applications in textile like curtains, panels, fixed structures, decorative clothes, light-emitting slippers, light plush toys, knitting products, embroidery products etc. It also has various applications in technical textiles for fire-fighting personals and military personals.

In the present work, PET luminescent fibres/filaments have been prepared by using rare-earth strontium aluminates, the main source of light emission Eu2+,Dy3+ were added as the luminescent material, fibre- forming polymer PET as the matrix by the process of melt spinning.

The structure, composition and properties of luminescent material and fibres/filaments have been done by SEM, XRD, DSC and persistence glowing effect.

Key words: Decorative, Functional Fibres, Luminescence, Light-emitting, Melt-Spinning

Graphene Oxide Membrane Decorated with Metal Oxide Nanoparticles by Scanning Electrochemical Microscopy

M.O. Concha-Guzmán, J.M. Mora-Hernández, M.E. Rincón

Instituto de Energías Renovables, Universidad Nacional Autónoma de México, Av. Xochicalco S/N, Col. Centro, Temixco, Mor. 62580 México.
maocg@ier.unam.mx

The combination of graphene oxide (GO) decorated with metal oxides provides the opportunity to develop novel and functional materials for energy and environmental applications [1]. In this work, we decorated GO membranes with metal oxide nanoparticles using scanning electrochemical microscopy. GO was prepared from graphite powder by the Hummers modified method [2]. Inks of various concentrations were spray-coated on carbon paper to form self-standing membranes. X-ray diffraction, FTIR and TGA studies were performed before and after decoration. In order to compare the performance of the physicochemical interfacial processes and determine the charge-transfer active regions, the scanning electrochemical microscopy technique was used to decorate and characterized the membranes [3].

Keywords: graphene oxide, carbon paper, membrane, surface.

[1] AANI, S. A., J.WRIGHT C., ATIEH M. A., HILAL N. 2017. Engineering Nanocomposite Membranes: Addressing Current Challenges and Future Opportunities, *Desalination*, 401,1–15.

[2] HUMMERS JR, W. S.; OFFEMAN, R. E. 1958. Preparation of Graphitic Oxide. *Journal of the American Chemical Society*, 80 (6), 1339.

[3] Gupta S., Price C. 2015. Scanning Electrochemical Microscopy of Graphene/Polymer Hybrid Thin Films as Supercapacitors: Physical-Chemical Interfacial Processes. *AIP ADVANCES*, 5, 107-113.

Ce-doped NiZn nanoferrites ($Ni_{0.8}Zn_{0.2}Ce_xFe_{2-x}O_4$) for Technological Applications: Synthesis, Structural and Magnetic Investigations

Majid Niaz Akhtar[a, *] *, Muhammad Azhar Khan*[b]

[a]*Department of Basic Sciences and Humanities , Muhammad Nawaz Sharif University of Engineering and Technology (MNSUET), 60000 Multan, Pakistan.*
[a]*Department of Physics, The Islamia University of Bahawalpur, Bahawalpur-63100, Pakistan.*

Corresponding author: majidniazakhtar@mnsuet.edu.pk
majidniazakhtar@gmail.com *Tel: +923336856069*

$Ni_{0.8}Zn_{0.2}Ce_xFe_{2-x}O_4$ nanoferrite samples with different compositions such as x=0, 0.1, 0.2, 0.3, 0.4 and 0.5 were synthesized using sol gel method. XRD (X-ray diffraction), FTIR (Fourier Transform Infrared Spectorscopy), FESEM (Field Emission Scanning Electron Microscopy) and VSM (Vibrating Sample Magnetometer) were used to investigate the phase, structure, metal stretching vibrations, morphology, dielectric and magnetic properties of $Ni_{0.8}Zn_{0.2}Ce_xFe_{2-x}O_4$ nanoferrites respectively. The crystallite size, lattice parameter (theoretical and experimental) and volume of the cell decreased with Ce^{3+} contents in the NiZn ferrite. The size of the crystallites were in the range of 41 to 9 nm respectively. The physical properties such as bulk density, X-ray density and porosity were also found to be decreased with Ce^{3+} substitution in the NiZn ferrites. However, the lattice strain were increased with Ce subsititution. The cation distributions at the tetrahedral and octahedral sites of the Ce doped NiZn nanoferrites were also determined. The force constant at tetrahedral and octahedral sites were also calculated from the FTIR analysis. The magnetic properties such as remanence, saturation, coercivity, Bohr magneton and magneto crystalline anisotropy constant (K) were evaluated from the magnetic hysteresis loops. Saturation magnetization, remanence were decreased whereas the coercivity were increased. Bohr magneton and initial permeability were decreased with the substitution of Ce^{3+} contents. Yaffet and Kittle (Y-K) angles were also calculated and were increased with Ce doped NiZn nanocrystalline ferrites. These Ce-doped NiZn nanoferrites with excellent properties have potential technological applications in various fields such as security, switching, core and microwave absorption applications and devices.

Keywords: Nanoferrites; X-ray Diffraction; Fourier Transform Infrared Spectroscopy; Scanning Electron Microscopy, Magnetic Properties

Development of A New Type of Magnetoelectric Coupling

Stephen S. Sasaki

University of California, Los Angeles

Experimental realization of a novel granular multiferroic composite has successfully demonstrated a new type of magnetoelectric coupling. The composite multiferroic consists of single domain Ni nanocrystals forced into close proximity by diacid linkers and subsequently surrounded by a ferroelectric. The theoretical model provides an excellent fit of the experimental results, with the composite multiferroic showing an enhanced coercivity as a function of temperature and a significantly increased onset of observable coercivity.

Metal/Semiconductor Hetero-nanocrystals: Hetero-Interface Control and advanced new energy Applications

Jiatao Zhang

Beijing Key Laboratory of Construction Tailorable Advanced Functional Materials and Green Applications, School of Materials Science and Engineering, Beijing Institute of Technology, Beijing, 100081, China

***Corresponding author. Tel: 86-10-68918065, Fax: 86-10-68918065 and** Email: zhangjt@bit.edu.cn*

Growth of monocrystalline semiconductor based metal/semiconductor hybrid nanocrystals （core/shell and heterodimer） with modulated composition, morphology and interface strain are the prerequisite for exploring their plasmon-exciton coupling, efficient electron/hole separation, and enhanced photoctalysis properties. By controlling soft acid-base coordination reactions between molecular complexes and colloidal nanostructures, we showed that chemical thermodynamics could drive nanoscale monocrystalline growth of the semiconductor shell on metal nano-substrates. We have demonstrated evolution of relative position of Au and CdX in Au-CdX from symmetric to asymmetric configuration, different kinds of phosphine initialized cation exchange reactions to precisely synthesize metal/semiconductor hetero-nanostructures and doped semiconductor nanostructures, heterovalent dopant engineering, and oriented attachment of doped Qds into micrometer nanosheets, which can further lead to fine tuning of doped level, plasmon-exciton coupling, different hydrogen photocatalytic performance and enhanced photovoltaic, electrical properties. The doped luminescence and p-/n-type electronic impurities in semiconductor nanostructures enabled the exploration of their photoelectric conversion applications.

References

J. Zhang, Y. Tang, K. Lee, M. Ouyang, *Nature* 2010, 466, 91.

J. Zhang, Y. Tang, K. Lee, M. Ouyang, *Science* 2010, 327, 1634.

Q. Zhao, J. Zhang*, etc., *Adv. Mater.* 2014, 26, 1387.

H.Qian, J. Zhang*, etc., *NPG Asian Mater.* 2014, accepted.

J. Gui, J. Zhang*, etc., Angew. Chem. Int. Ed. 2015, 54, 3683-3687.

J. Liu, Q. Zhao, J. Zhang*, etc., *Adv. Mater.* 2015, 27, 2753-2761.

M. Ji, M. Xu, **J. Zhang***, etc. ***Adv. Mater.*** 2016, 28, 3094–3101.

Sequential Processing for Production of BHJ Solar Cells and Electronic Doping of Conjugated Polymer Films

Benjamin Schwartz

University of California, Los angeles Campus, USA

One of the key issues with improving the efficiency of conjugated polymer-based phovoltaics is controlling the nm-scale morphology of the two active components. Typically, efficiency is optimized by trial-and-error: component weight ratios, solvent additives, post-processing thermal annealing, etc. are all used to attempt to obtain the desired bulk heterojunction (BHJ) interpenetrating network. In this talk, we discuss some of our recent work aimed at using alternate, more reproducible methods for controlling BHJ morphology. We show that sequential processing (SqP) of the polymer and fullerene components can provide an exquisite degree of control of the nm-scale morphology of a BHJ, and that the degree of crystallinity and swellability of the polymer controls both the amount of intercalated fullerene and the geometry of the interpenetrating network. We also demonstrate that SqP can be used to molecularly dope films of conjugated polymers, enabling control over the crystalline domain sizes and morphology, and enabling AC-field Hall effect and other measurements that directly address the nature of carrier transport.

Heteropolyacid Immobilized on Thiol-Functionalized Halloysite Clay Nanotubes: Efficient Catalyst for the Synthesis of Indeno[1,2-b]quinolines via Four-Component Reaction

Majid, M. Heravi [1a] Samahe Sadjadi [2], [,b] and Mansoureh Daraie[1,c]

[1] Gas Conversion Department, Faculty of Petrochemicals, Iran Polymer and Petrochemical Institute, PO Box 14975-112, Tehran, Iran

[2] Department of Chemistry, School of Science, Alzahra University, PO Box 1993891176, Vanak, Tehran, Iran

mmh1331@yahoo.com [a], samahesadjadi@yahoo.com [b], [c]daraie_m@yahoo.com

Keywords: Phosphotungstic acid, Halloysite Clay, Indeno[1,2-b]quinoline, Catalyst.

A novel heterogeneous hybrid catalyst was designed and synthesized by functionalization of halloysite clay nanotubes by 3-mercaptopropyl trimethoxysilane and subsequent immobilization of Keggin type heteropolyacid, phosphotungstic acid via wet impregnation method. The characterization of the catalyst was carried out by SEM/EDX, FTIR and XRD techniques. Moreover, the catalytic activity of the catalyst was investigated for four-component reaction of benzaldehydes, dimedone, 1,3-indandione, and amines to afford indeno[1,2-b]quinoline. The results indicated high catalytic activity and reusability of the catalyst which was superior compared to some previously reported catalysts. Relatively short reaction time as well as solvent-free condition was other merits of this protocol.

Hydrogen Storage Properties of Hollow Carbon Balls

Sang Kyoo Lim[1], Seong Hui Hong[1], Young Kwang Kim[1], Sung-Ho Hwang[1]
[1]Smart Textile Convergence Research Group, Daegu Gyeongbuk Institute of Science and Technology (DGIST), Daegu 42988, Republic of Korea
E Mail limsk@dgist.ac.kr

Hydrogen is an advantageous energy source because it is renewable and its use would reduce the emission of pollution. It has been considered as an ideal energy medium for replacing fossil fuels such as oil and coal. The success of hydrogen economy in the future depends on our ability to discover efficient and cost-effective hydrogen storage materials. Considerable scientific efforts have been made to study carbon materials, metal-organic frameworks (MOF), metal hydrides, and so on. Among the above promising materials, carbon-based materials have received continuous interest as potential hydrogen storage media due to their high surface areas, tunable texture structures and low gas-solid interactions, which provide high hydrogen uptake capacity. Hollow carbon balls were successfully synthesized via dispersion polymerization and carbonization of modified poly methyl methacrylate(PMMA). The hydrogen storage properties and morphological structure were investigated.

Keywords: Hydrogen storage, Carbon ball, Hollow, Dispersion polymerization

[1] [1] Niaz, S., Manzoor, T., Pandith, AH. 2015. Hydrogen Storage: Materials, Methods and Perspectives. *Renewable Sustainable Energy Rev*, 50, 457-469.
[2] [2] Zhang, F., Zhao, P., Niu, M., Maddy, J. 2016. The Survey of Key Technologies in Hydrogen Energy Storage. *Int J Hydrogen Energy*; 41, 14535-14552.
[3] [3] Sethia, G., Sayari, A. 2016. Activated Carbon with Optimum Pore Size Distribution for Hydrogen Storage. *Carbon;* 99, 289-294.

Acceptance ID: 23TP-P

On the Dislocation Contribution to the Dielectric Loss in the Materials with Piezoelectric Properties

V.N.Nechaev, V.V.Dezhin

Voronezh State Technical University, Voronezh, Russian Federation
viktor.dezhin@mail.ru

The dielectric dispersion is known to be due to both ferroelectric nature of a crystal and various impurities and defects within it occurs in ferroelectrics in the wide range of frequencies from 10^4 to 10^{12} s^{-1}. One should have the complete classification of the mechanisms of the dielectric dispersion and the dielectric loss to understand better the physical properties of ferroelectrics. This is of great importance for the polycrystalline ferroelectrics, where the concentration of defects of various kinds is very high. In the present report the dielectric loss and the dielectric dispersion in a ferroelectric crystal with dislocations are studied. The results may be applicable both to the paraelectric and ferroelectric states. However, if some ferroelectric is not a piezoelectric in paraelectric state, then the investigated effects in paraelectric state will be rather weak because of the weak electrostriction coupling. Let a variable electric field be applied to a crystal. This field gives rise – through the piezoelectric coupling – to the variable mechanical stresses. Then the dislocations in the crystal will be driven by Peach-Koehler force and will start moving, dissipating the external field energy. Connection of the electric field energy dissipated per unit time with the internal friction is found. The case of resonant loss (Granato-Lucke model) is considered. The loss related to this mechanism to be at frequencies of megahertz range. The relaxation processes being responsible for the Bordoni and Hasiguti peaks also are considered. The use of obtained equations makes it possible to distinguish the dislocation contribution to both dielectric loss and dielectric dispersion and, therefore, to derive additional information about the crystal structure in a sufficiently simple way in terms of only one method.

Keywords: Piezoelectrics, dielectric loss, dislocation, internal friction

Acceptance ID: 2GTY-P

Laminated Composite Beam Finite Element Formulation for Modeling Flexible Smart Structures Undergoing Large Deformations

Peter L. Bishay[1]; Ardalan R. Sofi[1]

[1]California State University, Northridge, CA, USA.

Smart material elements are embedded in many composite structures that undergo large deformations, such as hybrid polymer composites with embedded shape-memory alloy wires or piezoelectric fibers or patches, in robotic applications and morphing aerospace structures. Hence, it is critical to develop efficient computational tools to precisely and accurately predict the deformation of such composite structures subjected to any mechanical or hydrothermal loading. In this work, a finite element formulation of fiber-reinforced laminated composite beams undergoing large deformation and rotation, in response to mechanical or hydrothermal loads, is developed based on Von Karman nonlinear theory and the Updated Lagrangian (UL) approach. Stretching, bending, and torsion has been accounted for, and a closed form element tangent stiffness matrix has been derived. The model has been verified in different problems by comparison with Nastran-in-CAD results. In all problems, the difference in the resulting deformations is less than 10%. The major advantage of the proposed approach is that the composite beam is modeled using 1D elements rather than 2D elements with laminated composite material as in the case of using regular finite element software packages. Hence, the proposed model is highly efficient specially when dealing with large structures made of flexible composite beams.

Keywords: Flexible Composites; large deformation; geometric nonlinearity; finite elements.

Acceptance ID: 2PTL-O

Laminated composite for plain bearings

Kontsevoi, Mejlakh, Shubin, Pastukhov, Sipatov.

Institute of Metallurgy of Ural Branch of Russian Academy of Sciences.
kuv.45@mail.ru / Russia, 620016, Ekaterinburg,101 Amundsen st.

Today the topical problem of material science is development of new antifriction coatings and technology of their applying on substrate. Methods of powder metallurgy are most promising ones to solve the problem due to considerable opportunities in selection of composition and designing of materials structure. The new antifriction high-density powder composite material has been developed. Copper reinforced by particles of ferro-aluminides and iron serve as a basis for the composite. Lead inclusions are solid lubricant. Optimization of powder dispersiveness, parameters of Fe-Al intermetallides synthesis by mechanical technique, method of powders homogenization, schemes and regimes of heat treatment and forming operations of powder mixtures have established a foundation for production of the composite. To obtain coatings with relative density of 0.99-1.00 it is advantageous to make direct rolling of powder charge on a substrate with total cobbing of 75-80%. It was established in the result of investigation of influence of pressure in forming operations and rolling regimes (rate and deformation ratio) on compacting of powder mixtures. Whereas, solid additives (ferroaluminides and iron) are reduced in size in 8-9 times and aligned in rows along rolling axis. Microstructure takes the fibrous form shown in Fig., submicron intermetallic particles - dark dots, reinforcing iron inclusions of stripe form, and lead elongated in thin plates are evenly distributed at a composite body.

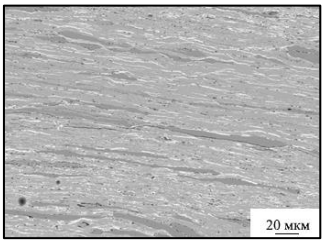

Fig. The sample composition (mass %) is 5 - Fe_2Al_5, 5 - Fe, 10 - Pb, Cu the balance.

The Brinell hardness and friction torque of the developed composite are 980÷1000 MPa and 0.4 N•m, respectively.

Keywords: antifriction coatings, reinforced composite, copper matrix, plain bearing, laminated structure

Acknowledgements: This work was supported by Russian Scientific Foundation, project № 15-13-00029.

Acceptance ID: 2SN4-P

Functional graded W-Cu materials prepared from Cu-coated W powders by microwave sintering

Huipei Chen[1] , Jigui Cheng[1,2], Wenchao Chen[1,2], Jianfeng Li[1,2], Laima Luo[1,2], Yucheng Wu[1,2]*

1. School of Materials Science and Engineering, Hefei University of Technology, Hefei, 230009, China.
2. Research Centre for Powder Metallurgy Engineering and Technology of Anhui Province, Hefei, 230009, China
Tel: +86 0551 62901793; fax: +86 0551 62901361
E-mail: jgcheng63@sina.com

In a fusion reaction device like Tokamak, tungsten has been considered to be one of the promising materials for the plasma facing materials (PFMs). In addition, copper and its alloys are often used as the heat sink materials. However, because of the differences in coefficient of thermal expansions (CTE) and Young's modulus, the joining of these two materials results in high residual and thermal stresses at the interface when exposed to high-heat loads. In order to overcome these drawbacks, functional graded W-Cu composite materials were used as an interlayer to relieve the thermal stress. Nevertheless, the distinct difference in physical properties between W and Cu, make different sintering shrinkage between W-Cu layers with different Cu content. Thus, it is still a challenging work to fabricate the W-Cu FGMs with wide compositional distribution and good properties.

In experimental, Cu-coated W powders with different Cu contents and particle size were prepared by an electro less process. Functional graded W-Cu composite materials were obtained by lamination pressed the W-Cu powders, and subsequently wave sintering. Microstructure of W-Cu FGM samples were observed by scanning electron microscope (SEM). The elementary distribution of the samples was characterized by energy dispersive spectrum (EDS). Density, physical property and mechanical property of the samples were also investigated.

The experiment results show that the W-Cu FGM samples which sintered at 1350˚C for 40 min reach relative density above 97%. The Cu element has a graded distribution in the thickness direction. The interfaces between layers bond well. Furthermore, the samples exhibit excellent physical and mechanical properties. The thermal conductivity of the samples reaches 210W•(m•K^{-1}). The maximum bending strength and hardness is 1004 MPa and 346HV, respectively.

Key words: W-Cu functionally gradient materials; Microwave sintering; Microstructure; Interface

Acceptance ID: 2TY9-P

Preparation of Epoxy-modified Silicone-treated Micro-/Nano-Silicas in Epoxy/Silica Composites for Electrical Insulators

Hong-Ki Lee[1], Jae-Young Lee[1] and In-Soo Jeong[2]

[1]Hydrogen Fuel Cell Center, Woosuk University, Korea
[2]Korea Institute of Science and Technology Information, Korea

The surface of micro-silica or nano-silica was modified with epoxy-modified silicone and their effect on the electrical breakdown strength was evaluated in epoxy/micro-/nano-silica composites (EMNC). Firstly, the surface of micro- or nano-silica was treated with hydroxy silane and then the hydroxy group of the silane was reacted with epoxy-modified silicone. And then the surface-treated micro- and nano-silica were mixed with epoxy resin and polyester-modified polydimethylsiloxane (PEM-PDMS) by using an ultrasonicator. Transmission electron microscope (TEM) was used to observe the even dispersion of nano-silica in an epoxy/micro-silica composite and it was found that the nanosilicas were well dispersed. Electrical breakdown strength of the epoxy/micro-silica (60 wt%)/nano-silica (1 phr)/PEM-PDMS (0.5 phr) system was 60.0 kV/2 mm, which was 13.6% higher than that of epoxy/micro-silica (60 wt%)/PEM-PDMS (0.5 phr) system, 52.8 kV/2 mm. And contact angle of neat epoxy was 77°, which was 132% higher than that of epoxy/micro-silica (60 wt%)/nano-silica (1 phr)/PEM-PDMS (0.5 phr) system, 101.6°.

Keywords: Micro-silica, Nano-silica, Epoxy-modified silicone, Epoxy/micro-/nano-silica composite (EMNC), Electrical insulation breakdown strength

Acceptance ID: 37EJ-P

Internet of Things (IoT) : Application and Challenge on the Growth of a Single CuO Nanowire Using Chemical Vapor Device (CVD) Method

Tai-Yue Li[1], *Da-Chi Luo*[1], *Sheng Yun Wu*[1,*]

[1]*Department of Physics, National Dong Hwa University, Hualien 97401, Taiwan.*
**Corresponding Email:sywu@mail.ndhu.edu.tw (SYW)*

A new IoT- chemical vapor device was designed and performed to synthesize well separate *in-plane* CuO nanowires with a high level of crystallinity using a copper grid substrate, avoiding the appearance of catalytic contamination. We compare and contrast two types of with- and without- IoT, to identify their potential for monitoring the size effects of growth mechanism. Two-dimensional EDS mapping with a diffusion model was used to obtain the diffusion length and the activation energy ratio. The ratio value is close to 0.3~0.4, revealing that the growth of CuO nanowires was attributed to the short-circuit diffusion. Confocal Raman spectroscopy is a powerful tool for probing the phonon confinement effect in a single CuO nanowire. The confocal Raman spectrometry results confirm the expected outcome, that reducing of the diameter of a cylindrical cross-section of a single nanowire results in Raman frequency downshifts. The applicability of investigating the size effects of the quantum confinement of a single nanowire with IoT big data recording is possible because the *in situ* detections for CVD enviroments are relatively straightforward and the reproduced well separated CuO nanowires can be obtained accoring big data analysis.

Keywords: Internet of Things, Nanowire, Chemical vapor device, Raman, EDS mapping

Acceptance ID: 38E9-P

Proliferation, morphology and gene expression of gingival fibroblasts on ceria-stabilized zirconia/alumina nanocomposite

Fuminori.I[1], *Yoko.O*[1], *Kazuyoshi.B*[1]

Depertment of Prothodontics,School of Dentistry,Showa University ,Tokyo,Japan[1]
ft.iwasa@dent.showa-u.ac.jp

The Ce-stabilized tetragonal zirconia polycrystals (Ce-TZP) nanostructured zirconia/alumina composite (Ce-TZP/Al_2O_3) is composed of 10 mol% cerium dioxide (CeO_2) stabilized TZP as a matrix and 30 vol% of Al_2O_3 as a second phase. Ce-TZP/Al_2O_3 exhibits greater flexural strength and fracture toughness than yttria-stabilized tetragonal zirconia polycrystals (3Y-TZP), and it is completely resistant to low temperature aging degradation, indicating its suitability for use in dental implants. [1,2] The acquisition of soft tissue seal plays a critical role in long-term success of dental implants. The periodontal attachment to Ce-TZP/Al_2O_3 implant surface treatments such as machined and mirror finishing have been a topic of particular interest in this respect. Considering the existing controversy regarding soft tissue behavior in contact with Ce-TZP/Al_2O_3 implant surfaces, this study aimed to assess the attachment, proliferation, morphology and extracellular matrix (ECM) synthesis of human gingival fibroblasts (HGFs) on different Ce-TZP/Al_2O_3 abutment surfaces.

In this in vitro, experimental study, HGFs were cultured on discs (machined titanium, machined and mirror polished zirconia). Cell viability, proliferation rate, morphology and ECM and proinflammatory cytokine synthesis were assessed by tetrazolium salt-based colorimetry (WST-1) assay, scanning electron microscopy (SEM), real-time polymerase chain reaction (PCR), and multiplex cytokine immunoassay system, respectively. Data were analyzed using ANOVA and Post Hoc test. Fibroblast initial attachment after 24h cultivation was markedly higher in both zirconia groups than that in titanium group. Proliferation rate on machined zirconia groups showed the greatest activity among three groups in 3days after seeding. In contrast to the typical spindle-shaped cells on the machined titanium surfaces, both zirconia surfaces had small circular/angular cells containing contractile ring-like structures and elongated, multi-shaped cells with a developed cytoskeletal network. Ce-TZP/Al_2O_3 surfaces were found to produce dermal-related ECM synthesis at both the protein and gene levels, without proinflammatory cytokine synthesis. Within the limitations of this study, HGFs on machined Ce-TZP/Al_2O_3 surfaces had a more mature morphology and greater proliferation and differentiation as compared to those on mirror polished zirconia and machined titanium surfaces. This indicates better attachment of these cells to machined Ce-TZP/Al_2O_3 surfaces, creating a more efficient soft tissue seal around dental implants.

Keywords: Ce-TZP/Al_2O_3, Gingival fibroblast, Zirconia implant

[1] Nawa M, Bamba N, Sekino T, Niihara K. The effect of TiO2 addition on strengthening and toughening in intragranular type of 12Ce-TZP/Al2O3 nanocomposited. J Eur Ceram Soc 1998;18:209-219.
[2] Tanaka K, Tamura J, Kawanabe K, Nawa M, Oka M, Uchida M, et al. Ce-TZP/Al2O3 nanocomposite as a bearing material in total joint replacement. Journal of biomedical materials research 2002;63:262-270.

Acceptance ID: 3S2C-P

Magnetite Nanoparticles Compounded Silica@Carbon Dots: Synthesis and Fluorescence Sensing of Fluoride Ions

An efficient, reusable and double fluorophore complexed magnetic fluoride nanoparticle has been designed with a chemical recognition receptor in charge of the exchange of fluorescent substance and F^- ions. Organosilane-functionalized carbon dots (SiCDs) are immobilized in outer mesoporous silica ($mSiO_2$) which is coated on the Fe_3O_4 core protected by an amorphous silica layer, and then compound as a fluorescent superparamagnetic nano-core (Fe_3O_4@SiO_2@$mSiO_2$-SiCDs) with a maximum excitation wavelength of 525 nm. A fluorescent fluoride probe composed of pure carbon quantum dots (pCDs) with a maximum excitation wavelength of 450 nm and Lanthanum coordinated diethylenetriaminepentaacetic acid (DTPA)-modified fluorescent core (Fe_3O_4@SiO_2@$mSiO_2$-SiCDs@DTPA−La^+, FSMN) has been realized. The probe could act as a concentration indicator since F^- ions are absorbed through the exchange reaction between the pCDs and fluoride ions. This method is extremely sensitive, fast, and selective for fluoride ions and could monitor the real-time concentration of nanoparticles in aqueous solution. The minimum detection limit of fluoride is 50 nM and the removal efficiency is higher than 96% when utilized in tap water. Excellent mesoporous and superparamagnetic properties of the receptor are advantageous for the removal and quantification of fluoride ions. Because of the high sensitive, reusable and biocompatible nature, FSMN-pCDs shows great potential to serve as fluorescent sensor for intracellular detection of fluoride and in drug delivery system.

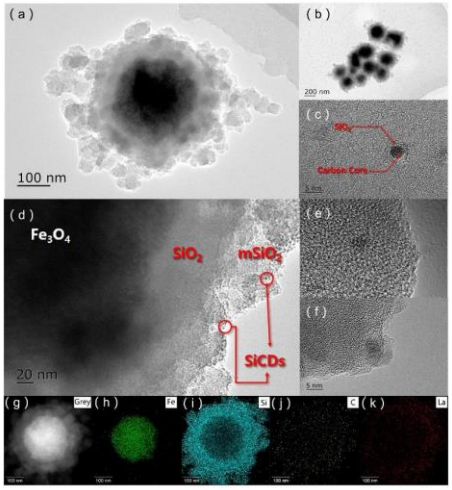

Figure 1 Nanostructure of Fe_3O_4@SiO_2@$mSiO_2$-SiCDs@DTPA−La^+: (a, b, d) Low magnitude TEM images, (c) HRTEM images of SiCDs, (e-f) HRTEM images of immobilized SiCDs in outer mesoporous silica coat, (g-k) SEDS images show the distribution of Fe, Si, C, La elements.

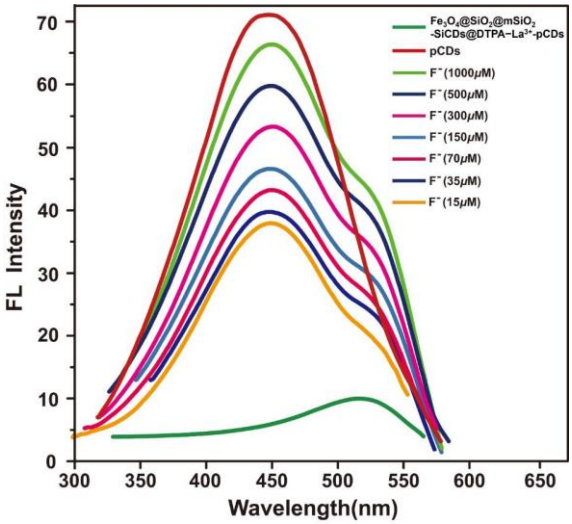

Figure 2 Fluorescence spectra of pCDs, Fe_3O_4@SiO_2@mSiO_2-SiCDs@DTPA−La^{3+}, and Fe_3O_4@SiO_2@mSiO_2-SiCDs@DTPA−La^{3+}-pCDs with gradual addition of F^- ions in Millipore water.

Acceptance ID: 3ZVP-O

Non-isocyanate polyurethanes and their self-healable properties

Sang Hyub Lee and Dai Soo Lee

Department of Semiconductor and Chemical Engineering, Chonbuk National University, 567 Baekje-daero, Deokjin-gu, Jeonju-si, Chonbuk, 54896, Republic of Korea
dslee@jbnu.ac.kr / 82-63-270-2310

Due to the outstanding physical properties, polyurethanes (PU) have been widely used in the various fields for coating, fiber, insulation, cushioning, and adhesives. Usually, the PU elastomers are synthesized by the reaction of isocyanate (N=C=O) terminated PU prepolymers and cross linking agent. In the application of PU system, moisture sensitivity of isocyanates is one of difficulities due to the high reacticity of N=C=O with moisture, resulting in undesirable product through the irreversible urea forming side reaction. And storage stability of PU prepolymers also could be negatively affected by moisture in the environments.

To overcome these drawbacks of conventional PU systems, non-isocyante PU (NIPU) system based on the end-capping of PU prepolymers with glycerol carbonate (GC) and curing by the reaction of cyclic carbonate and amine was developed. The capping of N=C=O groups with GC alleviate the moisture sensitivity and improve the storage stabilities of PU systems. [1-3]

Furthermore, hydrogen bonds in NIPU are largely increased compared with the conventional PUs due to the OH groups generated through the ring opening of cyclic carbonate by amines during the cure. The enhanced H-bonding in NIPU impart self-healable properties against damages such as micro-crack and cut in NIPU. The self-healing ability of NIPU is expected to extend the lifetime of NIPUs as well as extend the application of PUs in various fields. [4-5]

Keywords: Non-isocyanate polyurethane, Hydroxyl urethane, Hydrogen bonding, Self healing

[1] ALBERT LEE & YULIN DENG. 2015. Green polyurethane from lignin and soybean oil through non-isocyanate reactions. *European Polymer Journal*, 63, 67-73.
[2] JIN GUAN, YIHU SONG, YU LIN, XIANZE YIN, MIN ZUO, YUHUA ZAHO, XIAOLE TAO & QIANG ZHENG. 2011. Progress in study of Non-Isocyanate Polyurethane. *Ind Eng Chem Res* , 50, 6517-6527.
[3] LISE MAISONNEUVE, OCEANE LAMARZELLE, ESTELLE RIX, ETIENNE GRAU & HENRI CRAMAIL. 2015. Isocyanate-Free Routes to Polyurethanes and Poly(hydroxyl Urethane)s. *Chem Rev*, 115, 12407-12439.
[4] YULIN CHEN, AARON M. KUSHNER, GREGORY A. WILLIAMS AND ZHIBIN GUAN. 2012. Progress in study of Non-Isocyanate Polyurethane. *NATURE CHEMISRY*, 4, 467-472.
[5] YINLEI LIN & GUANGJI LI. 2014. An intermolecular quadruple hydrogen-bonding strategy to fabricate self-healing and highly deformable polyurethane hydrogels. *J Master Chem B*, 2, 6878-6885.

Acceptance ID: 42wQ-O

Application of SiC/Carbon Nanofiber composite for Thermal barrier

Sung-Ho Hwang[1], *Young Kwang Kim*[1], *Sang Kyoo Lim*[1]

[1]*Smart Textile Convergence Research Group, Daegu Gyeongbuk Institute of Science and Technology (DGIST), Daegu 42988, Republic of Korea*
E Mail hsungho@dgist.ac.kr

As prepared SiC/Carbon nanofiber composite (SiCNC) has superior thermal properties. SiCNC is prepared by electrospinning with the mixed solution of polyacrylonitrile (PAN) and tetraethyl orthosilicate (TEOS) and thereafter carbonization of electrospun fibers under N_2 flow. For an application to thermal barrier materials, thermal stability and conductivity of SiCNC were investigated depending on annealing time. In-plane thermal conductivity of SiCNC showed higher value with increasing of annealing time. Especially, SiCNC which was annealed for 10 hours at 1400°C has the highest thermal conductivity (0.674 W/m·K) and thermal stability, which is confirmed by thermal decomposing rate of materials calculated from TGA result (R_{TD} =1.883%/min). Whereas, annealing time of SiCNC are not correlated with through-plane thermal conductivity. We suggest intensively one-pot preparation of SiCNC with economic feasibility through its systematic comparison for the thermal properties enhancement. Furthermore, formation mechanism of SiCNC is discussed.

Keywords: Silicon carbide, Carbon nanofiber, thermal conductivity, electrospinning

[1] Nhut, J.-M., Vieira, R., Pesant, L., Tessonnier, J.-P., Keller, N., Ehret, G., Pham-Huu, C., Ledoux, M. J., Synthesis and catalytic uses of carbon and silicon carbide nanostructures. *Catalysis Today* **2002,** *76* (1), 11-32.
[2] Hmida, H. A. a. E. S. B. H., Silicon Carbide: Synthesis and Properties, Properties and Applications of Silicon Carbide, Prof. Rosario Gerhardt (Ed.), *InTech* **2011**.
[3] Matsumoto, H., Imaizumi, S., Konosu, Y., Ashizawa, M., Minagawa, M., Tanioka, A., Lu, W., Tour, J. M., Electrospun Composite Nanofiber Yarns Containing Oriented Graphene Nanoribbons. *ACS Appl. Mater. Interfaces* **2013,** *5* (13), 6225-6231

Acceptance ID: 45VT-P

Electric-field control of magnetism in multiferroic heterostructures

Y. G. Zhao[1], A. T. Chen[1], Y. Liu[1], P. S. Li[1], X. F. Han[2], D. T. Pierce[3], John Unguris[3], H. G. Piao[4], H. S. Luo[5], S. Y. Li[6], X. Z. Zhang[4], and C. W. Nan[4]

[1]*Department of Physics, Tsinghua University, Beijing 100084, China*
[2]*Beijing National Laboratory for Condensed Matter Physics, Chinese Academy of Sciences, Beijing 100190, China*
[3]*Center for Nanoscale Science and Technology, National Institute of Standards and Technology, Gaithersburg, Maryland 20899, USA*
[4]*School of Materials Science and Engineering and State Key Lab of New Ceramics and Fine Processing, Tsinghua University, Beijing 100084, China*
[5]*Shanghai Institute of Ceramics, Chinese Academy of Sciences, Shanghai 201800, China*
[6]*Department of Physics, Fudan University, Shanghai 200433, China*
ygzhao@tsinghua.edu.cn

With the fast development of information storage, exploiting new concepts for dense, fast, and non-volatile random access memory with reduced energy consumption is a significant and challenging task. To realize this goal, electric-field control of magnetism is crucial. In this regard, multiferroic materials, especially multiferroic heterostructures [1,2], composed of ferromagnetic (FM) and ferroelectric (FE) materials, provide an important way for manipulation of magnetism via electric fields, which is essential for the new generation information storage technology.

We have carried out electric-field control of magnetism in different FM/FE heterostructures in our previous work [3]. Recently, We study the angular dependence of electric-field-controlled exchange bias and magnetization reversal in CoFeB/IrMn/$Pb(Mg_{1/3}Nb_{2/3})_{0.7}Ti_{0.3}O_3$ [4], showing the control of exchange bias by electric fields, and electric-field-controlled magnetization reversal was realized at zero magnetic field. We also studied electric-field control of magnetism in multiferroic heterostructures composed of CoFeB and (1-x)$Pb(Mg_{1/3}Nb_{2/3})O_3$-x$PbTiO_3$ (PMN-xPT) with different ferroelectric phases via changing composition and temperature [4], demonstrating the coupling between magnetism and ferroelectric domains including macro and microdomains for different ferroelectric phases. We then studied electric-field control of magnetism in CoFeB/PMN-PT at the mesoscale using spatially-resolved techniques including scanning Kerr microscopy and scanning electron microscopy with polarization analysis with in situ electric fields [4], and revealed the domain-switching controlled magnetism, providing a path for designing magnetoelectric devices through domain engineering. Our work demonstrates the interesting new physics and potential applications of electric-field control of magnetism in the FM/FE multiferroic heterostructures and should be significant for spintronics.

Keywords: Electric-field control of magnetism, multiferroic heterostructure

[1] EERENSTEIN, W., MATHUR, N. D. & SCOTT, J. F. 2006. Multiferroic and Magnetoelectric Materials. *Nature*, 442, 759-765.
[2] RAMESH R. & SPALDIN N. A. 2007. Multiferroics: Progress and Prospects in Thin Films. *Nature Mater.*, 6, 21-29.
[3] ZHANG, S. et al., 2012. Electric-Field Control of Nonvolatile Magnetization in $Co_{40}Fe_{40}B_{20}$/$Pb(Mg_{1/3}Nb_{2/3})_{0.7}Ti_{0.3}O_3$ Structure at Room Temperature. *Phys. Rev. Lett.* 108, 137203; ZHANG, S. et al., 2014. Giant electrical modulation of magnetization in $Co_{40}Fe_{40}B_{20}$/$Pb(Mg_{1/3}Nb_{2/3})_{0.7}Ti_{0.3}O_3$(011) heterostructure. *Scientific Reports*, 4, 3727; YANG, L. F. et al., 2014. Bipolar loop-like non-volatile strain in the (001)-oriented $Pb(Mg_{1/3}Nb_{2/3})O_3$-$PbTiO_3$ single crystals. *Scientific Reports*, 4, 4591; LI, P. S. et al., 2014. Electric Field Manipulation of Magnetization Rotation and Tunneling Magnetoresistance of Magnetic Tunnel Junctions at Room Temperature. *Adv. Mater.* 46, 2340;
[4] CHEN, A. T. et al., 2016. Angular dependence of exchange bias and magnetization reversal controlled by electric-field-induced competing anisotropies. *Adv. Mater.* 28, 363; LIU, Y. et al., 2016. Electric-field control of magnetism in $Co_{40}Fe_{40}B_{20}$/(1-x)$Pb(Mg_{1/3}Nb_{2/3})O_3$-x$PbTiO_3$ multiferroic heterostructures with Different Ferroelectric Phases. *ACS Appl. Mater. Interfaces* 8, 3784 (2016). LI, P. S. et al., Spatially resolved ferroelectric domain-switching controlled magnetism in $Co_{40}Fe_{40}B_{20}$/$Pb(Mg_{1/3}Nb_{2/3})_{0.7}Ti_{0.3}O_3$ multiferroic heterostructure. to be published.

Acceptance ID: 4AMU-I

Electrical Properties of Urethane Composites with MWNT and piezoelectric materials

J.S. Kim[1,a], I. Choudhry[2,b] and H.K. Lee[3,c]

[1,2,3]Department of Civil & Environmental Engineering, KAIST, Daejeon 34141, South Korea,
[a]kjs3428@kaist.ac.kr, [b]iqra.choudhry@kaist.ac.kr, [c]haengki@kaist.ac.kr

Keywords: Energy harvesting, Electrical energy, Piezoelectric material, Urethane, MWNT

This paper summaries a portion of an experimental work conducted by the authors, in which piezoelectric properties of urethane composites with MWNT and piezoelectric materials were investigated [1]. The piezoelectric performances of composites composed of various types of piezoelectric materials, urethanes and multi-wall carbon nanotubes (MWNT) at various ratios were studied under different loading conditions. The foot stamping test results revealed that urethane composites embedded PZT nanopowder generated 0.4~0.6 V higher output voltages than those of ZnO and $BaTiO_3$. A positive correlation between the piezoelectric material content and the output voltage was observed. The incorporation of MWNT reduced the noise of the output voltage. Details of the test results will be presented.

Acknowledgement. This research was supported by the National Research Foundation of Korea (NRF) grant funded by the Korean government (Ministry of Science, ICT & Future Planning) (NRF-2015R1A2A1A10055694).

References

[1] Kim, J.S., Choudhry. I and Lee, H.K. (2017). "Evaluation on piezoelectric performance of nano-material & urethane based transducer for energy harvesting technique," in preparation.

Acceptance ID: 4FEC-O

Violet-blue Emission from ZnO-Graphene Hybrid Quantum Dot by Intrinsic Defect Control

Hong Hee Kim[1,2], Yeonju Lee[1], Cheolmin Park[2], Won Kook Choi[1]*

[1]Materials and Life Science Research Division, Korea Institute of Science and Technology (KIST), Korea
[2]Department of Material Engineering, Yonsei University, Korea

One of a wide-bandgap semiconductor, Zinc oxide (ZnO) has a near ultraviolet bandgap (3.37 eV) and an exciton binding energy of 60 meV at room temperature (RT), and has several favorable properties, such as high electron mobility, high oscillator strength, and good transparency. In the spectra of Hydrothermally synthesized ZnO nanoparticles showed an excitation dependent photoluminescence (PL): a strong yellow emission by excitation wavelength of 300-350 nm and violet-blue light emissions centered at 410, 435, and 465 nm at the excitation wavelength longer than 380 nm. From the pholtoluminescence excitation (PLE), it is confirmed that yellow emission and violet-blue emission correlated to Zn interstitial (Zn_i located in the conduction band)-oxygen vacancy (V_O) pair and the transition between Zn_i (located below conduction band) to Zn vacancy (V_{Zn}) respectively. After attaching graphene to ZnO, PL was not dependent on the excitation wavelength. Yellow emission completely disappeared whereas the intensity of blue emission was greatly increased by 10 times and quantum efficiency was measured as much as 92%. Based on ZnO NPs and ZnO-graphene hybrid quantum dots, the origin of visible range emissions long-standing controversy in ZnO academia was clearly revealed and controlled.

Acknowledgement: This work was financially supported from KIST Institutional Program.

Acceptance ID: 4H5J-O

The Hydrogen Embrittlement Susceptibility of High Strength Steels

Burak Bal[1,a], Ismail Alper Isoglu[2,b], Motomichi Koyama[3,c]

[1] Department of Mechanical Engineering, Abdullah Gul University, 38039 Kayseri, Turkey
[2] Department of Bioengineering, Abdullah Gul University, 38039 Kayseri, Turkey
[3] Department of Mechanical Engineering, Kyushu University, Nishi-ku, Fukuoka 819-0395, Japan
[a]burak.bal@agu.edu.tr, [b]alper.isoglu@agu.edu.tr, [c]koyama@mech.kyushu-u.ac.jp

Keywords: Hydrogen Embrittlement, High Strength Steels, Fracture Surface, Testing.

Hydrogen embrittlement is a mechanism which degrades the mechanical properties of metals and metallic alloys [1,2]. It is well-known that as the strength of materials increases, it becomes more vulnerable to hydrogen embrittlement because of the high diffusibility of hydrogen in the lattice [3,4]. Twinning induced plasticity (TWIP) steel is one of the new game changing materials which shows extraordinary strength levels with significant ductility [5,6]. Therefore, understanding the hydrogen embrittlement susceptibility of TWIP steels under different microstructural and environmental conditions is of utmost importance in order use these materials in any kind of applications such as automotive, aviation, or energy related applications without sacrificing from safety [7].

In the current study, several tensile tests were conducted to hydrogen-charged and hydrogen-uncharged specimens in order to observe the hydrogen embrittlement susceptibility of TWIP steels under different strain rates from 1×10^{-3} to 1×10^{-5} s^{-1} at room temperature. Hydrogen charging was carried out at high temperature (353 K), and high pressure to increase the hydrogen diffusibility and to diffuse the hydrogen homogenously inside the microstructure for 1 week, which satisfies the homogeneity of hydrogen distribution in material according to $\sqrt{DT}$ method. Strain rates were selected low enough to allow hydrogen to interact with moving dislocations and promote hydrogen embrittlement [8,9]. Microstructural investigations were carried out by electron-backscattered diffractometry (EBSD), scanning electron microscope (SEM), transmission electron microscope (TEM) and in-situ SEM.

In this study, we demonstrate that hydrogen embrittlement is much more pronounced at low strain rates. In particular, ductility was reduced by 15% at high strain rate whereas it was reduced by 40% at low strain rate. Moreover, hydrogen charging enhances microstructural interactions such as slip lines, twin formation, slip-twin interactions at both low & moderate strain values and high strain values based on in-situ SEM observations. It also decreases the twin thickness, which contributes further hardening, but it does not change the dislocation mobility based on TEM observations. Furthermore, hydrogen charging changes the fracture mode from ductile to quasi-cleavage. Quasi-cleavage facets sharpen as the strain rate decreases. One of the most significant outcomes of this work is a new hydrogen embrittlement mechanism proposed which proves the segregation of hydrogen on twin boundaries unlike previous studies. Specifically, slip lines distort the twin boundaries and create a trap sites for hydrogen. Overall, this study sheds light on the effect of strain rate on hydrogen embrittlement susceptibility of high-strength steels.

References

[1] M. Dadfarnia, P. Sofronis, B.P. Somerday, D.K. Balch, P. Schembri and R. Melcher: Eng. Fract. Mech. Vol. 78 (2011), p. 2429–2438.
[2] D. Shih, I.M. Robertson and H.K. Birnbaum: Acta Metall. Vol. 36 (1988), p.111–124.
[3] K. Horikawa, H. Okada, H. Kobayashi and W. Urushihara: Journal Japan Inst. Met. Vol. 74 (2010), p. 199–204.
[4] C. San Marchi, B.P. Somerday, X. Tang and G.H. Schiroky: Int. J. Hydrogen Energy. Vol. 33 (2008), p. 889–904.
[5] H. Idrissi, K. Renard, L. Ryelandt, D. Schryvers and P.J. Jacques: Acta Mater. Vol. 58 (2010), p. 2464–2476.
[6] T. Niendorf, C. Lotze, D. Canadinc, A. Frehn and H.J. Maier: Mater. Sci. Eng. A. Vol. 499 (2009), p. 518–524.
[7] B. Bal, B. Gumus, G. Gerstein, D. Canadinc and H.J. Maier: Mater. Sci. Eng. A. Vol. 632 (2015), p. 29–34.
[8] T. Michler and J. Naumann: Int. J. Hydrogen Energy. Vol. 33 (2008), p. 2111–2122.
[9] H.K. Birnbaum: Scr. Metall. Mater. Vol. 31 (1994), p. 149–153.

Acceptance ID: 4QZK-O

Photothermal properties of CdSe nanowires using Anodic Alumina Membrane

S. Ktifa(1) , F. Laatar(1), N. Yacoubi(2), H. Ezzaouia(1)*

(1) Photovoltaic Laboratory, Research and Technology Centre of Energy, Borj-Cedria Science and Technology Park, BP 95, 2050 Hammam-Lif, Tunisia
(2) Photothermal Laboratory, Nabeul, Tunisia

Much attention has been paid toward synthesis and characterization of one dimensional nanostructure mainly due to their unique magnetic, electronic and optical properties and their potential applications in different fields including magnetic, electronic and optical devices. CdSe nanorods array were prepared using impregnation in porous anodic aluminum oxide. CdSe is one of the II–IV semiconductors and because of high photosensitivity it has been widely used in photoconductive devices. Photothermal deflection technique (PTD) is used to determine thermal conductivity and diffusivity. It deduced from the photothermal deflection measurements by comparing experimental amplitude of the photothermal signal to the corresponding theoretical one. In this work we study the influence of thermal annealing from 150 0^C to 400 0^C on thermal properties. The morphology characterization studied by scanning electron microscopy (SEM), has been shown that the grain size of nanocrystallin growth with thermal annealing. It was observed an increase in CdSe NCs size from 2.22 to 2.56 nm when the average pores diameter of PAA increase from 30 to 180 nm. Thermal conductivity increase with thermal annealing from 10,5 $Wm^{-1}K^{-1}$ to 25 $Wm^{-1}K^{-1}$.

Acceptance ID: 4SCE-P

Single walled carbon nanotubes-reinforced various metal matrix composite materials fabricated by spark plasma sintering process

Hansang Kwon[1,2], Gwangjae Park[1], Jaehong Park[2], Marc Leparoux[3], Akira Kawasaki[4]

[1]Department of Materials System Engineering, Pukyong National University, Sinseonro 365, Namgu, 48547 Busan, Republic of Korea
[2]Next Generation Materials Co., Ltd., Sinseonro 365, Namgu, 48547 Busan, Republic of Korea
[3]Laboratory of Advanced Materials Processing, EMPA-Swiss Federal Laboratories for Materials Science and Technology, Feuerwerkerstrasse 39, 3602, Thun, Switzerland
[3]Department of Materials Processing Engineering, Graduate School of Engineering, Tohoku University, Sendai 980-8579, Japan

Various metal powders were mixed with single walled carbon nanotubes (SWCNT) by mechanical ball milling process and followed by spark plasma sintering (SPS) processes. Small amount of SWCNT additions (0.1 and 1 vol%) were well dispersed onto the pure aluminum (Al), 5052 Al alloy, pure titanium (Ti), Ti6Al4Vanadium alloy, pure copper (Cu), and stainless steel 316L (SUS316L). Each composite powders were SPSed at 600 oC, 50MPa and 5min. and the SPSed composites were well synthesized regardless of the matrices. Vickers hardness of the composite materials were measured and they exhibited higher values regardless of the SWCNT composition than those of the pure materials. The SWCNT reinforced Cu matrix composites showed highest strengthening comparing with the other metal matrices system. The SWCNT-reinforced various metal matrices composite materials could be offered as an engineering materials in many kind of industrial fields such as aviation, transportation and electro technologies etc. However, detail strengthening mechanism should be carefully investigated. However, we believe that powder metallugical processes are useful tool for fabricating of the SWCNT-reinforced metal matrix composite materials.

Keywords: single walled carbon nanotubes (SWCNT); Metal Matrix Composites (MMC); spark plasma sintering (SPS), Mechanical property, Vickers hardness

Acceptance ID: 58Y4-O

Giant Dielectric Permittivities in Functionalized Barium Titanate/Epoxy Resin Polymer Composites with Low Loss Tangent

Haiping Xu[*], *Cheng Xie, Guoyin Shi, Dandan Yang, Yue Zhai, Xiujuan Dai, Yanli Qin*

School of Environmental and Materials Engineering, College of Engineering, Shanghai Polytechnic University, Shanghai 201209, China;

The Barium Titanate ($BaTiO_3$, BT) was modified by solid phase reaction with different mass ratio mixture of niobium pentoxide (Nb_2O_5) and cobalt tetraoxide (Co_3O_4) as dopants, then the functionalized $BaTiO_3$ (BTNC) containing niobium (Ni) and cobalt (Go) on its surface was obtained. The BTNC/epoxy resin (BTNC/EPR) polymer-based composites with different composition and concentration of BTNC particles were fabricated via a simple physical mixing and subsequently hot-press processing. The surface morphology of BTNC and BTNC/EPR composites, respectively, were characterized by scanning electron microscopy (SEM). At the same time, the elemental composition on surface of BTNC was analyzed by energy dispersive spectrometer (EDS). The effects of constituent and doping amount of BTNC on dielectric properties of BTNC/EPR composites were investigated. The results show that there are Ni and Go elements on the surface of BTNC. When the BTNC is obtained with mass ratio of Nb_2O_5/Co_3O_4 is 4.5/1, as well as the total content of Nb_2O_5 and Co_3O_4 mixture is 1.0 wt%, the BTNC/EPR composite exhibit the best dielectric properties. The dielectric permittivity of BTNC/EPR composite with 80 wt% BTNC content is 75.8 on 100Hz, which is increased about 30 than BT/EPR composite at the same content of BT.

Key Words: Functionalized Barium Titanate; Dopant; Epoxy resin; Composite; Dielectric property

Acceptance ID: 5B6U-P

Durability of Advanced Composite Sheets in H_2SO_4

Yongcheng Ji[1] and Yail J. Kim[1]

[1]Department of Civil Engineering, University of Colorado Denver, 1200 Larimer Street, Denver, CO80217, USA
jimmy.kim@ucdenver.edu

This research presents the chemical, physical, and mechanical characteristics of advanced composite sheets made of carbon fiber reinforced polymer (CFRP) when subjected to sulfuric acid (H_2SO_4). Test coupons are submerged in a 5% H_2SO_4 solution for up to 6 weeks, and their responses are measured by Fourier transform infrared spectroscopy, thermogravimetric analysis, dynamic mechanical analysis, and destructive mechanical loading. Also examined are the pH variation of the solution and the microscopic surface textures of the specimens with an increase in exposure time. The aliphatic amine and alkane functional groups of the CFRP are activated by sulfuric acid, including chain scission reactions that cause interfacial deterioration between the carbon fibers and resin. The acid exposure decreases the energy storage and dissipation capacities of the CFRP, as well as its glass transition temperature. The chemically-induced damage in the fiber-resin interface is responsible for lowering the load-carrying capacity of the CFRP, along with strain-softening. An analytical model is developed based on a Weibull distribution, which quantifies the degree of reliability and hazard associated with acid-damaged CFRP. An environmental reduction factor is calibrated and proposed for CFRP-strengthening in chemical plants and wastewater treatment plants.

Keywords: chloride penetration; high performance concrete; internal curing; superabsorbent polymer

Acceptance ID: 5MM9-O

QSAR, Synthesis, Characterization and Pharmacological Evaluation of Substituted Indazole Derivatives as Antimicrobial Agents

Shekhar. S[1], Minu. M[1, 2], Singh.D[2], Dantu. PK[2], Sarkar. A[1]

[1] Department of Chemistry, School of Applied Science,
Netaji Subhas Institute of Technology, University of Delhi, India
[2]Department of Chemistry, Dayalbagh Educational Institute, U.P, India
E Mail (shashanks634@gmail.com)

A series of substituted Indazole having good electron withdrawing group affinities, were synthesized and tested for their *in vitro* antibacterial and antifungal activities. Quantitative Structure activity relationship was performed on a series of known substituted Indazole derivatives as antimicrobial agents. This study was performed on compounds having Indazole ring substituted moieties to find out the structural requirements for antimicrobial activity. Principal component regression, combined with stepwise forward-backward variable selection method resulted with r^2, q^2 and pred_r^2 values of 0.85, 0.70 and 0.75 respectively. The validation of models was performed through the leave-one-out cross technique in conjunction with external validation. The results thus obtained may provide useful substitution patterns on the hexahydroindazole skeleton and may also help to design more potent compounds. Quantitative Structure Activity Relationship (QSAR) investigations indicated that the QSAR model was effective in describing the antimicrobial (antibacterial and antifungal) activity.

Keywords: QSAR;PCR, Indazoles ;Antimicrobial compounds .

Acceptance ID: 63EC-P

LIGHT-EMITTING MATERIALS FOR TEXTILE APPLICATIONS

Pravin C. Patel, Hireni R. Mankodi, Anuradha Ajmera

Textile Engineering Department, Faculty of Technology and Engineering,
The M.S. University of Baroda, Vadodara:390001

Advance functional materials have attracted much attention as a next generation of textile fibres. The fibres functionality depends on end-use and covers wide range of applications. Luminous material is one of the functional materials in which rare earth minerals with luminescent properties are added in proper proportion to get desired luminescence. This type of material can be used to produce novel functional fibres also known as Luminescent Fibres. It is a fibre/filament which can emit its own light. Luminescent fibres have wide range of applications in textile like curtains, panels, fixed structures, decorative clothes, light-emitting slippers, light plush toys, knitting products, embroidery products etc. It also has various applications in technical textiles for fire-fighting personals and military personals.

In the present work, PET luminescent fibres/filaments have been prepared by using rare-earth strontium aluminates, the main source of light emission Eu2+,Dy3+ were added as the luminescent material, fibre- forming polymer PET as the matrix by the process of melt spinning.

The structure, composition and properties of luminescent material and fibres/filaments have been done by SEM, XRD, DSC and persistence glowing effect.

Key words: Decorative, Functional Fibres, Luminescence, Light-emitting, Melt-Spinning

Acceptance ID: 67FG-O

Preparation and Characterization of Fatty Acid Eutectic/Diatomite Filter Aid Form-stable Phase Change Material for Thermal Energy Storage

*Duo MENG *, Kang ZHAO, Dongxu Wang*

(School of Civil and Architectural Engineering, Liaoning University of Technology. Jinzhou 121000, China)

Form-stable phase change materials (PCMs) are a kind of thermal functional composites which can be applied in the latent heat thermal energy storage and prevent the flow and leakage of solid-liquid PCM. In this study, capric-lauric fatty acid (CA-LA)/diatomite filter aid form-stable PCM was prepared by vacuum impregnation method and its characteristics such as microstructure, thermo-physical properties, thermal stability were investigated by scanning electron microscopy (SEM), Fourier-transform infrared (FT-IR), Differential scanning calorimetry (DSC) and Thermogravimetric (TG) technique. The adsorption capacity of diatomite filter aid to CA-LA eutectic was 49wt%, and the composite PCM kept solid in macro-level even when the CA-LA melted due to the capillary and surface tension forces of diatomite filter aid. DSC analysis showed that phase change temperature and latent heat of the form-stable PCM was 21.8℃ and 75.45 J/g respectively. Mass loss temperature range of CA-LA in the composite was prolonged to 120~233℃ compare to that of the pure CA-LA eutectic in range of 120-195℃ though TG analysis. It indicated that the diatomite filter aid particles absorbed and constrained the CA-LA molecules in the pores and confirmed the form-stable property of the composite. After 100 times thermal cycling, the phase change temperature and latent heat of the form-stable PCM respectively decreased by 0.9% and 1.1%, which can be neglectable in the practical engineering application. Moreover, the heating/cooling test revealed that the form-stable PCM can absorb and release latent heat to adjust the environmental temperature in a certain period of time. Thus, it can be concluded that the prepared CA-LA/diatomite filter aid form-stable PCM is a promising thermal storage composite with the proper phase change temperature, good thermal capacity, thermal stability and reliability, and effective temperature regulation function to be applies in the building energy conservation and low temperature heat storage applications.

Keywords: Form-stable phase change material; Diatomite filter aid; Fatty acid eutectic; Thermal storage; Energy saving

Acceptance ID: 68XT-P

Multiferroics and Magnetoelectric Effects in Metal-Organic Frameworks

*Ying Tian, Yinina Ma, Liqin Yan, Yisheng Chai, and Young Sun**

Institute of Physics, Chinese Academy of Sciences, Beijing 100190

The hybrid metal-organic frameworks (MOFs) that combine both merits of inorganic and organic materials represent a new family of multifunctional materials. In this talk, we report the multiferroics (coexistence of magnetic order and ferroelectricity) and magnetoelectric effects in a series of MOFs with a perovskite structure. Single-crystal samples of MOFs were prepared by solvothermal methods. These MOFs show a magnetic ordering between 5-20 K, depending on the magnetic ions (Cu^{2+}, Mn^{2+}, Co^{2+} or Fe^{2+}). Meanwhile, they also exhibit a ferroelectric transition between 160-270 K. Both direct (magnetic field control of electric polarization) and converse (electric field control of magnetization) magnetoelectric effects have been observed in these MOFs. Especially, the Fe-based MOF exhibits the most interesting behaviors, such as resonant quantum tunneling of magnetization, electric control of magnetism, and resonant quantum ME effect. The possible origin of the multiferroics and magnetoelectric effects is discussed in terms of the role of hydrogen bonding and magnetoelastic coupling.

References

[1] Y. Tian et al., Observation of Resonant Quantum Magnetoelectric Effect in a Multiferroic Metal−Organic Framework, J. Am. Chem. Soc. 138, 782−785 (2016).
[2] Y. Tian et al., High-temperature ferroelectricity and strong magnetoelectric effects in a hybrid organic-inorganic perovskite framework. Phys. Status Solidi RRL 9, 62 (2015).
[3] Y. Tian et al., Cross coupling between electric and magnetic orders in a multiferroic metal-organic framework. Sci. Rep. 4, 6062 (2014).
[4] Y. Tian et al., Quantum Tunneling of Magnetization in a Metal-Organic Framework, Phys. Rev. Lett. 112, 017202 (2014).
[5] W. Wang et al., Magnetoelectric coupling in the paramagnetic state of a metal-organic framework, Sci. Rep. 3, 2024 (2013).

Acceptance ID: 6FEE-O

Bioinspired graphene-based nanocomposites

*Qunfeng Cheng**

Schoolo of Chemistry, Beihang University
Xueyuan Road No.37, Haidian District, 100191, Beijing, China
Email: cheng@buaa.edu.cn

With its extraordinary properties as the strongest and stiffest material ever measured and the best-known electrical conductor, graphene could have promising applications in many fields, especially in the area of nanocomposites. However, processing graphene-based nanocomposites is very difficult. So far, graphene-based nanocomposites exhibit rather poor properties. Nacre, the gold standard for biomimicry, provides an excellent example and guidelines for assembling two-dimensional nanosheets into high performance nanocomposites. The inspiration from nacre overcomes the bottleneck of traditional approaches for constructing nanocomposites, such as poor dispersion, low loading, and weak interface interactions. Herein, we summarizes recent research on graphene-based artificial nacre nanocomposites,[1-6] and focuses on the design of interface interactions and synergistic effects for constructing high performance nanocomposites.

References

[1]. Q. Cheng, L. Jiang, Angew. Chem., Int. Ed. 2017, 56, 934-935.
[2]. S. Gong, H. Ni, L. Jiang, Q. Cheng, Materials Today 2017, In press.
[3]. W. Sijie, X. Feiyu, J. Lei, C. Qunfeng, Adv. Funct. Mater. 2017, In press.
[4]. Y. Zhang, S. Gong, Q. Zhang, P. Ming, S. Wan, J. Peng, L. Jiang, Q. Cheng, Chem. Soc. Rev. 2016, 45, 2378-2395.
[5]. Y. Zhang, Y. Li, P. Ming, Q. Zhang, T. Liu, L. Jiang, Q. Cheng, Adv. Mater. 2016, 28, 2834-2839.
[6]. S. Wan, J. Peng, L. Jiang, Q. Cheng, Adv. Mater. 2016, 28, 7862-7898.

Acceptance ID: 6GR2-O

Design of Novel Composites by Using "MAB" Phases as a Functional Constituent

*M. Fuka, F. Al-Anazi, M. Dey, and S. Gupta**

Department of Mechanical Engineering
University of North Dakota, ND 58201
Corresponding author: surojit.gupta@engr.und.edu

It is well known that $M_{n+1}AX_n$ (MAX) phases (over 60+ phases), where n =1,2,3; M is an Early Transitional Metal, A is a Group A element (mostly groups 13 and 14); and X is C and/or N, are novel nanolaminate ternary carbides and nitrides (space group $P6_3/mmc$) bestowed with excellent properties like damage tolerance, thermal shock resistance and machinability [1-4]. However these solids do not have a ternary composition where X = B. Recently, Ade *et al.* [5] had successfully synthesized single crystals of $Cr_2AlB_2(CrB_2)_x$ (x = 0, 1, 2), M_2AlB_2 (M = Cr, Mn, Fe), and MAlB (M = Mo, W), and due to their similarity with MAX Phases classified these novel ternary solids as "MAB-phases". Kota el al. [6] reported dense and predominantly single-phase MoAlB by using a reactive hot pressing method. High temperature studies also indicated that the compound is stable to at least 1400 °C in inert atmospheres and had moderately low Vickers hardness values of (10.6 ± 0.3) GPa compared to other transition metal borides. In this paper, we will report novel structural composites by using MAB Phases a multifunctional functional constituent. There has been very limited or no studies on these novel composite systems.

References:
[4] "Elastic and Mechanical Properties of the MAX Phases", M.W. Barsoum and M. Radovic
[5] Annu. Rev. Mater. Res. 41, 195-227 (2011).
[6] "Synthesis and characterization of a remarkable ceramic: Ti_3SiC_2", M.W. Barsoum, T. El-Raghy, J. Am. Ceram. Soc. 79, 1953–1956 (1996).
[7] "The $M_{n+1}AX_n$ phases: a new class of solids; thermodynamically stable nanolaminates",
[8] M.W. Barsoum, Prog. Solid State Chem. 28, 201–281 (2000).
[9] "Synthesis and mechanical properties of fully dense Ti_2SC", S. Amini, M.W. Barsoum, T. El-
[10] Raghy, J. Am. Ceram. Soc. 90 (12), 3953–3958 (2007).
[11] "Ternary Borides Cr_2AlB_2, Cr_3AlB_4 , and Cr_4AlB_6: The First Members of the Series
[12] $(CrB_2)_nCrAl$ with n = 1,2, 3 and a Unifying Concept for Ternary Borides as MAB-Phases",
[13] M. Ade, & H. Hillebrecht, *Inorg. Chem.* 54, 6122–6135 (2015).
[14] "Synthesis and Characterization of an Alumina Forming Nanolaminated Boride: MoAlB",
[15] S. Kota, E. Zapata-Solvas, A. Ly, J. Lu, O. Elkassabany, A. Huon, W. E. Lee, L. Hultman,
[16] S. J. May & M. W. Barsoum, Scientific Reports, 6:26475, DOI: 10.1038/srep26475.

Acceptance ID: 6LCJ-O

Simultaneous Electrical/Mechanical Characterization of Smart Composites Composed of Cement-Based Materials and Shape Memory Alloys

Eui-Hyun Kim,[1] Ki-Won Seo,[1] Chan-Yeong Jeon,[2] Eunsoo Choi,[2] and Jinha Hwang[1]

[1]Department of Materials Science and Engineering, Hongik University, Seoul 04066, South KOREA
[2]Department of Civil Engineering, Hongik University, Seoul 04066, South KOREA

Self-healing is one of the critical functions required of smart concretes. Shape memory alloys (SMAs) offer two unique effects such as shape memory effects and superelastic effects, unlike other structural metals. Upon fabricating composites composed of SMA wires and conventional cements, the designed composites allow for overcoming the mechanical weaknesses encountered in conventional concretes which are associated with tensile fractures. Under specialized environments, the material interface between the cementitious component and SMA materials plays an important role in achieving the robustness of the SMA/cement interface, leading to the enhancement in mechanical performance. Traditionally, the material interface is evaluated in terms of mechanical aspects, i.e., using a strain-stress characteristic feature. However, the current work attempts simultaneous characterization involving mechanical load-displacement relations synchronized with impedance spectroscopy as a function of displacement. Frequency-dependent impedance spectroscopy is tested as an in-situ monitoring tool on structural variations encountered in smart composites composed of non-conducting cementitious materials and conducting metals.

Acceptance ID: 76R5-P

Evolution of 3D Nanoporosity and morphology in selectively dealloying gold-based bulk metallic glass

Yi Xu[1], Guangcun Shan[1,2], Pak Man Yiu[1], Tamaki Shibayama[3], Seiichi Watanabe[3], Masato Ohnuma[4], Chan-Hung Shek[1*]*

1Department of Physics and materials science, City University of Hong Kong, No.83 Tat Chee Avenue, Kowloon Tang, Hong Kong, China
2School of Instrumentation Science and Opto-electronics Engineering, Beihang University, No.37 XueYuan Road, Beijing 100095, China
3Laboratory of Quantum Energy Conversion Materials, Centre for Advanced Research of Energy and Materials, Division of Quantum Science and Engineering, Faculty of Engineering, Hokkaido University, Kita 13, Nishi 8, Kita Ku, Sapporo 0608628, Japan
4Laboratory of Quantum Beam System Engineering, Division of Quantum Science and Engineering, Faculty of Engineering, Hokkaido University, Kita 13, Nishi 8, Kita Ku, Sapporo 0608628, Japan

Current fabrication methods of nanoporous gold mainly rely on dealloying typical $Ag_{65}Au_{35}$ binary alloy precursor with the 'dealloying threshold or parting limt' more than 55%. Here we report a simple chemical dealloying process, through selective dissolution of single element from an Au-based ternary bulk metallic glass with low 'parting limit', for generating three-dimensional free-standing nanoporous metal (NPM) with high specific surface area and large overall thickness of the nanoporous structure. Our finding provides insights for understanding the underlying relationship between 'low parting limit' and atomic level structure of metallic glass. A comprehensive picture on the porosity evolution stages and the correlation between the 'cone shape protrusion' generation and potential energy landscape are illustrated. Additionally, this nanoporous structure was also duplicated through dealloying Pd based ternary intermetallic, however, which was correlated with bulk diffusion theory that dealloyed morphology consisting of "void-dendrites" structure penetrating into the solid.

Acceptance ID: 78B5-O

Photo-curable resins modified with in situ generated silver nanoparticles for additive manufacturing

Sciancalepore[1], *Taormina*[1], *Messori*[2], *Bondioli*[1]

[1] *Department of Engineering and Architecture, University of Parma, Italy*.
[2] *Department of Engineering "Enzo Ferrari", University of Modena and Reggio Emilia, Italy*.
National Interuniversity Consortium of Materials Science and Technology INSTM, Italy.
massimo.messori@unimore.it

The main objective of the present work is the preparation and characterization of innovative photo-curable resins modified with *in situ generated* silver nanoparticles and their use as raw materials for additive manufacturing technologies.

Photo-curable acrylic resins were formulated with different type and amount of silver salts for use in additive manufacturing technologies such as stereolitography (SLA) and digital light printing (DLP). Silver nanoparticles were *in situ* generated within the organic matrix during the photo-curing process by exploiting the tendency to reduction of silver ions to metallic silver under UV irradiation [1]. The obtained nanoparticle-filled composites were characterized in term of gel content and thermo-mechanical properties as well as electrical conductivity and antibacterial properties.

Keywords: Photo-curable resins, silver nanoparticles, additive manufacturing

[1] NAZAR, R., RONCHETTI, S., ROPPOLO, I., SANGERMANO, M., BONGIOVANNI, R.M. 2015. In situ synthesis of polymer embedded silver nanoparticles via photopolymerization. *Macromolecular Materials and Engineering*, 300, 226-233.

Acceptance ID: 78KD-P

COMPARITIVE STUDIES ON ADSORPTION OF DYE AND HEAVY METAL IONS FROM EFFLUENTS USING ECOFRIENDLY ADSORBENT

This paper describes to implement the kinetic model for adsorption of Malachite Green and heavy metal ions Cu (II) and Ni (II) from effluents using activated carbon prepared by chemical activation with phosphoric acid from Chrysopogon *zizanioides* roots (PCRAC). Supporting to this, results from Scanning Electron Microscopic (SEM) and Transmission Electron Microscopy (TEM) for PCRAC showed that the presence of heterogeneous and porous morphology on the surface of adsorbent indicated effective adsorption of dye and metal ions. Interestingly the maximum adsorption of both Cu(II) and Ni(II) ions was observed at 30°C and at P^H 6.6. From the kinetic studies, pseudo-second order kinetics was best suited for Malachite Green-PCRAC and PCRAC-metal ions system than Pseudo - first order kinetics. Equilibrium data for both the heavy metal ions and dye are satisfactorily fitted with Freundlich isotherm model than Langmuir isotherm, Elovich and intraparticle model.

Key words: PCRAC, (SEM), (TEM), MG and heavy metal ions, Langmuir and Freundlich isotherm models.

Acceptance ID: 7CKX-O

Nanoparticle/MOF composites: preparations and applications

*Huaiguo Xue and Huan Pang **

College of Chemistry and Chemical Engineering, Yangzhou University, Yangzhou, 225002, Jiangsu, China
**Email: huanpangchem@hotmail.com*

Within the last twenty years, MOFs have emerged as a new kind of promising porous materials in the areas of gas sorption and separation, catalysis, drug delivery, and molecule sensing. Meanwhile, nanomaterial also has attracted wide attention recent years. Owing to the porous structure of MOFs, we can combine nanoparticles with MOFs to get nanoparticle/MOF composites, which possess the advantages of both parent materials. In this work, there are mainly two methods to introduce nanoparticles into MOFs: employing MOFs as templates to hold gust nanoparticles in their channels or encapsulation of prey-synthesized nanoparticles. The former includes chemical vapor deposition technique, solid grinding technique, liquid impregnation method and double solvent method, the latter refers to some new techniques like self-sacrificing template technique. Here, we will also carefully give a review about their applications in hydrogen storage, ammonia adsorption, acidic gas adsorption, catalysis and energy storage area.

Acceptance ID: 7nbb-P

Tailoring the magnetic anisotropy and magnetoimpedance in amorphous microwires: experimental and theoretical investigations

A.M. Adam[1,4], L.V. Panina [1,2], M.G. Nematov[1], M.M. Salem[1,3], A. Uddin[1], A. Dzhumazoda[1]

[1]*National University of Science and Technology, MISiS, Moscow 119991, Russia*
[2]*Institute for Design Problems in Microelectronics RAS, Moscow 124681, Russia*
[3]*Physics Department, Faculty of Science, Tanta University, Tanta 31527, Egypt*
[4]*Physics Department, Faculty of Science, Sohag University, Sohag 82524, Egypt*

Enhancement and shaping of the magnetoimpedance (MI) response have attracted enormous attention due to potential technological applications, for instance, weak magnetic-field sensing, recording heads, and smart materials. Large MI can be observed in various materials, however, nearly-zero magnetostriction amorphous microwires show the best conditions for this effect in terms of controlling the sensitivity and the shape of MI characteristics [1]. In low magnetostrictive amorphous materials such as Co-based alloys, the effective anisotropy of a certain type can be induced using an appropriate heat treatment [2,4]. Typically, heat treatment is used to enhance a circumferential anisotropy. However, for many MI applications such as microwave stress-sensitive MI for smart materials a specific helical anisotropy is required. In this work we propose a dc current heat treatment of a Co-based microwire with small positive magnetostriction to induce a helical anisotropy with a controlled angle between the wire axis and the easy anisotropy direction. The heat treatment in our work was carried out during dc current of varying amplitude (30-55 mA) passing for a certain period of time. The hysteresis loop was transferred from a bistable type typical for axial anisotropy to inclined one which is consistent with the helical anisotropy. Additionally, the MI measurements confirmed the change. To understand the effect of current outflow in the wire under study, we propose the occurrence of some kind of annealing resulting from joule heating in a circular magnetic field generated by the current. In contrast to previously published related works which were aimed at refining circumferential anisotropy in negative magnetostrictive wires, we report the possibility to control the angle of the helical anisotropy in wires which in as-prepared state have an axial anisotropy. Furthermore, a theoretical model was proposed to describe the anisotropy and MI changes.

Kew words: Magnetoimpedance, anisotropy tailoring, helical anisotropy, current annealing

References

[1] M. H. Phan and H. Peng, 2008 "Giant magnetoimpedance materials: fundamentals and applications," *Prog. Mater Sci*., vol. 53, pp. 323-420.
[2] A. Zhukov, A. Talaat, M. Ipatov, J.M. Blancob and V. Zhukova, 2016 *ACTA PHYSICA POLONICA*, vol. 129, p. 694.
[3] J. Liu, H. Shen, D. Xing and J. Sun, 2014 "Optimization of GMI properties by AC Joule annealing in melt-extracted Co-rich amorphous wires for snsor applications," *Phys. Status Solidi* A, vol. 211, no. 7, pp. 1577-1582.
[4] A. Amirabadizadeh, R. Mardani, M. Ghanaatshoar, 2016 The effect of current frequency and magnetic field direction in alternative current-field annealing on the GMI and magnetic properties of Co-based wires, *Journal of Alloys and Compounds*: doi: 10.1016/ j.jallcom.2015.11.125.

Acceptance ID: 7UQQ-O

Construction of Bicomponent Interfacial Layers on Nanoparticles: Roles of 'Diluent' Ligands

*Sohyun Seo and Jae-Seung Lee**

Department of Materials Science and Engineering, Korea University
145 Anam-ro, Seongbuk-gu, Seoul, 02841, Republic of Korea
E Mail/ seosohyun94@gmail.com
jslee79@korea.ac.kr

DNA-gold nanoparticle conjugates (DNA-AuNPs) have been employed in various applications such as building blocks for nano-architecture, drug carriers for intercellular delivery, and multifunctional probes for biological target detection, based on their selective and sensitive binding properties. For this reason, controlling binding properties of DNA-AuNPs is one of the most significant subjects to achieve the aforementioned goals. Typically, construction of bicomponent layers employing non-functional chemicals, i.e. diluents, is widely devised, but further systematic examination of nanoparticle-conjugation conditions needs to be thoroughly carried out.

In this presentation, we investigate complicated interfacial interactions of non-functional diluent ligands, and eventually control overall conjugation of ligands to core nanoparticles. In particular, we demonstrate what exactly controls the construction of the bicomponent layers on the nanoparticle surfaces, and how the overall binding properties of the nanoparticles can be controlled, providing strong and general guidelines to effectively design nanoprobes for catalytically enhanced sensing applications. We also evaluated that polycytosine requires a careful handling when employed as a diluent on account of the possibility of *i*-motif formation.

Keywords: nanoparticle, DNA, diluent, binding properties, surface chemistry

Acceptance ID: 82KM-P

Rational design of hierarchical porous WO_3 microspheres with nanothorns and their functionalization with Pt catalyst for application in exhaled breath sensor

Hee-Jin (Cho)[1], Seon-Jin (Choi)[1], Won-Tae (Koo)[1], and Il-Doo (Kim)[1]*

[1] Department of Materials Science and Engineering, Korea Advanced Institute of Science and Technology, 291 Daehak-ro, Yuseong-gu, Daejeon 305-701, Republic of Korea
eriny@kaist.ac.kr *(presenting author) /* idkim@kaist.ac.kr *(corresponding author)*

Maximization of active surface area and porosity is of importance for enhancement of gas sensing performances, since the sensing reactions of analyte gases occur on the surface of metal oxides. In this work, a hierarchical porous WO_3 microspheres with nanothorns, which have highly improved surface area and porosity compared with dense WO_3 microspheres, were synthesized with spray pyrolysis and post heat-treatment. The hierarchical porous WO_3 microspheres consist of small WO_3 nanospheres, in which each nanospheres also consist of small WO_3 nanoparticles, and one dimensional (1D) nanothorns exist on the WO_3 microspheres. This unique morphology is attributed to excessive concentration of block co-polymer during spray pyrolysis in inert gas (N_2). As a result, multiple pores of meso- and macro-scale were loaded within WO_3 microspheres, which could facilitate easy gas penetration and diffusion. Each mesopores are located between small nanoparticles, on the other hand the macropores are located between nanospheres within large microspheres. Furthermore, the reactive surface area is highly enhanced owing to the 1D nanothorns at the surface of microspheres. In addition, we functionalized the hierarchical porous WO_3 microspheres with Pt catalyst during spray pyrolysis process. The Pt catalytic functionalization showed vastly improved sensing capability with superior acetone selectivity from the investigation of gas sensing characteristics in high humid atmospheres (90% RH), which is similar to exhaled human breath condition. Therefore this work demonstrates a facile synthesis of hierarchical porous WO_3 microspheres with 1D nanothorns using spray pyrolysis, and exhibits a significant potential for diagnosis of diseases by analyzing the exhaled breath.

Keywords: spray pyrolysis, WO_3 microspheres, hierarchical porous structure, nanothorn,

Acceptance ID: 89LQ-O

Graphene-MWNT-Poly(*p*-phenylenebenzobisoxazole) Multiphase Nanocomposite *via* Solution Prepolymerization with Superior Microwave Absorption Properties and Thermal Stability

*Hua, Feng, Xu, Wang, Huang, Zhuang**

The Key Laboratory of Advanced Polymer Materials of Shanghai, School of Materials Science and Engineering, East China University of Science and Technology, Shanghai, China, 200237

E-mail: jiasonghua@mail.ecust.edu.cn (presenting author)

qxzhuang@ecust.edu.cn (corresponding author)

With the exponential growth of electronic devices, electromagnetic pollution has become a major concern for human beings. Therefore, microwave absorption materials are highly demanded to eliminate unwanted radiation in both civilian and military fields. (Wei et al., 2015, Chen et al., 2014) Furthermore, in aerospace engineering, a high-performance microwave absorber is also essential for the stealth technology. (Liu and Huang, 2013) Here, we present a facile synthesis of the Graphene/MWNTs/PBO composite. To promote the integration of nanoparticles and PBO matrix, acid-modified MWNTs and Graphene Oxide (GO) were functionalized to constitute better bonding with the amino groups in PBO *via* $SOCl_2$. Then, functionalized MWNTs and GO were mixed together *via* ultrasonication to obtain the GO/MWNTs network. It is expected that the long one-dimensional MWNTs can bridge adjacent two-dimensional GO platelets and inhibit their aggregation, resulting in remarkable synergetic effects on the enhanced microwave absorption properties. (Singh et al., 2012)

Acknowledgements

This work was financially supported by the National Natural Science Foundation of China (51573045) and the International Collaboration Research Program of Science and Technology Commission of Shanghai (16520722000).

Keywords: PBO, graphene, carbon nanotubes, nanocomposites, microwave absorption

References

[1] WEI, J., ZHANG, S., LIU, X., QIAN, J., HUA, J., LI, X. & ZHUANG, Q. 2015. In situ synthesis of ternary $BaTiO_3$/MWNT/PBO electromagnetic microwave absorption composites with excellent mechanical properties and thermostabilities. *J. Mater. Chem. A,* 3, 8205-8214.

[2] CHEN, Y., LIU, X., MAO, X., ZHUANG, Q., XIE, Z. & HAN, Z. 2014. Gamma-Fe_2O_3-MWNT/poly(p-phenylenebenzobisoxazole) composites with excellent microwave absorption performance and thermal stability. *Nanoscale,* 6, 6440-7.

[3] LIU, P. & HUANG, Y. 2013. Synthesis of reduced graphene oxide-conducting polymers-Co_3O_4 composites and their excellent microwave absorption properties. *RSC Advances,* 3, 19033-19039.

[4] SINGH, V. K., SHUKLA, A., PATRA, M. K., SAINI, L., JANI, R. K., VADERA, S. R. & KUMAR, N. 2012. Microwave absorbing properties of a thermally reduced graphene oxide/nitrile butadiene rubber composite. *Carbon,* 50, 2202-2208

Acceptance ID: 8jpx-O

Highly Precise Detection of Colon Cancer Specific Biomarker from Patient's Serum Samples

Minhong Jeun[1], Hyunwoo Son[1], Jaewon Choi[1,2], Sungwook Park[1,2], Eun-Ju Do[3], Sang-Yeob Kim[3], Seung-Jae Myung[3], Kwan Hyi Lee[1,2,]*

[1]*Center for Biomaterials, Biomedical Research Institute, Korea Institute of Science and Technology (KIST), Seoul 02792 Republic of Korea.*
[2]*Department of Biomedical Engineering, Korea University of Science and Technology (UST), Seoul 02792, Republic of Korea.*
[3] *Department of Gastroenterology, Asan Medical Center, University of Ulsan College of Medicine, Seoul 05505, Republic of Korea*
mmhjeun@kist.re.kr / kwanhyi@kist.re.kr

Colon cancer is the third deadliest cancer that is affecting the United States population in both occurrence and fatality rate. The current method of identifying colon cancer initially relies on optical screening for polyp samples and then subsequent tissue evaluation. However, due to the highly invasive nature of the clinical methods, unwanted side effects may happen due to human errors in the medical field. Therefore, a new primary diagnostic tool are in high demand.

In this study, a transistor based bio-sensor capable of transforming a biological signal into an electrical signal for data identification is proposed. The bio-sensor in question is a dual-gate field-effect transistor (DGFET) which is capable of quantitatively identifying the colon cancer specific biomarker in a clinical sample.[1] The hardships that plague clinical application of field-effect transistors, such as the Debye length limit and the noise from the background ionic influence from clinical samples, have been minimized through our sensing platform. Without the need to change the background media from a highly complex solution to a more commonly utilized media such as PBS, we were able measure biomarker concentrations in physiological media.

Through rigorous testing, the limit of detection has been recorded to be substantial, being able to identify the biomarker concentration in a clinical sample even at the femto-molar level.

Keywords: Colon cancer, biomarker, transistor bio-sensor, serum sample, diagnosis

Acknowledgements: This research was supported by Korea Health Technology R&D Project through the Korea Health Industry Development Institute funded by the Ministry of Health and Welfare, Republic of Korea (HI15C-3078-020015).

[1] XIN, B., PLATZER, P., FINK, S. P., REESE, L., NOSRATI, A., KW WILSON, J., & MARKOWITZ, S. 2005. Colon Cancer Secreted Protein-2 (CCSP-2), a Novel Candidate Serological Marker of Colon Neoplasia. *Oncogene*, 24, 724-731.

Acceptance ID: 8MQP-O

Atomi/nano-scale structured titanium materials with high strength and excellent ductility

Powder metallurgy process was applied to fabricate atomi/nano-scale structured titanium (Ti) materials having high tensile strength (over 1200MPa) and excellent ductility (20% or more) at ambient temperature. Oxide (X-O) particles were mixed with pure Ti powder, and the elemental mixture powder was consolidated by solid-state sintering process. Oxide particles were completely dissolved and decomposed during sintering. Both oxygen and metal (X) atoms were uniformly solute into α / β -Ti crystals, and resulted in the remarkable increment of strength of Ti sintered materials by solid solution strengthening effect. In addition, the solute drag effect at the grain boundaries was also effective to obstruct the grain growth, and resulted in tensile strength improvement of Ti materials. In this presentation, the typical examples in use of TiO2 and ZrO2 particles as additive elements will be introduced to explain the microstructural and mechanical properties of Ti sintered materials.

Acceptance ID: 8MZH-I

Fabrication & Characterization of Graphene Oxide/ Polyvinyl Alcohol Nanocomposite

Bhasha, Jain.P

Department of Chemistry, School of Applied Science,
Netaji Subhas Institute of Technology, University of Delhi, India
E Mail (pj381970@gmail.com)

Polymer Nanocomposites employing carbon based nanofiller have been utilized to develop high strength materials for structural applications. In the present work, graphene oxide is used as a nano filler to fabricate PVA-GO nanocomposite. It exhibits a large aspect ratio, low density and high flexibility. The challenge in the current scenario is to achieve significant improvement in interfacial adhesion between polymer matrix and nanofiller. In this study, a simple and biocompatible approach to synthesize graphene oxide-reinforced poly (vinyl alcohol) (PVA) composite films has been developed. The preparation of PVA and Graphene Oxide nanocomposite were carried out using solution casting method by using deionized water as a solvent followed by ultrasonication & to make homogeneous dispersion of nanofiller. The composite samples were prepared using various wt% of graphene oxide content. The results showed that a small amount of graphene oxide content could enhance the properties of PVA-GO Nanocomposites. Surface characterization revealed the uniform distribution of graphene oxide and slight agglomeration of nanoparticles was observed. The mechanical & thermal properties were further investigated.

Keywords: Polyvinyl Alcohol, Graphene Oxide, Polymer Nanocomposite

Reference

[1] X. Zhao, Q. Zhang, Y. Hao, Y. Li, Y. Fang, and D. Chen "Alternate multilayer films of poly(vinyl alcohol) and exfoliated graphene oxide fabricated via a facial layer-by-layer assembly". *Macromolecules*, Vol. 43, No. 22, pp 9411-9416, 2010.
[2]
[3] Liang J., Huang Y., Zhang L., Wang Y., Ma Y., Guo T., Chen Y.: Molecular-level dispersion of graphene into poly(vinyl alcohol) and effective reinforcement of their nanocomposites. Advanced Functional Materials, 19, 2297–2302 (2009).

Acceptance ID: 8PSG-O

3D printing of various composite materials for electronic circuits

Kyung-Hyun Kim[*1], Kyu-Sung Lee[1], Ji-Young Oh[1], Yong-Seok Yang[1], Hyun-Woo Dang[1]*

[2]Chang-Woo Lee[2]

[1]Electronics and Telecommunications Research Institute (ETRI)
218 Gajeongno, Yuseong-gu, Daejeon, 34129, South Korea
[2]Korea Institute of Machinery and Materials (KIMM)
156 Gajeongbuk-ro, Yuseong-gu, Daejeon, 34103

Nowadays, 3D printing is one of the hot items in the whole world. These techniques can be used various application fields, which are making prototypes for medical and dental field, electronics, aerospace, automotive, design, architecture, and so on. In particular, we are interested in printing electronic circuits and are working on developing printing materials to replace printed circuit board (PCB) using 3D printers.

Therefore, we studied various composite materials, which are glass powder, carbon powder, carbon nanotube (CNT), and cellulose nanocrystal (CNC), for improving thermal, mechanical, and electrical properties of polylactic acid (PLA). We successfully maked thermoplastic filaments using a mini-extruder machine for fused deposition modelling (FDM) printer and also maked many 3D printed samples for thermal, mechanical, and electrical measurements. The 3D printed samples, which were included various composite materials, were investigated in terms of printing speed, printing temperature, and printing bed temperature. The 3D printed samples were measured by thermal mechanical analyzer (TMA), bending strength with micro-universal testing machine, dielectric constant with LCR meter. Surface morphology and composition of those are measured by scanning electron microscope (SEM) and energy dispersive X-ray spectroscopy (EDS).

This work was supported by the National Research Council of Science & Technology (NST) grant by the Korea government (MSIP) (No. CRC-15-03-KIMM).

Acceptance ID: 8RNU-P

Generalized Susceptibility of Screw Dislocation in Ferroelastic Crystal

V.V.Dezhin, V.N.Nechaev

Voronezh State Technical University, Voronezh, Russian Federation
viktor.dezhin@mail.ru

Of interest is the effect of dislocations on anomalous behavior of the physical properties of ferroelastic crystals in the vicinity of a structural phase transition. Earlier cases of static and moving with a constant speed of dislocation have been investigated. Bending vibrations of dislocations were not discussed in these papers. The authors investigated the bending vibrations of an edge dislocation in ferroelastics, ferroelectrics and ferromagnets in the works [1, 2], The present report considers small amplitude bending vibrations of a screw dislocation near the point of the structural phase transition, which is described by the order parameter. In the presence of dislocation in the ferroelastic crystal there appears a contribution to order parameter, which is generally coordinate-dependent and time-dependent. Solving the set of equations in Fourier representation and considering only summands linear over the dislocation displacement $u(q,\omega)$ we find $f(q,\omega)=\alpha^{-1}(q,\omega)u(q,\omega)$, where $f(q,\omega)$ is projection of Peach-Koehler force onto the dislocation slip plane, $\alpha(q,\omega)$ is the generalized susceptibility of the screw dislocation, describing its linear response to the external force, the space dependence of which is characterized by wave vector q and the time dependence – by frequency ω. Linear response function allows you to determine dynamic characteristics of a screw dislocation and give a correct description of the ferroelastic crystal behavior in external fields.

Keywords: Screw dislocation, bending vibrations, ferroelastic crystal, generalized susceptibility

[1] DEZHIN, V.V., NECHAEV, V.N., ROSCHUPKIN, A.M. 1989. Generalized Susceptibility of Dislocation in Ferroelectrics. *Ferroelectrics Letters*, 10, N 5, 155-160.
[2] DEZHIN, V.V., NECHAEV, V.N., ROSCHUPKIN, A.M. 1990. Generalized Susceptibility of Dislocation in Ferroelectrics and Ferromagnetics. *Zeitschrift für Kristallographie*, 193, 175-197.

Acceptance ID: 8UKL-P

TD-DFT study on chiral Schiff base Fe(II) complex for DSSC dyes

Shinnosuke TANAKA[1], Mauricio A. PALAFOX[2], Tomoyuki HARAGUCHI[1], and Takashiro AKITSU[1]

[1]Department of Chemistry, Tokyo University of Science, Tokyo, Japan.
[2]Departamento de Química-Física I Universidad Complutense de Madrid, Madrid, Spain.
akitsu@rs.kagu.tus.ac.jp

Chiral salen-type Schiff base Fe(II) complexes for dye-sensitized solar cells (DSSCs) were designed [1] for comparison with Co(II), Ni(II), Cu(II) and Zn(II) ones. The substituent effects on their absorption spectra as well as electrochemical behavior were evaluated by TD-DFT computational methods as well as some experimental ways. In Fe UV-vis-NIR spectra, Fe(II) complexes exhibited red-shift of absorption bands due to electron withdrawing groups. The magnitude of HOMO-LUMO gap, transition energies, and electric transition dipole moments calculated by TD-DFT were discussed. Optimized structures of Fe(II) complexes revealed that conformation of carboxyl groups is suitable for chemisorption onto TiO_2 surface.

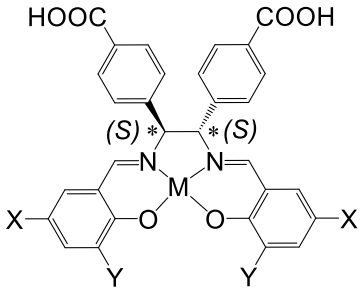

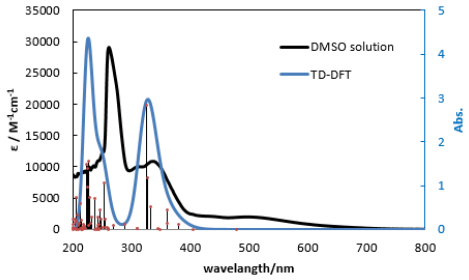

Keywords: DSSC, Schiff base, iron, TD-DFT

[1] SHOJI, R., IKENOMOTO, S., SUNAGA, N., SUGIYAMA, M. & AKITSU, T., Absorption wavelength extension for dye-sensitized solar cells by varying the substituents of chiral salen Cu(II) complexes. 2016. *J. Appl. Sol. Chem. Model.*, 5, 48-56.

Acceptance ID: 8XVM-O

Fabrication of organic thin film transistor based on organic-inorganic hybrid film as gate dielectrics

Wen-Chen Chien[*1], *Yang-Yen Yu*[*2,3] , *Chi-Ting Chiu*[2]

[1:]*Department of Chemical Engineering, Ming Chi University of Technology, 84 Gunjuan Rd., Taishan, New Taipei City 24301, Taiwan*
[2:] *Department of Materials Engineering, Ming Chi University of Technology, 84 Gunjuan Rd., Taishan, New Taipei City 24301, Taiwan*
[3:] *Department of Chemical and Materials Engineering, Chang Gung University, 259 Wenhua 1st Rd., Guishan, Taoyuan City 33302, Taiwan*

Organic thin film transistors (OTFTs) based on pentacene and hydroxyl-containing polyimide-zirconium dioxide (PI-ZrO_2) hybrid films were fabricated on silicon substrate in which the PI and ZrO_2 were as the semiconductor and the gate dielectrics, respectively. Zirconium butoxide ($Zr(OBu)_4$) was used as the precursor to synthesize nano-sized ZrO_2 colloid through the hydrolysis and condensation reaction in a sol-gel process. Then, PI-ZrO_2 hybrid solution was synthesized from a condensation reaction between hydroxyl-containing ZrO_2 and polyimide, followed by a spin coating to form the PI-ZrO_2 dielectric composites. Cyclic olefin copolymer (COC) was used as a modify layer to enhance the interface property between the semiconductor and the dielectric layer. In addition, PffBT4T-2OD was replaced by pentacene as semiconductor to expect a good performance on device. The thermal, optical, surface, dielectric, and electrical properties of the PI-ZrO_2 dielectric composites were investigated and correlated to ZrO_2 content. The PI-ZrO_2 hybrid dielectrics showed the tunable insulating properties, including high dielectric constants, high capacitances, and low leakage current densities. Besides, the bottom-gate top-contact OTFTs based on the PI-ZrO_2 hybrid dielectrics PZ30% and PZ30%-COC showed the best performance with the near zero threshold voltage. The best field-effect mobility (μ) and current on/off ratio (Ion/Ioff) of OTFTs were 1.12 $cm^2V^{-1}s^{-1}$ and $1.2x10^4$ for the dielectrics PZ30% and 3.25 $cm^2V^{-1}s^{-1}$ and $1.2x10^6$ for the dielectrics PZ30%-COC, respectively. The results showed that the OTFTs based on the PI-ZrO2 dielectrics and pentacene were fabricated successfully and the best performance for OTFTs was obtained when the ZrO2 content in hybrid films was 30 wt%.

Keywords: Polyimide, Zirconia, Hybrid thin film, Sol-gel method, Modify layer
Acceptance ID: 97YN-P

Bivalence Mn_5O_8 with hydroxylated interphase for high-voltage aqueous sodium-ion storage

Xiaoqiang Shan, Daniel Charles, Xiaowei Teng

Department of Chemical Engineering, University of New Hampshire, Durham, New Hampshire 03824, USA

Rechargeable aqueous electrochemical energy storage (EES) devices, especially ones using earth-abundant and non-toxic materials, have shown great promise for many applications owing to their high safety, low cost, and environmental friendliness. However, the thermodynamically stable potential window for aqueous EES has an intrinsic limit of 1.23 V, beyond which the hydrogen evolution reaction and oxygen evolution reaction occur. The evolved gas from electrolyte decomposition also severely deteriorates the electrode. A potential window of 1.23 V is too narrow for storage devices to achieve high energy and power performance. Extensive efforts have been made to break through this limit on the potential window while retaining the benefits of aqueous energy storage systems.

In this study, we report a high-rate high-voltage aqueous Na-ion full cell system based on a novel surface hydroxylated Mn_5O_8 electrode. As probed by synchrotron-based surface-sensitive soft X-ray spectroscopy, an ice-like surface hydroxyl layer is formed after cycling. Density functional theory (DFT) calculations show that the interplay between the hydroxylated interphase and the unique bivalence ($Mn^{2+}{}_2Mn^{4+}{}_3O_8$) layered structure suppresses the HER and OER with a stable potential window of 3.0 V. The system exhibits a two-electron charge transfer via Mn^{2+}/Mn^{4+} redox couple, and provides facile pathway for Na-ion transport at high-rate. The 3.0 V aqueous symmetric full cell exhibited a high energy density, 23 Wh kg^{-1} at a rate of 550 C, with nearly 100% coulombic efficiency and 85% energy efficiency after 25,000 charge-discharge cycles. Although the electrochemical properties of Mn_5O_8 have been largely overlooked since its structure was determined in 1965, our result shows that Mn_5O_8, the only bivalence layered manganese oxide, can serve as a new generation of pseudocapacitor electrode materials for enabling a stable potential window of 3.0 V for aqueous energy storage. This offers a new paradigm for developing electrode materials with a wide potential window and facile charge transfer for aqueous energy storage devices, which exhibits the performance comparable to that of non-aqueous Li-ion batteries, but is safe and environmentally benign. In addition, it will be an interesting topic for further studies on whether and how a well ordered hydroxylated interphase could form on the surface of other metal oxides, increase their overpotential towards gas evolution reactions, and therefore increase the potential window of aqueous energy storage.

Acceptance ID: 98ZY-O

Synthesis of water-soluble Fe-based fluorescent nanomaterials

*Junyoung Kwon[a], Seung Won Jun[a], Xiang Mao[a, b], Chang-Seok Kim[a], Jaebeom Lee[a]**

[a]Departments of Cogno-Mechatronics Engineering, Pusan National University, Busan 46241, Republic of Korea
[b]Key Laboratory of Luminescent and Real-Time Analytical Chemistry, Ministry of Education, College of Chemistry and Chemical Engineering, Southwest University, Chongqing, 400715, P.R. China

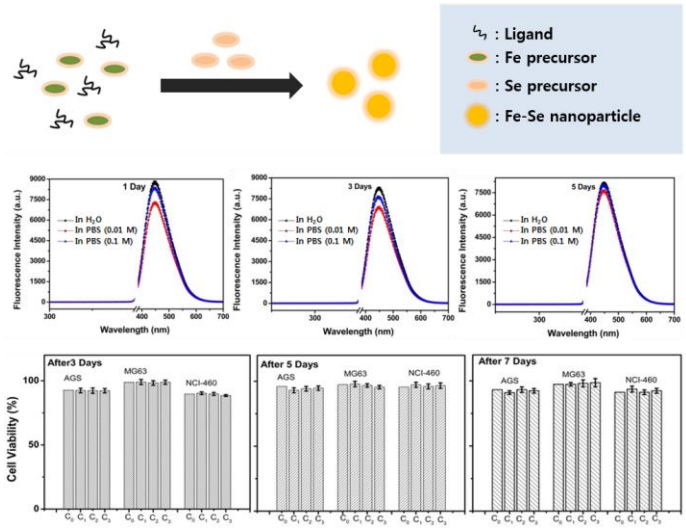

Iron chalcogenides possess substantial attractions because of their potential uses for biomedical, energy conversion and memory device application. Realization of this promise has been restricted by the lack of control over the crystallinity and nanoscale organization of iron chalcogenide films. High-quality nanoparticles (NPs) from these semiconductors will afford further studies of photophysical processes in them. NPs from these semiconductors can also serve as building blocks for mesoscale iron chalcogenide assemblies.

Here, we report a synthetic method for FeSe NPs that meet these needs with a diameter of ca. 5 nm in polar solvent and aqueous dispersions. The crystallinity of the individual NPs was confirmed by high resolution transmission electron microscopy (HR-TEM). The prepared FeSe NPs exhibit relatively high photoluminescence with a quantum yield of 4%, which was previously hard to attain for iron chalcogenides. Moreover, they also show offresonant luminescence due to two-photon absorption, which can be valuable for biological applications. To confirm biocompatibility of the FeSe NPs, cytotoxicity test was performed by using three different human cell lines which are AGS, MG63, NCI-460. As a result, FeSe NPs have over 90 % of cell viability.

Acceptance ID: 99LT-P

Wind effect of spoilers on the roof of gable low-rise buildings by converting wind energy

Gang LI[1], *Shi GAN*[1], *Zhi-qian DONG*[1]

[1] *Dalian University of Technology, Dalian, Liaoning Province 116024 China.*
469465077@qq.com

This paper presents the use of spoilers mounted at gable roof building for converting wind energy to reduce high wind-induced suctions occurring at roof-edge and ridge. A gable roof building model with spoilers of different dimensions was tested in a boundary layer wind tunnel. The influences of geometric dimensions and arrangement of spoilers on converting wind energy and mitigating high suctions on gable roof were be investigated. The experimental result show that the spoilers at gable wall have the greatest influences on wind pressures, followed by spoilers at eave. The angles between spoilers and roof are the most influencing geometrical factor for spoilers, which are recommended as 0-30° for spoilers at eave and 25-30° for spoilers at gable wall. The recommended ratio of spoilers height to eave height is between 1/70 and 1/12 and of spoilers width to the length of building is between 1/25 and 1/15. Although it have been proved that the spoilers have obvious effect on converting wind energy and mitigating high suctions on roof, the uplift force of spoilers can not be ignored. The spoilers should be connected with main structure of building to share the uplift force of spoilers.

Keywords: spoiler, wind energy, low-rise building, wind pressure, conversion devices

.

Acceptance ID: ae3r-O

Magnetic studies of Co_xCr_{1-x} thin films thermally evaporated under normal incidence

A. Kharmouche

Laboratory of Surfaces and Interfaces Studies of Solid Materials
Laboratoire d'Etudes des Surfaces et Interfaces des Matériaux Solides (L.E.S.I.M.S. Laboratory), Department of Physics, Ferhat Abbas University Setif1, 19000, Algeria.

We prepared series of Co_xCr_{1-x} thin films, using thermally evaporation under vacuum, onto Si(100) and glass substrates. To perform the static magnetic properties, Alternating Gradient Field Magnetometer (AGFM) and Vibrating Sample Magnetometer(VSM) measurements techniques have been used. The zero-field magnetic structure has been investigated by Magnetic Force Microscopy (MFM), using a Veeco 3100 apparatus. To perform the dynamic magnetic properties of the samples, we used Ferromagnetic Resonance(FMR) and Brillouin Light Scattering (B.L.S.) with a (2x3)–pass tandem Fabry-Perot interferometer techniques. In-plane easy magnetization axis was found for all samples. Using different spectra provided by these tools, we computed first, second and uniaxial magnetic anisotropy factors (K_1, K_2 and K_u) by way of several methods. Values of the computed effective magnetic anisotropy factors K_{ueff}, higher than 10^6 erg.cm^{-3}, have been found (see figure below). All these results will be discussed and correlated.

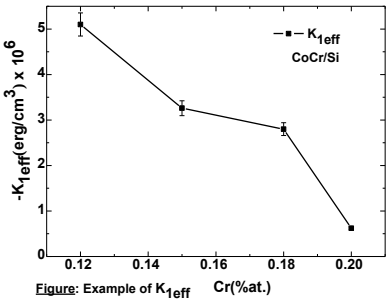

Figure: Example of K_{1eff}

Acceptance ID: ANXH-O

Structural and Optical characteristics of Cu^+-implanted AlN thin films

Arshad Mahmood[1], A. Shah[1], Zahid Ali[1] and I. Ahmad[2]*

[1]National Institute of Lasers and Optronics (NILOP), P.O. Nilore Islamabad
[2]National Center for Physics (NCP), Islamabad
[3]Pakistan Institute of Engineering and Applied Sciences (PIEAS), P.O. Nilore Islamabad

RBS/C, Raman, spectroscopic ellipsometry (SE) and spectrophotometer techniques have been used to investigate the impact of Cu implantation with varying ions fluences (5×10^{14}, 1×10^{15} and 5×10^{15} cm^{-2}) on the structural and optical properties of MBE grown AlN thin films. The level of implantation defects, as measured by RBS/C, gradually increases with the increasing of ions fluence, which is confirmed by Raman analysis. Further, it was observed that the implantation defects accumulate at the surface for the flux of 5×10^{14} cm^{-2} while the defect region shifts inside the film for the fluence higher than 5×10^{14} cm^{-2}. The basic Raman modes, E_2 (high) and A_1 (LO), for the wurtzite AlN crystal structure have been observed. It was found that both Raman modes shift with Cu^+ fluences, indicating that Cu atom substituted into Al sites, causes to produce mass defects. Similarly ellipsometric study explores that the optical constants (n and k) of the films vary with the increasing of Cu ion fluences. In comparison, the band gap energy was also determined by using transmission spectra and found to agree with that of the ellipsometric results. These analyses confirm that the band gap energy decreases after implantation of Cu ions in the AlN film.

Keywords: Cu^+ implantation; radiation defects; Raman scattering; Band gap energy; Optical constants.

**Corresponding Author: Dr. Arshad Mahmood*

Email: drarshadjanjua@gmail.com

Tel. 92-51-9248687

Acceptance ID: ARSH-O

Multifunctional materials inspired by salivary acquired pellicle

Xinyuan Xu[1], Yanpeng Liu[1], Jianshu Li[1,]*

[1] College of Polymer Science and Engineering, State Key Laboratory of Polymer Materials Engineering, Sichuan University, Chengdu, 610065, China.
jianshu_li@scu.edu.cn

Manipulation of the surface properties of biominerals is very important for their biomedical applications. However, the straightforward preparation of a multifunctional and stable coating on biominerals remains a challenge. Here, a rapid and universal method for multifunctional coatings was developed based on a salivary acquired pellicle (SAP) inspired dendrimer. Then, the SAP-inspired strategy was also applied to modify a series of materials such as tannin acid (TA) and oligomeric procyanidins (OPC). These materials have an external surface modified with DDDEEKC peptide sequence, which mimics the adsorption function of statherin as one of the main components of SAP, to endow the them with a universal capability for adhesion on biominerals. For example, the DDDEEKC modified PAMAM coating can be formed by a simple dip-coating method on various biominerals within 10 min, and is stable for more than one month. It provides a universal platform of secondary modifications for different applications. Also, the DDDEEKC decorated TA and OPC can be used as restorative biomaterials to resist bacterias and also induce the remineralization of tooth enamel.

Scheme 1. SAP-inspired multifunctional materials for biomineral coating, and dental restorative/antibacterial materials (SAP-TA and SAP-OPC) for example.

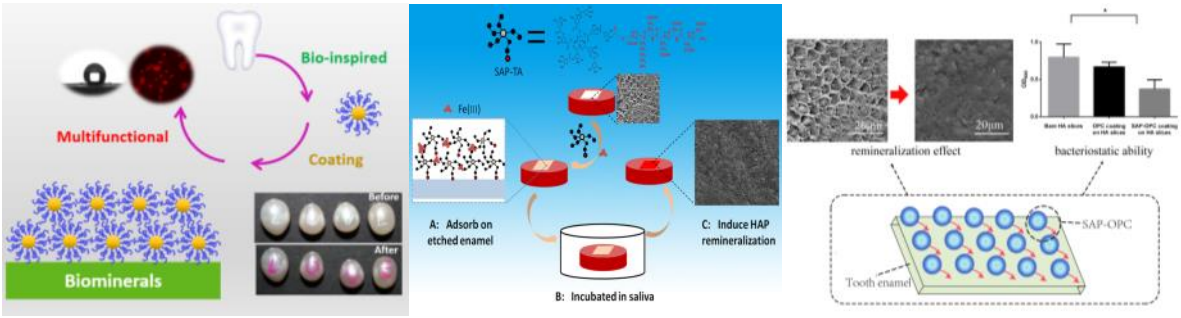

Keywords: Multifunctional, coating, restorative/antibacterial materials, salivary acquired pellicle, bio-inspired.

[1] ZHANG, S., HE, L., YANG, Y., YANG, B., LIAO, Y., XU, X., LI, J., YANG, X. & LI, J. 2016. Effective in-situ repair and bacteriostatic material of tooth enamel based on salivary acquired pellicle inspired oligomeric procyanidins. *Polymer Chemistry*, 7, 6761-6769.

Acceptance ID: B5ED-O

In-situ observation of lattice structure of PZT ceramic during the heating process

Mitsuhiro Okayasu, Kohei Bamba, Toshiki Yamazaki

Graduate School of Natural Science and Technology, Okayama University
3-1-1 Tsushimanaka, Kita-ku, Okayama, 700-8530, Japan
E Mail/ Contact Détails (mitsuhiro.okayasu@utoronto.ca / +81 86 251 8025)

To better understand the lattice characteristics of lead zirconate titanate (PZT) ceramics, the lattice orientations and domain-switching characteristics have been examined during loading and unloading process using various experimental techniques. Upon loading, linear and nonlinear fracture mechanics of the PZT ceramics are observed. The slope of the stress-strain response is attributed mainly to lattice strain and domain switching strain. During the loading process, electrical activity also occurs several times in the PZT ceramics. This activity is related to a lightning-like phenomenon and consists of a bright flash with a click. This electrogenerative event is caused by severe domain-switching. The characteristics of domain-switching and reverse switching are detected during the loading and unloading processes. The amount of domain-switching depends on the grain, due to different stress levels. In addition, two patterns of 90˚ domain-switching systems are characterized, namely (i) 90˚ turn about the tetragonal *c*-axis and (ii) 90˚ rotation of the tetragonal *a*-axis. There is strong domain switching when the domain (*c*-axis of the tetragonal structure) is orientated close to the loading direction. A large number of domains are switched between 85.4° and 90.0°, with many crossing the loading axis. In situ TEM observation of the domain switching characteristics of PZT ceramic has been conducted with increasing the sample temperature from 25°C to 300°C, and the domain switching like behavior is directly observed from the lattice image, where the severe domain switching occurs less than 100°C.

Keywords: piezoelectric ceramic; lead zirconate titanate ceramic; domain switching

[1] Okayasu, M., Ozeki, G., Mizuno, M., Fatigue failure characteristics of lead zirconate titanate piezoelectric ceramics, *J. Eur. Ceram. Soc*. 30(2010)713–725.
[2] Okayasu, M., & Bamba, K., Domain switching characteristics of lead zirconate titanate piezoelectric ceramics on a nanoscopic scale, *J. Eur. Ceram. Soc.* 37(2017)145–159.
[3] Okayasu, M., Sato, K., Mizuno, M., Influence of domain orientation on the mechanical properties of lead zirconate titanate piezoelectric ceramics, *J. Eur. Ceram. Soc.* 31(2011)141–150.

Acceptance ID: B85E-O

Magnetic Responsive Polyethylene Glycol Nanocomposite Actuators

Alfadhel[1], Hsu[1], Borkholder[1]

[1]Microsystems Engineering, Rochester Institute of Technology, Rochester, NY.
Presenting author: mh4060@rit.edu.
Corresponding author: ahaeen@rit.edu.

Multifunctional polymers have attracted attention as the need grows for materials to simultaneously demonstrate different capabilities [1]. Of those highly-demanded nanocomposites, magnetothermally-responsive materials demonstrate a promising application in drug delivery systems [2]. The quick reacting nature of magnetothermally-responsive polymers inspires us to present a one-of-a-kind nanocomposite valve that utilizes both the magnetic force attraction and the thermal-induced phase change for operation. Valves that show good performances are typically micromachined, however, they cannot be easily integrated with other components and fail to provide a simple solution for interconnecting channel systems [3,4]. Researchers have shown great interest in flexible magnetic valves, but have yet overcome the integration difficulty and the high power consumption [3]. The proposed valve based on magnetothermally-responsive nancomposites offers unique features and capabilities including easy integration, biocompatibility, scalability and a one-way passive operation. The valve is fabricated by incorporating Fe_3O_4 nanoparticles in polyethylene-glycol (PEG). Fe_3O_4 is biocompatible and can be easily dispersed and manipulated with external field due to its superparamagnetic nature. 2 µm Parylene encapsulates the nanocomposite to offer biocompatibility, enclosure and flexibility. The presented valve is designed to fit 0.7 mm in diameter channels, however, it can be customized to fit any microfluidic system. After the valve is injected in the channel and steered to the desired location, it is heated above the phase change temperature of PEG (e.g. body temperature). The valve expands and gets locked in place with a NdFeB permanent magnetic nanocomposite to attract the nanoparticles, sealing at one edge of the valve while keeping the other loose. The nanocomposite actuator, operated in liquid state, is stretched by the nanoparticles attracted toward the magnetic field source and sticks to the inner wall of the tube to realize one-way sealing. The presented magnetothermally-responsive actuator demonstrates a reliable operation as a passive one-way valve that exhibits steady flows from the inlet side, i.e. 5 µL/min at 14 kPa and robust sealing from the outlet side, i.e. 66 nL/min at 14 kPa min due to the difficulty for the flows to deform the actuator's outlet side where the nanoparticles are attracted toward the ring magnet to fully stretch the actuator at. The demonstrated performance indicates the valve is suitable to be integrated with implantable micropumps or drug delivery systems to prevent back flow of body fluids to the microfluidic systems.

Keywords: magnetic nanocomposites, thermosensitive polymers, valve, actuator

[1] THEVENOT, J., OLIVEIRA, H., SANDRE, O. & LECOMMANDOUX, S. 2013. Magnetic responsive polymer composite materials. *Chemical Society Reviews*, 42, 7099.
[2] BRAZEL, C. 2008. Magnetothermally-responsive Nanomaterials: Combining Magnetic Nanostructures and Thermally-Sensitive Polymers for Triggered Drug Release. *Pharmaceutical Research*, 26, 644-656.
[4] OH, K. & AHN, C. 2006. A review of microvalves", J. Micromech. Microeng.16, R13–R39.
[5] BENITO-LOPEZ, F., BYRNE, R., RADUTA, A., VRANA, N., MCGUINNESS, G. & DIAMOND, D. 2010. Ionogel-based light-actuated valves for controlling liquid flow in micro-fluidic manifolds, Lab Chip, 10, 195-201.
Acceptance ID: BDHA-O

Ferroelectric and Magnetic Properties of $BiFeO_3$-based Thin Films

Dalhyun Do[1], *Gwangho Park*[1], *Miju Kim*[1]

[1]*Department of Advanced Materials Engineering, Keimyung University, Daegu 42601, South Korea*
ddo@kmu.ac.kr

$BiFeO_3$ (BFO) has been extensively studied due to coupled electric, magnetic, and structural order parameters that result in simultaneous ferroic properties at room temperature. Although BFO thin films have great potential in multifunctional electronic devices, high leakage current and weak magnetization of BFO are major obstacles for the potential applications. Many efforts have been made to improve the phase purity, magnetic and electrical properties of BFO. It has been reported that the substitution of a small amount of ions at Bi and/or Fe sites can reduce leakage current and modify magnetic properties. Also, the properties can be improved by forming a solid solution with other perovskite. In this study, we prepared $BiFeO_3$, $Bi(Fe,Mn)O_3$, $0.67BiFeO_3$-$0.33BaTiO_3$ thin films by using RF magnetron sputtering. Crystal structure, microstructure, electric and magnetic properties are discussed in details.

Keywords: $BiFeO_3$, thin films, ferroelectricity, magnetism, sputtering

[1] CATALAN, G. & SCOTT, J. F. 2009. Physics and application of Bismuth Ferrite. *Advanced Materials*, 21, 2463-2485.
[2] LAHMAR, A., HABOUTI, S., DIETZE, M., SOLTERBECK, C.-H., & SE-SOUNI, M., 2009. Effects of Rare Earth Manganites on Structural, Ferroelectric, and Magnetic Properties of $BiFeO_3$ Thin Films. *Applied Physics Letters*, 94, 012903.
[3] WU, J., WANG, J., XIAO, D., & ZHU, J., 2011. Valence-driven Electrical Behavior of Manganese-modified Bismuth Ferrite Thin Films. *Journal of Applied Physics*, 109, 124118.

Acceptance ID: BK29-P

Modeling and Simulation of Contact Interaction between the Components of USDC

Zili Huang [1], Junkao Liu[2]

[1] State Key Laboratory of Robotics and System, Harbin Institute of Technology, Harbin 150001, Heilongjiang Province, China.
[2] State Key Laboratory of Robotics and System, Harbin Institute of Technology, Harbin 150001, Heilongjiang Province, China.
NOIRKILLER@outlook.com ***(corresponding author's)***
jkliu@hit.edu.cn ***(presenting author's)***

To address some of limitations of traditional drilling device, the Ultrasonic/Sonic Driller/Corer (USDC) was developed by NASA Jet Propulsion Laboratory as a special percussive mechanism for in-situ rock sampling. Generally, the USDC consists of three components, i.e., a piezoelectric ultrasonic transducer with a horn, a free-mass and a drill bit. The free-mass delivers energy from transducer to the surface of rock by bouncing between the horn and the drill bit. This paper presents simulation and analysis for the collisions of this novel drilling system. The collision force and duration of interactions are analyzed by using Finite element approach, meanwhile, effects of wastage of different components on the collision is also explored. A simplified integrated analysis is made to predict the characteristics of USDC and critical factors that affect drilling efficiency. The drilling testing platform is established and experimental data is applied to verify the simulation results.

Keywords: Ultrasonic/Sonic Driller/Corer; Collision; Piezoelectric transducer.

[1] E. Battistelli, P. Falciani, P. Magnani, B. Midollini, G. Preti, E. Re, Galileo Avionica's Technologies and Instruments for Planetary Exploration, Origins of Life and Evolution of Biospheres, 36 (2006) 587-596.
[2] Y. Bar-Cohen, S. Sherrit, B.P. Dolgin, N. Bridges, B. Xiaoqi, C. Zensheu, A. Yen, R.S. Saunders, D. Pal, J. Kroh, T. Peterson, Ultrasonic/sonic driller/corer (USDC) as a sampler for planetary exploration, Aerospace Conference, 2001, IEEE Proceedings., 2001, pp. 1/263-261/271 vol.261.
[3] M. Badescu, Y. Bar-Cohen, S. Sherrit, X. Bao, Z. Chang, C. Donnelly, J. Aldrich, Percussive augmenter of rotary drills (PARoD), Proc., SPIE Smart Structures and Materials, SPIE, San Diego, CA., 2012, pp. 83450J-83450J-83458.
[4] Y. Bar-Cohen, M. Badescu, S. Sherrit, K. Zacny, G.L. Paulsen, L. Beegle, X. Bao, Deep drilling and sampling via the wireline auto-gopher driven by piezoelectric percussive actuator and EM rotary motor, Proc., SPIE Smart Structures and Materials/NDE Symp., SPIE, Bellingham, WA, 8., 2012, pp. 83452A-83452A-83458.
[5] S. Sherrit, M. Badescu, X. Bao, Y. Bar-Cohen, Z. Chang, Novel horn designs for power ultrasonics, Ultrasonics Symposium, 2004 IEEE, 2004, pp. 2263-2266 Vol.2263.
[6] P. Harkness, M. Lucas, A. Cardoni, Architectures for ultrasonic planetary sample retrieval tools, Ultrasonics, 51 (2011) 1026-1035.
[7] B. Xiaoqi, Y. Bar-Cohen, C. Zensheu, B.P. Dolgin, S. Sherrit, D.S. Pal, D. Shu, T. Peterson, Modeling and computer simulation of ultrasonic/sonic driller/corer (USDC), IEEE Transactions on Ultrasonics, Ferroelectrics, and Frequency Control, 50 (2003) 1147-1160.

Acceptance ID: BK9Z-P

Recent Advances on Structural Health Monitoring of Civil Structures Using Piezoceramic Transducers

Linsheng Huo and Gangbing Song

School of Civil Engineering, Dalian University of Technology

The piezoceramic (Lead Zirconium Titanate, PZT) materials, due to their low costs and excellent dynamic properties, have broad application prospects in structural health monitoring of civil engineering. Nowadays, researchers have made great progress on the sensor exploiting and application in structural health monitoring. However, even though the PZT sensors have broad frequency responses, only partial frequency ranges of PZT signal tends to be used for structural health monitoring, which makes the monitoring target too single and the function too wasteful. There are still further studies to be done on the dynamic properties of sensors and multi-functional applications based on the broad frequency range of piezoelectric sensors. The authors developed the structural health monitoring methods using the broad-frequency responses of piezoelectric sensors in recent years. This paper introduced the recent advances on the structural health monitoring of civil structures using piezoelectric sensors, including bolt looseness detection, corrosion monitoring in steel bars, impact direction identification, and crack detection of concrete.

Acceptance ID: BLB4-O

Preparation of acrylate-based and alkali-soluble polymer coating ink

Chul Woo Lee

Department of Chemical & Biological Engineering/RIC, Hanbat National University, Daejeon, South Korea
cwlee@hanbat.ac.kr/corresponding author's

Alkali-soluble polymer coating is used to protect a plate glass during a cutting process for the production of a tempered glass. Alkali-soluble property is necessary to remove the polymer film after processing. In order to reduce a curing time, UV curable resins are preferred to thermosetting resins. Monomer, oligomer, acidic polymer, photo initiator, and additives are included in the coating ink. Uniformity of the coating, curing time, adhesive strength, hardness, and detachability are important factors to achieve good performance.

In this study, various acrylates were used as monomers and the effects of physical properties with variable monomer contents and mixing ratio of monomers were investigated. To provide an alkali-soluble property, acidic polyacrylates with various acid value and molecular weight were used and the relations between peering time and these properties were investigated as well. The number of functional groups of acrylate monomers, the type and the amount of photo initiator, the amount of talc additive had great effects on the physical properties such as adhesive strength, curing time, thickness, hardness and detachability of the polymer coating.

Keywords: alkali-soluble, acrylates, UV-curable, coating agent.

Acceptance ID: BPCQ-P

Piezoresistive Behavior of 3D Porous Carbon Nanotube Composite Structures

*Myoung-seok Kim, Jaebong Jung, and Ji Hoon Kim**

School of Mechanical Engineering, Pusan National University
Busandaehak-ro 63beon-gil, Geumjeong-gu, Busan 46241, Republic of Korea
** Corresponding author. kimjh@pusan.ac.kr*

In order to design flexible pressure sensors with high sensitivity, a multi-physics computational model for piezoresistivity was developed. The developed model was used to investigate the piezoresistive behavior of porous carbon nanotube composite structures. The effects of filling factor, orientation, and size distribution on the piezoresistivity were analyzed and an optimized structure with high sensitivity was proposed. For validation, the proposed structure was 3D printed and the piezoresistivity of the porous structure was evaluated.

Acceptance ID: BQ8Y-P

Optical Study of Oxygen-Incorporated ZnS Mixed Compound for Color Palette Visible-Light Emission Device

Min-Han Lin[1], *Ching-Hwa Ho*[1,2]

[1] *Graduate Institute of Applied Science and Technology, National Taiwan University of Science and Technology, Taipei 106, Taiwan*
[2] *Graduate Institute of Electro-Optical Engineering and Department of Electronic and Computer Engineering, National Taiwan University of Science*
E Mail: d10222604@mail.ntust.edu.tw*;* chho@mail.ntust.edu.tw.

Single crystal of oxygen-incorporated ZnS is an environmened friendly wide-band-gap semiconductor. The series of $ZnS_{1-x}O_x$ materials have considerable potential to be applied in solar cell and ultraviolet light-emitting devices. In this study, we have grown oxygen-incorporated ZnS crystals by chemical vapor transport (CVT) with iodine as a transport agent (I_2). Three types of crystals are discussed herein: the first type is an undoped ZnS, the second one is a $ZnS_{0.94}O_{0.06}$ compound, and the third crystal is $ZnS_{0.9}O_{0.1}$. The $ZnS_{0.94}O_{0.06}$ crystal is obtained by pre-oxidized Zn powder together with sulfur element using CVT growth. The $ZnS_{0.9}O_{0.1}$ was grown from source materials of ZnO powder, Zn powder and sulfur powder using CVT. The stoichiometry content of the three samples is determined by energy dispersive x-ray (EDX). We will further characterize the materials using transmission electron microscopy (TEM), thermoreflectance (TR) and photoluminescence (PL) measurements. Through the high resolution transmission electron microscopy (HRTEM) and selected area electron diffraction (SAED) results, we can see that the structure of the oxygen-incorporated ZnS belongs to zinc-blende phase. The lattice constant of the compounds can be further calculated to be a = 5.43Å (ZnS), 5.41Å ($ZnS_{0.94}O_{0.06}$) and 5.39Å ($ZnS_{0.9}O_{0.1}$), respectively. From the TR measurement results the transition energies of excitonic transitions are E_A = 3.864 eV (ZnS), 3.807 eV ($ZnS_{0.94}O_{0.06}$) and 3.786 eV ($ZnS_{0.9}O_{0.1}$), E_B = 3.918 eV (ZnS), 3.856 eV ($ZnS_{0.94}O_{0.06}$) and 3.786 eV ($ZnS_{0.9}O_{0.1}$), and E_C = 3.998 eV (ZnS), 3.940 eV ($ZnS_{0.94}O_{0.06}$) and 3.896 eV ($ZnS_{0.9}O_{0.1}$) at 40K, respectively.The transition energies of E_A are close to the positions of free-exciton emission peaks of the corresponding compound at low-temperature. Defect-state and surface-state emissions including sulfur vacancy (V_S in ZnS) and oxygen vacancy (V_O in ZnO) of the $ZnS_{1-x}O_x$ will emit red, yellow, green to violet visible emissions. The $ZnS_{1-x}O_x$ can be applied in fluorescent material and light-emitting device, and which becomes a further color-palette luminescence matter.

Keywords: II-VI compound semiconductor, Thermoreflectance, Photoluminescence, Color palette emissions.

[1] Chen, R., Li, D., Liu, B. & Peng, Z. 2010. Optical and excitonic properties of crystalline ZnS nanowires: Toward efficient ultraviolet emission at room temperature. *Nano Lett.* , 10, 4956-4961.
[2] Abounadi, A., Blasio, M. D., Bouchara, D., Calas, J., Averous, M., Briot, O., Briot, N., Cloitre, T., Aulombard, R. L. & Gil, B. 1994. Reflectivity and photoluminescence measurements in ZnS epilayers grown by metal-organic chemical-vapor deposition. *Phys. Rev. B*, 50, 11677-11683.
[3] Ho, C. H. & Lin, M. H. 2016. Synthesis and optical characterization of high-quality ZnS substrate for optoelectronics and UV solar-energy conversion. *RSC Advances*, 6, 81053-81059.

Acceptance ID: BUXU-O

Al-SUS316L composite materials fabricated by the spark plasma sintering process

Kwangjae Park[1], Jehong Park[2], Marc Leparoux[3], Akira Kawasaki[4], Hansang Kwon[1,2]*

[1]Department of Materials System Engineering, Pukyong National University, 365, Sinseon-ro, Nam-gu, Busan 48567, Korea
[2]Next Generation Materials Co., Ltd., 365, Sinseon-ro, Nam-gu, Busan 48547, Korea
[3]Laboratory of Advanced Materials Processing, EMPA-Swiss Federal Laboratories for Materials Science and Technology, Feuerwerkerstrasse 39, 3602, Thun
[4]Department of Materials processing Engineering, Graduate School of Engineering, Tohoku University, Sendai, 980-8579, Japan
**Corresponding author E-mail : kwon13@pknu.ac.kr*
Presenting author E-mail : pkj3678@naver.com

Aluminum(Al)-stainless steel 316L(SUS316L) composite materials was successfully manufactured using mechanical ball milling and spark plasma sintering (SPS). The composite materials comprised Al-20vol% SUS316L, Al-50vol% SUS316L, and Al-80vol% SUS316L, which were sintered at 600°C and 200 MPa for 5 min. The intermetallic compounds, such as $Al_{13}Fe_4$ and $AlFe_3$ were detected in the XRD patterns and exhibited in the composites due to the reaction between Al and SUS316L during the SPS process. The SEM(EDS), mapping and Fe-Al phase diagram results also indicated the presence of the intermetallic compound. The highest Vickers hardness (630 Hv) was achieved with the Al-50vol% SUS316L composite. In order to explain the increase in mechanical hardness, the strengthening mechanism, such as the Orowan looping mechanism was used in this work. Consequently, the SPSed Al-SUS316L composite materials are expected to be applicable in various fields of industrial engineering.

Keywords: Aluminum, Stainless steel 316L, Spark plasma sintering, Vickers hardness, Strengthening mechanism

Acceptance ID: C3MA-P

Structural transition, leakage, dielectric and magnetic properties of La/Cr-codoped $BiFeO_3$ ceramics

Fangting Lin

Key Laboratory of Optoelectronic Material and Device, and Department of Physics, Shanghai Normal University, Shanghai 200234, PR China
E Mail: nounou7@163.com; Tel.: +86 21 64322726

Single-phase $BiFeO_3$ (BFO) is one of the most widely studied multiferroic materials due to its fascinating fundamental physics as well as its potential applications in electronic devices. But there exist some problems such as large leakage current, high dielectric loss and weak ferromagnetism, which have seriously prohibited its practical use. Extensive reports showed that doping, especially codoping at the Bi/Fe sites, is an effective way to enhance the electrical and magnetic properties of BFO [1–14]. La [3–5] and Cr [7–11] are two common dopants for the Bi-site and Fe-site substitutions, respectively. However, the La/Cr codoping has been seldom reported until now.

In this work, BFO and $Bi_{1-x}La_xFe_{0.9}Cr_{0.1}O_3$ ($BLFC_{x=0.1–0.2}$) ceramics were prepared by modified solid-state reaction. The effect of La/Cr codoping on the microstructure, leakage, dielectric and magnetic properties of BFO was studied. The results show that the La/Cr codoping can induce a structural transition from a rhombohedral phase to a triclinic phase and thereby a series of changes in physical properties. The leakage current density can be reduced by over 2 orders of magnitude compared with undoped BFO, and are 1 to 4 orders of magnitude lower than those of Ba/Cr-codoped BFO ceramics [7], in a reasonable range for device applications [15]. The dielectric constant at 100 kHz of $BLFC_{x=0.2}$ is over 8 times larger than that of undoped BFO, and about 6, 3 and 2 times larger compared with Cr-doped [11], La/Gd-codoped [14] and Ba/Cr-codoped [7] BFO ceramics, respectively. The best remanent magnetization from $BLFC_{x=0.2}$ is over 4 orders of magnitude higher than that of undoped BFO, and 1 to 3 orders of magnitude higher compared with La-doped [3,4], La/Zr-codoped [5], La/Co-codoped [6] and Ba/Cr-codoped [7] BFO ceramics. The enhanced magnetization will be interesting for magnetic field sensor applications. These improvements can be attributed to the reduction of oxygen vacancies, the suppression of the spiral spin structure and a new ferromagnetic Fe^{3+}–O^{2-}–Cr^{3+} super-exchange interaction, induced by the La/Cr codoping. More interestingly, abrupt changes are observed around x=0.15, not only in microstructure but also in electrical and magnetic properties, which may suggest the coupling effect among them. The results indicate $BLFC_{x=0.1–0.2}$ ceramics as a promising candidate for magnetoelectric effect studies as well as for magnetoelectric device applications.

Keywords: multiferroic material, structural transition, leakage current, dielectric properties, magnetic properties

[1] SATI, P. C., KUMAR, M. & CHHOKER, S. 2015. Phase Evolution, Magnetic, Optical, and Dielectric Properties of Zr-Substituted $Bi_{0.9}Gd_{0.1}FeO_3$ Multiferroics. *J Am Ceram Soc*, 98, 1884-1890.
[2] YUAN, G. L., OR, S. W., LIU, J. M. & LIU, Z. G. 2006. Structural Transformation and Ferroelectromagnetic Behavior in Single-Phase $Bi_{1-x}Nd_xFeO_3$ Multiferroic Ceramics. *Appl Phys Lett*, 89, 052905.
[3] LIN, Y. H., JIANG, Q. H., WANG, Y., NAN, C. W., CHEN, L. & YU, J. 2007. Enhancement of Ferromagnetic Properties in $BiFeO_3$ Polycrystalline Ceramic by La Doping. *Appl Phys Lett*, 90, 172507.
[4] ZHU, J., Kumar, N. P., MIN, Z., HU, Y. M. & Reddy, P. V. 2015. Structural, Magnetic and Dielectric Properties of $Bi_{1-x}La_xFeO_3$ (x=0, 0.1, 0.15 and 0.2). *J Magn Magn Mater*, 386, 92-97.
[5] LAN, C. Y., JIANG, Y. W. & YANG, S. G. 2011. Magnetic Properties of La and (La, Zr) Doped $BiFeO_3$ Ceramics. *J Mater Sci*, 46, 734-738.
[6] GU, Y. H., ZHAO, J. G., ZHANG, W. Y., LIU, S. J., GE, S. P., CHEN, W. P. & ZHANG, Y. 2016. Improved Ferromagnetism and Ferroelectricity of La and Co Co-Doped $BiFeO_3$ Ceramics with Fe Vacancies. *Ceram Int*, 42, 8863-8868.
[7] WEI, J. Z., ZHANG, M., DENG, H. L., CHU, S. J., DU, M. Y. & YAN, H. 2015. Effect of Cr Doping on Ferroelectric and Magnetic Properties of $Bi_{0.8}Ba_{0.2}FeO_3$. *Ceram Int*, 41, 8665-8669.
[8] DONG, G. H., TAN, G. Q., LIU, W. L., XIA, A. & REN, H. J. 2014. Crystal Structure and Highly Enhanced Ferroelectric Properties of (Tb, Cr) Co-Doped $BiFeO_3$ Thin Films Fabricated by a Sol–Gel Method. *Ceram Int*, 40, 1919-1925.
[9] LIU, W. L., TAN, G. Q., XUE, X., DONG, G. H., REN, H. J. & XIA, A. 2014. Phase Transition and Enhanced Multiferroic Properties of (Sm, Mn and Cr) Co-Doped $BiFeO_3$ Thin Films. *Ceram Int*, 40, 12179-12185.

[10] LIU, W. L., TAN, G. Q., XUE, X., DONG, G. H. & REN, H. J. 2013. Structure Transition and Enhanced Ferroelectric Properties of (Mn, Cr) Co-Doped $BiFeO_3$ Thin Films. *J Mater Sci: Mater Electron*, 24, 4827-4832.
[11] CHANG, F. G., ZHANG, N., YANG, F., WANG, S.X. & SONG, G. L. 2007. Effect of Cr Substitution on the Structure and Electrical Properties of $BiFeO_3$ Ceramics. *J Phys D: Appl Phys*, 40, 7799-7803.
[12] SHI, X. X., QIN, Y. & CHEN, X. M. 2014. Enhanced Ferroelectric Properties in $Bi_{0.86}Sm_{0.14}FeO_3$–Based Ceramics. *Appl Phys Lett*, 105, 192902.
[13] KARPINSKY, D. V., TROYANCHUK, I. O., BUSHINSKY, M. V., GAVRILOV, S. A., SILIBIN, M. V. & FRANZ, A. 2016. Crystal Structure and Magnetic Properties of $Bi_{1-x}Ca_xFe_{1-x}Mn(Ti)_xO_3$ Ceramics across the Phase Boundary. *J Mater Sci*, 51, 10506-10514.
[14] SURESH, P., BABU, P. D. & SRINATH, S. 2016. Role of (La, Gd) Co-Doping on the Enhanced Dielectric and Magnetic Properties of $BiFeO_3$ Ceramics. *Ceram Int*, 42, 4176-4184.
[15] WANG, J. L., LI, L., PENG, R. R., FU, Z. P., LIU, M. & LU, Y.L. 2015. Structural Evolution and Multiferroics in Sr-Doped $Bi_7Fe_{1.5}Co_{1.5}Ti_3O_{21}$ Ceramics. *J Am Ceram Soc*, 98, 1528-1535.

Acceptance ID: cpyu-P

Novel Advance in (am-γ-,δ-,θ-,-α) Al_2O_3 nanoparticles recovering from synthetic polymer- A sol gel attempt

Ali Bumajdad[*a], *Fakhreia A. Sagheer*[a], *Shamsun nahar*[a]

[a]*Chemistry Department, Faculty of Science, P.O. Box 5969, Safat, State of Kuwait, Kuwait.*

Abstract: Alumina nanoparticles (NPs) have been the subject of researchers because of their temperature dependence unique properties (*e.g.*, variety of metastable structure including am-γ-,δ-,θ-,κ,-χ,-η- alumina and as well as stable α-alumina). Poly vinyl chloride (synthetic) polymers were subjected to synthesis alumina nanoparticles using sol gel process and aluminum ethoxide(AEO) as precursor. Hybrid films were thermally degraded by heating at different temperature (500º-1100ºC) in a dynamic atmosphere of air. The solid residues, with less aggregation forming nanoparticles, were assessed by thermogravimmetry (TG), X-ray diffractomertry (XRD) and electron microscopy to consist dominantly of uniformly agglomerated spherical, cubic, tetragonal, monoclinic and rhombohedral mesoporous Al_2O_3 nanoparticles, irrespective of the alumina in the film. The recovered alumina particles morphology and surface microstructure were scanned by field emission scanning and high resolution transmission electron microscopy, respectively. Whereas the particle surface chemistry and texture were delved into, respectively, by means of X-ray photoelectron spectroscopy (XPS) and N_2 sorptiometry. The recovered alumina was found, irrespective of the film content of alumina, to enjoy not only a high temperature (up to 1100ºC) stable nanoscopic with γ-,δ-,θ-,α-alumina structure but also a high temperature stable chemical composition (lattice Al^{3+} and O^{2-} and absorbed OH). Amorphous; 440, 400-δ alumina; 401δ-, 113α- alumina faceted microstructure and highly accessible (127-6m^2/g) with average pore diameter in the range 4-6nm. Different polymorphs of alumina are important for different application with successful application.

Key words: Surface properties, PVA-film, γ-alumina, α-alumina

**Corresponding Author: Dr. Ali Bumajdad*
E-mail: bumajdad@gmail.com, Tel: + 965-99411998

Acceptance ID: D8RQ-O

Reprogrammable phononic metamaterial

Osama R. Bilal, André Foehr and Chiara Daraio

Phonons are the lattice vibrations that are responsible for the propagation of sound, vibrations and heat at higher frequencies. Phononic crystals and acoustic metamaterials are material systems that exploit the geometry and elastic properties of basic building blocks (the unit cells), often repeating in space, to manipulate phonons and redirect energy. While there exist demonstrations of tunable phononic metamaterials by means of piezoelectric shunting, cell symmetry relaxation, static loading, granular contacts and acoustic trapping. They either lack the locality of element-wise programming, the ability to switch between desired material functionalities in real-time or continuously consume energy. Moreover, the existing solutions require direct contact between the metamaterial and the programming method. Obtaining element-wise and real-time programmability of metamaterials, in a reversible manner, would allow their applications to extend to new sensors, filters, and switches. In this work, we present the experimental realization of a 3D printed metamaterial plate that uses nonlinear interactions between its unit cells and an external magnetic potential, to dynamically tune wave propagation, controlling the frequency range of subwavelength band gaps.

Acceptance ID: DDTM-O

Characterization on Acoustic Emission Identification of MgO-C Refractory Damage Based on Principal Component Analysis and Empirical Mode Decomposition

Abstract: The presence of this high amount of MgO-C in the refractory can be responsible for micro damage occurrence during the repeated loading step after melt casting (annealing), exhibiting highly nonlinear behavior. Set aside the temperature factor for the moment, it might be a more feasible way to study the micro damaging mechanism from the point of view of micromechanics in advance in virtue of AE experimental characterization. This time domain method is used to determine new relevant descriptors to be introduced in the classification process to improve the characterization and the discrimination of the damage mechanisms. A major issue in the use of AE technique is how to discriminate the AE signatures due to the different damage mechanisms. Besides for the disturbances (e.g. scattering attenuation due to damage accumulation, viscous damping, inhomogeneity of concrete, internal sample structure defects, etc.) giving rise to misleading data if they are not well accounted and minimized, there are also 15 parameters in the identifying the damage in the process of the AE data, which complicate the work. Accordingly, AE with a clustering procedure is an effective tool that provides a better discrimination of damage mechanisms in refractory composite materials. The purpose of this work was to construct a properly labelled learning database of AE signals where each group was associated with identified damage mechanism. High dimensional feature space reduction was a remaining challenge to statistical processing and classification of AE data. An improvement was the use of classifiers able to group signals which have similar shapes into clusters. In the present study, unsupervised pattern recognition techniques, i.e., EMD with PCA, were used for the analysis of AE data. First, scattering AE signals were decomposed into different time scales of the intrinsic component through the empirical mode decomposition method. Secondly, the Hilbert-Huang transform was used to obtain the instantaneous frequency function component. Additionally, the time and the frequency domain characteristic values were calculated to construct the feature matrix. Thirdly, the PCA was adopted to generate a set of artificial variables made of a linear combination of the input features depicting the largest variance by using complete link hierarchical clustering in order to merge the correlated features into groups. Those applied a greedy approach that generated all possible feature combinations and then selected the one which optimized a given criterion. Finally, the support vector machine was employed to classify the damage signals. The classification was validated by the scanning electron microscopy. The results showed that there was a good result between the clustering groups and damage mechanisms with the observational results: the considered damage processes were primary matrix cracking and interfacial damage.

Acceptance ID: E8LD-P

Modulating Antimicrobial Activity and Mammalian Cell Biocompatibility with Glycosylated Miktoarm Star Polymers

*Edgar H. H. Wong** [1,2], *Zhangyong Si* [1,2], *Mary B. Chan-Park** [1,2]

[1] *School of Chemical and Biomedical Engineering, Nanyang Technological University, Singapore 637459*
[2] *Centre for Antimicrobial Bioengineering, Nanyang Technological University, Singapore 637459.*
Author correspondence: wonghoehon@gmail.com; mbechan@ntu.edu.sg
Author presenting : SIZH0001@e.ntu.edu.sg

The development of novel reagents and antibiotics for combating multi-drug resistance bacteria has been receiving significant attention in recent years. The use of synthetic biomacromolecules/nanoparticles prepared via controlled polymerization techniques is regarded as one of the most promising approaches to overcome such challenge because of the ability to precisely engineer the chemical functionality, and hence the biological properties of the nanomaterial (Lam et al., 2016). Several research groups have reported on the synthesis of antimicrobial polymers to combat the rise of antibiotic-resistant pathogens. However, the majority of these materials exhibit poor selectivity (Hancock and Sahl, 2006). Even though they are effective in killing bacteria, they are inherently harmful towards healthy mammalian cells, which hinder their potential for clinical applications.

In here, we describe the fabrication of new antimicrobial star polymers (< 30 nm in size) consisting of mixtures of polylysine and glycopolymer arms that not only possess good antimicrobial efficacy towards Gram-positive bacteria, including methicillin-resistant Staphylococcus aureus (MRSA) and vancomycin-resistant Enterococci (VRE) (with MIC values as low as 16 μg mL-1), but are also non-hemolytic (HC50 > 10000 μg mL-1) and exhibit excellent mammalian cell biocompatibility. This new class of antimicrobial star polymers is prepared via a strategic combination of modern synthetic polymer chemistry protocols that entails click chemistry, reversible addition fragmentation chain transfer (RAFT) polymerization, N-carboxyanhydride ring-opening polymerization (NCA-ROP), and macromolecular assembly/cross-linking. The antimicrobial activity and mammalian cell biocompatibility of the star nanoparticles can be tuned efficiently depending on the molar ratio of polylysine to glycopolymers arms and the type of sugars employed (e.g., glucosamine, glucose and galactose). The technology described herein thus represents an innovative and effective approach in fighting deadly infectious diseases.

Keywords: glycosylation, miktoarm star, antimicrobial agent

[1] LAM, S. J., O'BRIEN-SIMPSON, N. M., PANTARAT, N., SULISTIO, A., WONG, E. H., CHEN, Y.-Y., LENZO, J. C., HOLDEN, J. A., BLENCOWE, A. & REYNOLDS, E. C. 2016. Combating multidrug-resistant Gram-negative bacteria with structurally nanoengineered antimicrobial peptide polymers. Nature microbiology, 1, 16162.
[2] HANCOCK, R. E. & SAHL, H.-G. 2006. Antimicrobial and host-defense peptides as new anti-infective therapeutic strategies. Nature biotechnology, 24, 1551-1557.

Acceptance ID: EE53-O

Microwave Absorbance of Polymer Composites Containing SiC Fibers Coated with Ni-Fe Thin Films

Tian Liu[1], Woo-cheal Choi[2], Byungil Yoon[2], Sung-Soo Kim[1]

[1] Department of Advanced Materials Engineering, Chungbuk National University, Cheongju 361-763, Korea
[2] DACC Carbon Co. Ltd., Unam-ro 30, Deokjin-gu, Jeonju 561-202, Korea
E mail: sskim@chungbuk.ac.kr/*Tel: +82-43-261-2418, Fax: +82-43-271-3222*

SiC is a good potential material as microwave absorbers due to its sufficient dielectric loss in microwave radiation [1]. However, the absorption capability of SiC is not satisfactory as a single constituent. It is generally utilized as an auxiliary absorbent in other materials or after surface treatments to enhance the absorption capacity. In this study, Ni-Fe films are coated on SiC chopped fibers through electroless plating for the control of high-frequency electromagnetic properties and its effect on microwave absorbance is investigated. The electroless plating of Ni-Fe films is conducted using a two-step process of surface sensitizing and metal plating. The complex permeability and permittivity was measured in the composite specimens with the metalized SiC chopped fibers dispersed in a silicone rubber matrix. The original non-coated SiC fibers exhibit a considerable value of dielectric loss. The complex permeability spectrum is not greatly changed with Ni-Fe coating. On the while, dielectric constant is sensitively increased with Ni-Fe coating, due to the enhancement of the space charge polarization. The improvement in absorption capability (lower reflection loss and small matching thickness) is evident with Ni-Fe coating on SiC fibers. For the composite of Ni-Fe coated SiC fibers, –35 dB reflection loss less is predicted at 7.6 GHz with a matching thickness of 4 mm.

Keywords: silicon carbide, copped fibers, nickel-iron plating, microwave absorbers

[1] ZHANG, B., LI, J., SUN, J., ZHANG, S., ZHAI, H., & DU, Z., 2002, *J. Europ. Cer. Soc*. 22, 93-98.

Acceptance ID: EEBZ-P

Magnetic irreversible behavior and spin dynamics in iron-doped $EuCrO_3$

F. L. A. Machado, D. R. Ratkovski, P. R. T. Ribeiro and J. M. M. Ramírez

Departamento de Física, Universidade Federal de Pernambuco, 50670-901, Recife, Pernambuco, Brazil
and
H. V. S. Pessoni and A. Franco Jr
Instituto de Física, Universidade Federal de Goiás, C.P. 131, 74001-970 Goiânia, Goiás, Brazil

The rare-earth orthochromite $EuCrO_3$ is an orthorhombic distorted perovskite that has been attracting considerable attention because of its potential in application as a multifunctional material. It shows physical and chemical properties that are strongly influenced by the rare-earth ion lying on the A-site of a perovskite structure. $EuCrO_3$ does also present a rich variety of magnetic spin interactions, namely Cr^{3+} - Cr^{3+}, Cr^{3+} - Eu^{3+} and Eu^{3+} - Eu^{3+}, which are highly temperature dependent leading to a spin-canting antiferromagnetic phase below a Néel temperature T_N at low temperatures. In this work, the magnetic properties of nanopowders of pure and Fe-doped europium chromite samples prepared by a combustion reaction technique were investigated. The samples were characterized by X-ray diffraction and FTIR spectroscopy. The dc magnetization was measured for temperatures in the range $0 < T < 300$ K by using the zero-field and field-cooled procedures for applied magnetic fields H up to 85 kOe. Below some temperature T_{irr} (H) an irreversible behavior was observed and the data was fitted to a de Almeida-Thouless line yielding a critical exponent $\Phi = 2.5$ and a glassy temperature T_G of 170 K. The dynamics of the spins was investigated by measuring the T-dependence of the ac magnetic susceptibility χ_{ac} near T_N for frequencies f in the range $10\text{-}10^4$ Hz. It was found that the maximum in χ_{ac} shifts to higher values of T for increasing values of f, yielding a shift per decade of frequency of about 0.003. Two theoretical models, namely, the Voguel-Fulcher law and the power-law critical dynamics law where used for analyzing the shifting in χ_{ac} yielding $\tau_0 = 1.8 \times 10^{-9}$ s (= 1.6×10^{-15} s) for the characteristic relaxation time, $E_a/k_B = 39.23$ K for the activation energy and $T_G = 165.9$ K (= 167.5 K) for the Voguel-Fulcher (power law) model. Besides, the power law fitting yielded 5.62 for the product of the correlation length critical exponent (z) with the dynamical critical exponent (μ). The irreversible behavior and the shifting in χ_{ac} are signatures of spin-glass systems while the values found for X and for the other fitting parameters are comparable to the ones measured in other spin-glass systems. Finally, the correlation among the bonding angle Cr^{3+} - O^{2-}- Cr^{3+} and T_N was investigated. T_N was found to increase with increasing values of the bonding angle. This work was partially supported by the Brazilian Agencies CNPq, CAPES, FACEPE and FINEP.

Acceptance ID: F7UJ-O

Magneto-dielectric coupling in LSMO-PZT nanocomposites

O. P. Thakur[1], Manish Kumar[1,2,3], S. Shankar[2,3], A. K. Ghosh[1*]*

[1]Department of Physics, NSIT, New Delhi 110078, India
[2]Materials Research Laboratory, Department of Physics, Banaras Hindu University, Varanasi 221005, India
[3] Department of Physics, ARSD College, University of Delhi, New Delhi 110021, India
E Mail/ Contact Détails : opthakur@yahoo.com *, +91-9205475014 (Presenting Author)*
opthakur@yahoo.com ,anupkg66@gmail.com*; (Corresponding authors)*

Ferromagnetic-piezoelectric nanocomposites of $La_{0.7}Sr_{0.3}MnO_3$–$PbZr_{0.52}Ti_{0.48}O_3$ (LSMO–PZT) were synthesized by sol–gel route. The powder X-ray diffraction studies confirm the phase purity and the particle size in nanometer range. The coupling between the coexisting phases was achieved at magnetic transition temperature from the magnetic, dielectric and magneto-dielectric studies of LSMO–PZT nanocomposites. The quantitative magneto-dielectric coupling was found to be maximum value and decrease with increase in frequency. This provides the signature of magneto-dielectric coupling qualitatively as well as quantitatively in LSMO–PZT nanocomposites.

Keywords: Nanocomposites, magneto-dielectric, dielectric.

References

[1] KUMAR M,, SHANKAR S., DWIVEDI G. D., ANSHUL A., THAKUR O. P. & GHOSH A. K. 2015. Magneto-dielectric coupling and transport properties of the ferromagnetic-$BaTiO_3$ composites. *Appl. Phys. Lett.*, 106, 072903.
[2] HOON Y. S., KIM S. H., LEE S. J., KIM H. K. & LEE M. 2006. Fabrication and frequency response of dual-element ultrasonic transducer using PZT-5A thick film. *J. Sens. Actuators A*, 125, 463.
[3] TANG Z. H., TANG M. H., LV X. S., CAI H.Q., XIAO Y. G., CHENG C. P., ZHOU Y. C. & HE J. J. Enhanced magnetoelectric effect in $La_{0.67}Sr_{0.33}MnO_3$/$PbZr_{0.52}Ti_{0.48}O_3$ multiferroic nanocomposite films with a $SrRuO_3$ buffer layer. 2013. *Appl. Phys*., 113, 164106.
[4] DWIVEDI G. D., KUMAR M., SHAHI P., BARMAN A., CHATTERJEE S. & GHOSH A. K. Low temperature magnetic and transport properties of LSMO–PZT nanocomposites. 2015. *RSC Adv.* 5, 30748.
[5] B.D. CULLITY,1978. Elements of X-Ray Diffraction, *Addison-Wesley:* MA.

Acceptance ID: F86C-O

Functional Metal-organic frameworks and their applications in gas adsorption, catalysis and molecular sensing

Ali Morsali

Department of Chemistry, Faculty of Sciences, Tarbiat Modares University, P.O. Box 14115-175, Tehran

Metal-organic frameworks (MOFs) are a class of porous materials with great potentials in catalysis, gas storage and sensing.[1] An important feature of MOFs over other porous materials is the ability to tune their pore size, topology and functionality by the deliberate design and selection of organic and inorganic molecular building blocks from which the network is constructed.[2] Taking advantage of this feature, chemists have tried to design and synthesize novel MOFs having particularly desired and predetermined functions and properties. MOFs containing functional groups, such as urea, amide, imine, and other groups are currently in the spotlight due to their potential applications in different areas including molecular sensing and catalysis.[3-5] Thus, MOF containing one of these functional groups offers a convenient platform for designing supramolecular recognition units with adjustable specificity.[6] It is now well-established that MOFs containing functional groups offers a convenient platform for designing supramolecular recognition units with adjustable specificity for guest recognition. These frameworks may provide better performance than MOFs based on non-functionalized carboxylate linkers for a wide variety of applications, including gas storage, organocatalysis and molecular sensing. The presentation will provide an outlook of future research in which the incorporation of supramolecular recognition unit can provide new MOF platforms for different applications.

References:

[1] L. R. MacGillivray, Metal-organic frameworks: design and application, John Wiley & Sons, 2010.
[2] R. Cook, Y.-R. Zheng and P. J. Stang, Chem Rev, 2013, **113**, 734-777.
[3] A. Azhdari Tehrani, S. Abedi, A. Morsali, J. Wang and P. C. Junk, Journal of Materials Chemistry A, 2015, **3**, 20408-20415.
[4] Y. Xiong, Y.-Z. Fan, R. Yang, S. Chen, M. Pan, J.-J. Jiang and C.-Y. Su, Chem Commun, 2014, **50**, 14631-14634.
[5] H. Deng, C. J. Doonan, H. Furukawa, R. B. Ferreira, J. Towne, C. B. Knobler, B. Wang and O. M. Yaghi, Science, 2010, **327**, 846-850.
[6] K. Kim, Nat Chem, 2009, **1**, 603-604.

Acceptance ID: F9YN-I

Preparation, structure, and functional properties of NBT- and KNN- based perovskite ceramics

E.D. Politova[1], N.V. Golubko[1], G.M. Kaleva[1], A.V. Mosunov[1], S.P. Kabanov[1], N.V. Sadovskaya[1], S. Yu. Stefanovich[1,2], D.A. Belkova[2], D.A. Strebkov[2], P.K. Panda[3]

[1]*Karpov Institute of Physical Chemistry; Vorontsovo pole, 10, Moscow, 105064, Russia*
[2]*Lomonosov Moscow State University; Leninskie gory, 1, Moscow, 119992, Russia*
[3]*National Aerospace Laboratories, Kodihalli, Bangalore-560017 India*
Corresponding& presenting author politova@cc.nifhi.ac.ru

Increasing concern on the environment safety stimulated investigations of lead-free ferroelectric materials on the base of barium titanate $BaTiO_3$ (BT), bismuth-sodium titanate $(Na_{0.5}Bi_{0.5})TiO_3$ (NBT) and sodium-potassium niobate $(K_{0.5}Na_{0.5})NbO_3$ (KNN) perovskites in order to replace widely used Pb-containing materials.

In this work, influence of donor (Nb^{5+}) and acceptor dopants (Mn^{3+}, Fe^{3+}, Ni^{3+}) on structure, dielectric and ferroelectric properties of compositions close to Morphotropic Phase Boundaries (MPB) in KNN-BT and NBT-BT systems have been studied. Over stoihiometric additives (KCl, LiF, Bi_2O_3, V_2O_5) were used to improve sintering of ceramics. Ceramic samples were prepared by the two-step solid state reaction method at temperatures of 970–1470 K.

The samples were characterized by the X-ray Diffraction, Scanning Electron Microscopy, Second Harmonic Generation, and Dielectric Spectroscopy methods. Piezoelectric properties of poled samples were measured using the YE2730A d_{33}-meter.

Ferroelectric phase transitions were revealed at ~ 350-400 K and at ~ 550 K (NBT-BT), and at ~700 K (KNN-BT). Using the SHG method, increase in the spontaneous polarization value was observed in NBT-based ceramics with Na/Bi content >1 mainly due to presence of admixture phases with ferroelectric properties ($Na_2Ti_6O_{13}$ and $Bi_4Ti_3O_{12}$). Effects of dielectric relaxation at high temperatures were observed in ceramics with deficiency in the A-sites and containing cations with mixed valence in the B-sites of the perovskite lattice. At the room temperature, improvement of functional parameters was observed in modified ceramics. This confirms prospects of new lead-free piezoelectric materials development on the base of modified KNN-BT and NBT-BT compositions close to the MPB.

Keywords: perovskite, ceramic, ferroelectrics, piezoelectrics

Acknowledgment

The work was supported by the Russian Fund for Basic Research (Projects 15-03-03269 and 16-53-48009).

Acceptance ID: FA2P-O

Investigation on microstructure and dehydrogenation performance of magnesium borohydride for hydrogen energy storage

Z Wu[1*], *L Zhu*[1], *F Yang*[1], *Z Zhang*[1,2], *Y Wang*[3]

[1]*School of Chemical Engineering and Technology, Xi'an Jiaotong University, Xi'an 710049, P.R. China*.
[2]*State Key Laboratory of Multiphase Flow in Power Engineering, Xi'an Jiaotong University, Xi'an 710049, P.R. China.*
[3]*School of Chemical Engineering, Northwest University, Xi'an 710069, P.R. China*.
Presenting and corresponding author's E-mail: wuz2015@mail.xjtu.edu.cn

Hydrogen energy is viewed as one of the most promising secondary energy sources in the 21st century due to the advantages of abundant resources, high conversion efficiency and non-pollution [1,2]. However, the technologies used for hydrogen storage are still deficient, impeding the large-scale applications of hydrogen energy [3], and an efficient, economic and safe hydrogen storage material has been the focus of attention. $Mg(BH_4)_2$ material, having a high hydrogen capacity (14.8 wt.% in theory) and low hydrogen binding enthalpy [4,5], has been recognized as one of the potential candidates for hydrogen storage. Nevertheless, the existence of boron element could easily result in the generation of various B-based products during dehydrogenation of $Mg(BH_4)_2$ due to the metalloid character of B, which makes the dehydrogenation process become complex. The decomposition path of $Mg(BH_4)_2$ during the dehydrogenation is still controversial thus far. In the present study, the dehydrogenation of $Mg(BH_4)_2$ is experimentally investigated from the point of view of pressure-composition isotherm and simultaneous thermal analysis. The decomposition mechanism of $Mg(BH_4)_2$ is discussed based on these analyses and the evolution of microstructure during the dehydrogenation. In addition, the important thermodynamic and kinetic parameters, such as reaction enthalpy, entropy and apparent activation energy, are determined for each decomposition step of $Mg(BH_4)_2$.

Keywords: Magnesium based materials, Hydrogen storage, Microstructure, Reaction enthalpy

[1] SCHLAPBACH, L. & ZüTTEL, A. 2001. Hydrogen-Storage Materials for Mobile Applications. *Nature*, 414, 353-358.
[2] CHO, E. S., RUMINSKI A. M., ALONI S., LIU Y. S., GUO J. H. & URBAN J. J. 2016. Graphene Oxide/Metal Nanocrystal Multilaminates as the Atomic Limit for Safe and Selective Hydrogen Storage. *Nat Commun*, doi: 10.1038/ncomms10804.
[3] JEON K. J., MOON H. R., RUMINSKI A. M., JIANG B., KISIELOWSKI C., BARDHAN R. & URBAN J. J. 2011. Air-Stable Magnesium Nanocomposites Provide Rapid and High-Capacity Hydrogen Storage without Using Heavy-Metal Catalysts. *Nat Mater*, 10, 286-290.
[4] SEVERA, G., RöNNEBRO, E. & JENSEN, C. M. 2010. Direct Hydrogenation of Magnesium Boride to Magnesium Borohydride: Demonstration of > 11 Weight Percent Reversible Hydrogen Storage. *Chem Commun*, 46, 421-423.
[5] ZAVOROTYNSKA, O., EL-KHARBACHI, A., DELEDDA, S. & HAUBACK, B. C. 2016. Recent Progress in Magnesium Borohydride $Mg(BH_4)_2$: Fundamentals and Applications for Energy Storage. *Int J Hydrogen Energy*, 41, 14387-14403.

Acceptance ID: FGHY-O

Free-standing undoped ZnO microtubes with rich and stable shallow acceptors

Yijian Jiang[1, 2] , Qiang Wang[2], Yinzhou Yan[2]*

[1] Beijing Institute of Petrochemical Technology, Beijing 102617, China
[2] Institute of Laser Engineering, Beijing University of Technology, Beijing 100124, China

Fabrication of reliable large-sized *p*-type ZnO is the major challenge to realise ZnO-based electronic device applications. Here we report a novel technique to grow high-quality free-standing undoped acceptor-rich ZnO (A-ZnO) microtubes with dimensions of ~100 μm in diameter and 5 mm in length by optical vapour supersaturated precipitation. The A-ZnO exhibits long lifetimes (>1 year) against compensation/lattice-relaxation and the stable shallow acceptors with binding energy of ~127 meV are confirmed from Zn vacancies. The A-ZnO provides a possibility for a mimetic *p*-*n* homojunction diode with n^+-ZnO:Sn. The diode threshold voltage, turn-on voltage, reverse saturated current and reverse breakdown voltage are 0.72 V, 1.90 V, <10 μA and >15 V, respectively. The high concentrations of holes in A-ZnO and electrons in n^+-ZnO make the dual diffusion possible to form a depletion layer. The A-ZnO also demonstrates quenching-free donor-acceptor-pairs (DAP) emission located in 390-414 nm with temperature of 270-470 K. Combining the temperature-dependent DAP violet emission with native green emission, the visible luminescence of A-ZnO microtube can be modulated in a wide region of colour space across white light. The present work opens new opportunities to achieve ZnO with rich and stable acceptors instead of *p*-ZnO for a variety of potential applications.

Acceptance ID: FUK3-P

[*] Corresponding author: yjjiang@bjut.edu.cn

High Performance Flexible Piezoelectric Generator Based on the CNTs-doped PZT/Epoxy Nanocomposite

H. J. Kim[1] *and B. Yeon*[1]

[1]*Electronics and Telecommunications Research Institute, 218 Gajeong-ro, Yuseong-gu, Daejeon, Rep. Korea*
Corresponding author: nolawara@etri.re.kr */ 82-42-860-6152*

Recently, polymer-based piezoelectric nanocomposites have received a great deal of attention for sensors, actuators and transducers[1]. Typically, 0-3 piezoelectric nanocomposite consisting of a particulate ceramic randomly dispersed within a polymer matrix has many advantages of better flexibility, easier manufacturing and lower cost, compared to other types. However, it still has critical drawbacks of poorer piezoelectric properties since the ceramic particles within a polymer matrix are hard to be fully polarized. In this paper, the CNTs-doped PZT/Epoxy nanocomposites with PZT ceramic fillers of 81 wt.% and various amounts of carbon nanotubes (CNTs) additives are studied to achieve high performance flexible piezoelectric energy harvesters. To prepare the CNTs-doped PZT/Epoxy nanocomposite, various volume fractions of CNTs up to 0.4 wt.% were added to the nanocomposites. The electrical conductivity and dielectric constant results show that increase of the CNTs content can improve the electrical conductivities and, as a result, they can increase the poling efficiency of the composites. Based on the highest piezoelectric performance of the CNTs-doped nanocomposite (CNTs contents of 0.08 wt.%), it was shown that the flexible piezoelectric generator fabricated with the CNTs-doped nanocomposite film can generate an open-circuit voltage of 2.5 V and a short-circuit current of 25 mA.

Keywords: Generator, Piezoelectric, Nanocomposite, PZT/epoxy, Carbon nanotube

[1] K.I. PARK, S.B. BAE, S.H. YANG, H.I. LEE & S.J. LEE 2014. Lead-free BaTiO3 nanowires-based flexible nanocomposite generator. *Nanoscale*, 6, 8962-8968.

Acceptance ID: GK2J-P

Preparation of Plate Ceramic coated with metal oxide nanoparticles and Its Various Applications

Dae-Sung Kim

Eco-Composite Materials Center, Korea Institute of Ceramic Engineering and Technology(KICET), Jinju-si, Gyeongsangnam-do, 52851, Republic of Korea
dskim@kicet.re.kr

Titanium dioxide nanopowder has received much interest. This is due to its use in various applications such as cosmetics, high reflective coatings, and medical devices coating and gas sensors. Rutile TiO_2 exhibits an excellent refractive index, high whiteness, higher hiding power and superior chemical stability. In addition, Mica-based pearlescent pigments, which are Mica coated by TiO_2 or metal oxide nanoparicles, are widely applied in plastics, cosmetics, automobiles coatings among others, but they seem to be not explored by the ceramic industry. Herein I would like to introduce the potential of Infrared(IR) reflecting pigment and phosphorous effect pigment, along with the coating technology of plate ceramic coated by metal oxide nanoparticles. IR reflecting pigments have increasingly been used in external wall and roof of building in order to reduce heat build up caused by the absorption of the sun's energy and the occurrence of "urban heat islands effect". Moreover, any printable surface of valuable products are subject to forgeries. Luminescent pigments as identification items are discussed among of various method that is magnetism, hologram, etc. In this presentation, rutile TiO_2 or phosphorous mateirals as nano-sized metal oxide was prepared by sol-gel or template method. The nanosized materials were coated on plate ceramic to apply IR reflection, isolation-heat, special area with pearlescent or phosphorous effect. The various pigments were characterized by X-ray diffraction, FE-SEM, zeta potential, and a UV-Vis-NIR spectrophotometer, Refratometer, Fluorescence spectrometer.

Keywords: TiO2, Rutile, refractive index, Infrared reflection, identification pigment

[1] SYNNEFE, A., SANTAMOURIS M., APOSTOLAKIS, K. 2007. *Sol Energ*., 81(4), 488-497.

Acceptance ID: H276-P

Microstructure, relaxor-like behavior and electrical properties of Gd-doped $(Ba_{0.85}Ca_{0.15})(Zr_{0.1}Ti_{0.9})O_3$ lead-free piezoceramics

Buyin Li, Zhikang Hu, Qi Xiao, Siyuan Yu, Yuanzheng Luo, Shanshan Li, Yebin Xu*

School of Optical and Electronic Information, Huazhong University of Science and Technology, Wuhan 430074, PR China

Lead-free $(Ba_{0.85}Ca_{0.15})(Zr_{0.1}Ti_{0.9})O_3$+ x mol% (x=0–0.6) Gadolinium ceramics (BCZT-G) were fabricated via the conventional oxide-mixed method and the effects of gadolinium on the phase structure, microstructure, dielectric, ferroelectric and piezoelectric properties were investigated. The XRD patterns showed that the single perovskite phase was achieved in all compositions. The SEM images indicate that a small addition of Gd_2O_3 greatly affects the microstructure. The diffusive phase transition was enhanced with increasing the Gd content. The phenomena were explained well by defect chemistry .The BCZT ceramics with 0.2 mol% Gd content sintered at 1450℃ showed excellent piezoelectric properties with d_{33}=432 pC/N and k_p=43%. Besides these, a low dielectric loss (tanδ=0.019), a low coercive field (Ec=0.30 kV/mm) and high remanent polarization values ($2P_r$~20.3 μC/cm^2) were also obtained on BCZT+0.2 mol% Gd content lead-free ceramics. As a result, the performance of a small amount of the amphoteric rare earths ion Gd^{3+} doped BCZT ceramics have significantly enhanced compared to the undoped BCZT ceramics.

Key words: Lead-free, Gd-doped, Dielectric relaxor, Piezoelectric, defect chemistry

* Corresponding author. Tel.&Fax: +86 27 87542994; E-mail address: libuyin@hust.edu.cn

Acceptance ID: H7QQ-O

Stimuli-response targeted calcium nanoparticles for tumor therapy

*Jing Yao *, Hui Xiong, Shi Du*

Department of Pharmaceutics, China Pharmaceutical University, Nanjing 210009, China
** Correspondence to: Jing Yao, E-mail: yaojing@cpu.edu.cn (J. Yao). Tel.: +86 25 83271059; Fax: +86 25 83301606.*

The therapeutic strategy attacking double key site of the tumor cells (i.e. both mitochondria and nuclei) to achieve enhanced anticancer efficacy was attracting much attention. Calcium-based nanoparticle was a potential nanocarrier for drug delivery and tumor therapy. Hydroxyapatite (HAP), a hydroxylated calcium phosphate-based material which could be used as drug carrier to load drugs by means of adsorption, has long been known for its excellent biocompatibility, non-toxicity and non-mutagenicity. HAP nanoparticles could induce apoptosis of the tumor cells by a mitochondrial pathway, and also enter into the nuclei to impede the proliferation of tumor cells. However, lacking of active targeting effect, drug burst release, aggregation and low water-solubility limited the application of HAP nanoparticles in the field of drug delivery. In our studies, biocompatible and water-soluble functional materials such as tumor targeted peptides and hyaluronic acid were designed to coat on the surface of HAP nanoparticles by covalent bond to improve water solubility of HAP nanoparticles and facilitate its tumor targeting delivery. Furthermore, stimuli-response drug release from the nanoparticles based on the tumor microenvironment was expected to enhance the in vivo efficacy of HAP nanoparticles. Such functional materials modified HAP (HAP-FM) nanoparticles were used for the delivery of doxorubicin (DOX) to liver tumor to enhance the therapeutic effect of DOX by mitochondrial and nuclei dual-targeted strategy and reduce the side effects of chemotherapy. Our study showed that DOX-loaded HAP-FM nanoparticles exhibited good stability, favorable biocompatibility and the obvious distribution of DOX in both mitochondrial and nuclei of tumor cells as well as good antitumor efficacy with reduced the DOX-induced toxicity. In conclusion, HAP-FM nanoparticles were promising targeted nanocarriers for tumor therapy of antitumor drugs.

Acknowledgements:
This work was supported by the 12th of Six Talent Peak Foundation of Jiangsu Province (YY-001), Qing Lan Project and the Project Program of State Key Laboratory of Natural Medicines, China Pharmaceutical University (JKGQ201107).

References:

[1] H Xiong, S Du, J Ni, J Zhou, J Yao*. Mitochondria and Nuclei Dual-targeted Heterogeneous Hydroxyapatite Nanoparticles for Enhancing Therapeutic Efficacy of Doxorubicin. *Biomaterials*, 2016, 94: 70-83.

[2] J Yao, Y Zhang, S Ramishetti, Y Wang, L Huang*. Turning an antiviral agent into an anticancer drug: Nanoparticles delivery of ancyclovir monophosphate. *J Control Release*, 2013, 170(3): 414-420.

Acceptance ID: HB2W-O

Water-soluble carbohydrate substituted A_3B type tetrapyrazinoporphyrazine Zn complexes

*Jong Min Park, Chang Young Jung, Joong Hyun Cho, Dae Hyun Kim, Jae Yun Jaung**

Organic and Nano Engineering, Hanyang University
jjy1004@hanyang.ac.kr

Tetrapyazinoporphyrazines (TPPs), which have similar structure and properties with phthalocyanines, are remarkable compounds possessing photophysical, semiconducting, and photoconducting properties due to their 18π-electron aromatic macrocyclic structures. The solubility of TPP in various solvents is critical for application in PDT. However, many TPPs are not soluble in common organic but also aqueous solvents. Peripheral or axial substituents such as long alkyl, alkoxy, and other bulky groups can improve the solubility of tetrapyrazinoporphyrazines [1]. In this study, we synthesized asymmetric A_3B-type TPP Zn complexes incorporating bornanes and carbohydrate units, β-D-glucose and β-D-galactose, to investigate important properties with applications in PDT sensitizers. The synthesized compounds did not show aggregation in DMSO and were slightly soluble and aggregated in water. Future testing of the TPPs complexes against different cancer cell lines is being progressed to determine their potential targeting selectivity.

Keywords: tetrapyrazinoporphyrazine, photodynamic therapy, carbohydrate, hydrophilicity

[1] JONG MIN PARK, CHEOL JUN SONG, WANG YAO, CHANG YOUNG JUNGM IN HO HYUN, DONG HOON SEONG, JAE YUN JAUNG. 2015. Synthesis of carbohydrate-conjugated azaphthalocyanine complexes for PDT. Tetrahedron Letters, 4967-4970.

Acceptance ID: HE5V-P

One-Step Electrospun Nano-Net (ENN) Reinforced Microfiber Structure for Cabin Air Filtration Application

Sung Won (Ko)[1], Ji Yeon (Lee)[2], Woo Jin(LEE)[2], Chan Hee (Park)[1,3], Cheol Sang (Kim)[1,3]

[1]Bionanosystem Engineering Department, Chonbuk National University, Republic of Korea.
[2] Mechanical Design Engineering Department, Chonbuk National University, Republic of Korea.
[3]Division of Mechanical Design Engineering, Chonbuk National University, Republic of Korea.
swc2736630@gmail.com, biochan@jbnu.ac.kr, chskim@jbnu.ac.kr / +82-63-219-5293, +82-63-270-2395, +82-63-270-4284

Recent researches in membrane which coexisting with microfiber and nano-net have introduced various materials and they have been applied to a variety of applications. Particularly, researches in the field of filtration applications have been actively carried on because it can observe these phenomena which are transition/free molecular flow regime, Brownian diffusion, particle-fiber interactions, aerodynamic slip and sieve to occur that are required for the filtration application. Also, in the case of filtration applications using conjugated nano-net and microfiber, they exhibit improved mechanical strength and higher filtration efficiency than nanofibers alone. In this study, we report the development of conjugated nano-net and microfiber by electrospinning process for filtration application. We fabricated the conjugated nano-net and microfiber membrane samples with different content of cellulose nanocrystals (CNCs). It was observed that the formation of nano-net between microfibers which was affected by content amount of CNCs and the optimum CNC amount could be determined by this experiment. And the nano-net thus formed has an influence on the performance of the filtration application. We compare the characteristics of each samples and effectiveness as filtration applications were verified by the following experiments. The morphology of samples was characterization with a Field emission scanning electron microscopy (FE-SEM) and the diameter of fibers was presented as mean diameter±standard deviation. The structural characteristics of samples was performed with Fourier transform infrared spectroscopy(FT-IR), Universal testing machine(UTM), and Thermogravimetric analysis(TGA). And to measure the efficacy as filtration application, we fabricate the filter samples on nonwoven fabric and pressure drop and quality factor for all tested filter samples was measured. Finally, excellent properties of prepared conjugated nano-net and microfiber could be effective for filtration application and we expect them to overcome the limits of filtration application using nanofibers.

Keywords: Nano-net, filter, filtration, CNC

[1] Sambaer, W., et al. 2012. 3D air filtration modeling for nanofiber based filters in the ultrafine particle size range. Chemical Engineering Science 82: 299-311.
[2] Gopal, R., et al. 2006. Electrospun nanofibrous filtration membrane. Journal of Membrane Science 281(1): 581-586.

[3] Patanaik, A., et al. 2010. Performance evaluation of electrospun nanofibrous membrane. Journal of Membrane Science 352(1): 136-142.

Acceptance ID: HJ6D-P

Rechargeable anti-bacterial efficacy of montmorillonite modified with cetylpyridinium chloride for dental materials

YOSHIHARA[1], *ABE*[2], *NAGAOKA*[1], *MAKITA*[3], *OBIKA*[3], *VAN MEERBEEK*[4], *YOSHIDA*[2]

[1]*Okayama University, 2-5-1 Shikata-cho, Kita-ku, Okayama 700-8558 Japan.*
[2]*Hokkaido University, Kita 13, Nishi 7, Kita-ku, Sapporo, 060-8586, Japan.*
[3] *National Institute of Advanced Industrial Science and Technology (AIST), 2217-14 Hayashi-cho, Takamatsu 761-0395, Japan.*
[4] *KU Leuven, Kapucijnenvoer 7, BE-3000 Leuven, Belgium*
E Mail/(presenting and corresponding author: Kumiko YOSHIHARA, k-yoshi@md.okayama-u.ac.jp)

Cetylpyridinium chloride (CPC) is a cationic quaternary ammonium compound with antiseptic properties, typically used in mouth rinses and tooth pastes. While CPC could theoretically provide antibacterial properties to dental materials, such as dental adhesives, cements and composites, a main difficulty is its limited release in particular after curing [1]. We developed rechargeable CPC-loaded montmorillonite (CPC-Mont) in order to ensure a long-term antibacterial effect. In this study, we characterized CPC-Mont and investigated the anti-bacterial efficacy of CPC-Mont added to PMMA resin.

Keyword: antibacterial agent, recharge, cetylpyridinium chloride, montmorillonite, X-ray diffraction

[1] NAMBA, N., YOSHIDA, Y., NAGAOKA, N., TAKASHIMA, S., MATSUURA-YOSHIMOTO, K., MAEDA, H., VAN MEERBEEK, B., SUZUKI, K., TAKASHIBA, S.. 2009. Antibacterial effect of bactericide immobilized in resin matrix. *Dent Mater*. 25:424-30.

Acceptance ID: HJMM-O

Visual Spectral Analysis of Polymer Blend Dispersion in Microcompounder

Won Taek Oh[1], Hee Yeon Jeong[1], Bo Kyung Kim[2], Myung Ho (Kim)[2], Tae-Dong Kim[1,]*

[1]Department of Advanced Materials and Chemical Engineering, Hannam University, Daejeon 305-811, Republic of Korea.
[2]MKE, Daejeon 305-811, Republic of Korea.
Onechoice92@gmail.com / tdkim@hnu.kr

Microcompounders are the most common compounding machines for making polymer composites. The torque rheometry is an effective tool for predicting the processing characteristics of thermoplastic polymers. It provides continuous monitoring of torque and temperature data during compounding which is a measure of processability. In this work, we have studied the influence of processing parameters on the dispersion degree of an anthracene derivative in polystyrene matrix with respect to the rheological, structural, and optical properties and to develop an approach for the rapid analysis of the progress of dispersion. An anthracene derivative, AMA, was synthesized as a tracer. The chemical structure of the synthesized AMA was confirmed by 1H-NMR and thermal properties were examined by DSC. In addition, a blend of polystyrene and AMA was spin-coated on the film, and heat and oxidation stability were confirmed by UV measurement. The film was prepared by mixing PS and AMA through a microcompounder, and the dispersibility was confirmed by SEM and UV measurement. AMA were indicated high thermal and oxidation stability. By using microcompounder, the polymer blend with the AMA tracer was mixed and it was visually indicated by fluorescent images.

Keywords: Microcompounder, Polymer Blend, Tracer, Processability

[1] BOUQUEY, M., LOUX, C., MULLER, R., & BOUCHET, G. 2011. Morphological Study of Two-Phase Polymer Blends During Compounding in a Novel Compounder on the Basis of Elongational Flows. *Journal of Applied Polymer Science*, 119(1), 482-490.

[2] BANERJEE, S., JOSHI, M., & GHOSH, A. K. 2010. A Spectroscopic Approach for Structural Characterization of Polypropylene/Clay Nanocomposite. *Polymer Composites*, 31(12), 2007-2016.

[3] MARIC, M., & MACOSKO, C. W. 2001. Improving Polymer Blend Dispersion in Mini-mixers. *Polymer Engineering & Science*, 41(1), 118-130.

Acceptance ID: HNYJ-P

A Peridynamic Plate Formulation to Couple Delamination and In Plane Failures for Composite Laminates

Ugur YOLUM[1,2], Mehmet Ali GULER[1]

[1]Department of Mechanical Engineering, TOBB University of Economics and Technology, Söğütözü, Ankara 06560, Turkey.
[2]Helicopter Group, Turkish Aerospace Industries (TAI), Kazan, Ankara 06980, Turkey.
Email : mguler@etu.edu.tr/ Tel.: +90-312-292-4088; Fax: +90312-292-4091

Composite materials are commonly used in critical aerospace applications. They exhibit a complex failure behavior that is in general interaction of in plane failures and delamination of layers. In plane failures occur as matrix cracks and fiber breakage. Depending on the type of loading, a complex interaction of different failure modes are observed. Analytical tools are not mature enough to account for that behavior. Thus determination of load carrying capacity of composite structures are primarily based on test data in aerospace industry. Peridynamic theory that is proposed by Dr. Silling is capable of simulating crack growth in both isotropic and orthotropic media [1]. Peridynamic Theory (PD) is a nonlocal version of Classical Continuum Mechanics. In PD, equations of motion is formulated using interactions of material points in a finite horizon. By that aspect, PD resembles to molecular dynamics.

In this study, a PD Orthotropic plate formulation is proposed to capture in plane failure modes of composites. PD estimation of crack propagation in 45^0 oriented 1m x 1m orthotropic plate with a thickness of t=0.05 m under bending loading is illustrated in Fig.1.

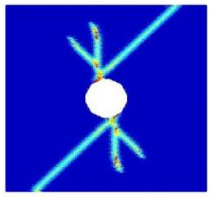

Figure 1 PD Prediction of Crack Propagation in 45^0 ply under bending loading

Interlayer interactions of different plies will be added to plate formulation to consider both in plane and out of plane failures in composite materials. The formulation will be validated with experiments from literature. This research is supported by TÜBİTAK (The Scientific and Technological Research Council of Turkey), under award MAG 115M585.

Keywords: Peridynamic Theory, Bending Failure, Delamination

[1] SILLING, S.A. 2000. Reformulation of elasticity theory for discontinuities and long-range forces. J. Mech. Phys. Solids

Acceptance ID: HVTW-O

Laser-assisted immobilization of nanoparticles on polymer carrier

Jakub (Siegel)[1], *Oleksiy (Lyutakov)*[1], *Tomáš (Hubáček)*[2], *Václav (Švorčík)*[1]

[1]*University of Chemistry and Technology Prague, Technicka 5, 166 28 Prague, Czech Republic.*
[2]*Biology centre CAS, SoWa National Research Infrastructure, Na Sadkach 7, 370 05 Ceske Budejovice, Czech Republic.*
Jakub.siegel@vscht.cz

Immobilization of nanoobjects on the surface of underlying material belongs to current issues of material science [1]. Such altered materials exhibits completely exceptional properties exploitable in a broad spectrum of industrially important applications ranging from catalysts up to health-care industry. In this work we present unique approach for immobilization of electrochemically synthesized silver nanoparticles on polyethyleneterephthalate (PET) foil which lies in physical incorporation of particles into thin polymer surface layer induced by polarized excimer laser light. Changes in chemical composition and surface structure of polymer after particle immobilization were recorded by wide range of analytical techniques such as ARXPS, EDX, RBS, AAS, Raman, ICP-MS, DLS, UV-Vis, SEM, TEM, and AFM. Thorough analysis of both nanoparticles entering the immobilization step as well as modified PET surface allowed revealing the mechanism of immobilization process itself. Silver nanoparticles were physically embedded into a thin surface layer of polymer reaching several nanometers beneath the surface rather than chemically bonded to PET macromolecules. Laser-implanted nanoparticles open up new possibilities especially in the development of the next generation cell-conform antimicrobial coatings of polymeric materials, namely due to the considerable immobilization strength which is strong enough to prevent particle release into the surrounding environment.

Keywords: Silver nanoparticles; Polyethyleneterephthalate; Excimer laser; Immobilization

[1] SLEPICKA, P., KASALKOVA, N. S., SIEGEL, J., KOLSKA, Z., BACAKOVA, L. & SVORCIK, V. 2015. Nano-structured and functionalized surfaces for cytocompatibility improvement and bactericidal action. *Biotechnology Advances*, 33, 1120-1129.

Acceptance ID: HVTZ-O

EGF-loaded Hyaluronic acid based microparticles as effective carriers in wound model

Sun-Woong Kang[1, 2†], Jong-Jin Choi[3†], Ha-Na Kim[3], Joseph Seo[3], Soon-Jung Park[3], Hyung-Min Chung[3], Kang Moo Huh[4], Ho Yun Chung[5,], Sung-Hwan Moon[3,*]*

[1]*Next-generation Pharmaceutical Research Center, Korea Institute of Toxicology, Daejeon, Republic of Korea.*
[2]*Department of Human and Environmental Toxicology, University of Science and Technology, Daejeon, Republic of Korea*
[3]*Department of Stem Cell Biology, Konkuk University School of medicine, Seoul, Republic of Korea*
[4]*Department of Polymer Science and Engineering, Chungnam National University, Daejeon, Republic of Korea;*
[5]*Kyungpook National University School of Medicine, Daegu, Republic of Korea*
[†,*]*These authors contributed equally to this work as first and corresponding authors, respectively.*

Epidermal growth factor (EGF) is widely recognized to be involved in the regenerative process, but only a few studies document its effect on acute wounds when EGF release is sustained over a period of time by encapsulation in an emulsion based hydrogel. Among hydrogels, hyaluronic acid (HA) is a promising carrier because it is biodegradable and known to bind to the components of the ECM which undergoes remodeling during regeneration. Coupled with EGF in micro-particulates, it may serve to directly deliver the cytokine to the impaired ECM to stimulate cells for ECM remodeling. In this study, we demonstrate a very simple and effective way to produce EGF conjugated HA microspheres for the purpose of targeted and sustained EGF delivery to damaged ECM in acute wounds. This approach is advantageous due to its simplicity which may serve to accelerate research in wound regeneration and relevant drug discovery.

This research was supported by a grant (HI14C-3309) of the Korea Health Technology R&D Project through the Korea Health Industry Development Institute (KHIDI) and from a National Research Foundation of Korea (NRF) grant funded by the Korean government (MSIP No. 2016M3A9B4919616).

Keywords: Hyaluronic acid, wound healing, Epidermal growth factor, microparticle, delivery system

Acceptance ID: J3HY-P

Nanocarriers for corrosion control in reinforced concrete

D. A. Koleva

Delft University of Technology, Faculty of CiTG, Department Materials & Environment;

Stevinweg 1, 2628 CN, Delft, The Netherlands

Corrosion of steel reinforcement and subsequent degradation of reinforced concrete structures, subjected to aggressive environment, represents a major concern in relation to infrastructure durability. In this regard, there is an increasing need of improving civil structures performance by using new materials with specifically tailored properties, establishing optimum regimes of construction and maintenance and ideally, making use of possible self-repair or self-healing in these structures in the event of detrimental influence and/or internal damage.

Gaining control or altering materials' behaviour at the nano-level results in traditional materials with radically enhanced properties. Nevertheless, nano-technology applications are still rare in construction, which would otherwise break new ground in the engineering practice. A recent approach to control corrosion-related ageing of materials and structures was based on the synergetic action of electrochemistry, cement chemistry and nano-technology. The approach proved to be realistic, resulting in encouraging and unforeseen possibilities. The application of polymeric nano-materials to simultaneously control electrochemical phenomena at the steel surface and pore network development of the bulk cement-based matrix was studied. Among other formations, specific nanocarriers i.e. polymeric micelles and vesicles, were employed. This contribution presents the main concept of employing polymeric nanocarriers for reinforced concrete structures and briefly reviews some main outcomes of this research.

KEYWORDS: micelles; vesicles; corrosion ; concrete ; self-healing

Acceptance ID: J9A3-O

Removal of organochlorine pesticides using green synthesized magnetic mesoporous silica nanocomposite

Waleed Ahmed El-Said, Dina M. Fouad, Mohamed H. Ali, Mohamed A. El- Gahami*

Department of Chemistry, Faculty of Science, Assiut University, Assiut, 71516, Egypt
Email: dinafouad93@hotmail.com

Green synthesis of nanomaterials has received increasing attention as an eco-friendly technology in materials science. Here, we have used two types of extractions from green tea leaf (i.e. total extraction and tannin extraction) as reducing agents for a rapid, simple and one step synthesis method of mesoporous silica nanoparticles (MSNPs)/iron oxide (Fe_3O_4) nanocomposite based on deposition of Fe_3O_4 onto MSNPs. MSNPs/Fe_3O_4 nanocomposite were characterized by X-ray diffraction, Fourier transform infrared spectroscopy, scanning electron microscopy, energy dispersive X-ray, vibrating sample magnetometer, N_2 adsorption, and high-resolution transmission electron microscopy. The average mesoporous silica particle diameter was found to be around 30 nm with high surface area (818 m^2/gm). MSNPs/Fe_3O_4 nanocomposite was used for removing lindane pesticide (an environmental hazard material) from aqueous solutions. FTIR, UV-vis, High-performance liquid chromatography and gas chromatography techniques were used to confirm the high ability of MSNPs/Fe_3O_4 nanocomposite for sensing and capture of lindane molecules with high sorption capacity (more than 89%) that could develop a new eco-friendly strategy for detection and removing of pesticide and as a promising material for water treatment application.

Keywords: Green synthesis; mesoporous silica; magnetic iron oxide NPs; Lindane

[1] Bretcanu, O., Verne, E., Coisson, M., Tiberto P., Allia, P., 2006, Magnetic properties of the ferrimagnetic glass-ceramics for hyperthermia. *Journal of Magnetism and Magnetic Materials*. ;305:529–533.

[2] Johannsen, M., Gneveckow, U., Taymoorian, K., Thiesen, B., Waldofner, N., Scholz, R., Jung, K., Jordan, A., Wust, P., Loening, S.A., 2007, orbidity and quality of life during thermotherapy using magnetic nanoparticles in locally recurrent prostate cancer: results of a prospective phase I trial. Int J Hyperthermia., 23, 315-23.

[3] Akhtar, N., El-Safty, S.A., Khairy, Md., El-Said, W.A., Akhtar, N., El-Safty, S.A., Khairy, Md., El-Said, W.A., 2015. Fabrication of a highly selective nonenzymatic amperometric sensor for hydrogen peroxide based on nickel foam/cytochrome c modified electrode , *Sensors and Actuators B: Chemical*, , 207, 158-166

[4] El-Said, W.A., Yea, C.-H., Jung, M., Kim, H.-C., Choi, J.-W., 2010, Analysis of effect of nanoporous alumina substrate coated with polypyrrole nanowire on cell morphology based on AFM topography. Ultramicroscopy, 110, 676-681

Acceptance ID: JBDX-I

Mechanical properties and failure characteristics of titanium based bulk metal glass

Tomoki Shigeoka, Mitsuhiro Okayasu

Graduate School of Natural Science and Technology, Okayama University
3-1-1 Tsushimanaka, Kita-ku, Okayama, 700-8530, Japan
E Mail/ Contact Détails (p1fd4z52@s.okayama-u.ac.jp / +81 80 5620 8448)

Mechanical properties of titanium based bulk metal glass (Ti-BMG) are investigated experimentally, in which tensile and fatigue test are carried out. To understand the mechanical characteristics of the Ti-BMG clearly, those properties of three commercial crystalline materials (64-Ti: titanium alloy, A5056: aluminum alloy and S45C: medium carbon steel) are also investigated. The ultimate tensile stress of Ti-BMG is about 1400MPa, which is about 30% higher than that for the crystalline 64-Ti, and more than 200% higher than that for other conventional metals. Due to amorphous structure of Ti-BMG, no clear plastic deformation is detected while severe plastic deformation can be seen for the crystalline metals. In contrast, the fatigue strength of the Ti-BMG drops sharply in the later fatigue stage and the fatigue limit for Ti-BMG is the lower than that for the commercial metals, even though the high tensile strength is obtained for Ti-BMG. Furthermore, to examine the fatigue properties of Ti-BMG in detail, fatigue crack growth properties are investigated together with 64-Ti. The obtained crack growth characteristics are different trend, e.g., the low crack growth resistance is obvious for Ti-BMG compared to that for 64-Ti. Because the roughness of the fatigue fracture surface of 64-Ti is twice as high as that of Ti-BMG (namely different extent of crack closure), the high crack driving force is obtained for Ti-BMG, leading to the high crack propagation speed or the low fatigue strength.

Keywords: titanium based bulk metal glass; fatigue property; crack driving force; crack closure

[1] M. Okayasu, S. Takasu, T. Bitoh, D.H. Shin, M. Makabe, Fatigue and tensile properties of titanium based bulk glassy alloys, Int. J. Mater. Eng. Tech. 5(2011)77-90.

Acceptance ID: JZL2-P

Stretchable Supramolecular Hydrogels with Triple Shape Memory Effect

Xiaoxia Le[1], *Jiawei Zhang*[1], *Tao Chen*[1]

[1]*Division of Polymer and Composite Materials, Ningbo Institute of Material Technology and Engineering, Chinese Academy of Science, Ningbo, P.R. China*
E Mail: lexiaoxia@nimte.ac.cn; *tao.chen@nimte.ac.cn*

Shape memory polymers on the basis of reversible supramolecular interactions have invoked growing research interest, but still suffer from limitations such as poor mechanical strength and finite shape memory performance.[1,2] Here, we present a novel mechanical stretchable supramolecular hydrogel with triple shape memory effect at macro/micro scale. The introduction of double network concept into supramolecular shape memory hydrogels endows them with excellent mechanical properties. Design of two non-interfering supramolecular interaction systems of both dynamic phenylboronic (PBA)-diol ester bonds and the chelation of alginate with Ca2+ endue the hydrogel with outstanding triple shape memory functionality, as shown in Figure1.[3]

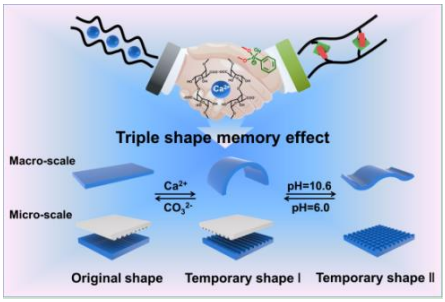

Figure1 the scheme of triple shape memory effect

Keywords: Supramolecular hydrogel, triple shape memory effect, good mechanical properties

[1] MENG, H., XIAO, P., GU, J. C., WEN, X. F., XU, J., ZHAO, C. Z., ZHANG, J. W. & CHEN, T. 2014. Self-healable Macro-/microscopic Shape Memory Hydrogels Based on Supramolecular Interaction. *Chem. Commun*. 50, 12277-12280

[2] MENG, H., ZHENG, J., WEN, X. F., CAI, Z. Q., ZHANG, J. W. & CHEN, T. 2015. pH- and Sugar-induced Shape Memory Hydrogel Based on Reversible Phenylboronic Acid-diol Ester Bonds. *Macromol. Rapid Commun*. 36, 533-537

[3] LE, X., LU, W., ZHENG, J., TONG, D. Y., ZHAO, N., MA, C. X., XIAO, H., ZHANG, J. W., HUANG, Y. J., CHEN, T. 2016, Stretchable Supramolecular Hydrogels with Triple Shape Memory Effect. *Chem. Sci.* 7, 6715-7-6720

Acceptance ID: K7NG-P

Redox-Tunable Cationic Materials for Environmental Applications

Ali Trabolsi

New York University Abu Dhabi (NYUAD)

Immobilizing molecular switches within materials can give rise to new bulk properties that are useful for a variety of applications. Here, we report the preparation of amorphous and crystalline viologen-based extended networks with controlled morphology. The viologens allow access to three distinct redox states: dicationic, radical-cationic and neutral. With viologens in their dicationic state, the particles were used for inkless printing, gaseous amine sensing, and efficient oxoanion capture. With viologens in any oxidation state, the materials were capable of (200-400 wt %) vapor iodine capture. Iodine capture within these newly developed systems was fast, requiring minutes, compared to capture by previously reported materials that typically takes hours. With viologens in their neutral state, the polymers exhibited the highest iodine loadings reported to date. Upon one and two-electron reduction, the polymers lose partially or completely their cationic character and therefore their anion removal capability.

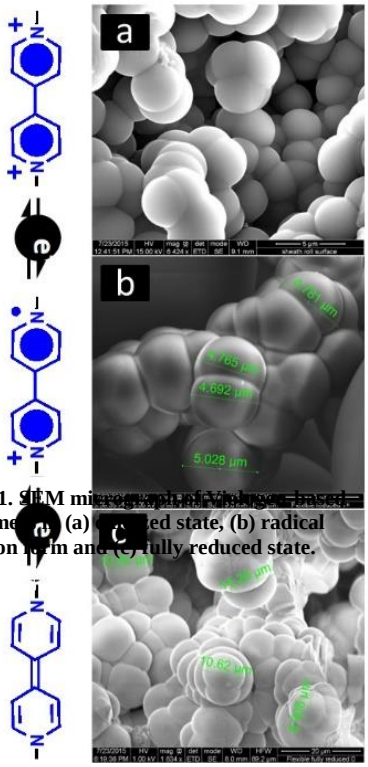

Figure 1. SEM micrograph of Viologen-based polymer (a) oxidized state, (b) radical cation form and (c) fully reduced state.

1. ***Radical-Cation Dimerization Overwhelms Inclusion in [n]Pseudorotaxanes***
K. Nchimi Nono, P. Dalvand, K. Wadhwa, S. Nuryyeva, S. Alneyadi, T. Prakasam, A. C. Fahrenbach, J.-C. Olsen, Z. Asfari, C. Platas-Iglesias, M. Elhabiri, A. Trabolsi, *Chem. Eur. J.*, **2014**, *20*, 7334-7344.

2. ***Intramolecular Redox-Induced Dimerization in a Viologen Dendrimer*** K. Wadhwa, S. Nuryyeva, A. C. Fahrenbach, M. Elhabiri, C. P.-Iglesias, A. Trabolsi, *Journal of Materials Chemistry C* **2013**, *1*, 2302–2307.

Acceptance ID: K9Q8-O

A DFT Investigation of Conjugated Polymers/Oligomers and Fullerenes Interactions in Bulk Heterojunction Organic Solar Cells

Sarah A. (Ayoub)[1,2], *Jolanta B. (Lagowski)*[1]

[1] *Department of Physics and Physical Oceanography, Memorial University, St. John's, NL A1B 3X7, Canada.*
[2] *Department of Physics, King Abdulaziz University, Jeddah 21589, Kingdom of Saudi Arabia.*
s.ayoub@mun.ca , jolantal@mun.ca

The performance of bulk heterojunction organic solar cells made of conjugated polymers/oligomers and fullerenes has significantly improved in the last few years (with PCE exceeding 10%).[1] Experiments suggest that the intermolecular interactions between polymers and fullerenes are critical to the design of (even) more efficient organic photovoltaic cells.[2] However, a detailed understanding of these intermolecular interactions is still lacking. In this work, we employ dispersion corrected density functional theory (DFT) methods, wB97xD, B3LYP-D3, B97D3, and PBE1PBE-D3, to investigate the properties of these heterogenous interactions in various promising oligomer/fullerene combinations (e.g. a pair of PC71BM and a copolymer based on thieno[3,4-b]thiophene/benzodithiophene (PTB7)[3], PCBM and a copolymer based on 2,7-carbazole/dithienyl-2,1,3-benzothiazole (PCDTBT)[4], and PC71BM and a copolymer based on difluorobenzothiadizole/quaterthiophene (PffBT4T-2OD)[1]). In particular, we determine and analyze the conformational and electronic structures, and binding energies of these combinations. We obtain the most preferred orientations of oligomers with respect to fullerenes and analyze the connection between their electronic structures and device performances. Using binding energies, we assess the strength and stability of the oligomer/fullerene intermolecular interactions. Finally, we investigate the effect of (linear and branched) side-chains of oligomers on the binding energies of these combinations.

Keywords: Polymer/Fullerene Interactions, Organic Solar Cells, DFT

[1] LIU, Y., ZHAO J., LI, Z., *et al.* 2014. *Nature Communications.*
[2] HUANG, Y., KRAMER, E., HEEGER, E., *et al*. 2014. *Chemical Reviews.*
[3] HE, Z., ZHONG, C., SU, S., *et al*. 2012. *Nature Photonics*.
[4] BEAUPR´E, S. & LECLERC, M. 2013. *Journals of Materials Chemistry*.

Acceptance ID: KCF4-O

Enhanced Dielectric and Energy Storage Performance of Polymer-based Composites Containing Inorganic 3D-network

Suibin Luo,[a] Yanbin Shen[a], Shuhui Yu,[a] , Yanjun Wan [a,b], Wei-Hsin Liao[b], Rong Sun,[a] Jianbin Xu[c], and Ching-Ping Wong[ac]*

a. Center for Advanced Materials, Shenzhen Institutes of Advanced Technology, Chinese Academy of Sciences, Shenzhen, China, 518055.
b. Department of Mechanical and Automation Engineering, The Chinese University of Hong Kong, Hong Kong, China.
c. Department of Electronics Engineering, The Chinese University of Hong Kong, Hong Kong, China.

Flexible nanocomposites with high permittivity (ε_r), low loss and high voltage breakdown strength are highly desired in microelectronics, medical instruments, and hybrid electric vehicles etc. Miniaturization of the electrical and electronic systems calls for materials with improved permittivity and energy storage density. The conventional polymer-based composites containing dispersed ceramic particles suffer from low permittivity (mostly <50) even with a high filler loading (>50vol%). In this study, by constructing a 3D-network of high-ε_r ceramic fillers in the polyvinylidene fluoride (PVDF)-epoxy matrix, composites with an ultra-high permittivity of over 200 and a low loss of less than 0.1 were obtained with the inorganic filler loading of only 30vol%. The energy storage density was enhanced by more 5 times larger in comparison with the polymer matrix. $BaTiO_3$ (BT), $SrTiO_3$ (ST) and BT-ST 3D-network were constructed and the properties of their corresponding composites including dielectric performance, energy storage density and discharge-charge efficiency were compared and analyzed.

Acceptance ID: KP6Q-O

Processing and characterization of LaFeSi compounds synthesized by ball-milling technique

H. Takama, M. Muralidhar and M. Murakami

Shibaura Institute of Technology, Graduate School of Science and Engineering, 3-7-5 Toyosu, Koto-ku, Tokyo 135-8548, JAPAN

Advanced magnetic refrigerants like $La(Fe,Si)_{13}$ require large entropy and adiabatic temperature changes connected with the phase change and hysteresis. In order to advance their incorporation in prototypes and industrial applications, low cost, high performance, single phase materials are needed. In this work, $LaFe_{11.5}Si_{1.5}$ starting powders were mixed and ball milled for 2 hours and sintered at the temperatures 900 ºC, 1150 ºC, and 1250 ºC for 0.5 h. Eventually, the sintered pellets were crashed and milled in a planetary ball mill for 0.5 hour and sintered at 1150 ºC and 1250 ºC for 1 h, 2 h, and 5 h to find optimum processing conditions for the single phase material production. X-ray diffraction analysis confirmed that almost single phase 1:13 was obtained by annealing at 1150 ºC for 0.5 h and with the ball milling time 1 h. The study of the micro-structural observation by optical and scanning electron microscopy showed a uniform microstructure of these samples. SEM by EDX analysis of this material showed a uniform chemical composition in various locations on the pellet surface. These results implied that a proper sintering temperature combined with ball milling are crucial for obtaining the single 1:13 phase of $La(FeSi)_{13}$ material by a simple scalable solid state sintering method.

Acceptance ID: KWDF-P

Carbon Felt Electrodes Electric and Hydraulic Properties under Different Compression Conditions Studied Experimentally

A.Krasnopolski, A.Kosenko, S.Lugovskoy, M.Averbukh

Ariel University, Israel

Carbon felt is a widespread material for electrodes in redox flow batteries, fuel cells etc. Its regnant use is determined by the numerous affirmative properties such as sufficient electrical conductivity, hydraulically permeable structure and significant superficial surface as well as the ability to endure strong acids and alkali solutions comprising the most of well-known batteries electrolytes. Bonded together relatively long carbon filaments compose its internal framework, which represents a cluster of narrow twisting channels with significantly varying cross-section. Therefore, hydraulic permeability of a felt is similar to that of a porous media and is determined by a ratio of internal empty volume regarding entire volume as well as by the arrangement of carbon fibers. Felt electro-conductivity is ensured by the concentration of carbon filaments though mostly by the density of electrical interconnections between fibers. Both of these properties are extremely important for the efficient activities of electrochemical appliances where carbon felt comprises electrodes. However aiming to improve electrode conductivity and electrical contact between felt to substrate of electrodes a designer has to squeeze carbon felt to some extent. Unfortunately, felt squeezing immediately decreases hydraulic permeability of electrodes owing to diminishing empty volume and cross-sections of intrinsic channels. Therefore, both of these properties are contradicting one to another under compression.

Designer of a specific electrochemical system has to take into account this circumstance for providing optimal development of electrochemical cell. The task is complicated by the fact that both of these characteristics depend on physical parameters of electrolyte such as its density and electrical permittivity. The last as it seems can influence the density of interconnections between carbon filaments. Consequently, electrical and hydraulic parameters of carbon felt need to be tested in different environmental conditions.

Presented article provides the results of measurements of carbon felt electrical conductivity like a dry and immersed in several non-conductive liquids having various electrical permittivity. Hydraulic permeability was evaluated by the water flow having a given temperature through carbon felt and induced by different pressure. It is enough since this parameter for other liquids and other conditions could be recalculated using well-known relations.

Keywords: Carbon felt, electrical conductivity, hydrodynamic permeability.

Acceptance ID: LJQS-O

Core/double-shell-structured hyperbranched aromatic polyamide functionalized graphene nanosheets-poly(*p*-phenylene benzobisoxazole) nanocomposite films with improved dielectric properties and thermostability

*Feng, Hua, Zhang, Liu, Zhuang**

The Key Laboratory of Advanced Polymer Materials of Shanghai, School of Materials Science and Engineering, East China University of Science and Technology, Shanghai, China, 200237
E-mail: harryfeng@mail.ecust.edu.cn (presenting author)
qxzhuang@ecust.edu.cn (corresponding author)

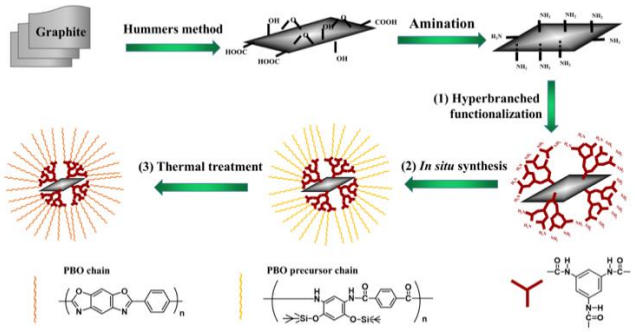

Fig. 1 The fabrication of core-double-shell structured GNs-HAP-PBO nanocomposites

Keywords: PBO, graphene, dielectric constant, energy density, nanocomposites

[1] CHEN, Y., LIU, X., MAO, X., ZHUANG, Q., XIE, Z. & HAN, Z. 2014. gamma-Fe2O3-MWNT /poly(p-phenylenebenzobisoxazole) composites with excellent microwave absorption performance and thermal stability. *Nanoscale,* 6**,** 6440-7.

[2] CHEN, Y., ZHANG, S., LIU, X., PEI, Q., QIAN, J., ZHUANG, Q. & HAN, Z. 2015. Preparation of Solution-Processable Reduced Graphene Oxide/Polybenzoxazole Nanocomposites with Improved Dielectric Properties. *Macromolecules,* 48**,** 365-372.

[3] CHEN, Y., ZHUANG, Q., LIU, X., LIU, J., LIN, S. & HAN, Z. 2013. Preparation of thermostable PBO/graphene nanocomposites with high dielectric constant. *Nanotechnology,* 24**,** 245702.

[4] ZHUANG, Q., LIU, X., WANG, Q., LIU, X., ZHOU, J. & HAN, Z. 2012. Synthesis of acid-soluble graphene and its use in producing a reduced graphene oxide–poly(benzobisoxazole) composite. *Journal of Materials Chemistry,* 22**,** 12381.

Acceptance ID: LWZY-O

Adhesive Contact and Instability of a Pre-deformed Soft Electroactive Half-space

G. Z. Xia[1], *W. Q. Chen*[1, 2, 3, 4]

[1]*Department of Engineering Mechanics, Zhejiang University, Hangzhou 310027, China*
[2]*Soft Matter Research Center, Zhejiang University, Hangzhou 310027, China*
[3]*Key Laboratory of Soft Machines and Smart Devices of Zhejiang Province, Zhejiang University, Hangzhou310027, P. R. China*
[4]*State Key Laboratory of Fluid Power and Mechatronic Systems, Zhejiang University, Hangzhou 310027, P.R. China*
E-mail: guozhan_xia@zju.edu.cn

Soft electroactive materials are one of the most representative soft matter, becoming increasingly important in advanced electronic devices, such as artificial muscle and flexible wearable sensing suit [1-2]. However, due to the inherent electromechanical coupling and nonlinear large deformation, it's not easy to theoretically predict its responses in practical applications and accurately characterizing their properties in scientific experiments.

On the other hand, the breakthrough in piezoresponse force microscopy (PFM) and other electromechanical scanning probe microscopes (SPMs) [3] may enlighten us a robuster way to obtain the properties of soft electroactive materials. Accordingly, the pressing demand of efficient theoretical models catering for such new indentation techniques must be prudently considered where, in contrast to hard materials, the adhesive effect is quite indispensable at nano-scale. [4]

In this report, we focus on the adhesive contact between a pre-deformed compressible soft electroactive half-space and a rigid axisymmetric indenter. Unlike the published work [5], the adhesion in the contact is considered by using a modified JKR model [6, 7]. With the help of new results of potential theory method in piezoelectricity [8], all physical quantities are expressed in terms of elementary functions, especially for three common types of indenter (flat-ended circular, conical, and spherical). Moreover, instability of an electroactive half-space subject to large deformation is also investigated carefully under diverse electrical boundary conditions, which is necessary to explain the critical phenomenon observed in the contact load-depth relations.

For illustration, numerical results are presented for a compressible electroelastic neo-Hookean model. The present theoretical analysis is first verified by comparing with facile FEM simulations. Second, for the instability of the half-space, a tiny difference in the curve of critical stretch is observed between the electrically conducting boundary conditions and the insulating ones. Third, some results for spherical and conical indentations are given and discussed, which incidentally indicates significant influence of adhesion on the contact at nano-scale.

Keywords: Soft electroactive material, indentation, adhesive effect, buckling instability

[1] TSE, T. C. H., O'BRIEN, B., MCKAY, T. & ANDERSON, I. A. 2011. A Validated Finite Element Model of a Soft Artificial Muscle Motor. *Proc. SPIE*, 7976, 79761Q-79761Q-9.

[2] MENGÜÇ, Y., PARK, Y. L., PEI, H., et al. 2014. Wearable Soft Sensing Suit for Human Gait Measurement. *Int. J. Rob. Res.*, 33(14), 1748-1764.

[3] KARAPETIAN, E., KACHANOV, M. & KALININ, S. V. 2005. Nanoelectromechanics of Piezoelectric Indentation and Applications to Scanning Probe Microscopies of Ferroelectric Materials. *Phil. Mag*., 85(10), 1017-1051.

[4] EBENSTEIN, D. M. & PRUITT, L. A. 2006. Nanoindentation of Biological Materials. *Nano Today*, 1(3), 26-33.

[5] ZHANG, W. L, QIAN, J. & CHEN, W. Q. 2012. Indentation of a Compressible Soft Electroactive Half-space: Some Theoretical Aspects. *Acta Mech. Sin.*, 28(4), 1133-1142.

[6] MAUGIS, D. 2013. *Contact, Adhesion and Rupture of Elastic Solids.* Springer Science & Business Media.

[7] LU, P., FOO, Y. L., SHEN, L., et al. 2011. A General Relation for Contact Stiffness Including Adhesion in Indentation Analysis.

J. Mate. Res., 26(11), 1406-1413.

[8] CHEN, W. Q. 2009. Adhesive Contact between a Rigid Punch and a Piezoelectric Half-space. In: Yang W., Feng, X. Q., & Qin Q. H. (eds.). *Advances in Damage, Fracture and Nanomechanics*. Tsinghua University Press. 58-65. (In Chinese)

Acceptance ID: m2s6-O

A functional buffer with traveling wave dielectroporesis to overturn specimen

Po-Jen Shih[1], *Shih-Wei Wang*[1]

[1]*National University of Kaohsiung, 700, Kaohsiung University Rd., Nanzih District, Kaohsiung, Taiwan*
pjshih@nuk.edu.tw/ 886-7-5916592

Specimen preparation is one of the most important processes; and to achieve reliable measurements, the specimen is needed to fixed on a substrate and to satisfy the placed requirement through applying a polycationic adhesive coating on the substrate. Thus one side of the specimen could be observed, but the adhered side facing the substrate cannot be measured, especially when the scanning probe microscope is applied to measure elevation contour. We develop a three-dimensional device containing a functional buffer (or liquid) which can take on the specimens and trap single particle (or cell). The functional buffer is triggered by the traveling wave dielectrophoresis, and thus one single particle is trapped in the dielectrophoretic force filed with slowly rotation. The dielectophoretic fore filed is constructed by five electrodes within hundreds of microns, and it includes the conventional dielectrophoretic force and the traveling-waved dielectrophoretic force. This total dielectrophoretic force could apply a force and a torque to the target subject without contacting the subject directly. Thus the particle can translate or rotation with certain paths in three-dimensional space when we applying functional commands. Thus the adhered side of the particle could be rotated and measured. Numerical simulation contained the finite element method analysis is presented to predicted the particle translating and rotating paths, and the experimental tests of the functional buffer of the device also demonstrate the specimen's translation and rotation in certain paths.

Keywords: Travelign wave dielectrophoresis, rotation, translation

[1] HUGHES, M. P., 1994. Computer-aided analyses of electric fields used in electrorotaton studies. *J. Phys. D: Appl. Phys.*, 27, 1564-1570.

[2] HUGHES, M. P. and MORGAN, H. 1998. Dielectrophoretic trapping of single sub-micrometre scale bioparticles. *J. Phys. D: Appl. Phys.* 31, 2205-2210.

Acceptance ID: M2WJ-P

Multiparticle Scattering Effects and Relaxation Pathways in Semiconducting Carbon Nanotubes and Graphene

Leonas Valkunas,

Department of Theoretical Physics, Vilnius University, Vilnius, Lithuania;
Department of Molecular Compounds Physics, Center for Physical Sciences and Technology, Vilnius, Lithuania

Keywords: Single-walled and double-walled carbon nanotubes, one-color and two-color transient absorption, theoretical simulations of excitation kinetics

We present a thorough analysis of one- and two-color transient absorption measurements performed on single- and double-walled semiconducting carbon nanotubes [1, 2]. By combining the currently existing models describing exciton–exciton annihilation—the coherent and the diffusion-limited ones—we are able to simultaneously reproduce excitation kinetics following both E11 and E22 pump conditions. Our simulations revealed the fundamental photophysical behavior of one-dimensional coherent excitons and non-trivial excitation relaxation pathways. In particular, we found that after non-linear annihilation a doubly-excited exciton relaxes directly to its E11 state bypassing the intermediate E22 manifold, so that after excitation resonant with the E11 transition, the E22 state remains unpopulated. A quantitative explanation for the observed much faster excitation kinetics probed at E22 manifold, comparing to those probed at the E11 band, is also provided. Effects caused by multiparticle scattering on the linear and nonlinear spectral properties of graphene are also theoretically discussed.

[1]. M. W. Graham, J. Chmeliov, Y.-Z. Ma, H. Shinohara, A. A. Green, M. C. Hersam, L. Valkunas and G. R. Fleming, *J. Phys. Chem. B*, **2011**, 115, 5201–5211.
[2]. J. Chmeliov, J. Narkeliunas, M. W. Graham, G. R. Fleming, L. Valkunas, *Nanoscale* **2016**, 8, 1618-1626.

Acceptance ID: MBFT-O

The giant magnetoelectric effect in the YIG/Terfenol-D/PZT structure

Jingjing Lu, Jing He, Changcheng Ma, Shilin You, Xing Zhang, Jie Zhu, Zuoqi Hu†

School of Optical and Electronic Information, Huazhong University of Science and Technology, Wuhan, 430070, China.
E Mail/lu_2014@hust.edu.cn; hu_zuoqi@hust.edu.cn

A multilayer magnetoelectric (ME) composite with a high ME coefficient is proposed based on YIG/Terfenol-D/PZT structure. The equivalent circuit approach, which is based on the constitutive equations and the motion equations in the piezoelectric and magnetostrictive layers, was used to analyze the ME effect of the ME composite. The ME coefficient of the YIG/Terfenol-D/PZT structure is higher than one of the YIG/PZT structure because of the giant magnetostriction of the Terfenol-D interlayer and the exchange coupling action in the YIG/Terfenol-D bilayers. The exchange coupling action was discussed via calculating the free energy of the YIG/Terfenol-D bilayers on the based of the minimum energy principle, and the magnetization M_s of the YIG layer followed the one of the Terfenol-D layer due to the exchange coupling action. The magnetization M_s of the Terfenol-D layer was changed by the ME effect of the Terfenol-D/PZT layers. Combined the ME effect and the exchange coupling action, the external electric field could change the direction of the YIG magnetization M_s, which influences the ferromagnetic resonance (FMR) of the YIG layer. Therefore the YIG/Terfenol-D/PZT structure can be used to build an electric and magnetic field dual-tunable microstrip filter with a wide electric-adjustable range. Fig. 1 shows that a larger defection angle in the YIG of YIG/Terfenol-D/PZT is changed than the one of YIG/PZT by the electric field on the PZT. For the giant magnetostrictive Terfenol-D layer joins, the ME coefficient of YIG/Terfenol-D/PZT is higher than the one of YIG/PZT.

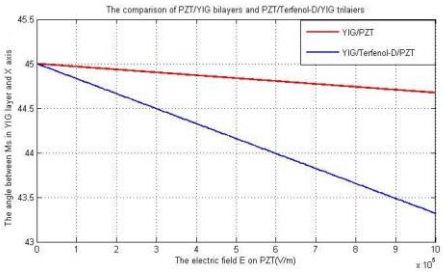

Fig.1 The direction of the YIG magnetization M_s in the YIG/Terfenol-D/PZT and YIG/PZT vs. the external electric field on PZT

Acknowledgments

This work was funded by the National Natural Science Foundation of China (NSFC) No.61271072.

Keywords: magnetoelectric effect, exchange coupling action, equivalent circuit approach

[1]LU, C., LI, P., WEN, Y., YANG, A., HE, W., ZHANG, J., 2013. Investigation of magnetostrictive/piezoelectric multilayer composite with a giant zero-biased magnetoelectric effect. Applied Physics a-Materials Science & Processing. 113(2), 413-21.

[2] FETISOV, Y. K., SRINIVASAN, G., 2006. Electric field tuning characteristics of a ferrite-piezoelectric microwave resonator. Applied Physics Letters. 88, 143503.

[3] PETTIFORD, C., DASGUPTA, S., LOU, J., YOON, S. D., SUN N. X., 2007. Bias field effects on microwave frequency behavior of PZT/YIG magnetoelectric bilayer. IEEE Transactions on Magnetics, 43(7), 3343-5.

Acceptance ID: mcbj-O

Magneto-Optically Active Magnetoplasmonic Graphene

Jaewook Lee and Jaebeom Lee

Two-dimensional nanocomposites with magnetic and optical properties were investigated for novel magneto–optical (MO) applications. Such MO effect could be induced and enhanced by synergic property with magnetic and plasmonic coupling. In this study, magnetoplasmonic graphene (MPGRP) decorated with Au nanoparticles (NPs) and magnetic NPs (MNPs) was simply prepared as 2D MO active material. This MPGRP exhibited superparamagnetic behaviour at room temperature and strong MO activity resulting from magnetic spin from the MNPs and electron spin from the Au NPs on one graphene sheet, which is beneficial for memory or optoelectronic devices, sensing platforms, energy harvesting, and biomedical MO devices.

Acceptance ID: MDX3-P

Electronic and Mechanical Properties of various phases of $MoSe_2$

Sumandeep Kaur[1], Ashok Kumar[2], Sunita Srivastava[1] and Tankeshwar[3]

[1]Department of Physics, Panjab University, Chandigarh-160014, India
[2]Centre for Physical Sciences, Central University of Punjab, Bathinda, 151001, India.
[3]Department of Physics, Guru Jambheshwar University of Science and Technology, Hisar- 125001, Haryana, India.

Corresponding Author E-mail: sunita@pu.ac.in

Using first principle calculations, we have constructed three structurally stable phases of $MoSe_2$ i.e., trigonal prismatic phase (h-$MoSe_2$), octahedral coordinated phase (t-$MoSe_2$) and square octagon phase (so-$MoSe_2$). We have studied the electronic and mechanical properties of these phases. The h-$MoSe_2$ is a semiconductor while the other two are metallic. Also the so-$MoSe_2$ phase depicts a Dirac cone like feature at its Fermi level. In order to check the mechanical strength we have calculated the stress-strain relation for these structures. Also the in-plane stiffness, poisson's ratio and young's modulus have been calculated for these phases as these parameters are the ones the charactrizes the mechanical flexibility of the sheets. For t-$MoSe_2$, we found anisostrpic mechanical strength while for the other two structures it is found to be isotropic. These interesting properties could find important applications in the area of nanoelectronic-device fabrication.

Acceptance ID: MLVQ-O

Fabrication of a Novel 3D Electrospun Nanofibrous Scaffolds via a Convenient Method for Tissue Engineering

Sung Won Ko[1], Serim Jang[1], Joshua Lee[1], Ji Yeon Lee[2], Chan Hee Park[1, 3] and Cheol Sang Kim[1, 3]

[1]Bionanosystem Engineering Department, Chonbuk National University, Jeonju 561-756, Republic of Korea.
[2] Mechanical Design Engineering Department, Chonbuk National University, Jeonju 561-756, Republic of Korea.
[3]Division of Mechanical Design Engineering, Chonbuk National University, Jeonju 561-756, Republic of Korea.
tpfla6020@gmail.com, biochan@jbnu.ac.kr, chskim@jbnu.ac.kr / +82-63-219-5293, +82-63-270-2395, +32-63-270-4284

Recently, many research groups have studied creating three-dimensional (3D) structures by micro and nanoscale fibrous membranes for tissue engineering applications. Conventional electrospun scaffolds have significant problems such as poor cellular infiltration and difficulty in filling three-dimensional volumes. In this study, we fabricated poly caprolactone (PCL)/ Cellulose acetate (CA) composite nanofibers by electrospinning. To improve biocompatibility and water uptake property, samples were prepared with different PCL/CA ratios (100/0, 70/30, 50/50, 30/70) and filled in different molds. The thin PCL/CA nanofibrous membrane becomes a 3D structure by convenient physical treatments, i.e. via orbital shaker and ultra-sonicator. The pore size and nanofiber diameters before and after treatment was compared by scanning electron microscopy (SEM) images. The characterizations of 3D nanofibrous scaffolds were fulfilled by Fourier transform infrared spectroscopy (FT-IR) and thermogravimetric analysis (TGA). To evaluate biocompatibility and infiltration of cells, we seeded fibroblasts (NIH-3T3) on the electrospun nanofibrous membranes by using CCK-8 analysis and confocal laser scanning microscopy. The convenient 3D nanofibrous scaffold fabricated herein can be applied in tissue engineering.

Keywords: Swelling rate, 3D scaffold, nanofiber, highly water absorption.

[1] JOSHI, M. K., PANT, H. R., TIWARI, A. P., MAHARJAN, B., LIAO, N., KIM, H. J., PARK, C. H. & KIM, C. S. 2016. Three-dimensional cellulose sponge: Fabrication, characterization, biomimetic mineralization, and in vitro cell infiltration. *Carbohydrate Polymers,* 136**,** 154-162.

Acceptance ID: MWTN-P

Preparation and characterization of carboxymethyl cellulose based carbon foam obtained via electron beam irradiation

Yong-Sun Kim[a], Hong Gun Kim[a,b], Lee Ku Kwac[a,c], Si Hwan Lee[a], Hye Kyoung Shin[a,]*

[a] *Institute of Carbon Technology, Jeonju University, 303 Cheonjam-ro, Wansan-gu, Jeonju-si, Jeollabuk-do 55069, Republic of Korea,*
[b] *Department of Mechanical & Automotive Engineering, Jeonju University,303 Cheonjam-ro, Wansan-gu, Jeonju-si, Jeollabuk-do 55069, Republic of Korea*
[c] *Department of Manufacturing Technology and Design Engineering, Jeonju University,303 Cheonjam-ro, Wansan-gu, Jeonju-si, Jeollabuk-do 55069, Republic of Korea*

Carbon foams were prepared by facile method without stabilization from CMC composites of biopolymer obtained according to various EBI doses and CA concentration. Gel fraction to study cross-linking degree in CMC increased with the increase of CA concentration and EBI doses between 20 kGy and 80 kGy. Among samples, CMC composite with 4 wt% CA via 80 kGy represents the highest gel fraction value of about 98%, showing the highest carbon yields and compressive strength due to lower break defects after carbonization by the increase of cross-linked parts in carbon foam obtained from CMC composites with 4 wt% CA via 80 kGy. In addition, BET analysis for carbon foam obtained from CMC composite with 4 wt% via 80 kGy was also observed the highest specific surface area of 372.06 m^2/g and adsorption pore size of 2.20 nm by interaction of the more gas with further carbon atoms.

[*] *Author to whom correspondence should be addressed.*
Fax: +82 63220 3161.
E-mail address: jokwanwoo@jj.ac.kr (H.K. Shin)

Acceptance ID: MWWF-P

Surface modification effects on the magnetic and optical properties of ZnCoO/2D hybrids

*Yifan Xu[1], Jun Qian[1], Jiang Sun[1], Peng Wang[1], Wenzhe Wang[1], Xinzhi Shi[2], Chang Qi[2], Shuangli Ye[1,2]**

[1]School of Printing and Packaging, Wuhan University, Wuhan 430072, China
[2] Institute of Microelectronics and Information Technology, Wuhan University, Wuhan 430072, China
E-Mail:slye@whu.edu.cn (corresponding author's)
E-Mail:xuyifan8@whu.edu.cn ***(prensenting author's)***

The ZnCoO/2D (graphene, B-doped graphene and MoS2) hybrids have been synthesized successfully by a facile chemical process, respectively. The structure, morphology, and chemical composition of the as-prepared hybrids are characterized by HRTEM, XRD, XPS and Raman techniques. It can be found that these hybrids consist of wurtzite ZnCoO and 2D materials without the impurity phase. The ZnCoO/graphene and ZnCoO/B-doped graphene hybrids show quasi-core-shell structure [1]. The p-n junction is formed in ZnCoO/B-doped graphene hybrid. These hybrids display diverse magnetic and optical properties due to the different surface modifications by the 2D materials. Antiferromagnetic, paramagnetic and superparamagnetic properties can be found in these hybrids. Particularly, a significantly enhanced photoluminescence (PL) phenomenon is observed in the ZnCoO/MoS_2 hybrid at room temperature. The temperature-dependent PL experiments verify that the origin of this emission band can be attributed to the intra-center optical transitions of the Co^{2+} ions in ZnCoO core. The diverse magnetic properties and the enhanced PL phenomenon suggest the existence of the significant interplay between the ZnCoO and the 2D materials[2]. These tunable optical and magnetic properties have a promising application in multi-functional ZnCoO–based semiconductor and spintronic devices.

Keywords: Surface modification, ZnCoO, 2-dimensional (2D) material, magnetic property, photoluminescence

[1] XIANG, Z., QIAN, J., ZHOU, Y., LIU, F., QI, C., SHI, X., ... & YE, S. (2015). Synthesis of quasi-core–shell Co-doped ZnO/graphene nanoparticles.*Materials Letters, 161, 286-288.*
[2]MOURI,S.,MIYAUCHI,Y., & MATSUDA, K. (2013). Tunable photoluminescence of monolayer MoS_2 via chemical doping. *Nano letters, 13(12), 5944-5948.*

Acceptance ID: NQKH-O

Hierarchical Self-assembly of Highly Active and Stable Materials

Xiao-Yu Yang, Jie Ying, Yu-Xuan Xiao, Hao Wei*
State Key Laboratory of Advanced Technology for Material Synthesis and Processing,
Wuhan University of Technology, Wuhan, China
Email: xyyang@whut.edu.cn

Herein, we present our recent work on design of a series of self-assembled hierarchical nanomaterials at micro/nano scale, which their activity and stability can be greatly enhanced. Firstly, hierarchical micro-meso-macroporous materials with zeolite architectures have been designed and synthesized by using self-assembly method [1, 2]. These materials exhibit high activity and high stability in catalysis, which can be attributed to the unique and stable hierarchically porous structure.

References

[1] X.Y. Yang, Y. Li, G. Van Tendeloo, F. Xiao and B.L.Su, "One-pot synthesis of catalytically stable and active nanoreactors: encapsulation of size-controlled nanoparticles within a hierarchically macroporous core@ordered mesoporous shell system," Adv. Mater., vol. 21, pp. 1368–1372, 2009.

[2] L.H. Chen, X.Y. Li, G. Tian, Y. Li, J.C. Rooke, G.S. Zhu, S.L. Qiu, X.Y. Yang and B.L.Su, "Highly stable and reusable multimodal zeolite TS-1 based catalysts with hierarchically interconnected three-level micro–meso–macroporous structure," Angew. Chem. Int. Ed., vol. 50, pp. 11156–11161, 2011.

Acceptance ID: NSVZ-O

Three-dimensional graphene networks grown by chemical vapor deposition

Li Zheng[1,2], Xinhong Cheng [1,], Yahong Xie[3,*], Peiyi Ye[3], Qian Wang[1,2], Dongliang Zhang[1,2], Ziyue Gu[1,2], Qingchang Li[1,2], Hongyue Zhu[1,2], Ru qian[1,2] and Yuehui Yu[1]*

[1] State Key Laboratory of Functional Materials for Informatics, SIMIT, Chinese Academy of Sciences, Changning Road 865, Shanghai 200050, P. R. China
[2] University of Chinese Academy of Sciences, Beijing 100049, P. R. China
[3] Department of Materials Science and Engineering, UCLA, Los Angeles, 90095, USA
Presenting author: zhengli@mail.sim.ac.cn
Corresponding author: xh_cheng@mail.sim.ac.cn; yahong.xie@gmail.com

Graphene, an atomic monolayer composed of the honeycomb structure with sp^2 hybrid has attracted increasing attention. The unique two-dimensional (2D) structure and excellent chemical and physical properties of graphene have made it a promising candidate for a broad range of application in many fields. However, the irreversible agglomeration or restacking of graphene sheets severely suppress its intrinsically high conductivity, reduce its mechanical strength and diminish its accessible surface area. One effective method to tackle this challenge is to engineer a graphene material in which individual graphene sheets are bonded together to construct three-dimensional (3D) networks. On the other hand, the applications of graphene-based materials in energy, environment, sensing and biology also require assembly of 2D graphene into 3D architectures to achieve high specific surface areas, strong mechanical strengths and fast mass and electron transport kinetics. Owing to the ease of preparation and processing, chemical exfoliation of graphite oxide has been used for integration of 3D macroporous structure of graphene. However, the chemically derived graphene shows poor electrical conductivity owing to severe defects in graphene sheets introduced during exfoliation and reduction processes. Recently, chemical vapor deposition (CVD) has been performed to grow large-area and high-quality 3D graphene networks using methane as the carbon source. However, the decomposition temperature of methane is generally 1000℃ even with catalysis of metal substrates. Such a high temperature may damage metal structure when its dimension is down to micron level due to drastic atomic diffusion. In this work, we use camphor to grow 3D graphene macroscopic structure on nickel foam by template-directed CVD. Usually, PMMA is required to prevent graphene from collapsing during the metal templates etching process. The residue of PMMA will contaminate graphene and there is so far no way to completely remove PMMA on graphene without damage its structure. For our grown 3D graphene, no PMMA is required to act as the support layer during nickel etching. Except the partial slight cracks of outmost graphene, other graphene inherits the continuous and interconnected 3D scaffold structure of nickel foam. All the graphene sheets in the 3D macroscopic structure are in direct contact with one another and well separated, indicating high quality of 3D graphene networks.

Acceptance ID: NZMU-O

Transparent nanofiber composites for organic electronics

Hak Yong Kim and Su Hyeong Chae

Department of BIN Convergence Technology
Chonbuk National University, Jeonju 561-756, South Korea

Transparent nanofiber composites were successfully synthesized by easy electrospinning technique. The keratin was extracted from discarded wool hair by the sulphitolysis process and the glyoxal solution was used as a cross-linking agent. Discarded wool hair based keratin/poly(vinyl alcohol) blended nanofibers (WH/PVA NFs) were fabricated via electrospinning technique and characterized by several techniques. The resulting WH/PVA NFs composite mats showed good uniformity in fiber morphology and suitable mechanical strength. More importantly, composite nanofiber with excellent optical transmittance were achieved by a simple water treatment called 'dip and dry' process. In order to study the transparent property of optically transparent NFs for applying in transparent wearable devices, we fabricated a transparent flexible Organic Photovoltaics (OPV) substrate. The obtained results showed that the WH/PVA NF composites could be considered as a potential candidate in transparent wearable devices. This study suggests a simple approach to utilize a waste material in an eco-friendly way for electronics applications.

Acceptance ID: T7JL

Design with Purpose - A design : STEM responsive, bioresilient soft matter platform that can contribute positively to both compelling human centric needs and economic prosperity

Raymond Oliver (Prof)

Chair, Active and Interactive Materials, Director, Design:STEM Studio-Lab, School of design, Northumbria University, Newcastle upon Tyne, NE1 8ST

The application of soft, programmable material, making and machines that integrate with creative design principles to engage and unlock a broad set of opportunities and application spaces addressing human centred needs, habits and behaviours.

We question how best to probe, interrogate, explore, interpret and demonstrate tangible material benefits that contribute to improved ways of living in both urban and rural/remote environments and communities and have developed a framework approach based on 'Pasteur's Quadrant' coupled to a creative and social design practice to generate a distinct pathway towards realisable societal and economic product and service solutions.

In particular, how best to design with purpose. Exploring programmable materials and new fabrication tools that builds across multiple length scales that are both familiar and experiential.

Examples will be illustrated with evidence based Natural and Responsive material systems including shape memory applications for everyday living and new uses of polysaccharides including nano cellulose, chitosan and novel biocomposites.

The processes of knowledge acquisition, interpretation and demonstration is undertaken by a well equipped group of innovators which is highly multidisciplinary in form. New results pertaining to the future of paper will be discussed and illustrated with material examples.

Acceptance ID: OLIV-O

Facile Synthesis of Layered $Ni(OH)_2$/Graphene from Expanded Graphite

Shuihua Tang[a,b,], Jiawei Yuan[a,b], Renjie Qu[a,b], Xiaolong Qin[a,b], Lingshan Wu[a,b]*

[a] State Key Lab of Oil and Gas Reservoir Geology & Exploitation, [b] School of Materials Science and Engineering, Southwest Petroleum University, Chengdu 610500, China.

In recent years, tremendous research efforts have been attempt to design excellent performance composites through incorporating carbon materials with conducting polymers and transition-metal oxides/hydroxides. NiO or $Ni(OH)_2$ is a promising electrode material in alkaline electrolyte due to its high theoretical specific capacitance, low toxicity and cost, but it is still subjected to poor conductivity, large particle size and particle aggregation during a charging-discharging process. Therefore, NiO or $Ni(OH)_2$/carbon-based composite has been intensively explored. Graphene has been regarded as an ideal EDLC electrode material owing to its high specific surface area and good electrical conductivity, but it is very expensive and has a tendency to re-stack back to graphite. Expanded graphite (EG) has been commercialized with illegible cost compared to graphene, and it possesses wider interlayer spacer than graphite. In this work, we address several routes to use inexpensive EG as the starting subtance, then layered $Ni(OH)_2$/graphene composites were synthesized by electrochemical depositition, microwave-assistant heating precipitation and hydrothermal methods. These procedures are simple, cost effective, environmental friendliness, and easily scaled-up. With carbon nanotubes (CNTs) as the conductive additive, the schematic structure of the final composite is shown in **Fig. 1**.

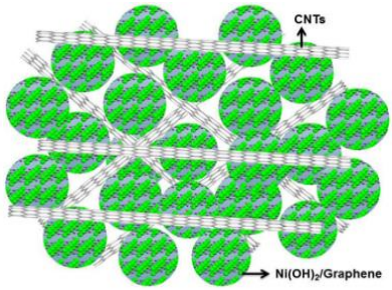

Fig. 1 Schematic structure of $Ni(OH)_2$/graphene-CNTs composite.

The obtained layered $Ni(OH)_2$/graphene-CNTs composite exhibits a maximum specific capacitance of 1580 F g^{-1} at 1 A g^{-1} in 6 M KOH, due to the adequate utility of electroactive specific area of graphene and $Ni(OH)_2$ with smaller particle size. After 3000 cycles at scan rate of 100 mV s^{-1}, 90 % specific capacitance was retained, this is mainly due to EG could effectively prevent $Ni(OH)_2$ nanoparticles from aggregation and CNTs construct a network-like electrode. These results indicate that the $Ni(OH)_2$/G has a promising application for supercapacitor.

Acceptance ID: PLTF-O

First-Principles Study of La-substitution Doping Effect on Magnetic Transition Temperature of Hexagonal $YMnO_3$ Films

D. Chen[1], *Y. L. Zhu*[1], *X. L. Ma*[1]

[1]*Division of Solids Atomic Imaging, Institute of Metal Research, Chinese Academy of Sciences, Wenhua Road 72, Shenyang, Liaoning, 110016 China.*
*E Mail/ Contact Détails (**dchen@imr.ac.cn**)*

Recently, multiferroic manganites have attracted a great deal of attention both theoretically and experimentally [1-3]. Hexagonal $YMnO_3$ is the most extensively studied multiferroic material among all hexagonal manganites, which possesses magnetism and ferroelectricity simultaneously with a high ferroelectric transition temperature (~900 K) and a low antiferromagnetic transition temperature (~70 K). Accordingly, we have been devoted to exploring the possibility of tuning magnetic transition (Néel) temperature towards the room temperature functionality of $YMnO_3$ thin film [3]. The objective of the work is to study La-substitution doping effects on electronic structures and magnetic transition temperature in the hexagonal $YMnO_3$ superlattice films with first-principles method. Based on the density functional theory, we calculated the formula $Y_{1-x}La_xMnO_3$ (x = 0, 0.167, 0.333 and 0.5) and pay attention to the lattice constants and the substitution energy. The monotonous evolution of the parameters suggests a random distribution of the La atom on the Y-sites whatever x ($0 \le x \le 0.5$) preserves the $YMnO_3$ hexagonal structure, but the substitution energy (per La atom) will do not change monotonously and have a minimum with doping dependence x increasing. When x=0.167, the value of substitution energy is negative and favorable as compared to other doping dependences. Then, we choose the nominal doping dependence (x=0.167) to study the doping effect on the electronic structures and magnetic state transitions of hexagonal $YMnO_3$ films. As results, we found that the substitution doping effects on magnetic transition temperature depend on the interface strain types in the hexagonal $YMnO_3$ films, which provides possibilities to improve the multiferroic properties of hexagonal $YMnO_3$.

Acknowledgments: This work is supported by the National Natural Science Foundation of China (NSFC) (51231007, 51171190 and 51371176), the Special Program for Applied Research on Super Computation of the NSFC-Guangdong Joint Fund (the second phase). We especially thank Dr. T. Sasaki and Dr. I Solovyev (Computational Materials Science Unit, National Institute for Materials Science, 1-1 Namiki, Tsukuba, Japan) for good suggestions and fruitful discussions.

Keywords: Substitution doping, magnetic transition temperature, hexagonal $YMnO_3$ film, first-Principles

[1] FONTCUBERTA, J. 2015. Multiferroic $RMnO_3$ thin films. *C. R. Physique*, 16, 204-226

[2] CHOI, T., HORIBE, Y., YI, H. T., CHOI, Y. J., WU, W., & CHEONG, S. W. 2010. Insulating interlocked ferroelectric and structural antiphase domain walls in multiferroic $YMnO_3$. *Nat. Mater.*, 9, 253-258

[3] CHEN, D., ZHU, Y. L., MA, X. L. 2017. Effects of the Interface Strain on the Magnetic Transition Temperature of Hexagonal $YMnO_3$ Films: A First-Principles Study. *Submitted to* 2017 Joint IEEE International Symposium on Applications of Ferroelectrics (ISAF), Atlanta, GA, USA.

Acceptance ID: PNQV-O

Magnetic properties and hyperfine interaction of Y-type $BaSrCo_2(Fe_{0.9}Al_{0.1})_{12}O_{22}$ hexaferrite investigated by Mössbauer spectroscopy

Jung Tae (Lim), In-Bo (Shim), and Chul Sung (Kim)

Department of Physics, Kookmin University, Seoul 02707, Republic of Korea.
hisashi@kookmin.ac.kr / presenting author
cskim@kookmin.ac.kr / corresponding author

Y-type hexagonal ferrite has been studied for magnetoelectric effect in interesting physics properties. Recently, some of Y-type hexagonal ferrite single crystal such as $Ba_{0.5}Sr_{1.5}Zn_2(Fe_{0.92}Al_{0.08})_{12}O_{22}$, and $BaSrCo_2Fe_{11}AlO_{22}$ have been extensively studied due to the reduction of the in-plane orbital moment via Aluminum substitution[1]. Therefore, $BaSrCo_2(Fe_{0.9}Al_{0.1})_{12}O_{22}$ polycrystalline sample was synthesized by polymerizable complex method and investigated the magnetic properties and hyperfine interaction by using x-ray diffractometer (XRD), vibrating sample magnetometer (VSM) and Mössbauer spectrometer. From the refined XRD patterns of $BaSrCo_2(Fe_{0.9}Al_{0.1})_{12}O_{22}$, the crystal structure was confirmed to be rhombohedral structure (space group : *R-3m*), and lattice constant a_0, c_0, and bulk density were 5.87, 43.55 Å and 5.21 g/cm^3, respectively. Base on the field-dependent magnetization curves of $BaSrCo_2(Fe_{0.9}Al_{0.1})_{12}O_{22}$ sample up to 15 kOe at various temperatures ranging from 4.2 to 295 K, showing that sample was not saturated and magnetic phase transitions from conicalmagnetic state to ferromagnetic state with increasing applied field. The magnetization at 15 kOe (M_{15kOe}) and coercivity (H_c) of $BaSrCo_2(Fe_{0.9}Al_{0.1})_{12}O_{22}$ sample decrease from M_{15kOe} = 24.93 emu/g, H_c = 775.23 Oe at 4.2 K to M_{15kOe} = 21.08 emu/g, H_c = 428.43 Oe at 295 K. We have obtained Mössbauer spectra of sample at various temperatures ranging from 4.2 and 700 K. From the analyzed Mössbauer spectra, we expect that non-magnetic Al ions preferentially occupy the up-spin site of $18h_{VI}$, $3b_{VI}$, and $3a_{VI}$.

Keywords: Y-type hexaferrite, Mössbauer spectroscopy, Spin transition

[1] NAKAJIMA, T., TOKUMAGA, Y., MATSUDA, M., DISSANAYAKE, S., FERNANDEZ-BACA, J., KAKURAI, K., TAGUCHI, Y., TOKURA, Y., and ARIMA, T. 2016. Magnetic structures and excitations in a multiferroic Y-type hexaferrite $BaSrCo_2Fe_{11}AlO_{22}$. *Phys. Rev. B* 94, 195154.

Acceptance ID: PX47-P

Structural Degradation Assessment of Reinforced Concrete Structures using Self-diagnosis Technology

An Cheng[1], *Wei-Ting Lin*[1], *Sao-Jeng Chao*[1], *Hui-Mi Hsu*[1]

[1] *Department of Civil Engineering, National Ilan University, No.1, Sec. 1, Shennong Rd., Yilan City, Yilan County 260, Taiwan.*
ancheng@niu.edu.tw/ phone :+886-3-9317557

The accumulation of internal defects in materials often results in degraded performance and the prevention of sudden material failure has become an important issue in materials research. This study added graphite to cement-based materials to investigate conductivity behavior and sensitivity to the effects of pressure.

This study examined the influence of graphite content on the workability, durability, and mechanical properties of concrete using specimens with water cementitious ratios of 0.4. The preparation of specimens containing 4 %, 8%, 12% and 16 % of the cement was replaced with graphite. We then investigated the influence of graphite content on the electrical resistivity of the concrete and conducted cyclic loading tests to determine the relationship between and the application of load and the resulting changes in resistivity to indicate the existence and development of internal cracking. Our results show that the addition of graphite to concrete significantly reduces fluidity. In addition, the compressive strength of the concrete presented a linear decline proportional to the addition of graphite. The addition of graphite powder also increased the porosity of the specimens, and the difference in porosity between graphite mixtures and the control group increased with age. With regard to resistivity, concrete with 8 % graphite content reached the percolation threshold of the concrete, and with an increase in the amount of graphite, resistivity gradually decreased. In cyclic loading tests with a fixed load, specimens with 5 % or more graphite content were better able to reflect the relationship between loading and resistivity.

In inclusion, the mixture in which 8% of the cement was replaced by graphite provided the best tradeoff between strength and sensitivity to the effects of cracking, making it the best option for practical use in construction.

Keywords: Pressure-sensitive materials, graphite powder, resistivity change rate, cyclic loading test

Acceptance ID: QAXE-P

Design of Organic-Inorganic Heterojunctions Toward High Performance Field Effect Transistor Applications

Chao Jiang, Jiawei Wang, Fengjing Liu, Ji Dong

National Center for Nanoscience and Technology, CAS Center for Excellent in Nanoscience, Beijing 100190, China

A hybrid structure of organic-inorganic heterojuctions has been highly expected to realize more flexible design of functional devices in opto-electronics and electronics for ubiquitous applications in reality. Especially, with tremendous increasing of novel materials, the novel device applications are coming true. Here, we present several examples to illustrate the possible strategy of design in phototransistors and ambipolar transistors.

Organic/Perovskite hybrid thin film transistor photodetectors consist of C8BTBT molecular film and CH3NH3PbI3 film prepared by two-step vacuum deposition. By implementing perovskite CH3NH3PbI3 film onto the organic active layer, the organic/perovskite hybrid photodetector exhibited a photoresponsivity of 33 A/W and fast response time and well gate tunable ability. Improvement of photodetection performance is attributed to the balance between light absorption in perovskite layer and an effective transfer of photogenerated carriers entering from perovskite into organic C8BTBT channel.

Secondly, as showing large potentials for applications in integrated logic circuits with low power dissipation, wide noise margins, and higher robustness, ambipolar transistors have attracted widely attentions in recent. Here, we utilize IGZO and organic semiconducting material--DNTT, to fabricated ambipolar transistors. The transistors show balance mobilities for n- and p-type channels, in addition, ideal reliability was observed in the prolonged bias stress test. Converters based on above were also built up, which showed promising behaviors with gain value as high as 30. The organic-inorganic hybrid heterostructures may open up a path way for the flexible design of functional devices and its integrations.

Acceptance ID: QGBU-O

Experimental Analysis of Curved FRP Panel Behavior

Woo-tai Jung[1] , *Hee beom Park*[1], *Jong-sup Park*[1], *and Jae-yoon Kang*[1]

[1]*Structural Engineering Research Institute, Korea Institute of Civil Engineering and Building Technology, Goyang, Republic of Korea.*
woody@kict.re.rk

The purpose of this study is to verify performance through various experiments such as materials, connected parts, and real size specimens in order to apply an eco tunnel with curved FRP panels. FRP is checked to apply in many sites because of strong points such as high strength, light weight, chemical resistance and need to secure reliability through real size test because of low applications, low construction cases, problems with design criteria. This study tested for members unit, panel unit and real size specimens and the following conclusions can be drawn. The result of this study showed that bond performance and bond length are satisfied through direct tensile test of connected members. It can be seen that the connection between pannels can apply the resin bonding method through the small scale model and the cross-connection in connected member of fiber direction is better than consecutive connection. Also, sand coating in panel improve composite behavior interface of FRP, and concrete and performance of parallel connection is good through real size test.

Keywords: Curved FRP, panel, connected member, Sand coating

Acceptance ID: QUB9-P

Activated carbons made from natural carbonaceous sources such as wood, coal, coconut shell, etc.

E.A. Kiseleva, R.I. Nafikov, V.Y.Lobov, T.N.Guseinova

Advanced Electrodes – Fuel Cell (ADEL-FC), 119002, 2/24 Kaloshin Lane, Moscow, Russia.
kanna787@mail.ru

Activated carbon, also known as activated charcoal, is a form of highly porous carbon. The highly porous character of activated carbon makes it useful in a variety of applications which require a highly adsorptive surface, such as a media for purification, solvent recovery, deodorization, and as an antidote for certain poisons. Additionally, activated carbon may be used as electrode material, such as in double layer capacitance applications, where high surface area allows for increased charge storage density compared to less porous materials. Activated carbons made from non-synthetic sources (i.e., natural carbonaceous sources such as wood, coal, coconut shell, etc.), are typically attractively priced and are available with sufficiently high surface area. Electrodes are based on original wood (coconut shell)-derived activated carbon, produced by potassium hydroxide high-temperature activation in ADEL-FC. Porous structure and specific surface area can be controlled by changing activation process parameters. This method include: (i) carbonizing a carbonaceous source material to generate a char; (ii) activating the char to form an activated carbon; and (iii) washing the activated carbon with a plurality of increasingly basic solutions. Electrodes were prepared from slurry by cold-rolling. Such electrodes may be incorporated into various devices, including electric double-layer capacitors, fuel cell. For electrode characterization cyclic voltammetry, impedance spectra analysis, ESR and galvanostatic charge–discharge were used.

Keywords: Activated carbon, electrodes materials, double-layer capacitors, fuel cell

Acceptance ID: QWAS-P

Ferromagnetism on mechanically-exfoliate in CVD-carbon film prepared by using adamantane as precursor

S. Sangphet[1], D. Doonyapisut[1], S. Siriroj[1], N. Sriplai[2], S. Maensiri[1], S. Pinitsoontorn[2], W. Meevasana[1]

[1]School of Physics, Institute of Science, Suranaree University of Technology, Nakhon Ratchasima, 30000 Thailand.
[2]Departmant of Physics, Faculty of Science, Khon Kaen University, Khon Kaen, 40002 Thailand
suppanut.tone@gmail.com

The common ferromagnetic materials usually contain elements whose d- or f-orbital is incompletely filled (e.g. iron, nickel, and cobalt). Interestingly carbon-based materials without such magnetic element (e.g. Q-carbon [1], graphene[2], Teflon[3], or diamond with defects[4]) can also exhibit ferromagnetism at room temperature. In this work, by using chemical vapor deposition (CVD) technique, we have grown carbon films with adamantane as the precursor and have observed room-temperature ferromagnetism; adamantine is the smallest member of the saturated nano-hydrocarbon known as "diamondoid" series (nano-diamond structures). We prepared carbon films on various substrates, e.g. silicon, quartz, and sapphire. The signature of moderately strong ferromagnetism is observed with saturated magnetization as large as 6.2 $emu \cdot cm^{-3}$. By using energy dispersive x-ray spectroscopy (EDX), we have found no evidence of conventional magnetic elements (e.g. Fe, Co, and Ni) whose amount is high enough to explain such strong signal; for an example, if Fe impurity were the origin, there should be around 10,000 ppm of Fe, which could easily be detected by EDX.

Intriguingly, this ferromagnetism could be further enhanced when the carbon film is mechanically exfoliated; the saturated magnetization of the remaining film could increase by six times. We believe that the origin of this observed ferromagnetism is similar to the case of the stretching Teflon film [3] where the study suggests that the ferromagnetism comes from the dangling bonds with localized magnetic moments. In our case, by using Raman spectroscopy, the data suggest that these similar dangling bonds were created during the CVD process. The localized magnetic moment from these bonds may then give the observed magnetization and after the mechanical exfoliation, the orientation of the dangling bonds could become aligned and hence the magnetization is further enhanced. Regardless of the origin, our finding already suggests an inexpensive way to create thin film with moderately strong ferromagnetism which could be used in applications of magnetic coating.

Keywords: Adamantane, Diamondoid, Raman spectroscopy, ferromagnetism, dangling bond

[1] NARAYAN, J. and BHAUMIK, A. 2015. Novel phase of carbon, ferromagnetism and conversion into diamond *J. Appl. Phys.*, 118, 215303-12.

[2] YAZYEV, O. V. and HELM, L. 2007. Defect-induced magnetism in graphene *Phys. Rev. B*, 75, 125408-4.

[3] MA, Y. W., LU, Y. H., YI, J. B., FENG, Y. P., HERNG, T. S., LIU, X., GAO, D. Q., XUE, D. S., XUE, J. M., OUYANG, J. Y. & DING, J 2012. Room temperature ferromagnetism in Teflon due to carbon dangling bonds *Nat. Commun*, 3, 727-734

[4] TALAPATRA, S., GANESAN, P. G., KIM, T., VAJTAI, R., HUANG, M., SHIMA, M., RAMANATH, G., SRIVASTAVA, D., DEEVI, S. C. & AJAYAN, P. M. 2005. Irradiation-induced magnetism in carbon nanostructure *Phys. Rev. Lett.*, 95, 97201-4.

Acceptance ID: QZPS-O

Functionalised Silica Nanoparticles as Fouling Resistant Surface Coatings

Paul J Molino[1], *Brianna Knowles*[1], *Binbin Zhang*[1], *Michael J Higgins*[1], *Gordon G Wallace*[1],

[1]*ARC Centre of Excellence for Electromaterials Science, Intelligent Polymer Research Institute, University of Wollongong, Wollongong, Australia*
pmolino@uow.edu.au

Critical to the development of antifouling coatings technologies for biomedical and terrestrial/aquatic applications is the coupling of effective materials and functional chemistries with coating fabrication techniques, providing a clear avenue for the application of these coatings to industrially relevant processes. One approach that is gaining increasing interest is the application of nanomaterials to generate antimicrobial interfaces. Nanomaterials can be employed to provide specific functionality to the coating interface (i.e. catalytic interfaces), they can be modified to present appropriate surface chemistries at the material interface, and the coating fabrication method may be tailored to generate specific interfacial topographies and surface morphologies. In this talk we present silica nanoparticles as a highly tuneable coating system through which nanopartricle size and surface functionality, generated through the tethering of various chemistries using silane chemistry, can be tailored to enable control over the nano- and micro-interfacial properties of nanoparticle coatings. Through modifying silica nanoparticles with hydrophilic chemistries (e.g. poly(ethylene glycol and zwitterions), we show the coatings comprised of functionalised silica nanoparticles are highly effective at resisting adsorption from organics, and adhesion and colonisation by microbial organisms. We also demonstrate this nanoparticle system to be highly amenable to a range of fabrication technologies, such as spray coating and inkjet printing.

Keywords: biofouling, nanoparticle, zwitterion, surface functionalization

Acceptance ID: RSR5-O

Porous ZnO Nanowire Arrays: Ultrahigh Broadband Antireflection and Full Range Visible-Light Photodetection

*Kapil Gupta and Chuan-Pu Liu**

Department of Materials Science and Engineering, National Cheng Kung University, Tainan 70101, Taiwan

Porous ZnO nanowire arrays (PZNA) were synthesized by hydrothermal method followed by controlled hydrogen annealing for different durations. Internal and external pores of the PZNA were formed with a gradient distribution from top to bottom of the nanowires. This pore density gradient distribution in PZNA serves as a new mechanism to achieve graded-refractive-index for broadband antireflection with the smallest reflectance of less than 5% at 800 nm. Moreover, the cathodoluminescence spectra suggest the emergence of numerous surface defects in PZNA, contributing to defect state excitation phenomena. Owing to the unique geometric and microstructural features associated with PZNA, the PZNA devices exhibit an exceptional capability for steady photodetection over the entire visible light range through the synergetic actions of antireflection, multiple scattering and defect state excitations.

Acceptance ID: S4AF-O

Effects of Chemical Reduction on Graphene Oxide Reinforced Poly (vinyl alcohol) Nanocomposite Thin Films

Jain.P, Bhasha

Department of Chemistry, School of Applied Science,
Netaji Subhas Institute of Technology, University of Delhi, India
E Mail (pj381970@gmail.com)

Biopolymer based nanocomposites are of prime importance in the present scenario due to their environmental friendly impact on various applications. Nanofiller incorporated Poly (vinyl alcohol) thin films have been fabricated by solution casting technique. Graphene Oxide was prepared by modified Hummer's method which was further chemically reduced by using hydrazine. Dispersion of graphene oxide into PVA matrix is facilitated by hydrogen bonding due to the presence of hydroxyl groups. The composite samples were prepared using a range of wt% of reduced graphene oxide content respectively and water is used as a processing solvent. The results showed a significant improvement of mechanical strength on addition of small amount of reduced graphene oxide as compared to neat PVA. The increase in tensile strength is attributed to the enhancement in crystallinity. SEM analysis revealed that the nanofiller particles are uniformly distributed throughout the surface. Degree of crystallinity and melting enthalpy of PVA – Graphene Oxide nanocomposites were investigated by thermal analysis.

Keywords: Polyvinyl Alcohol; Graphene Oxide; Nanocomposite

Reference

[1] S. K. SHARMA, J. PRAKASH & P.K.PUJARI, Effects of the molecular level dispersion of graphene oxide on the free volume characteristics of poly(vinyl alcohol) and its impact on the thermal and mechanical properties of their nanocomposites: **Phys. Chem. Chem. Phys**, 2015,**17**, 29201-29209.

Acceptance ID: S66P-O

Curing behaviors of epoxidized soybean oil with isosorbide as a hardener

Hanna Kim and Dai Soo Lee

Department of Semiconductor and Chemical Engineering, Chonbuk National University, 567 Baekje-daero, Deokjin-gu, Jeonju-si, Chonbuk, 54896, Republic of Korea
dslee@jbnu.ac.kr / 82-63-270-2310

Recently, renewable resources based biopolymers are attracting attentions of scientists and industry engineers due to the sustainability of the biomass. Many of the candidates of biopolymers to replace the polymers from petroleum oils are based on the fatty acids. But, the biopolymers based on the fatty acids are mechanically weak and frequently the heat resistance is not good enough for the applications. Isosorbide is produced from sorbitol by bioprocess and many reports on the application of the isosorbide are available in the literatures.[1,2]. Typical applications of isosorbide for polymer systems are based on the reaction of two hydroxyl groups for the esterification and carbamation to prepare polyesters and polyurethanes.[3,4] We have paid attentions on the potentioal of isosorbide as a hardener of epoxy resin to replace phenolic hardeners. It is interesting to note that rigid back bone can be introduced by incorporating isosorbide in biopolymer systems. But we found that isosorbide is immisible with most of the epoxy resins. Thus, adduct of isosorbide with epoxy resin was investigated to prepare epoxy resin systems based on the biomass. In order to prepare adducts of epoxy resin and isosorbide, cationic polymerization of epoxidized soybean oil and isosorbide was carried out with boron trifluoride in chloroform. Molecular weight of adduct could be adjusted by varying the initiator concentration and the reaction time. The adduct could be cured into network structure of high mechanical strength and heat resistance. Curing behaviors of the epoxidized soybean oil adduct was studied emplying differential scanning calorimetry. It was found that curing behavior of the adduct based on the biomass was similar to the bis-phenol A based epoxy resins, i.e., autocatalytic second order reactions. It is postulated that isosorbide can be useful hatdener of epoxy resins with sustainability.

Keywords : Bio-resource, flexible thermoset, Isosorbide, Epoxidized soybean-oil

[1] JOO RAN KIM, SURAJ SHARMA. 2012. The development and comparison of bio-thermoset plastics from epoxidized plant oils. *Industrial Crops and Products*, 36, 485-499.

[2] JOSHUA M. SADLER, ANH-PHUONG T. NGUYEN, FAYE R. TOULAN, JEFFREY P. SZABO, GIUSEPPE R. PALMESE, CAROLINE SCHECK, STEVE LUTGEN, JOHN J. LA SCALA. 2013. Isosorbide-methacrylate as a bio0based low viscosity resin for high performance thermosetting applications. *Jouranl of Materials Chemistry A*, 1, 12579-12586.

[3] NAO HOSODA, HISAO HAYASHI, TAKASHI TSUJIMOTO. 2016. Bio-based flexible network polymer from epoxidized soybean oil reinforced by poly(butyl methacrylate). *International Journal of Chemistry*, 8, 159-164.

Acceptance ID: SK9M-O

The Study on 1-1-3 Piezoelectric Composite

Lei Qin[1,], Xu-hui Mi[1], Chuanxin-Gu[1], Chao Zhong[1]*

[1] Research Center of Sensor Technology, Beijing Information Science & Technology University, Beijing, China 100101

1-1-3 piezoelectric composites with PMN-PT single crystal, epoxy and silicone rubber were prepared by using the modified 'slice and fill' technique. The effect of the volume percentage of PMN-PT single crystal on the properties of the composite was analyzed by experiments. The experimental results show that the change of the volume percentage of the epoxy has no effect on the piezoelectric properties of the composites, which only affects the acoustic impedance. For comparison, 1-3 piezoelectric composites with PMN-PT and epoxy were prepared. The electromechanical coupling coefficient of 1-1-3 piezoelectric composites is higher than 1-3 composite, and also the acoustic impedance Z of 1-1-3 composite is lower than 1-3 composite. The 1-1-3 composite can be used to design high performance hydrophone than 1-3 composite.

Keywords: piezoelectric composite; electromechanical coupling coefficient; acoustic impedance

* *Corresponding author's email:* ***qinlei@bistu.edu.cn***

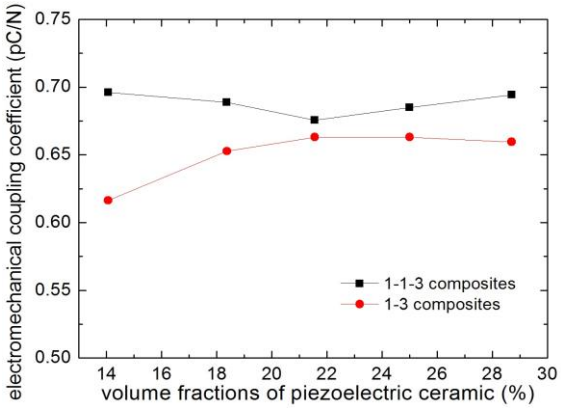

Acceptance ID: SWNH-O

SiO_2@TiO_2 core-shell aerogels: Enhanced thermal stability and photocatalytic activity

Ferreira-Neto E.P [1,2], *Worsley, M.A.*[2], *Rodrigues-Filho U.P.*[1]

[1]*Instituto de Química de São Carlos, Universidade de São Paulo, São Carlos, SP, Brazil*
[2] *Physical and Life Sciences Directorate, Lawrence Livermore National Laboratory, Livermore, CA, USA*
Contact : eliaspaiva@usp.br, uprf@iqsc.usp.br

Owing to their highly porous nature and unique structural properties, TiO_2 aerogels prepared by sol-gel method and supercritical drying are interesting choices for development of high performance photocatalysts for environmental remediation and solar energy conversion processes [1]. Nevertheless, controlled formation of nanocrystalline TiO_2 aerogels is challenging as the required crystallization by post-synthesis high temperature thermal treatments may lead to uncontrolled crystallite growth and sintering, as well as irreversible anatase-to-rutile phase transformation, structural changes which are highly detrimental to photocatalytic performance [2,3]. To address such drawbacks, in the present study we report new routes for the preparation of SiO_2@TiO_2 core-shell structured aerogels aiming to improve thermal stability and photoactivity of titania by using silica aerogel as a functional support for titania [4]. SiO_2@TiO_2 aerogels synthesis was carried out by soaking SiO_2 wet gels in $TiCl_4$/DMF followed by epoxide-assisted gelification (Route 1) or thermo-induced hydrolysis at 80ºC (Route 2). The obtained gels were subsequently washed by solvent-exchange in ethanol and acetone, dried in supercritical CO_2 and calcined at 600ºC or 1000ºC. Characterization by Raman spectroscopy and x-ray diffraction analysis indicated exclusive formation of anatase nanocrystallites in the heat-treated SiO_2@TiO_2 aerogels, which demonstrate exceptionally high thermal stability as crystallize size did not increased past 10 nm even after the materials were submitted to 1000ºC thermal treatment. On the other hand, unsupported TiO_2 aerogel sample undergoes crystallite growth (>100nm) and extensive rutile formation, including total conversion of anatase into rutile at 1000 ºC. Moreover, the prepared SiO_2@TiO_2 core-shell aerogels showed remarkably higher photocatalytic activity as compared to unsupported TiO_2 aerogels treated at 600ºC or 1000ºC, as demonstrated by Rhodamine B photodegradation essays. Highest photocatalytic activity was achieved for SiO_2@TiO_2 prepared by thermohydrolysis method (Route 2). Superior photocatalytic performance of SiO_2@TiO_2 aerogels is assigned to the high photoactivity of silica supported anatase nanocrystals, efficient light harvesting due to the difference in refraction index between silica and anatase as well as improved Rhodamine B adsorption capacity by SiO_2 aerogel support.

Keywords: SiO_2, TiO_2, sol-gel, aerogel, photocatalysis

[1] CHEN, L., ZHU, J., LIU, Y. M., CAO, Y., LI, H.X., HE, H.Y., DAI, W. L., FAN, K.N., 2006. Photocatalytic activity of epoxide sol–gel derived titania transformed into nanocrystalline aerogel powders by supercritical drying. *J. Mol. Catal. A Chem.* 255, 260–268.

[2] ZHAO, L., WANG, S., WANG, Y., LI, Z., 2016. Thermal stability of anatase TiO2 aerogels. *Surf. Interface Anal.* In press

[3] HANAOR, D.A.H., SORRELL, C.C., 2010. Review of the anatase to rutile phase transformation. *J. Mater. Sci.* 46, 855–874.

[4] KIBOMBO, H.S., PENG, R., RASALINGAM, S., KOODALI, R.T., 2012. Versatility of heterogeneous photocatalysis: synthetic methodologies epitomizing the role of silica support in TiO2 based mixed oxides. *Catal. Sci. Technol*. 2, 1737–1766.

Acceptance ID: SYXP-P

Solution-processed zinc oxide as an electron transporting layer for improving the performance of perovskite solar cells

Yang-Yen Yu[1,2],Chia-Fen Teng* [1]

[1] *Department of Materials Engineering, Ming Chi University of Technology*
84 Gunjuan Rd., Taishan Dist., New Taipei City 24301, Taiwan
[2:] *Department of Chemical and Materials Engineering, Chang Gung University,*
259 Wenhua 1st Rd., Guishan Dist., Taoyuan City 33302, Taiwan
[*]*Corresponding author's e-mail: yyyu@mail.mcut.edu.tw*

Organic−inorganic perovskite solar cells have recently emerged at the forefront of photovoltaics research due to its dual electron and hole mobility. Organo-metal halide perovskites were composed of an ABX_3 (e.g. $CH_3NH_3PbI_3$) structure in which A represented a cation, B a divalent metal cation (e.g. Pb^{2-}) and X a halide (e.g. F, Cl, Br, I). Zinc oxide (ZnO) was used as the perovskite electron transport layer of the solar cell in this study. The active layer of perovskite solar cells here were fabricated by two step process. To investigate the effect of mixed solvent on the performance of perovskite active layer, different ratios of toluene and isopropyl alcohol (IPA) were used in the preparation of composite perovskite film. We found that the optimum volume ratio of isopropyl alcohol and toluene could result in the higher PCEs. The best performance of perovskite solar cells with the structure, ITO/ZnO/Perovskite/Spiro-OMeTAD/Ag, prepared at volume ratio of isopropyl alcohol and toluene (9:1) are: PCE=13.2 %, Jsc=20.1 mA/cm^2, Voc=1.1 V, and Fill Factor=0.60.

Keywords: Solar cell, Perovskite, Zinci oxide, Electron transport layer

Acceptance ID: SZDE-P

Scanning Probe Lithography for Production of 3D Mesoscale Materials

Gang-yu Liu

Department of Chemistry, University of California, Davis, CA 95616

Scanning probe microscopy (SPM) has been widely used by the research and development community to visualize specimens with unprecedented resolution: reaching nanometer levels routinely and atomic and molecular levels on occasion. The localization of SPM at atomic and molecular scale has been harnessed to control interactions of molecules towards 2D and 3D nanolithography. Combining SPM's spatial precision with the advanced local delivery methodologies including microfluidics, this work reveal how the molecules assemble from nano- to meso-scale. Layer-by-layer nanoprinting of various structures with designed functionalities will be presented, and potential applications will also be discussed.

Acceptance ID: T43X-I

Effect of Particle Shape and Size on the Structure and Optical Band-Gap of Zinc Oxide Nanoparticles

T.E.P. Alves[1,2] and A. Franco Jr[2]

[1]Instituto Federal de Educação, Ciências e Tecnologia de Goiás, Anápolis-GO - Brazil
[2]Instituto de Física, Universidade Federal de Goiás, Goiânia-GO, Brazil.
franco@ufg.br

In this study we prepared zinc oxide (ZnO) nanoparticles by polyol method using zinc acetate and sodium acetate in a propylene glycol medium with control on the hydrolysis reaction (HR) time [1]. It was observed that the hydrolysis reaction time and acetate ions had a strong effect on the morphology and size of ZnO nanoparticles (NPs). For instance, Transmission Electron Microscope (TEM) images revealed that ZnO NPs synthesized by short HR time (10 min) and long HR time (300 min) crystallized in small rods and elongated rods shape, respectively. On the other hand, using only zinc acetate reagent the ZnO NPs crystalized in roughly spherical shape. These differences may be attributed to the high polarization of acetate compared to propylene glycol, i.e. the huge amount of acetate present in the solution affects the oriented attachment growth of the ZnO NPs [2]. In addition the HR time played import rule on the optical-band gap, (E_g) of ZnO NPs. E_g values determined by means of Kubelka-Munk model decreased from 3.31 eV to 3.28 eV for short HR time and long HR time, respectively. This can be explained in terms of structural defects and mainly due to difference between particle sizes [3]. The X-ray diffraction (XRD) patterns revealed that all samples crystalized in the typical ZnO wurtzite structure. However, the (002) diffraction peak intensity of ZnO NPs synthesized only with zinc acetate was higher than those synthesized by using both zinc acetate and sodium acetate. This may be an indication that the c axis was the preferential crystal growth direction. Therefore, the ZnO NPs morphology can be tailored by using the polyol method, thus physical properties that are important for some technological applications were controlled.

Keywords: Polyol, zinc oxide, propylene glycol, optical band-gap

[1] POUL, L.; AMMAR, S.; JOUINI, N. AND FIEV, F. 2003. Synthesis of Inorganic Compounds (Metal, Oxide and Hydroxide) in Polyol Medium: A Versatile Route Related to the Sol-Gel Process. *Journal of Sol-Gel Science and Technology*, 26, 261–265.

[2] WANG, Z.L. 2004. Zinc oxide nanostructures: growth, properties and applications. *Journal of Physics: Condensed Matter*, 16, R829–R858.

[3] FRANCO Jr., A. and PESSONI, H.V.S. 2014. Optical band-gap and dielectric behavior in Ho – doped ZnO nanoparticles. *Materials Letters*, 180, 305–308.

Acceptance ID: TFEF-P

Exfoliated Nanocomposites Based on Polypyrrole and Graphene Analogous Molybdenum Disulfide

R. Bissessur[1*], *J. Hong*[1] *and D. C. Dahn*[2]*

[1]*Department of Chemistry, University of Prince Edward Island, Charlottetown, Canada*
[2]*Department of Physics, University of Prince Edward Island, Charlottetown, Canada*
**Author for correspondence e-mail: rabissessur@upei.ca*

Exfoliated nanocomposites consisting of polypyrrole (PPy) and molybdenum disulfide (MoS_2) were synthesized. The MoS_2 was first prepared in an exfoliated state by reacting molybdic acid with a huge excess of thiourea at 500°C under nitrogen flow [1]. The PPy-MoS_2 nanocomposites were prepared by polymerization of pyrrole with ammonium peroxydisulfate, in the presence of the exfoliated MoS_2 [2]. The amount of MoS_2 in the reaction mixture was systematically varied to produce a range of nanocomposite materials ranging from 1 to 50% by mass of MoS_2. The nanocomposites were characterized by Fourier transform infrared spectroscopy, powder X-ray diffraction, scanning electron microscopy, and van der Pauw electrical conductivity measurements. Powder X-ray diffraction provided evidence that the nanocomposites are exfoliated. The diffractograms of the nanocomposites were completely amorphous, suggesting lack of structural order in these materials and indicating the formation of genuine exfoliated systems. It was intriguing to observe that the nanocomposites exhibited enhanced electronic conductivity when compared to the pure polymer.

References:

1. Ramakrishna Matte, H. S. S.; Gomathi, A.; Manna, A. K.; Late D. J.; Datta, R.; Pati, S. K.; Rao, C. N. R. *Angew. Chem*. **2010**, 122, 4153.

2. *Exfoliated Polypyrrole-MoS_2 Nanocomposites: Preparation and Characterization.* Hong, J.; Bissessur, R; Dahn, D.C. In *Molybdenum Disulfide: Synthesis, Properties and Industrial Applications*, McBride J. (Ed.) Publisher: Nova Science, **2016**. (**Invited Contribution**).

Acceptance ID: THVB-O

Evaluation of Ceramic/Ceramic (Al2O3/Al2O3) Joint Interface Prepared Via Brazing

M. Leylaz Mehrabadi [(1)], A. Ghazi Daryani and [(2)] A. Nemati [(3)]

(1) Researcher in Department of Material Science & Eng., University of Tehran, Tehran, Iran

(2) Researcher in Ceramic Eng. group, Department of Material Science & Eng., Sharif University of Technology, Tehran, Iran

(3) Center of Excellence for Advanced Materials Sharif University of Technology, Tehran, Iran
majid.behzad@outlook.com

Recent investigations show that ceramic/ceramic joints have high potential for applications in industry. Cost and difficulty in manufacturing complex components, either in one-step or by joining of ceramic-metal and ceramic-ceramic, have inhibited more widespread use. It is important to know how to join components without problems and understand the role of the interface as a main factor of controlling the properties in these joints.

The main aim of preparing this paper has been investigating of joining two ceramics with metal fillers (Al_2O_3 to Al_2O_3), the interface of Al_2O_3/ Al_2O_3 with the same metal interlayer (Ag-Cu-Ti) and the effects on the properties as well.

The results showed that the optimum joining of Al_2O_3/Al_2O_3 was obtained by applying a metal layer of Ag-Cu as well as an active metal of Ti-6Al-4V. The second filler was used to increase wet ability and improve strength.

Microscopic investigations revealed penetration and activation of elements from the interface to bulk of ceramic body and it was the major reaction in the joints. Both joints showed the deepest penetration of Ti atoms from interface into the ceramics. According to the XRD results, TiO and V_2O_5 were the most important phases in the Al_2O_3/Al_2O_3 interface. The strength of both joints increased until an optimum time and temperature condition and decreased after that by forming of other phases, which inhibited the formation of a stronger interface. The optimum time and temperature is suggested to be 900°C and 60 min for Al_2O_3/ Al_2O_3.

Keywords: Ceramic/Ceramic Joints, Interface, XRD, EDAX, strength

Acceptance ID: U28B-P

Quinone derivatives for supercapacitor electrodes

Sang Jun Kim, Mohammed Latifatu, Sujeong Shin, Louis Hamenu, Alfred Madzvamuse, Choong Sup

Department of Applied Chemistry & Biotechnology, Hanbat National University, San 16-1, Dukmyung-Dong, Yusung-Gu, Daejeon 305-719, South Korea
jmko@hanbat.ac.kr

We have synthesized various quinone derivatives for the supercapacitor electrode with high capacitance and investigated the capacitance enhancement of activated carbon by physically blending it with a quinone derivative. The properties of the electrode designed were investigated in terms of amount of quinone derivative added, redox behavior and specific capacitance against scan rate and cycle life. The potential of physically mixing quinone with carbon materials simplifies the electrode design process and makes it more cost effective and environmentally friendly. Details on electrochemical properties will be discussed in the presentation.

Acceptance ID: U356-O

Facile Synthesis & Characterization of Poly (Vinyl Alcohol)/Graphene Oxide Nanocomposite reinforced with Ag Nanoparticles.

Gautam.S[1], *Bhasha*[1], *Srivastav.C*[2], *Jain.P*[1]

[1]*Department of Chemistry, School of Applied Science,*
[1]*Netaji Subhas Institute of Technology, University of Delhi, India*
[2]*Department of Applied Chemistry & Polymer Technology*
[2]*Delhi Technological University, Delhi, India*
E-Mail (prnm_j@yahoo.co.in)

In the present work, we have reported fabrication of Poly (Vinyl Alcohol)/ Graphene Oxide Nanocomposite incorporated Silver Nanoparticles (Ag NPs) via solution casting approach to make desired film membrane. GO-Ag Nanocomposite (NPs) has good Biological & Mechanical property which can be used in packaging applications. The obtained thin film was characterized by thermal & mechanical analysis. The melting point peak of the film is shown at 260^0C observed by Differential Scanning Calorimeter (DSC) analysis. Tensile strength as well as thermal stability of Nanocomposite was increased due to the existence of GO & Ag which has strong hydrogen bonding interaction within Nanofiller & matrix. Antimicrobial activity was carried out by employing *E. coli* bacteria against neat PVA and integrated Nanocomposite film.

Keywords: Graphene Oxide, Nanocomposite, Poly (Vinyl Alcohol), Antibacterial Property

Acceptance ID: UEWS-P

Highly ion transportable membranes prepared by pore-fillied technique for reverse elecreodialysis

Young-Woo Choi[1,], Misoon Lee[2], Nam-Jo Jeong[1], Chan-Soo Kim[1], Pil Kim[2]*

[1]***Korea Institute of Energy Research***, *152 Gajeong-ro, Daejeon, South Korea.*
[2]***Chonbuk National University***, *567 Backje-daero, Jeonju-si, South Korea.*
[1,*]*E-Mail : cozmoz67@kier.re.kr*

As a key element in the RED process, the membrane influences the overall power output of the RED stack. Especially, the membrane resistance is one of important properties of the membrane. In this study, CEM and AEM consisting of cross-linked polymers in a porous polyolefin substrate were simultaneously used for application in RED. Physico-chemically stable and ultrathin ion exchange pore filling membranes (cation exchange membranes and anion exchange membranes) with high ion transfer coefficients have been developed for reverse electrodialysis as an energy conversion system. The polymer electrolytes in both cases of cation exchangeable and anion exchangeable ones consisting of the whole hydrocarbon materials were introduced into porous hydrocarbon substrates and crosslinked by radical polymerization in this work. The thickness of the prepared pore filling membranes was controlled between 16 and 23 micrometers to extremely lower membrane resistance and to increase ion transfer. All the properties of the prepared membranes were compared with commercial membranes obtained from Tokuyama, Fuji, and Fuma-Tech. Furthermore, RED cell performance and energy efficiency using the prepared pore filling membranes were also evaluated.

Keywords: Reverse electrodialysis, ion exchange membrane, Resistance

[1] KIM, H. K., LEE, M. S., LEE, S. Y., CHOI, Y. W., JEONG, N. J., KIM, C. S. 2015. High power density of reverse electrodialysis with pore-filling ion exchange membranes and a high open-area spacer *J. Mater. Chem. A, 3*, 16302-10552-16306.

Acceptance ID: UMXP-P

Compression Failure of Carbon Fabric/Polyurethane Composite Tubes

Shun-Fa Hwang, Bo-Hao Chiu, Hui-Lun Yu

Department of Mechanical Engineering, National Yunlin University of Science and Technology, 123 University Road, Sec. 3, Douliu, Yunlin 64002, Taiwan, ROC
hwangsf@yuntech.edu.tw

Recently, it's popular to use composite tubes as energy absorbing components for car crashworthiness. In the present work, the composite tubes consist of polyurethane (PU) resin and carbon fiber fabric, because PU resin is superior in impact, viscosity, low curing temperature, and short curing time. Vacuum assisted resin transfer method is used to fabricate these braided composite tubes because of short cycle time. To investigate the mechanical behavior of these braided composite tubes, static compression loadings are applied to them until failure. In addtion to experimental tests, finite element analysis is executed to simulate the failure processes. Since they are braided composite, different braid angles are created by different tube diameters. To discuss the effect of different braid angles in finite element analysis, the effective elastic constants and strengths of the braided composites predicted by basic finite element analyses are adopted. When the tube diameters are 25, 28.5, and 33 mm, the measured failure loads are 49059, 46300, and 38500 N, while the predicted values are 50897, 47026, and 37945 N. It shows that the simulation results are very close to the experiment values. In addition, the final failure scenarios are similar from both the experiment and the simulation. Therefore, it verifies the progressive failure simulation of the finite elment analysis for the braided composite tubes.

Keywords: braided composite, tube, compression, progressive failure, finite element analysis

Acceptance ID: W7NE-P

Triboelectric generator using a paper

*Wonkyeong Son[1], Sungwoo Chun[1], Soa Bang[1], and Wanjun Park[1]**

[1]Department of Electronics and Computer Engineering, Hanyang University,
Wangsimni-ro, Seoul, South Korea, 04763
Fax: +82(31)-2220-4319 E-mail address: wanjun@hanyang.ac.kr

Energy harvesting using triboelectric generator (TEG), which converts external mechanical energy into electrical power, has attracted considerable attention as a viable route to meet rapidly increasing energy demands [1]. Until now, many attempts have been focused on improving the output power with variable frictive layers exhibiting a difference of distinct electron affinity [2]. To utilize the TEG as an environmental and more feasible energy harvester, eco-friendly materials have also been searched for those frictive layers.

In this study, we propose a triboelectric generator with a regular paper for the one side of the frictive layer which provides large enough electronegativity difference with polyimide (PI) film for the other side. A hydrophobic coating is applied with trichloro(1H,1H,2H,2H-perfluorooctyl) silane (FOTS) to increase generating power without degradation by humidity. The proposed TEG reached to 300 V for the maximum $V_{open\text{-}circuit}$ (V_{oc}) and ~175 mA/m^2 for $J_{short\text{-}circuit}$ (J_{sc}) with the applied force of 0.12 MPa which are comparable to other conventional TEGs [3-4]. Furthermore, the TEG shows superior stability with maintaining uniform output during repetition operations over 10,000 cycles. Finally, a visible performance of the output is successfully demonstrated with capability for lighting of 150 red light-emitting-diodes (LEDs).

Keywords: paper, triboelectric generator, energy harvesting

[1] Fan, F., Tian, Z., Wang, Z. 2012. Flexible triboelectric generator! *Nano Energy*, 1, 328.

[2] Wang, S., Lin, L., Wang, Z. 2015. Triboelectric Nanogenerators as Self-Powered Active Sensors. *Nano Energy*, 11, 436–462.

[3] Zhu, Z., Pan, C., Guo, W., Chen, C., Zhou, Y., Yu, R., Wang, Z. 2012. *Nano Lett.*, 12, 4960-4965.

[4] Lee, C., Choi, Y., Choi, C., Sim, H., Kim, S., Kim, Y. 2016. *RSC Adv.*, 6, 10094.

Acceptance ID: WC7V-P

Crystal Structure and Photoluminescence of an A Unusual 12-fold Cationic Coordination Titanate Host

Liumei Su[1], Gemei Cai[1,], Zhanpeng Jin[1]*

[1]School of Materials Science and Engineering, Central South University, Changsha, 410083, China
E-mail addresses: caigemei@csu.edu.cn (Gemei Cai)

Developing new solid-state lighting host materials is one of the significant and intriguing aspects in the field of luminescence materials[1]. Herein, this paper reports a novel LiInTi2O6 host for phosphors in solid state lighting. The sub-solidus phase relationships, thermal stability, crystal structure, as well as composition-, and temperature-dependent luminescence were investigated and discussed by means of various analytic techniques, including powder X-ray diffraction (XRD), differential scanning calorimetry (DSC), structure solution, photoluminescence excitation (PLE) and emission (PL) spectrum, decay lifetime, high-temperature luminescence, and chromaticity coordinate. LiInTi2O6 crystallizes in a trigonal unit cell with lattice parameters of a = b = 5.1058(7) Å, c = 28.568(4) Å, and Z = 6 in space group R-3m (No. 166), consisting of an unusual 12-fold coordination hexagonal prisms structural framework. Taking LiInTi2O6 as host, a series of Dy3+/Tm3+ singly-doped and co-doped phosphors were successfully synthesized. With increasing Dy3+ concentration, emission colors of LiInTi2O6:Tm3+,Dy3+ phosphors can be appropriately tuned from blue to yellow going through the white region based on the principle of energy transfer. Energy transfer efficiencies were calculated and the mechanism was discussed. Configurational coordinated diagram was employed to explain the thermal quenching behaviour of the white lighting phosphor.

Keywords: LiInTi2O6,crystal structure, energy transfer mechanism, luminescence properties

[1] Bardsley, N.; Bland, S.; Hansen, M.; Pattison, L.; Pattison, M.; Stober, K.; Yamada, M., Solid-State Lighting R&D Plan. Solid-State Lighting Program, Building Technologies Office, Office of Energy Efficiency and Renewable Energy, U.S. Department of Energy 2015, Washington D.C.

Acceptance ID: WDKT-O

Synthesis of Sulfonamide Derivatives and Application to Water Treatment System

Seong Ik (Jeon)[1], *Cheol-Hee (Ahn)*[1*]

[1]*Research Institute of Advanced Materials (RIAM), Department of Materials Science and Engineering, College of Engineering, Seoul National University, Seoul 151-744, Korea.*
meteor424@snu.ac.kr *(Seong Ik Jeon) /* chahn@snu.ac.kr *(Cheol-Hee Ahn)*

Removal of metal ions in water for industrial use, called water softening, is an important procedure since ions are known to cause significant problems on operation and maintenance of equipment or piping in facilities. Though ion exchange or chelate resin is one of the widely used methods for desalination, it has some limitations in ion selectivity and regeneration. Especially, huge amount of salt or strong acidic/basic condition needs to be applied iteratively for reuse of the resin. In this research, sulfonamide-derived cation capturing system is suggested as an alternative to relieve these drawbacks. Sulfonamide derivatives show sharp transition from charged to uncharged form at certain pH, which alleviates the condition of regeneration. Moreover, chemical modification of sulfonamide had been fully established so that diverse functionalities such as antimicrobial effect, ion specificity or ion sensing property can be easily introduced in chelation system. Small molecular sulfonamide was synthesized with various Schiff bases to check the basic ion capturing property and product was analyzed with ^{1}H NMR. Cation chelating capacity of product was quantified by solvent extraction method, and appropriate types of sulfonamides were chosen as candidates. The selected sulfonamide types were formulated into particular structure such as microbead, membrane, or hydrogel and the ratio of ion capturing moiety was defined with FT-IR. Finally, their metal ion capturing capacity in actual circumstances and regeneration property in moderate acidic pH were verified. In conclusion, we confirmed the potential of these sulfonamide-functionalized structures to be used for water treatment, which can overcome the disadvantages of conventional water softening system.

Keywords: Sulfonamides, Chelating Ligand, Water Softening

Acceptance ID: WEPJ-P

Superior plastic deformability of shape memory Ni-Mn-Ga alloys near chemical ordering transition temperatures

X. X. Zhang[1], L. S. Wei[1], M. F. Qian[1,2], P. G. Martin[3], L. Geng[1], T. B. Scott[3], H. X. Peng[4]*

[1]School of Materials Science and Engineering, Harbin Institute of Technology, Harbin 150001, P.R. China
[2] Advanced Composites Centre for Innovation and Science (ACCIS), University of Bristol, Bristol BS8 1TR, United Kingdom
[3] Interface Analysis Centre, University of Bristol, Bristol BS8 1TL, United Kingdom
[4]Institute for Composites Science Innovation (InCSI), School of Materials Science and Engineering, Zhejiang University, Hangzhou, 310027, China
**Corresponding author. Tel: +86-451-86415894, Fax: +86-451-86413921, E-mail: xxzhang@hit.edu.cn*

Ni-Mn-Ga ferromagnetic shape alloys (FMSAs) exhibit large magnetic-field-induced strain (MFIS) and are attractive for applications in sensors, actuators and dampers operating at high frequencies. The requirement of such devices with complex shapes is growing. However, the plastic forming of polycrystalline Ni-Mn-Ga alloys is difficult due to their intrinsic brittleness and thus low plasticity. Here, high-temperature deformation behaviors of a polycrystalline $Ni_{51.3}Mn_{27.6}Ga_{21.1}$ alloy were investigated based on the processing map and microstructural observations. The processing map was built from the isothermal compressive curves tested at temperatures within 600 - 1000 °C and strain rates of 0.001 - 1 s^{-1}. The corresponding microstructural evolution with temperature and strain rate was systematically analyzed. The hot deformation mechanism of the Ni-Mn-Ga alloy was strongly dependent on the Zener-Hollomon parameter Z: the dynamic recrystallization was the dominant mechanism at low *Z* region in the disordered B2 state, then with increasing Z, dynamic recovery occurred and transition to ordered $L2_1$ state, and finally only dynamic recovery existed at high *Z* region. This proved that the intrinsic brittle polycrystalline Ni-Mn-Ga alloys are strikingly facile for large plastic deformation in the B2 state by dynamic recrystallization at temperatures 950 - 1000 °C and strain rates 0.02 - 0.3 s^{-1}, which opens a temperature and strain rate processing window for this intrinsic brittle alloys.

Acceptance ID: WFJ9-O

Investigation on Actuation Characteristics and life cycle behavior of Thin Film CuAlNi/Polyimide Shape Memory Alloy Bimorph and their application towards developing Flappers for Aerial Robots

Akash Kumar Jain, Akash K , Gaurav Karmarkar, Aniket Jadhav and

I A Palani

Mechatronics and Instrumentation lab, Discipline of mechanical Engineering·Indian Institute of Technology Indore, India
email: palaniia@iiti.ac.in

Two-way displacing Cu-Al-Ni Shape Memory Alloy/Polyimide composite films were developed by thermal evaporation. During actuation, the shape memory effect was observed and the return stroke during cooling was primarily due to the flexible substrate. Two different thicknesses of 25 μm and 50 μm Polyimide sheets were used as substrates. The fatigue life of the developed films was tested up to 1000 cycles. The results displayed no loss in shape memory effect, proving it can be used in MEMS devices. The actuation temperature of the Cu-Al- Ni film was around 250°C and due to this high actuation temperature the micro-flapper mechanism is hardly affected by ambient temperature changes thus making it robust and highly reliable over a vast range of extreme/challenging environments. The actuation properties during joule heating were studied for voltages ranging from 3 V – 8 V. To control the flapping frequency of wings, an electronic system has been designed to provide desired voltages in square wave form with control over pulse width and amplitude.

Keywords: Shape Memory Alloy, Bimorph, Micro Flapper, Micro Aerial Robot, Micro Actuator

Acceptance ID: X5FQ-O

Effect of Li Substitution on the Magnetic Properties of $Na_{1-x}Li_xFeSO_4F$ by Mössbauer spectroscopy

Hyunkyung (Choi), Sam Jin Kim, Chul Sung (Kim)

Department of Physics, Kookmin University, Seoul, Republic of Korea
newton@kookmin.ac.kr / presenting author
cskim@kookmin.ac.kr / corresponding author

Iron based fluorosulfate, *M*$FeSO_4F$ (*M*=Na, Li) compounds has been known as theoretical positive electrode material with high operating voltage [1]. The addition of Li ions engenders a charge difference and modification to the dimensionality of the lattice along with an redox potential, thus offering the new architectures and electrochemical behavior [2]. In this study, the crystal and magnetic structure of $Na_{1-x}Li_xFeSO_4F$ fluorosulfates has been investigated with the XRD, VSM and Mössbauer analysis. The $Na_{1-x}Li_xFeSO_4F$ (x=0.01, 0.05, 0.1) samples were synthesized by ionothermal method due to the poor hydrolytic stability. The prepared $Na_{1-x}Li_xFeSO_4F$ samples have monoclinic strucutres with space group of $P2_1/c$. The lattice constants and volume of the $Na_{1-x}Li_xFeSO_4F$ samples decreased with increasing Li concentrations. According to the temperature dependent magnetic susceptibility of $Na_{1-x}Li_xFeSO_4F$ samples showed abnormal antiferromagnetic behaviors with decreasing Néel temperture (T_N) due to Li substitution. For $Na_{1-x}Li_xFeSO_4F$, the T_N ordering temperatures, determined to be 33, 32.5, and 32 K for x=0.01, 0.05, and 0.1, respectively. In order to investigate the magnetic structure in terms of Fe nucleus, temperature dependent Mössbauer spectrum recorded at various temperatures ranging from 4.2 to 295 K. The Mössbauer spectrum of $Na_{1-x}Li_xFeSO_4F$ at room temperature consists of two doublets, indicating the existence of Fe^{2+} sites. Each spectrum of $Na_{1-x}Li_xFeSO_4F$ in the $T< T_N$ was fitted to two set(A, B-site) of asymmetrical 8 lines, considering the magnetic hyperfine field(H_{hf}) and electric quadrupole splitting(ΔE_Q) interaction. The H_{hf} and ΔE_Q values of $Na_{0.95}Li_{0.05}FeSO_4F$ at 4.2 K were determined to be $H_{hf,A}$ = 245 kOe, $\Delta E_{Q,A}$ = 2.76 mm/s and $H_{hf,B}$ = 312 kOe, $\Delta E_{Q,B}$ = 2.77 mm/s. From these results, these chagnes in $Na_{1-x}Li_xFeSO_4F$ are originated from the strong electric crystalline field which can be enhanced the asymmetric Mössbauer spectra below T_N.

Keywords: Antiferromagnetism, Cathode, Mössbauer spectroscopy

[1] TRIPATHI, R., RAMESH, T. N., ELLIS, B. L., NAZAR. L. F. 2010. Scalable Synthesis of Tavorite $LiFeSO_4F$ and $NaFeSO_4F$ Cathode Materials. *Angew. Chem. Int. Ed*., 49, 8738-8742.

[2] XIE, Y., YU, H. T., YI, T. F., WANG, Q., SONG, Q. S., LOU, M., ZHU, Y. R. 2015. Thermodynamic stability and transport properties of tavorite $LiFeSO_4F$ as a cathode material for lithium-ion batteries. *J. Mater. Chem. A*, 3, 19728-19737.

Acceptance ID: X9TQ-P

ASSESSMENT OF THE OPTICAL AND SOLID STATE PROPERTIES OF MANGANESE SULPHIDE (MnS) THIN FILM; THEORETICAL APPROACH.

[1, 2,]*Emmanuel Ifeanyi Ugwu,*

[1]*Department of Industrial Physics, Ebonyi State University, P.M.B 53, Abakaliki, Nigeria.*
[2]*Dept.of Physics, University of Jos, Jos, Nigeria.*
[1]*ugwuei@yahoo.com ;ugwuei2@gmail.com +2348059265326*

Assessment of the optical and Solid State properties of MgS thin film using theoretical approach of beam propagation technique in which a scalar wave is propagated through the material thin film deposited on a substrate with the assumption that the dielectric medium has homogenous reference dielectric constant term, ε_{ref} and a perturbed dielectric term, $\Delta\varepsilon_p(r)$ representing the deposited thin film medium is presented in this work. These two terms, constituted arbitrary complex dielectric function that describes dielectric perturbation imposed by the medium of for the system. This is substituted into a defined scalar wave equation in which the appropriate Green's Function was defined on it and solved using series solution technique in conjunction with Born approximation method in order to obtain a model equation of wave propagating through the thin film. This was used in computing the propagated field for different input regions of field wavelength such as ultraviolet, visible and infrared region respectively during which the influence of the dielectric constants of the thin film on the propagating field were considered. The results obtained from the computed field were used in turn to compute the band gaps, solid state and optical properties of the thin film such as reflectance, Transmittance and reflectance. The electrical and optical conductance was also computed.

Keywords; Scalar wave, optical and Solid State properties, Manganese Sulphide thin film, *Dielectric medium, Perturbation, Green's function, Band gap, Transmittance* Conductance.

Acceptance ID: XFUM-O

Aerosol assisted fabrication of Ag@SiO2 for catalytic reduction of 4-nitrophenol and antibacterial applications

Prof. Xingmao Jiang

Wuhan Institute of Technology
jxm@wit.edu.cn

Ag-decorated silica nanoparticles have been successfully fabricated by an aerosol method. The size of Ag nanoparticles (AgNPs) can be well controlled by tuning the precursor composition and calcination temperature and the AgNPs on the surface of silica can be gradually grown with the increase of the calcination temperature. The as-prepared nanocomposites with well dispersed AgNPs possessed distinguished catalytic activities in catalysing for the reduction of 4-NP by $NaBH_4$ in the aqueous phase. The nanostructured particles showed outstanding antimicrobial properties. Through the coupling of contact triboelectrification and electrostatic induction, the self-charging capability has been realized due to the ambient wind-induced vibrations of a triboelectric membrane between the two supercapacitors.

Acceptance ID: XYEH-O

Crystal growth-based methods used for manufacturing of volumetric composite nanomaterials for plasmonics/metamaterials

D. A. Pawlak [1,2], K. Sadecka [1], P. Osewski [1], M. Gajc [1], Nowaczynski [1,2], M. Kurowska [1], P. Paszke [1,2], B. Surma [1], A. Klos [1], J. Toudert [3]

[1]Institute of Electronic Materials Technology, Wolczynska 133, 01-919 Warsaw, Poland.
[2]Centre of New Technologies, University of Warsaw, Banacha 2C, 02-097 Warsaw, Poland.
[3]The Institute of Photonic Sciences, 08860 Castelldefels, Barcelona, Spain.
Dorota.Pawlak@itme.edu.pl

Novel research areas have been developed in the field of photonics: metamaterials and nanoplasmonics.

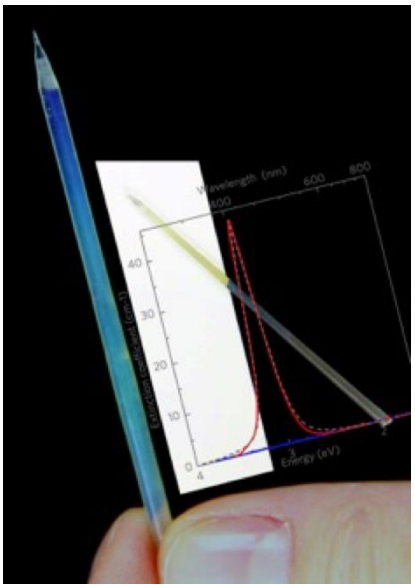

Figure 1: Nanoplasmonic composite with a localized surface plasmon resonance at 405 nm obtained by the Nanoparticle Direct Doping method [3]

By utilizing the ideas developed in these research areas and using specially-designed materials, unusual electromagnetic properties such as artificial magnetism, negative refractive index, cloaking and squeezing photons through subwavelength holes have been demonstrated. These novel fields need new material fabrication techniques, especially bottom-up approaches such as self-organization. Two novel bottom-up manufacturing methods will be presented: (i) method based on directionally-grown self-organized eutectic structures [1, 2]; and (ii) NanoParticles Direct Doping method (NPDD) [3] based on directional solidification of dielectric matrices doped with various nanoparticles. In both cases we apply one of the crystal growth methods - the micro-pulling down method - to create the material. We will discuss: (i) Volumetric materials based on bulk glasses doped with plasmonic nanoparticles obtained by NPDD, with localized surface plasmon resonance at visible and IR wavelengths [3]; (ii) Bi_2O_3-Ag eutectic-based composite exhibiting tunable localized surface plasmon resonance ~600 nm [4, 5, 6], and second harmonic generation [7]; (iii) materials with enhanced luminescence eg. at 1.5 um wavelength, and up-conversion processes due to plasmonic resonances [3, to be published]; (iv) Eutectic material with subwavelength transmission at IR frequencies [8, to be published]; (v) Eutectic materials with enhanced Faraday effect [unpublished]; (vi) Pivotal for metamaterials structures such as split-ring resonators obtained in eutectic composites [2]. Utilizing

crystal growth application for manufacturing of novel photonic composites may enable their easy application.

Keywords: Nanocomposites, plasmonics, metamaterials, eutectic composites, nanoparticles

[1] PAWLAK, D. A., KOLODZIEJAK, K., TURCZYNSKI, S., KISIELEWSKI, J., ROZNIATOWSKI, K., DIDUSZKO, R., KACZKAN, M., MALINOWSKI, M., 2006. Self-organized, rod-like, micron-scale microstructure of $Tb_3Sc_2Al_3O_{12}$-$TbScO_3$:Pr eutectic, *Chem. Mat.* 18, 2450-2457.

[2] PAWLAK, D. A., TURCZYNSKI, S., GAJC, M., KOLODZIEJAK, K., DIDUSZKO, R., ROZNIATOWSKI, K., SMALC J., VENDIK, I., 2010. How far are we from making metamaterials by self-organization? The microstructure of highly anisotropic particles with an SRR-like geometry, *Adv. Funct. Mat.* 20, 1116-1124.

[3] GAJC, M., SURMA, B., KLOS, A., SADECKA, K., ORLINSKI, K., NIKOLAENKO, A. E., ZDUNEK, K., PAWLAK D. A., 2013. NanoParticle Direct Doping: Novel method for manufacturing three-dimensional bulk plasmonic nanocomposites, *Adv. Funct. Mat.* 23, 3443-3451.

[4] SADECKA, K., GAJC, M., ORLINSKI, K., SURMA, B., KLOS, A., JOZWIK-BIALA, I., SOBCZAK, K., DLUZEWSKI, P., TOUDERT, J., PAWLAK, D. A., 2015. When Eutectics Meet Plasmonics: Nanoplasmonic, Volumetric, Self-Organized, Silver-Based Eutectic, *Adv. Opt. Mat.* 3, 381-389.

[5] SADECKA, K., TOUDERT, J., SURMA, B., PAWLAK, D. A., 2015. Temperature and atmosphere tunability of the nanoplasmonic resonance of a volumetric eutectic-based Bi_2O_3-Ag metamaterial, *Opt. Exp.* 23, 19098-19111.

[6] SADECKA, K., BERGER, M. H., ORLINSKI, K., JOZWIK-BIALA, I., PAWLAK, D. A., 2015. Evolution of silver in a eutectic-based Bi_2O_3–Ag metamaterial, 2017. *J. Mat. Sci.* in press.

[7] DESKA, R., SADECKA, OLESIAK-BANSKA, J., MATCZYSZYN, K., PAWLAK, D. A., SAMOC, M., 2017. Nonlinear plasmonics in eutectic composites: second harmonic generation and two-photon luminescence in a volumetric eutectic-based Bi_2O_3-Ag metamaterial, 2017. *Appl. Phys. Lett.* 110, 031102- 031105.

[8] MYROSHNYCHENKO, A., STEFANSKI, A., MANJAVACAS, A., KAFESAKI, M., MERINO, R. I., ORERA, M., PAWLAK, D. A., GARCIA DE ABAJO, E. J., 2012. Interacting plasmon and phonon polaritons in aligned nano- and microwires, 2012. *Opt. Exp.* 20, 10879-10887.

[8], MYROSHNYCHENKO, A., STEFANSKI, A., MANJAVACAS, A., KAFESAKI, M., MERINO, R. I., ORERA, M., PAWLAK, D. A., GARCIA DE ABAJO, E. J., 2012. Interacting plasmon and phonon polaritons in aligned nano- and microwires, 2012. *Opt. Exp.* 20, 10879-10887.

Acceptance ID: XYZA-I

A highly efficient absorbent for hydrophobic liquids using graphene-sponge composite

*Sungwoo Chun[1], Hyungjune Lee[1], Wonkyeong Son[1], Soa Bang[1], and Wanjun Park[1]**

[1]Department of Electronics and Computer Engineering, Hanyang University,
Wangsimni-ro 04763, Seoul 133-791 South Korea
Fax: +82(31)-2220-4319 E-mail address: wanjun@hanyang.ac.kr

Due to water pollution with environmentally hazardous liquids, purifying technologies have attracted considerable interest. In the typical method, hydrophobic or oleophilic absorbents have been developed for selective removal of hydrophobic contaminants, including oils and organic solvents, in order to purify polluted water. In general, absorbents require a porous structure to increase absorption efficiency. Zeolite, fabrics, and sawdust have been used for the purifying process. To increase filtration efficiency, it is critical to develop a material that possesses high selectivity and capacity to absorb the polluted liquids from water. Besides microporous polymer-based materials, which have already been intensively studied for this purpose, graphene has recently attracted great interest as the most effective absorbent material due to its large surface area and strong hydrophobicity. Of the many approaches evaluated, graphene composites introduced into a porous substance using a facile dip-coating method with graphene oxide (GO) nanoparticles emerged as the preferred absorbent to increase the absorption of pollution liquids (34–140 times of its own weight for chloroform) [1-2]. The approaches should also contain a reduction process for converting hydrophilic GO to hydrophobic reduced GO (rGO) in order to increase the selective capturing capability.

In this work, we propose an absorbent composed of hydrophobic graphene-sponge composite (GSC) by embedding graphene flakes (GFs) directly into a polyurethane sponge (PS) acting as a porous substance. With the self-aggregation nature of GFs in dispersion, the dip-coating method easily enhances graphene concentration, thereby increasing the capturing capability for polluted liquids. Furthermore, the hydrophobicity of the GFs directly reflected by the absorbent capacity is attributed to the selective capture of the polluting liquids mixed in the water, with no additional process to obtain the hydrophobic character. The adsorption capability and selectivity of the proposed absorbent was tested for various hydrophobic liquids common in water.

Keywords: Graphene composite, Graphene absorbent, Hydrophobic coating

[1] Zhu, H., Chen, D., An, W., Li, N., Xu, Q., Li, H., He, J. & Lu, J. 2015. A robust and cost-effective superhydrophobic graphene foam for efficient oil and organic solvent recovery. *Small*, 11, 5222-5229.

[2] Tjandra, R., Lui, G., Veilleux, A., Broughton, J., Chiu, G. & Yu, A. 2015. Introduction of an enhanced binding of reduced graphene oxide to polyurethane sponge for oil absorption. *Ind. Eng. Chem. Res*., 54, 3657-3663.

Acceptance ID: XZXZ-P

The Spectral Heterogeneity and Size Distribution of the Fluorescent Carbon Dots Derived from Spectroscopic Methods

Chih-Wei Chang[1]

[1]*Department of Chemistry, National Changhua University of Education, No1, Jinder Road, Changhua, Taiwan, 50058*
cwchang@cc.ncue.edu.tw

We have performed comprehensive studies on the photoluminescence properties of the carbon dots prepared from citric acid (C-dots^{CA}) and citric acid+ethylenediamine (C-dots^{CA+EDA})[1]. The cryogenic experiment confirms that the excitation dependent fluorescence and the spectral relaxation dynamics of the C-dots are associated with the presence of multiple emissive states/species in the C-dots instead of solvation dynamics. Moreover, we have also compared the size of the C-dots estimated from the TEM images and fluorescence anisotropy methods. Our experimental results indicate that the fluorescence anisotropy method not only avoids the formation of aggregates during the sample preparation processes, but also selectively detects the size of the emissive C-dots in the solution; therefore, the fluorescence anisotropy method is ideal for studying the size dependent optical properties of the C-dots.

Keywords: Carbon dots, fluorescence anisotropy, time-resolved emission spectra,

[1] YING-FENG HSU., YU-HSUN CHEN.&CHIH-WEI CHANG. 2016. The spectral heterogeneity and size distribution of the carbon dots derived from time-resolved fluorescence studies. Phys. Chem. Chem. Phys. 18, 30089-30092

Acceptance ID: Y2G6-O

Wearable graphene/polydimethylsiloxane (PDMS) composite for pressure sensor

Soa Bang[1], Sungwoo Chun[1], Wonkyeong Son[1], and Wanjun Park[1]*

[1]Department of electronic and computer Engineering, Hanyang University
Wangsimni-ro, Seoul, South korea, 04763
**E-mail: wanjun@hanyang.ac.kr*

Development of wearable piezoresistive pressure sensors is an emerging field for various future applications, such as electronic skin and soft robotics [1]. As materials for these sensors, graphene/polymer composites are one of the best candidates because of its low-cost, super-elastic, superb electrical property, and easy fabrication. In this work, we propose a wearable pressure sensor using conductive graphene/PDMS composite especially for the application of pressure sensor which is expected to open a new route for low-cost pressure sensors with potential facile integration into future wearable sensors such as flexible touch-on displays, human–machine interfacing devices and prosthetic skins.

The composite was fabricated by dispersing the graphene flakes and PDMS separately in hexane, thus reducing a percolation threshold to 0.87 vol% due to uniform dispersion. After configuring the pressure sensor by adding Pt electrodes on both sides of the composite, the sensor demonstrates sensitive responses in resistance for the vertically applied pressure to 100 Pa from 1 MPa which exceeds general human perception range for touch. The sensor also shows reliable characteristics with 1500 cycles of repeated measurements. Finally, after the attachment on biological skin, the sensor demonstrates to detect the movements of fingers and arms and to monitor the cardiovascular health from the detection of wrist pulse.

Keywords: flexible composite, graphene, conductive polymer

[1] GONG, S., SCHWALB, W., WANG Y., CHEN Y., TANG Y., SI J., SHIRNAZADEH, B & CHENG W. 2013. A wearable and highly sensitive pressure sensor with ultrathin gold nanowires. *Nature.Com*., 10.1038.

Acceptance ID: YA82-P

Synthesis & Characterization of TiO_2 Nanoparticles by Neem Leaves (Azadirachta Indica) Extract.

Bhasha [a], Rukmani Sharma[a], *Santosh Singh*[b], *Anjana Sarkar*[a] ,Purnima Jain[a]
[a]Netaji Subhash Institue of Technology, Dwarka Sec-3, *University* of Delhi,INDIA
CSIR-National Physical Laboratory, New Delhi, INDIA
Presenting author's email- rukmanis13@gmail.com

The synthesis of nanoparticles from plant extract through eco-friendly green chemistry has recently drawn attention of researchers with a view to develop TiO_2 nanoparticles. Many plants extracts like Lemon Grass, Indian Gross berry and Neem Leaves have been tried for the synthesis of TiO_2 nanoparticles. Neem has chosen because of its functional antinoceptive,antioxidant,anti-inflammatory, antidiabetic, antifungal and antimicrobial properties. In the present paper, we reported the synthesis of TiO_2 Nanoparticles by using extracts of Neem Leaves and Titanium isopropoxide as a precursor. The characteristic properties of TiO_2 nanoparticles were studied by XRD, SEM/EDX, TEM, UV-VIS and FTIR analytical techniques to confirm their structural, morphological and optical attributes. The sharp peak of XRD pattern exhibits the polycrystalline nature and formation of TiO_2 rutile structured nanoparticles. SEM/EDX and TEM images revealed the spherical structure of nanoparticles with size varying in the range of 10-20 nm. UV-VIS spectrum recorded in 1100 – 200 nm region showed the excitonic emission peak at about 380 nm while IR transmission spectrum showed the characteristic stretching modes of TiO_2.The green route approach increases the economic viability of a material. These results confirmed the synthesis of TiO2 nanoparticles via non-hazardous green chemistry route by using neem leaves extract

Keywords: TiO_2 Nanoparticles, Neem (Azadirachta Indica) Extracts, Titanium Isopropoxide, Green Chemistry

Reference

1. X. Zhao, Q. Zhang, Y. Hao, Y. Li, Y. Fang, and D. Chen "Alternate multilayer films of poly(vinyl alcohol) and exfoliated graphene oxide fabricated via a facial layer-by-layer assembly". *Macromolecules,* Vol. 43, No. 22, pp 9411-9416, 2010.

2. Liang J., Huang Y., Zhang L., Wang Y., Ma Y., Guo T., Chen Y.: Molecular-level dispersion of graphene into poly(vinyl alcohol) and effective reinforcement of their nanocomposites. Advanced Functional Materials, 19, 2297–2302 (2009).

Acceptance ID: YN4G-O

An Experimental Study on Reinforced Concrete Beams Strengthened with Prestressed NSM CFRP Tendon

Woo-tai Jung[1] , *Hee-beom Park*[1], *Jong-sup Park*[1], *and Jae-yoon Kang*[1]

[1]*Structural Engineering Research Institute, Korea Institute of Civil Engineering and Building Technology, Goyang, Republic of Korea.*
woody@kict.re.rk

FRP(fiber reinforced polymer) is one of functional materials to replace steel such as reinforcing bar and tendon. Mostly FRP materials are applied in the repair and strengthening area. This study investigated on the flexural strengthening performance of reinforced-concrete beams strengthened with prestressed near-surface mounted (NSM) tendon. Two prestressing systems are used to introduce prestressing force to specimens in this study. One is pre-tension system and the other is new prestressing system with anchorage like post-tension. The test results revealed that the surface treatment of the CFRP tendon improved the strengthening performance by 13% and anchorage needed to enhance strengthening effect. Also in case of using the CFRP tendon with low bond strength, it shows that strengthening effect can be improved by executing beforehand surface treatment of the tendon on site.

Keywords: FRP, tendon, nsm, strengthening, prestress

Acceptance ID: YQRA-P

Low Density Composite and Hybrid Foams Based on Aligned Carbon Nanotube Sheets

Bradford [*1], *Lubna*[1], *Faraji* [1], *Yildiz* [1], *Stano* [1], *Aly*[1] *and Jur*[1]

[1] *Department of Textile Engineering, Chemistry and Science, North Carolina State University, Campus Box 8301, Raleigh, NC 27695, USA*
*E-mail: philip_bradford@ncsu.edu**

Ultralow density foams with multifunctional and tunable properties are desirable for many engineering applications. We have previously demonstrated (and presented at AFM 2015) the ability to fabricate stable, ultralow density carbon nanotube (CNT) foams by stacking aligned CNT sheets and then coating with a conformal carbon coating [1]. While those foams are very interesting by themselves, there has arisen a need to hybridize them with other materials to optimize their properties for applications in energy absorption materials, filtration and separation, catalysis, sensors, supercapacitors and batteries. In addition, even though those foams were stable under pure compression loading, their overall durability needs improvement. Our presentation will detail two approaches using the CNT foams as the primary scaffold for the deposition of other functional and stabilizing materials.

In the first, atomic layer deposition (ALD) was used to coat the interconnected CNT structure with thin coatings of ceramic oxide materials. Even thought the foam samples are large and have a significant surface area, their ultralow density enables very conformal deposition throughout the foam. Even when ceramic coated, the hybrid foams continued to exhibit elastic recovery due to the underlying CNT network. The compressive mechanical properties of the foams became, to a degree, tunable by changing the thickness of the oxide. The thermal stability increased and the hybrid was demonstrated as a catalytic material.

In the second approach, a new technique was used to solution coat the ultralow density CNT foams with polymer coatings. Low viscosity polymer solutions were used to fully wet and fill the foam structure. As the solvent was rapidly evaporated, the CNT foams remained dimensionally stable. This resulted in very low density CNT structures where the individual CNTs in the CNT foam network were coated with polymer. Composite foams were prepared with polydimethylsiloxane solutions concentrations ranging from 2.5% to 50% by weight. This method dramatically increases the durability of the materials and allowed for a wide range of composite foam densities and mechanical properties.

Keywords: Carbon nanotube, foam, anisotropic, tunable, multi-functional

[1] FARAJI, S., STANO, K., YILDIZ, O., LI, A., ZHU, Y., , & BRADFORD, P. 2015. Ultralight Anisotropic Foams from Layered Aligned Carbon Nanotube Sheets. *Nanoscale*, 7, 17038-17047.

Acceptance ID: YXD7-O

Enhanced electro-dynamic responses of relaxor and normal ferroelectric polymer blends

Hung Viet (Tran)[1], *Quang Van (Duong)*[1], *Fabrice (Domingues Dos Santos)*[2], *Seung Tae (Choi)*[1]

[1] *School of Mechanical Engineering, Chung-Ang University, 84 Heukseok-Ro, Dongjak-Gu, Seoul 06974, Republic of Korea*

[2]*Piezotech S.A.S., Arkema-CRRA, Rue Henri Moissan, 69493 Pierre-Benite Cedex, France*

trantomhung@cau.ac.kr (presenting author: Hung Viet Tran)

stchoi@cau.ac.kr (corresponding author: Seung Tae Choi)

The electromechanical properties of relaxor ferroelectric polymers (RFPs) such as poly(vinylidene fluoride-trifluoroethylene-chlorofluoroethylene) [P(VDF-TrFE-CFE)] and poly(vinylidene fluoride-trifluoroethylene-chlorotrifluorethylene) [P(VDF-TrFE-CTFE)], can be strongly influenced by blending with a small amount of normal ferroelectric polymers (NFPs) such as poly(vinylidene fluoride-trifluoroethylene) [P(VDF-TrFE)]. NFPs with different compositional ratios of VDF and TrFE were blended into RFPs with different compositional ratios of VDF, TrFE and CFE or CTFE monomers, with which bimorph actuators were fabricated. Dynamic strain response of blended polymer bimorph actuators was measured with a confocal laser displacement sensor, from which strain amplitude, frequency response, and phase delay were evaluated. Interestingly, the effect of P(VDF-TrFE) (75:25) and P(VDF-TrFE) (55:45) on the electro-dynamic responses of the blended polymers is quite opposite even they are both normal ferroelectric. The P(VDF-TrFE) (55:45) enhances the strain amplitude and mechanical energy density of the blended polymers, but the P(VDF-TrFE) (75:25) reduces. The optimum combination of NFPs and RFPs was proposed for enhanced electro-dynamic responses of the blended polymers.

Acceptance ID: Z2XU-O

Synthesis of Au modified SnO_2 nanoflowers and its gas sensing performances toward SO_2

*Lingyue Liu, Wei Yang, Shaoming Shu, Shantang Liu**

Email: stliu@wit.edu.cn
Key Laboratory for Green Chemical Process of Ministry of Education and School of Chemistry and Environmental Engineering, Wuhan Institute of Technology, Xiongchu Avenue, Wuhan, 430073, PR China

Au modified tin dioxide(SnO_2) nanoflowers were synthesized by a hydrothermal process and a solution reduction process. The obtained products were characterized by X-ray diffraction(XRD), scanning electron microscopy(SEM), X-ray photoelectron spectroscopy(XPS), photoluminescence spectra(PL), electron spin resonance(ESR) and in-stiu diffuse reflectance FTIR spectra technique. Results demonstrated the Gold nanoparticles(AuNPs) were perfectly embedded in the surface of SnO_2 nanoflowers. The sensor based on the Au-SnO_2 nanoflowers showed a high sensitivity about 10 to 20 ppm of sulfur dioxide and the minimum detectable concentration about 1 ppm at the work temperature of 200°C. The enhanced SO_2 sensitive properties of Au-SnO_2-based sensor could be attributed to the appropriate content of oxygen vacancies and the potential spillover effect of AuNPs. Therefore, this work demonstrates that the appropriate amount of oxygen vacancies in Au-SnO_2 nanocomposites can efficiently improve the response of sensor for detection of the harmful and poisonous sulfur dioxide.

Acceptance ID: Z82N-P

Zn-Poly(Aniline-Co-5-Aminosalicylic Acid) Battery

Zhuan Hu Jinqing Kan *

School of Chemistry and Chemical Engineering, Yangzhou University, Yangzhou, 225002, China

Zn-PANI secondary batteries have shown many excellent characteristics, such as high reversible energy density and columbic efficiency, long cycle life and low self-discharge rate [1-3]. However, polyaniline has an electrochemical activity and low conductivity at pH > 4, while zinc is easily corroded in acidic aqueous electrolytes (pH≤4), which limits the commercialization of the secondary batteries. Synthesizing new types of the aniline-based copolymers has greatly attracted the recent researchers. The copolymerization of aniline and other monomers (such as -OH, -SO_3H, -COOH) have been widely used for the synthesis of aniline-based copolymers with improved electroactivity.

The copolymer, poly(aniline-co-5-aminosalicylic acid), was prepared by the methods potentiostatic electrochemical copolymerization in a three-electrode cell. The poly(aniline-co-5-aminosalicylic acid), A zinc sheet and polypropylene non-woven fabric were mounted in a transparent vessel. The structure diagram of the Zn-poly(aniline-co-5-aminosalicylic acid) secondary battery is as follows (Fig.1). The relationship between coulombic efficiency and cycle number was shown Fig.2.

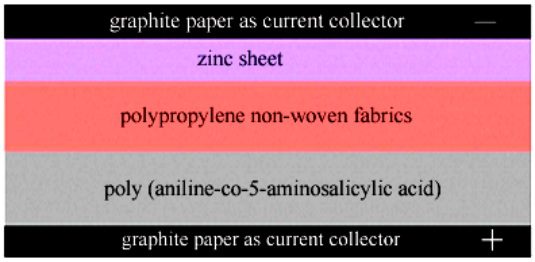

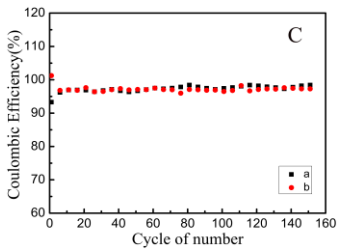

Fig.1 The structure schematic of the battery; Fig.2 The relationship between coulombic efficiency and cycle number

The Zn-poly(aniline-co-5-aminosalicylic acid) secondary battery has an output large-capacity of 145 mAh g^{-1} with a Columbic efficiency of >97% after 150 cycles between 0.75 V and 1.5 V. The new secondary battery will possess broad commercial application prospect.

Acknowledgements：This project was supported by the National Science Foundation of China (No.20873119), and by the Priority Academic Program Development of Jiangsu Higher Education Institutions. Part of the data was from the Testing Center of Yangzhou University.

References

[1] M.Chen, G.A.Rincon-Mora, IEEE T. Energy Conver.21 (2006) 504.
[2] B.Z.Jugovic, T.L.Trisovic, J.S.Stevanovic, M.D.Maksimovic, B.N.Grgur, Electrochim. Acta 51 (2006) 6268.
[3] M.Pasta, C.D.Wessells, R.A.Huggins, Y.Cui, Nat. commun. 3(2012) 1149.
Acceptance ID: Z9E4-P

* Corresponding author, e-mail: jqkan@yzu.edu.cn, Tel: 86 514 87975590 9415.

Novel Properties of cluster-based nanostructures

Wang Guanghou

National Laboratory of Solid State Microstructures
& Department of Physics
Nanjing University, Nanjing 210093

Atomic clusters consist of a few to thousands of atoms and/or molecules, and attract a great attention in nanoscience and nanotechnology since they can be used as building blocks to assemble various kinds of nanostructures with novel properties. One of strategies for growing nanostructures with cluster beams consists in depositing low-energy particles. Ideally, by depositing the clusters with low kinetic energies, one would like to conserve the memory of the free-cluster phase to form thin films with their original properties. Since the kinetic energy is of the order of eV per cluster, i.e., a few meV per atom, which is negligible compared to the binding energy of an atom in the cluster, no fragmentation of the clusters is expected upon impact on the substrate [1]. In this talk we would like to present some of our work as examples to show how this can be realized.

1) Quantization of surface modes of silicon clusters

2) Multi-channel Conductance Resonance of Au cluster-based nanostructures

3) Strong magnetoelectric effect in Tb-Fe/(Zr0.52Ti0.48)O3 heterostructures by alloy clusters.

4) Coupling enhancement of plasmon between Ag nanoclusters

5) Quantum modification on surface states of Dirac systems by atomic clusters.

It demonstrated that production, manipulation and deposition of gas phase clusters is of primary importance for the synthesis of nanostructured materials and for the development of industrial processes based on nanotechnology [2].

References:
[1] P. Jensen, Review of Modern Physics 71(5), 1695 (1999).
[2] K. Wigner P. Piseri, H. Vakedi Tafreshi, P. Minani, J. Phys. D. Appl. Phys. 39, R439 (2006)

Acceptance ID: Z9QA-O

Self-Multiplying Fractal Machining of Silicon

Erwin Berenschot[1], Rolf Vermeer[2], Henri Jansen[3], Roald Tiggelaar[4], Han Gardeniers[1], Niels Tas[1]

[1] MESA+Institute for Nanotechnology, Mesoscale Chemical Systems Group University of Twente, 7522 NB Enschede, The Netherlands
[2] Micronit BV, Colosseum 15, 7521 PV, Enschede, Netherlands
[3] DTU Danchip National center for Micro and Nanofabrication, Technical University of Denmark, 2800 Kgs. Lyngby, Denmark
[4] MESA+ Institute for Nanotechnology, NanoLab Cleanroom, University of Twente 7522 NB Enschede,The Netherlands
E Mail : n.r.tas@utwente.nl

The main aim of our work is to develop wafer-scale nanofabrication strategies for formation of small (down to sub-10 nm level) and complex 3D-nanostructures in mono-crystalline substrates. By combine anisotropic etching of silicon with so called "corner lithography" we have shown the formation of 2D-extruded (fig. 1a) as well as full-3D concave fractal structures in silicon [2, 3]. For example, based on only one micro-sized photo-lithographic opening, we were able to machine a template for formation of a folded silicon oxide shell having 625 nano-apertures on all the apices (fig. 1b). These 3D-fractal structures can be formed in large numbers in parallel (fig. 1c)Currently, we would like to introduce the formation of *convex* 3D-fractal structures in silicon based on a modified corner lithography process, fig. 2. Starting with the formation of a micron sized tetra-hedron on a {111} silicon wafer [4], we are able to selectively open the silicon oxide mask at the apex, and form three tetrahedrons with a size of the order of 100 nm (fig. 2a, b). In a similar fashion we can form two nano-ridges from a single ridge (fig. 2c, d). This is the first and essential step showing that multiple self-similar substructures can be formed from a convex silicon structure.

a)

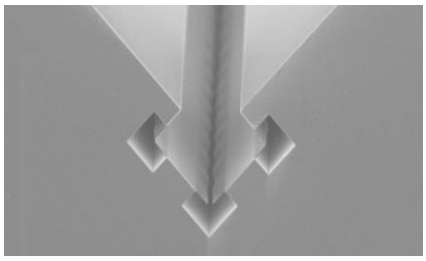

b)

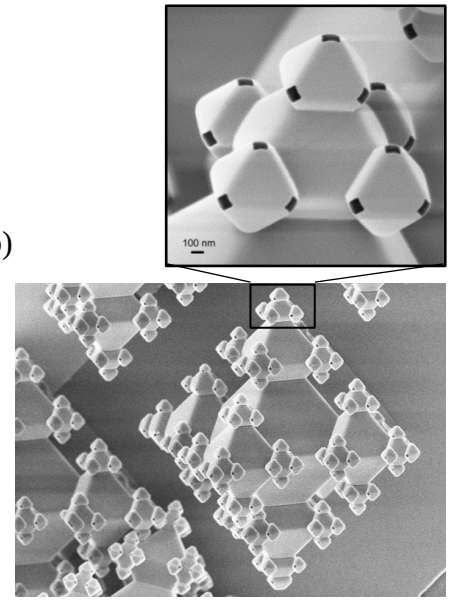

c)

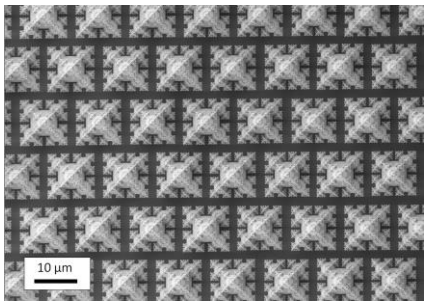

Fig. 1: a) Self-multiplying channel structure fabricated in silicon, b) 3D-octahedral fractal structure (silicon oxide shell formed in a concave silicon mold) [2, 3], c) Overview of many fractal structures which were fabricated in parallel.

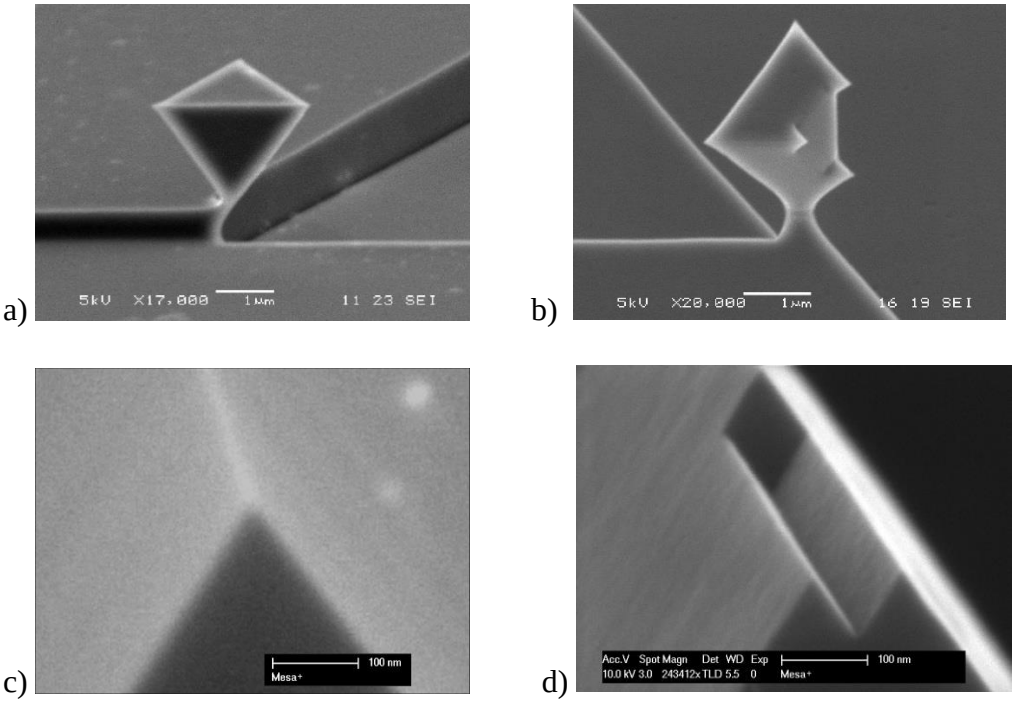

Fig. 2: a) Original tetrahedral silicon structure, b) After formation of self-similar substructures. c) Original nano-ridge silicon structure, d) After formation of two self-similar nano-ridges.

The significance of the proposed fabrication route is the self-multiplying formation of convex nanostructures in crystalline materials such as silicon. This is important for applications where such small convex sub-structures are essential for a specific functionality. One could think of silicon nanocrystals, employed in components like single electron transistors and quantum dots, and silicon nanowires as transistors or chemical sensors. Strategies for self-multiplying 3D-nanostructuring are expected to have significant impact in the field of energy storage and energy conversion.

Keywords: Silicon, anisotropic etching, fractal, 3D machining

[1] BERENSCHOT, E.J.W., BUROUNI, N., SCHURINK, B., VAN HONSCHOTEN, J., SANDERS, T.G.P., TRUCKENMULLER, R., JANSEN, H.V., ELWENSPOEK, M.C., VAN APELDOORN, A.A., TAS, N.R. 2012. 3D Nanofabrication of Fluidic Components by Corner Lithography. *SMALL*, 8, No. 24, 3823-3831.

[2] BERENSCHOT, E.J.W., JANSEN, H.V., TAS, N.R. 2013. Fabrication of 3D fractal structures using nanoscale anisotropic etching of single crystalline silicon. *J. Micromech. Microeng.*, 23, 055024 (10pp).

[3] BERENSCHOT, E.J.W., YAGUBIZADE, H., JANSEN,H.V., DIJKSTRA, M., TAS, N.R. 2014. Fabrication of 2D-extruded fractal structures using repeated corner lithography and etching. *9th IEEE International Conference on Nano/Micro Engineered and Molecular Systems, IEEE-NEMS*, 6908830, 374-377.

[4] KOZHUMMAL, R., BERENSCHOT, E., JANSEN, H., TAS N.,
ZACHARIAS, M., ELWENSPOEK, M. 2012. Fabrication of micron-sized tetrahedra by
Si<1 1 1> micromachining and retraction edge lithography. *J. Micromech. Microeng.*, 22 085032 (7pp)

Acceptance ID: ZG42-O

SYMPOSIUM 2: Advances in Thin Films

Transmittance enhancement in two-dimensional chalcogenides

A.M. Adam[1,2], L.V. Panina [1,3], P. Petkov[4]

[1] National University of Science and Technology, MISiS, Moscow 119991, Russia
[2] Physics Department, Faculty of Science, Sohag University, Sohag 82524, Egypt
[3] Institute for Design Problems in Microelectronics RAS, Moscow 124681, Russia
[4] Physics Department, University of Chemical Technology and Metallurgy, Sofia 1000, Bulgaria

Graphene, a single atomic layer of graphite, demonstrate remarkable electronic properties due to its energy band structure. Graphene is a perfect electronic and thermal conductor, and that is why graphene-based materials have been proposed for many applications ranging from transparent conductors, thermal interface materials to barristor transistor-like devices [1-4]. A large number of other layered materials can be thinned down into two-dimensional nanostructures and monolayers [1-3]. Two-dimensional (2D) materials can be assembled layer by layer to form a van der Waals heterostructure [3,4]. As a member of the 2D materials family, Bi_2X_3 (X= Se, Te) has been widely investigated for thermoelectricity [5]. Moreover, they have been discovered to be topological insulators and have led to an intensive research [6]. Bi_2X_3 based chalcogenides exhibit a layered, rhombohedral crystal structure, each layer consists of five covalently bonded atomic planes, X-Bi-X-Bi-X, known as a quintuple layer. Experimentally, it was stated that 3D materials which are held together by the weak van der Waals forces can be exfoliated into thin flakes by mechanical or chemical exfoliation methods, a method known as a top-down process. Thus, it is possible to create few quintuple layers from bulk Bi_2Se_3 with ‘‘graphene-inspired’’ exfoliation methods as bulk Bi_2Se_3 possesses the graphene-like layered structure [7]. Miniaturizing the source bulk materials down to few nanometers would result in a significant enhancement of light transmission through the prepared layers. In our work, thickness reduction as well as simultaneous annealing led to an optical transmission of 99.6%. Such significant enhancement can be ascribed to nanophotonic effect of zero-wave anti-reflection unique to ultra-small thicknesses. With such kind of transmissivity enhancement, optoelectronic applications including transparent electrode can be met.

Keywords: 2D Chalcogenides; light transmission; thickness reduction; annealing; band gap.

[1] Yang, H.; Heo, J.; Park, S.; Song, H. J.; Seo, D. H.; Byun, K. E.; Kim, P.; Yoo, I.; Chung, H. J.; Kim, K. 2012 Graphene Barristor, a Triode Device with a Gate Controlled Schottky Barrier. *Science*, 336, 1140–1143.

[2] Andreas Pospischil and Thomas Mueller, 2016, Optoelectronic Devices Based on Atomically Thin Transition Metal Dichalcogenides *Appl. Sci*. 6, 78.

[3] Novoselov, K.S.; Jiang, D.; Schedin, F.; Booth, T.J.; Khotkevich, V.V.; Morozov, S.V.; Geim, A.K. 2005Two-dimensional atomic crystals. *Proc. Nat. Acad. Sci*., 102, 10451–10453.

[4] Geim, A.K.; Grigorieva, I.V. 2013 Van der Waals heterostructures. *Nature*, 499, 419–425.

[5]. Mishra, S. K., Satpathy, S. & Jepsen, O. 1997 Electronic structure and thermoelectric properties of bismuth telluride and bismuth selenide. *J. Phys. Condens. Mat*. 9, 461–470.

[6] Jie Yao, Kristie J. Koski, Weidong Luo, Judy J. Cha, Liangbing Hu, Desheng Kong, Vijay Kris Narasimhan, Kaifu Huo, Yi Cui, 2014 *NATURE COMMUNICATIONS*, 5:5670, 1-7.

[7] Liping Sun, Zhiqin Lin, Jian Peng, Jian Weng, Yizhong Huang, Zhengqian Luo, 2014, *SCIENTIFIC REPORTS*, 4: 4794, 1-9.

Acceptance ID: 2KLW-O

Functional Conductive Polymer Thin Film for Impedimetric Screening of Biorecognition Interfaces

Ramazan KIZIL[1], Fatma G. GÜLER[2], Sezai SARAÇ[2]

Istanbul Technical University, Chemical Enginering Department[1], Chemistry Department[2], Maslak, 34469 Istanbul, Turkey, correspondence: kizilr@itu.edu.tr

There are ingenious approaches for fabricating novel electrical or optical sensing platforms with enhanced sensitivity and selectivity by incorporation of a functional thin film of organic transducing molecules in the device architecture. Electroactive polymers, which are capable of transporting redox species on their side chains, are becoming promising film materials for the construction of electron transferring interfaces for electrochemical sensing. The attractiveness of such an inherently conductive polymeric thin film interface between a metal measurement electrode and a biological system lies in its unmatched surface tailoring convenience through derivatization of the polymer backbone with a range of different chemical functional groups.

We used electroactive copolymers of thiophene (Th) , 3-thiophene carboxylic acid (3-ThCA), and 3,4-thiophene dicarboxylic acid (3,4-ThDCA) grown on a gold coated glass by electro-oxidative polymerization. Electrochemical co-polymerization of these monomers was characterized by electrochemical impedance spectroscopy (EIS), FTIR, FE-SEM and AFM. The film morphology of the Poly(Th-co-,3.4-ThDCA) and Poly(Th-co-,3-ThDCA) copolymers was found to be different. While the surface morphology of Poly(Th-co-,3-ThDCA) layer was reminiscent of typical cauliflower like spherical growth of conductive polymers in low donicity solvent, acetonitrile, the polymer film of Poly(Th-co-,3.4-ThDCA) copolymer exhibited a porous columnar structure. The carboxylic groups in the film were well characterized from the C=O stretch in the IR spectra. EDC/NHS chemistry was used to attach a well known biorecognition element, strepatvidin, to the electroactive polymer film. FTIR and FE-SEM were employed to characterize chemical attachment of this protein to the polymer surface. The surface morphology has found to be changed after the protein attachment, making the surface smoother. This interface was also screened by impedimetric methods to investigate the electrochemical sensor potential of the system.

This talk will cover growth of thin electroactive copolymer films from two different carboxylic acid functionalized monomers. The morphology of these copolymer films will be compared using AFM and FE-SEM images. The substitute dependent polymer film properties will be discussed, illustrating their protein anchoring capacity. Techniques employed for incorporation of a biorecognition layer made up of streptavidin to the copolymer film and its characterization will be introduced. The talk will discuss the potential of this biorecognition element modified electroactive copolymer film as a capacitive sensor for non-faradaic impedimetric analysis of biotinylated target molecules.

Acceptance ID: 2v2t-O

Unveiling of Crystal Structure and Growth Mechanism within Highly Strained $BiFeO_3$ Grown on $LaAlO_3$

I.-T. Bae[1], A. Kovács[2], H. J. Zhao[3], J. Íñiguez[3], S. Yasui[4], T. Ichinose[5], and H. Naganuma[6]

[1]S[3]IP Center, State University of New York at Binghamton, Binghamton, USA
[2]ER-C, Peter Grünberg Institute, Forschungszentrum Jülich, Jülich, Germany
[3]Materials Research and Technology Dept., Luxembourg Institute of Science and Technology, Belvaux, Luxembourg.
[4]Dept. of Innovative and Engineered Materials, Tokyo Institute of Technology, Yokohama, Japan
[5]Dept. of Applied Physics, Graduate School of Engineering, Tohoku University, Sendai, Japan
[6]Dept. of Applied Physics, Graduate School of Engineering, Tohoku University, Sendai, Japan and Unit´e Mixte de Physique, CNRS, Thales, Univ. Paris-Sud, Universit´e Paris-Saclay, Palaiseau, France
E Mail/ itbae@binghamton.edu

$BiFeO_3$ is a multiferroic material with ferroelectricity and antiferromagnetism. A great deal of recent research activity on $BiFeO_3$ has been triggered by an article published in *Science* [1]. It demonstrated that the ferroelectricity of $BiFeO_3$ can be enhanced more than ten times when $BiFeO_3$ is epitaxially grown as thin film. Ever since, extensive studies have tried to further enhance its physical properties as well as to interpret the reason for physical properties enhancement found in thin film $BiFeO_3$. When $BiFeO_3$ grows epitaxially, it inevitably goes through lattice stress/strain imposed by the substrate materials that usually have different crystal structure and/or lattice parameter. Thus, a number of studies have tackled this challenging task of understanding of structural modification occurring within $BiFeO_3$ thin films. While $BiFeO_3$ thin films' physical properties are rather well established in terms of epitaxial growth conditions, film thickness, and the types of substrate materials, the fundamental question of "*what is the mechanism of physical property enhancement?*" still remains elusive. In order to answer this question, precise structural analysis about stress/strain effect on epitaxially grown $BiFeO_3$ film is imperative. It is worth noting that a couple of recent review articles pointed out that despite extensive theoretical and experimental studies, the crystal structure(s) of $BiFeO_3$ thin films are still unclear owing to its crystallographically complex nature [2,3]. As a result, publications dealing with the structural characterization have not waned at all over the years [3]. In this study, we investigate, for the first time, the *complete crystallographic detail* of so called "*highly strained $BiFeO_3$*" grown on $LaAlO_3$ substrate by using multi zone axes transmission electron microscopy, (= experiment), combined with first-principles calculation (= theory). Detailed electron diffraction analysis combined with first-principles calculation allow us to determine the *highly strained $BiFeO_3$* exhibits a *monoclinic structure* with space group of *Cm*. Complete crystallographic information including the locations of all the basis atoms within the monoclinic unit cell will be presented. We will further discuss the growth mechanism as well as electronic structure of the "*highly strained $BiFeO_3$*" using advanced electron microscopy techniques such as aberration corrected transmission electron microscopy and electron energy loss spectroscopy.

Keywords: highly strained $BiFeO_3$, crystal structure, transmission electron microscopy, structure factor calculation, first-principles simulation.

[1] WANG, J., NEATON, J. B., ZHENG, H., NAGARAJAN, V., OGALE, S. B., LIU, B., VIEHLAND, D., VAITYANATHAN, V., SCHLOM, D. G., WAGHMARE, U. V., SPALDIN, N. A., RABE, K. M., WUTTIG, M., & RAMESH, R. 2003. Epitaxial $BiFeO_3$ muliferroic thin film heterostructures. *Science*, 299, 1719-1723.

[2] SANDO, D, BARTHÉLÉMY, & A, BIBES, M. 2014. $BiFeO_3$ epitaxial thin films and devices: past, present and future. *J. Phys.: Conden. Matter.*, 26, 473201.

[3] SANDO, D, XU, B, BELLAICHE, L, & NAGARAJAN, V. 2016. A multiferroic on the brink: Uncovering the nuances of strain-induced transitions in $BiFeO_3$. 2016. *Appl. Phys. Rev.*, 3, 011106.

Acceptance ID: 2WDB-O

P-doped silicon carbide films as prospective transmission photocathodes

Jozef Huran[1], Nikolay I. Balalykin[2], Alexander A. Feshchenko[2], Pavol Boháček[1], Juraj Arbet[1]

[1]Institute of Electrical Engineering, Slovak Academy of Sciences, Dúbravská cesta 9, 84104 Bratislava, Slovakia
[2]Joint Institute for Nuclear Research, Joliot-Curie 6, 141980 Dubna, Moscow Region, Russian Federation

For each accelerator facility, e.g. the light source and the future electron-ion collider, the development of the photo injector is a key technology. Semiconductor photocathodes are widely used in various scientific experiments for the generation of ultracold, short bunched, and spin-polarized high-density electron beams.

Phosphorus doped silicon carbide films were deposited on silicon substrate for structural characterization and on double side polished quartz glass (10x10 mm) for transmission photocathode preparation. Thickness of the films was in the region 250-2000 nm. On one side of quartz glass was deposited Ti very thin film, thickness 5 nm, as adhesion film, before SiC film deposition. Ti film was deposited by electron beam evaporation. PECVD technology was used for SiC thin film growth. Concentration of elements in the films was determined by RBS and ERD analytical method simultaneously. The quantum efficiency was calculated from the measured laser energy and the measured cathode charge. RBS and ERD analysis indicated that the films contain silicon carbon, hydrogen, phosphorus and small amount of oxygen. Lift off technique was used for Al mesh preparation on SiC/quartz structures. Dry etching was used for SiC mesh preparation on quarzt glass using Al mask prepared by photolitography and lift off technique. Lift off technique was used for Al mesh preparation as contact on SiC mesh/quartz structures (transmission photocathode). The prepared transmission photocathode is placed on the hollow cathode assembly of the Pierce structure DC gun to produce photoelectrons. The 15 ns UV laser pulses (quadrupled Nd:YAG laser, 266 nm) with laser spot size ≤ 5 mm are used to backside photocathode illumination. To draw the electrons from the photocathode a negative voltage was placed on the cathode. The bunch charge is measured by using Faraday cup (FC). Perspectives for implementation of P-doped SiC thin films on quartz glass transmission photocathode in DC gun technology and vectorial effect of laser pulse interaction with different thickness SiC wall mesh are discussed.

This research has been supported by the Slovak Research and Development Agency under the contracts APVV-0443-12 and has been executed in the framework of the Topical Plan for JINR Research and International Cooperation (Project 02-0-1067-2013/2017).

Acceptance ID: 36GE-O

Ternary Solar Cells with a Mixed Face-On and Edge-On Enable an Unprecedented Efficiency of 12.1%

*Tanya Kumari, Sang Myeon Lee, So-Huei Kang, Shanshan Chen and Changduk Yang**

Department of Energy Engineering, School of Energy and Chemical Engineering, Perovtronics Research Center, Low Dimensional Carbon Materials Center, Ulsan National Institute of Science and Technology (UNIST), 50 UNIST-gil, Ulju-gun, Ulsan 44919, South Korea.
*tanyaisara@unist.ac.kr (yang@unist.ac.kr)**

Ternary organic solar cells (OSCs), with a simple structure, can be easily adopted as sub-cells in a tandem design, thereby further enhancing the power conversion efficiency (PCE) [1, 2]. Ternary blend OSCs comprising two donors and one acceptor (or one donor and two acceptors) are emerging as a fascinating alternative to overcome the challenges encountered during spectrally broad light harvesting using multi-junction OSC processing while retaining the simplicity of a single-step processing of the active layer. Despite some successful examples of ternary OSCs achieved by carefully selecting multiple components [3, 4], the current PCEs generally continue to be far less than the state-of-the-art binary and tandem systems. This is because the third component within the host binary systems can act as a recombination center or a morphological trap rather than a control agent to extend the absorption of the solar spectrum, since unfavorable interactions between the third component and host blend are inevitable. Therefore, the molecular compatibility of the active materials used in ternary OSCs is believed to be critical in achieving high PCEs [5, 6]. We speculate that in a vast pool of available active materials, the use of an archetype of high-performance poly(4,8-bis(5-(2-ethylhexyl)thiophen-2-yl)benzo[1,2-*b*;4,5-*b*']dithiophene-2,6-diyl-alt-(4-(2-ethylhexyl)-3-fluorothieno[3,4-*b*]thiophene-)-2-carboxylate-2-6-diyl)) (PTB7-Th):[6,6]-phenyl-C_{71}-butyric acid methyl ester ($PC_{71}BM$) binary host can pave a shortcut for discovering ideal ternary systems. In addition to its appropriate energy level alignment and high-crystalline characteristics, a benzo[1,2-*b*;4,5-*b*']dithiophene (BDT)-based small molecule, namely DR3TSBDT, is intuitively expected to have good compatibility with PTB7-Th because of the molecular similarity in their backbones, which is based on identical BDT units.

Given this background, a ternary OSC was designed and fabricated by incorporating DR3TSBDT as the additional donor into the PTB7-Th:$PC_{71}BM$ host matrix. The photovoltaic performance of OSCs fabricated using different DR3TSBDT concentrations was evaluated using a conventional architecture of indium-tin oxide (ITO)/PEDOT:PSS/active layer/Al under simulated AM 1.5G irradiation (100 mW cm^{-2}). This paper presents a discussion on the representative ternary blend systems (0, 10, 25, 30, 40, and 100 wt.% DR3TSBDT loading ratios). PCEs of additional DR3TSBDT loading ratios are also examined in this study. Using highly optimized conditions for PTB7-Th:$PC_{71}BM$ binary OSCs, a maximum PCE of 10.10% was obtained, The PCE value reported in this study is comparable with that of the previous best OSCs based on PTB7-Th:$PC_{71}BM$. Upon the addition till 25 wt.% DR3TSBDT into the host system, J_{SC} increases continuously together with a moderate enhancement in FF (up to 70.44%), whereas a marginal decrease in V_{OC} was observed in the range of 0.794–0.772 V. Meanwhile, at DR3TSBDT loadings higher than 30 wt.%, a large drop in J_{SC} was observed. Therefore, ternary OSCs with a 25 wt.% DR3TSBDT content exhibited the best photovoltaic performance with an unprecedented PCE of 12.1% (average PCE = 11.78 ± 0.34%). The best device was sent to confirm the notable PCE from an independent laboratory. Our in-depth study reveals that the exceptionally high PCE results from not only improving the photon absorption range but also facilitating charge transport while reducing recombination. This is achieved through a combination of cascade energy levels and optimized morphology. To understand the working mechanism and the different photovoltaic performances in the tested OSCs, we characterized the charge transport property and recombination dynamics. The similar surface energies of 28.4 and 30.6 mJ m^{-2} for DR3TSBDT and PTB7-Th:$PC_{71}BM$ host blend, respectively, calculated using Young's equation provide additional proof of the good miscibility in ternary systems. This is further evidenced from energy dispersive X-ray analysis (EDAX) and optical microscopy. The EDAX elemental mapping indicates that the nitrogen signals from DR3TSBDT are well-spread and are adjacent to the fluoride peaks of PTB7-Th in the ternary blends. Each ternary film appears to be uniformly blended, at least at the scale shown in the optical microscopy, lacking any gross aggregation. The morphology and microstructure of the blend films were further characterized using atomic force microscopy (AFM), high-resolution transmission electron microscopy (HR-TEM), and grazing incidence wide-angle X-ray scattering (GIWAXS). Unlike common high-performance OSCs that favor face-on orientation, our

ternary OSCs have a mixed orientation, which is a combination of face-on and edge-on orientations, thus enabling much higher PCEs compared to the preferentially face-on orientated host system.

Keywords: Ternary blend, high efficiency, face-on and edge-on, organic solar cell

[1] CHA, H., CHUNG, D. S., BAE, S. Y., LEE, M.-J., AN, T. K., HWANG, J., KIM, K. H., KIM, Y.-H., CHOI, D. H. & PARK, C. E. 2013. Complementary Absorbing Star-Shaped Small Molecules for the Preparation of Ternary Cascade Energy Structures in Organic Photovoltaic Cells. *Adv. Funct. Mater.*, 23, 1556-1565.

[2] LU, L., CHEN, W., XU, T. & YU, L. 2015. High-performance ternary blend polymer solar cells involving both energy transfer and hole relay processes. *Nature Commun.*, 6, 7327.

[3] LU, L., XU, T., CHEN, W., LANDRY, E. S. & YU, L. 2014. Ternary blend polymer solar cells with enhanced power conversion efficiency. *Nature Photon.*, 8, 716-722.

[4] XIAO, L., GAO, K., ZHANG, Y., CHEN, X., HOU, L., CAO, Y. & PENG, X. 2016. A complementary absorption small molecule for efficient ternary organic solar cells. *J. Mater. Chem. A*, 4, 5288-5293.

[5] AN, Q., ZHANG, F., ZHANG, J., TANG, W., DENG, Z. & HU, B. 2016. Versatile ternary organic solar cells: a critical review. *Energy Environ. Sci.*, 9, 281-322.

[6] ZHANG, J., ZHANG, Y., FANG, J., LU, K., WANG, Z., MA, W. & WEI, Z. 2015. Conjugated Polymer–Small Molecule Alloy Leads to High Efficient Ternary Organic Solar Cells. *J. Am. Chem. Soc.*, 137**,** 8176-8183.

Acceptance ID: 4T2B-O

Ultra-low Operating Voltage of Thin-Film Transistors Enabled by Sputtered Electrolyte Dielectrics

Xiaochen (Ma)[1], Hanbin (Wang)[2], Qian (Xin)[2], Aimin (Song)[1,2]

[1]School of Electrical and Electronic Engineering, University of Manchester, Manchester, M13 9PL, United Kingdom
[2] Center of Nan electronics and School of Microelectronics, Shandong University, Jinan, 100083, China
E Mail: xinq@sdu.edu.cn; A.Song@manchester.ac.uk

In the last decade, oxide-semiconductor based thin-film transistors (TFTs) have attracted much attention for large-area applications such as flat-panel display drivers thanks to their high performance, low deposition temperature and low cost. In many of these applications, particularly portable/wearable electronics and low-power electronics, it is highly desirable for the TFTs to be capable of operating at low voltages. This generally requires a very thin gate dielectric layer, which however may cause gate leakage and low yield due to material surface inhomogeneity issues or in some cases mechanical stress when flexibility is required. High k dielectrics are also used to increase the gate specific capacitance and hence reduce the voltage required to switch TFTs on and off. However, they are typically grown by atomic-layer deposition (ALD) and require either an elevated substrate temperature during deposition or in post-deposition annealing. Furthermore, despite producing high-quality highly-conformal films, it is still challenging to apply ALD technique in high-throughput manufacturing with large-sized substrates.

One interesting approach to achieving low-voltage operation is the use of ionic liquid or polymer electrolyte as gate dielectric, which can form an electric double layer with very high gate capacitance. However, in real applications, it is challenging to pattern and control the shape of ionic liquids or polymer electrolytes. Here, we present a controllable oxide electrolyte deposited by sputtering technique as the gate dielectric in InGaZnO TFTs. The TFTs show excellent properties with a threshold voltage close to 0 V, a low operating voltage of 1V, a low subthreshold swing below 80 mV/dec, and a high on/off ratio. The structure of the sputtered electrolyte was characterized by scanning electron microscopy and transmission electron microscopy. The results demonstrate the promise of high-performance, fully-sputtered oxide-semiconductor TFTs for low-power applications.

Keywords: Oxide semiconductor, thin-film transistor, operating voltage, gate dielectric, electrolyte

Acceptance ID: 5D2Q-O

Compostie thin films based on the 2D FRET process: assembly, luminescence properties and its VOC sensoring performance

*Y.-M. Qin[1], Z. Li[1], and J. Lu[1,2]**

[1] State Key Laboratory of Chemical Resource Engineering, [2]Beijing Advanced Innovation Center for Soft Matter Science and Engineering, Beijing University of Chemical Technology,15 Beisanhuan East Road, Beijing , 100029, China.

(*) lujun@mail.buct.edu.cn

Nowadays, volatile organic compounds(VOCs) became a kind of important environmental pollutes, and the detection and treatment of which was very significant for environmental protection and human health. This work focused on the design and construction of inorganic/organic composited thin films formed by organic luminescence molecules and layered double hydroxides(LDHs) nanosheets. This composite thin film exhibited the outstanding luminescence properties, and aggregative/restrict induced luminescence and 2D Föster energy transfer process were realized within the LDHs interlayers. This composite thin film showed the prominent luminescence response for the occurrence, polarity of common VOCs, and have the ability to selective probe for four VOCs vapor.

References

[1] Y.-M Qin, J. Lu* et.al., *Adv. Funct. Mater.* 26, (2016), 6752

[2] Y.-M Qin, P. Zhang, J. Lu*. et.al., *J. Mater. Chem. C*, 3 (2015), 5246.

[3] Y.-M. Qin, J. Lu*, S.-D. Li, Zhen Li, S.-F. Zheng. *J. Phys. Chem. C.* 118(2014), 20538

[4] Z. Li, J. Lu, Y.-M Qin, S.-D. Li. *J. Mater. Chem. C*, 1(2013), 5944.

[5] Z. Li, J. Lu*, S.-D. Li , S.-H Qin , and Y.-M Qin. *Adv. Mater.* 24(2012), 6053

Acceptance ID: 6RCQ-P

Characteristics of the Flexibility of Mogul-Patterned Structure Under the Influence of External Forces

Yeon-Ho Lee[1] and Youn-Jea Kim[2]

[1]Graduate school of Mechanical Engineering, Sungkyunkwan University, Suwon 16419, Republic of Korea
[2]School of Mechanical Engineering, Sungkyunkwan University, Suwon 16419, Republic of Korea
yjkim@skku.edu

Electrodes of the mogul-patterned structure are characterized by high degree of flexibility compared to other configurations. The flexibility performance is an important design factor in the semiconductor and biomedical devices. In this study, the structural characteristics of a mogul-patterned electrode were investigated with various geometrical aspect ratios and film thicknesses under the influence of external tensile force or compressive force applied to the heater. In addition, structural stability of the mogul-patterned electrode was evaluated using von Mises stress criterion. Numerical analysis was carried out using COMSOL ver. 5.2, and the results were graphically depicted.

Keywords: Mogul-patterned structure, Aspect ratio, Mechanical characteristics

[1] H. B. Lee, C. W. Bae, L. T. Duy, I. Y. Sohn, D. I. Kim, Y. J. Song, Y. J. Kim & N. E. Lee, **(2016)**, Mogul-Patterned Elastomeric Substrate for Stretchable Electronics, *Advanced Materials*, 28, 3069-3077.

Acceptance ID: 76KP-O

The growth mechanism of wafer-scale atomic layer epitaxy of copper using the sputtering method

Ho-Yeol (Park)[1], Seunghun (Lee)[2], Miyeon (Cheon)[3], Hyangsook (Lee)[4], Ik-Jae (Lee)[5], Eunha (Lee)[4], Young Hee (Lee), Se-Young Jeong[1,7]

[1]Department of Cogno-mechatronics Engineering, Pusan National University, Busan 46241, Republic of Korea.
[2]Department of Materials and Engineering, University of Maryland, College Park, MD 20742, USA.
[3] Crystal Bank Research Institute, Pusan National University, Miryang, 627-706, Republic of Korea
[4]Analytical Engineering Group, Samsung Advanced Institute of Technology (SAIT)
Samsung Electronics Co., Suwon 443-803, Republic of Korea.
[5]Pohang Accelerator Laboratory, Pohang University of Science and Technology, Pohang 790-784, South Korea.
[6]Center for Integrated Nanostructure Physics Institute for Basic Science (IBS) Sungkyunkwan University Suwon 16419, Republic of Korea
[7]Department of Optics and Mechatronics Engineering, Pusan National University, Busan 46241, Republic of Korea.

syjeong@pusan.ac.kr

The copper is deteriorated by the grain boundaries (GBs) and the oxidation at GBs. So, the growth of the thin film without any GBs and any defects has been a dream for a long time. Especially, the fabrication of GB-free wafer scale metal film has never been reported. Therefore, our realization of the single crystal copper film of wafer-scale with RMS of 1 Å and FWHM of 0.018˚ using conventional sputtering system is considered to be mysterious. Our detailed structural study on the copper thin film reveals how the nucleations initially build up, connected each other by epitaxial lateral overgrowth (ELO) and GBs disappear, which finally leads to single crystal film. This study is applied to making transparent conducting electrode, meta material, growing single crystal graphene and also the grain-free wafer scale growth of other metal films such as silver, aluminum and nickel.

Keywords: Single crystal thin film, copper, sputtering, grain-free, wafer scale

[1] KIM, W. K., LEE, S., LEE, D. H., PARK, I. H., BAE, J. S., LEE, T. W., KIM, J. Y., PARK, J. H., CHO, Y. C., CHO, C. R., JEONG, S. Y. 2015. Cu Mesh for Flexible Transparent Conductive Electrodes. *Scientific Reports* 5, 10715 (2015)

[2] LEE, S., KIM, J. Y., LEE, T. W., KIM, W. K., KIM, B. S., PARK, J. H., BAE, J. S., CHO, Y. C., KIM, J. D., OH, M. W., HWANG, C. S. & JEONG, S. Y. 2014. Fabrication of high-quality single-crystal Cu thin films using radio-frequency sputtering. *Scientific Reports* 4, 6230 (2014)

[3] NGUYEN, V. L., Perello, D. J., LEE, S., NAI, C. T., SHIN B. G., KIM, J. G., PARK, H. Y., JEONG, H. Y., ZHAO. J., VU, Q. A., LEE, S. H., LOH, K. P., JEONG, S. Y. & LEE, Y. H. 2016. Wafer-scale single-crystalline AB-stacked bilayer graphene, *Advanced Materials*, 28, 8177-8183.

Acceptance ID: 7VJL-O

The influence of oxygen flow ratio on the optoelectronic properties of p-type NiO_x thin films deposited by ion beam assisted RF sputtering

Sheng-Chi Chen [1, 2], Hui Sun [3], W. C. Peng [1], C. K. Wen [4], T. H. Chuang[4]

[1] Department of Materials Engineering and Center for Thin Film Technologies and Applications, Ming Chi University of Technology, Taipei 243, Taiwan
[2] Department of Electronic Engineering, Chang Gung University, Taoyuan 333, Taiwan
[3] Institute of Materials Science and Engineering, Ocean University of China, 238 Songling Road, Qingdao 266100, P. R. China
[4]Institute of Materials Science and Engineering, National Taiwan University, Taipei 106, Taiwan
chensc@mail.mcut.edu.tw

p-type transparent conductive oxides (TCOs) have aroused people's attention due to their potential applications in the fields of photovoltaics, transparent displays, sensor arrays, photocatalysts and invisible integrated circuits [1]. Among various p-type TCOs, NiO is an attractive candidate. Its advantages include: wide bandgap above 3.6 eV, intrinsic p-type conductivity, abundant availability, chemical stability, non-toxicity, low-cost, easy to produce etc. [2]. Recently, it was proposed that interstitial oxygen plays an important role on NiO film's electrical properties. Holes can be generated from interstitial oxygen and are responsible for the film's p-type conductivity [3]. Thus, how to introduce interstitial oxygen into NiO films has become a hot subject for researchers. In the current work, oxygen ion beam assisted RF sputtering is employed to deposit NiO thin films. Through this technology, O-rich NiO films are realized. The influence of the oxygen flow ratio (f_{O2}) on the films' optoelectronic properties is studied. The films' structural, morphological, optical and electrical properties are investigated by X-ray diffractometer (XRD), field emission scanning electron microscope (FE-SEM), UV-Vis spectrophotometer and Hall measurement, respectively. The results show that with an increase in f_{O2}, a degradation in the film's crystallization is detected, which is assumed to be caused by the introduction of interstitial oxygen. Meanwhile, the carrier concentration enhances significantly and the carrier mobility reduces, and the film's conductivity improves. Whereas, the films' optical transmittance decreases when the f_{O2} rises. This is attributed to more scattering of the visible light in the films with poor crystallinity deposited under higher f_{O2}. When the f_{O2} reaches 100%, the optimal p-type conductivity of 25 $S \cdot cm^{-1}$, with a carrier concentration of 8.1×10^{19} cm^{-3} and a carrier mobility of 2.0 $cm^2V^{-1}s^{-1}$ is achieved. In this condition, the film's optical bandgap is around 3.95 eV.

Keywords: NiO films, oxygen ion assisted, optoelectronic properties, p-type conduction

[1] Frenzel H., Lajn A., Grundmann M., 2013. One decade of fully transparent oxide thin-film transistors: fabrication, performance and stability. Phys. Status Solidi R 7, 605-615.

[2] Loukil A., Boukhachem A., Ben Amor M., Ghamnia M., Raouadi K., 2016. Effects of potassium incorporation on the structural, optical, vibrational and electrical properties of NiO sprayed thin films for p-type optical windows. Cream. Int. 42, 8274-8289.

[3] Chen S.C., Kuo T.Y., Sun T.H., 2010. Microstructures, electrical and optical properties of non-stoichiometric p-type nickel oxide films by radio frequency reactive sputtering. Surf. Coat. Technol. 205, S236-S240.

Acceptance ID: 82FR-P

Improved performance of AlGaN-based ultraviolet light-emitting diodes using electrical doping effects

T. H. Kim, K. H. Kim, H. J. Choi, Kim, T. G. Kim

School of Electrical Engineering, Korea University, Seoul 02841, Korea
tgkim1@korea.ac.kr

Recently, glass-based transparent conductive electrodes (G-TCEs) with high electrical conductivity and optical transmittance in the ultraviolet (UV) region have been reported and successfully applied to AlGaN-based UV light-emitting diodes (LEDs) as top electrodes [1]. In this device scheme, direct ohmic contact to p-AlGaN was obtained via conducting filament (CF) formed between the metal and p-AlGaN using an electrical breakdown (EBD) method. During the EBD process, metal atoms can be diffused and electrically doped in the p-AlGaN layer across the G-TCE such as AlN film. This electrical doping not only provide a channel for carrier injection but also improve ohmic behavior on p-AlGaN layers by electrical doping effects. In this study, we report electrical doping effects using various metals such as Pt, Ni, Ti, and Mg for 365 nm near-UV LEDs with AlN TCEs and demonstrate the improved performance when compared to the LEDs with typical ITO TCEs.

Keywords: Conducting filaments, electrical breakdown method, ultraviolet light-emitting diodes, transparent conductive electrodes

[1] TAEHO, K., KYEONGHEON, K., BYEONGRYOUNG, L., JUHYUN, P., FREDSCHUBERT, E., TAEGEUN, K. 2017. Glass-Based Transparent Conductive Electrode: Its Application to Visible-to-Ultraviolet Light-Emitting Diodes. *ACS Appl. Mater. Interfaces, in press.*

Acceptance ID: 89NJ-P

Realizing High Performance InGaZnO Schottky Diodes by Substrate and Anode Treatments

Lulu (Du)[1], He (Li)[1], Qian (Xin)[1], and Aimin (Song)[2]

[1]School of Microelectronics, Shandong University, Jinan 250100, China
[2]School of Electrical and Electronic Engineering, University of Manchester, Manchester M13 9PL, United Kingdom
Correspondence author's electronic mail: xinq@sdu.edu.cn
Presenting author's electronic mail: luludu_5313@163.com

In contrast to well-studied oxide semiconductor based thin film transistors, very limited efforts have been made on oxide based diodes, although they are essential for transparent and low cost integrated circuits. Here, high performance Schottky diodes based on 100-nm InGaZnO (IGZO) and 50-nm Pd anode on SiO_2/Si substrate have been realized.[1,2] Our results indicate that substrate annealing (300 ^oC, 30 min, in air) decreases Pd surface roughness and lead to 30 meV increase in Schottky barrier height (Φ_B) and one order of magnitude increase in rectification ratio ($I_{on/off}$). Oxidation treatments, including oxygen plasma and UV-Ozone treatments, on Pd anode improve diode performance. Oxygen plasma treatment is more effective than UV-ozone treatment, and it leads to 150 meV increase in Φ_B and two orders of magnitude increase in $I_{on/off}$. X-ray photoemission spectroscopy results show that oxygen plasma treatment induces more complete Pd oxidation, and thus ensures better oxygen stoichiometry at Schottky interface and higher anode work function. Using the optimized substrate and Pd treatments, we have achieved high performance IGZO diode with an extremely high $I_{on/off}$ of 7.2×10^7 and a near unity ideality factor of 1.09. This is, the highest performance among the reported as-deposited IGZO Schottky diodes.

Keywords: InGaZnO(IGZO), Schottky diode, annealing, oxidation treatments.

[1] DU, L., LI, H., YAN, L., ZHANG, J., XIN, Q., WANG, Q., & SONG, A. 2017. Effects of substrate and anode metal annealing on InGaZnO Schottky diodes. *Appl. Phys. Lett*., 110(1), 011602.

[2] XIN, Q., YAN, L., LUO, Y., & SONG, A. 2015. Study of breakdown voltage of indium-gallium-zinc-oxide-based Schottky diode. *Appl. Phys. Lett.*,106(11), 113506.

Acceptance ID: 8HZ2-O

Hydrogen sensors of metal-oxides on SiC substrate operating directly at high temperature

Seongjeen Kim[1], *Sangcheol Kim*[2]

[1]*Department of Electronic Engineering, Kyungnam University, Changwon, Korea 51767*
[2]*Power Semiconductor Research Center, Korea Electrotechnology Research Institute (KERI), Changwon, Korea 51543*
E-mail: sjk1216@kyungnam.ac.kr

In the last years, a particular attention has been devoted to hydrogen detection. Hydrogen is the most promising clean renewable energy for the new transportations based on fuel cells. We fabricated Pd/metal-oxides/SiC-based hydrogen sensors operating directly at high temperatures around the vehicle engine. In this work, silicon carbide (SiC) was used as a substrate instead of silicon as the maximum operating temperature of the silicon for electronic devices is limited below 250 ℃ owing to its narrow bandgap energy. We investigated different thin metal oxides, such as Ta_2O_5, TiO_2, and SiO_2 layers, on a SiC substrate. To estimate response characteristics of the sensor, variations in capacitance and current-voltage characteristics after exposure to different hydrogen concentrations up to 2,000 ppm were examined at temperatures ranging from room temperature to 600 ℃ which is the maximum operating temperature of the SiC substrate.

Keywords: hydrogen sensor, high temperature, metal oxides, SiC, palladium

[1] SOO, M. T., CHEONG, K. Y. & NOOR, A. F. M. 2010. Advances of SiC-based MOS capacitor hydrogen sensors for harsh environment applications: S. Seal: *Sens. Actuators B*, 151, 39-55.

[2] KIM, S., CHOI, J., JUNG, M., JOO, S. & KIM, S. 2013. Silicon carbide-based hydrogen gas sensors for high-temperature applications: *Sensors*, 13, 13575-13583.

Acceptance ID: 8ZLA-P

Epitaxy of GaN films on MoS_2/c-sapphire substrate by PA-MBE

Ken-Yuan Kan[1], Iwan Susanto[1], Yen-Ten Ho[2], Ping-Yu Tsai[3], Ing-Song Yu[1,]*

[1] Department of Materials Science and Engineering, National Dong Hwa University, Hualien 97401, Taiwan.
[2] Department of Materials Science and Engineering, National Chiao Tung University, Hsinchu 30010, Taiwan.
[3] Electronic Systems Research Division, Chung-Shan Institute of Science & Technology, Tao-Yan 325, Taiwan.
[*]isyu@gms.ndhu.edu.tw

Gallium nitride (GaN) semiconductor is one of the popular functional materials due to its various applications in optoelectronic and electronic devices. GaN films can be deposited by plasma-assisted molecular beam epitaxy (PAMBE) on different substrates, i.e. Si (111), Sapphire (0001) and 4H-SiC. Due to the lattice mismatch between GaN films and substrates, the substrates profoundly affect the growth mechanism of GaN films during the epitaxy[1]. Recently, two-dimensional layered transition metal dichalcogenides has attracted significant attentions for their potential applications in nanoelectronics, optoelectronics and spintronics. Layered growth molybdenum disuphide (MoS_2) can be grown by pulsed laser deposition (PLD), chemical vapor deposition, or two-step sulfurization with molybdenum oxide [2]. This two dimensional material can be integrated in the growth of GaN films on c-Sapphire, but the limitation of growth temperature. In this work, GaN films were grown at low temperature (750 °C) by PAMBE on c-sapphire substrates with two-dimensional MoS_2 which can be prepared by PLD and two-step sulfurization methods. The surface condition of the substrates and epi-layers were investigated by *in-situ* reflection high energy electron diffraction (RHEED) as shown in Figure 1. Scanning electron microscopy (SEM) and atomic force microscopy (AFM) were used for the observation of surface morphorlogy. High resolution X-ray diffraction (HRXRD) was also conducted to determine crystal orientations and defect densities of the GaN films. Their residual strains and optical properties were studied by photoluminescence (PL) spectra. X-ray photoelectron spectroscopy (XPS) was used for the analysis of surface composition of GaN epi-layers. The purpose is to study the influence of these MoS_2 layers on the growth mechanism of GaN films by PAMBE for the diverse applications in the future.

Keywords: GaN, molecular beam epitaxy, MoS_s, pulsed laser deposition, sapphire

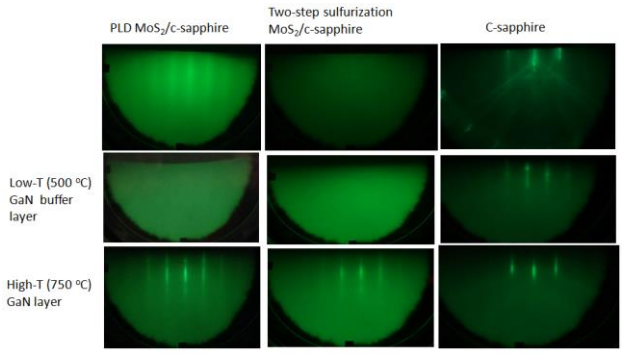

Figure 1. RHEED patterns of PLD MoS_2/c-sapphire, two-step sulfuriczation MoS_2/c-sapphire and c-sapphire as substrates for the epitaxy of GaN films.

[1] Yang Z.-P., Tsou T.-H.,Lee C.-Y., Kan K.-Y., Yu I.-S. 2016. Effects of Substrate and Annealing on GaN Films Grown by Plasma-Assisted Molecular Beam Epitaxy. *Surface & Coatings Technology*. in press, http://dx.doi.org/10.1016/j.surfcoat.2016.11.019.

[2] Ho Y.-T., Ma C.-H., Luong T.-T., Wei L.-L., Yen T.-C., Hsu W.-T., Chang W.-H., Chu Y.-C., Tu Y.-Y., Pande K. P., Chang E. Y. 2015. Layered MoS_2 grown on c-sapphire by pulsed laser deposition. *Phys. Status Solidi RRL*, 9, No. 3, 187-191.

Acceptance ID: 9BMD-P

Second Harmonic Generation in mesostructured SIO2:DR1:CTAB films as function of the incidence angle

J. A. Garcia- Macedo, J. A. Luna S.

Departamento de Estado Solido. Instituto de Fisica, Universidad Nacional Autonoma de Mexico. Circuito Exterior Cd. Universitaria, 04510 Mexico D.F.
**:e-mail gamaj@fisica.unam.mx, phone (5255) 56225103*

Non-linear optical (NLO) response of materials is opening new technological applications, in optical communications, data storage and development of new sensors, for example. The presence of a mesostrucure in the material can change its NLO response. We prepared films of SiO2:DR1 with a hexagonal structure by using CTAB surfactact. The surfactanct was taken out by thermal and chemical treatment. The mesostructure was probed by X-ray diffraction. The thickness of the films was determined by SEM. We studied the second harmonic generation (SHG) of these films at different incident angles, under a Corona poling. The time response of SHG is reported at each angle. These results show a saturable curve as function of the angle.

We acknowledge support from PAPIIT IN113917, CONACyT 179607, Bilateral Mexico-Italia 174506 and SECITI 053. And we acknowledge the technical assistance from Diego Quiterio (SEM samples preparation), Roberto Hernandez (SEM) and Antonio Morales (XRD).

Acceptance ID: 9HWH-O

Graphene based solutions for corrosion protection on low alloy steel

Krupa Balakrishnan and Sutapa Roy Ramanan

Dept. of Chemical Engineering, BITS Pilani Goa Campus

Corrosion is a major problem in modern societies costing nations more than billions of dollars every year. Various approaches are undertaken for corrosion protection, protective coating being one of them. The different types of protective layers used, metallic or alloy based organic layers, polymeric films, paints and varnishes, anodized oxide layers etc., depend upon their ability to form a barrier between the active metal surface and the atmosphere [1-3]. Apart from general coating failures like flaking or cracking disposal of coating baths, like chromates, have serious environmental impacts. Moreover, most of the conventionally used protective coatings result in increased thickness as well as changes in optical, electrical and thermal properties of the base material. Graphene, in single and multilayer form has the potential to form ultrathin coatings which does not alter the properties of the underlying material [4-6]. Graphene is considered to be inert under various atmospheres along with being impermeable to gas molecules thereby forming a natural diffusion barrier [7]. These properties make graphene a potentially important candidate for anticorrosion films. Graphene layers have been investigated on copper, nickel, aluminum and stainless steel substrates using CVD, Langmuir-Blodgett method, electrophoretic deposition, electrospray etc. [4-6] of which CVD has emerged as the most favored method. Elaborate and expensive experimental arrangements and precise control of temperature, concentration of precursor material and time of exposure is required to generate good quality films using CVD. However, to make use of graphene films for anti-corrosion properties more viable it is necessary to develop a low temperature, fast and effective method of film deposition so that all kinds of substrates can be easily coated.

We report a simple low temperature cost effective method of fabricating anti-corrosion films of graphene prepared through wet chemical synthesis. Graphene/graphene-TiO_2 films were developed on low alloy steel coupons via dip coating technique and were subsequently dried in air oven at 75ºC. The process was repeated to develop multiple coating layers. The formation of graphene was confirmed using XRD and Raman spectroscopy. The coated substrates were tested for their corrosion resistance under different environments. The corrosion rate was determined using Tafel extrapolation method. Cyclic voltammetry studies were conducted to study the oxidation behavior under corrosive environments and AC impedance spectroscopy analysis was carried out to estimate the polarization resistance. Reduction of up to 70% in corrosion rate was noticed for composite graphene coatings.

References:

1. Rao, B. V. A.; Iqbal, M. Y.; Sreedhar, B. Self-assembled Monolayer of 2-(octadecylthio) benzothiazole for Corrosion Protection of Copper. Corrosion Science 2009**,** 51, 1441-1452.
2. Stratmann, M.; Feser, R.; Leng, A. Corrosion Protection by Organic Films. Electrochimica Acta 1994, 39, 1207-1214.
3. Merkula, D. M.; Novikov, P. D.; Ivanenkov, V. N.; Sapozhnikov, V. V.; Lyakhin, Y. I. Utilization of Edn Varnish for Protection of Metal Sea-Water Sampling Bottles Against Corrosion. Oceanology-Ussr 1974, 14, 299-300.
4. Shanshan Chen, Lola Brown, Mark Levendorf, Weiwei Cai, Sang-Yong Ju, Jonathan Edgeworth, Xuesong Li, Carl Magnuson, Aruna Velamakanni, Richard R. Piner, Jiwoong Park, Rodney S. Ruoff, Oxidation resistance of graphene-coated Cu and Cu/Ni alloy, ACS Nano 2011, 5, 1321–1327.
5. Prasai D, Tuberquia JC, Harl RR, Jennings GK, Rogers BR, Bolotin KI, Graphene: corrosion-inhibiting coating. ACS Nano. 2012; 6: 1102-1108.
6. Hu J, Ji Y, Shi Y, Hui F, Duan H and Lanza M. A Review on the use of Graphene as a Protective Coating against Corrosion. Ann J Materials Sci Eng. 2014;1(3): 16.
7. Bunch, J. S.; Verbridge, S. S.; Alden, J. S.; van der Zande, A. M.; Parpia, J. M.; Craighead, H. G.; McEuen, P. L. Impermeable Atomic Membranes from Graphene Sheets. Nano Lett. 2008, 8, 2458–2462.

Acceptance ID: AZZR-O

Organic Mechano-Responsive Luminescent Materials

Zhiyong Yang, Juan Zhao, Tao Yu, Shizhao Zheng, Yi ZHANG, Jiarui XU, Zhenguo Chi

PCFM Lab, GD HPPC Lab, Guangdong Engineering Technology Research Center for High-performance Organic and Polymer Photoelectric Functional Films, State Key Laboratory of Opto-electronic Material and Technologies, School of Chemistry, Sun Yet-sen University, Guangzhou 510275, China.
chizhg@mail.sysu.edu.cn (Prof. Zhenguo Chi)

Mechano-responsive luminescent materials are a class of "smart" materials with luminescent properties that change in response to external force stimuli. These materials are widely used in sensors, memory chips, and security inks. However, organic mechano-responsive luminescent materials were very limited several years ago. In recent years, our group have synthesized many organic mechano-responsive luminescent materials covering fluorescence, phosphorescence and thermally activated delayed fluorescence (TADF), including mechanoluminochromic materials, mechanoluminescent materials, and mechano-responsive afterglow materials.

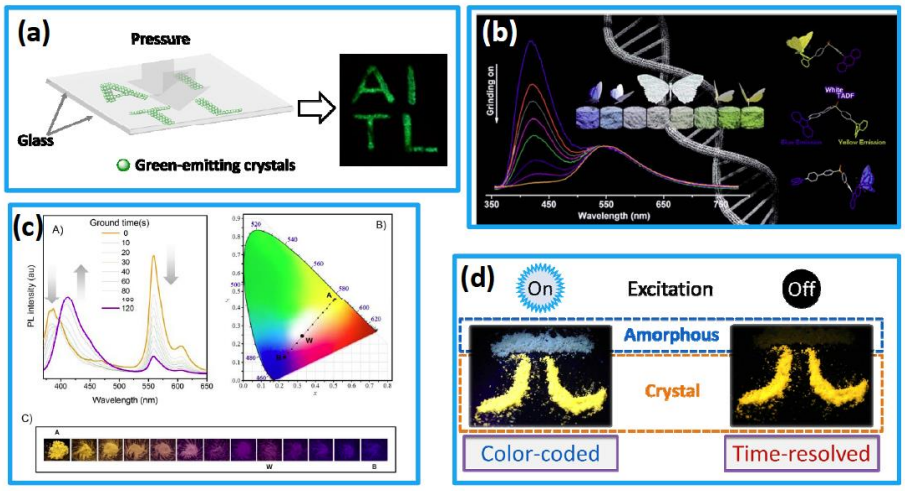

Figure 1 (a) Mechanoluminescence, (b) Mechano-responsive AIE-TADF dual-emission, (c) Mechano-responsive fluorescence/phosphorescence dual-emission, (d) Mechano-responsive afterglow.

Keywords: Organic luminescent materials, mechano-responsive, mechanoluminochromism mechanoluminescence

REFERENCES

[1] CHI, Z. G., ZHANG, X. Q., XU, B. J., ZHOU, X., MA, C. P., ZHANG, Y., LIU, S. W., XU, J. R. 2012. Recent advances in Organic Mechanofluorochromic Materials. *Chem. Soc. Rev.*, 41, 3878-3896.

[2] XU, S. D., LIU, T. T., MU, Y. X., WANG, Y. F., CHI, Z. G., LO, C. C., LIU, S. W., ZHANG, Y., LIEN, A., XU, J. R. 2015. An Organic Molecule with Asymmetric Structure Exhibiting Aggregation-induced Emission, Delayed Fluorescence, and Mechanoluminescence. *Angew. Chem. Int. Ed.*, 54, 874-878.

[3] MAO, Z., YANG, Z. Y., MU, Y. X., ZHANG, Y., WANG, Y. F., CHI, Z. G., LO, C. C., LIU, S. W., LIEN, A., XU, J. R. 2015. Linearly Tunable Emission Colors Obtained from a Fluorescent-phosphorescent Dual-emission Compound by Mechanical Stimuli. *Angew. Chem. Int. Ed.*, 54, 6270-6273.

[4] YANG, Z. Y., MAO, Z., ZHANG, X., OU, D. P., MU, Y. X., ZHANG, Y., ZHAO, C. Y., LIU, S. W., CHI, Z. G., XU, J. R., Bryce, M. R. 2016. Intermolecular Electronic Coupling of Organic Units for Efficient Persistent Room-temperature Phosphorescence. *Angew. Chem. Int. Ed.*, 55, 2181-2185.

[5] XIE, Z. L., CHEN, C. J., XU, S. D., LI, J., ZHANG, Y., LIU, S. W., XU, J. R., CHI, Z. G. 2015. White-light Emission Strategy of Single Organic Compound with Aggregation-induced Emission and Delayed Fluorescence Properties. *Angew. Chem. Int. Ed.*, 54, 7181-7184.
[6] XU, B. J., HE, J. J, MU, Y. X., ZHU, Q. Z., WU, S. K., WANG, Y. F., ZHANG, Y., JIN, C. J., LO, C. C., CHI, Z. G., LIEN, A., LIU, S. W., XU, J. R. 2015. Very Bright Mechanoluminescence and Remarkable Mechanochromism Using a Tetraphenylethene Derivative with Aggregation-induced Emission. *Chem. Sci.*, 6, 3236-3241.

Acceptance ID: B4ZH-I

Thermal Tuning of Infrared Absorption Based on Retarded Insulator-to-Metal Transition of Vanadium Dioxide

Peiheng Zhou[1], *Lin Yang*[1,2], *Guoshuai Zhen*[2], *Lei Bi*[1,2], *Taixing Huang*[1,2], *Longjiang Deng*[1,2]

[1]*National Engineering Research Center of Electromagnetic Radiation Control Materials, University of Electronic Science and Technology of China, Chengdu, 610054.*
[2]*State Key Laboratory of Electronic Thin Film and Integrated Devices, Chengdu 610054, China.*
phzhou@uestc.edu.cn/ +862883201893

Recently, vanadium dioxide (VO_2) has been extensively concerned and studied for its insulator-to-metal transition (IMT) near the room temperature at picosecond time scales. This phase transition can be induced thermally, optically or electrically. As a result of IMT, the conductivity of VO_2 can increase by four orders of magnitude and the optical transmission in the near-IR will decrease significantly. Utilizing the IMT in VO_2, frequency-tunable metamaterials with arrays of Ag split ring resonators (SRRs) have been reported in the near-IR range from 1.5 to 5 microns [1]. Mikhail A. Kats fabricated Y-shaped antennas on a 180-nm-thick VO_2 film deposited on sapphire substrate, and achieved approximately 10% tunability of the resonance frequency at the center wavelength of 10 μm [2]. With the development of practical application of VO_2, VO_2 has been used in many research hotspots. For example, a sandwiched structure ZnO/VO_2/ZnS forming a VO_2-based smart window exhibited a high solar modulation ability (ΔT_{sol} = 13.01%), and maintained a high T_{lum} at 63.24% and 57.39% both in semiconducting and metallic phases [3]. However, most of the reported metamaterials based on VO_2 are worked on the complete IMT effect. As a matter of fact, it has been proved that the insulating and metallic phases coexist in VO_2 around the phase transition temperature T_c [4]. Dielectric properties determined by the volume fractions of insulating and metallic phases in VO_2 should also change correspondingly. Utilizing this property of VO_2, ultra-thin perfect absorber with a single VO_2 layer of thickness much smaller than the incident wavelength on an opaque sapphire substrate realized a large continuous tuning range (from ~80% to 0.25% in reflectivity) at λ = 11.6 μm [5]. Moreover, our recent work [6] has found a new Raman peak at 166 cm^{-1} in over oxidized VO_2, which was attributed to the characteristic peak of V^{4+}/V^{5+} mixed valence states. Therefore, it becomes more significant and interesting to have further study on the dielectric properties of VO_2 and utilize them to redesign our tunable or active devices.

In this work, effect of the retarded IMT of VO_2 caused by the dual-phase properties were concentrated on the thermal tuning of mid-infrared absorption. Here, we firstly deposited the over oxidized VO_2 by pulsed laser deposition (PLD), and conducted the dielectric analysis by a Drude-Lorentz classical oscillator model [7]. Secondly, the dielectric constants with different metallic phase volume fraction were calculated by the Bruggeman formula [8]. Then, the VO_2-based infrared metamaterial absorber was fabricated, tested and studied to support the retarded IMT in VO_2 near Tc.

Acknowledgments

The authors are grateful to the supported of National Natural Science Foundation of China (NSFC) (61471097, 61475031, 51302027), and the Program for Changjiang Scholars and Innovative Research Team in University.

Keywords: VO_2 thin film, insulator-to-metal transition, infrared absorber, metamaterial

[1] DICKEN, M. J., AYDIN, K., PRYCE, I. M., SWEATLOCK, L. A., BOYD, E. M., WALAVALKAR, S., MA, J. & ATWATER, H. A. 2009. Frequency tunable near-infrared metamaterials based on VO2 phase transition. *Optics Express*, 17, 18330-18338.

[2] KATS, M. A., BLANCHARD, R., GENEVET, P., YANG, Z., QAZILBASH, M. M., BASOV, D. N., RAMAMNATHAN, S. & CAPASSO, F. 2013. Thermal tuning of mid-infrared plasmonic antenna arrays using a phase change material. *Optics Letters*, 38, 368-370.

[3] ZHAO, Y., XU R., ZHANG X., HU, X., KNIZE, R. J. & LU, Y. 2013. Simulation of smart windows in the ZnO/VO_2 /ZnS sandwiched structure with improved thermochromic properties. *Energy & Buildings*, 66, 545-552.

[4] QAZILBASH, M. M., BREHM, M., ANDREE, G. O., FRENZEL, A., HO, P. C., CHAE, B. G., KIM, B. J., YUN, S. J., KIM, H. T., BALATSKY, A. V., SHPYRKO, O. G., MAPLE, M. B., KEILMANN, F. & BASOV, D. N. 2009. Infrared spectroscopy and nano-imaging of the insulator-to-metal transition in vanadium dioxide. *Physical Review B*, 79, 7715-7722.

[5] KATS, M. A., SHARMA, D., LIN, J., GENEVET, P., BLANCHARD, R., YANG, Z., QAZILBASH, M. M., BASOV, D. N., RAMANATHAN, S. & CAPASSO, F. 2012. Ultra-thin perfect absorber employing a tunable phase change material. *Applied Physics Letters*, 101, 221101.

[6] HUANG, T. X., YANG, L., QIN, J., HUANG, F., ZHU, X. P., ZHOU, P. H., PENG, B., DUAN, H. G., DENG L. J., BI, L. 2016. Study of the Phase Evolution, Metal-Insulator Transition and Optical Properties of Vanadium Oxide Thin Films by Confocal Raman Microscopy Mapping. *Optical Materials Express*, 6, 3609-3621.

[7] VERLEUR, H. W., BARKER, A. S. & BERGLUND, C. N. 1968. Optical Properties of VO2 between 0.25 and 5 Ev. *Physical Review*, 172, 788-798.

Acceptance ID: BPQQ-O

Plasmonic Ag-TiAlN based nanocermet thin films with robust selectivity and thermal stability for Solar Thermal Applications

Abdul Ghafar (Wattoo)[a,b], *Cheng (Xu)*[a,b], *Lijing (Yang)*[a,b], *Zhenlun (Song)*[a,b,*]

[a]*Key Laboratory of Magnetic Materials and Devices, Ningbo Institute of Materials Technology & Engineering, Chinese Academy of Sciences, Ningbo, Zhejiang 315201, China*
[b]*Zhejiang Province Key Laboratory of Magnetic Materials and Application Technology, Ningbo Institute of Materials Technology & Engineering, Chinese Academy of Sciences, Ningbo, Zhejiang 315201, China*
(abdul@nimte.ac.cn and songzhenlun@nimte.ac.cn)

Growing plasmonic materials as cermet composites is attractive for selective solar absorbers. Silver nanoparticles/alumina cermet shows reasonable resistance to high-temperature oxidation; however, an inherent long-range inter-layer diffusion confines their applications at elevated temperatures. In this work, a well-designed Ag-TiAlN and AgAl-TiAlN nanocermets exhibit stable plasmonic absorption characteristic with ignorable degradation at 550 °C for 6 h in air. Based on this cermet, TiAlON/Ag-TiAlN/AgAl and TiAlON/AgAl-TiAlN/AgAl tandem absorbers were constructed successfully, representing a high solar absorptance (≈94%) and a low infrared emittance (≈8%) in the whole spectrum of solar light. Thermally induced out-diffusion of Al atoms and their oxidation in air afford an opportunity to form alumina capped Ag nanoparticles. Alumina capped Ag nanoparticles agglomerate together suppressing the long distance diffusion of active layer. TiAlN layer acts as an absorber layer as well as diffusion barrier for the base layer. Photoluminescence and ellipsometery techniques were employed to study the optical properties of the cermet absorber. UV-Visible spectroscopy, micro-Raman spectroscopy and X-ray photoelectron spectroscopy techniques were used to test the thermal stability. These results proved that the cermet absorber is highly efficient for low-mid-high temperature applications.

Keywords: Nanocermet, titanium aluminum nitride, thermal stability, solar selective absorber

Acceptance ID: cucz-P

Perhydropolysilazane Derived Thin, Transparent, Abrasion and Atomic Oxygen Resistant Silica Coating

Zongbo Zhang[1], *Dan Wang*[1,2], *Wenwen Huang*[1], *Yongming Luo*[1], *Caihong Xu*[1,2]

[1]*Institute of Chemistry, Chinese Academy of Science, Beijing 100190, China.*
[2] *University of Chinese Academy of Sciences, Beijing 100049, China.*
Zongbo@iccas.ac.cn, *Fax/Tel.: +86-01-62554487*

Polymer based materials face severe damage from atomic oxygen (AO) in low earth orbit (LEO). In this work, a novel solution based coating method has been proposed, which adopted the inorganic polymer of perhydropolysilazane(PHPS) as precursor material, then coated it on the polyimide film by dipping process, and finally cured the coating under moisture atmosphere. The cured PHPS converted into silica with O/Si ratio of 1.9. The coating is dense and transparent with excellent adhesion to the commercial Kapton polyimide film. The coated Kapton film exhibited not only excellent atomic oxygen resistant properties with only 4% weight loss under radiation of atomic oxygen with fluence of 1.2E21 atoms/cm^2, but also superior abrasion resistant ability with only slight scratches after 2000 times abrasion test under load of 15000N/m^2 with a face to face testing mode. This work has provided a new choice for robust, easy-implement, atomic oxygen resistant coating for the polymer based materials used on the spacecrafts.

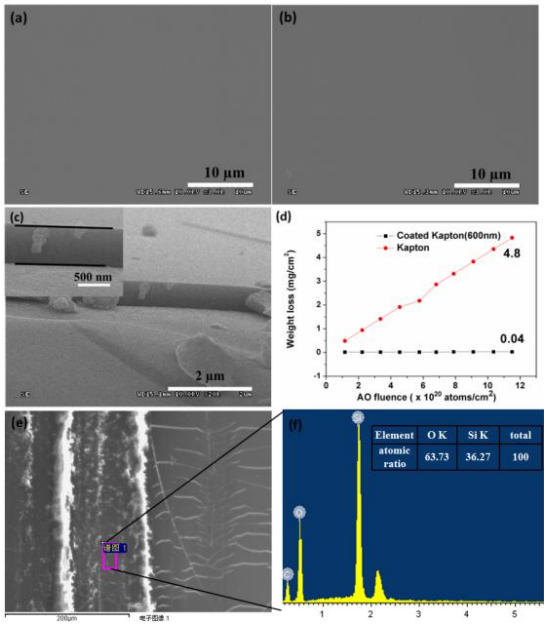

Fig.1 (a) The SEM image of the obtained coating, (b) The SEM image of the coating after AO radiation test, (c) The cross-section the coating, (d) The weight loss of the bare Kapton film and coated Kapton film with coating thickness of 600nm under AO radiation, (e) The SEM image of the coated Kapton after abrasion test, (f) The EDS spectrum of trench area caused by friction, inset is the element composition.

Keywords: low earth orbit, atomic oxygen, perhdropolysilazane, silica coating, abrasion resistant

[1] MINTON T. K., WU B., ZHANG J., LINDHOLM N. F., ABDULAGATOV A. I., O'PATCHEN J., GEORGE S. T. & GRONER M. D. 2010. Protecting Polymers in Space with Atomic Layer Deposition Coatings. *ACS Applied Materials & Interface*, 9, 2515-2520.

[2] GOUZMAN I., GIRSHEVITZ O., GROSSMAN E., ELIAZ N. & SUKENIK C. N. 2010. Thin Film Oxide Barrier Layers: Protection of Kapton from Space Environment by Liquid Phase Deposition of Titanium Oxide. *ACS Applied Materials & Interface*, 7, 1835-1843.

[3] ZHANG H. T., GUO Z., CHEN Q., WANG X. W., WANG Z. D. & LIU Z. W. 2016. Deposition of Silicon Oxide Coatings by Atmospheric Pressure Plasma Jet for Oxygen Diffusion Barrier Applications. *Thin Solid Films*, 615: 63-68.

[4] LOEBLEIN M., BOLKER A., TSANG S. H., ATAR N., UZAN-SAGUY C., VERKER R., GOUZMAN I., GROSSMAN E. & TEO E. H. T. 2015. 3D Graphene-Infused Polyimide with Enhanced Electrothermal Performance for Long-Term Flexible Space Applications. *Small*, 48: 6225-6234.

[5] PENG D. Q., QIN W. & WU X. H. Improvement of the Atomic Oxygen Resistance of Carbon Fiber-reinforced Cyanate Ester Composites Modified by POSS-graphene-TiO2. 2016. *Polymer Degradation and Stability*, 133: 211-218.

Acceptance ID: D528-O

The influence of nitrogen pressure on formation of niobium nitride by thermal processing

Ashraf H. Farha[1,3], Hani E. Elsayed-Ali [1] and Yüksel Ufuktepe [2,]*

[1]Department of Electrical and Computer Engineering and the Applied Research Center, Old Dominion University, Norfolk, Virginia 23529, USA
[2]Department of Physics, Cukurova University, Adana, 01330, TURKEY
[3]Department of Physics, Faculty of Science, Ain Shams University, Cairo 11566, EGYPT
[*]E Mail : ufuk@cu.edu.tr

Transition metal nitrides exhibit many important mechanical and chemical properties for technological applications, such as superconductivity, extreme hardness and wear resistance. The attractive structural properties of niobium nitride make it possible for many applications. As is well known, niobium nitride thin films could be used as gas sensors, diffusion barriers in Josephson junctions, possible cathode materials in vacuum microelectronic devices and coatings for superconductive cables. NbN_x crystallize in different phases, including β-Nb_2N (hexagonal), γ-Nb_4N_3 (tetragonal) δ-NbN (face-centered cubic), δ´-NbN (hexagonal), ε-NbN (hexagonal) and η-NbN (hexagonal) structure. The diffusion of nitrogen onto the niobium surfaces can be created by high substrate temperature with suitable nitrogen background gas pressure.

In the present work the nitridation of niobium films by thermal processing at 1300°C in different nitrogen pressures ranging from 2.6×10^{-4} to 3.3 Pa was investigated. The NbN_x films were successfully deposited by thermal heating on niobium substrates. The effect of nitrogen background pressure was compared with regard to NbN_x phase and reaction with the Nb substrate. The formed phases were characterized by X-ray diffraction (XRD) and atomic force microscope (AFM). Electronic structure of the NbN_x films was investigated by X-ray absorption near edge structure (XANES). The phase transition followed a sequence of α-NbN → β-Nb_2N when nitrogen pressure was increased. As pressure increases to more than 0.13 Pa the samples are having α-NbN phase mixed with β-Nb_2N phase. Increasing nitrogen pressure results more α-phase concentration accompanied with increase of other phases.

Keywords: NbN, thin films, thermal diffusion, surface morphology, X-ray absorption spectroscopy

Acceptance ID: EZ3L-O

Solid Particle Erosion of ZrN Coating Material on GF/EP and CF/EP Composites by Using PVD

Mehmet Bagci

Mechanical Engineering Department, Selcuk University, Alaeddin Keykubad Campus, 42075, Selcuklu, Konya, Turkey

Email: mehmetbagci@selcuk.edu.tr

Solid particle erosion influences many industries such as aerospace, power generation, coal mining, as well as in manufactured goods like pipe line in petroleum refining, helicopter rotor blades, pump impelling blades, rocket nozzles in jet engines, which caused great economic losses. Therefore, many researchers have investigated the solid particle erosion behavior of metal, polymer and their composite materials worn by solid particle. While fiber reinforced polymers take place in most of the studies conducted on solid particle erosion of composites, studies involving erosion on composites with coating materials can hardly be encountered. The poor erosion resistance of thermoplastic composites causes severe problems if the material is subjected to solid particle erosion. To overcome this problem, erosion resistant magnetron sputtered PVD coatings were deposited on GF/EP and CF/EP substrates. This is due to the fact that it is not easy to clearly understand erosion mechanisms of these types of composites, properties of their components and their interface interactions. The world of advanced science and technology has always been in need of materials with superior properties for better operational performances. Parallel to such needs, the importance and industrial usage of polymer composites have tremendously increased. The composites are extensively used as structural materials in various components and engineering parts in automobile, space craft industry, marine and energy conversion systems due to their excellent specific properties. The underlying reason for this is the fact that these composite materials exhibit high strengths, possess better coating properties and are economic as well. Meanwhile, advanced scientific researches on these materials are progressively carried out. Protective coatings produced by Physical Vapour Deposition (PVD) can increase the life time of the components. Therefore; in this study, ≈0.15 μm thickness ZrN coatings are applied on GF/EP and CF/EP by magnetron sputtering to gain an improved understanding of the erosion resistance. The impingement angles used in the tests were 30°, 60° and 90°, while the impact velocity was 34 m/s. Al_2O_3 particles with an average diameter of 400 μm was used. All test specimens regardless of their various properties exhibit maximum erosion rates at 30° impingement angle and thus exhibiting similar behavior as that observed for ductile materials. SEM views were performed on the surfaces in order to characterize the erosion mechanism. The erodent particles of the both coating layer and composite matrix were found of main role in governing the wear progression. The measured erosion rates were sensitively correlated with the material removal process in order to explain the changes within the interfaces.

Keywords: Solid particle erosion, ZrN coating, GF/EP, CF/EP, PVD, Erosion rate.

Acceptance ID: G294-O

Threshold Voltage Modulation of Polymer Transistors by Photo-induced Charge-Transfer between Donor-Acceptor Dyad

Juho Kim[1], Ji Eon Kwon[2], Soo Young Park[2], and Jong H. Kim[3], Tae-Dong Kim[1]*

[1]Department of Advanced Materials and Chemical Engineering, Hannam Unversity, Daejeon, 305-811, Korea
[2]Department of Materials Science and Engineering, Seoul National University, Seoul, 151-744, Korea
[3]Department of Molecular Science and Technology, Ajou Univerity, Suwon, 443-749, Korea
kjuho91@gmail.com / tdkim@hnu.kr

Since the first report on the organic field-effect transistor (OFET) in 1986, conjugated semiconducting polymers have attracted significant attraction as active layers of field-effect transistors (FETs) in recent years because of their excellent charge carrier transport ability, simple solution processibility, and uniform large-area printability. In addition, mechanical durability, flexibility and facile chemical structure modification of semiconducting polymers make them an emerging candidate material for next-generation optoelectronic devices. In order to minimize power consumption of integrated circuits in electronic devices driven by PFETs, particularly for portable devices, lowering V_{th}s or precise adjustment of V_{th}s of PFETs is necessary. So far, a number of experimental approaches have been envisioned for reducing V_{th}s, such as employing floating gate, high-dielectric constant (k) gate insulators, layered device structures, and photo-induced charge-transfer effect. Among them, because of its effectiveness, photo-induced charge-transfer, which utilizes inducing enhanced mobile charge carrier concentration in the FET channels for the V_{th} modulation, has received particular attention. In this work, we have studied photo-induced optoelectronic properties of conjugated polymers from device characterization and quantum calculation on the polymers. It was demonstrated that the photo-sensitive conjugated polymer with electron donor-acceptor dyads can modulate charge accumulation by photo-irradiation resulting in threshold voltage shift in the polymer field-effect transistors (PFETs) while this effect of the photo-inactive polymer is relatively low. These results suggest that the feasible molecular design strategies can provide an effective platform to achieve controllable threshold voltage modulation in PFETs.

Keywords: Conjugated polymers, Polymer field-effect transistors, Threshold voltage, Photo-induced charge-transfer

[1] TSUMURA, A., KOEZUKA, H. & ANDO, T. 1986. Macromolecular electronic device: Field-effect transistor with a polythiophene thin film. *Applied Physics Letters*, 49, 1210-1212.

[2] BABEL, A. & JENEKHE, S. A. 2003. High electron mobility in ladder polymer field-effect transistors. *Journal of the American Chemical Society*, 125, 13656-13657.

[3] MEI, J., KIM, D. H., AYZNER, A. L., TONEY, M. F. & BAO, Z. 2011. Siloxane-terminated solubilizing side chains: bringing conjugated polymer backbones closer and boosting hole mobilities in thin-film transistors. *Journal of the American Chemical Society*, 133, 20130-20133.

Acceptance ID: G4S9-P

Improved Performance of Nitride-based UV LED with MOCVD Grown Tin-doped Indium Oxide as UV Transparent Conductive Layer

*Yi Zhuo, Zimin Chen, WenbinTu and Gang Wang**

State Key Lab of Optoelectronics Materials & Technologies, Sun Yat-Sen University, Guangzhou 510275, China
e-mail: zhuoyi@mail2.sysu.edu.cn; stswangg@mail.sysu.edu.cn

Recently, the growing demand for ultraviolet optoelectronic devices, such as UV-LEDs, promotes call for suitable transparent conductive material. Tin-doped indium oxide (ITO) with low resistivity and high transparency has been widely used as transparent conductive layer in visible region[1]. However, the traditional ITO shows serious absorbance in the UV range because of an optical bandgap of 3.8 eV[2]. By extending the transmission window into UV range, ITO would become a promising UV-TCL material. In this work, we studied the electrical and optical properties of the ITO thin films grown by metal-organic chemical vapor deposition (MOCVD) and their application to UV-LEDs.

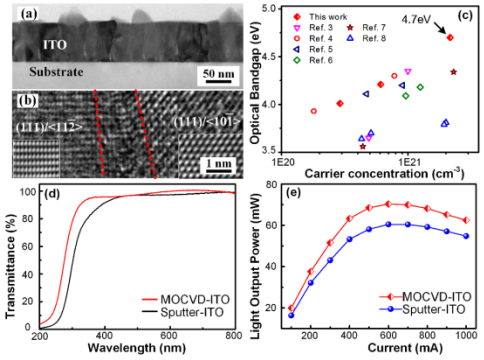

Figure 2 (a, b) Cross-sectional (High Resolution) TEM measurements; (c) The comparison of the optical bandgap of ITO grown by different techniques; (d) Transmittance spectrum of ITO deposited by MOCVD and sputtering; (e) I-L measurement of UV-LEDs with MOCVD-ITO and Sputter-ITO TCL.

ITO thin film was grown on double-side polished c-plane sapphire by MOCVD. The as-grown ITO is polycrystalline (Fig. 1(a)&(b)) and the resistivity of the film is 2.75×10^{-4} Ω·cm. Significant widening of optical bandgap from the well-known 3.8 eV to 4.7 eV have been observed. Because of the difference in preparing methods and conditions, the reported optical bandgap of ITO thin films conflicts seriously even for samples with similar electron concentration and conductivity. In Figure 1(c), the optical bandgap Eg is, together with some results reported by other groups, plotted as a function of carrier concentration *n*. For the samples grown by MOCVD in our work, the widening of bandgap as large as ΔE_g=0.98 eV is at least 0.4 eV larger than the reported value [3-8]. Thus, high transmittance at UVA/UVB region is achieved, which make it promissing for UVA/UVB optoelectronic device application.

Table 1. Comparison of UVA transmittance for different conductive materials.

	Thickness (nm)	Sheet Resistance (Ω/sq)	Averaged UVA Transmittance (%)
Textured ITO (this work)	90	30.6	94
MgZnO:Al	500	49	70
Silver Nanowire		32	89.9
Carbon Nanotube	100	53	<50
Graphene	3.5	520	<85

Correlated Metal $SrVO_3$	10	45	40

Furthermore, we fabricated UV-LEDs with two different ITO layers, one is grown by MOCVD and the other one is deposited by magnetic sputtering. As shown in Fig. 1(d), the ITO deposited by MOCVD shows show great enhancement in UVA/UVB transmittance. The I-V characteristics of two LED sampes are similar while the sample with MOCVD-grown ITO has slight lower foward voltage. The I-L measurement shows that the light output power of the UV-LEDs with MOCVD-grown ITO increased by 16.8% at 600 Ma (Fig. 1(e)). These results strongly suggest that ITO is a promising transparent conductive material for optoelectronic devices.

Keywords: ITO, UV transparent conductive, UV light emitting diode

[1] CHANG, S. J., SHEN, C. F., CHEN, W. S., KUO, C. T., KO, T. K., SHEI, S. C. & SHEU, J. K. 2007. Nitride-based light emitting diodes with indium tin oxide electrode patterned by imprint lithography. *Applied Physics Letters,* 91**,** 3.

[2] KUO, C. H., CHEN, C. M., KUO, C. W., TUN, C. J., PAN, C. J., PONG, B. J. & CHI, G. C. 2006. Improvement of near-ultraviolet nitride-based light emitting diodes with mesh indium tin oxide contact layers. *Applied Physics Letters,* 89.

[3] FUJIWARA, H. & KONDO, M. 2005. Effects of carrier concentration on the dielectric function of ZnO : Ga and In2O3 : Sn studied by spectroscopic ellipsometry: Analysis of free-carrier and band-edge absorption. *Physical Review B,* 71.

[4] HAMBERG, I., GRANQVIST, C. G., BERGGREN, K. F., SERNELIUS, B. E. & ENGSTROM, L. 1984. Band-gap widening in heavily Sn-doped In2O3. *Physical Review B (Condensed Matter),* 30**,** 3240-9.

[5] KIM, H., GILMORE, C. M., PIQUE, A., HORWITZ, J. S., MATTOUSSI, H., MURATA, H., KAFAFI, Z. H. & CHRISEY, D. B. 1999. Electrical, optical, and structural properties of indium-tin-oxide thin films for organic light-emitting devices. *Journal of Applied Physics,* 86**,** 6451-6461.

[6] KIM, H., HORWITZ, J. S., KUSHTO, G., PIQUE, A., KAFAFI, Z. H., GILMORE, C. M. & CHRISEY, D. B. 2000. Effect of film thickness on the properties of indium tin oxide thin films. *Journal of Applied Physics,* 88**,** 6021-6025.

[7] RAY, S., BANERJEE, R., BASU, N., BATABYAL, A. K. & BARUA, A. K. 1983. Properties of tin doped indium oxide thin films prepared by magnetron sputtering. *Journal of Applied Physics,* 54**,** 3497-501.

[8] TUNA, O., SELAMET, Y., AYGUN, G. & OZYUZER, L. 2010. High quality ITO thin films grown by dc and RF sputtering without oxygen. *Journal of Physics D-Applied Physics,* 43.

Acceptance ID: G53V-P

Effects of Thermal Annealing on Electrostatic Capacitance Properties for High-k ZrO_2 Layers Grown on Ge

Youngmin Lee,[1] *Dong Jin Lee*,[1] *Hwauk Lee*,[2] *Sejoon Lee*[1,2,*]

[1] *Quantum-functional Semiconductor Research Center, Dongguk University, Seoul 04623, Korea*
[2] *Department of Semiconductor Science, Dongguk University, Seoul 04623, Korea*
**E-Mail: sejoon@dongguk.edu*

We investigated the effects of thermal annealing on the electrostatic capacitance properties of the high-*k* ZrO_2 layers grown on *p*- Ge at 500°C by r.f. magnetron sputtering. During the growth of ZrO_2, we maintained the higher oxygen-partial pressure (*i.e.*, O_2/Ar > 1) so as to avoid oxygen deciciencies in ZrO_2. The samples were subsequently annealed at 600-700°C for 60 s in Ar ambience. For the as-grown ZrO_2 layer, the maximum capacitance (*i.e.*, C_{max} at the accumulation mode) was observed to drastically decrease with increasing frequency of *ac* signals. After thermal annealing at temperatures above 600°C, however, the dielectric characteristics of the ZrO_2 layers were much improved. Namely, after annealing at 600 - 650°C, C_{max} was more than 3-times-increased and was much stabilized at wide frequency ranges. These indicate that the defect density was effectively decreased through thermal annealing. From results of x-ray photoelectron spectroscopy, we confirmed the above features to arise from the stabilization of Zr-O bonds. The best electrostatic permittivity was ~24, the equivalent-oxide-thickness was <4 nm, and the dielectric breakdown field was >1 MV/cm. The results suggest that the dielectric characteristics of ZrO_2 can be effectively improved through thermal annealing.

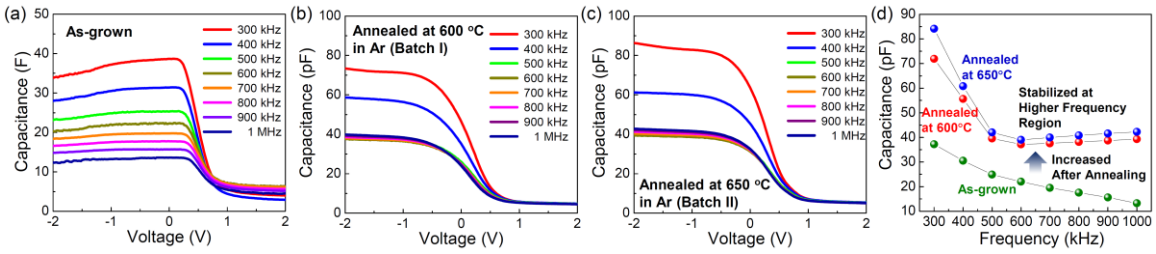

Fig. 1. C-V characteristic curves of (a) as-grown, (b) 600°C-annealed, (c) 650°C-annealed ZrO_2 layers. (d) Dependence of C_{max} on frequencies for the as-grown and annealed ZrO_2 layers.

Keywords: High-k ZrO_2, Ge, Thermal Annealing, Electrostatic Capacitance

Acceptance ID: GYKB-P

Surface film characterization and secondary electron emission properties of Ag-Mg-Al alloy

Fan Zhou, Quan Zhang, Feifei Wang, Wei Liu, and Jinshu Wang

School of Materials Science and Engineering
Beijing University of Technology
Beijing, China
zhoufan@bjut.edu.cn

Secondary electron emission (SEE) materials have broad applications in various vacuum electronic devices, such as electron and photoelectron multipliers and plasma display panels. Among various SEE materials, Ag-Mg alloy has been utilized due to the advantage of high secondary electron yields (δ) of MgO film developed on the alloy conventionally through a thermal activation process in various atmospheres, such as oxygen, carbon dioxide and water vapor. Depending upon the activation parameters, Ag-Mg alloys with MgO films of 20-200 nm thick and δ values in the range of 3-12 can be obtained. However, poor resistance to electron/ion bombardment and short lifetime of the Ag-Mg alloy cathodes restrict their practical application. In this study, MgO thin film of ~50 nm containing alumina were developed on a Ag-Mg-Al alloy through an activation process performed at 550°C for 30 min under oxygen pressures of 20.0 Pa. Surface film composition and component distribution for the alloy are also characterized by Auger Electron Spectroscopy (AES). SEE property and preliminary electron bombardment testing for the alloy after proper activation are also investigated. Element depth profiles of the activated alloy derived from AES reveal that the top surface consists of pure MgO and alumina locates beneath the top surface MgO layer, which is due to higher migration rate of magnesium than aluminum during activation. The activated aluminum-containing alloy exhibit superior secondary electron yield of 7.9 and better resistance to electron bombardment comparing to conventional Ag-Mg alloy cathode, which is attributed to the alumina present in the surface MgO film, resulting in increased bonding energy and consequently better working stability of the film.

Keywords: MgO thin film; Ag-Mg-Al alloy; activation; secondary electron yield; electron bombardment

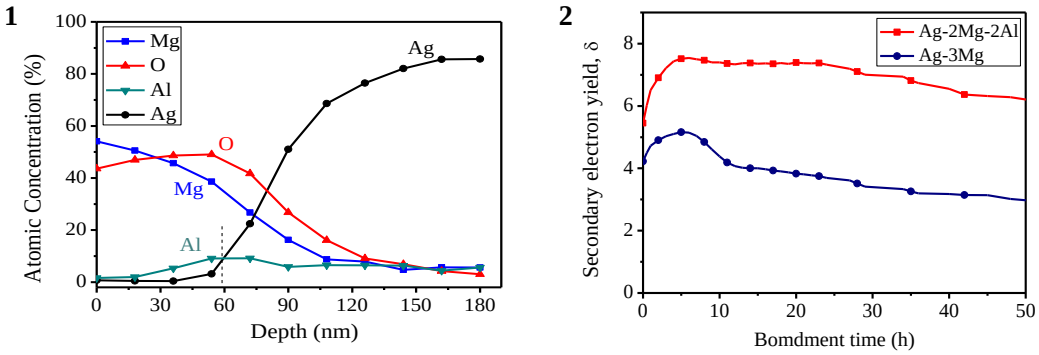

Fig. 1 Element depth profiles of the Ag-2Mg-2Al activated at 500°C for 30 min at P_{O2}=20 Pa.
Fig. 2 Secondary electron yields for the activated alloy specimens under constant electron bombardment for 50 h.

References

[1] F. Yang, J.S. Wang, W. Liu, X. Liu, M. Zhou, "Studies on the pressed yttrium oxide-tungsten matrix as a possible dispenser cathode material" Mater. Chem. Phys., vol. 149-150, pp. 288-294, October 2015.

[2] P. Wargo, B.V. Haxby, W.G. Shepherd, "Preparation and properties of thin film MgO secondary emitters" J. Appl. Phys., vol. 27, pp. 1311-1316, November 1956.

[3] Q. Zhang, J.S. Wang, F. Zhou, W. Liu, F.F. Wang, C. Lai, "Influence of activation parameters on the thickness of MgO thin film on Ag-3Mg alloy and its secondary eelctron emission property" Mater. Res. Bull., in press.

Acceptance ID: HCB8-O

Black diamond: A piece of jewelry for science and technology

Gufei Zhang[1], Tomas Samuely[2], Jozef Kacmarcik[2], Paul W. May[3], Evgeny A. Ekimov[4], Johan Vanacken[1], and Victor V. Moshchalkov[1]*

[1]INPAC-Institute for Nanoscale Physics and Chemistry, KU Leuven, Belgium
[2]Centre of Low Temperature Physics, Institute of Experimental Physics, Slovak Academy of Sciences & Faculty of Science, P. J. Safarik University, Slovakia
[3]School of Chemistry, University of Bristol, UK
[4]Vereshchagin Institute for High Pressure Physics, Russian Academy of Sciences, Russia

Since the preparation of synthetic diamond by Dr. H. T. Hall at General Electric in 1954, industry has benefited more and more from this material. With a low fabrication cost, synthetic diamond brings in nearly all the unique advantages of natural diamond, e.g., the robust mechanical strength, the extraordinarily high thermal conductivity, the remarkable resistance to contamination and chemical etching, and so on. Besides, the remarkable electronic properties of blue diamond (lightly boron-doped diamond), has made this cost-effective semiconductor a promising candidate for the 21st-century microelectronics and power electronics. After 2004, the application range of artificial diamond has been further extended owing to the superconductivity discovered in black diamond (heavily boron-doped diamond). For example, well functional superconducting quantum interference device (SQUID) and local probing tips have been made of black diamond.

Black diamond also provides a powerful stage for solving some interesting puzzles, which are not only relevant for practical concerns but also significant in fundamental science. The observation of superconductivity in *bad* conductors (doped insulators such as high temperature superconductors and black diamond) is an intriguing question directly linked to the origin of superconductivity. In addition, the influence of disorder on the quantum condensate of Cooper pairs still remains an attractive topic, after accompanied the ever growing list of superconductors for nine decades. Note that as a result of the used preparation method, synthetic black diamond is generally granular disordered. Here we present the observation of a series of anomalous electrical transport, magnetic, specific heat and local superconducting properties of granular black diamond. These anomalies, demonstrating a bosonic nature, are interpreted as a result of quantum confinement and coherence effects in the presence of intrinsic and extrinsic granularity. Our data, obtained for black diamond, provide a reference for understanding the superconductivity in other granular disordered systems.

Acceptance ID: HLTJ-O

A graphene superficial layer for the advanced electroforming process

Hokyun Rho[1,2], Mina Park[1], Seungmin Lee[1], Sukang Bae[1], Tae-Wook Kim[1], Jun-Seok Ha[2] and Sang Hyun Lee[1]*

[1] Applied Quantum Composites Research Center, Korea Institute of Science and Technology, Jeollabuk-do 565-905, Republic of Korea
[2] Department of Advanced Chemicals & Engineering, Chonnam National University, Gwangju 61186, Republic of Korea
**E-mail : sanghyun.lee@kist.re.kr*

Electroforming process is a specialized electroplating technology for the development of micronscale-sophisticated metal architectures using a cathode mandrel or template.[1] In combination with lithography technology, electroforming has been widely used for development of microelectromechanical systems (MEMS), as part of a process called LIGA.[2] In order to fabricate metal thin structure, the separation of the metal film from the mold without deformation or damage is one of the most important steps in the electroforming process. In addition, the mold has to be electrically conductive to draw metal ions from the solution, while the deposited metals must have less adhesion with the mold to facilitate its removal.

In this study, we introduced a chemical vapor deposition (CVD) graphene grown on a Cu foil as a template, which provides high electrical conductivity and low adhesive force with the template, thus enabling an effective electroforming process. Graphene provides the required conductivity for electrodeposition, as well as a low adhesive force for effective delamination from the thin film, which enables continuous processing. The adhesion between an electroplated Cu film and graphene is much less than that between graphene and the Cu foil that was used for CVD. The surface morphology of the deposited Cu film resembles the flat surface of the graphene/Cu template. This study effectively connects the electroforming process aided by graphene to the concept of flexible electronic devices and provides an approach for the practical implementation of a conducting line or frame in electronics packaging of a flexible circuit board for LED arrays.[3]

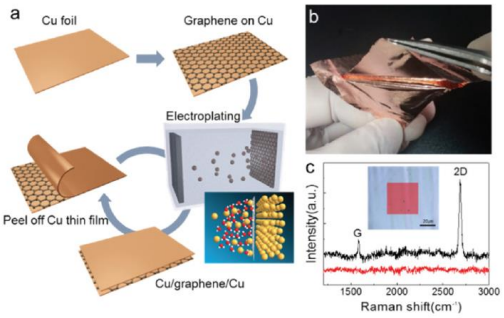

Figure 1. Free-standing Cu thin film from an electroforming process.

Keywords: Electroforming process, graphene, copper, electrodeposition, flexible circuit board

[1] MACGEOUGH. J. A., LEU. M. C., RAJURKAR. K. P., DE SILVA. A. K. M., LIU. Q. 2001. Electroforming Process and Application to Micro/Macro Manufacturing. CIRP Ann.-Manuf. Technol., 50, 499-514.
[2] ROMANKIW. L. T. 1997. A path: from electroplating through lithographic masks in electronics to LIGA in MEMS. Electrochim. Acta, 42, 2985-3005.
[3] RHO. H., PARK. M., LEE. S., BAE. S., KIM. T.-W., HA. J.-S., LEE. S. H. 2016. A graphene superficial layer for the advanced electroforming process. Nanoscale, 8, 12710-12714.
Acceptance ID: J6G9-P

Preparation, structure and properties of sputtered thin films of titania and titanium suboxides

*Yu-Jen Lin, Mikhail Pylnev, Wei-Zen Kang and Ming-Show Wong**

Department of Materials Science and Engineering, National Dong Hwa University, Hualien, Taiwan-974, ROC

Corresponding author's e-mail: mswong@gms.ndhu.edu.tw

TiO_2 has been widely investigated due to its versatile functional properties for applications energy and environment. Recently, black and colored titania oxides exhibiting exceptional photocatalytic properties were reported. A series of TiO_x ($0<x\leq2$) thin films with different Ti/O ratio were deposited on Si substrates by reactive magnetron sputtering of Ti metal in the $Ar+O_2$ plasma. The influence of the deposition/annealing temperatures and oxygen flow rate on the structure, and mechanical, electrical and photocatalytical properties of the films was studied. With increasing the oxygen flow rate, the following phases appeared in the following order: Ti metal, Ti-O solid solution, TiO, Ti_2O_3, Ti_3O_5, Magnéli phases (Ti_4O_7 and Ti_5O_9) and rutile and anatase TiO_2. With increasing the processing (deposition or annealing) temperatures, the crystallinity of the films was improved, which resulted in changes of film properties. The trends of hardness and electrical conductivity of the ceramic TiO_x films were $TiO>Ti_2O_3>$Magneli phases and then the rutile phase. The mixed Magneli films exhibited superior photocatalytical properties to those of pure titania films.

Keywords : Titania; TiO_x, Titanium suboxide; Reactive sputtering; Magneli phase; Nanoindentation.

Acceptance ID: JPKD-P

Molecular Self-Assembly on Two-Dimensional Atomic Crystals

Organic molecular self-assembly on two-dimensional (2D) materials has wide potential applications, such as passivation layers, organic electronics, photonic devices, solar cells, and graphene-based devices, while understanding the dynamic mechanism of the self-assembly falls far behind its application. Therefore, it is crucial and urgent to understand the physical mechanisms on the self-assembly. Via molecular dynamics simulation, we successfully visualize the nanoscale self-assembly of organic molecules on graphene and boron nitride monolayer from a disordered state to an ordered structure.[1,2] On the basis, we reveal that the intermolecular hydrogen-bonds play a key and positive role in the self-assembly.[3] They can significantly broaden the nucleation area, raise the stability-metastability critical temperature, accelerate the nucleation process, and guide the nucleation direction.[3] Moreover, we propose an effective passivation approach, self-assembly of organic molecules on black phosphorus (BP), to protect BP from the degradation without breaking the original electronic properties of BP.[4]

1. **Zhao, Y.**; Wu, Q.; Chen, Q., Wang, J. Molecular Self-Assembly on Two- Dimensional Atomic Crystals: Insights from Molecular Dynamics Simulations. *J. Phys. Chem. Lett.* **2015**, *6*, 4518-4524.
2. Wu, B.; **Zhao, Y.**; Nan, H.; Yang, Z.; Zhang, Y.; Zhao, H.; He, D.; Jiang, Z.; Liu, X.; Li, Y.; Shi, Y.; Ni, Z.; Wang, J.; Xu, J.-B.; Wang X. Precise, Self-Limited Epitaxy of Ultrathin Organic Semiconductors and Heterojunctions Tailored by van der Waals Interactions. *Nano Lett.* **2016**, *16*, 3754-3759. (Co-first author)
3. **Zhao, Y.**; Wang, J. How to Obtain High-Quality and High-Stability Interfacial Organic Layer: Insights from the PTCDA Self-Assembly. Accepted by *J. Phys. Chem. C* DOI: DOI: 10.1021/acs.jpcc.7b00606.
4. **Zhao, Y.**; Zhou, Q.; Li, Q.; Yao, X.; Wang, J. Passivation of Black Phosphorus via Self-Assembled Organic Monolayers by van der Waals Epitaxy. *Adv. Mater.* **2016**, DOI: 10.1002/adma.201603990.

Acceptance ID: JV69-O

High performance, low-cost top-contact Pentacene-based Organic Thin Film Transistor with oxidized MoO_3/Au bilayer source-drain electrode

Ranjit Sarma & Tribeni Borthakur*

Thin Film Lab. Department of Physics, Jagannath Barooah College(Autonomous), Jorhat785001, Assam, India
**rsarmajrt@gmail.com*

We have proposed an improved Pentacene-based Organic Thin Film Transistor (OTFT) with oxidized MoO_3/Au bilayer source-drain. A low-cost deposition method developed in the laboratory is used to prepare oxidized MoO_3/Au bilayer source-drain. OTFT devices with the oxidized MoO_3/Au bilayer source/drain electrode exhibit better performance than the lab made MoO_3/Au bilayer source/drain OTFT devices. The field-effect-mobility, on-off ratio, threshold voltage and subthreshold slope of devices with oxidized MoO_3/Au bilayer source/drain electrode OTFT are $1.7 cm^2 v^{-1} s^{-1}$, 2.5×10^6, -3.5 volts and .39 v/decade respectively.

Acceptance ID: KG4A-O

Characterization of Cu Thin Film on Invar Sheet by Finite Element Analysis and Dynamic-Nano Indentation Method

B. K. Kang[1], Y. Baik[1], and Yong Choi[1,]*

[1]Department of Materials Science and Engineering, Dankook University, Cheonan, Chungnam, 31116, Korea

The surface properties of a thin film were determined by dynamic-nano indentation method, which was verified by finite element analysis. The specimens were magnetron sputtered Cu thin film on Invar (Fe-35%Ni) sheet which was prepared by electroforming. The deposit rate of copper on electroformed Invar thin sheet increase with sputter power. The surface resistance of Cu/Invar sheet was reduced to 67% comparing to that of Invar sheet. The elastic stiffness, friction coefficient and fatigue limit of the Cu/Invar were 45, 0.130, 0.093, respectively. The load-time-displacement curves of the bulk, the hard coating deposit and the thin film determined by dynamic-nano indentation method well described their elastic stiffness. The micro-Vickers hardness of the Cu thin film was 240 [Hv], respectively. The empirical equation between micro-Vickers hardness and nano-hardness was $Y[GPa]=9.18x10^{-3}X[Hv]$. The finite element analysis of a load distribution at the nano indenter tip based on static linear and non-linear conditions showed that 1 mN-loading made 486 [mN] at copper. The load estimation by finite element analysis was well agreement with the dent deformation observed by surface probe microscopy.

Acceptance ID: KPZL-P

Synthesis and properties of two-dimensional layered arsenic monosulfide (As_4S_4) possessing strong structural luminescence

Leonid Mochalov, Aleksey Nezhdanov, and Aleksander Mashin

Lobachevsky State University of Nizhny Novgorod, Nizhny Novgorod, Russia.
E Mail: **mochalovleo@gmail.com**

The novel physical properties of two-dimensional and layered "beyond graphene" chalcogenide materials suggest a strong base to study new fundamentals underlying condensed matter physics. Among these materials layered arsenic monosulfide is a key to advancing 2-D photosensitive devices [1, 2] such and quantum computer [3]. Here we demonstrated the synthesis of two dimensional arsenic monosulfide (As_4S_4) via interaction of elemental arsenic and sulfur in low-temperature non-equilibrium plasma discharge at low pressure.

Plasma samples were prepared by a set-up with scheme shown on Fig.1.

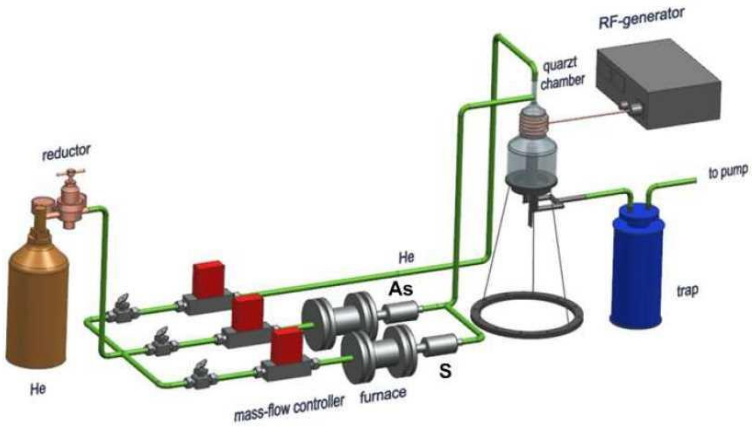

Fig. 1. Principal scheme of the PECVD setup.

The study of the samples macro-composition was carried out by X-ray microanalysis using a scanning electron microscope JSM IT-300LV (JEOL) with an energy-dispersion detector for elemental analysis X-MaxN 20 (Oxford Instruments) under high vacuum and at accelerating voltage of 20 kV.

IR spectrum of prepared on sodium chloride substrate As_4S_4 thin film is presented in fig. 2a. There are no lines of own or selective absorption bands in the range of 2-17 microns and degree of transparency reaches the value of 90 %. High parameters of IR transparency may be explained by high purity of the initial substances, their additional purification in plasma discharge and small thickness (about 500 nm) of the thin film. Strong structural photoluminescence of As-S thin films deposited on SiO_2 and NaCl substrates with maximum on 575 nm was measured at excitation of 473 nm laser (fig. 2b).

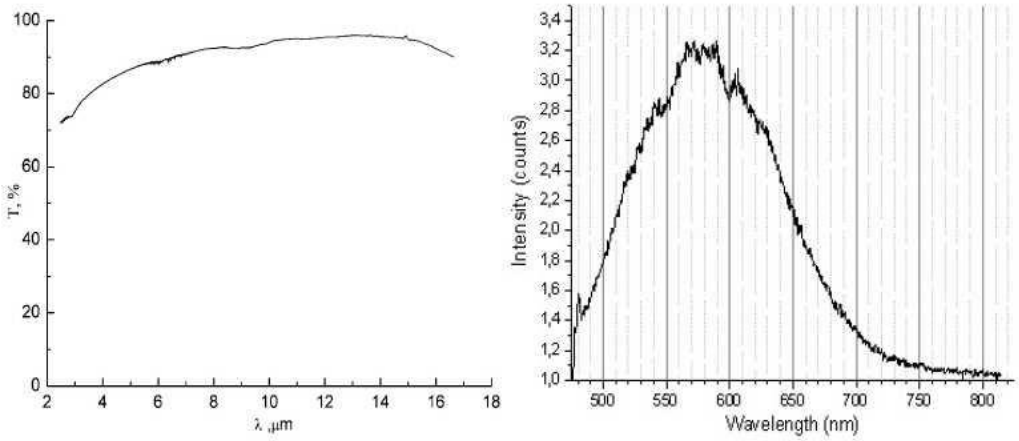

Fig. 2. IR absorption spectra of prepared As_4S_4 thin films (a) and photoluminescence of As-S thin films deposited on SiO_2 and NaCl substrates (b)

The surface of thin film was studied by Atom Forced Microscopy (figure 2). Thin film consists of structural units of 100 nm size and roughness value is equal to 3 nm.

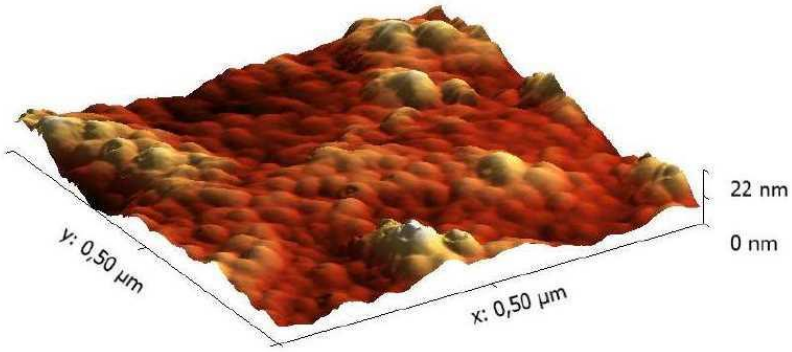

Fig. 3. The results of AFM surface study

According to the data obtained the surface quality of the thin film obtained by PECVD via elemental arsenic and sulfur is comparable with the same for the other methods [3].

The results of Electron Scanning Microscopy investigations a presented on fig .4.

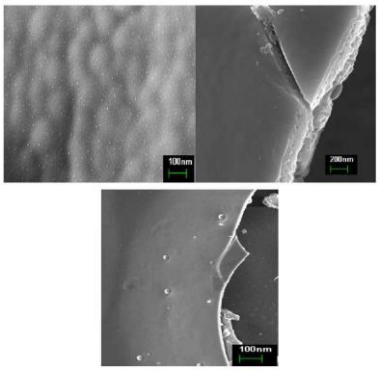

Fig. 4. The results of ESM

It is shown that the obtained As_4S_4 films possess 2-D layered structure.

Keywords: arsenic monosulfide films, PECVD, luminescence

[1] FRUMAR, M., FRUMAROVA, B., NEMEC, P., WAGNER, T., JEDELSKY, J., HRDLICKA, M. 2006. Thin chalcogenide films prepared by pulsed laser deposition – new amorphous materials applicable in optoelectronics and chemical sensors. *J. Non-Cryst. Solids*, 352, 544–561

[2] GONZÁLEZ-LEAL, J. M., PRIETO-ALCÓN, R., ANGEL, J. A., AND MÁRQUEZ, E. 2003. Optical properties of thermally evaporated amorphous as 40 S 60-x Se x films. *J. Non-Cryst. Solids*, 315, 134–143.

[3] GONZÁLEZ-LEAL, J., PRIETO-ALCÓN, R, VLCEK, M. AND MARQUEZ, E. 2004. Structural and optical characterization of amorphous AsS and AsSe films prepared by plasma-enhanced chemical vapor deposition. *J. Non-Cryst. Solids*, 345–346, 88–92.

Acceptance ID: KUGU-I

Synthesis and characterization of As-Te phase-changing chalcogenide materials prepared via Plasma-enhanced Chemical Vapour Deposition

Leonid Mochalov, Aleksey Nezhdanov, and Aleksander Mashin

Lobachevsky State University of Nizhny Novgorod, Nizhny Novgorod, Russia.
E Mail: mochalovleo@gmail.com

Tellurium-based chalcogenide materials are of proper interest, since they possess a wider transparency window in IR region and lower phonon energy values compared with sulfur and selenium based glasses [1-6]. In combination with a relatively narrow bandgap, these materials have got a great potential for application in IR optoelectronics and photonics. The effect of threshold switching was first noted for the As-Te-I glasses in 1964 [7], and for the As-Te-Se glasses in 1966 [8]. However, exactly the As-Te binary system causes the particular interest of researchers because it seems, in fact, to be a model for understanding of the glass-forming properties of the entire family of the chalcogenide tellurium based materials [9]. In this paper we report that first time As-Te phase-changing materials were prepared via plasma-enhanced chemical vapor deposition (PECVD) by low-temperature non-equilibrium RF plasma at low pressure. First time volatile elements As and Te were the initial substances. Fine phase tailoring of As-Te films was implemented by means of changing of the parameters of deposition. Phase modification of the films by 632.8 nm laser irradiation was demonstrated.

The synthesis was carried out by the plasma-chemical setup shown in Fig1.

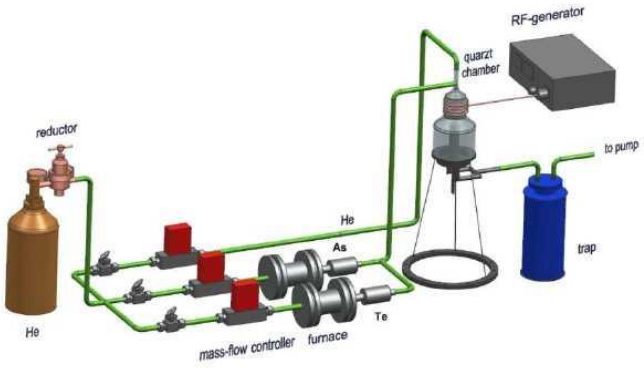

Fig. 1. Scheme of the plasma-chemical setup for As-Te film preparation.

Keywords: tellurium-based glasses, phase-changing materials, chalgogenides, PECVD

[1] OVSHINSKY, S.R. 1968. Reversible electrical switching phenomena in disordered structures. *Phys. Rev. Lett.*, 21, 1450-1453.

[2] FEILEIB, J., DE NEUFVILLE, J, MOSS. S.C., OVSHINSKY, S.R. 1971. Rapid reversible light-induced crystallization of amorphous semiconductors. *Appl. Phys. Lett.*, 18, 254-257.

[3] NALIVAUKO, V.I. 2007. Materials for Optical Information Recording on the Base of Subnanostructured Chalcogenide Films. *J. of Nuclear Instruments and Methods in Physics Research (NIMA)*, 575, 113.

[4] ADAM, J-L, ZHANG, X. 2014. Chalcogenide Glasses: Preparation, Properties and Applications, *Handbook.* *Woodhead Publishing*.

[5] KOLOBOV, A.V. 2003. Photo-Induced Metastability in Amorphous Semiconductors, Wiley.

[6] CORNET, J., ROSSIER, D. 1973. Properties and structure of As Te glasses (II). Local order parameters and structural model. *J. Non-Cryst. Solids*, 12, 85-99.

[7] CHANG, J., DOVE, D.B. 1974. Electron diffraction RGF analysis of amorphous As_2Se_3, As_2Se_2Te, As_2SeTe_2 and As_2Te_3 films. *J. Non-Cryst. Solids*, 16(1), 72–82.

[8] MA, Q., RAOUX, D., BENAZETH, S. 1993. Local structure of As_xTe_{100-x} glasses studied by differential x-ray anomalous scattering and x-ray absorption spectroscopy, *Phys. Rev. B*, 48(22), 16332.

[9] KUMEDA, Y., USUKI, T., UEMURA, O. 1996. TOF-neutron diffraction study of liquid TI-As_2X_3 systems (X: Se, Te). *J. Non-Cryst. Solids*, 205–207(1), 130–134.

[10] TITUS, S. K., ASOKAN, S. 1992. Thermal crystallization behavior of As-Te glasses. *Physical Review B*, 46(22), 14493-14500.

Acceptance ID: KUGU-I

Graphene-templated Laterally Continuous Growth of Ultrathin Metal film For Bio-Implantable Thermal heater

Soo Sang Chae and Jeong-O Lee

Korea Research Institute of Chemical Technology, 141 Gajeong-ro, Yuseong-gu, Daejeon 34114, Korea

Tel.:82-42-860-7303, E-mail: jolee@krict.re.kr

Metal thin films as a most essential materials in numerous present electronics has been evolving over the decades. However, their use in future electronics including biological and photonic electronics is limited due to its opacity and low flexibillity. Changing the thickness of metal to the nanometer scale, approximately to underneath 10 nm, can cause them to display unexpected properties, which may be a semi-transparency and bendability. However, most metal growth mechanisms (e.g. Island growth model) lead to conductivity loss within the thikcness-scale because of those high cohesive energy. In this study, we present that graphene may be seen as a template for realizing laterally continuous ultrathin metal films by suppressing the island formation, which become conducting at a thikncess much smaller than the percolation threshold. Graphene that is atomically flat as well as chemically inertness can make the incident metal atoms to minimize surface diffusion and nucleation density. Furthermore, as motivated by graphene's transparecy, the percolation threshold thinkness of metal thinfilm is strongly influenced by the chemical functionallity of underlying substrate. Finally, we demonstrated that the resulting ultrathin metal film exhibits a superior thermal-heater performance with low operating voltage, which allow to be used in bio- implantable thermal heater for crytherapy or thermotherapy.

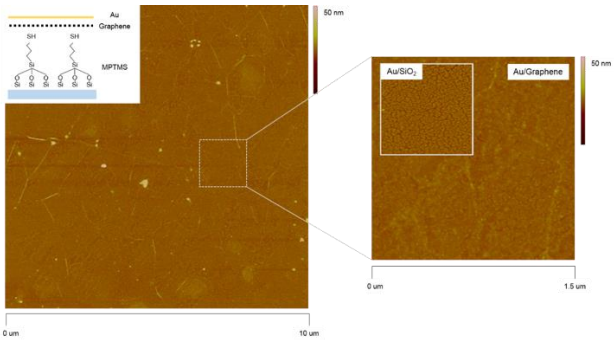

Fig. 1. AFM topographic images of 6 nm gold thin film deposited on Graphene.

Ultrathin and smooth gold thinfilm was achieved on graphene template over large area (left). Graphene that is atomically flat can allow the incident metal atoms to minimize surface diffusion and nucleation density, which result in ultrathin smooth metal film formation (right) as comparison that on bare SiO_2 substrate (inset).

Acceptance ID: lm6b-O

Effect of layer boundaries of ALD processed multilayered inorganic thin films on environmental protection

*Saya Lee and Sang Ouk Ryu**

Dept. of Electronics and Electrical Engineering, Dankook University
** corresponding and presenting author*

Recently, a protective thin film coating for organic devices has drawn great attention due to their vulnerable nature against humidity and atmosphere. The protective coating on glass substrates is now readily commercialized. However, the coatings on flexible substrates for the application of foldable devices are still huge technical challenges.

To impose a flexibility to inorganic thin films they must have the lowest possible thickness yet maintain physical protection requirements against environmental issues. Multilayer inorganic thin films were deposited by means of atomic layer deposition(ALD) technique. The layer consists of Al_2O_3(50nm)/TiO_2(5nm)/Al_2O_3(50nm) thin films. Measured water-vapor transmission rate(WVTR) by means of MOCON Aquatron2 has shown well below its detection limit which is known to be 5 x 10^{-5} g/m^2 day. Two different examinations were performed to figure out origin of the physical capabilities of environmental protection of the coatings. Is it from densities of each coated thin films or layer boundaries normal to penetration direction of the multilayered thin films?

Acceptance ID: LWRG-P

Improvement of perovskite solar cell efficiency via surface modification

Sang-Hun Nam[1], Ki-Hwan Hwang[1,2], Dong In Kim[1,2], Jin-Hyo Boo[1,2]

[1]Institute of Basic Science, Sungkyunkwan University, Suwon 440-746, Korea
[2]Department of Chemistry, Sungkyunkwan University, Suwon 440-746, Korea
E Mail : jhboo@skku.edu

Recently, perovskite materials have attracted great attention due to its outstanding light-harvesting characteristics. Especially, methylammonium lead halide perovskites are a new family of photovoltaic materials with advantages of efficient light absorption, easy solution processability, extremely long ambipolar carrier diffusion lengths, etc. In this work, we have tried to improve current density and efficiency via glass texturing, soft-lithograph and solvent engineering technique in two different cell structures, based on mesoscopic metal oxides and planar heterojunction solar cells. The glass substrates were textured by wet etching process using diluted HF solution at a constant concentration of etchants ($HF:H_2O=1:1$). Then, the light trapping properties of suitable films were controlled over a wide range by varying the etching time (1~5 min, interval 1 min). The surface texturing changed the reflected light in an angle that it can be reflected by substrate glass surface. As a result, current density and cell efficiency were affected by light trapping layer. We also fabricated perovskite solar cell with a high-quality three dimensional photonic crystal nanostructures embossed in the mesoporous TiO_2 layer. The effect of photonic crystal with round-shaped of various size (400~1600 nm, interval 400 nm) have enhanced optical absorption, resulting that the current density is greatly improved while the open-circuit voltage of the cell maintain. Thus, power conversion efficiency was greatly improved. Lastly, in the case of solvent engineering, we made the dense perovskite layer through fast-dipping method into diethyl ether at planar heterojunction structures. In this reason, it was confirmed that effective action of ether fast dipping treatment on the perovskite morphology control and solar cell property. On the basis of the recent achievements, a power conversion efficiency with over 20% is achieved based on optimized perovskite solar cells.

Keywords: Perovskite solar cell, Glass texture, Soft-lithograph, Solvent engineering, Efficiency

Acceptance ID: MUGP-I

Fabrication of SiC based AFM cantilever for NSOM application

Sang-Hun Nam[1], Ki-Hwan Hwang[1,2], Jung-Hoon Yu[1], Dong In Kim[1,2], Ji Won Lee[1,2], Jin-Hyo Boo[1,2]

[1]Institute of Basic Science, Sungkyunkwan University, Suwon 440-746, South Korea
[2]Department of Chemistry, Sungkyunkwan University, Suwon 440-746, South Korea
E Mail : jhboo@skku.edu

Silicon carbide thin films were deposited on Si(100) substrates by metal-organic chemical vapor deposition(MOCVD) in high vacuum condition(2.0×10^{-7} Torr) using 1,3-disilabutane as a single source precursor which contains silicon and carbide in 1:1 ratio at various temperature in the range of 700 ~ 1000 °C. The XPS result shows that the SiC thin film grown at 950 °C which have carbon rich for silicon and carbon at 1:1.2 ratio. XRD result shows that the SiC thin film grown at 900 °C which appeared at 2 = 41.6° for SiC (200) reflection at a large intensity and a single shape diffraction peck. SEM images result show that the SiC thin film grown at 900 °C which has influence on the small grain size and single crystallinity. AFM images result show that the SiC thin film has smooth surface at RMS = 20nm. In this paper, we fabricated the small aperture for the better performance such as less noise, higher resonant frequencies and fast imaging. We will apply that silicon carbide thin film has smooth surface on NSOM application.

Keywords: SiC, Thin Film, AFM, Cantilever, NSOM

Acceptance ID: MUGP-P

Pattern formation of a dried droplet of suspension solution

Chen-Zhe Wang[1,2], Kun Zhang[2,3], and Ru-Wen Peng[3]

1) Department of Physics, University of California, Berkeley, CA 94720, USA
2) NSF Nanoscale Science and Engineering Center, University of California, Berkeley, CA 94720, USA.
3) National Laboratory of Solid State Microstructures and School of Physics, Nanjing University, Nanjing 210093, China

When a droplet of suspension solution of solid particles, such as coffee or soy sauce, is dried on table surface, very often a ring-shaped stain is formed. Although the phenomenon has been known for centuries, the problem was carefully studied only in recent decades. In this work we use polystyrene spheres and water as a model suspension solution to study stain pattern of the droplet. Two types of substrates with different wetting features have been used. For hydrophilic surface, conventional ring-shaped patterns are observed. For hydrophobic surface the dried pattern becomes a solid 'pancake' instead of a ring. The influence of concentration of suspension solution and gravity on stain pattern has also been investigated. This study might be enlightening in improving printing quality and painting homogeneity.

Acceptance ID: N5G3-O

A novel *in-situ* Al-doped ZnO films by atomic layer deposition with an interrupted flow method

Jheng-Ming Huang[1], Ching-Shun Ku[2], Hsin-Yi Lee[2,3], Chih-Ming Lin[3], San-Yuan Chen[4]

[1] Program for Science and Technology of Accelerator Light Source, National Chiao Tung University, Hsinchu 300, Taiwan.
[2]2National Synchrotron Radiation Research Center, 101 Hsin-Ann Road, Hsinchu Science Park, Hsinchu 30076, Taiwan.
[3]Department of Applied Science, National Hsinchu University of Education, Hsinchu 30014, Taiwan
[4] Department of Materials Science and Engineering, National Chiao Tung University, Hsinchu 300, Taiwan.
e-mail: hylee@nsrrc.org.tw

In this study, we developed a novel *in situ* doping method with an interrupted flow for an atomic layer deposition (ALD) system. *In situ* aluminium-doped ZnO (AZO) films were grown on glass substrates at temperatures in range 200-280 °C; the optimal temperature, 260 °C, depended on the electrical properties. To assess the effect of the ratio of pulses of diethylzinc (DEZn) and trimethylaluminium (TMA) on the structural, optical and electrical properties, we grew AZO films with various pulse doping ratios of DEZn:TMA in a range from 3:1 to 10:1 at 260 °C. These properties and the content of Al were investigated with X-ray diffraction, X-ray reflectivity (XRR), a high-resolution transmission electron microscope (HRTEM), a secondary-ion mass spectrometer (SIMS), transmission spectra, Hall measurements and X-ray photoelectron spectra (XPS). The electrical resistivity was least, 5.7×10^{-4} Ω cm, for ALD-AZO films with pulse ratio 6:1; the carrier mobility was 8.80 $cm^2\ V^{-1}\ s^{-1}$ and optical transmittance up to 94 %. The epitaxial AZO films grown in situ also on m-plane sapphire exhibited the two-fold symmetry of ZnO (110) in the orthorhombic crystal system. All results show that a novel in situ doping method with an interrupted flow method controls the Al content of AZO films more easily, and is more usefully applicable for a structure with a large aspect ratio for an advanced photoelectric device. We expect that this novel in situ doping method with an interrupted flow is applicable to not only ALD AZO films but also other ALD doping, such as Ga, In (n-type) or P, N (p-type) for ALD epitaxial growth.

Keywords: thin films; X-ray scattering; electrical conductivity; atomic layer deposition

[1] Liu, Y. T., Ku, C. S., Chiu, S. J., Lee, H. Y., & Chen, S. Y. 2014. Ultrathin Oriented $BiFeO_3$ Films from Atomic Layer Deposition with Greatly Improved Leakage and Ferroelectric Properties. ACS *Appl. Mater. Interfaces*, **6** 443−449.

[2] Huang, J. M., Ku, C. S., Lin, C. M., Chen, S. Y., & Lee, H. Y. 2015. In situ Al-doped ZnO films by atomic layer deposition with an interrupted flow, Mater. Chem. Phys. **165**, 245-252.

[3] Huang, J. M., Tsai, S. Y., Ku, C. S., Lin, C. M., Chen, S. Y., & Lee, H. Y. 2016. Enhanced Electrical Properties and Field Emission Characteristics in AZO/ZnO-nanowires Core-shell Structures. Phys. Chem. Chem. Phys. **18**, 15251-15259.

Acceptance ID: NFMC-P

Characterization of IBAD Titanium Nitride Nano-Scale Thin Films.

I. Odeh[1], R. Elian[1], F. Aljamal[1], H. Al Ghanem[2]

Department of Physics, Yarmouk University, Irbid 21163, Jordan.
Department of Applied Physical Sciences, Jordan University of Science and Technology, Irbid 22110, Jordan

Titanium Nitride nano-scale thin films have been prepared by ion beam assisted reactive DC magnetron sputtering. The films are characterized by XRD, SEM and TEM. The films are found to be amorphous. The effect of the ion beam during deposition was evident from smoothness of film surface (SEM and TEM images) and modifications in optical properties. Investigation of the optical constants shows stable refractive index, 2.3, dominating most of the visible range. The films are not highly absorptive in the visible range. The extinction coefficient k in the visible region is negligibly small. A slightly wide energy gap of 2.9 ± 0.1 eV is estimated for the IBAD amorphous titanium nitride nano-thin films.

In an additional set of AC conductivity measurements, the impedance and permittivity of the as- prepared films are measured as a function of frequency. The results reveal that Titanium Nitride nano thin films are highly resistive.

The stability of the films at normal room environment in addition to the golden color makes the nano-thin films suitable for hard and decorative coatings.

Acceptance ID: NV2Q-P

Development of circularly polarized UV-visible absorption spectroscopy for probing magnetic properties

A. Rasritat[1], *W. Meevasana*[1]

[1]*School of Physics, Institute of Science, Suranaree University of Technology, Nakhon Ratchasima, Thailand 30000*
E Mail : Aissara.22@gmail.com

In this work, we have developed a technique called circularly polarized UV-visible absorption spectroscopy to study electronic structure of magnetic materials, focusing on band gap and low-energy excitation. Using the concept of magnetic circular dichorism, circularly left (CL) and circularly right (CR) polarization will couple differently to electrons with opposite spins. When a magnetic material is in external magnetic field, absorption spectra with energy scale near the band gap are then expected to be different between the circularly left and right polarizations. We have developed an instrument with this capability. We have performed a test measurement on ferromagnetic $Y_3Fe_5O_{12}$ [1] thin film on $Gd_3Ga_5O_{12}$ substrate which its thickness on both side as 4-5 μm and found that the absorption edges with CR and CL polarizations can already be different as large as 40 meV in energy under magnetic field (B) of 0.15 T. We also expect that this technique may also be used to observe other low-energy magnetic excitations which will be discussed.

Keywords: magnetic properties, UV-visible absorption

[1] TOMITA, S., KATO, T., TSUNASHIMA, S., IWATA, S., FUJII, M., & HAYASHI, S. Magneto-Optical Kerr Effects of Yttrium-Iron Garnet Thin Films Incorporating Gold Nanoparticles. PRL **96,** 167402 (2006).

Acceptance ID: P7PX-O

Different Performance and Current Collapse Suppression of Al_2O_3/AlGaN/GaN HEMTs with SiNx passivation grown by PECVD, Amorphous AlN and Monocrystal-like AlN passivation grown by PEALD

Dongliang Zhang[1,2], Xinhong Cheng [1,], Li Zheng[1,2], Lingyan Shen[1,2], Qian Wang[1,2], Jingjie Li[1,2], Ru qian[1,2] ,Ziyue Gu[1,2] and Yuehui Yu[1]*

[1] State Key Laboratory of Functional Materials for Informatics, SIMIT, Chinese Academy of Sciences, Changning Road 865, Shanghai 200050, P. R. China
[2] University of Chinese Academy of Sciences, Beijing 100049, P. R. China
Presenting author: dlzhang@mail.sim.ac.cn
Corresponding author: xh_cheng@mail.sim.ac.cn

Gallium nitride-based metal-insulator-semiconductor high-electron-mobility transistors (MIS-HEMTs) have been widely explored as attractive candidates for next-generation high-efficiency power switching and microwave applications, owing to the superior material properties, including high breakdown electric field, high switching frequency and low on-resistance. Compared to the conventional Schottky gate HEMTs, MIS-HEMTs offer lower gate leakage, higher switching frequency and higher breakdown voltage (BV). The common gate insulating layers are some high-k dielectric materials, such as Al_2O_3, HfO_2, but the growth process will induce the unacceptable Ga-O bonds on the GaN surface. These defects will increase the surface donor-like states (SDS), which is relative to current collapse (CC) and it is a critical challenge to improve the performance of GaN HEMTs devices. Therefore, it is essential to consider how to reduce the GaN surface state density and control the formation of Ga-O bonds to suppress CC.

Recently, PECVD-grown SiNx films have been widely applied on GaN surface passivation to suppress CC. However, the PECVD growth process will induce surface damage by high-energy plasm, making SiNx/GaN interface a challenging task. Whereas, AlN grown by the remote plasm used in ALD will remove native oxide with minimum surface damage. Particularly, with Rapid Annealing Temperature (RTA) over 1000°C, the AlN film will be monocrystal-like.T he monocrystal-like AlN film can also form heterojunction with GaN cap, supply fixed charges, suppress surface states and control CC effectively.

In this work, we manufacture three Al_2O_3/AlGaN/GaN HEMTs devices structures with different passivation layers: one is SiNx passivation grown by PECVD, and the other two are amorphous and monocrystal-like AlN passivation grown by PEALD. Therein, the monocrystal-like AlN is treated by RTA over 1000°C. HRTEM can clearly reveal the crystallinity. Using probe station and semiconductor parameter analyzer operation, the direct current (DC) performance, BV, and CC are analyzing, indicating the superiority of AlN passivation on GaN HEMTs surface.

Acceptance ID: PG66-O

Surface Modification of Conducting Polymer Nanoparticles with Polymeric Thiols

Brandon DiTullio[1], Leah Pendleton[1], Paige Whitehead[1], Paul Molino[2], Timothy Hanks[1]

[1]Department of Chemistry, Furman University, Greenville, SC USA.
[2] ARC Centre of Excellence for Electromaterials Science, Intelligent Polymer Research Institute, University of Wollongong, AUS.
Prof Timothy Hanks, tim.hanks@furman.edu; tel.: +1 864-294-3373

Thin films of electrically conducting polymers, such as polyaniline and polypyrrole, readily react with thiols to give materials with dramatically altered surface properties, including surface energies and susceptibility to fouling from biological organisms. [1, 2] We have previously shown that such films can be made highly hydrophobic by exposure to thiol solutions or vapors and that electroactive moieties can be affixed to the surface while remaining in electronic communication. [3] Here we show that nanoparticles and fibers of the polymers are also readily modified with both small thiols and thiol-terminated macromolecules. The extent and rate of the modification reaction is dependent upon the size of the thiol and the reaction temperature. In addition to grafting too conducting polymer surfaces, polymer brush-type structures may be from them through surface-initiated polymerizations reactions, particularly the atom transfer radical polymerization (ATRP) process. The rate of the ATRP reaction is similar to that on gold, though the increased roughness of the surface results in an increased number of surface-attached chains per nominal 2D surface area. The derivatized particles may find use as additives in conventional paints and coatings.

Keywords: conducting polymer, nanoparticle, surface modification, anti-fouling

[1] BERGMAN, B., HANKS T. W. 2000, Spectroscopic, Microscopic and Surface Analysis of Alkanethiol- and Fluoroalkanethiol-Modified Conducting Polymer Thin Films. *Macromolecules,* 33, 8035-8042.

[2] ZHANG, B.; NAGLE, A.; WALLACE, G.G.; HANKS, T.W.; MOLINO, P.J 2015. Functionalised Inherently Conducting Polymers as Low Biofouling Materials. *Biofouling,* 31, 493-502.

[3] HANKS, T.; GLISH, L.; SINGH, S.; JOHNSON, D.; WRIGHT, L. 2005, Conducting Polymers as Substrates for Surface-Mounted Molecular Devices. *Synth. Metals*, 153, 177-180.

Acceptance ID: QYVL-O

Atomic-Layer-Deposition of Indium Oxide Films for Thin-Film Transistors

Qian Ma, He-Mei Zheng, Wen-Jun Liu[1], Shi-Jin Ding[2]

State Key Lab ASIC & Syst., School of Microelectronics, Fudan University, Shanghai 201203, China
[1]Email: wjliu@fudan.edu.cn; [2]Email: sjding@fudan.edu.cn

Abstract: Recently, In_2O_3 has attracted many interests for various applications such as photovoltaic devices, electrochemical sensors, and flat panel displays [1-2]. However, there are few reports on the atomic-layer-deposited In_2O_3 thin-films. In this work, atomic-layer-deposition (ALD) of In_2O_3 thin-films was investigated using cyclopentadienyl indium (InCp) and hydrogen peroxide (H_2O_2) as precursors, and the deposited films were characterized with ellipsometry, atomic force microscope, X-ray photoelectron spectrum, X-ray diffraction, Hall effect measurement etc. Subsequently, the In_2O_3 channel-based thin-film transistors (TFTs) with an Al_2O_3 gate dielectric were demonstrated successfully. The In_2O_3 thin films can be deposited at relatively low temperatures of 150-210 ºC, exhibiting a growth rate of 1.4-1.7Å/cycle and a root-mean-square (RMS) roughness of 0.25-0.41nm. To increase deposition temperature can effectively reduce oxygen vacancies and C impurity, thus significantly improve the quality of the sample. The optical band gap of the In_2O_3 film can be modulated by the deposition temperature, which can shift from 3.3 eV to 3.8 eV as the deposition temperature increases from 150 to 210 ºC. This is mainly related to the concentration changing of oxygen vacancies in the films. Furthermore, the electron mobility and conductivity increase with increasing the deposition temperature, but the carrier concentration does not change apparently. Finally, the fabricated bottom-gate In_2O_3 TFTs after the proper annealing exhibit field-effect mobility of 7.8cm^2/V·s, a threshold voltage of -3.7 V, a subthreshold swing of 0.32 V/dec, and an on/off current ratio of 10^7. Figure 1 (a) and (b) show the typical transfer and output curves of the fabricated TFT, respectively. In a word, the current study provides an insight into ALD In_2O_3 film as a promising candidate for transparent electronics in the future.

Keywords: In_2O_3, ALD, Thin-film transistors

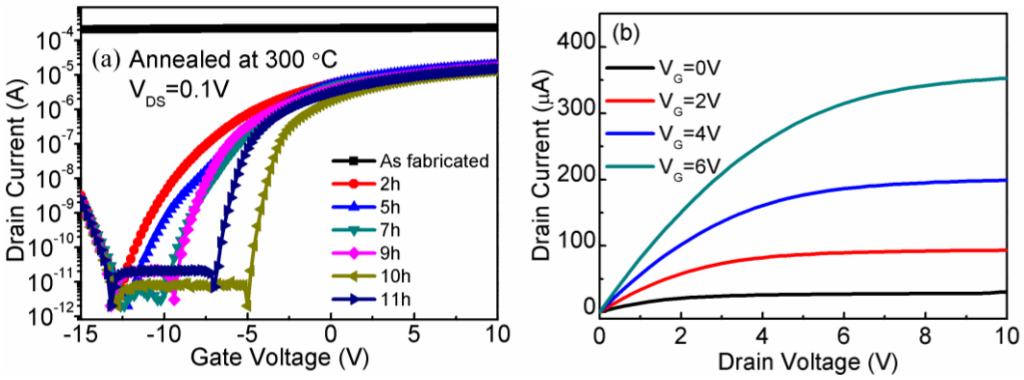

Fig. 1(a) Transfer characteristics of In_2O_3 TFTs annealed at 300ºC for different time in air. (b) Output characteristics of the In_2O_3 TFT annealed for 11h in air.

References:

1. M. Gebhard, M. Hellwig, H. Parala, K. Xu, M. Winter and A. Devi, Dalton Trans., 43, 937 (2014)
2. D.-J. Lee, J.-Y. Kwon, J. Lee, and K.-B. Kim, *J. Phys. Chem. C*, 115, 15384 (2011).

Acceptance ID: SAF7-P

Thickness Dependence of Electrical Properties in Sol-Gel-Derived $(Na_{0.85}K_{0.15})_{0.5}Bi_{0.5}TiO_3$ Thin Films

*Yunyi Wu, Siu Wing Or**

Department of Electrical Engineering, The Hong Kong Polytechnic University, Hung Hom, Kowloon, Hong Kong
**E Mail: eeswor@polyu.edu.hk (S. W. Or; Corresponding Author)*

$(Na_{0.5}Bi_{0.5})TiO_3$-modified $K_{0.5}Bi_{0.5}TiO_3$, namely $(1-x)(Na_{0.5}Bi_{0.5})TiO_3–x(K_{0.5}Bi_{0.5})TiO_3$, is found to exhibit improved dielectric and piezoelectric properties at the morphotropic phase boundary (MPB) region (x=0.15) recently [1],[2]. It is generally believed that a thin nonferroelectric or nonswitchable ferroelectric layer with low dielectric constant and located at the interface between the electrodes and the film will have a significant influence on the ferroelectric and dielectric properties. Thus, such a ferroelectric capacitor can be modeled as a stacked structure, formed by a bulk ferroelectric layer in series with a low dielectric interfacial passive layer [3],[4]. Moreover, the stability of the temperature dependence of ferroelectric properties is one of the important characteristics in view of both scientific knowledge and engineering applications.

In this work, $(Na_{0.85}K_{0.15})_{0.5}Bi_{0.5}TiO_3$ (NKBT) thin films with different thicknesses are fabricated on Pt/Ti/SiO_2/Si substrates via an aqueous sol-gel method, and the effect of thickness on the electrical properties of the NKBT thin films is investigated. The ferroelectric and dielectric behaviors are studied in a wide temperature range of 20–150ºC (Figs. 1–3). NKBT thin films with different thicknesses show a desirable perovskite structure with no detection of preferential orientations. Since the motion of domain walls in the thinner films will be blocked by the presence of the passive layer or by the charged defects located at the interface, there will be a larger domain wall motion contribution to the dielectric response in the thicker films and at higher temperature. Both thickness and temperature are found to affect the ferroelectric properties of the films. The remnant polarization (P_r) is enhanced when the film thickness is increased, while P_r is weakened when the temperature is elevated from -150 to 20 ºC (Figs. 1 & 2). The piezoelectric response with increasing film thickness exhibits a similar quantitative trend with the dielectric response, and the effective constant d_{33}* increases from 34 pm/V for a 2-layer film to 65 pm/V for a 14-layer film (Fig. 3).

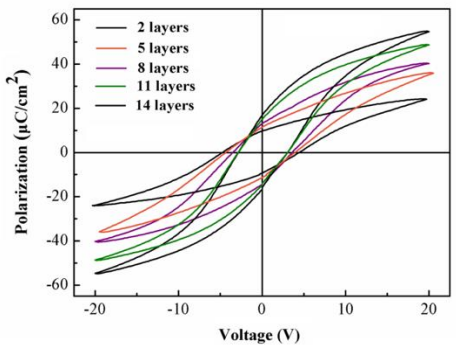

Fig. 1 Ferroelectric hysteresis loops for NKBT films with different thicknesses at room temperature.

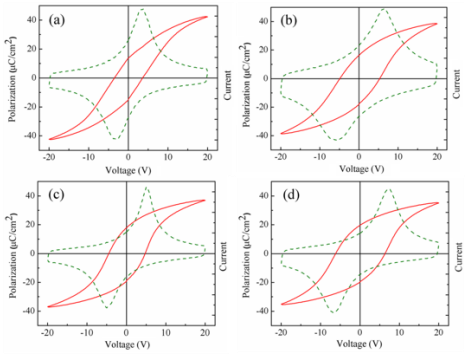

Fig. 2 Polarization–applied voltage hysteresis loops and their corresponding current loops at different temperatures: (a) 20, (b) -50, (c) -100, and (d) -150 ºC.

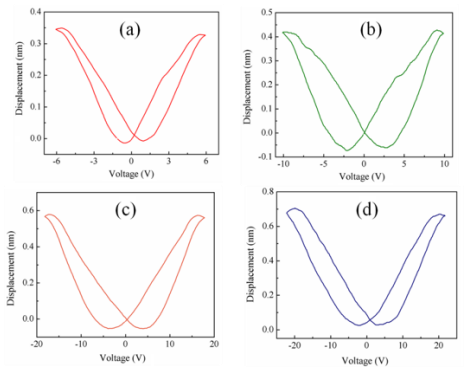

Fig. 3 Local displacement–voltage loops of for NKBT thin films with various thicknesses: (a) 2 layers, (b) 5 layers, (c) 11 layers, and (d) 14 layers.

This work was supported by the Research Grants Council of the HKSAR Government under Grant No. PolyU 5228/13E

Keywords: Sol-gel; Thin films; Ferroelectrics; Thickness dependence; Electrical properties.

[1] SASAKI, A., CHIBA, T., MAMIYA, Y. & OTSUKI, E. 1999. Dielectric and Piezoelectric Properties of $(Bi_{0.5}Na_{0.5})TiO_3$-$(Bi_{0.5}K_{0.5})TiO_3$ systems. *Jpn. J. Appl. Phys.* 38, 5564-5567.

[2] YU, T., KWOK, K. W., **&** CHAN, H. L. W., 2007. The Synthesis of Lead-free Ferroelectric $Bi_{0.5}Na_{0.5}TiO_3$-$Bi_{0.5}K_{0.5}TiO_3$ Thin Films By Sol-Gel Method. *Material letters* 61**,** 2117-2120.

[3] TAGANTSEVA, A. K. **&** GERRA, G. 2006. Interface-Induced Phenomena In Polarization Response of Ferroelectric Thin Films. *J. Appl. Phys.* 100, 051607.

[4] SINNAMON, L. J., BOWMAN, R. M. **&** GREGG, J. M., 2001. Investigation of Dead-Layer thickness in thin-film capacitors. *Appl. Phys. Lett.* 78, 1724-1726.

Acceptance ID: SSND-P

Multi-physical Field Coupling Characteristics of a Piezoelectric Film Driven Micro-jet

Kai Li, Jun-kao Liu, Wei-shan Chen

[1] State Key Laboratory of Robotics and System, Harbin Institute of Technology, Harbin 150001, China;
*E Mail：**sdcxlikai@126.com;** Tel: **+86-13101615682 (corresponding author)***
E Mail：cws@hit.edu.cn; Tel: +86-451-8641-6119 (presenting author)

Thanks to its advantages of high injection accuracy, fast response, and achieving on-demand injection, the piezoelectric micro-jet, based on piezoelectric inkjet technology, is wildly applied in various fields (Yang et al., 2016, Kwon et al., 2015, Fribourg-Blanc et al., 2013, Caro et al., 2016). A piezoelectric micro-jet, which takes piezoelectric thin film as the driving element, is proposed in this paper. The designed micro-jet has the advantages of simple structure, easy assembly and discharging the bubbles which are formed from nozzle part and have negative influences on the injection.

For the current researches, the analysis models are mainly two-dimensional, and the effect of fluid solid coupling effect are always ignored (Wijshoff, 2010, Tsai and Hwang, 2008, Li et al., 2016). However, the fluid solid coupling effect has a great influence on the simulation results. In order to accurately analyze the injection performance of the piezoelectric micro-jet, a two way multi-physical field coupling analysis method is proposed in this paper.

The effects of fluid solid coupling on the operating frequency of the micro-jet and dynamic characteristics of the vibrator are analyzed by the proposed method. And, in order to obtain the excitation signals to meet different injection requirements, the transient injection characteristics of the micro-jet under different excitation are analyzed as well. Firstly, the nozzle pressures under different excitation signals are obtained based on the transient analyses of the acoustic structure coupling characteristics of the micro-jet. Then, through the analysis of hydrodynamic characteristics of the nozzle part, the droplet velocity, mass flow of nozzle, and the molding time of the droplet, under different excitation parameters, are gained.

According to the obtained results, the adjustment method of the excitation parameters for different injection requirements are given. The experimental prototype is manufactured and experiments are carried out. The reliability of the proposed two way multi-physical field coupling analysis method is verified by comparing the experimental results with simulation results.

Keywords: multi-physical field, piezoelectric film, actuator, acoustic

[1] CARO, N., MEDINA, E., DIAZ-DOSQUE, M., LOPEZ, L., ABUGOCH, L. & TAPIA, C. 2016. Novel active packaging based on films of chitosan and chitosan/quinoa protein printed with chitosan-tripolyphosphate-thymol nanoparticles via thermal ink-jet printing. *Food Hydrocolloids,* 52**,** 520-532.

[2] FRIBOURG-BLANC, E., DANG, D. M. T. & DANG, C. M. 2013. Characterization of silver nanoparticle based inkjet printed lines. *Microsystem Technologies-Micro-and Nanosystems-Information Storage and Processing Systems,* 19**,** 1961-1971.

[3] KWON, Y. T., LEE, Y. I., LEE, K. J., CHOI, Y. M. & CHOA, Y. H. 2015. A Novel Method for Fine Patterning by Piezoelectrically Induced Pressure Adjustment of Inkjet Printing. *Journal of Electronic Materials,* 44**,** 2608-2614.

[4] LI, K., LIU, J.-K., CHEN, W.-S., YE, L. & ZHANG, L. 2016. Research on the Injection Performance of a Novel Lubricating Device Based on Piezoelectric Micro-Jet Technology. *Journal of Electronic Materials,* 45**,** 4380-4389.

[5] TSAI, M. H. & HWANG, W. S. 2008. Effects of pulse voltage on the droplet formation of alcohol and ethylene glycol in a piezoelectric inkjet printing process with bipolar pulse. *Materials Transactions,* 49**,** 331-338.

[6] WIJSHOFF, H. 2010. The dynamics of the piezo inkjet printhead operation. *Physics Reports,* 491**,** 77-177.

[7] YANG, H. S., KANG, B. J. & OH, J. H. 2016. Control of Evaporation Behavior of an Inkjet-Printed Dielectric Layer Using a Mixed-Solvent System. *Journal of Electronic Materials,* 45**,** 755-763.

Acceptance ID: SZ3E-P

Electronically Pure Semiconducting Single-Walled Carbon Nanotube Ink for Large Scale Electronics

Huaping Li

Atom Nanoelectronics Inc. 440 Hindry Avenue, Unit E, Inglewood, California 90301 USA
Email: huaping.li@atomnanoelectronics.com

Carbon nanotube thin film transistors (TFTs) with characteristics resembling those of TFTs constructed on amorphous silicon, low-temperature polycrystalline silicon and metal oxides were fabricated on (6,5) single chirality single-walled carbon nanotube (SWCNT) thin film deposited from electronically pure semiconducting (6,5) single chirality single-walled carbon nanotube (SWCNT) ink. This ink was extracted in industrial scale from raw SWCNTs produced using high pressure carbon monoxide conversion, and deposited on pretreated substrates to form uniform and consistent (6,5) HiPCO SWCNT thin film using solution process. The (6,5) HiPCO SWCNT thin films were characterized as pure semiconductor without metallic impurities showing classic nonlinear current-bias curves in Schottky-type diodes. Both N-type and P-type (6,5) HiPCO SWCNT TFTs were fabricated with femto Ampere off-current and I_{ON}/I_{OFF} ratio of 10^8 by depositing SiN_x and HfO_2 dielectrics on the top of (6,5) HiPCO SWCNT thin films, respectively. The (6,5) HiPCO SWCNT inverter with voltage gain of 52 was also demonstrated by wire-bonding one P-type HiPCO SWCNT TFT to one N-type HiPCO SWCNT TFT.

Acceptance ID: UGE2-O

Incorporation and effect of inorganic polyphosphate on the surface of implant materials by bio-inspired supramolecular nanofilm

Xinyuan Xu[1], *Yanpeng Liu*[1], *Jianshu Li*[1,*]

College of Polymer Science and Engineering, State Key Laboratory of Polymer Materials Engineering, Sichuan University, Chengdu, 610065, China.
xinyuanxu22@163.com, jianshu_li@scu.edu.cn

Implant materials have been widely used as a type of restoration approach. However, they may cause peri-implantitis, which is related to lesions of peri-implant attachment, presence of aggressive bacterial strains, excessive mechanical stress, and corrosion. There are some approaches to reduce the morbidity such as eliminating the inflammatory lesion, CO_2 laser and so on. We attemped to reduce the disease via enhancing the antibacterial properties and osseointegration. Lysozyme, as a natural protein, has been used for preparing thin supramolecular nanofilm, which can adsorb on the surface of metal, ceramic, PTFE, PET, etc., and have great antibacterial properties. And the inorganic polyphosphate (polyP), found in every cell in nature and likely conserved from prebiotic times, has been demonstrated the ability of promoting periodontal tissue regeneration. Hence, we coated a layer of nanofilm on the surface of implant materials by incorporating lysozyme and polyP via electrostatic interaction. This work will provide a simple and effective method to modify the surface of implant materials and reduce the peri-implantitis.

Scheme 1. The preparation and biological evalution of impant materials coted by lysozyme and polyphosphate.

Keywords: Multifunctional, coating, restorative/antibacterial surface, bio-inspired.

[1] Wang D, Ha Y, Gu J, et al. 2D Protein Supramolecular Nanofilm with Exceptionally Large Area and Emergent Functions[J]. Advanced Materials, 2016, 28(34): 7414-7423.

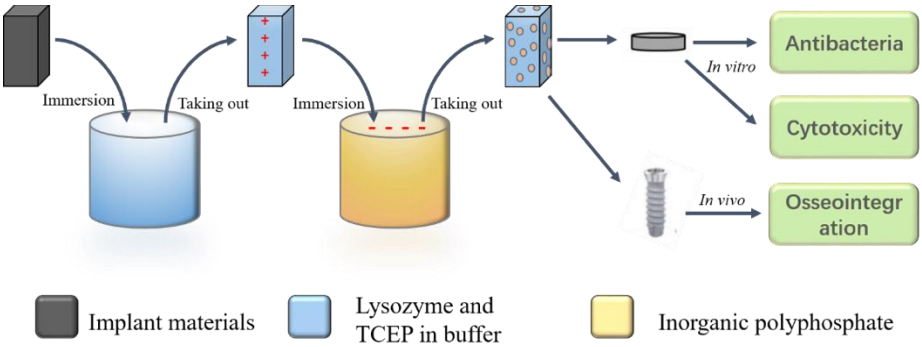

Acceptance ID: UJP8-P

Effect of Isosorbide-based Dimethacrylate on the Water-resistant Polymer Thermoelectric Devices

Recently, a considerable effort has been devoted to the implementation of PEDOT:PSS as an organic-thermoelectric active material due to its high electrical conductivity. However, most of conventional PEDOT:PSS films with the enhanced conductivity have poor stability and durability to moisture due to hygroscopic PSS. In this study, we introduced 2,5-bis(2-hydroxy-3-methacryloyloxypropoxy)-1,4:3,6-dianhydro-sorbitol (Iso-GMA) as an additive to give the film with mechanical durability for rainy outdoor use and simultaneously higher thermoelectric properties compared to the pristine PEDOT:PSS film without additives. The structural and morphological evolution of the films according to the additive concentration plays a key role in determining the characteristics for water-resistant polymer thermoelectric devices.

Acceptance ID: UK2Y-P

A Bandgap-Tunable Layered Organic-inorganic Perovskite-like Hybrids, $(C_6H_5C_2H_4NH_3)_2Sn_xPb_{1-x}I4$ (x=0,0.3,0.5,0.7,1)

Liling Guo[a], *Hanxing Liu*[a], *Xiaoyan Gan*[a,b,c]

a. School of Material Science and Engineering, Wuhan University of Technology, 122 Luoshi Road, Wuhan 430070, China;
b. Hubei Key Laboratory of Advanced Technology for Automotive Components, Wuhan University of Technology, 122 Luoshi Road, Wuhan 430070, China;
c. Hubei Collaborative Innovation Center for Automotive Components Technology, Wuhan University of Technology, 122 Luoshi Road, Wuhan 430070, China
E Mail/ Contact Détails : gll@whut.edu.cn, *ganxiaoyan@whut.edu.cn*

Layered organic-inorganic perovskite-like hybrids $(C_6H_5C_2H_4NH_3)_2Sn_xPb_{1-x}I_4$ (x=0,0.3,0.5,0.7,1) were synthesized by a hydrothermal method. Structures and optical properties of these hybrids were studied by using X-ray diffraction (XRD), scanning electron microscopy (SEM), X-ray fluorescence spectroscopy(XRF) and ultraviolet-visible adsorption spectroscopy(UV-Vis). Changing the amount of Sn from 0 to 1, the interlayer distance d of these hybrids varied from 16.36Å to 16.27Å and the bandgaps tuned from 2.40eV to 1.78eV. The results demonstrate that the different ratios of Pb and Sn can change the interlayer distances and tune bandgaps of these hybrids.

Keywords: Organic-inorganic, perovskite-like, hybrids, Layered structure, Bandgap

[1] GAN, X.Y., WANG O., LIU K.Y., DU, X.J., GUO, L.L., & Liu, H.X. 2017. 2D Homologous Organic-Inorganic Hybrids as Light-Absorbers for Planer and Nanorod-based Perovskite Solar Cells, Solar Energy Materials and Solar cells, DOI: 10.1016/j.solmat.2016.12.047

[2] GUO, L.L., Wang, X.Q., Wang, Q., GAN, X.Y., Liu, H.X. 2015. Synthesis and Characterization of New Functional Material $(4\text{-}XC_6H_4C_2H_4NH_3)_2SnI_4$ (where X=H, F, Cl), *Polyhedron*, 85, 874–879.

Acceptance ID: VB4B-P

A New Green Phosphor of Semiconductive Nanoporous ZnMnO:P

Sejoon Lee,[1,2] *Youngmin Lee,*[2] *Dong Jin Lee,*[2] *Hwauk Lee*[1]

[1] *Department of Semiconductor Science, Dongguk University - Seoul, Seoul 04623, Korea*
[2] *Quantum-functional Semiconductor Research Center, Dongguk University - Seoul, Seoul 04623, Korea*
E-Mail: sejoon@dongguk.edu

A new green phosphor of semiconductive nanoporous ZnMnO:P was prepared through high-dose P^+ ion implantation into ZnMnO and subsequent annealing at 1000°C. The nanoporous ZnMnO:P phosphor exhibited a semiconducting behavior with the carrier concentration of ~10^{18} cm^{-3} and displayed a strong green luminescence at the wavelength of ~520 nm. Through analyzing the panchromatic cathodoluminescence properties, we confirmed that the strong green emission arises from the nanosized pores in ZnMnO:P. During high-temperature annealing, lattice atoms and implanted ions should thermally migrate toward metastable lattice points so as to recover the implantation damage. This promotes the thermal nucleation of nanopores in ZnMnO:P. Since the oxygen vacancies and the dopant ions are enriched in nanopores, the green luminescence centers are created in nanoporous ZnMnO:P. As a result, the green band could be localized within the bandgap, in which band-filling will occur *via* the photon confinement. This allows nanoporous ZnMnO:P to act as a semiconducting green phosphor.

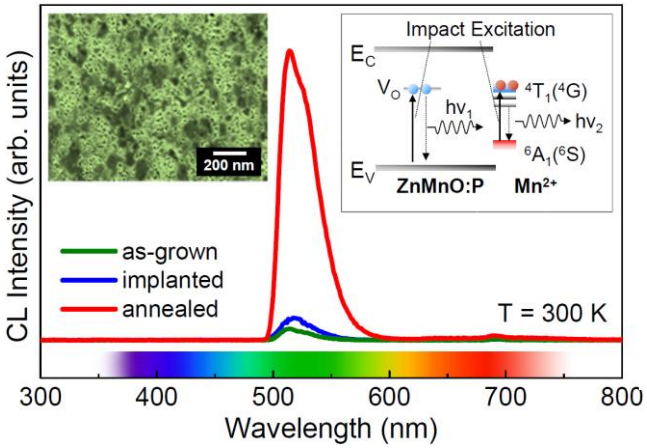

Fig. 1. CL spectra at 300 K of as-grown ZnMnO, P^+-implanted ZnMnO, and nanoporous ZnMnO annealed at 1000°C. The left-hand-side inset displays the top-view scanning electron microscopy image of nanoporous ZnMnO:P used for the cathodoluminescence measurement. The right-hand-side inset illustrates the green luminescence-related optical transitions in ZnMnO:P represented in the energy-band scheme.

Keywords: Nanoporous ZnMnO, Strong green emission, Semiconductive Phosphor

Acceptance ID: VJDQ-P

Influence of Sputtering Pressure of Channel Layer on the Performance of Hafnium-doped Zinc Oxide TFTs

Dedong Han[1], Jing Wu[1,2], Yingying Cong[1], Junchen Dong[1], and Yi Wang[1]*

[1]*Institute of Microelectronics, Peking University, Beijing 100871, China*.
[2]*Shenzhen Graduate School, Peking University, Shenzhen 518055, China*.
E Mail: handedong@pku.edu.cn

In recent years, with the development of active-matrix display system, the demand for high-performance thin film transistors is increasing in the industry. As conditional channel materials, Si-based TFTs have reached their limits. For recent years, oxide semiconductor thin film transistors have attracted much attention for the better performance than Si-based TFTs and potential use in the application of high resolution AMLCDs and AMOLEDs. Oxide TFTs have higher mobility and most oxide semiconductors are transparent in the visible light region and thereby they can be used to realize transparent displays. A large amount of researches have been carried out on oxide TFTs, especially ZnO-based TFTs. Among these materials, IGZO TFTs has been regarded as the most promising candidate to replace Si-based TFTs, and even had already been put into actual use by the industry. But in fact, Indium and Gallium are toxicants, rare elements on earth and going to be exhausted, hence people are searching for a non-In and non-Ga active channel layer which offers competitive advantages, such as lower cost, higher throughout, and safety. ZnO-based TFTs have many advantages, for example, it is possible to growth at room temperature and ZnO is a wide band gap material (3.4eV) and it is transparent in the visible region. In our experiment, we choose Hafnium-doped ZnO as the channel material since Hafnium (Hf) is harmless to human and environment. Because of the high interest of this material in the future display application, it is very important to analyze the key factors that have influence on the electrical properties of the transistors. We have fabricated Hafnium-doped Zinc Oxide thin film transistors (HZO TFTs) using RF magnetron sputtering. Influence of sputtering pressure during the deposition of HZO thin films by RF magnetron sputtering on the performance of HZO TFTs was researched. And we found that sputtering gas pressure has a very large effect on the characteristics of the TFT device. The performance of HZO TFT reach the best when the sputtering pressure is 0.8 Pa, which exhibit the subthreshold swing of 0.25 V/decade, the saturation mobility of 268 $cm^2/V•s$, the threshold voltage of 4.7 V and the on/off current ratio of 10^9. At higher sputtering pressure, the more collisions of sputtered molecules with Ar molecules resulted in low deposition rate, high resistivity and low mobility. Meanwhile, we also researched the device stability over time. And HZO TFTs fabricated on glass exhibited high stability.

Keywords: Hf-doped Zinc-Oxide, Thin film transistors, sputtering gas pressure, high performance, fully transparent.

Acceptance ID: VU6Z-P

Comparative Study with a Unique Arrangement to Tap Piezoelectric Output to Realize a Self Poled PVDF Based Nanocomposite for Energy Harvesting Applications

Pusty[1], *Sharma*[1,], *Shirage*[1,2]

[1] *Discipline of Metallurgy Engineering and Materials Science, Indian Institute of Technology (IIT) Indore, Indore-453552, Madhya Pradesh, India.*
[2] *Discipline of Physics, Indian Institute of Technology (IIT) Indore, Indore- 453552, Madhya Pradesh, India.*

mpusty@gmail.com, paras.shirage@gmail.com

In this work we present a comparative study on the enhanced piezoelectric performance between Carbon Nanotubes (CNT) doped as well as Iron-Reduced Graphene Oxide (Fe-RGO) doped PVDF nanocomposite. The enhanced performance is realized by a unique device structure, in which the bottom electrode is physically not in contact with the piezoelectric film until external excitation is applied. FTIR characterization shows the enhancement of polar crystallization phases due to electrostatic interactions in PVDF by the addition of CNT and Fe-RGO. Raman Spectroscopy indicates the formation of good quality FeRGO nanosheets and also shows high crystalline quality of CNTs. Raman Spectroscopy identifies the interaction between CNTs and Fe-RGO nanosheets with the polymer that supports the piezoelectric current generation mechanism. Conductivity measurements show that addition of CNT and Fe-RGO in PVDF increases the conductivity of the nanocomposite films. The CNT/PVDF and Fe-RGO/PVDF piezoelectric energy harvesting device produced an open circuit output voltage of 2.5 V and 1.2 V respectively. A short circuit rectified current of nearly 700 nA and 300 nA was detected by the CNT/PVDF and Fe-RGO/PVDF based piezoelectric energy harvesting device.

Keywords: nanocomposite, energy harvesting, piezoelectricity, CNT, Fe-RGO

[1] ADHIKARY, P., GARAIN, S. & MANDAL, D. 2015. The co-operative performance of a hydrated salt assisted sponge like P(VDF-HFP) piezoelectric generator: an effective piezoelectric based energy harvester. *Phys.Chem.Chem.Phys.*, 17, 7275-7281.

Acceptance ID: VZHX-O

A miniaturized energy-harvesting device

Zara Koochak, Rahim Esfandyarpour, James Harris, Ron Davis, Stanford University

A key challenge in designing a broad range of implant biomedical devices is limited power source. Most of existing biomedical devices rely on batteries with limited lifetime and negative effect on miniaturization potential of the device. To overcome this issue, in this paper we have designed, fabricated and tested a miniaturized flexible device to harvest and convert body generated mechanical energy into electrical energy.

The device works based on the piezoelectric property of a novel nano material, Molybdenum disulfide (MoS2), which is deposited on a flexible substrate. We demonstrated stretching and releasing of deposited single layer of MoS2 in our device can generates power during each pulse of human heartbeat, which can be stored and potentially be used to drive a large set of biomedical devices.

Acceptance ID: WEJE-P

Growth and some characterization of nanocrystalline ZnO/CoO and C-nanotube/CoO bilayers: synthesis, surface features and XPS studies

B.A. Taleatu[1,2], L. Cozzarini[2], G. Bertolini[2], S. Adewinbi[1] and A. Okunola[1]

[1]Department of Physics and Engineering Physics, Obafemi Awolowo University Ile-Ife, Nigeria
[2]Sincrotrone Trieste S.C.p.A., s.s 14 Km 163.5 in Area Science Park, 34149 Trieste, Italy

Zinc Oxide and carbon nanotube (C-nanotube) have been separately grown on Cobalt Oxide (CoO) thin film as bilayer structures. Two samples of CoO film were pre-deposited on ITO coated glass and Si (111) wafer from solution electrolyte. The structures were characterized by some surface probing techniques. Surface morphology shows that particles of CoO film are evenly distributed across the substrate, its average size increases between 60 and 73 nm with increase in deposition voltage. A transparent thin layer of ZnO completely laminated the CoO underlayer. The thickness of evaporated C-nanotube is about 16 nm. Interdispersion of C-nanotube within the crystallites of CoO was also observed. Optical measurement indicated that both the CoO film and the ZnO/CoO bilayer are fairly transparent to visible light. The energy badgap was estimated as 2.28 and 2.19 eV respectively. Photoemission studies revealed possible interaction between CoO and ZnO atoms but not with the ITO glass constituents. The study suggests that both CoO and C-nanotube could be a recipe for effective charge separation in nanostructured photonic devices.

Acceptance ID: X3QL-O

Synthesis and characterization of tungsten particles-containing diamond coating by hot filament chemical vapor deposition

Naichao Chen, Yingchao Chen, Jun Ai, Ping He, Jianxing Ren

School Energy and Mechanical Engineering, Shanghai University of Electric Power, Shanghai, 200090, China.

Diamond coating has gained an intensive attraction in the tribological fields due to its high hardness. However, its weak toughness always gives arise to the fragile crack under the external load, which causes the delamination and peeling off from substrate. In this work, a novel deposition method combining the conventional hot filament chemical vapor deposition (HFCVD) and particles-doping technique is proposed to balance the hardness and toughness for diamond coating, with which the tungsten particles-containing diamond coating is deposited on the silicon carbide substrate. The as-deposited diamond coating is characterized by scanning electron microscope (SEM), surface profilometer, X-ray diffraction (XRD) and Raman spectrum. Rockwell C indentation tests are conducted to evaluate the adhesion of diamond. The results indicate that tungsten carbide (WC) may be formed between tungsten particles and diamond coating. Then, the relative soft WC particles provide the suitable sites to release the residual stress in coating. Furthermore, the impact load is imposed on the as-deposited diamond coating. The results show that the W-WC-diamond structural coating can validly inhibit the crack propagation. Hence, adding particles into the diamond coating may provide an useful way in enhancing the mechanical properties of diamond coating.

Acceptance ID: xgxv-P

Metal-insulator transition of Ru-doped VO_2 epitaxial films grown on sapphire substrate.

Jong-Gul Yoon and Hyuna Im

Department of Physics, University of Suwon, Gyunggi-do 445-743, Republic of Korea.
jgyoon@suwon.ac.kr

Effects of Ru-doping on the structure and metal-insulator transition (MIT) of vanadium dioxide (VO_2) are investigated by changing Ru-doping concentration in VO_2 epitaxial films grown on c-sapphire substrate. X-ray diffraction study at room temperature showed that (010) VO_2 grew on (0001) sapphire and the out-of-plane lattice constant of Ru-doped VO_2 films decreased with the increase in Ru-doping concentration up to 3 atomic %. Critical temperature (T_C) of MITs for the Ru-doped VO_2 is found to decrease with the increase in Ru-doping concentration, which is crtical for technological application of VO_2. A nonmonotomic decrease in surface rsisistivity was also observed up to around 3 atomic % of Ru-doping and a metallic phase at room temperature was obtrained. Optical reflectance measurements at several different temperatures showed that the decrease in reflectivity at longwavelength region was accompanied by the MITs of the films. We discuss the mechanism of Ru-doping induced reduction of T_C for Ru-doped VO_2 MIT in conjunction with the experimental results.

Keywords: Metal-insulator transition, vanadium oxide, thin film, doping effects

Acceptance ID: XKZR-O

Photoprecursor Approach toward Controlled Deposition of Organic Small-Molecule Semiconductors for Photovoltaic Applications

Mitsuharu Suzuki[1], *Ken-ichi Nakayama*[2,3], *Hiroko Yamada*[1]

[1]*Graduate School of Materials Science, Nara Institute of Science and Technology, Ikoma, Nara 630-0192, Japan*
[2]*Department of Organic Device Engineering, Yamagata University, Yonezawa, Yamagata 992-8510, Japan*
[3]*Department of Material and Life Science, Osaka University, Suita, Osaka 565-0871, Japan*
Email: msuzuki@ms.naist.jp

The active layer in organic photovoltaic cells is typically a blend of p-type and n-type semiconductors, and the arrangement of these materials critically affects the device performance. As a means for controlled preparation of organic photovoltaic layers, we have proposed a 'photoprecursor approach' in which α-diketone-type photoprecursors of acenes are solution-deposited and then converted quantitatively to target acene-based semiconducting materials by in-situ photoreaction.[1] α-Diketone-type photoprecursors of acenes are in general more soluble than corresponding photoreaction products, and thus this method allows indirect solution processing of highly crystalline, scarcely soluble acene compounds. Indeed, the photoprecursor approach enables preparation of well-performing bulk-heterojunction (BHJ) layers containing terribly self-aggregating acenes.[2] Note here that the morphology of resulting BHJ layers can be controlled by tuning photoreaction conditions. The photoprecursor approach can also be employed for the layer-by-layer deposition of different materials by solution processes, given that the solubility of photoreaction product is sufficiently low. By taking advantage of this feature, we have prepared p–i–n-type photovoltaic layers in which a BHJ layer (i-layer) is sandwiched between neat p- and n-type materials.[3] In our proof-of-concept system, the p–i–n-type active layers gave power conversion efficiencies (PCEs) of up to 5.9%, while the corresponding BHJ active layer afforded the maximum PCE of only 3.0%. These examples demonstrate the effectiveness of the photoprecursor approach in controlling morphology and material distribution in photovoltaic active layers.

Keywords: organic semiconductors, solar cells, solution process, small molecules, morphology

[1] SUZUKI, M., AOTAKE, T., YAMAGUCHI, Y., NOGUCHI, N., NAKANO, H., NAKAYAMA, K., YAMADA, H. 2014. Synthesis and Photoreactivity of α-Diketone-Type Precursors of Acenes and Their Use in Organic-Device Fabrication. *J. Photochem. Photobiol. C*, 18, 50–70.

[2] SUZUKI, M., YAMAGUCHI, Y., TAKAHASHI, K., TAKAHIRA, K., KOGANEZAWA, T., MASUO, S., NAKAYAMA, K., YAMADA, H. 2016. Photoprecursor Approach Enables Preparation of Well-Performing Bulk-Heterojunction Layers Comprising a Highly Aggregating Molecular Semiconductor. *ACS Appl. Mater. Interfaces*, 8, 8644–8651.

[3] YAMAGUCHI, Y., SUZUKI, M., MOTOYAMA, T., KATAGIRI, C., TAKAHIRA, K., IKEDA, S., YAMADA, H., NAKAYAMA, K. 2014, Photoprecursor Approach as an Effective Means for Preparing Multilayer Organic Semiconducting Thin Films by Solution Processes. *Sci. Rep.*, 4, 7151.

Acceptance ID: YDQK-P

N-, P- Type and Ambipolar Properties of Sputtered SnO_x Thin-Film Transistors

Yunpeng (Li)[1], *Jia (Yang)*[1], *Yunxiu (Qu)*[1], *Qian (Xin)*[1], *Aimin (Song)*[2]

[1] *School of Microelectronics, Shandong University, Jinan 250100, China*
[2] *School of Electrical and Electronic Engineering, University of Manchester, Manchester M13 9PL, United Kingdom*
E-mail: ypli2013@126.com, xinq@sdu.edu.cn, A.Song@manchester.ac.uk

Transparent oxide-semiconductor thin-film transistors (TFTs) have shown huge potential in flat-panel displays and integrated circuits. However, the lack of high-performance p-type and ambipolar oxides hampers the development of transparent CMOS circuits. SnO has shown the most promise among the very limited number of p-type and ambipolar oxides. Up to date, how to achieve p-type SnO TFTs with high on/off ratio (e.g. $>10^3$) or ambipolar SnO TFTs is still a challenge. Here, we have discovered that even a tiny (2%) increase of sputtering power could sharply switch the film conduction from n-type to p-type and increase the on/off ratio by orders of magnitude (FIG. 1). The highest on/off ratio of the fabricated p-type TFT with an active layer of 27-nm SnO and gate insulator of 300-nm thermally grown SiO_2 was 1.79×10^4, which is among the best values of reported single-gated TFTs. Moreover, we have found a new way to achieve ambipolar SnO_x TFTs by importing n-type SnO_2 into SnO-dominated films.

Keywords: SnO, thin film transistors, p-type, ambipolar, sputtering

[1] Li, Y., Xin, Q., Du, L., Qu, Y., Wang, Q. & Song, A. 2016. Extremely Sensitive Dependence of SnO_x Film Properties on Sputtering Power. *Sci. Rep.*, 6, 36183-36191.

[2] Zhang, J., Kong, X., Yang, J., Li, Y., Wilson, J., Liu, J., Xin, Q., Wang, Q. & Song, A. 2016. Analysis of carrier transport and band tail states in p-type tin monoxide thin-film transistors by temperature dependent characteristics. *Appl. Phys. Lett.* 108, 263503.

Acceptance ID: Z7DE-O

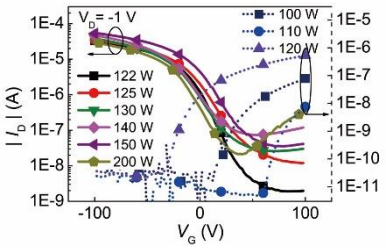

FIG. 1 Transfer curves of SnO_x TFTs with different sputtering powers.

Room temperature ferromagnetism and ferroelectricity in strained multiferroic $BiFeO_3$ thin films on $La_{0.7}Sr_{0.3}MnO_3/SiO_2/Si$ substrates

M. C. Ramírez-Camacho[1,2], C. F. Sánchez-Valdés[2], J. J. Gervacio-Arciniega[2], R. Font[3], C. Ostos[4], D. Bueno-Baques[5], M. Curiel[6], J. L. Sánchez-Llamazares[7], J. M. Siqueiros[2], O. Raymond-Herrera[2]

[1]*Posgrado en Física de Materiales, Centro de Investigación Científica y de Educación Superior de Ensenada, Carretera Tijuana-Ensenada 3918, Zona Playitas, 22860 Ensenada, B. C., México.*
[2]*Centro de Nanociencias y Nanotecnología, Universidad Nacional Autónoma de México, AP 14, Ensenada 22860, Baja California, México*
[3]*Facultad de Física, Universidad de La Habana, San Lázaro y L, 10400 La Habana, Cuba*
[4]*Instituto de Química, Universidad de Antioquia, UdeA, Calle 70 No. 52-21, Medellín, Colombia*
[5] *Center for Advanced Technologies and Optical Materials, Dept. of Physics and Energy Science, University of Colorado, Colorado Springs, Colorado 80918, USA.*
[6]*Instituto de Ingeniería, Universidad Autónoma de Baja California, Mexicali 21280, Baja California, México*
[7]*Instituto Potosino de Investigación Científica y Tecnológica A.C., Camino a la Presa San José 2055, Col. Lomas 4ª, San Luis Potosí 78216, México.*

A novel ferromagnetic state coexisting with ferroelectric ordering at room temperature in strained $BiFeO_3$ (BFO) thin films grown using a sputtering technique on $La_{0.7}Sr_{0.3}MnO_3/SiO_2/Si(100)$ (LSMO/SOS) substrates is reported. The properties of BFO films with different thicknesses (t_{BFO} = 15, 50, 70, 120, and 140 nm) on 40 nm LSMO layers are explored. [012] *out-of-plane* highly textured BFO/LSMO stacks grew with rhombohedral structures. LSMO layers are nanostructured in nature, constituted by ferromagnetic single-domain nanoregions induced by the constrain of the SiO_2 surface, with T_C ~ 200 K and high coercive field (H_C) of ~ 1100 Oe at 2.5 K. BFO films grew epitaxially nanostructured on LSMO, exhibiting ~ 4 nm spherical nanoregions. The BFO layers show typical antiferromagnetic behavior (in a greater volume fraction) when made thicker (t_{BFO} > 70 nm).

The thinner films (t_{BFO} < 50 nm) display ferromagnetic behavior with T_C > 400 K, H_C ~ 1600 Oe for 15 nm and ~1830 Oe for 50 nm. We propose that such ferromagnetic behavior is originated by the establishment of a new magnetic configuration in the Fe^{3+}-O-Fe^{3+} sublattice of the BFO structure, induced by strong hybridization at the interface as consequence of superexchange coupling interactions with the ferromagnetic Mn^{3+}-O-Mn^{3+}/Mn^{4+} sublattice of LSMO. All BFO layers show excellent ferroelectric and piezoelectric properties (coercive field ~ 740 kV/cm, and d_{33} = 23 pm/V for 50 nm; ~ 200 kV/cm and 55 pm/V for 140 nm), exhibiting 180º and 109º DWs structures depending on the thickness. Such multiferroic properties predict the potential realization of new magneto-electronic devices integrated with Si technology.

This work was supported by DGAPA-UNAM Grants (IN110315 and IN106414) and Conacyt Grants (127633 and 166286). The authors thank the technical support from CIQA (Saltillo), the Laboratorio Nacional de Investigaciones en Nanociencias y Nanotecnología (LINAN, IPICyT), and the Laboratorio Nacional de Nanotecnología (CIMAV-Chihuahua), in Mexico. The authors thank the technical assistance from A.G. Rodriguez, E. Murillo, E. Aparicio, P. Casillas, I. Gradilla, F. Ruiz, J. López-Mendoza, G.F. Hurtado (CIQA), O.O. Solís and J.G. Murillo-Ramírez (CIMAV-Chihuahua). C.F. Sánchez-Valdés thanks CTIC-UNAM for supporting his postdoctoral position at CNyN-UNAM.

KEYWORDS: multiferroic, BFO/LSMO thin film, rf sputtering, interlayer exchange coupling, superexchange

Acceptance ID: Z8TB-P

Various soft X-ray spectroscopy study of WO_3 thin film depending on growth conditions

Sunwoo (Ahn)[1], Chang Jin (Lim)[1], Simhee (Ryu)[1], Bokyung (Ryu)[1], Soohaeng (Cho)[1], Sang Wan (Cho)[1], Hirohito (Ogasawara)[2]

[1] *Department of Physics, Yonsei University, 1 Yonseidae-gil, Wonju-si, Gangwon-do, 26493, Republic of Korea.*
[2] *Stanford Synchrotron Radiation Lightsource, SLAC National Accelerator Laboratory, 2575 Sand Hill Road, Menlo Park, CA 94025, USA.*
dio8027@yonsei.ac.kr

Electronic structures of WO_3 thin film have been studied using x-ray photoelectron spectroscopy (XPS), x-ray absorption spectroscopy (XAS), and x-ray emission spectroscopy (XES) in an attempt to understand the influence of growth conditions on the electrical properties. The influence of growth oxygen pressure on the metal–insulator transition was investigated. It found that the conductivity of WO_3 films increases remarkably with the increase of the oxygen pressure during the growth and the decreased oxygen vacancies are induced by lower growth oxygen pressure. In conclusion, the origin of the metal-insulator transition was verified by XPS, XAS and XES.

Keywords: XES, XAS, XPS, WO_3, Electronic structure

[1] Wang, F., Valentin, C. D. & Pacchioni, G. 2012. Doping of WO_3 for Photocatalytic Water Splitting: Hints from Density Functional Theory. *The Journal of Physical Chemistry*, 116, 8901-8909.

[2] Qian, J., Peng, Z., Shen, Z., Zhao, Z., Zhang, G. & Fu, X. 2016. Positive impedance humidity sensors via single-component materials. *Scientific Reports*, 6, 25574.

Acceptance ID: ZE7S-P

Spectral Engineering of Microwaves through Varying Chemical Potential of Graphene in Double Meta Surface Graphene-Cone CIC Absorber

Arash Dehzangi[1], *Masih Ghasemi*[2], *Yiyun Zhang*[1], *Lina Ayat*[3], *P.K. Choudhury*[2]

[1]*Center for Quantum Devices, Department of Electrical Engineering and Computer Science, Northwestern University, Evanston, 60208, IL, USA*
[2]*Institute of Microengineering and Nanoelectronics, National University of Malaysia, UKM Bangi, 43600 Selangor, Malaysia*
[3]*EASi Engineering LCC, 226 Airport Parkway, San Jose, 95110, CA, USA*
(ghasemi.masih61@gmail.com)

Tuning the chemical potential of graphene and varying surface plasmon polariton (SPP) waves over the effective contact area of micro-cone graphene layers with silicon substrate are the two ways to control the peak absorptivity of the structure at a certain wavelength over the infrared and microwave regimes in a double layer graphene-cone metasurface based conductor-insulator- conductor (CIC) absorber. The graphene cone is assumed as made of hundreds of mono-layer grapheme, and at temperature, each cone is treated by an electrical source for tuning the chemical potential of graphene at 0 eV (the normal condition), 0.25 eV (which is the band gap of graphene; lack of carries density) and 1 eV (existence of carrier density). Polarized microwave at different incident angles plays the role of variable Hall effect sources [1,2]. The three-layer CIC absorber hosts a thick (1 mm) substrate for efficient trapping of electromagnetic waves between the two graphene metasurface layers, which are not good reflectors. The symmetrical structure of the cone in the x- and y-directions treats the polarized microwaves almost in the similar manner as that at the normal incident angle. However, the spectral features alter due to changes in the resonance condition, which causes spectral shift of the sharp peaks with different magnitude in the absorption spectrum over the far-infrared range. Results also confirm the negative impact of increasing the chemical potential on the performance of CIC absorber within the aforesaid regimes. Narrow spectral filtering of this device over far-infrared band makes it prominent for the application related to space observatory and far-infrared spectroscopy.

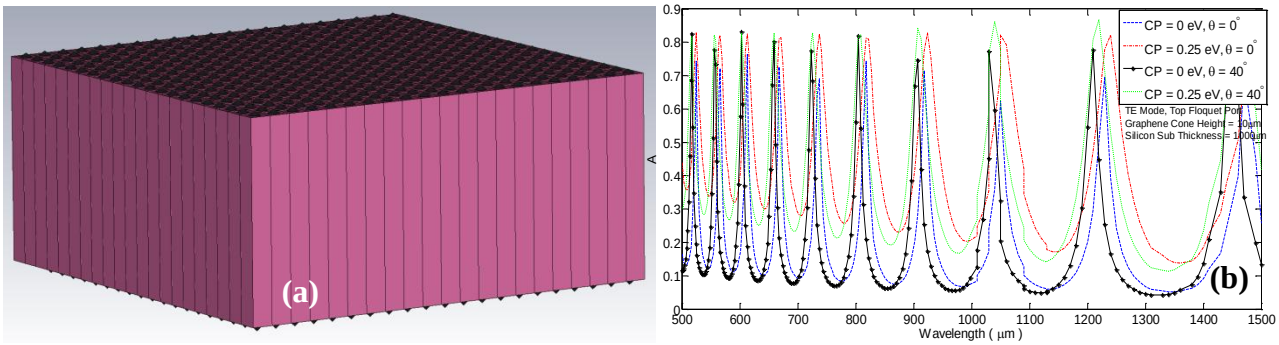

Figure 1. Schematic of CIC Absorber (a), and its absorption spectrum of at different CP values (0 eV and 0.25 eV) and incident angles (0° and 40°) (b).

References:

1. Hajaj, E. M., O. Shtempluk, V. Kochetkov, A. Razin, and Y. E. Yaish. "Chemical potential of inhomogeneous single-layer graphene." Physical Review B, Vol. 88, Issue. 4 (2013).

2. Lin, Xiao, Yang Xu, Baile Zhang, Ran Hao, Hongsheng Chen, and Erping Li. "Unidirectional surface plasmons in nonreciprocal graphene." New Journal of Physics, Vol. 15, Issue. 11 (2013).

Acceptance ID: ZJ6H-P

SYMPOSIUM 3: Advances in Polymers & Ceramics

Sulfur polymers for mercury capture

Parker[1], *Smith*[1], *Hasell*[1]

[1] *Department of Chemistry, University of Liverpool, Crown Street, Liverpool, L16 7ZD, UK,*
**t.hasell@liverpool.ac.uk*

Heavy metal contamination exists in the waste streams of many industries, and mercury is of particular concern for human health. Sulfur is an industrial by-product, removed as an impurity in oil-refining. This has led to vast unwanted stockpiles of sulfur, and resulted in low bulk prices. Sulfur is therefore a promising alternative feedstock to carbon for polymeric materials. Inverse vulcanisation has made possible the production of sulfur polymers, stabilised against depolymerisation by crosslinking.[1,2] Supercritical CO_2 can be used to foam inverse vulcanised polymers – making them macroporous.[3] These high sulfur-foams show excellent potential as low cost water filters to remove Hg. Alternative crosslinkers for inverse vulcanisation, from industrial by-products or bio-renewable sources, can be used to reduce the cost and improve the properties of the resultant polymers.[4] Carbonisation can be used to induce microporosity in the polymers, generating sulfur doped activated carbons with narrow pores size distributions.[5]

Keywords: Inverse vulcanization, porous, sulfur, polymer, mercury

[1] CHUNG, W. J. *et al*., A., 2013. The use of elemental sulfur as an alternative feedstock for polymeric materials. *Nature Chemistry*, 5, 518–524.

[2] CROCKETT, A. M., *et al.*, 2016. Sulfur-Limonene Polysulfide: A Material Synthesized Entirely from Industrial By-Products and Its Use in Removing Toxic Metals from Water and Soil. *Angew. Chem., Int. Ed.*, 55, 1714-1718.

[3] HASELL, T., PARKER, D. J., JONES, H. A., MCALLISTER, T., HOWDLE, S. M., 2016. Porous inverse vulcanised polymers for mercury capture. *Chemical Communications*, 55, 1714-1718.

[4] PARKER, D. J., JONES, H. A., PETCHER, S., CERVINI, L., GRIFFIN, J. M., AKHTAR, R., HASELL, T., 2016. Low cost and renewable sulfur-polymers by inverse vulcanisation, and their potential for mercury capture. *Journal of Material Chemistry A*, DOI: 10.1039/c6ta09862

Acceptance ID: 22XZ-O

Colloidal Photonic Crystal Enhanced Fluorescence for Efficient Optical Devices

Mingzhu Li, Yanlin Song*

Institute of Chemistry, Chinese Academy of Sciences (ICCAS)
Beijing Engineering Research Center of Nanomaterials for Green Printing Technology
Beijing National Laboratory for Molecular Sciences (BNLMS)
Beijing 100190, P. R. China

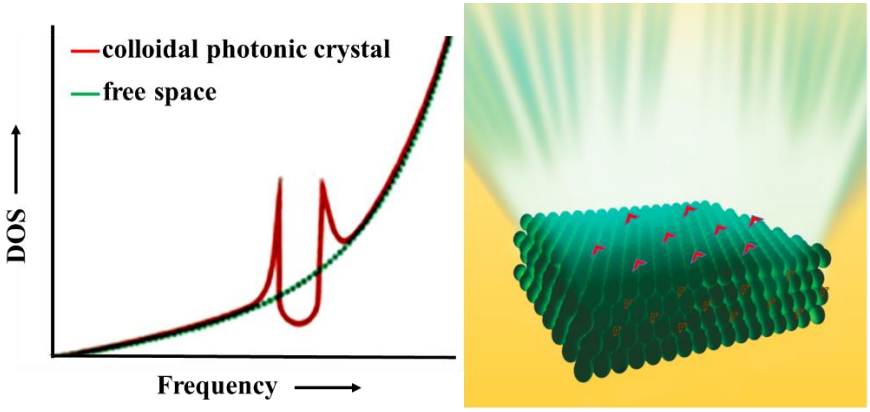

Fluorescence detections have high sensitivity and ease of operation, which are widely used for molecular diagnosis and environment monitor. High fluorescence signal and ultra-high sensitivity are of an enormous demand for luminescent devices and the bio/chem sensors in many areas and disciplines. Fluorescence emission is crucially depended on its surroundings besides the intrinsic property of fluorophore, known as Purcell effect. Photonic crystal (PC) has attracted tremendous attention for fluorescence enhancement, for PC microcavities combine high quality factors with small effective modal volumes that lead to enhanced values of the spontaneous emission rate through the Purcell effect. Additionally, slow photon effect of PC can enhance the extraction efficiency which is another crucial factor to achieve the enhancement of fluorescence.

We developed serials of fluorescence sensors and devices based on colloidal photonic crystals (CPCs) enhanced fluorescence, and exploited it into displays, optical devices, chemical and biological sensors. The best enhancement of fluorescence can be achieved by modifying the relationship between the photonic band gap and the excitation light and spontaneous emission to appreciate enhanced excitation and enhanced extraction at the same time. Additionally, CPC can serve as an effective dielectric mirror for high light extraction due to its ability to forbid the photon propagation in the photonic band gap, which is of great meaning for high efficient luminescence and display. Besides spontaneous emission, CPCs present another noticeable ability of boosting energy transfer between atoms and the energy from chemical reaction to the fluorophore. The self-assembled photonic structure from colloidal sphere can be constructed into various forms according to the demand of various bio/chem molecular diagnosis, which was demonstrated by ultra-sensitive detection of HIV, SARS, TNT, cocaine and various metal ions.

Colloidal photonic crystals are efficient optical antennas for fluorescence and can be easy compatible with traditional light trapping structures. Versatile CPCs patterns provide an alternate strategy to construct optical

integrated devices and accelerate their practical application. The presented CPC-assisted fluorescence sensors are low-cost and easy-to-use devices and will take great advantages for practical application such as point-of-care. It is evident that the whole field is still a juvenile one and offers ample opportunity for optical device design and discovery.

Acceptance ID: 2PCT-O

Medical carbon/oxygen dosimetry using OSL technique from easily prepared α – Al_2O_3 doped by carbon using ion implantation

Mini Agarwal[1], K Asokan[2], and Pratik Kumar[1],

[1]Medical Physics Unit, IRCH, AIIMS, New Delhi- 110 029, India
[2] Inter-University Accelerator Centre, Aruna Asaf Ali Marg, New Delhi-110 06, India

The goal of this work is to characterize augmented optically stimulated luminescence (OSL) micro crystalline (α – Al_2O_3 with 99 and 99.5% purity) and nano crystalline phosphor (single crystal, sapphire and poly crystal α –Al_2O_3 commercially purchased) as reusable and highly sensitive radiation dosimeter for low dose measurement in medical (diagnostics) applications. All present OSL phosphors suffer one or other lacuna prompting us to synthesizes α –Al_2O_3 nano phosphor which promises to be a cheap and have the capability to measure small and large radiation dose simultaneously with extraordinary efficiency. All the present OSL phosphors tend to saturate at higher doses (≈ 5-10 Gy) if they are able to measure small doses (≈ 1μGy). However, α –Al_2O_3 nano phosphor defies this and can measure doses in hundreds of KGy due to the incorporation of carbon as stable defects. In this study, attempts will be made to improve the characteristics of the commercially available OSL phosphors for their applications in medical dosimetry. α –Al_2O_3:C is a well known phosphor (only one commercially available) in OSL technique. However, a few complex issues are associated in the synthesis of the present phosphor such as complex doping process in the reducing atmosphere of graphite at very high temperature. The present work attempts to make an efficient OSL dosimeter by using well known and precisely controlled ion implantation for carbon doping (at 100 and 500 keV with three different fluencies in the range of 2.5 x 10^{15} to 6.25 x10^{15} ions/cm^2 as a function of dopant concentration in mol% to obtain the optimized one) to address the issues. Analysis of the new product α –Al_2O_3:C (optimized dopant concentration ~1% at 6.25 x10^{15} ions/cm^2) would be carried out by using RISO TL/ OSL reader. For cancer therapeutic applications, high energy heavy charged particles such as protons, helium, carbon and oxygen are at the verge of taking off because heavy ions (HCPs) exhibit an increased RBE in Braggs peak region as compared to entrance region. Therefore, we had been irradiated our newly meant phosphor by 80 MeV carbon and oxygen ion beam with four different fluencies in the range of 1x10^{11} – 2x10^{13} ions/cm^2 as a function of doses. It has been observed the high luminescent signal intensity at high fluence of high energy heavy charged particle in case of carbon ion beam irradiation than oxygen ion beam. So, there is an urgent need of an easily available, cheap, reproducible, and suitable radiation measuring materials for HCPs. This work seeks to develop a phosphor for HCP which may not only be sensitive for low doses medical investigation but also an invaluable tool for charged HCP dosimetry.

Chondrocyte aggregates incorporated with hyaluronic acid particles for cartilage regeneration

*Hae-Eun Shim, Sun-Woong Kang**

Predictive Model Research Center, Korea Institute of Toxicology, Daejeon, Korea
E Mail: swkang@kitox.re.kr , Tel : +82-42-610-8209, Fax : 82-42-610-8157

Articular cartilage has limited self-healing potential because cartilage has neither vascular supply nor resident stem cells. Autologous chondrocyte implantation (ACI) is one of the promising technologies for cartilage regeneration. Several studies have reported on the successful repair of cartilage defects by transplantation of cultured chondrocytes. One of the major thrusts in cartilage regeneration using ACI is to prevent dedifferentiation of chondrocyte and preserve viability of chondrocytes after transplantation. Attempts have been made to promote viability and therapeutic potential, including the use of 3D aggregates and spheroids, but more extensive studies are required to fully exploit the therapeutic potential offered by transplanted chondrocytes for cartilage regeneration because more dead cells are expected at the inner core of spheroids by hypoxic condition and limitation of nutrient diffusion in the cores of the spheroids. Therefore, in this study, we hypothesized that hyaluronic acid (HA) particles, an important component of hyaline articular cartilage, can serve to make the chondrocytes “feel more at home”. In this study, we demonstrate that incorporation of HA particles in multicellular aggregate is able to enhance viability and therapeutic efficacy of chondrocytes. This work was supported by Project No. 2016-02-DD-016.

Keywords: Hyaluronic acid, 3D culture, Cartilage regeneration, Tissue engineering

[1] Cho, M.O., Li, Z., Shim, H.E., Cho, I.S., Nurunnabi, N., Park, H., Lee, K.Y., Moon, S.H., Kim, K.S., Kang, S.W., Huh, K.M. 2016. Bioinspired tuning of glycol chitosan for 3D cell culture. *NPG Asia Materials*, 8, e309, 1-10.

Acceptance ID: 3C5U-P

Polymer Based Stacked Multilayer Transparent Electrode for Organic Optoelectronics

Vikas Sharma[1], *Kanupriya Sachdev*[1, 2]

[1]*Department of Physics, Malaviya National Institute of Technology, Jaipur 302017, INDIA*
[2]*Materials Research Centre, Malaviya National Institute of Technology, Jaipur 302017, INDIA*
Email: phyvikas@gmail.com

Polymer based optoelectronic devices have generated a large academic and industrial attention because of their technological advantages. Metal embedded polymer hybrid materials have found applications in a large number of energy conversion and display applications requiring organic transparent electrode. Here we report the result of investigations on Polystyrene-Silver- Polystyrene (P-A-P) multilayer structure which shows promising electrical and optical properties for its use as a transparent electrode for flexible optoelectronic devices. Polystyrene (PS) is used as the polymer layer with silver layer embedded in between the two polymer layers to form the stacked multilayer structure. Thin films of Polystyrene (PS) were coated by spin coating and silver layer was deposited by DC sputtering. Ag layer thickness was varied from 4 nm to 30 nm to optimize the middle layer thickness for best properties. The overall thickness of the multilayer was <100 nm. These films of varying Ag thickness were then characterized by XRD, Raman, FESEM and AFM for their structural and morphological investigations. Optical and electrical properties were measured using UV-Vis spectrophotometer and Hall measurement technique respectively. Average transparency of PAP structure is found to be ≥ 70 % for visible spectrum for 8nm thick Ag layer. Minimum value of obtained resistivity for 8 nm thickness reflects the formation of a continuous layer. The films are shown to have smooth morphology from FESEM images and have very low roughness as calculated using AFM technique. This feature is useful for growth of further layer for device fabrication. XPS was used to reveal the chemical state of the trilayer. Depth profiling was performed to check the stability of the trilayer. The importance of the present investigation underlies in the process which is easy, low cost and allows tunability of properties of TCE as per of the application.

Keywords: Polymer, Multilayer, Transparent Electrode, Hall measurement, XPS.

[1] ELLMER, K. 2012. Past achievements and future challenges in the development of optically transparent electrodes. Nat. Photonics 6, 808–816.

[2] SHARMA, V., VYAS, R., BAZYLEWSKI, P., CHANG, G.S., ASOKAN, K., SACHDEV, K., 2016. Probing the highly transparent and conducting SnO_x/Au/SnO_x structure for futuristic TCO applications. RSC Adv. 6, 29135–29141.

[3] Hedayati, M.K., Javaherirahim, M., Mozooni, B., Abdelaziz, R., Tavassolizadeh, A., Chakravadhanula, V.S.K., Zaporojtchenko, V., Strunkus, T., Faupel, F., Elbahri, M., 2011. Design of a Perfect Black Absorber at Visible Frequencies Using Plasmonic Metamaterials. Adv. Mater. 23, 5410.

Acceptance ID: 6G7Q-O

Preparation and Characterization of Nonwoven for Recyclable Cushion Material

Jung Yeon Kim[1], Jeong Rak Choi[2], Yeong Og Choi[1]*

[1]Technical Textile & Materials Group, Korea Institute of Industrial Technology, Korea
[2]Environment Textile Research Team, Korea Textile Development Institute, Korea
**yochoi@kitech.re.kr*

Due to health hazards and sustainability associated with PU foam, nonwovens are being developed as a replacement cushion material in car seats. For this application, the nonwoven needs to have stability under repeated dynamic loads and a good recovery capacity. For sustainability, it is desirable that nonwoven is made from uni-material. In this study, nonwovens for cushion material were prepared from poly(ethylene terephthalate)(PET) based fibers and their properties were characterized in aspects of process conditions. Two PET hollow fibers which are different in diameter were mixed with three kinds of PET-based elastic binding fibers in several ratios. The binding fibers used in this study are bi-component sheath-core structure. The evenly mixed fibers were carded to form web, cross lapped and then bonded to form nonwoven through needle punching, flat-bed bonding or hot air-through bonding process. The nonwovens prepared have a basic weight of 600 g/m2 and a thickness of 10 mm and are composed of 100 % PET-based fibers. The nonwovens prepared from just one component polymer (uni material) could be easily recyclable after use. The bulky nonwovens prepared to replace PU form were characterized in tensile, stiffness, compression and compared with PU foam. They showed lower compression shrinkage after long term compression than that of PU form, indicating their better compression recovery. They also showed good recovery capacities under dynamic compression.

Keywords: Hollow fiber, Nonwoven, Cushion, compression recovery

Acceptance ID: 6QJN-P

Polypyrrole/Graphene/Cadmium Sulphide Based Polymeric Nanocomposites for Optoelectronic Device Fabrication.

Dr. R. B. Choudhary

Nanostructured Composite Materials Lab, Department of Applied Physics (APH), Indian Institute of Technology (IIT-ISM), Dhanbad-82600 (Jharkhand) INDIA.
E-mail address: <rbcism@gmail.com>

Polymeric nanocomposites of polypyrrole/graphene/cadmium sulphide (PPY/GN/CdS) with varying concentration of CdS (2 wt%, 5 wt%, 10 wt % and 20 wt%) were synthesized via *in-situ* polymerization method. These nanocomposites were characterized using X-ray diffraction (XRD), energy dispersive x-ray (EDX), Fourier transform infrared spectroscopy (FTIR) and field emission electron microscopic (FESEM) techniques. The XRD results revealed broad peaks following the formation of graphene from graphene oxide and confirmed semi-crystallization behaviour of the nanocomposites. The elemental composition of the nanocomposites was assessed using EDX analysis and the chemical structures were studied by FTIR analysis. The FESEM images showed good dispersion of CdS nanoparticles with GNs and PPY. The optical properties were studied using ultraviolet-visible (UV-visible) spectroscopy and the bands gaps were calculated by *Tauc* plots. The nanocomposite sample with 5 wt % CdS showed the lowest band gap and revealed that it has higher absorption coefficient compared to other nanocomposites. The electrical properties were studied using current-voltage (I-V) measurement method. The I-V plots showed *ohmic* nature for electrical properties of the polymeric nanocomposite optimized at 5wt% CdS. These results lead to the understanding that polymeric PPY/GN/CdS nanocomposite can serve as one of the most promising materials for fabrication of optoelectronic devices.

Acceptance ID: 76R9-O

Aerosol Jet Printing and Photonic Sintering of Lead Zirconate Titanate Films

Jing (Ouyang)[1], Denis (Cormier)[2], Scott A (Williams)[3], David A (Borkholder)[1]

[1]Microsystems Engineering, Rochester Institute of Technology, Rochester, NY.
[2]Industrial and Systems Engineering, Rochester Institute of Technology, Rochester, NY.
[3]Chemistry and Materials Sciences, Rochester Institute of Technology, Rochester, NY.
Presenting author: jxo711@rit.edu.
Corresponding author: david.borkholder@rit.edu.

Lead Zirconate Titanate (PZT) has been widely used in actuators [1], sensors [2], and energy harvesters [3], due to its high piezoelectric response. PZT aerosol jet printing and photonically pulsed sintering technique has been demonstrated, which significantly shortens the processing time, enhances the film piezoelectric performance, and allows realizing devices on flexible and non-planar substrates [4]. However, it is presented that the depth of photonic sintering did not extend through the full thickness of the film. Therefore, it limits the film to obtain a further higher piezoelectric response. In this paper, a fully photonically sintered PZT film is reported giving rise to a superior piezoelectric performance. The commercially available nano-scaled PZT powders (average diameter = 480 nm) were used to mix with DI water, sintering aid (Cu_2O and PbO with molecular weight percentage of 1:4), and binder (polyvinylpyrrolidone) to formulate the aerosol-jet printable ink. Aerosol jet printing technique (Aerosol Jet 300, Optomec, Inc., USA) was adopted to deposit the film on a stainless steel substrate resulting in an approximately 5 µm thickness film. After drying at 200 °C for 1 hour in the atmospheric environment, the film was sintered photonically with the optimized sintering parameter combination (voltage = 550 V, duration = 170 µs, frequency = 2 Hz, number of pulses = 20 × 2) in less than 1 minute. With assistance of Scanning Electron Microscopic images, a fully sintered PZT film was observed. After poling the samples with 20 kV/cm electric filed for 1 hours at 170 °C in the atmospheric environment, the piezoelectric voltage constant (g_{33}) was measured yielding -23.8×10^{-3} V-m/N. This greatly improves the previousely reported result (17.9×10^{-3} V-m/N) [4]. This optimized fabrication process enables to use short time to obtain an enhanced piezoelectric response providing more potentials for better piezoelectric performance devices.

Keywords: PZT, film, photonic sintering, piezoelectric, voltage

[1] KOCH, M., EVANS, A. G. R. & BRUNNSCHWEILER, A., 1998. The dynamic micropump driven with a screen printed PZT actuator, *Journal of Micromechanics and Microengineering*, 8, 119-122.

[2] DEFAY, E., MILLON, C., MALHAIRE, C. & BARBIER, D., 2002. PZT thin films integration for the realization of a high sensitivity pressure microsensor based on a vibrating membrane. *Sensors and Actuators A: Physical*, 99, 64-67.

[3] OUYANG, J., PENMETCHA, A. R., CORMIER, D. & BORKHOLDER, D. A., 2015. Photonically sintered PZT energy harvester. *ASME 2015 International Mechanical Engineering Congress and Exposition*. V010T13A024-V010T13A024.

Acceptance ID: 7JNN-O

Synthesis and Self-organization of comb-like polymers possessing amphiphilic diblock polymeric side chain

Wen-Li Wang, Ren-Hua Jin

Graduate School of Engineering, Kangawa University, Rokkakubashi, Yokohama 221-8686, Japan
[phone/Fax : 81-45-481-5661; E-mail : rhjin@kanagawa-u.ac.jp]

Block copolymers or graft copolymers, which combine two or more types of homopolymer subunits with different properties, can easily form various self-assembled entities such as micelles, vesicles and lamellar structure via micro-phase separation. Consequently, they are very useful to construct nano/micro-structured and hierarchical materials. For this purpose, the structure-controllable living polymerization reactions are indispensable to design desired copolymers. Comb polymers, which possess a linear backbone and densely grafted side chains, can show unusual conformations different from those of linear and starlike polymers because of the steric repulsion among side chains. And they have attracted a great deal of attention recently.

Recently, we have developed a chemistry related to the properties and functions of linear poly(ethyleneimine) (LPEI). LPEI can be dissolved in water as heated to 80 °C while crystallizes to form aggregates with various morphologies when returned to room temperature. Interestingly, these morphologies can be easily transformed into silica when the crystalline aggregates mixed with silica sources. [1,2] In this study, we used poly(choloromethylstyene) obtained via RAFT polymerization as a macroinitiator for block copolymerization of methyloxazoline (MOZ) and phenyloxazoline (POZ). This resulted in comb-polymers possessing polystyrene as a backbone and block-copolymers PMOZ-b-PPOZ as side chains. Then the block of PMOZ was selectively hydrolyzed to polyethyeleimine (PEI). The obtained comb-polymers with PEI block showed remarkable self-assembly property and chemical function in silica mineralization in aqueous media.

Keywords: Comb-like copolymer, amphiphilicity, template, silica

[1] Jian-Jun Yuan and Ren-Hua Jin. 2005. Fibrous Crystalline Hydrogels Formed from Polymers Possessing A Linear Poly(ethyleneimine) Backbone. *Langmuir*, 21, 3136-3146.

[2] Dong-Dong Yao and Ren-Hua Jin. 2015. Synthesis of comb-like poly(ethyleneimine)s and their application in biomimetic silicification. *Polymer Chemistry*, 6, 2255-2263.

Acceptance ID: 8SMC-P

Self-reduction and luminescence properties of Ce^{4+}→Ce^{3+} based on novel layered compound $MgIn_2P_4O_{14}$

Jing Zhang[1], *Gemei Cai*[1,*], *Zhanpeng Jin*[1,*]

[1] *School of Materials Science and Engineering, Central South University, Changsha, 410083, China*
E-mail addresses: caigemei@csu.edu.cn (Gemei Cai), jin@csu.edu.cn (Zhanpeng Jin), beihaishamo@csu.edu.cn (Jing Zhang).

In present work, a novel layered phosphate $MgIn_2P_4O_{14}$ was found and synthesized for the first time, with the crystal structure solved by the powder X-ray diffraction method. It crystallizes in the monoclinic *C*2/*c* (No. 15) space group with lattice parameters of a = 9.8733(3) Å, b = 8.7595(2) Å, c = 12.5931(3) Å, β = 108.546(2) °, and Z = 4.

In $MgIn_2P_4O_{14}$, the self-reduction phenomenon of Ce^{4+}→Ce^{3+} was observed with the underlying mechanism investigated. Rather than the stressed importance of AO_4 (A = P, B, Al, etc.) 3-dimensional network to the protection of the doping ions from the oxygen in the air in the previous researches [1], we advance a new proposal to describe how AO_4 groups and layered structural features promote the electron transfer from the cation vacancies to Ce^{4+}.

Moreover, a set of luminescence properties of $MgIn_2P_4O_{14}$: Ce_x phosphors were investigated by means of various analytic techniques, including photoluminescence excitation and emission spectrum, decay lifetime, low-temperature VUV luminescence, high-temperature luminescence and so on.

Keywords: $MgIn_2P_4O_{14}$, crystal structure, self-reduction, mechanism, luminescence properties

[1] Pei, Z., Su, Q., Zhang, J. 1993. The valence change from RE^{3+} to RE^{2+} (RE= Eu, Sm, Yb) in SrB_4O_7: RE prepared in air and the spectral properties of RE^{2+}. *Journal of alloys and compounds*, 198, 51-53.

Acceptance ID: 959C-P

Preparation of novel polymer materials via manipulating their chain sequence

Xiang Gao[*]**,** *Zhenan Zheng and Hongze Li*

The State Key Laboratory of Chemical Engineering, College of Chemical and Biological Engineering, Zhejiang University, Hangzhou, China
[*]*gaox@zju.edu.cn*

The polymer chain sequence has significant impact on the properties of copolymers through affecting the mobility and interaction of polymer chain segments. With the development of controlled/living radical polymerizations, the polymer chain sequence of copolymers can be manipulated more easily than ever before. With the innovation on the design of polymer chain sequence, novel high performance or functional polymer materials have been prepared. The current work will show our recent efforts on the modification of polymer chain sequence through living radical polymerization method and introduction of novel properties into conventional polymer materials through the innovation on their chain sequence.

A many-shot living radical emulsion polymerization method is proposed to synthesize copolymers with high molecular weight and well-controlled chain sequence. In this method each shot consisting of comonomers with different fractions is added in stepwise manner during the reaction. High conversions over 95% are achieved in 35 min after each shot. The compositional variation along the polymer chain is then directly determined by the comonomer fractions added at each shot. With this method, a conventional methyl acrylate/styrene copolymer is changed to multi-shape memory smart materials, polymer electrolyte with high ionic conductivity for lithium-ion battery, high-performance electrode binder for lithium-ion battery and 3D printable multi-shape memory materials by simply redesigning its polymer chain sequence.

Keywords: polymer materials, chain sequence, living radical polymerization, lithium-ion battery binder, shape memory polymer

Acceptance ID: 9RV8-O

Fabrication of conductive fabric heaters using PEDOT:PSS

Changbong Yeon[1,2], *Gayoung Kim*[1,2], *Jung Wook Lim*[1,2], *and Sun Jin Yun*[1,2,*]

[1]*ICT Materials & Components & Research Laboratory, Electronics and Telecommunications Research Institute, 218 Gajeongno, Yuseong-gu, Daejeon 34129, Korea.*
[2]*Department of Advanced Device Engineering, University of Science and Technology, 217 Gajeongno, Yuseong-gu, Daejeon 34113, Korea.*
E Mail: Sjyun@etri.re.kr

Wearable and stretchable heaters are currently attracting a lot of interests as demands for wearable devices rapidly grow in market. Among the various heating materials, conducting polymers having processability, flexibility, and light weight are the most promising materials for the wearable applications. Most fabrics can be simply impregnated with poly(3,4-ethylenedioxythiophene):poly(4-styrenesulfonate) (PEDOT: PSS) solution which is the most successfully commercialized conducting polymer due to its high mechanical flexibility and excellent thermal stability.[1] However, the electrical conductivity of pristine PEDOT:PSS is below 1 S/cm which is too low to be utilized in heaters. The conductivity of PEDOT:PSS has been reported to be increased by the addition of dielectric organic solvents, such as dimethyl sulfoxide (DMSO),2 or by post-treatment with strong acids.3,4 However, residual DMSO may irritate human skin and fabrics are easily damaged by the acids. Therefore, it is necessary to develop a method to increase the conductivity of PEDOT:PSS causing no damage to the fabrics. The technique should be also simple and cost-effective to be successfully utilized for practical applications.

In this work, we investigated a very effective method for increasing the conductivity of PEDOTPSS using sodium dodecyl sulfate (SDS), one of the ionic surfactants that have been generally used in detergents for laundry, and firstly suggested the combination of blending and dipping methods using SDS. The results clearly showed that the conductivity of PEDOT:PSS was dramatically increased to ~1335 S/cm and the mechanism of conductivity enhancement of PEDOT:PSS was also clearly revealed. Then, we fabricated the highly conductive and stretchable fabric heaters using SDS-modified PEDOT:PSS. The fabric heaters exhibited reversible electrical behavior even with a cyclic loading of a tensile strain larger than 80%. The heaters fabricated using this method can be adaptable for the finger joint or elbow requiring very high stretchability. We are confident that the method suggested in this work is not only efficient for greatly improving the conductivity but also simple and cost-effective method for fabricating highly conductive and stretchable fabrics with various e-textile applications.

Keywords: conducting polymer, conducting fabric, PEDOT:PSS, sodium dodecyl sulfate, Fabric heater

[1] Ding, Y., Invernale, M. A. & Sotzing, G. A. 2010. Conductivity trends of PEDOT-PSS impregnated fabric and the effect of conductivity on electrochromic textile, *ACS appl. Mater. Inter.*, 2, 1588-1593.

[2] Reyes-Reyes, M., Cruz-Cruz, I. & Lo´pez-Sandoval, R. 2010. Enhancement of the electrical conductivity in PEDOT:PSS films by the addition of dimethyl sulfate, *J. Phys. Chem. C*, 114**,** 20220-20224.

[3] Xia, Y., Sun, K. & Ouyang, J. 2012. Solution-processed metallic conducting polymer films as transparent electrode of optoelectronic devices, *Adv. Mater.*, 24, 2436-2440.

[4] Yeon, C., Yun, S. J., Kim, J. & Lim, J. W. 2015. PEDOT :PSS films greatly enhanced conductivity via nitric acid treatment at room temperature and their application as Pt/TCO-free counter electrodes in dye-sensitized solar cells, *Adv. Electron. Mater*., 1, 1500121

[5] Yeon, C., Kim, G., Lim, J. W. & Yun, S. J. 2016. Highly conductive PEDOT :PSS treated by sodium dodecyl sulfate for stretchable fabric heaters, *RSC Adv.*, DOI: 10.1039/C6RA24749K.

Acknowledgement: This work was supported by Institute for Information & Communications Technology Promotion (IITP) grant funded by the Korea government (MSIP) (B0117-16-1003, Fundamental technologies of two-dimensional materials and devices for the platform of new-functional smart devices).

Acceptance ID: C7ND-O

High Contrast, Low-power Consuming Electrochromic Polymer Display

*Younghoon Kim, Minsu Han, Yeonghwan Heo, Woojae Lee, Chihyun Park, and Eunkyoung Kim**

Department of Chemical and Biomolecular Engineering, Yonsei University, 50 Yonsei-ro, Seodaemun-gu, Seoul 120-749, Republic of Korea.
E-mail:eunkim@yonsei.kr

Electrochromic polymers offer low-cost solution process for applications such as smart windows, electrochromic sunglasses, and displays. Among the electrochromic (EC) materials, π-conjugated polymers(CPs) are promising materials for electroactive layer in electrochromic devices (ECDs), demonstrating a high coloration efficiency, fast response, and high reversibility.[1, 2)] As these properties are influenced by not only the chemical structure of EC materials but also by the EC reaction in a device, both factors are crucial. Of the various electrochromic CPs, the transmittance changes of the poly(3,4-propylenedioxythiophene) derivatives (PRs) can reach high color contrast maintaining the high cycle stability.[3)] We synthesized several PRs for high color contrast and bistability. Further control on the EC material combination, through charge balancing reactions, afforded ECDs with a high color contrast, long stability, and high bistability. Here, the optimum material combination will be discussed along with charge balancing mechanism and demonstrate the application of the low-power consuming display into an automatic EC windows.

Reference

1) E. Kim et al, ACS Appl. Mater. Interf., 2012, 4, 1, 185-191.

2) E Kim et al, Angew. Chem. Int. Ed., 2013, 52, 4, 1180-1184

3) E.Kim et al, Energy Environ. Sci., 2016, 9, 117-122

Acceptance ID: CPSA-P

A study on the manufacturing method of 3D scaffold based on wrinkled nanofiber for promoting nerve regeneration

Jun Hee Lee[1], Seo Yeon Lee[2], Deock Hee Youn[2], Ji Yoon Lim[2], Chan Hee Park[1,2,] and Cheol Sang Kim[1,2,*]*

[1]Department of Mechanical Design Engineering, Chonbuk National University, Korea
[2]Department of Bionanosystem Engineering, Chonbuk National University, Korea
C.H.Park[*](biochan@jbnu.ac.kr), C.S.Kim[*] (cskim@jbnu.ac.kr)

Scaffolds with nano-sized patterns can be used to aid or inhibit cell proliferation. Electrospinning can produce continuous mats with nanopatterns and can control fiber diameter, density and alignment in a variety of ways. Previous studies have shown that ordered nanofibers promote cell regeneration and studies on how to fabricate aligned nanofibers have been extensively studied, but studies on the fabrication of 3D scaffolds with excellent physical properties are rare. In this study, a nanofiber mat was fabricated using collectors surrounded by circularly arranged metal rods, and aligned nanofibers and irregular nanofibers were formed between the metal rods and the metal rods, respectively. The mat, which was separated from the collector, was wrinkled by the shrinkage of the alignment part, and the irregularly formed part and the aligned part were repeated at regular intervals. The completed nerve conduit showed a cross-section with multiple layers of nanofibres, with wrinkled fibers and irregular fibers repeated at regular intervals. The aligned nanofibers were formed in the circumferential direction and were able to expand and contract in the circumferential direction. The nerve conduit developed through this study will be applied to future neuro - regeneration and artificial cardiovascular research.

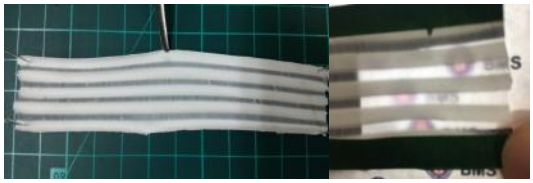

<Fig. 1. Wrinkled nanofibrous mat>

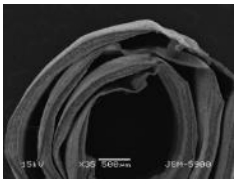

<Fig. 2. Wrinkled nanofibrous tube>

Keywords: Wrinkled nanofiber, Aligned nanofiber, Nerve regeneration, Nanofibrous tube

Acceptance ID: EF7X-P

Structure and Physical Properties of a New Multiblock Copolymers Based on Bio Poly(trimethylene furanoate)

Anna Szymczyk[1], *Magdalena Kwiatkowska*[2], *Iwona Kasprowiak*[1], *Sandra Paszkiewicz*[2]

[1]*Institute of Physics, Faculty of Mechanical Engineering and Mechatronics, West Pomeranian University of Technology, Av. Piastów 48, 70-310 Szczecin, Poland.*
[2]*Institute of Material Science and Engineering, Faculty of Mechanical Engineering and Mechatronics, West Pomeranian University of Technology in Szczecin, Av. Piastów 19, 70-310 Szczecin, Poland.*
*E Mail/ Contact Détails (**anna.szymczyk@zut.edu.pl**)*

Nowadays, in the new materials' syntheses, one can observe a new trend associated with the development of the technologies for the production of monomers from renewable resources and their use in the synthesis of new materials, or the substitution of monomers of petrochemical origin with the monomers obtained from these materials. Partially and fully bio based new multiblock copolyesters were synthesised and the effect of their chemical structure, morphology, and resulting supermolecular structure on their physical and elastic properties were investigated. These new block copolymers are composed of poly(trimethylene furanoate) (PTF) as rigid block and polydiols such as poly(tetramethylene ether) glycol (PTMG) or fatty acid dimer diol (FADD) as flexible block. The poly(trimethylene *furanoate*) (PTF) is a polyester synthesized from monomers (2,5-furandicarboxylic acid, 1,3-propanediol) obtained from renewable materials, which can bring notable ecological and energy effects from the point of view of using this material in practical applications. Recently, synthesis of furanoates (poly(ethylene furanoate) (PEF), poly(butylene furanoate) (PBF)) has been reported in a number of reports and considered as biobased alternatives to their terephthalate homologues. In our work we made an effort to study of structure and properties of PTF homopolymer and PTF based block copolymers.

Keywords: bio based copolyesters, poly(trimethylene furanoate), phase structure

Acceptance ID: FYV5-O

Development of Customized Biomedical Devices with Biocompatible Materials on the Basis of 3D Imaging and 3D Printing Techniques

Suk Hee (Park) [1], *Han Bit (Lee)* [1], *Ji Eun (Lee)* [1], *Seung Woo (Chun)* [1], *Yong (Son)* [1], *Jeanho (Park)* [1], *Nak Kyu (Lee)* [1]

[1]*Micro/Nano Scale Manufacturing R&D Group, Korea Institute of Industrial Technology, Ansan-si, Gyeonggi-do 426-910, Korea.*
selome815@kitech.re.kr / +82-31-8040-6829

Recently, three-dimensional (3D) printing technology has received a great deal of attention in customized products, which require arbitrary and adaptive shaping. In this respect, its application can be classified into two categories depending on their body contact manner: 1) implantable devices, and 2) wearable or patchable devices. Here, we present an integrative approach to the implementation of the 3D and flexible biomedical devices, which were separately realized for implantable and wearable devices but commonly characterized by use of 3D printed templates.[1]

1) Implantable device : A representative application in 3D printing of biomaterials is fabrication of tissue engineering scaffold. Despite the extensive utilization of 3D printing, the direct printing of biomaterials has a limitation in terms of flexibility due to the original stiffness of material and limit of processing resolution. We overcame this limitation by incorporating dip-coating process with 3D printing of template. Briefly, 3D design was carried out on the basis of medical image data. According to the designed morphology, a sacrificial construct was 3D-printed using a water-soluble material. Thereafter, the 3D template was dip-coated with a solution of biomaterials. After the sacrificial template was removed by water, a micrometer-scale thin film tube could be obtained with retaining the 3D morphology. Owing to its thin geometry, the resulting structure exhibited a sufficient flexibility and suitable applicability to tubular scaffolds for tissue engineering. We demonstrated the feasibility by conducting animal surgery experiments and expect the universal applicability in other tubular tissue engineering such as vascular, airway, and abdominal organs.

2) Wearable device : We also present a 3D-printing-based technique for fabricating 3D and flexible wearable devices. Like the 3D-printing-based scaffold above, our approach employed a 3D-printed template, which was used for elastomer casting process. With the aid of a recently introduced 3D printing machine, the molding template could be fabricated as a multi-material form with flexible, semi-flexible and rigid materials for its parts. Owing to the robust single-entity mold with multi-material characteristics, the elastomer molding and demolding processes could be successfully performed without any notable defects, thickness. With the defect-free and 3D-curved elastomer sheets, a sandwich-form device was integrated using a piezoelectric layer between the sheets with gold-sputtered electrodes. Based on the piezoelectric functionality, we showed several conceivable applications of the 3D flexible sensors to wearable electronics or human-like soft robotics, such as monitoring of heart pulse on skin and perception of external force while wearing. We expect our achievements will open up a variety of new applications for wearable electronic devices, particularly in the fields of health monitoring medical devices.

Keywords: 3D printing, biomedical device, template, scaffold, wearable device

[1] LEE, H. B., KIM, Y. W., YOON, J., LEE, N. K., & PARK, S. H. 2017. 3D customized and flexible tactile sensor using a piezoelectric nanofiber mat and sandwich-molded elastomer sheets. Smart Materials and Structures, 26, 045032.

Acceptance ID: G24M-P

The investigation of Ce/Gd-codoped YAG transparent ceramic for the excellent white LED

Shengming Zhou, Yanru Tang, Xuezhuan Yi, Shuai Zhang, Deming Hao, Xiuchen shao, Jie Chen

Shanghai Institute of Optics and Fine Mechanics, Chinese Academy of Sciences, Shanghai 201800, China.

The transparent ceramic phosphor samples with chemical formula $(Ce_{0.001}Gd_xY_{0.999-x})_3Al_5O_{12}$ and the two-phase $(Ce_{0.001}Gd_xY_{0.999-x})_3Al_5O_{12}$-$Al_2O_3$ were synthesized by the vacuum sintering method, and their crystal structure, grain morphology, and luminescence properties, are investigated. XRD spectra showed that the diffraction peaks shift slightly toward the smaller diffraction angles with increasing Gd concentration. The grain size of all samples ranges from 5μm to 15μm. The photoluminescence (PL) spectra of the ceramic phosphor with different Gd doping concentrations are measured and it showed that the peaks of yellow-green light are red-shifed, which helps to improve the color-rendering properties. Ceramic plate phosphors able to produce white light when directly combined with commercially available blue light emitting diodes were tested. The $(Ce_{0.001}Gd_xY_{0.999-x})_3Al_5O_{12}$-$Al_2O_3$ ceramic phosphor has a better luminous efficacy than that without the second phase of Al_2O_3 under the same test condition. The Al_2O_3 particle plays an important role in promoting the luminous efficacy, it changes the propagation of the light in ceramic, reduces the total internal reflection, and consequently improves extraction efficiency of light. Therefore, the $(Ce_{0.001}Gd_xY_{0.999-x})_3Al_5O_{12}$-$Al_2O_3$ ceramic phosphor is promising for the application of high-power density illumination.

Acceptance ID: GDLB-O

Nanocelluloses with Tunable Amphiphilicity and Functionality

You-Lo Hsieh

University of California at Davis, Davis, CA 95616
ylhsieh@ucdavis.edu

Cellulose, the nature's most abundant polymer, is naturally synthesized in highly oriented and crystalline structures that can be isolated into among the most unique nano-biomaterials. This paper presents diverse and efficient strategies to generate 1D nano-arrays of designed nanocelluloses from agricultural crop residues and food processing wastes. Cellulose nanofibrils (CNFs) and nanocrystals (CNCs) in varied aspect ratios and surface chemistries have been derived by a newly developed green process, solid acid catalyst[1] as well as common sulfuric acid hydrolysis, 2,2,6,6-tetramethylpyperidine-1-oxyl (TEMPO) mediated oxidation and shear forces. Both methods of derivation and fractionation govern not only the yields but also the quality attributes of nanocelluloses. Nanocelluloses can also be derived from less pristine biomass to give higher yields as well as advatnageous properties, such as higher thermally stability and hydrophobicity[2]. These nanocelluloses have shown to be effective dispersing and emulsifying agents for oil-water emulsions[3,4], coagulants for microbes[5] as well as templates for nanoparticles and nanoprisms[6]. Ways to assemble nanocellulose into hybrid and porous structures with novel functional properties, such as highly crystalline nanofibers[7], super-absorbent hydrogels and amphiphilic aerogels[8,9], will be demonstrated for applications including nano-hybrids, oil recovery and separation, water purification, etc. These versatile nanocelluloses and their facile conversion into advanced materials not only highlight the vast potential of these unique biologically derived nanomaterial building blocks for the future but also offer means to minimize the impact of the food production system on our environment.

Keywords: Nanocellulose, amphiphilic, aerogel, hydrogel, renewable

[1] HU, S., JIANG, F., HSIEH, Y.-L. 2015. 1D Lignin based solid acid catalysts for direct hydrolysis of crystalline cellulose, *ACS Sustainable Chemistry & Engineering*, 3:2566-2574.

[2] GU, J., HSIEH, Y.-L. 2017. Alkaline cellulose nanofibrils from streamlined alkali treated rice straw, *ACS Sustainable Chemistry & Engineering*, 5: 1730-1737.

[3] GU, J., HSIEH, Y.-L. 2015. Surface and structure characteristics, self-assembling and solvent compatibility of holo-cellulose nanofibrils, *ACS Applied Materials & Interfaces*, *7*(7), 4192–4201.

[4] JIANG, F., HSIEH, Y.-L. 2015. Novel holocellulose nanocrystals: amphiphilicity, O/W emulsion and self-assembly, *Biomacromolecules*, 16, 1422-1441.

[5] WANG, M.S., JIANG, F., HSIEH, Y.-L., Nitin, N. 2014. Cellulose nanofibrils improve dispersibility and stability of silver nanoparticles and induce production of bacterial extracellular polysaccharides, *Journal of Materials Chemistry B*, 2 (37), 6226-6235.

[6] JIANG, F., HSIEH, Y.-L. 2014. Synthesis of cellulose nanofibril bound silver nanoprism for surface enhanced Raman scattering, *Biomacromolecules*. 15 (10), 3608-3616.

[7] JIANG, F., HAN, S., HSIEH, Y.-L. 2013. Controlled defibrillation of rice straw cellulose and self-assembly of cellulose nanofibrils into highly crystalline fibrous materials, *RSC Advances*, 3(30): 12366-12375.

[8] JIANG, F., HSIEH, Y.-L. 2014. Amphiphilic superabsorbent cellulose nanofibril aerogels, *Journal of Materials Chemistry A*, 2: 6337-6342.

[9] JIANG, F., HSIEH, Y.-L. 2017. Cellulose nanofibril aerogels: synergistic improvement of hydrophobicity, strength, thermal stability via crosslinking with diisocyanate, ACS Applied Materials & Interfaces, *9* (3), 2825–2834.

Acceptance ID: H2RL-O

Novel Stable-Jet Electrospinning of Microfiber Bundles for Tissue Engineering Applications

Do Hee Lee[1], Joshua Lee[1], Seoyeon Lee[1], Chan Hee Park[1,2,], Cheol Sang Kim[1,2,*]*

[1]Department of Bionanosystem Engineering, Graduate School, Chonbuk National University, Jeonju, Republic of Korea
[2]Division of Mechanical Design Engineering, Chonbuk National University, Jeonju, Republic of Korea
Email : jjangwon21@gmail.com, biochan@jbnu.ac.kr, chskim@jbnu.ac.kr

Electrospinning utilizes high voltage to create nanofibers from a polymer solution. The threads of nanofibers start off as a stable jet, but starts to whip as it gets further away from the tip of the nozzle. A metal circular disk that acts as a base electrode that helps maintain a stable electric field was installed near the end of the nozzle tip to increase the length of this stable jet. In this preliminary study, we were able to create fibers with a unique morphology by utilizing the interface at which the stable jet transitions into an unstable whip. In electrospinning without the electrode, that interface is too close to the nozzle tip, which does not allow for sufficient evaporation of the solvent and thus results in thicker fibers or a melt. However, with the base electrode, the stable-unstable interface is farther from the tip and allows for proper fiber formation. The resulting microfibers bunch together to form unique bundles that exhibit strong mechanical strength and high cell viability rates. The unique morphology of the bundles was confirmed via SEM and cell viability through CCK. We foresee application of these fiber bundles in tissue engineering and possibly in the field of stents.

Keywords: Stable-jet electrospinning, base electrode, microfiber bundles, tissue engineering

[1] SUN, D., CHANG, C., LI, S., & LIN, L. 2006. Near-Field Electrospinning. *Nano Lett.*, 6 (4), 839-842.

Acceptance ID: KKKJ-P

New luminescent cyanopyridine based conjugated polymers: Synthesis, structure, photophysical and electrochemical properties

Airody Vasudeva Adhikari[a*], *Naveenchandra Pilicode*[a], *Madhukara Acharya*[a]

[a]*Organic Materials Laboratory, Department of Chemistry, National Institute of Technology Karnataka, Surathkal, Mangalore-575 025, India*

[*]*Corresponding author, Tel.: +91-824-2474000, Ext[n]: 3203; Fax: +91-824-2474033.*

E-mail: avadhikari123@yahoo.co.in, avchem@nitk.ac.in, avachem@gmail.com

Mobile: +91 9448627138

In recent years, there have been immense research interests in the electroluminescent and photoluminescent properties of conjugated heteroaromatic polymers, as they are promising candidates for several electronic applications such as light-emitting devices, transistors, photovoltaic cells, polymer memory and switches. It has been well-established that the incorporation of cyanopyridine ring system into polymeric framework would enhance the optical properties remarkably mainly because of its stable structure, powerful electron with-drawing nature and extended conjugation together with rigidity induced by heteroatom participation in the conjugation, avoiding energy dissipation through vibration. On the basis of the above considerations and in the context of our efforts on developing a novel blue light emitting polymer, we have designed three new conjugated polymers (**P**$_{1\text{-}3}$) carrying cyanopyridine moiety in their backbone and synthesized them in good yield *via* solution condensation polymerization technique. Structurally, they differ by vinylene linkages and were shown to exhibit good solubility in common organic solvents like THF, $CHCl_3$, DMF etc., largely due to presence of long alkoxy chains. These polymers were characterized using UV-Visible, PL, FTIR, and ^{1}H NMR spectroscopy and GPC technique followed by elemental analysis. Further, they were subjected to electrochemical and thermal analyses. The newly synthesized polymers displayed good thermal stability with onset decomposition temperature above 350 ^{0}C. Electrochemical band gap of these polymer were found to be in the range of 2.5-2.7. The polymers **P**$_{1\text{-}3}$ showed absorption maxima at 390 nm, 365 nm and 375 nm and emission bands at 418, 440 and 479 nm in THF, respectively. The spectral results reveal that they are strong blue light emitters. In order to acquire a deeper understanding of the electronic and optical properties of the polymers, density functional theory (DFT) calculations were performed.

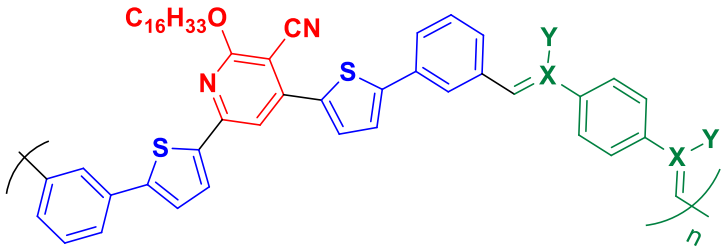

Where P_1: X = C and Y = CN

P_2: X = C and Y = H

P_3: X = N and Y = H

Key words: Cyanopyridine, conjugative polymers, PLED, DFT, band gap.

References:

K.A. Vishnumurthy, M.S. Sunitha, K. Safakath, Reji Philip, **Airody Vasudeva Adhikari***, (2011). "Synthesis, electrochemical and optical studies of new cyanopyridine based conjugated polymers as potential fluorescent materials." *Polymer*, 52 (2011), 4174-4183

Chao Tank, Tao Yang, Xudong Cao, Youtian Tao, Fangfang Wang, Cheng Zhong, Yan Qian Xinwen Zhang, Wei Huang, "Tuning a Weak Emissive Blue Host to Highly Efficient Green Dopant by a CN in Tetracarbazolepyridines for Solution-Processed Thermally Activated Delayed Fluorescence Devices", *Advanced optical materials*, 3, 6, (2015), 786-790

Xiao-Ling Liu, Dan Wu, Rui Sun, La-Mei Yu, Jian-Wen Jiang, Shou-Ri Sheng, "Synthesis and properties of novel soluble fluorinated polyamides containing pyridine and sulfone moieties", *Journal of Fluorine Chemistry*, 154, (2013), 16-22

Madiha Irfan, Iqbal Ahma, Shahid Ameen Samra, Aamer Saeed, "Study on the synthesis andc haracterization of 3,3′-bicarbazole and pyridine based luminescent copolymers", *Materials Letters*, 161 (2015) 37-40

Acceptance ID: MHZC-O

Syringeless Electrospinning for Easy and Versatile Preparation of Nanofibers

Kyung Jin Lee

Kyonggi University
kjlee@cnu.ac.kr

We report a syringeless electrospinning method using a rotating, helically probed cylinder. This method provide several advantages over general and needleless electrospinning with respect to various experimental parameters, such as processibility, selection of materials and solvent, and productivity as well. This method makes the electrospinning process a batch-based continuous system, and thus make it possible to avoid tedious optimization. With this system, comparable result to those of conventional electrospinning can be realized and one can produce more functional nanofiber webs when combined with other techniques such as colloidal electrospinning, the preparation of nanofiber webs with several different materials and highly crystalline polymers. This syringeless electrospinning procedure will contribute to the mass production of nanofiber webs and new applications for nanofibers in biological, chemical, and medical fields.

Acceptance ID: MW2E-P

Chiral transfer systems based and mediated on silica frames

Seiji Tsunega and Ren-Hua Jin

Department of Material and Life Chemistry, Faculty of Engineering, Kanagawa universityKanagawa University, 3-27-1 Rokkakubashi, Kanagawa-ku, Yokohama, Kanagawa 221-8686, Japan
Phone/Fax: +81-45-481-5661; E-mail: r201570113pa@jindai.jp

Chiral inorganic materials have attracted great interest because of their unique structures and optical activities as well as potential applications such as chiral catalysis, sensor, optical resolution etc. However, most of reports on chiral inorganic materials put the focus on controlling the chiral morphology like a helical or twisted structure. Therefore, chiroptical properties would disappear with the corruption of chiral morphology. In our previous work, we have reported nano-fiber based chiral silica materials with strong chiroptical activities which can be easily prepared by using nano crystalline aggregates composed of linear polyethyleneimine (LPEI) and chiral (L- and D-) tartaric acid as catalytic templates in silica deposition.

In this report, we further synthesized functional SiO_2@metal composites and investigated their chiroptical activities. The integration of metal NPs into silica was carried out without any additional reductants because of the amine groups in LPEI encapsulated in chiral silica working as a reduction sites. Interestingly, chiral SiO_2@metal composites and free metal nanoparticles synthesized in chiral silica frame exhibited unique optical activities in CD spectra.

Keywords: nano gold, nano silver, chiral silica, polyethyleneimine, tartaric acid

[1] H. MATSUKIZONO & R.-H. JIN 2012. High-Temperature-Resistant Chiral Silica Generated on Chiral Crystalline Templates at Neutral pH and Ambient Conditions. *Angew. Chem. Int. Ed.*, 51, 5862 –5865.

Acceptance ID: NNC3-P

Effect of as-received IGCC slag addition in geopolymer

Seongyeol Kim[1] and Yooteak Kim[1]

[1]Kyonggi University, Department of Materials Engineering, Suwon, Republic of Korea 16227
E-mail : ytkim@kgu.ac.kr, *Contact Details : +82-70-4024-9765*

It is well known fact that the cement production is responsible for almost 5% of total CO_2 emission in the world and which mainly affects to global warming. Geopolymers were worth as ordinary portland cement (OPC) substitutes because geopolymers release 80% less CO_2 than OPC and have sufficient mechanical properties like OPC. Therefore, geopolymers have attracted from eco-friendly construction industries. Geopolymers can be fabricated by aluminum silicate materials with alkali activators such as fly ash, blast furnace slag and so on. IGCC (Integrated Gasfication Combined Cycle) slag was used for fabricating geopolymers in this study. Geopolymers were fabricated with finely grounded and sieved (under 128mesh) IGCC slag. The grinding process of as-received IGCC slag would be one of the main costs for production of geopolymer. Therefore, the idea of using as-received IGCC slag (before grinding IGCC slag) as aggregates in the matrix of geopolymer was introduced to reduce the production cost as well as to enhance the compressive strength. As-received IGCC slag (0, 10, 20, 30, 40wt %) was added in the mixing process of geopolymer and compared. The compressive strength of geopolymers with an addition of 10wt% of as-received IGCC slag increased by 20% compared to that of no addition one and reached up to 41.20MPa. The enhancement of compressive strength would be caused by as-received IGCC slags acting as aggregates in the geopolymer matrix as in those of concrete. Density of geopolymers slightly increased to 2.1-2.2g/cm^3 with an increase in addition. Therefore, it is concluded that small addition of as-received IGCC slag in the geopolymer could increase compressive strength and decrease the total cost of the product. Moreover, the direct use of as-received IGCC slag may contribute the environment protection by reducing process time and CO_2 emission.

Keywords: Geopolymer, IGCC slag, Aggregates, As-received IGCC slag

Acceptance ID: PTGU-P

Inorganic Impurities in Isolated Polymers from Renewable Biomass Resources

S.Yaman, H.Haykiri-Acma, S. Kucukbayrak*

Istanbul Technical University, Faculty of Chemical and Metallurgical Engineering, Department of Chemical Engineering, 34469, Maslak, Istanbul, Turkey
Phone: 90 212 2853351 Fax: 90 212 2852925
e-mail: yamans@itu.edu.tr

Woody biomass that is regarded as a renewable and sustainable energy source is mainly consisted of several polymeric materials such as lignin, cellulose, and hemicellulose. Therefore, the term of ‘‘lignocellulosic’’ is used for a number of biomass species. Cellulose $(C_6H_{10}O_5)_n$ is the primary structural component in the cell wall of biomass, and it is a long chain polymer with high degree of polymerization. Hemicellulosics are complex polysaccharides with the generic formula $(C_5H_8O_4)_n$ found in the cell walls, and xylan is the most abundant form of hemicellulosics. Besides, lignin is the second most abundant renewable polymer after cellulose and nature’s most abundant aromatic (phenolic) polymer. These polymers are connected with weak ether bonds and they can be separated from each other by suitable techniques which mostly base on chemical disintegration methods. In this way, each individual natural polymer can be isolated and characterized.

However, these isolated ingredients have always been regarded as pure, and so far potential inorganic impurities resulting from the parent biomass have been ignored. For this reason, this study focuses on the inorganics in the isolated polymers. In this context, two different biomass species such as hybrid poplar wood and apricot stones which are renewable sources were subjected to sequential isolation procedures of ASTM D1105, Wise’s Chlorite Method, and van Soest’s Method. The isolated holocellulose (hemicellulose + cellulose) and lignin were then characterized mineralogically by X-ray Diffraction (XRD) and X-ray Fluorescence (XRF) techniques, and the results were compared with those for the parent biomass species. It was determined that the isolated holocelluloses and lignins are not just ash-free and they have ash contents up to 2.2% and 4.0%, respectively. Also, various minerals including potassium chloride, several phosphate minerals, and alumina silicates were found to survive after chemical treatments applied during isolation. In addition, the presence of several heavy metals was also detected. These results reveal that minerals cannot be eliminated entirely because of the natures of the chemicals used, and they unavoidably remain in the isolated natural polymers.

***** corresponding author

Acceptance ID: PVGP-O

The Development of Immaculate Denture with the 2-Methacryloyloxyethyl Phosphorylcholine Polymer

Ikeya[1], Iwasa[1], Fukunishi[1], Tsukahara[1], Inoue[2], Ishihara[2], Baba[1]

[1]Department of Prosthodontics, School of Dentistry, Showa University, Kitasenzoku 2-1-1, Oota-ku, Tokyo 145-8515, Japan
[2]Department of Materials Engineering School of Engineering, The University of Tokyo
Presenting author: Kenji Ikeya. ikeya0306@dent.showa-u.ac.jp
Corresponding author: Kazuyoshi Baba. kazuyoshi@dent.showa-u.ac.jp

Denture plaque-associated infections are regarded as one of important social problems in a super-aged society, because they can cause a variety of health problem, such as denture stomatitis and aspiration pneumonia. The polymers composed of 2-methacryloyloxyethyl phosphorylcholine (MPC), well-known biomedical polymeric materials, have blood compatibility and tissue compatibility based on their resistance to protein adsorption, and several medical devices with the MPC polymer layer have already been used in clinical settings. The objective of this study was to evaluate the effects of the treatment with the photoreactive MPC polymer on plaque deposition on complete dentures based on poly (methyl methacrylate) (PMMA).

Keywords: MPC polymer, Biofilm formation, Denture plaque, Complete denture

[1] TAKAHASHI, N., IWASA, F., INOUE, Y., MORISAKI, H., ISHIHARA, K., BABA, K. 2014. Evaluation of the durability and antiadhesive action of 2-methacryloyloxyethyl phosphorylcholine grafting on an acrylic resin denture base material. J Prosthet Dent , 112, 194-203.

Acceptance ID: PYTV-P

Phytoncide-releasing nanotextiles and their antimicrobial properties

Jiyoung Shin (Shin) and Seungsin Lee (Lee)

Department of Clothing and Textiles, Yonsei University, Seoul, Korea
SL158@yonsei.ac.kr

It has been reported that plant-derived essential oils possess multiple properties such as antibacterial and antifungal activities, and antioxidant effects [1, 2]. Phytoncides are terpene-based volatile organic compounds released from various trees and plants, and they are well known for their natural characteristics of antimicrobial effects. Incorporating phytoncide into nanofibrous structures, which are ultrathin and lightweight with a large specific surface area, would create functional nanotextiles with intrinsic antibacterial properties based on natural substance and have high potential in medical and healthcare applications. This research investigates incorporating phytoncide into a polymetric matrix via electrospinning for the development of environmentally friendly, antimicrobial textile materials. Emulsion electrospinning method was employed to incorporate phytoncide into PVA nanofibrous matrix. An emulsion consisting of PVA solution as the aqueous phase and phytoncide oil as the oil phase was prepared. Nonionic surfactant was added to stabilize the emulsion. Electrospinning was conducted under a variety of spinning conditions to find an optimum spinning condition. The morphology of PVA nanofibers containing phytoncide oil was examined using a field emission scanning electron microscope (FE-SEM) and a transmission electron microscope (TEM). Heat treatment was carried out to stabilize the PVA-based nanofibers against dissolution in water. The release profile of phytoncide from the core of nanofibers was assessed by gas chromatography. The antimicrobial activities of phytoncide/PVA nanofibers were evaluated quantitatively in accordance with ASTM E 2149-01 by measuring the bacterial reductions of a Gram-positive bacterium (*Staphylococcus aureus*) and a Gram-negative bacterium (*Escherichia coli*). The SEM images of phytoncide oil/PVA nanofibers showed that the emulsion yielded relatively uniform nanofibers with diameters of 250-350 nm. The PVA nanofibers containing phytoncide were further characterized by a TEM to verify the inner structure of the fibers. TEM images illustrated that the resulting electrospun nanofibers are composed of uniform core and sheath structures and phytoncide was efficiently incorporated in the core. The release profile of phytoncide from the nanofibrous membranes showed continuous emission over 0 to 21 days through GC-MS analysis. The antimicrobial activity of phytoncide/PVA nanofibrous membranes at 3.0 g/m^2 web area density exhibited a 99.9 % reduction rate against both *Staphylococcus aureus* and *Escherichia coli*. The results demonstrate that the successful imparting of antimicrobial functions to nanofibrous membranes is achievable through simultaneous electrospinning of the polymer material with phytoncide oil.

Keywords: Functional textile, nanofibrous membrane, phytoncide, natural antibacterial substance

[1] WANG, S. Y., LAI, W. C., CHU, F. H., LIN, C. T., SHEN, S. Y., & CHANG, S. T. 2006. Essential oil from the leaves of Cryptomeria japonica acts as a silverfish (Lepisma saccharina) repellent and insecticide. *Journal of Wood Science*, 52, 522-526.
[2] ABE, T., HISAMA, M., TANIMOTO, S., SHIBAYAMA, H., MIHARA, Y., & NOMURA, M. 2008. Antioxidant effects and antimicrobial activities of phytoncide. *Biocontrol science*, 13, 23-27.

Acceptance ID: R488-P

Self-Propelled Water Droplets on A Structured Shape Memory Polymer Surface

Park[1], and Kim[1]

[1] Department of Mechanical Science and Engineering, University of Illinois at Urbana-Champaign, Urbana, Illinois, 61801, USA.
Presenter : jpark323@illinois.edu *Corresponding author : skm@illinois.edu*

While methods for dynamic tuning of surface wettability to manipulate water droplets have been widely explored for many applications including digital microfluidics, [1,2] those based on dynamically changeable surface morphology have remained challenging to achieve. In this work, we present a structured shape memory polymer (SMP) surface which shows dynamically tunable surface wettability enabled by surface morphological gradients in order to self-propel water droplets. The structured SMP surface involves a SMP pillar array consisting of nanotextured small and large pillars which can change its morphology between permanent and temporary shapes upon thermomechanical loading. [3,4] Specifically, the structured SMP surface dynamically creates a surface morphological gradient and changes its surface wettability during thermally induced shape recovery of the SMP pillar array. Different wetting characteristics of the structured SMP surface between permanent and temporary shapes are theoretically predicted and experimentally verified. Based on these findings, the structured SMP surface is designed and demonstrated such that the morphological difference between two shapes under a water droplet base overcomes contact angle hysteresis, resulting in self-propelling a water droplet, when combined with the thermal Marangoni effect.

Keywords: shape memory polymer, tunable surface wetting, droplet manipulation, lab-on-a-chip, hierarchical structure

[1] Seo, J., Lee. S. K., Lee, J., Lee, J. S., Kwon, H., Cho, S. W., Ahn, J. H., and Lee, T., 2015. Path-programmable water droplet manipulations on an adhesion controlled superhydrophobic surface. Sci Rep, 5.

[2] Huang, C. J., Fang, W. F., Ke, M. S., Chou, H. Y. E., and Yang, J. T. 2014. A biocompatible open-surface droplet manipulation platform for detection of multi-nucleotide polymorphism. Lab Chip, 14, 2057.

[3] Eisenhaure, J. D., Xie, T., Varghese, S., and Kim, S. 2013. Microstructured shape memory polymer surfaces with reversible dry adhesion. ACS Appl. Mater. Interfaces, 5, 7714-7717.

[4] Chen, C. M., & Yang, S. 2014. Directed water shedding on high-aspect-ratio shape memory polymer micropillar arrays. Advanced materials, 26, 8, 1283-1288.

Acceptance ID: rtmx-O

Synthesis of Basic Microgel with Polyethyleneimine Brushes and It's Template Function in mineralization

Daiki Soma, Ren-Hua Jin

Graduate School of Engineering, Kanagawa University, Rokkakubashi, Yokohama 221-8686, Japan
[Phone/Fax: 81-45-481-5661; E-mail: rhjin@kanagawa-u.ac.jp]

We have reported the preparation of various inorganic hybrid materials by using linear polyethyleneimine (LPEI) obtained from hydrolysis reaction of polyoxazoline. When cooling hot aqueous solution of LPEI to room temperature, the LPEI can grow into nano crystallites via crystallization-driven self-assembly process. These nano crystallites can play as catalytic templates in hydrolytic condensation of inorganic sources to produce various inorganic nano materials. Silica hybrid with versatile morphology can be prepared by changing self-assembly conditions of LPEI.

We also synthesized a variety of LPEI derivatives such as star-shaped PEI [1)] and comb-like PEI [2)] to fabricate silica with various morphologies. We found that molecular design of PEI is important strategy to fabricate inorganic hybrid materials. In this study, polystyrene microgel grafted PEI (μ-PSt-*g*-PEI) was synthesized by three steps of combination of dispersion polymerization of 4-choloromethylstyrene (CMS), cation ring-opening polymerization (CROP) of methyloxazoline and hydrolysis reaction. The inorganic hybrid materials such as silica, titanium dioxide (TiO_2) and nano silver (Ag^0) were fabricated by using the μ-PSt-*g*-PEI as template.

For synthesis of μ-PSt-*g*-PEI, μ-PStCl obtained by dispersion polymerization of CMS as monomer and divinylbenzene (DVB) as cross-linker in the mixture solvents of ethanol and DMAc was used as microgel type initiator for polymerization of methyloxazoline. And then the formed polymethyloxazoline-grafted microgel (μ-PSt-*g*-PMOZ) was transformed to μ-PSt-*g*-PEI via hydrolyzation. μ-PSt-*g*-PEI were in the range of 2.0 ~ 2.3 μm. In the case of silica mineralization, spherical micro silica hybrids were rapidly produced only by mixing TMOS and dispersed μ-PSt-*g*-PEI and their size could be tuned in the various aqueous media and calcination temperature under ambient conditions. Remove of the template of μ-PSt-*g*-PEI by calcination resulted in shrunken silica but remaining microsphere structure with different surface area. TiO_2 also deposited on the microgel of μ-PSt-*g*-PEI and microspheres with anatase or rutile phase were produced after calcination. Ag^0 prepared using μ-PSt-*g*-PEI as a reductive template also offered microball structure. We are sure that the μ-PSt-*g*-PEI would be a universal template directing ceramic micro-ball.

Key words: Polyethyleneimine brushes, polystyrene, microgel, template, inorganic microparticles

[1] JIN, R.-H. & YUAN, J.-J., 2005, Simple Synthesis of Hierarchically Structured Silicas by Poly(ethyleneimine) Aggregates Pre-Organized by Media Modulation, *ChemComm.*, 206, 1399.

[2] YAO, D.-D. & JIN, R.-H., 2015, Synthesis of comb-like poly(ethyleneimine)s and their application in biomimetic silicification, *Polym. Chem.*, 6, 2255.

Acceptance ID: S7S9-P

Development of hemostatic dressing based on calcium carboxymethyl cellulose fiber and chitosan

Song Jun (Doh)[1], Ga Hee (Kim)[1], Jung Nam (Im)[1], Tae Hee (Kim)[1], Gyu Dong (Lee)[1], Chae Hwa (Kim)[1], Yoon Jin (Kim)

[1]*Technical Textile & Materials Group, Korea Institute of Industrial Technology, Ansan, 15588, Republic of Korea.*
wolfpack@kitechc.re.kr

Various composite hemostats composed of carboxymethyl cellulose and chitosan were prepared and their mechanical properties in addition to blood clotting performances were investigated. In the in vitro blood clotting tests, the composite hemostats immediately absorbed blood and exhibited efficacious blood clotting characteristics. When compared with those of commercial nonwoven-type hemostatic agents, composite hemostats showed much faster blood clotting. The formation of polyelectrolyte complexes between carboxymethyl cellulose and chitosan after the absorption of water is believed to have contributed to the structural integrity in the wet state. Considering both the blood clotting performance and mechanical properties, composite hemostats were found to be effective hemostatic agent, and have high commercial availability.

Keywords: Carboxymethyl cellulose, chitosan, hemostat, polyelectrolyte, blood clotting

Acceptance ID: SRZ9-P

Controllable Energy Transfer of Novel DAE-TPE-Based Polymer by Optical Switching of Diarylethene (DAE) Unit and Aggregation Induced Emission of Tetraphenylethene (TPE) Unit

*Ravinder Singh,[a] Hsin-Yen Wu,[a] Atul Kumar Dwivedi,[a] Ashutosh Singh,[a] Chien-Min Lin,[a] Reguram Arumugaperumal,[a] Putikam Raghunath,[b] Ming-Chang Lin,[b] Jacek Gliniak,[c] Tung-Kung Wu,[c] Hong-Cheu Lin[a]**

[a] *Department of Materials Science and Engineering, National Chiao Tung University, Hsinchu, Taiwan. (*Corresponding author: E-mail: linhc@mail.nctu.edu.tw)*

[b] *Center for Interdisciplinary Molecular Science, Department of Applied Chemistry, National Chiao Tung University, Hsinchu, Taiwan.*

[c] *Department of Biological Science and Technology, National Chiao Tung University, Hsinchu, Taiwan.*

A novel polymer **P-PHT** consisting of an optical switchable diarylethene (DAE) unit and an aggregation induced emission (AIE) tetraphenylethene **(**TPE) unit connected by a triazole linker was designed and synthesized. Upon the irradiation of UV light (λ=346 nm), the DAE unit of **P-PHT** was cyclized with simultaneously decreasing AIE behavior in the TPE unit (with 90% water) due to the energy transfer from the TPE unit to the DAE unit. As a proof of this concept, the protonable nitrogen moiety either with the TPE unit or the DAE unit favored the AIE quenching of TPE more strongly, which was attributed to the cyclization of the DAE unit under acidic conditions. Therefore, the DAE unit in **P-PHT** was cyclized more significantly in water in comparison with traditionally reported organic media. Interestingly, the cyclization events of the DAE unit in **P-PHT** at 90% water content generated a rare example of monomeric emission of the TPE unit in such a new combination of both DAE and TPE chromophores in the polymeric system of **P-PHT**. Furthermore, the monomeric emission became more prominent (three times higher) under acidic conditions. The generation of the monomeric emission in the TPE unit through the cyclization of the DAE unit via energy transfer events was further verified by theoretical calculations. Accordingly, the theoretical results fully supported the obtained experimental results of both energy transfer and monomeric emission phenomena. Even due to energy transfer events from TPE to DAE, more AIE quenching of the TPE unit in polymer **P-PHT** could be further induced via the irradiation of **P-PHT** (open form) on solid films. Consequently, the energy transfer between the DAE unit and the TPE unit in polymer **P-PHT** could be manipulated not only by the close and open forms of the optical switchable DAE unit (via the irradiation of UV light) but also by the aggregation induced emission under various water contents and acidic conditions.

Acceptance ID: SW46-O

Carbon nanofibers based wearable patch for bio potential monitoring

H.C. JUNG[1], S. H. LEE[1] and D. H. KWON[1]
[1] Osong medical innovation foundation, medical device development center, Cheongju-Si, South Korea
hacher99@kbiohealth.kr

We fabricated a wearable patch including novel patch type flexible dry electrode based on carbon nanofibers (CNFs) and silicone-based elastomer (MED 6215) for long-term bio potential monitoring. There are many methods to make flexible conductive polymer by mixing metal or carbon based nanoparticles. In this study, CNFs are selected for conductive nanoparticles because carbon nanotubes (CNTs) are difficult to disperse uniformly in elastomer compare with CNFs and silver nanowires are relatively high cost and easily oxidized in the air. Wearable patch is composed of 2 parts that dry electrode parts for recording bio signal and sticky patch parts for mounting on skin. Dry electrode parts were made by ultrasonic wave and baking in prepared mold. To optimize electrical performance and diffusion degree of uniformity, we developed unique mixing and baking process. Secondly, sticky patch parts were made by patterning and detaching from smooth surface substrate after spin-coating soft skin adhesive. In this process, attachable and detachable strength of sticky patch are measured and optimized them for using a monitoring system. Manufactured two parts are aligned and make a hole in center point of them. To connect easily with conventional signal processing system without any adapters, we insert conventional snap into the hole. Assembled patch is flexible, stretchable, easily skin mountable and connectable directly with system. To evaluate performance of electrical, mechanical and adhesive characteristics, wearable patch were tested by changing concentrations of CNFs and thickness of dry electrode. The performances of electrodes were evaluated by using 9 types of electrodes with different concentrations of CNF and thickness. Also ECG (Electrocardiography) signals, motion artifact and sweat effect were tested by using 9 types of electrodes to evaluate performance of bio potential electrodes. In this results, the CNF concentration and thickness of dry electrodes were important variables to obtain high-quality ECG signals without incidental distractions. Cytotoxicity test are conducted to prove biocompatibility and long-term wearing test showed no skin reactions such as itching or erythema. To sum up, we could fully utilize fabricated wearable for the long-term bio potential monitoring easily.

Keywords: Carbon nanofibers, wearable patch, ECG, Bio potential monitoring

Acceptance ID: SYV5-P

Oxygen defects and optical properties of tungsten bronze nanoparticles

Machida,[1] *Okada,*[2] *Adachi*[1]

[1] *Sumitomo Metal Mining Co., Ltd., Ichikawa Research Center, Ichikawa, Chiba, Japan*
[2] *Ohkuchi Electronics Co., Ltd., Ink Materials Department, Isa, Kagoshima, Japan*
keisuke_machida@ni.smm.co.jp/kenji_adachi@ni.smm.co.jp

Tungsten bronze nanoparticles (TB NPs) are known to absorb near-infrared light at high luminous transmittance[1]. Optical absorptions in TB NPs have been reported both in terms of localized surface plasmon resonance (LSPR) and polaron mechanism[2]. In the present work the mechanism of optical properties are investigated for NPs of hexagonal TB, $Cs_{0.3}WO_{3-y}$, with different degree of oxygen deficiency.

Precursors composed of Cs_2CO_3 and H_2WO_4 were heated in reducing atmosphere at 550 °C followed by annealing in neutral atmosphere at 800 °C to obtain $Cs_{0.3}WO_{3-y}$ powders of different amount of oxygen content. Chemical analyses for Cs, W and O were independently performed, informing the reduction of O with increasing duration at 550 °C. XRD Rietveld analysis indicated systematic change in lattice parameters with reduction time. Molar absorption coefficients measured for the dispersions prepared from these samples exhibit LSPR peaks at around 0.9 eV and polaron peaks at around 1.4 eV, both increasing with increasing degree of reduction. Oxygen vacancies are thus considered to provide both conduction and localized electrons. We have deconvoluted the absorption peaks and analyzed the characteristic energies for plasmons and polarons corresponding to the respective excitation processes.

Keywords: near-infrared, tungsten bronze, nanoparticle.

[1] TAKEDA, H, ADACHI, K. 2007. Near Infrared Absorption of Tungsten Oxide Nanoparticle Dispersions. *J. Am. Ceram. Soc.*, *90*, 4059-4061.
[2] MACHIDA, K, ADACHI, K. 2016. Ensemble Inhomogeneity of Dielectric Functions in Cs-Doped Tungsten Oxide Nanoparticles. *J. Phys. Chem. C*, 120, 16919-16930.

Acceptance ID: THLS-O

Fabrication and Evaluation of Biodegradable Nanofiber as a Surgical Sealant for Hepatic Trauma by Solution Blow Spinning

Sang Eun (Hong)[1], *Ok Hee (Kim)*[2], *Ha Eun (Hong)*[2], *Say June (Kim)*[2], *Kuk Ro (Yoon)*[1]

[1]*Chemistry Based Bio Hybrid Sensor Research Team(BK21 plus), Organic Nano Material Lab, Department of Chemistry, Hannam University, 1646 Yuseong-daero, Yuseong-gu, Daejeon, 305-811, Korea.*
[2]*Department of Surgery, Daejeon St. Mary's Hospital, The Catholic University of Korea.*
sehong1892@gmail.com, kryoon@hnu.kr

Nanofiber and scaffolds have been widely demonstrated for biomedical applications. Solution blow spinning is a technique for depositing polymer fibers with promising potential use as a surgical sealant. This work reports the use of solution blow spinning to fabricate potential nanofiber surgical sealant on any surface substrate, utilizing only a commercial airbrush and compressed CO_2. Solution and deposition conditions of biodegradable polymer nanofibers were optimized and mechanical properties characterized with dynamic mechanical analysis. Nanofibers degradation condition was monitored for morphology and molecular weight different in vitro. Biocompatibility of nanofibers onto cell lines was indicated in vitro and blood interaction was evaluated with FE-SEM(Field-emission Scanning Electron Microscopy). For surgical sealant feasibility testing in a mouse model study was then used to demonstrate some of the possible surgical applications including use as a surgical hemostatic, a surgical sealant, and for tissue reconstruction. The physicochemical properties of the surgical sealant nanofiber was confirmed by EDS(Energy Dispersive X-ray Spectroscopy), FT-IR(Fourier Transform Infrared Spectroscopy), TGA(Thermogravimetric Analysis), Contact angle, Tensile strength.

Keywords: Biodegradable nanofiber, solution blow spinning, surgical sealant

[1] Adam M. Behrens, Brendan J. Casey, Michael J. Sikorski, Kyle L. Wu, Wojtek Tutak, Anthony D. Sandler, Peter Kofinas. 2014. In Situ Deposition of PLGA Nanofibers via Solution Blow Spinning. *ACS Macro Lett*, 3, 249-254.

Acceptance ID: U234-P

Structure – Property Relation of Natural Fiber Coir under Mercerization and Thermal Treatment

D. N. Mahato

Post Graduate Department of Physics,
Kolhan University, Chaibasa,
Jharkhand, India , PIN-833202,
e-mail – dn.mahato08@yahoo.com

Coir is an abundantly available natural fiber with immense potential for making a composite material for domestic and industrial use. The alkali treatment of coir fiber is known as mercerization,named after the scientist Mercer. Mercerization drastically changes the physical properties like breaking strength, young's modulus, thermal stability, activation energy and electrical properties of the fiber. The changes in physical properties are in consonance to the change in the structure of the fiber. The major component of the fiber is cellulose, which is crystalline in nature. The mercerization changes the crystallinity, crystallite size and molecular structure. A systematic study has been made of the change in inter-atomic distance, coupling constant and co-ordination number of the fiber by RDF (Radial Distribution Function) analysis of the XRD pattern of different degree of mercerization. Crystallite size and crystallinity of the fiber of different degree of mercerization has been studied by XRD pattern.

IR studies have been carried out to find the change in molecular structure at different concentration of alkali. DTA and DSC studies reveal the phase transitions and amount of heat energy evolved or absorbed during the processes and finally the activation energy and thermal stability of the fiber. The change in properties of the fiber is reflected with the change of structure due to mercerization and thermal treatment.

Acceptance ID: UGGR-O

Stimuli-Responsive Dendronized Polymers for Next Generation Biomaterials

Wen Li, Kun Liu, Afang Zhang

Shanghai University, Shangda Street No. 99, Shanghai 200444, China
E-mail: azhang@i.shu.edu.cn

Dendronized polymers are formed through densely attaching dendrons along a linear polymer main chain, which adopt cylindrical wormlike morphology with tunable thickness.[1] Inspired from the smart properties of biomacromolecules in nature, an intriguing class of stimuli-responsive dendronized polymers were constructed through combination of dendritic oligoethylene glycols (OEG) with various kinds of polymer backbones. Due to the densely covered OEG pendants, these macromolecules show unprecedented thermoresponsiveness and excellent biocompatibility.[2] This presentation will discuss our findings in developing versatile thermoresponsive warm-like dendronized polymethacrylates and polypeptides by decorating with dendritic OEG pendants through covalent linkages, dynamic covalent linkages or supramolecular interactions (Figure 1).[3] Depending mainly on the molecular topology, amphiphilic structure in these dendronized polymers plays different roles on mediating their stimuli-responsive properties. Based on the thickness effects, dendronized polymers undergo heterogeneous dehydration and collapse on individual molecular level. Therefore, guest molecules can be encapsulated and released through the phase transition, heating rate and thickness of the polymers, resulting in interestingly the formation of molecular containers. This encapsulation property afford these thick polymers tunable shielding ability to protonation and metal coordination in aqueous solutions. In a word, combination of unique thermoresponsive behavior, reversible encapsulation and switchable shielding to guests, protonation as well as metal coordination from these OEGylated dendronized polymers may lead to their promising applications in biomaterials, including drug delivery and targeting, enzyme activity control and transportation.

Keywords: smart polymers, dendritic polymers, controlled release, molecular shielding, thermoresponsive hydrogels

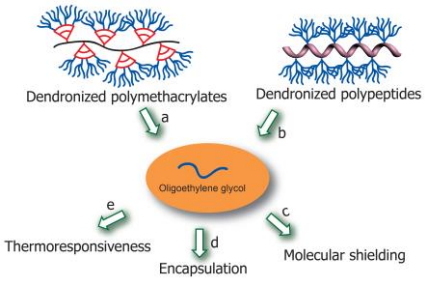

Fig. 1 Cartoon presentation of OEGylated stimuli-responsive macromolecules: a) thermoresponsive dendronized polymethacrylates, b) thermoresponsive dendronized polypeptides, c) molecular shielding, d) encapsulation, e) thermoresponsiveness.

[1] (a) Schlüter, A. D. & Rabe, J. P. 2000. *Angew. Chem. Int. Ed. 39*, 864–883; (b) Zhang, A. 2005. *Prog. Chem. 17*, 157–171. (c) Yan, J., Li, W. & Zhang, A. 2014. *Chem. Commun. 50*, 12221–12233.

[2] (a) Li, W., Zhang, A. & Schlüter, A. D. 2008. *Chem. Commun.* 5523–5525; (b) Junk, M. J. N., Li, W., Schlüter, A. D., Wegner, G., Spiess, H. W., Zhang, A. & Hinderberger, D. 2010. *Angew. Chem. Int. Ed. 49*, 5683–5687; (c) Junk, M. J. N., Li, W., Schlüter, A. D., Wegner, G., Spiess, H. W., Zhang, A. & Hinderberger, D. 2011. *J. Am. Chem. Soc. 133*, 10832–10838.

[3] (a) Yan, J., Liu, K., Li, W., Shi H. & Zhang, A. 2016. *Macromolecules 49*, 510–517; (b) Zhang, X., Yan, J., Li, W. & Zhang, A. 2016. *RSC Adv.* ***6***, 44216–44223.

Acceptance ID: y5c6-O

Inkjet Printing of Polyethylene Glycol as a Sacrificial Material for Flexible Microsystems

Ouyang[1], Mahajan[2], Alfadhel[1], Cormier[2], Borkholder[1]

[1]Microsystems Engineering, Rochester Institute of Technology, Rochester, NY.
[2] Industrial and Systems Engineering, Rochester Institute of Technology, Rochester, NY.
Presenting author: jxo711@rit.edu.
Corresponding author: ahaeen@rit.edu.

Microfluidics-based electronics have shown great potential in numerous applications such as energy harvesters, bio-inspired devices, and wearable healthcare sensors [1,2]. Microfluidic electronics have been realized using conventional microfluidic fabrication techniques. However, fabrication challenges and material incompatibilities pose barriers to achieving the full potential of this emerging field and limit the device capabilities and scalability [3].

This paper demonstrates a novel and simple processing technique for the realization of scalable and flexible microfluidic microsystems by inkjet-printing polyethylene-glycol (PEG) as a sacrificial template. Planar and out-of-plane structures can be directly printed on a wide range of substrate materials, including nonplanar surfaces, and embedded in a variety of soft (e.g. elastomeric) or rigid (e.g. thermoset) polymers. PEG can be removed through heating above its phase-change temperature after the formation of the structural layer. The developed technique allows easy modulation of the shape and dimensions of the pattern with the ability to generate complex 3D architectures without using lithography, and at low cost and short manufacturing time. The method produces robust structures that can be realized on electrodes and transducers directly without requiring any bonding or assembling steps which often limit the materials selection in conventional microfluidic fabrication [4.5].

The inkjet printing of PEG was optimized to print features with 50 μm width resolution, and 6 μm thickness per printed layer, with the ability to print multilayers and align features. Multilayer Polydimethylsiloxane (PDMS) microfluidic channels were created using this technique on several substrates such as glass, Polyethylene terephthalate (PET), PDMS and non-planar surfaces (including the tip of a cardiac catheter) to demonstrate the capability of the concept to directly realize microfluidic electronics and lab-on-a-chip devices on any surface. Moreover, the biocompatibility of PEG makes it attractive for medical and biological applications. By utilizing liquid metals (i.e. E-GaIn) as the filling material of the channels, flexible and stretchable devices have been realized such as pressure sensors with a sensitivity of 0.24 kPa^{-1}, and strain gauges that exhibit changes up to 10 $\%\Delta R/R_0$.

Keywords: Microfluidic electronics, flexible electronics, inkjet-printing, PEG, fabrication

[1] YEO, J. C., KENRY & LIM, C. T. 2016. Emergence of microfluidic wearable technologies, *Lab Chip*. 16, 4082-4090.

[2] CHENG, S. & WU, Z. 2012. Microfluidic electronics, *Lab Chip*, 12, 2782–2791.

[3] GO, J. S. & SHOJI, S. 2004. A disposable, dead volume-free and leak-free in-plane PDMS microvalve, *Sensors and Actuators A: Physical.* 114, 438-444.

[4] CHANG, W. H., WANG, C. H., LIN, C. L., WU, J. J., LEE, M.S. & LEE, G.B. 2015. Rapid detection and typing of live bacteria from human joint fluid samples by utilizing an integrated microfluidic system. *Biosensors and Bioelectronics*, 66, 148-154.

[5] DUFFY, D. C., McDonald, J. C., Schueller, O. J.A. & Whitesides, G. M. 1998. Rapid prototyping of microfluidic systems in poly (dimethylsiloxane). *Analytical chemistry*, 70, 4974-4984.

Acceptance ID: YQSY-O

Cenospheres Separation from High CaO Fly Ash: Surface Reaction and Materials Composition

Sorachon Yoriya, Angkana Chumphu, and Phattarathicha Tepsri*

National Metal and Materials Technology Center, National Science and Technology Development Agency, 114 Thailand Science Park, Pahonyothin Road, Khlong 1, Khlong Luang, PathumThani 12120, Thailand
**E-mail: sorachy@mtec.or.th*

Cenospheres are the value-added components within coal combustion fly ash produced by thermal power plant. With an aim to respond to the industrial expansion of cenospheres utilization, this work presents a study on recovery process of porous, hollow-sphere structured cenospheres from Class C high CaO fly ash, focusing on separation mechanism and efficiency, and (calcium, aluminium, silicon) compound composition relating to their surface reaction. Approaches to improving the cenospheres separation efficiency have been investigated, combining with a characterization of physical and chemical properties, spherical morphologies, and elemental composition of those collected cenospheres. This work has made a systematic comparison of cenospheres separation efficiency among those obtained recovery percentages. Wall thickness-size-density relationship of the porous cenospheres has been established as a function of the key wet separation parameters, demonstrating an insight regime into the intrinsically physical nature of cenospheres in coal fly ash. The results have revealed that the optimum ratio of fly ash to water is a considerable factor determining both quality and quantity of cenospheres, herein found it a direct result from the wet separation mechanism as basically depending upon the material-medium density difference. The recovery percent of cenospheres has appeared to relate, to some extent, to their chemical composition. The chemical reactions occurring on the cenospheres surface during the wet separation has been presumed to significantly contribute their effect on the recovery percent. Furthermore, mechanically compressive strength of the recovered fly ash from the wet separation process has been examined.

Acceptance ID: YSFZ-O

SYMPOSIUM 4: Advances in Energy Storage & Conversion Devices

Synthesis and Characterization of Pendant Disulfonated Block Copolymers Using Suzuki-Miyaura Coupling Reaction

Kyu Ha Lee[1], *Dong Jin Yoo*[1,2*]

[1]*Graduate School, Department of Energy Storage/Conversion Engineering, Hydrogen and Fuel Cell Research Center, Chonbuk National University, Jeollabuk-do 561-756, Republic of Korea*
[2]*Department of Life sciences, Chonbuk National University, Jeollabuk-do 561-756, Republic of Korea*
djyoo@jbnu.ac.kr

We synthesized a block copolymer containing pendant di-sulfonated monomer for fabrication of membrane for polymer electrolyte membrane fuel cells (PEMFCs). The pendent di-sulfonated monomers were synthesized through three step reaction. The F-terminated oligomers were synthesized using pendant di-sulfonated monomer and 4 4'-(hexafluoroisopropylidene) diphenol through nucleophilic aromatic substitution reaction and OH-terminated oligomers were synthesized using 4,4'-difluorobenzophenone and bisphenol A. Flexible membranes were then obtained by solution casting of multi-block copolymers. The morphologies, chemical structure, molecular weight, and intermolecular bond stretching of the copolymer membranes were characterized using AFM, ^{1}H- NMR, GPC, and FT-IR instrumentations. TGA and DSC based thermal properties were investigated and the all the prepared membranes exhibit good thermal stabilities with the first degradation of 150℃. Membranes specimens were extensively studied for ion exchange capacity (IEC), water uptake, dimensional stability, oxidative stability, and temperature dependent proton conductivity; all the membranes exhibit significant improvements.

Keywords: presulfonation, pendant, polymer electrolyte membrnae fuel cell, proton conductivity

[1] CHENYI, W, DONGWON, S, SOYOUNG, L, NA RAE, K, YOUNGMOO, L, MICHAEL, D.G., 2012, Poly(arylene ether sulfone) proton exchange membranes with flexible acid side chains, Journal of membrane science, 421-422, 375

Synthesis and characterization of fluorinated and sulfonated Poly(arylene biphenylsulfone) Block Coploymers for Polymer electrolyte membrane

Ji Young Chu[1], *Dong Jin Yoo*[1,2,3 *]

[1]*Graduate School, Department of Energy Storage/Conversion Engineering, Hydrogen and Fuel Cell Research Center, Chonbuk National University, Jeollabuk-do 561-756, Republic of Korea*
[2]*Department of Life sciences, Chonbuk National University, Jeollabuk-do 561-756, Republic of Korea*
djyoo@jbnu.ac.kr

The proton exchange membrane is one of the key materials of a polymer electrolyte membrane fuel cell (PEMFC). Among the different types of membranes, Nafion has been primarily used as a standard PEMFC membrane. However, the high cost, low glass transition temperature, and environmental incompatibility of the membranes have impeded the widespread commercialization of PEMFCs. In order to overcome these demerits, a number of alternative membranes have been developed for use in PEMs. Recently, to improve physical and electrochemical properties the precise control of morphology has been suggested as a strategy. Mutiblock copolymer containing hydrophilic and hydrophobic segments were developed to mimic the nano-separated morphology of Nafion. These membranes produced higher conductivity than their randomly sulfonated analogs due to the formation of well-connected water domains. Related to these reports, we synthesized newly designed and highly sulfonated block copolymers. Here, we report the sulfonated poly(arylene biphenyl ether sulfone) block copolymers and their major characteristics. We prepared directly a new series of sulfonated perfluorinated poly(biphenylsulfone) block copolymers as proton exchange membrane materials from hydrophilic and hydrophobic polymer via a nucleophilic aromatic substitution reaction. First, A sulfonated 4,4'-bis[(4-chlorophenyl)sulfonyl]-1,1'-biphenyl compound as a monomer was synthesized by using a fuming sulfuric acid and hydrophilic polymers were synthesized through polymerization of the monomer and 4,4'-(hexa-fluoroisopropylidene) diphenol. Second, hydrophobic polymers were synthesized from decafluorobiphenyl and 4,4'-(hexafluoroisopropylidene) diphenol. Finally we synthesized the block copolymers from hydrophilic polymers and hydrophobic polymers. The copolymers were characterized by proton NMR, FT-IR, GPC, thermogravimetric analysis (TGA), and differential scanning calorimetry (DSC) thermograms. Proton NMR, FT-IR and GPC were used for DS determination and structural analysis. The membranes showed excellent thermal and oxidative stability; e.g., TGA and DSC demonstrated that all sulfonated block copolymers exhibited good thermal stability with an initial weight loss at temperatures above 200℃. The performance of the membranes was measured in terms of water uptake, ion exchange capacity, proton conductivity and single cell test. The conductivity is greatly influenced by ion exchange capacity, temperature, and water activity. The proton conductivity of the block copolymer-21 was 129 mS cm^{-1} at 90℃ and 100% relative humidity. The new copolymers, which contain ion conductivity sites on the deactivated positions of the arylene sulfone ether backbone rings, are candidates as new PEMFC.

Keywords: proton exchange membrane, block copolymer, ion conductivity, morphology, AFM, ion channel

[1] JIYOUNG, C., AERHAN, K., KEESUK, N., HONGKI, L., DONGJIN, Y., 2013, Synthesis and characterization of partially fluorinated sulfonated poly(arylene biphenylsulfone ketone) block copolymers containing 6F-BPA and perfluorobiphenylene units, International journal of hydrogen energy, 38, 6268-6274

Flexible and Weaveable Wire-shaped Capacitor with High Energy Density

Bin Wang[1*] *Jianli Cheng1*

Institute of Chemical Materials, China Academy of Engineering Physics, Mianyang, Sichuan, China 621900
E-mail：binwang@caep.cn

Fiber-shaped supercapacitors (FSCs) that have the merits of tiny volume, high flexibility and wearability are attractive as power sources for miniaturized electronic devices, such as micro-robots, wearable electronic textiles and implantable medical devices. However, compared with batteries or traditional capacitors, FSCs show much lower-energy density and suffer from extra challenges in mechanical performance. According to the equation ($E = 0.5CU^2$), energy is proportional to capacitance. So it is crucial to explore high capacitance fibers with high operating voltage and good mechanical properties for FSCs.

In our study, we try to increase the capacitance and energy density of Electric-double layer capacitors (EDLCs) by increasing the fiber interfacial area. We adopt a simple pipe mold method to fabricate hollow RGO/PEDOT-PSS composite fibers with excellent flexibility and conductivity. The symmetric solid-state FSCs composed of two HCFs reveal a high specific areal capacitance of 304.5 mF cm^{-2} at 0.08 mA cm^{-2}, corresponding to an ultra-high energy density of 6.8 μWh cm^{-2} at a power density of 16.6 μW cm^{-2}.

Furthermore, PEDOT-PSS fibers with operating voltage of 1.8V will displayed. By increasing the operating voltage up to 1.8V, the energy density of the FSCs is increasing to 7.3μWh cm^{-2} at a power density of 20 μW cm^{-2}.

In this presentation, we will discuss the fiber formation mechanism, charge storage mechanism and we will display the flexible wire-shaped energy device constructed by the one-dimensional fiber micro-supercapacitors.

Keywords: graphene/polymer fiber; wire-shaped capacitor; wearable; high energy density

Acknowledgements

This work is supported by This work was supported by the Applied Fundamental Foundation of Sichuan Province (2014JY0202), the R&D Foundation of China Academy of Engineering Physics(2014B0302036), the Science Foundation for Distinguished Young Scholars of Sichuan Province(2016JQ0025) and National Natural Science Foundation of China (No. 21401177 and 21501160), the “1000plan” from the Chinese Government, and the Collaborative Innovation Foundation of SiChuan University(XTCS2014009).

Platinum nano-flowers with controlled facet planted in titanium dioxide nanotube arrays bed and their high electro-catalytic activity

Hongyi Li, Fei Wang, Man Liu, Junshu Wu, GuannaZu, Jinshu Wang**

Key Laboratory of Advanced Functional Materials, School of Materials and Engineering, Beijing University of Technology, Beijing 100124, P.R. China

Reprint Author: lhy06@bjut.edu.cn; wangjsh@bjut.edu.cn

Tel & Fax: +8610-67391101

To better platinum's (Pt's) electro-catalytic activity for oxidizing methanol, nano-flowers structured Pt catalysts with controlled facet had been planted onto titanium dioxide nanotube array (TNA) bed via a pulse electrodepositing method in an acid electrolyte containing chloroplatinic acid (H_2PtCl_6). The facet of Pt nano-flowers can be tuned as (111) or (100) by adding sulfuric acid (H_2SO_4) or hydrochloric acid (HCl) respectively into the precursor. It has been discovered that the nano-flower structured Pt catalysts with (111) facet generates a current density peak of 243.16 $mA \cdot mg^{-1}$(~2 times that of Pt catalysts with (200) facets) for catalytic oxidizing methanol in electrolyte containing 1 M methanol and 0.5 M H_2SO_4. In addition, the concentration of sulfuric acid in electrolyte has an effect on electrode's morphology, its electro-catalytic capability and stability. The mechanism of sulfuric acid anion for bettering Pt's electro-catalytic activity was comparatively studied by adding HCl into precursor instead of H_2SO_4.

Keywords: titanium dioxide nanotube arrays, platinum nano-flowers, pulse electro-deposition, direct methanol fuel cells

Acceptance ID: 2VE7-O

Conductivity measurement of PEMFC catalytic layers based on carbon xerogels and carbon black

F.Deschamps[1], N.job[1]

[1] University of Liège, Department of Chemical Engineering – Nanomaterials, Catalysis, Electrochemistry (NCE), Building B6a, B-4000 Liège, Belgium,
fabien.deschamps@ulg.ac.be

Proton exchange membrane fuel cells (PEMFC) are promising candidates for applications in mobile devices and transportations. The fuel cell market is growing [1]; however, for successful large-scale commercialization, significant cost reduction and durability improvement are needed. An optimization of the electrode structure is required to fulfill these goals [2]. Catalytic layers are generally prepared by mixing a protonic conductor ionomer, such as Nafion®, with a platinum catalyst supported on carbon black [3]. Nanostructured carbons allow for a better control of the textural properties, such as pore size and pore volume. More precisely, using carbon xerogels as support is a good way to improve the mass transport in catalytic layers [4,5].

In this communication, we present the elaboration and the characterization of catalytic layers based on carbon xerogels. For that purpose, carbon xerogels were synthesized by polymerization of resorcinol and formaldehyde in aqueous solution to form an organic gel. The latter was dried and pyrolyzed under inert atmosphere to obtain a porous carbon. By modifying the pH of the initial solution, several carbon xerogels with different pore sizes were synthesized. The grinding of these porous carbons in a planetary mill is required to get particle sizes (~10 µm) compatible with the thickness of the catalytic layers. Catalytic layers based on carbon xerogel and carbon black XC-72R were made on Kapton substrate by robotic spray. The inks for the spray were composed of carbon, Nafion water and isopropanol. These catalytic layers were characterized by profilometry on their whole surface to evaluate their homogeneity and their thickness. Then, measurements of electrical and ionic resistances were performed by four point measurements to estimate their influences in fuel cell performances.

Keywords: Nanostructured carbon, Catalytic layer, Fuel Cells, ionic conductivity, electrical conductivity

[1] HORWITZ J., FORD S. 2010. Developments in PEM Fuel Cells, Pira International.

[2] GASTEIGER H.A., KOCHA S.S., SOMPALLI B., et al. 2005. Activity benchmarks and requirements for Pt, Pt-alloy, and non-Pt oxygen reduction catalysts for PEMFCs. *Appl. Catal,* 56,9-35.

[3] SHARMA S., POLLET B.G. 2012. Support materials for PEMFC and DMFC electrocatalysts—A review. *J. Power Sources,* 208,96-119.

[4] JOB N., MARIE J., LAMBERT S. et al. 2008. Carbon xerogels as catalyst supports for PEM fuel cell cathode. *Energ. Convers. Manage,* 49,2461-2470.

[5] MARIE J., CHENITZ R., CHATENET M. et al. 2009. Highly porous PEM fuel cell cathodes based on low density carbon aerogels as Pt-support: Experimental study of the mass-transport losses. *J. Power Sources,* 190, 423-434.

Acceptance ID: 3858-O

Oxygen Evolution and Reduction Activity of Pyrochlore-based Oxide Catalysts

*Sung Ryul Choi, Nam-In Kim, Sung Won Lee, and Jun-Young Park**

HMC, Department of Nanotechnology and Advanced Materials Engineering, Sejong University, 209 Neungdong-ro, Gwangjin-gu, Seoul, 05006, Republic of Korea

In recent years, because of the issues of environmental pollutions and global climate changes, unitized regenerative fuel cells (URFCs) have been received many attentions for as renewable electrochemical devices for production of electricity and hydrogen gas [1]. In particular, the URFCs are an eco-friendly method to produce hydrogen and electricity. However, there are some technical issues for making commercialization of URFCs. Slow kinetics of oxygen evolution and reduction reactions (OERs and ORRs) for the oxygen electrode catalysts cause low cell performances with high polarization resistances [2]. Furthermore, the noble metal (iridium, ruthenium, platinum, and alloys)-based carbon-supported catalysts have still used for OER and ORR catalysts. But high cost and limited resource of noble metal catalysts prevent making commercialization of the bi-functional electrochemical cells [3]. Hence, pyrochlore-based oxide catalysts are considered as the alternative bi-functional catalytic materials, due to the unique crystalline structure of plentiful oxygen vacancies and electron pathways [4]. The pyrochlore-based catalysts are synthesized by the solid-state reaction and hydrothermal method with various A-site materials (eg. Y, Nd, and La) and B-site materials (Zr, Ti, and Sn) in $A_2B_2O_7$ structure [5, 6]. In the solid-state reaction, a stoichiometric mixture of A_2O_3 and B_2O_3 are mixed with ethanol for ball-milling during overnight. Then, ball-milled mixtures are dried in electric oven at 80 ℃ for 10 h. As prepared powders are heated at 1,100 ℃ for 10 h in air atmosphere. In the hydrothermal reaction, nitrate and chloride precursors are used with NaOH for alkaline condition. All of precursors are dissolved in deionized water, then the NaOH solution is added into the prepared solution. After forming of precipitations, final solution is transferred into hydrothermal reactor, sealed, and heated at 200 ℃ for 4h. The physicochemical properties of the final products are obtained by various analysis tools such as X-ray diffraction, scanning electron microscopy, transmission electron microscopy, and BET. For the electrochemical investigations, a rotating disk electrode (RDE) system is used with a 0.1 M KOH solution, an Hg/HgO and a Pt wire for electrolyte, reference electrode and counter electrode, respectively. The pre-conditioning of catalysts is carried out by cyclic voltammetry (CV) at a scan rate of 100 mV/s for 50 cycles with nitrogen purged electrolyte. The OER (1.2-1.7 V) and ORR (0.05-1.2 V) activities are analyzed by linear sweep voltammetry (LSV) at a scan rate of 5 mV/s for the performance and long-term stability [7, 8].

1. G. Chen, S.R. Bare, and T.E. Mallouk, *J. Electrochem. Soc.*, **149**, A1092 (2002).
2. D. Chen, C. Chen, Z.M. Baiyee, Z. Shao, and F. Ciucci, *Chem. Rev.*, **115**, 9896 (2015).
3. Y. Lee, J. Suntivich, K.J. May, E.E. Perry, and Y. Shao-Horn, *J. Phys. Chem. Lett.*, **3**, 399 (2012).
4. S. H. Oh, R. Black, E. Pomerantseva, J.-H. Lee, and L. F. Nazar, *Nat. Chem.*, **4**, 1004 (2012).
5. P.A. Fuierer and R.E. Newnham, J. Am. Ceram. Soc., **74**, 2876 (1991).
6. R. Trujillano, J.A. Martín, and V. Rives, Ceram. Int., **42**, 15950 (2016).
7. N.-I. Kim, Y.J. Sa, S.-H. Cho, I. So, K. Kwon, S.H. Joo, and J.-Y. Park, *J. Electrochem. Soc.*, **163**, F3020 (2016).

***** Corresponding authors: jyoung@sejong.ac.kr (J.-Y. Park)

Acceptance ID: 3GKV-P

Flexible B-doped graphene aerogel as a current collector and interlayer for high-performance lithium sulfur batteries

LuoYuanzheng[1], Xiaoqi[2] and LiBuyin[*]

Huazhong University of Science and Technology, Wuhan, Hubei, China

In this work, we synthesized a 3D porous boron-doped graphene aerogel(3D-BG) through a modified two-step hydrothermal reduction method, which has been simultaneously used as the matrix to load sulfur and the interlayer between cathode and separator. The sulfur contained 3D-BG was mechanically pressed to circular disc and directly used as a current collector-free cathode, which has high sulfur content, good flexibility and electrical conductivity. Since no extra conductive additive and binder are needed, the method is also more facile than general process. The interlayer was prepared through the same method, which was used as lithium polysulfides absorber and to suppress the shuttle effect. With the novel cathode and battery structure, the lithium-sulfur battery could deliver a high initial specific capacity more than 1100mAh/g. More importantly, compared with general cathode and non-interlayer battery, the dissolution of lithium polysulfides and shuttle effect are suppressed effectively by the porous structure and various functional groups of 3D-BG matrix and interlayer, greatly improving the utilization of active material and cycling stability.

Acceptance ID: 3UAM-P

Nanomaterials as high-capacity lithium-ion batteries anodes

*Hsing-Yu Tuan**

Department of Chemical Engineering, National Tsing Hua University, Taiwan, 30013, ROC
** E-mail: hytuan@che.nthu.edu.tw*

In this talk, we demonstrate that both dedecanethiol-passivated Ge nanowires and graphene-germanium composites can serve as excellent LIB anodes. Germanium (Ge) is considered as a high-capacity anode materials for lithium-ion batteries (LIBs) due to its high theoretical capacity of 1384 mAh/g, which is four times larger than graphite anode (372 mAh/g). However, the dramatic volume changes (~300 %) of Ge during the insertion/extraction usually cause crack and pulverization of electrode, and loss of electrode contact, making the capacity fade rapidly after several cycles. Ge nanostructures can effectively accommodate the volume changes, tolerate relaxed mechanical strain, and provide channels for efficient electron transport, but the anode performance still decayed rapidly within a few tens of cycles. Dodencanethiol-passivated Ge nanowires exhibit an excellent electrochemical performance with a reversible specific capacity of 1130 mAh/g. The functionalized Ge nanowires show high-rate capability having charge and discharge capacities of ~555 mAh/g at rates as high as 11 C. An aluminum pouch type lithium cell using a LiFePO4 cathode was assembled to provide larger current (~30 mA) for uses on light-emitting-diodes (LEDs) and audio devices. This study shows that organic monolayer-coated Ge nanowires represent promising Ge-C anodes with very low carbon content (~2-3 wt %) for high capacity, high-rate lithium-ion batteries and are readily compatible with commercial slurry-coating process for cell fabrication. Carbon-coated Ge nanoparticles/RGO (Ge/RGO/C) sandwich structures were formed via a carbonization process. The high nanoparticle-loading nanocomposites exhibited superior Li-ion battery anode performance when examined with a series of comprehensive tests, such as receiving a practical capacity of Ge (1332 mAh/g) close (96.2%) to its theoretical value (1384 mAh/g) when cycled at a 0.2 C rate and having a high-rate capability over hundreds of cycles. Furthermore, the performance of the full cells assembled using a Ge/RGO/C anode and an LiCoO2 cathode were evaluated. The cells were able to power a wide range of electronic devices, including an light-emitting-diode (LED) array consisting of over 150 bulbs, blue LED arrays, a scrolling LED marquee, and an electric fan.

Keywords: lithium, battery, anodes, nanowires, composites

[1] Guo-An Li, Chiu-Yen Wang, Wei-Chung Chang, Hsing-Yu Tuan. (2016, Aug). Phosphorus-Rich Copper Phosphide Nanowires for Field-Effect Transistors and Lithium-Ion Batteries. ACS Nano, 2016, 10, pp 8632–8644.
[2] Fang-Wei Yuan and Hsing-Yu Tuan. Scalable Solution-Grown High Germanium Nanoparticle Loading Graphene Nanocomposites as High-Performance Lithium Ion Battery Electrodes: An Example of Graphene-Based Platform towards Practical Full Cell Applications.Chemistry of Materials, 2014, 26 (6), pp 2172–2179

[3] Fang-Wei Yuan, Hong-Jie Yang, and Hsing-Yu Tuan, Alkanethiol-Passivated Germanium Nanowires as High-Performance Anode Materials for Lithium-Ion Batteries: The Role of Chemical Surface Functionalization, ACS Nano, 2012, 6, 9932

Acceptance ID: 3WB5-O

Sorption Study of Biopolymer (High Amylose Starch) as an Alternative Desiccant for Rotary Desiccant Wheels

Farhad Fathieh,[1] Leila Dehabadi,[2] Lee D. Wilson*,[2] Richard W. Evitts,[3] Carey J. Simonson[3]*

[1] Department of Chemistry, University of California, Berkeley, 419 Latimer Hall, Berkeley, CA 94720, USA
[2] Department of Chemistry, University of Saskatchewan, 110 Science Place, Saskatoon, SK. Canada S7N 5C9
[3] Department of Mechanical Engineering, University of Saskatchewan, 57 Campus Drive, Saskatoon, SK, Canada, S7N 5A9

Denotes corresponding author, underscore indicates presenting author

In a recent study (*ACS Sustainable Chem. Eng.*, **2016**, 4 (3), 1262) starch biopolymer desiccants displayed enhanced sorption capacity and regeneration ability when compared against commercial silica desiccant materials. Wide applications and projected growth in the global market are anticipated for solid desiccant materials, especially those derived from renewable resources that serve as alternative environmentally friendly bio-desiccants. In this research, the sorption of water vapor on high amylose starch is investigated as an alternative desiccant for air to-air energy exchangers used in ventilation units. Sorption performance of micron size mesoporous high amylose starch (HAS15) and two mesoporous silica gel samples were studied and compared. Transient water vapor sorption tests were performed using small-scale energy exchangers coated with HAS15 and the silica gel samples. Although N_2 gas adsorption tests showed lower sorption capacity for HAS15 compared to the silica gel samples, higher sorption rates and uptake capacity were shown for HAS15, when measured by water vapor transient sorption results. In addition, the latent effectiveness, an indicator of moisture recovery efficiency for exchangers was calculated for each exchanger. With the same amount of desiccant coated on the energy exchanger channels, the latent effectiveness of the HAS coated material was 2-13% greater than that of the silica gel materials, depending on the operating conditions.

Electrochemical Properties of NbO_2 as a Negative Electrode Material for Lithium-Ion Batteries

Yong Hoon Cho, Soon-Ki Jeong

Department of Chemical Engineering, Soonchunhyang University, Asan, 336-745, Republic of Korea.
hamin611@sch.ac.kr/ +82-41-530-1313

In recent years, global warming and increasing oil prices have highlighted the need for electric vehicles. In order to commercialize electric vehicles, it is very important to develop lithium-ion batteries (LIBs) with high-energy density. There are two approaches for achieving high-energy density LIBs: (1) by searching for new or improving existing positive electrode materials, or (2) searching for alternatives to carbonaceous negative electrode materials, which should have high capacity and low redox potential. In this study, we investigated alternatives to carbonaceous negative electrode materials. Graphite has been used as a negative electrode for LIBs. However, it does not meet the high-energy density requirements because it has a low theoretical capacity of 372 mA h g^{-1}, which was confirmed in practice [1].

Transition metal oxides such as MoO_2, MoO_3, and Co_3O_4 have much higher capacities than graphite because they can react with one or more Li^+ per formula unit [2]. Niobium dioxide (NbO_2) has a theoretical capacity of 429 mA h g^{-1}, assuming that it reacts with two Li^+. This can be converted to a volumetric capacity of 2531 mA h cm^{-3} (calculated using the density of NbO_2 (5.9 g cm^{-3})), more than three times greater than that of graphite (833 mA h cm^{-3}). Given its high capacity, NbO_2 is a promising candidate to replace graphite.

In this work, we investigated the electrochemical mechanism of lithium ion into NbO_2 as a negative electrode material in LIBs by in-situ X-ray diffraction. Electrochemical properties are obtained by charge and discharge test at various C-rates. Surface oxidation state was analyzed by X-ray photoelectron spectroscopy.

Keywords: Lithium secondary batteries, negative electrode, niobium oxides, in-situ XRD, interfacial reactions

[1] IDOTA, Y., KUBOTA, T., MAATSUFUJI, A., MAEKAWA, Y. & MIYASAKA, T. 2011. Tin-Based Amorphous Oxide: A High-Capacity Lithium-Ion-Storage Material. *Science*, 276, 1395-1397.

[2] WU, Z., REN, W., WEN, L., GAO, L., ZHAO, J., CHEN, Z., ZHOU, G., LI, F. & CHENG, H. 2010. Graphene Anchored with Co3O4 Nanoparticles as Anode of Lithium Ion Batteries with Enhanced Reversible Capacity and Cyclic Performance. *Science*, 4, 3187-3194.

Acceptance ID: 4AKD-P

Improved Cell Conversion Efficiency in Fabrication of Dye Sensitized Solar Cell Using Organic Dyes as Energy Materials in Different Solvents

K.R. Genwa[1] , *Chanchal Mahavar*[2],

[1,2] *Depatment Of Chemistry, Jai Narain Vyas University, New Campus, Bhagat Ki Kothi, Jodhpur-342005 INDIA*
Email: krg2004@rediffmail.com

Solar cells based on organic dyes offer a photovoltaic module with low hazard risk components, low production cost and easy manufacturing technique. We report organic-dye sensitized solar cells (O-DSSC)fabricated with various individual organic dyes and mixture of dyes in different solvents in conjunction with iodide/tri-iodide redox electrolyte and various catalytic material as a counter electrode. This technique was first developed by M. Grätzel and co-workers in 1991 thus also called as Grätzel cell. [1]

In DSSC different materials were evaluated as semiconductor, such as ZnO, TiO_2, Nb_2O_5 [2] [3] from which TiO_2 is most commonly used semiconductor. Using Triton-X as a thickener or stabilizer, the photoelectrodes of semiconductor thin film of DSSC is fabricated from TiO_2 nanoparticles paste, above which photosensitizer is allowed to adsorb. The incident sunlight is absorbed by sensitizer for photocurrent and sensitizer should be chosen the way that it could able to inject e^- in to conduction band of semiconductor. [4]

We evaluated result with various organic sensitizers such as Phloxin B (η=0.1142% in ethanol), Amido Black (η=0.146% in DMSO), Indigo carmine (η=0.0825% in DMSO), Birbeich Scarlet (η=0.167% in DMSO), Alizarin cyanine Green (η= 0.178% in DMSO), Evans Blue (η=0.148% in DMSO)[5] in suitable solvent using PEDOT: PSS-Graphite as a counter electrode. For each electron photogenerated from dye, an electron is injected into conduction band of semiconductor. These electron then are collected for powering a load via transparent (FTO) electrode, and arrive at counter electrode, which is coated by catalyst (PEDOT: PSS-Graphite) to speed up the redox reaction with electrolyte. The electrolyte with addition of additives can improve the efficiency of solar cells, another key component to obtain high efficiency of solar cell. The electrolyte phase can be liquid, quasi-solid and solid containing redox couple. Some type of redox couples are I^{3-}/I^-, Br^-/Br_2, $SCN^-/ (SCN)_2$, $SeCN^-/ (SeCN)_2$ & bipyridyl cobalt (III/II) [6]. We used I^{3-}/ I^- as electrolyte, far known for the best results concerning the efficiency of DSSC. Later the effects of the solvents on the performance of cells using mixture of dyes were studied. In present work five sets of organic dyes with different solvents were prepared from which Sudan Black B and Azur B individually tested (η=0.15% and η=0.21% in DMSO respectively) and obtained results compared with the results of mixture of same dyes in distilled water (η= 0.11%), ethanol (η= 0.20 %), and DMSO (η= 0.24%) [7]. High efficiencies for mixture of dyes are obtained when compared to results of their individual dyes, thus, showing the influence of mixture of dyes. The counter electrode and electrolyte were kept same in all these cells. Furthermore, variations were made both in solvents and counter electrode and crystal violet & Azur A were used as photosensitizer. Here we studied the effect of different catalytic material such as Platinum, Graphite-PEDOT: PSS, Graphite using mixture of two above dyes in different solvents (Distilled water, Ethanol DMSO). Obtained conversion efficiency (η) of CELL 1 [Crystal Violet + Azur A in Distilled H_2O]: Platinum (η=0.37%), Graphite-PSS:PEDOT (η=0.33%), Graphite (η=0.29%); CELL 2 [Crystal violet + Azur A in ethanol]: Platinum (η=0.26%), Graphite-PSS:PEDOT (η=0.23%), Graphite (η=0.16%); CELL 3 [Crystal violet + Azur A in DMSO]: Platinum (η=0.31%), Graphite-PSS:PEDOT (η=0.29%), Graphite (η=0.21%). Comparing the result it was found that platinum electrode consistently increases the cell performance as compared to Graphite, but showed results nearly equal to Graphite-PEDOT:PSS) concluding that PEDOT:PSS can take over the costly Platinum counter electrode with good efficiency.

Keywords: DSSC, thin film semiconductor, organic dyes, photoelectrods, solar cell

References:

[1] REGAN, B. O. & GRÄTZEL M. 1991. Dye Sensitized Solar Cell. *Nature*, 353, 737-740.

[2] TENNAKONE, K., KUMARA, G. R. R., KOTTEGODA, I. R. M., & PERERA, V. S. P. 1999. An efficient dye-sensitized photoelectrochemical solar cell made from oxides of tin and zinc. *Chem. Commun.*, 35, 15-16.

[3] SAYAMA, K., SUGUHARA, H. & ARAKAWA H. 1998. Photoelectrochemical properties of a porous Nb_2O_5 electrode sensitized by a ruthenium dye. *Chem. Mater.* 10, 3825-3832.

[4] GRATZEL, M. 2004. Conversion of sunlight to electric power by nanocrystalline dye sensitized solar cell. *J. Photochem. Photobiol. A: Chem.* 164, 3-14.

[5] KONG, F. T., DAI, S. Y. & WANG, K. J. 2007. Review of recent progress in dye-sensitized solar cells. Adv. OptoElectron. 2007, 75384-1-75385-13.

[6] BOSE, S. & GENWA, K. R. 2016. New metal free organic dyes based DSSC with graphite-PSS PDOT counter electrode. *IRJPAC*, 11, 1-10.

[7] SONI, V., MAHAVAR, C. & GENWA, K. R. 2017. Effect of solvents on mixture of azur B and sudan black B photosensitizer in fabrication of DSSC. *IJRASET.* 5, 135-144.

Acceptance ID: 5DNC-O

DC Energy Storage and AC Line Filtering of Graphene Micro-sheets Prepared with Plasma Micro-discharges

Allagui A.[1,2], *Said Z.*[1], *Abdelkareem M. A.*[1], *Elwakil A.S.*[3], *Yang M.*[4] *Alawadhi H.*[2,5]

[1]*Dept. of Sustainable & Renewable Energy Eng., University of Sharjah, UAE*
[2]*Center for Advanced Materials Research, University of Sharjah, UAE*
[3]*Dept. of Electrical and Computer Eng., University of Sharjah, UAE*
[4]*Ningbo Institute of Materials Technology & Engineering, CAS, Ningbo, China*
[5]*Applied Physics Dept., University of Sharjah, UAE*
aallagui@sharjah.ac.ae / +1 919-883-4281

In this work, we show the preparation of multi-layer graphene sheets (MLG) from a carbon graphite electrode used alternatively as cathode and anode in a submerged micro-plasma setup [1]. Apart from the common atomic hydrogen, oxygen and molecular OH emissions obtained from optical emission spectroscopy, the cathodic micro-plasma shows richer and more intense spectral response when compared to the anodic one, including the molecular features of C_2. TEM results show for the material prepared by anodic micro-plasma relatively large lateral size sheet-like MLG without major structural distortions, whereas with the cathodic configuration, tiny flakes of graphite are seen to be attached to large lateral size MLG (see figure 1). Furthermore, we observe in the latter negative Raman shifts of the G peak and the appearance of the T peak at 1100 cm^{-1}, which are attributed to thermal-induced strains in the graphene crystal lattice, as well as to some C-C sp^3 bonds content. This suggests that MLG produced using the anodic micro-plasma is mainly through electro-assisted volume expansion of graphite by anions/solvent intercalation, followed by the destructive fragmentation and exfoliation of the anode [2]. Whereas MLG produced using the cathodic configuration is obtained through both intercalation/exfoliation, and degradation of the working electrode through localized heating and material evaporation. Cyclic voltammetry, constant-current charging/discharging and electrochemical impedance spectroscopy were used to evaluate the time- and frequency-domain behaviors of symmetric MLG-based supercapacitors. We also tested the behavior of the devices in an inverting integrator circuit using up to 5000 Hz bipolar excitations. MLG material produced using cathodic graphite showed superior performance at close-to-dc (< 1 Hz), whereas the anodic MLG is better suited for higher frequencies (see figure 1). This indicates the possibility of using MLG-based supercapacitors for both dc energy storage and ac filtering applications.

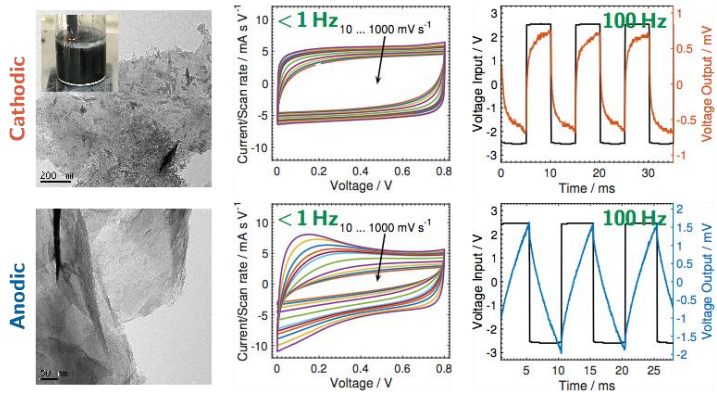

Figure 3: Morphological and electrochemical characterization of MLG sheets prepared with cathodic and anodic micro-plasma. The irregular structure of MLG sheets (top left) hosts some sp^3 C-C content (from Raman spectroscopy measurements, not shown here) contribute to outstanding 3 F/g device capacitance at low and close-to-dc frequencies. Whereas the smoothness of the MLG sheets prepared with anodic micro-plasma (bottom left) makes the material suitable for both reasonable energy storage (2.5 F/g device capacitance) as well as for high-frequency applications (compare results obtained from the inverting integrator circuit at 100 Hz).

Keywords: Graphene, Plasma micro-discharges, Supercapacitor, AC line filtering

[1] ALLAGUI, A., SALAMEH, T., ALAWADHI, H. 2015. One-pot Synthesis of Composite NiO Nanomaterials/Graphitic Carbon Flakes with Contact Glow Discharge Electrolysis for Electrochemical Supercapacitors, *Int. J. Energy Res.*, 39, 1689-1697.

[2] PARVEZ, K., WU, Z.-S., LI, R., LIU, X., GRAF, R., FENG, X., MULLEN, K. 2014. Exfoliation of Graphite into Graphene in Aqueous Solutions of Inorganic Salts, *J. Am. Chem. Soc.*, 136, 16, 6083-6091.

[3] WU, Z.-S., LIU, Z., PARVEZ, K., FENG, X., MULLEN, K. 2015. Ultrathin Printable Graphene Supercapacitors with AC Line-Filtering Performance, *Adv. Mater.*, 27, 24, 3669-3675.

Acceptance ID: 8BEJ-O

Synthesis of $CuInS_2$ quantum dots with gradient band gap and their application in solar cells

Quantum dots (QDs) hold promising for fabricating low-cost and high efficient solar cells for their tunable band gap, multiple exciton generation and hot electron injection. However, the most well studied QDs used in solar cells are CdS and PbS, which contain toxic element, and because of the mismatch energy gap of these QDs with solar spectrum, they suffer from incomplete coverage of the solar spectrum. That severely limit the application of solar cells on a large scale. As an alternative, $CuInS_2$ (CIS) QDs do not contain heavy toxic element, and the large absorption cross-section is well matched for harvesting solar energy that make it a promising material for solar cells. In this work, the CIS QDs with gradient band gap are synthesized simply by tuning the reaction time via hot-injection method. A serious of measurements such as XRD, TEM, PL spectra are conducted to characterize the composition, structure and optical properties of CIS QDs. High-performance chalcopyrite structure CIS QDs were obtained with band gap range from 1.46 to 1.86 eV. Finally, the multilayer of QDs with gradient band gap are applied on solar cells for their better coverage of solar spectrum and it shows photon-to-electron conversion (PCE) of 4.21 % which is about 20 % higher than that of monolayer CIS QDs. It offers the opportunity to further improve the efficiency simply by controlling band gap of QDs.

Keywords: $CuInS_2$ quantum dots, gradient band gap, characterization, solar cells, efficiency.

Acceptance ID: 9AEF-P

Photoelectrochemical Cell of Cu_2O Based Bi-Layer Photocathode with Sb Doped Cu_2O Seed Layer

Joo Sung Kim, Young Been Kim,[1] Seung Ki Baek,[1] Young Dae Yoon,[1] and Hyun Koun Cho[1,,**]*

[1]School of Advanced Materials Science and Engineering, Sungkyunkwan University, 2066, Seobu-ro, Jangan-gu, Suwon, Gyeonggi-do 16419, Republic of Korea.
** presenting author (chohk@skku.edu)*
*** corresponding author (chohk@skku.edu)*

Basically, Cuprous oxide (Cu_2O), which is a p-type oxide and suitable to an absorption layer of photovoltaic cell and photoelectrochemicall (PEC) cell for hydrogen generation, because it has an appropriate direct band-gap of 2eV and can absorb a large part of the solar spectrum and have an appropriate energy band position. The conduction band (CB) lies at -0.7 V of the hydrogen generation potential. Thus, the electrons excited by the CB of Cu_2O are energetic enough to be transferred to water for hydrogen evolution. Nevertheless, Cu_2O photoelectrodes have critical limitations in term of high PEC performance. First, the Cu_2O film is chemically unstable due to its self-photo deterioration mechanism. Because photo-corrosion is inevitable under visible light illumination because the redox potential of Cu_2O from self-reduction (Cu_2O to Cu) or self-oxidation (Cu_2O to CuO) by photo-generated electrons or holes is within its bandgap. Thus, an additional thin protective layer based on TiO_2 was used on top of the Cu_2O film to prevent direct contact between Cu_2O and the electrolyte. However, TiO_2 with high resistance requires a high growth temperature, resulting in an electrically resistive Cu_2O film, and an appropriate film thickness, which reduces the photocurrent. Second, the electrodeposited Cu_2O films generally exhibit low electrical conductivity and short minority-carrier diffusion lengths, which cause low photocurrents because of frequent non-radiative recombination. The high performance of electrodeposited cuprous oxide (Cu_2O) based photoelectrochemical (PEC) cells has been limited due to low electrical conductivity hindering effective carrier transport to electrodes and chemically unstable properties in aqueous environments, despite their several advantages such as suitable band gap, band position, and cost-effective and environmentally friend elements. The Cu_2O: Sb bi-layer improved the crystal growth of Cu_2O as well as the desirable crystal growth along the [111] direction. These microstructural changes showed high electrical conductivity due to the suppression of high hole mobility and instability associated with the surface.

Keywords: Cuprous oxide, Photoelectrochemical cell, Water splitting system, Sb Doped Cu_2O

Acceptance ID: 9ZUP-P

Materials and Architecture Perspectives for On-Chip Energy Storage and Power Generation

Chunlei Wang

Department of Mechanical and Materials Engineering
Florida International University

Conventional electrochemical double-layer capacitors (EDLCs) are well suited as power sources for devices that require large bursts of energy in short time periods. However, EDLCs suffer from low energy densities as compared to their battery counterparts, which restrict their applications in devices that require a simultaneous supply of high power and high energy. In the wake of improving the energy density of EDLCs, the concept of hybridization of lithium-ion batteries (LIBs) and EDLCs has attracted considerable attention in recent years. Such a hybrid known as a Lithium-ion capacitor (LIC) comprises a Li-ion intercalating anode and a fast charging-discharging EDLC cathode. Although quite ideal in theory, such a system poses major challenges, most of which are a result of the mismatch between the specific capacities and power densities of the LIB and EDLC electrodes. In this talk, the challenge and our recent progress on developing various on-chip energy storage and power generation systems will be discussed. We have demonstrated that high performance nanocomposites enabled carbon micropillar arrays as well as TiN passivated porous Si could be two promising platforms for on-chip application. In addition, a hybrid capacitor that utilizes a $Li_4Ti_5O_{12}$ (LTO) based anode and a graphene and carbon nanotube (G-CNT) composite based cathode will also be highlighted.

Acceptance ID: ADXC-I

In situ transmission electron microscopy study of porous Si nanostructures and investigation on porous Si-S full cells

Chenfei Shen[1], *Mingyuan Ge*[1], *Langli Luo*[3], *Anyi Zhang*[1], *Xin Fang*[1], *Yihang Liu*[2], *Jiepeng Rong*[1], *Chongmin Wang*[3], *Chongwu Zhou*[1,2,*]

[1]*Mork Family Department of Chemical Engineering and Materials Science, University of Southern California, Los Angeles, California 90089, United States.*
[2]*Ming Hsieh Department of Electrical Engineering, University of Southern California, Los Angeles, California 90089, United States.*
[3]*Environmental Molecular Sciences Laboratory, Pacific Northwest National Laboratory, Richland, Washington 99352, United States.*
[*]*Corresponding author.*
Email: chongwuz@usc.edu

Lithium-ion batteries have attracted great attention as one of the most versatile electrochemical energy storage devices. However, to meet the ever-growing energy needs for wide applications, further improvements on energy density of batteries are expected, which requires the development of innovative high-energy electrode materials. Silicon (Si) and sulfur (S) are two promising candidates and have been studied intensively as anode and cathode materials in lithium-ion batteries. In this work, we first discuss the lithiation behaviours of both porous silicon (Si) nanoparticles and porous Si nanowires by in situ and ex situ transmission electron microscopy (TEM) and compare them with solid Si nanoparticles and nanowires. The in situ TEM observation reveals that porous Si nanostructures has better capability to accommodate volume expansion, to suppress c-$Li_{15}Si_4$ formation during the first lithiation process, and to suppress pore evolution during cycling than solid Si nanoparticles.

On this basis, we use porous Si as anode material to pair up with S cathode to form Si-S full cells. We will discuss the challenges in the Si-S full cell integration, and a failure mechanism of Si-S full cell is proposed. On this basis, we report one prototype of Si-S full cells using lithiated Nafion-coated porous Si as anode and sulfur as cathode, and our study on the functionality of Nafion in shielding Si from reaction with polysulfides. With optimized mass ratio between sulfur and silicon, the full cell yields specific capacity of 330 mAh/g and energy density of 590 Wh/kg after 100 cycles based on the total mass of sulfur and silicon. The achieved energy density is more than 2 times higher than commercially available lithium-ion batteries. The investigation of issues in Si-S full cell research and the proposed full cell prototype will shed light on the development of next-generation lithium-ion batteries.

Acceptance ID: AU44-P

Finding Lead Free Halide Perovskites via Trivalent Metal Cations: A Theoretical Study

Ki-Ha Hong (Hong)[1] and Choong-Heui Chung (Chung)[1]

[1]Department of Materials Science and Engineering, Hanbat National University, 125 Dongseo-daero, Yuseong-Gu, Daejeon, 34158, Korea.
kiha.hong@hanbat.ac.kr

Organic-inorganic hybrid perovskite (OIPVK) are one of strong candidates for the next generation photovoltaic materials. Since the Miyasaka group first implemented methylammonium (MA, $CH_3NH_3^+$) lead tri-iodides ($MAPbI_3$) as a sensitizer in dye sensitized solar cells, there have been dramatic increases in the power conversion efficiency (PCE) of perovskite based solar cells, of which the certified PCE has already exceeded 20%. Stability and non-toxicity are the key factors affecting the commercialization of OIPVKs. Among various efforts to develop Pb-free perovskite solar cells, Sn based materials have shown the PCE. However, the stability of Sn-based perovskites is worse than Pb-based solar cells and the multivalent features of Sn are considered to be the origin of the unstable performance.

Recently, tri-valent metal halide perovskites ($A_3X_2I_9$, A=$CH_3NH_3^+$(MA)/Cs, X=Bi/Sb) have attracted considerable attention because they exhibit better stability and less toxicity than Pb halide perovskites. While the PCE of $A_3X_2I_9$ has not been able to compete with that of Pb/Sn based solar cells up to now, the stability of the perovskites has been significantly improved.

The fundamental bottleneck limiting the use of $A_3X_2I_9$ perovskites in solar cell applications is their large band gap, which can rarely be manipulated to less than 1.9 eV. This study presents a computational screening of Pb-free hybrid perovskites containing trivalent metal cation using density functional theory. The band structures of $Cs_3XX'I_9$ (X & X'= trivalent metal cations) were evaluated within $P6_3/mmc$ and $P\bar{3}m1$ lattice symmetries. Computational screening has been conducted considering proper band gap, absorption coefficient, formation energies and effective masses. Among the various tri-valent atoms investigated, In and Ga doping in Bi and Sb based perovskites showed very promising band gap modulation behaviors.

Keywords: Perovskite, solar cell , density functional theory, Pb-free, computational screening

Acceptance ID: AXCX-P

Bioelectrochemical system using inexpensive materials

Surajbhan Sevda

Dr B R A National Institute of Technology Jalandhar
sevdasuraj@gmail.com

In an era of climate change, alternate energy sources are desired to replace oil and carbon resources. Subsequently, climate change effects in some areas and the increasing production of biofuels are also putting pressure on available water resources. Microbial Fuel Cells have the potential to simultaneously treat wastewater for reuse and to generate electricity; thereby producing two increasingly scarce resources. Microbial fuel cell consists of anode and cathode, connected by an external circuit and separated by Proton Exchange Membrane. Anodic material must be conductive, bio compatible, and chemically stable with substrate. Metal anodes consisting of noncorrosive stainless steel mesh can be utilized, but copper is not useful due to the toxicity of even trace copper ions to bacteria. The simplest materials for anode electrodes are graphite plates or rods as they are relatively inexpensive, easy to handle, and have a defined surface area. Much larger surface areas are achieved with graphite felt electrodes

The most versatile electrode material is carbon, available as compact graphite plates, rods, or granules, as fibrous material (felt, cloth, paper, fibers, foam), and as glassy carbon. Proton Exchange Membrane is usually made up of NAFION or ULTREX. Microbial Fuel Cells utilise microbial communities to degrade organics found within wastewater and theoretically in any organic waste product; converting stored chemical energy to electrical energy in a single step. Oxygen is most suitable electron acceptor for an microbial fuel cell due to its high oxidation potential, availability, sustainability and lack of chemical waste product, as the only end product is water.

Acceptance ID: B2X3-O

Multi-yolk−shell SnO_2/Co_3Sn_2@C Nanocubes as Anode Materials for High Performance Lithium ion Batteries

Lianbang Wang, Yawei Xu, Liwei Su

(State Key Laboratory Breeding Base of Green Chemistry-Synthesis Technology, College of Chemical Engineering, Zhejiang University of Technology, Hangzhou, P. R. China, 310014, E-mail: wanglb99@zjut.edu.cn)

As a potential alternative of the limited capacity of graphite-based materials, SnO_2 has drawn researchers' great attention in terms of promising theoretical capacity and appropriate operation voltages.[1-2] Most of the works focus on large volume swings and the enhance of capacities, however, the challenging problems of SnO_2 anode material for lithium ion batteries are the poor electronic conductivity and the low oxygen reutilization due to the irreversibility of Li_2O generated in the initial discharge leading to a theoretical initial coulombic efficiency of only 52.4%. If the oxygen can be totally reutilized, the theoretical capacity of SnO_2 is as high as 1494 mA h g^{-1} (≈4 times that of graphite) rather than the limited theoretical capacity of 781 mA h g^{-1}. It is significant but remains a challenge to accomplish 100% reutilization of the oxygen in SnO_2 until now.[3-4]

We propose a novel strategy to improve the oxygen reutilization in SnO_2 by introducing oxygen-poor metals or alloys. According to this protocol, multi-yolk−shell SnO_2/Co_3Sn_2@C nanocubes are designed and successfully prepared using hollow $CoSn(OH)_6$ nanocubes as precursors followed by a facile hydrothermal and calcination treatment. The Co_3Sn_2 nanoalloys are uniformly dispersed in the matrix of SnO_2 and can release Co and Sn during discharging; the newly released Co can react with Li_2O to form CoO_x in charging. The efficient reutilization of oxygen allows a high initial coulombic efficiency of 71.7% and a reversible capacity of 1003 mA h g^{-1} after 200 cycles. The removal of Li_2O surrounding Sn nanocystals enables a high electronic conductivity for good rate performances. The unique multiyolk−shell nanostructure offers adequate breathing space for the volume wings during long-term cycling. This strategy employing oxygen-poor metal components provides a novel approach to enhance the oxygen reutilization in SnO2 for higher reversibility.

References:

1. L. Wang, W. Tang, Y. Jing, L. Su, Z. Zhou, *ACS Appl Mater Interfaces* 2014, *6*, 12346-12352.

2. L. Su, Y. Jing, Z. Zhou, *Nanoscale* 2011, *3*, 3967-3983.

3. R. Huang, L. Wang, Q. Zhang, Z. Chen, Z. Li, D. Pan, B. Zhao, M. Wu, C. M. Wu, C. H. Shek, *ACS*

Nano 2015, *9*, 11351-11361.

4. Z. X. Chen, M. Zhou, Y. L. Cao, X. P. Ai, H. X. Yang, J. Liu, *Adv. Energy Mater.* 2012, *2*, 95-102.

Acknowledgments: This work was supported by the National Natural Science Foundation of China (21403195 and 21421001) and the Key Research and Development Program (2015C01001 and 2016C01SA500898) of Science and Technology Department of Zhejiang Province.

Acceptance ID: BETY-P

Effect of Microstructure on the Performance of a LA92 Alloy Anode for Mg-Air Battery Application

L. C. Tsao[1]

[1]*Institute of Materials Engineering, National Pingtung University of Science & Technology, 1 Shuefu Road, Neipu, 91201 Pingtung, Taiwan.*
E Mail : tlclung@mail.npust.edu.tw

Owing to the growing concern on the energy crisis, Mg–air battery is considered as a promising power source and energy storage device, because of its high theoretical voltage, high specific energy, light weight, low cost and no pollution [1–3]. However, the Mg anode has some problems [4, 5]: (1) the discharge products adhered to the anode surface; (2) the self discharge occurring on the Mg anode. Therefore, the present work aims to investigate the performance of Mg–air battery based on Mg9Li2Al (LA92) alloys with different microstructures. In the present study, three unique microstructures (i.e. β-fine equiaxed, β-coarse equiaxed, and α + β coexist) achieved via different heat treatments, were included in the evaluation. The potentiodynamic polarization and electrochemical impedance spectroscopy tests show that the β-*coarse* microstructure enhances the electrochemical activity of the LA92 alloys. An Mg–air battery based on the processed LAZ92 alloys was prepared and the battery performance was investigated by constant current discharge test. The β-coarse LA92 alloy exhibited superior discharge properties compared to the other samples. In β-*coarse* LA92 alloys, the discharge product is loosely adhered to the alloy surface, and thus could keep high discharge activity during discharge. And the corrosion products are mainly $Mg(OH)_2$.

Keywords: Mg9Li2Al, Mg-Air battery, microstructure, corrosion behavior

[1] BLURTON, K.F., SAMMELLS, A.F. 1979. Metal/air batteries: Their Status and Potential - A review. *J. Power Sources*, 4, 263–279.

[2] LINDEN, D., REDDY, T.B. 2002. Handbook of Batteries, 3rd ed., McGraw-Hill.

[3] PENG, B., CHEN, J. 2009. Functional materials with high-efficiency energy storage and conversion for batteries and fuel cells. *Coordination Chemistry Reviews*, 253, 2805–2813.

[4] WANG, N., WANG, R., PENG, C., FENG, Y. 2014. Enhancement of the discharge performanceof AP65 magnesium alloy anodes by hot extrusion. *Corrosion Science*, 81, 85–95.

[5] ZHANG, T., TAO, Z., CHEN, J. 2014. Magnesium-air batteries: from principle to application. *Materials Horizons*, 1, 196-216.

Acceptance ID: BL4S-P

Perovskite Single-Crystalline Thin Films: On-Chip Fabrication and Properties

Yao-Xuan Chen[1], Qian-Qing Ge[1], Jin-Song Hu[1]

[1] Institute of Chemistry, Chinese Academy of Science, Beijing, 100190, China.
E Mail/ hujs@iccas.ac.cn

The organic-inorganic hybrid perovskites have been demonstrated many optoelectronic applications including high-efficiency perovskite solar cells (PSCs), solid-state lasers, light-emitting diodes and highly sensitive photodetectors, due to their superior photoelectric properties such as high absorption coefficient, long carrier lifetime, and highly balanced hole and electron mobility simultaneously. The organic-inorganic hybrid perovskite single-crystalline thin films (SCTFs) are promising for enhancing the photoelectric device performance due to the higher carrier mobility, longer diffusion length and carrier lifetime arising from the reduced trap-state densities compared with polycrystalline films. However, bulk perovskite single crystals available today are not suitable for direct fabrication of practical devices due to the unfavorable thickness.

In this presentation, we will present a facile space-confined solution-processed strategy to fabricate hybrid perovskite SCTFs with the following features: i) facile solution-processing method; ii) perovskite SCTFs in sub-millimeter scale; iii) adjustable thickness from nanometers to micrometers with an aspect ratio up to ~10^5; iv) thickness-dependent color for direct visual inspection of suitable thickness for diverse device applications; v) air-stable perovskite SCTFs; vi) on-substrate growth for direct practical device fabrication; vii) substrate-independent growth with potentials for various applications; viii) general method for fabricating various hybrid perovskite SCTFs. The structural, optical and electronic transport property characterizations revealed that the prepared perovskite SCTFs exhibited the excellent air stability and comparable quality to bulk single crystals with a low trap density of 4.8 x 10^{10} cm^{-3}, high carrier mobility of 15.7 $cm^2V^{-1}s^{-1}$, and long carrier lifetime of 84 μs. The further investigation showed that the developed space-confined strategy could also be applied to on-substrate single crystalline inorganic perovskite structures. These results might inspire the further exploration of on-chip fabrication of high-performance PSCs and diverse devices with perovskite SCTFs.

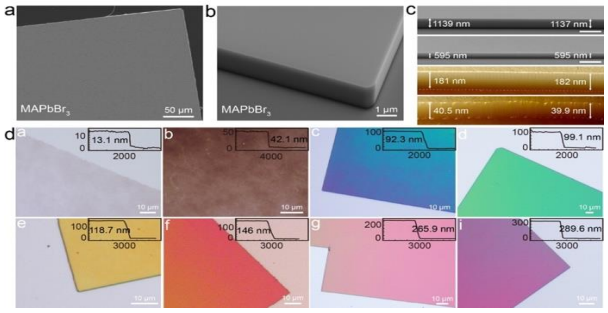

Keywords: Perovskite, single-crystalline, thin film, solar cell, photovoltaics

[1] CHEN, Y.-X., GE Q.-Q., SHI Y., LIU J., XUE D.-J., MA J.-Y., DING J., YAN H.-J., HU J.-S., WAN L.-J. 2016. General Space-Confined On-Substrate Fabrication of Thickness-Adjustable Hybrid Perovskite Single-Crystalline Thin Films. *J. Am. Chem. Soc.*, 138, 16196-16199.

[2] GE Q.-Q., DING J., LIU J., MA J.-Y., CHEN, Y.-X., GAO X.-X., WAN L.-J., HU J.-S. 2016. Promoting crystalline grain growth and healing pinholes by water vapor modulated post-annealing for enhancing the efficiency of planar perovskite solar cells. *J. Mater. Chem. A*, 4, 13458-13467.

Acceptance ID: BPFU-O

Recent Progress on Multi-Dimensional Nanocarbons and Their Applications in Electrochemical Capacitors

Churl Seung Lee [1], *and Joonho Bae* [2*]

[1] *Energy Nanomaterials Research Center, Korea Electronics Technology Institute, Seongnam, 463-816, Korea*

[2]*Department of Nano-physics, Gachon University, Seongnam, 461-701, Korea*

**Email (J. Bae):jnana2k@gmail.com,baejh2k@gachon.ac.kr*

In order to realize next generation energy storage devices with high efficiency, large energy/power density, and long life cycle, novel carbon-based nanomaterials are needed as electrodes. In here, we present interesting multidimensional carbon nanostructures which could find potential applications in electrodes for energy storage devices. Besides basic descriptions on their synthesis, characterizations, and capacitor electrodes performance, their possible applications in the next generation Li ion energy storage devices will be discussed. We prepared carbon nanoplatelets (CNPs) by simple thermal treatment of expandable graphites. By using carbon nanoplatelets (CNPs), multi- dimensional (1D+2D) carbon nanostructures (CNP-CNTs) were synthesized by use of metal catalysts and CVD process. Basic cyclic voltammetry study on the CNPs and CNP-CNTs reveals that CNP-CNTs possessed enhanced mass specific capacitances compared to those of CNPs. Our multi-dimensional carbon nanostructures showed excellent electrochemical properties probably due to large surface area and unique geometry. These results suggest that our multi-dimensional nanocarbons could be promising in their applications in electrochemical capacitors.

Acceptance ID: LQD3-O

The Study of Solar Cells Based on 2D Materials MoS2, WS2 and Graphene with Bulk Semiconductors

*Cheng-Lun Tsai, Yi-Hsien Lee, Jin-Hua Huang**

Department of Materials Science and Engineering, National Tsing Hua University, Hsinchu, Taiwan
**E-mail address: jihhuang@mx.nthu.edu.tw*

Graphene has shown superior properties suitable for photovoltaic devices, including high optical transmittance, high mechanical flexibility, low resistivity, and high carrier mobility. In theory, with the property of semi-metal, graphene is able to form a Schottky junction with any semiconductor having moderate carrier density. Monolayer Transition Metal Dichalcogenides (TMDs) are also promising two-dimensional materials in optoelectronic devices. Monolayer TMDs are semiconductors with direct bandgaps which are beneficial to optoelectronic usage. Combination of 2D materials and bulk semiconductors can potentially overcome the limited absorption problem and difficulties in mass production of 2D materials.

This work consists of two studies: Transferring the chemical vapor deposition (CVD) grown TMDs onto p-type Si substrates to produce heterojunction p-n solar cells, and transferring graphene which is also grown by CVD onto n-type GaAs to produce Schottky junction solar cells. In TMDs/p-Si heterojunction p-n solar cells, various back electrode materials and top electrode structures were investigated. The best power conversion efficiencies obtained for the MoS_2 and WS_2 heterojunction solar cells were 4.23 and 2.08 %, respectively. In grapheme/GaAs Schottky junction solar cells, the best power conversion efficiency was 2.08 %. This study demonstrates the potential application of 2D materials in photovoltaic devices.

Acceptance ID: C28M-O

Facile Fabricating Ternary Mo-based Oxides for Energy Storage Application

Gan Qu[1, 2], Jianbo Wang[2], and Yiwen Tang[1]

[1]Institute of Nano-Science & Technology, Department of Physics and Technology, Central China Normal University, Wuhan 430079, China.
[2]School of Physics and Technology, Center for Electron Microscopy, MOE Key Laboratory of Artificial Micro- and Nano-structures, and Institute for Advanced Studies, Wuhan University, Wuhan 430072, China.
Email address: ywtang@phy.ccnu.edu.cn

Ternary Mo-based oxides, such as $NiMoO_4 \cdot xH_2O$,[1] $CoMoO_4$,[2] and $MnMoO_4$,[3] have aroused a great deal of attention in energy storage field on account of the excellent electrochemical performance. However, the reported strategies for fabricating ternary Mo-based oxides are complicated, higher energy consumption, and time consuming, which restrict the industrial application of the materials. Here, we report an innovative method to synthesize the ternary Mo-based oxides nano-materials, which process is rapid, facile, and energy free. Furthermore, the strategy is not only low-cost, but also high-yielding, which displays a great potential for application. The formation mechanism has been discussed to reveal the evolution process of $NiMoO_4 \cdot xH_2O$ nanorods and sycamore fruit like $CoMoO_4$ and $MnMoO_4$ materials in this reaction system. In addition, the obtained ternary Mo-based oxides exhibit high specific capacitance and outstanding cyclic stability, making them attractive for application as energy storage materials.

Keywords: Molybdenum, ternary Mo-based oxides, energy storage

[1] PENG, S. J., Li, L. L., WU, H. B., MADHAVI, S. & LOU, X. W. 2015. Controlled Growth of $NiMoO_4$ Nanosheet and Nanorod Arrays on Various Conductive Substrates as Advanced Electrodes for Asymmetric Supercapacitors. *Adv. Energy Mater.*, 5, 1401172.

[2] MAI, L. Q., YANG, F., ZHAO, Y. L., XU, X., XU, L. & LUO Y. Z. 2011. Hierarchical $MnMoO_4/CoMoO_4$ Heterostructured Nanowires with Enhanced Supercapacitor Performance. *Nat. Commun.*, 2, 381.

[3] GHOSH, D., GIRI, S., MONIRUZZAMAN, M., BASU, T., MANDAL, M. & DAS C. K. 2014. α $MnMoO_4$/Grapheme Hybrid Composite: High Energy Density Supercapacitor Electrode Material. *Dalton Trans.*, 43, 11067-11076.

Acceptance ID: C4VA-P

Toward controlled growth and enhanced lithium storage capability of hybrid SnO_2-Co_3O_4 nanotubes

Xiaoxiao Yan, Jingfei Zhang, Dongmei Sun, Lin Xu, Yawen Tang*

Jiangsu Key Laboratory of New Power Batteries, Jiangsu Collaborative Innovation Center of Biomedical Functional Materials, School of Chemistry and Materials Science, Nanjing Normal University, Nanjing 210023, P.R. China
Corresponding author: sundongmei@njnu.edu.cn

Development of transformative technology capable of producing inexpensive superior lithium electroactive anode material with low volume changes and stable performance on cycling is an important step on the path to advanced application of lithium ion batteries (LIBs)[1-3]. In this work, a new synthetic strategy for hybrid SnO_2-Co_3O_4 nanotubes, based on electrospun polyvinylpyrrolidone (PVP) fibers with simultaneously evenly embedded metal precursors of Sn(IV) and Co(II) followed by two-step gradual pyrolysis in nature air, was developed. The formation mechanism, chemical composition, morphology and structure of the hybrid SnO_2-Co_3O_4 nanotubes were investigated by techniques, such as transmission electron microscopy (TEM), scanning electron microscopy (SEM), X-ray diffraction (XRD), and nitrogen adsorption-desorption isotherms (SADI). Control experiments show that the heat-treatment atmosphere, is the key for the in situ growth of the one-dimensional (1D) hollow hybrid SnO_2-Co_3O_4 nanotubes in a large yield.

The obtained hollow and flexible one-dimensional nanotubes effectively lessen the effects caused by volume change of the conversion reaction $Sn+xLi^+ + xe^- \leftrightarrow Li_xSn$ ($0 \le x \le 4.4$), and significantly shorten the solid-state diffusion length of Li ions upon cycling. The near neighbor Co nanophase, in situ generated from the co-component of Co_3O_4, is thought to catalytically promote the conversion of Sn to SnO_2 over $SnO_2+4Li^+ + 4e^- \rightarrow Sn+2Li_2O$ and enhance the reversible reduction of Li_2O during delithiation. These alleviate the degrading of the electrodes, thus improving the lithium insertion and extraction reversibility. The retained reversible capacity of the prepared hybrid nanotubes as an anode can reach 891 $mAh \cdot g^{-1}$ even after 200 cycles at a current density of 100 $mA \cdot g^{-1}$, showing tendency to further top the level up. The proposed method paves the way for rational design of 1D hollow hybrid nanotubes as a cost-effective and environmentally-friendly efficient anode for LIBs.

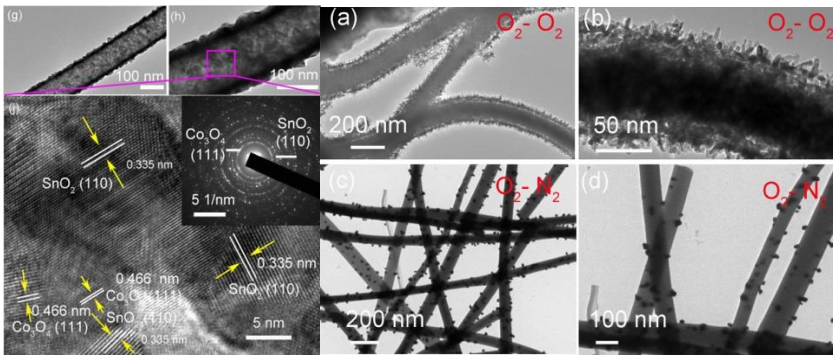

Figure 1 TEM images of hybrid SnO_2-Co_3O_4 composite under different experimental conditions

This work was supported by the National Natural Science Foundation of China (Grant Nos. 21576139, 21503111, and 21376122)

Keywords: Electrospinning, Kirkendall effect, SnO_2-Co_3O_4 nanotubes, Synergistic effect, Lithium ion battery

[1] WANG, X., FENG, J., BAI, Y., ZHANG, Q. & YIN, Y. 2016. Synthesis, Properties, and Applications of Hollow Micro-/Nanostructures. *Chemical Reviews*, **116**(18), 10983-11060.

[2] GOODENOUGH, J. B. & PARK K.-S. 2013. The Li-Ion Rechargeable Battery: A Perspective. *Journal of the American Chemical Society*, **135**(4): 1167-1176.

[3] WANG, W., DAHL, M. & YIN, Y. 2013. Hollow Nanocrystals through the Nanoscale Kirkendall Effect. *Chemistry of Materials*, **25**(8), 1179-1189.

Acceptance ID: CQ8Y-O

Superwetting electrodes for Gas-involved Electrocatalysis

*Wenwen Xu, Zhiyi Lu, Yingjie Li, Xiaoming Sun**

State Key Laboratory of Chemical Resource Engineering, Beijing University of Chemical Technology, Beijing 100029, China

Electrochemical gas-involved reactions, including gas-evolution reaction and gas-consumption reaction, are essential parts in current energy conversion processes and industries. Although the exploration of the highly active catalysts has been very mature, less attention was paid on the gas management during the gas-involved reactions. Inspired from bio-inspired materials, scientists find that bio-mimicked electrodes with superwetting property will influence the gas transportation process during the electrochemical reactions. Our group fortunately found that the interface behavior of electrode could be tuned by surface architecture construction, for example, transferring from aerophobic to superaerophobic by engineering a series of superwetting micro-/nanostructured electrodes, eg. MoS_2. Cu nanoarray and Pt pine-like films [1-4]; transferring from aerophibic to superaerophibic by poly(tetrafluoroethylene)(PTFE) modifying, eg. CoNCNT@CFP.[5] For gas-evolution reaction, constructing nanostructured superaerophobic electrodes is effective to improve the performance by enlarging the bubble contact angle and reducing the bubble adhesion force with the surface of the electrode, thus insuring smooth leaving of the gas products. As to the gas consumption reactions, the superaerophibic electrodes are able to improve the performance by providing an unblocked gas diffusion pathway and a smooth electron transport. Therefore, construction of superwetting surface (auperserophobic for gas evolution reaction and superaerophibic for gas consumption reaction) can boost the performances of the electrodes by managing the surface bubbles.

References

[1] Z. Lu, W. Zhu, X. Yu, H. Zhang, Y. Li, X. Sun, X. Wang, H. Wang, J. Wang, J. Luo, X. Lei, L. Jiang. *Adv. Mater.* **26**(2014) 2683-2687.
[2] Y. Li, H. Zhang, T. Xu, Z. Lu, X. Wu, P. Wan, X. Sun, L. Jiang. *Adv. Funct. Mater.* **25**(2015) 1737-1744.
[3] Z. Lu,M. Sun, T. Xu, Y. Li, W. Xu, Z. Chang, Y. Ding, X. Sun, L. Jiang. *Adv. Mater.* **27**(2015) 2361-2366.
[4] X. Liu, Z. Chang, L. Luo, T. Xu, X. Lei, J. Liu, X. Sun. *Chem. Mater.*, **26**(2014) 1889-1895.
[5] Z. Lu, W. Xu, J. Ma, Y. Li, X. Sun, L. Jiang. *Adv. Mater*, **28**(2016)155-7161.

Acceptance ID: EAHB-I

Observation of partial reduction of manganese in the lithium rich layered oxides during the first charge

Hyung Cheoul Shim,[a] Chang-Su Woo[a] and Seungmin Hyun[a]*

[a] *Department of Nano-Mechanics, Korea Institute of Machinery & Materials (KIMM), 156, Gajeongbuk-ro, Yuseong-gu, Daejeon, 305-343, Republic of Korea.*

Lithium rich layered oxides significant attention as energy harvesting materials due to their large capacities, which are, however, consist of queries on the large irreversible loss in capacities for the first charge/discharge cycle with oxygen removal in lattices related to layered Li_2MnO_3. Herein we present detailed studies on the Li-rich Mn based layered oxides of $0.4Li_2MnO_3$-$0.6LiNi_{1/3}Co_{1/3}Mn_{1/3}O_2$ that were electrochemically activated between 2.5 V and 4.3 or 4.7 V *vs*. Li^+/Li. Electron energy loss spectroscopy (EELS) and X-ray absorption spectroscopy (XAS) revealed unusual Mn reduction after first charging up to high voltage of 4.7 V. Moreover, its electronic structures are not fully recovered to original pristine of Mn^{4+} state when they were discharged again. High-angle annular dark-field image in scanning transmission electron microscopy (HAADF-STEM) and electron dispersive spectra (EDS) also show dramatic decline of oxygen contents with many porous morphologies which associated with oxygen vacancies formation by following oxidation of O^{2-} ions to O_2. Our analysis suggests that unstable superficial Mn valence state with severe defects due to oxygen vacancies may lead the large irreversible capacity loss during the first charge/discharge cycle of Li-rich layered oxide.

Acceptance ID: EHEC-P

The Influence of Active Material Weight Ratios and Thermal Expansion of Constituting Particles on a Newly Developed Li-ion Battery in the Shape of Textile Fibers

Seongmin Yun, Seunghwan Bang, Cheol Kim

Department of Mechanical Engineering, Kyungpook National University, 80 Daehak-Ro, Book-Gu, Daegu 41566, South Korea
kimchul@knu.ac.kr

In an effort to develop flexible rechargeable batteries, a new fiber-type flexible lithium-ion battery that consists of wound carbon nanotube fibers and active materials, has been developed and fabricated. The CNT fiber materials replace the conventional metal current collector, due to that CNT has high strength and outstanding electrical conductivity. Additionally, $LiMn_2O_4$ and $Li_4Ti_5O_{12}$ are coated on the surface of the CNT fiber as an active material in cathode and anode, respectively. Cathode and anode materials consist of active materials, a conductive agent and a binder, and the weight ratio of three different materials have a strong influence on mechanical and electrical performance, as well. Moreover, silicon is used as another kind of an anode material, which is deposited on the surface of CNT fibers using the electron beam evaporation method. Eight cases of weight ratios were investigated to find good weight ratio. Mechanical and electrochemical performances were also tested with respect to each weight ratio. The tensile strength of the CNT fiber coated with active materials was measured by a tensile testing machine to check the mechanical properties. Electrochemical property was also measured by a battery tester. Fiber-type full cells were fabricated to test relative chemical reaction between cathode and anode. Also, pouch-type half cells were produced to measure independent performance of cathode and anode, respectively. The pouch-type half-cell could make a LED bulb lightened. Discharge capacity for the case with a weight ratio (active material: conductive agent: binder = 70: 15: 15) showed 21mAh/g among 8 cases of cathode half-cell tests. When the lithium-ion battery is repeatedly charged and discharged, its average temperature varies from -20 to 60 ℃ and the electrode material with $LiMn_2O_4$ goes through thermal expansion. It may affect the concentration of diffusivity and lithium in the electrode. In this study voltage and temperature were compared with and without considering thermal expansion effects.

Keywords: Textile battery, fiber-type, active material, lithium ion, thermal expansion

[1] RAMADESIGAN, V., NORTHROP, P. W. C., DE, S., SANTHANAGOPALAN, S., BRAATZ, R. D. & SUBRAMANIANA, V. R. 2012. Modeling and Simulation of Lithium-Ion Batteries from a Systems Engineering Perspective. *J. Electrochem. Soc*., 159, 3, R31~R45.

(2) CHO, M., SON, Y. M., NAH, D. B., KIL, S. C. & KIM, S. W. 2010 Lithium-Ion Batteries for Plug-In Hybrid Electric Vehicle. *J. Energy Engineering*, 19, 2, 81~91.

Acceptance ID: F3R9-O

Development of Metal Oxide-Supported Metal and Ordered Intermetallic Nanoparticles to Enhance the Oxygen Reduction Reaction in PEMFC

Fuma Ando (Kanagawa University, Japan)

Recently, there has been an increased interest in polymer electrolyte membrane fuel cells (PEMFCs). PEMFCs have energy conversion efficiencies as high as 80%. However, the durability of PEMFCs has been recently recognized as one of the most important issues to be addressed before the commercialization of PEMFCs. Pt surface area loss due to carbon corrosion and Pt nanoparticle (NP) dissolution from the carbon support and/or aggregation on the carbon support are considered one of the major problems to address. Carbon black (CB) is normally used as a support material for the Pt catalyst to maximize the mass activity of the catalyst. However, the oxidized sites of the CB accelerate the degradation of the support material for Pt NPs. The CB will oxidize at edge sites because polar functional groups can form at those sites. The polar functional groups will be further oxidized and finally corroded away. Recently, carbon nanotubes (CNTs) have been proposed as promising support materials for Pt NPs because the CNT supports exhibit high conductivity and mass transport capability as well as high chemical stability. However, there are no novel binding sites for adsorbing Pt ions on the CNT surfaces, although the surfaces of CNT are composed of non-oxidized graphitic carbon. Usually, functional groups are generated on the external walls to make the binding sites for Pt source using harsh oxidative treatments, such as refluxing in HNO_3 or H_2SO_4-HNO_3. However, the treated CNT surfaces will suffer serious carbon corrosion under conditions such as low pH, high potential, high humidity, and high temperature (~80 °C). A new methodology for the deposition of catalyst NPs on CNT surfaces should be developed that satisfies both requirements for high NP dispersion and chemical stability. Recently, nanocrystalline TiO_2 as a catalyst support has received increasing attention due to its inherent stability in the electrochemical environment, its commercial availability, and its enhancement of electrocatalytic activity due to its corrosion resistance and the synergistic effect between NPs and TiO_2. We considered the preparation of PtPb/TiO_2 on cup-stacked carbon nanotube (CSCNT) to enhance the oxygen reduction reaction (ORR). CSCNTs are tubular carbon nanostructures with a stacked cup arrangement of graphene layers. Therefore, the edges of the graphene layers are densely exposed on the surface of the CSCNT. The graphene edges are used as scaffolds to thoroughly coat the CSCNT surface with TiO_2 layers. The PtPb ordered intermetallic NP electrocatalyst was selectively deposited on the TiO_2 layers. The CSCNT functions as an electron conducting path. Recently, we reported that PtPb/TiO_2 showed enhancement of electrocatalytic activity for the ORR [1]. The nature of the support, the composition of catalytic sites, the sites' interaction with the support, and the electronic structure of the catalytic sites all most likely influenced the observed electrochemical behavior. In this study, PtPb NPs were chemically deposited on small, thin TiO_2 layers that were prepared on CSCNTs. The unique catalytic property of PtPb ordered intermetallic NPs and the strong interaction between PtPb NPs and TiO_2 layers successfully achieved the enhancement of ORR in acidic aqueous solutions. The improved ORR performance of PtPb NPs/TiO_2/CSCNT is not an effect of the CSCNT support material. Rather, the higher performance is due to the interaction between PtPb NPs and TiO_2 [2,3]. The CSCNTs can provide a large amount of structure to PtPb NPs on TiO_2 on the CSCNT surface.

[1] T. Gunji, G. Saravanan, T. Tanabe, T. Tsuda, M. Miyauchi, G. Kobayashi, H. Abe, F. Matsumoto, *Catalysis Science and Technology*, **2014**, **4**, 1436.

[2] Fuma Ando, Takao Gunji, Hikaru Fujima, Tsuyoshi Takeda, Toyokazu Tanabe, Shingo Kaneko, Futoshi Matsumoto, Preparation of PtPb/TiO_2/Cup-Stacked Carbon Nanotube Composite for Enhancement of Electrocatalytic Reaction of Oxygen Reduction Reaction, *Chem Lett.*, **44(12)**, 1741-1743(2015).

[3] Fuma Ando, Toyokazu Tanabe, Takao Gunji, Takashi Tsuda, Shingo Kaneko, Tsuyoshi Takeda, Takeo Ohsaka, Futoshi Matsumoto, Improvement of ORR Activity and Durability of Pt Electrocatalyst Nanoparticles Anchored on TiO_2/Cup-Stacked Carbon Nanotube in Acidic Aqueous Media, *Electrochimica Acta*, **232**, 404-413(2017).

Acceptance ID: FL7Y-P

One-Dimensional Nanomaterials for Energy Storage

Liqiang Mai[*], *Yunlong Zhao*

122 Luoshi Road, Wuhan 430070, Hubei, China
** Email: mlq518@whut.edu.cn*

One-dimensional nanomaterials can offer large surface area, facile strain relaxation upon cycling and efficient electron transport pathway to achieve high electrochemical performance. Hence, nanowires have attracted increasing interest in energy related fields. We designed the single nanowire electrochemical device for in situ probing the direct relationship between electrical transport, structure, and electrochemical properties of the single nanowire electrode to understand intrinsic reason of capacity fading. The results show that during the electrochemical reaction, conductivity of the nanowire electrode decreased, which limits the cycle life of the devices.[1] We have fabricated hierarchical $MnMoO_4/CoMoO_4$ heterostructured nanowires by combining "oriented attachment" and "self-assembly".[2] The asymmetric supercapacitors based on the hierarchical heterostructured nanowires show a high specific capacitance and good reversibility with a cycling efficiency of 98% after 1,000 cycles. Then, we designed the general synthesis of complex nanotubes by gradient electrospinning, including $Li_3V_2(PO_4)_3$, $Na_{0.7}Fe_{0.7}Mn_{0.3}O_2$ and Co_3O_4 mesoporous nanotubes, which exhibit ultrastable electrochemical performance when used in lithium-ion batteries, sodium-ion batteries and supercapacitors, respectively.[3] In addition, we have successfully fabricated a field-tuned hydrogen evolution reaction (HER) device with an individual MoS_2 nanosheet to explore the impact of field effect on catalysis.[4] We also constructed a new-type carbon coated $K_{0.7}Fe_{0.5}Mn_{0.5}O_2$ interconnected nanowires through a simply electrospinning method. The interconnected nanowires exhibit a discharge capacity of 101 mAh g^{-1} after 60 cycles, when measured as a cathode for K-ion batteries.[5] Our work presented here can inspire new thought in constructing novel one-dimensional structures and accelerate the development of energy storage applications.

Keywords: One-dimensional nanomaterials, electrochemical device, K-ion batteries

Reference

[1] L. Q. Mai, Y. J. Dong, L. Xu, C. H. Han. *Nano Lett*. 2010, **10**, 4273;
[2] L. Q. Mai, F. Yang, Y. L. Zhao, X. Xu, L. Xu, Y. Z. Lou. *Nature Commun*. 2011, **2**, 381;
[3] C. J. Niu, J. S. Meng, X. P. Wang, C. H. Han, M. Y. Yan, K. N. Zhao, X. M. Xu, W. H. Ren, Y. L. Zhao, L. Xu, Q. J. Zhang, D. Y. Zhao, L. Q. Mai. *Nature Commun*. 2015, **6**, 7402;
[4] J. H. Wang, M. Y. Yan, K. N. Zhao, X. B. Liao, P. Y. Wang, X. L. Pan, W. Yang, L. Q. Mai. *Adv. Mater*. 2017, DOI: 10.1002/adma.201604464;
[5] X. P. Wang, X. M. Xu, C. J. Niu, J. S. Meng, M. Huang, X. Liu, Z. A. Liu, L. Q. Mai. *Nano Lett*. 2017, **17**, 544.

Acceptance ID: G8Y8-P

Graphene-platelets-wrapped Li3VO4 as an applicable anode for high-performance lithium ion batteries

X. J. Zhu

College of Chemistry, Central China Normal University
xjzhu@mail.ccnu.edu.cn

A simple sol-gel method following heat treatment is utilized to synthesize reduced-graphene-oxide-wrapped Li_3VO_4 (Li_3VO_4@rGO). X-ray diffraction, Raman spectroscopy and high resolution transmission electron microscopy show that Li_3VO_4 particles are tightly wrapped by rGO platelets, and the size of Li_3VO_4 is tuned with the fraction of rGO in the hybrid. Electrochemical measurements show that the Li_3VO_4@rGO hybrid with 11.0 *wt*.% rGO displays a reversible capacity of 579.8 mAh g^{-1} in the first cycle, and 489.0 mAh g^{-1} after 50 cycles, much higher than theoretical capacity of 394 mAh g^{-1} from Li_3VO_4. In a Li_3VO_4@rGO-$LiFePO_4$/C full cell, the anode delivers a capacity of 499.1 mAh g^{-1} at a rate of 0.05 C and 354.4 mAh g^{-1} at a rate of 0.5 C, as well as a capacity of 310.0 mAh g^{-1} after 100 cycles (@0.5 C), indicating that Li_3VO_4@rGO hybrids can be used as a practically high-performance anode material for lithium ion batteries.

Acceptance ID: gchk-O

Iron series metal-organic frameworks for electrochemical energy storage

*Huan Pang, Huaiguo Xue**

College of Chemistry and Chemical Engineering, Yangzhou University
Yangzhou, 225009, Jiangsu, P. R. China
E Mail/ Contact Détails: ***chhgxue@yzu.edu.cn***

Iron series metal-organic frameworks materials with controllable structures, large surface areas and adjustable pore sizes have attracted wide public concern for next-generation electrochemical energy-storage devices. Based on the current most advanced research, this review mainly introduces the application of iron series metal-organic frameworks and their derivatives in supercapacitors and batteries. The most recent advances in the area of iron series metal-organic frameworks electrode materials for supercapacitors and batteries are summarized.

Keywords: Iron series, metal-organic frameworks materials, supercapacitors, batteries

Acceptance ID: GFWG-P

Role of dyes as energy materials in photogalvanic cells for solar energy conversion and storage

Chhagan Lal

Department of Chemistry, Harcourt Butler Technical University, Kanpur, India
E-mail: c.lal9940@gmail.com /c_lal12@rediffmail.com

First of all in 1925 Rideal and Williams [1] observed the photogalvanic effect but it was systematically investigated by Rabinowitch [2] in iron thionine system long back.It was followed by other investigators from time to time [3-7].Photogalvanic effect was studied in photogalvanic cell containing EDTA as reductant, mixed dyes (combination of two dyes) as phtotosensitizer i.e. EDTA-NMB-SFO, EDTA-NMB-FG, EDTA-BG-FG, EDTA-BG-CB, EDTA-NMB-CB. The used reductant was Ethylene diamine tetra acetic acid and photosensitizers were new methylene blue (NMB), Safranine-O-(SFO), Fast Green (FG), Brilliant Green (BG), Celestine Blue (CB), in different combinations. The photopotential, photocurrent, conversion efficiency, power of the cells and performance of the photogalvanic cells were determined. The effects of various parameters on the electrical output of the cell were observed and a mechanism has also been proposed for the generation of photocurrent in photogalvanic cells using dyes as photosensitizers. The role of dyes as energy materials was investigated and energy conversion and storage potential of photogalvanic cell was also investigated. The photogalvanic cells (systems) can be used at power level for 95.0, 90.0, 72.0, 65.0, 45.0 minutes in the dark respectively.

Mechanism: The mechanism of generation of photocurrent in photogalvanic cells can be proposed as follows:

Illuminated Chamber

$$D + D^1 \xrightarrow{h\nu} + D^{1*} \quad (1)$$

$$D^* + D^{1*} + 2R \longrightarrow D^- + D^{1-} + 2R^+ \quad (2)$$

At Platinum electrode

$$D^- + D^{1-} \longrightarrow D + D^1 + 2e^- \quad (3)$$

Dark Chamber

Counter electrode

$$D + D^1 + 2e^- \longrightarrow D^- + D^{1-} \quad (4)$$

$$D^- + D^{1-} + 2R^+ \longrightarrow D + D^1 + 2R \quad (5)$$

Where $D + D^1$, $D^* + D^{1*}$, $D^- + D^{1-}$, R and R^+ are the mixed dyes, their excited forms, leuco or semi leuco forms and reductant and its oxidized form, respectively.

Key words: Photosensitizer, photogalvanic cell, conversion efficiency, fill factor

References:

[1] Rideal, E.K. and Williams, D.C., 1925. The action of light on the ferrous ferric iodine iodide equilibrium, *J. Chem. Soc.Trans.*, 127,258-269.

[2] Rabinowitch E., 1940.The photogalvanic effect, part I & II, *J.Chem.Phys.* 8,551-559,560-566.

[3]Kaneko M. and Yamada A., 1977.Photopotential and photocurrent induced by a tolusafranine-ethylenediaminetetraaceticacid system *J. Phys. Chem.*, 81, 1213-1215.

[4]Albery, W.J., Archer, M.D., 1977. Optimum efficiency of photogalvanic cells for solar energy conversion, *Nature*, 270,399-402.

[5] Gangotri, K.M. and Lal, C., 2000. Studies in photogalvanic effect and mixed dyes system: EDTA-methylene blue +toluidine blue, *Int. J. Energy Res.*, 24,365-371.

[6] Lal**,** C., 2007. Use of mixed dyes in a photogalvanic cell for solar energy conversion and storage: EDTA-thionine-azur-B system, *J. Power Sources*, 164,926-930.

[7]Yadav, S. and Lal, C., 2013.Optimization of performance characteristics of a mixed dyes based photogalvanic cell for efficient solar energy conversion and storage, *J.Energy Conversion and Management*, 66,271-276.

Acceptance ID: GU9F-O

Carbon nanofiber networks for stable lithium metal anodes with high coulombic efficiency and long cycle life

*Anyi Zhang†, Xin Fang†, Chenfei Shen†, Yihang Liu‡, Chongwu Zhou‡**

Lithium metal is considered as one of the most promising candidates as anode material for high-energy-density Li-ion batteries. However, the dendritic growth of Li metal during the plating/stripping process has severely reduced the Coulombic efficiency and caused safety problems, which has for a long time been a key issue that limited the application of Li metal anodes. Herein, we demonstrate a distinctive design for dendrite-free deposition of Li by modifying the Cu current collector with a three-dimensional carbon nanofiber (CNF) network. Due to the large surface area and high conductivity of the CNF network, Li metal can insert into and deposit onto CNF directly and no dendritic Li metal was observed, leaving a flat Li metal surface. With Li metal as the counter electrode for Li deposition, an average Coulombic efficiency of 99.9% was achieved for over 300 cycles, at a large current density of 1 mA/cm^2 and 2 mA/cm^2 with a high loading of 1 mAh/cm^2 of deposited Li. The scalable preparation method and impressive results achieved here demonstrated the potential of applying our design in the development of dendrite-free Li metal anode in future.

Acceptance ID: GW2B-P

Electrochemical Fabrication of Nanostructured Iron Oxide for Capacitive Application

Xiao-Chun Lu, Xiaoxia Liu

Department of Chemistry, Northeastern University, Shenyang, 110819, China
xxliu@mail.neu.edu.cn

Iron oxide/oxyhydroxides, hematite (α-Fe_2O_3) in particular, with the advantages of earth abundant, low cost and environmental friendliness have been widely studied as electrode materials for electrochemical energy storage (*e.g.* supercapacitors, Ni-Fe batteries and Li-ion batteries). However, during synthesis processes, hematite particles usually suffer from self-aggregation because of their high surface energy and thus grow into large blocks, leading to large "dead volume" which is inaccessible for electrolyte ion. Their advantage of the high theoretical capacity is also offset by the poor electrical conductivity.

In this work, nanostructured α-Fe_2O_3 was fabricated on conductive graphite foil through electrochemical deposition and following thermal treatment. Influences of pH value and iron source concentration in electrochemical deposition solution, as well as annealing temperature, on iron oxide/iron oxide precursor nanostructure fabrication and their pesudocapacitive performance were studied by cyclic voltammetry, constant current charge-discharge and electrochemical impedance spectroscopy. The annealed α-Fe_2O_3 electrode with 3D nanorod network architecture displayed a high specific capacitance of 622 F g^{-1} at 2 A g^{-1} and good cycling stability (87.5% capacitance retention after 5000 charge-discharge cycles). We believe this electrochemistry-annealing approach could open up new opportunities for fabricating high-performance hematite based materials for electrochemical energy storage.

Acknowledgement

We gratefully acknowledge financial supports from the National Natural Science Foundation of China (Grant No. 21673035).

Keywords: Electrochemical deposition, nanostructured iron oxide, graphite foil, supercapacitor

Acceptance ID: H7EA-P

Film and Interface Engineering for Efficient Planar Heterojunction Perovskite Solar Cells

*Yangyang Wang, Ningning Song, Sen Wang, Zengrong Li and Xianyu Deng**

Research Center for Advanced Functional Materials and Devices, Shenzhen Key Laboratory of Advanced Materials, School of Materials Science and Engineering, Shenzhen Graduate School, Harbin Institute of Technology, Shenzhen, 518055, (PR China)

Email: xydeng@hit.edu.cn

KEYWORDS: Crystal growth; Organic amine; Hydrochlorides; Interface; MoS_2

The film quality of perovskite ($CH_3MH_3PbI_3$) is very crucial to the performance of perovskite solar cells. Here we present two methods to grow high quality perovskite films *via* a simple and rapid process. Polymer PAN and a series of hydrochlorides with different organic amine cations were introduced into $CH_3NH_3PbI_3$ solution as a additive to obtain solar cells with high power conversion efficiency (PCE). Based on the device performance, a 2D material MoS_2 as an interfacial layer makes perovskite solar cells with a planar heterojunction have high PCE up to 17.06% as well as a significant enhancement of stability.

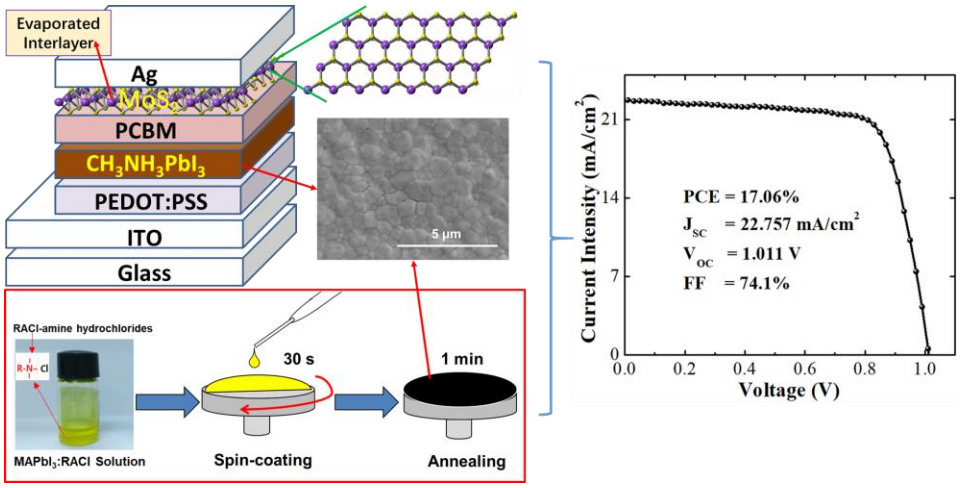

Acceptance ID: JWRR-P

Effects of Residual Lithium in the Precursors of $Li[Ni_{1/3}Co_{1/3}Mn_{1/3}]O_2$ on Their Lithium-ion Battery Performance

Minsang Jo[1], Heesuk Ku[1], Sanghyuk Park[1], Junho Song[2], Kyungjung Kwon[1,]*

[1]Department of Energy & Mineral Resources Engineering, Sejong University, Seoul 05006, Republic of Korea.
[2]Korea Electronics Technology Institute, 25, Saenari-ro, Bundang-gu, Seongnam-si, Gyeonggi-do 13509, Republic of Korea.
M. Jo; e-mail: alstkdtkd@gmail.com
K. Kwon; Fax: 82-2-3408-4344, Tel.: 82-2-3408-3947, e-mail: kfromberk@gmail.com

As the consumption of lithium-ion batteries (LIBs) increases, the recycling of spent LIBs becomes necessary. Because there are valuable metals such as Li, Ni and Co in the cathode active materials of LIBs, the recycling of LIB cathode has gathered more attention than other components, and can be conducted via hydrometallurgical route comprising leaching and co-precipitation processes. If the leach liquor of spent LIB cathode is directly used as a co-precipitation solution for the precursor of LIB cathode active materials, Li ions usually exist, which is not the case for the synthesis of new cathode active materials. In the usual preparation of Li cathode active materials such as $Li[Ni_xCo_yMn_z]O_2$ (NCM), Li ions are introduced after the synthesis of precursors. In this paper, the effect of residual Li in precursors on their LIB performance was investigated.

We synthesized precursors by hydroxide co-precipitation method using aqueous solutions including $NiSO_4$, $CoSO_4$, $MnSO_4$, and Li_2SO_4, which could simulate the leach liquor of NCM with sulfuric acid. To control the Li content of precursors, they were washed with distilled water for multiple times. A mixture of precursor and Li_2CO_3 was heated at 1000℃ for 8 hours to synthesize cathode active materials. The Li content of three kinds of precursors (one without Li_2SO_4, one with Li_2SO_4 and 6 time washing, and one with Li_2SO_4 with no washing) was 0, 0.15 and 1.44 mol% respectively. The corresponding active materials from the above precursors showed the initial discharge capacity of 161.08, 159.56 and 150.79 mAh/g respectively. The rate capability of the active materials also became aggravated with the increase in the amount of Li in the precursors although the Li content in the active materials was nominally identical. This decrease in the LIB performance can be attributed to cation mixing in the active materials, which were confirmed by the calculated intensity ratio of (003) and (104) peaks in XRD analysis. In summary, the LIB performance of NCM active materials can be aggravated by the presence of Li in precursors, and this aspect should be considered in the resynthesis of cathode active materials for LIB recycling.

Acknowledgements
This study was supported by the R&D Center for Valuable Recycling(Global-Top R&BD Program) of the Ministry of Environment.

Keywords: lithium ion battery, cathode, precursor, recycling, lithium

[1] LEE, M.-H., KANG, Y.-J., MYUNG, S.-T. & SUN, Y.-K. 2004. Synthetic optimization of $Li[Ni_{1/3}Co_{1/3}Mn_{1/3}]O_2$ via co-precipitation. *Electrochimica Acta*, 50, 939–948.

[2] ZHANG, X., XIE, Y., LIN, X., LI, H. & CAO, H. 2013. An overview on the processes and technologies for recycling cathode active materials from spent lithium-ion batteries. *Journal of Material Cycles and Waste Management*, 15, 420-430.

[3] PARK, S.-H., KANG, S.-H., BELHAROUAK, I., SUN, Y.K. & AMINE, K. 2008. Physical and electrochemical properties of spherical $Li_{1+x}(Ni_{1/3}Co_{1/3}Mn_{1/3})_{1-x}O_2$ cathode materials. *Journal of Power Sources*, 177, 177-183.

Acceptance ID: K9PF-P

A simple approach to fabricate an efficient polymer solar cells with non-conjugated electrolytes as the cathode buffer layer

Joo Hyun Kim[*], *Youn Hwan Kim, Mutia Anissa Marsya, Nadhila Sylvianti*

[1]*Department of Polymer Engineering, Pukyong National University, Busan 48547, Korea*
**e-mail :jkim@pknu.ac.kr*

Recently, bulk-heterojunction (BHJ) polymer solar cells (PSCs) have attracted attention due to their high potential for application as clean energy sources, as they are lightweight, flexible, and capable of large-area fabrication. The power conversion efficiencies (PCEs) of PSCs have improved rapidly. PCEs of over 10% have been reported, due to tremendous efforts made in areas such as the synthesis of new conjugated polymers / oligomers and interface engineering. Charge transport and collection properties at both electrode interfaces are crucial factors for improving the efficiency of PSCs. Significant work has been undertaken to improve interfacial properties, such as alcohol / water soluble conjugated polymer electrolytes (CPEs), non-conjugated polymers, alcohol / water soluble conjugated or non-conjugated small molecules (SMs), and polar solvent treatment. These materials enable the fabrication of a multilayer device without destroying a pre-coated organic semiconducting layer by orthogonal solubility in the processing solvents. PSCs with a thin film of these materials as an interlayer at the cathode interfaces show dramatically improved performance, relative to the devices manufactured without these materials as an interfacial layer. It has been reported that the ionic functionalities, at the end of side chains on the conjugated polymer backbone, induce the formation of favorable interface dipole, which leads to a decrease in the work function of the cathode. Non-conjugated polymers or SMs[8] can also reduce the work function of the cathode due to the formation of an interface dipole. In comparison with polymeric materials, SMs have advantages such as ease of synthesis and purification. In addition, SMs do not have batch-to-batch variation, or broad molecular weight distribution.

In this presentation, various type of cathode buffer layer materials based on either conjugated or non-conjugated electrolytes and their applications in organic solar cells will be discussed.

Keywords : Polymer Solar Cell, Bulk-heterojuction, Cathode buffer Layer

A simple approach to fabricate an efficient polymer solar cells with non-conjugated electrolytes as the cathode buffer layer

Joo Hyun Kim, Youn Hwan Kim, Mutia Anissa Marsya, Nadhila Sylvianti*

1Department of Polymer Engineering, Pukyong National University, Busan 48547, Korea
**e-mail: jkim@pknu.ac.kr*

Recently, bulk-heterojunction (BHJ) polymer solar cells (PSCs) have attracted attention due to their high potential for application as clean energy sources, as they are lightweight, flexible, and capable of large-area fabrication. The power conversion efficiencies (PCEs) of PSCs have improved rapidly. PCEs of over 10% have been reported, due to tremendous efforts made in areas such as the synthesis of new conjugated polymers / oligomers and interface engineering. Charge transport and collection properties at both electrode interfaces are crucial factors for improving the efficiency of PSCs. Significant work has been undertaken to improve interfacial properties, such as alcohol / water soluble conjugated polymer electrolytes (CPEs), non-conjugated polymers, alcohol / water soluble conjugated or non-conjugated small molecules (SMs), and polar solvent treatment. These materials enable the fabrication of a multilayer device without destroying a pre-coated organic semiconducting layer by orthogonal solubility in the processing solvents. PSCs with a thin film of these materials as an interlayer at the cathode interfaces show dramatically improved performance, relative to the devices manufactured without these materials as an interfacial layer. It has been reported that the ionic functionalities, at the end of side chains on the conjugated polymer backbone, induce the formation of favorable interface dipole, which leads to a decrease in the work function of the cathode. Non-conjugated polymers or SMs8 can also reduce the work function of the cathode due to the formation of an interface dipole. In comparison with polymeric materials, SMs have advantages such as ease of synthesis and purification. In addition, SMs do not have batch-to-batch variation, or broad molecular weight distribution.

In this presentation, various type of cathode buffer layer materials based on either conjugated or non-conjugated electrolytes and their applications in organic solar cells will be discussed.

Keywords: Polymer Solar Cell, Bulk-heterojuction, Cathode buffer Layer

Acceptance ID: KL7D-P

Novel metal oxide interfacial materials for solution process solar cell

Pingli Qin [1,3], Guang Yang[1,2], Guojia Fang[2] and Gang Li[1]

The Department of Electronic and Information Engineering, The Hong Kong Polytechnic University, Hong Hum, Kowloon, Hong Kong SAR, China
School of Physics and Technology, Key Laboratory of Artificial Micro- and Nano-structures of the Ministry of Education and School of Physics and Technology, Wuhan University, Wuhan 430072, P. R. China
School of Science, Wuhan Institute of Technology, Wuhan, Hubei 430073, P. R. China

Carrier transport material plays critical role in solution processed advanced solar cells such as organic polymer solar cell (OPV) and hybrid perovskite solar cells. High mobility, earth-abundant, environmentally-stable and nontoxic are the focus of electron transport and hole transport materials (ETMs and HTMs) research.

In this talk, we will present our work on low temperature, solution processed metal oxides as ETM and HTM in organic polymer solar cell and hybrid perovskite solar cells. Copper based binary metal oxide HTMs has achieved perovskite solar cell PCE of over 17% on glass, and 15.53% on flexible PET/ITO substrate. Solution processed Tin oxide (SnO_2) nanostructures are also applied in OPV and provskite solar cells as ETM, and show promising results in efficiency, stability and processability. We will also discuss the potential of these interfacial materials in tandem solar cells.

Acceptance ID: M6AD-P

Synthesis of CoNi Binary hydroxides Hetero-structure via Electrodeposition and Precursor Adjustment with Enhanced Capacitive Performance for Asymmetric Supercapacitor

Min Wei[1], Qingsong Huang[1], Yanping Zhou[2], Zhu Peng[1], Wei Chu[1]*

[1]School of Chemical Engineering, Sichuan University, Chengdu 610065, China
[2]School of Electronics and Information Engineering,
Sichuan University, Chengdu 610064, China
** Presenting & Corresponding author. E-mail: chuwei1965@scu.edu.cn*
Tel.: +86 028 85403836; Fax: +86 028 85461108

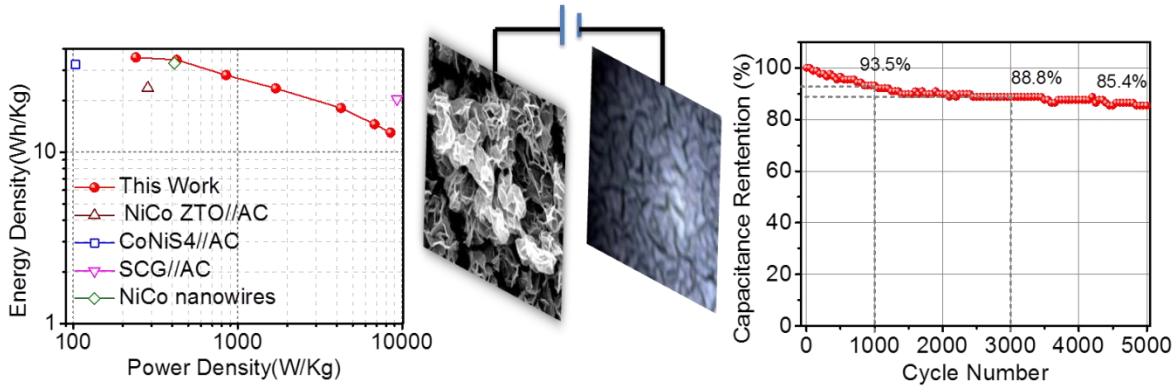

Figure 1

A hierarchical structure composed of the cobalt-nickel binary hydroxides (BH) supported on a nickel foam scaffold (CoNi BHs/NF) was synthesized by a controllable electrodeposition technique, using precursors with different anions, for high efficiency electrode materials in the asymmetric supercapacitor. The morphology and electrochemical performance of the CoNi BHs can be controlled by adjusting the molar ratio of precursors with different anions during the electrodeposition. In the investigation of cyclic voltammetry tests and galvanostatic charge-discharge, for the optimized sample, the hybrid delivered a high specific capacitance of 1587.5 F g^{-1} at a current density of 0.5 A g^{-1} and remained 1155 F g^{-1} at high current density of 10 A g^{-1}. The good performances were enabled and explained as that there were increased interlayer spacing, special structure and synergistic effects. Furthermore, there were a high energy density of 34.5 Wh kg^{-1} and a power density of 6800 W kg^{-1} in our experiments of asymmetric supercapacitor device.

Keywords: CoNi binary hydroxides, Electrodeposition synthesis, High performance electrode material, precursor, Asymmetric supercapacitor device

[1] WU, X., JIANG, L., LONH, C., WWI, T. & FAN, Z. 2015. Dual Support System Ensuring Porous Co–Al Hydroxide Nanosheets with Ultrahigh Rate Performance and High Energy Density for Supercapacitors. *Advanced Functional Materials*, 25, 1648-1655.

[2] YAN, J., WANG, Q., WEI, T., & FAN, Z. J. 2014. Recent Advances in Design and Fabrication of Electrochemical Supercapacitors with High Energy Densities. *Advanced Energy Materials*, 4, 1300816-1300859.

[3] WANG, X., SUMBOJA, A., LIN, M., YAN, J. & LEE, P. S. 2012. Enhancing Electrochemical Reaction Sites in Nickel–cobalt Layered Double Hydroxides on Zinc Tin Oxide Nanowires: a Hybrid Material for An Asymmetric Supercapacitor Device. *Nanoscale*, 4, 7266-7272.

[4] PENG, Z., GUO, Z. L., CHU, W. & WEI M. 2016. Facile Synthesis of High-Surface-area Activated Carbon from Coal for Supercapacitors and High CO_2 Sorption. *RSC Adv*ances, 6, 42019–42028.

[5] ZHU, Y. C., CHU, W., WANG, N., LIN, T., YANG, W., WEN, J. & ZHAO, X. S. 2015. Self-Assembled Ni/NiO/RGO Heterostructures for High-performance Supercapacitors. *RSC Adv*ances, 5, 77958–77964.

Acceptance ID: MCE5-I

Subphthalocyanines and Phthalocyanines for Molecular Photovoltaics

Hector Carrascosa, Giulia Lavarda, Lara Tejerina, D. Paola Medina, German Zango, Olga Trukhina, Mine Ince, M. Victoria Martínez, Tomás Torres[1]

[1] *Autonoma University of Madrid and IMDEA-Nanoscience, 28049 Madrid, Spain.*
E Mail : tomas.torres@uam.es

Subphthalocyanines (SubPcs)[1-3], phthalocyanine analogues, are intriguing compounds made of three diiminoisoindoline units N-fused around a boron atom. Their 14 pi-electron aromatic core associated with their curved structures render them appealing building blocks for the construction of multicomponent photo- or electroactive assemblies. SubPc pi-systems can be also organized at supramolecular level and used and active elements in molecular photovoltaics, in both SHJ and BHJ. On the other hand, engineered phthalocyanines has been used as Hole-Transporting Materials in Perovskite Solar Cells reaching Power Conversion Efficiency of 17.5% [3].

Keywords: Subphthalocyanines, Phthalocyanines, Solar Cells, Perovskites

[1] VERREET, B., CHEYNS, D., HEREMANS, P., STESMANS, A., ZANGO, G., CLAESSENS, C. G., TORRES, T. & RAND, B. P. 2014. Decreased Recombination Through the Use of a Non-Fullerene Acceptor in a 6.4% Efficient Organic Planar Heterojunction Solar Cell. *Adv. Energy Mater.* 4, 1301413.

[2] CHO, K., TRUKHINA, O., ROLDÁN-CARMONA, C., INCE, M., GRATIA, P., GRANCINI, G., GAO, P., MARSZALEK, T, PISULA, W., REDDY, P. Y., TORRES & T, NAZEERUDDIN, M. K. 2016. Molecularly Engineered Phthalocyanines as Hole-Transporting Materials in Perovskite Solar Cells Reaching Power Conversion Efficiency of 17.5%. *Adv. Ener. Mater.* In press. DOI: 10.1002/aenm.201601733465.

[3] DUAN, C., ZANGO, G., GARCÍA IGLESIAS, M., COLBERTS, F. J. M., WIENK, M. M., MARTÍNEZ-DÍAZ, M. V., JANSSEN, R. A. J. &TORRES, T. 2017. The Role of the Axial Substituent in Subphthalocyanine Acceptors for Bulk-Heterojunction Solar Cells" *Angew. Chem. Int. Ed*. 56, 148–152.

Acceptance ID: NHTA-O

Solid Flexible Supercapacitors Based on Organized Mesoporous TiN Films and Nanostructural Graft Copolymer Electrolytes

*Jung Yup Lim, Jin Kyu Kim, Chang Soo Lee, Jong Hak Kim**

Department of Chemical and Biomolecular engineering, Yonsei University
E-mail: jonghak@yonsei.ac.kr

We prepared organized mesoporous titanium nitride (om-TiN) films with large surface area, high porosity, and good interconnectivity on Ti substrates by nitration of TiO_2 templated by an amphiphilic graft copolymer, poly(vinyl chloride)-*graft*-poly(oxyethylene methacrylate) (PVC-*g*-POEM). This resulted in a much higher specific capacitance compared with randomly organized TiN (ran-TiN) films. Large electrodes (15 cm×15 cm) were successfully fabricated and their electrochemical performance did not change when bent. We also synthesized a highly ionic conductive amphiphilic nanostructured polymer electrolyte with good flexibility for solid-state flexible supercapacitors. It is based on a block-graft copolymer, i.e., poly(styrene-*b*-butadiene-*b*-styrene)-g-poly(oxyethylene methacrylate) (SBS-g-POEM) synthesized via one-pot free-radical polymerization. A well-defined microphase-separated structure with good interconnectivity at the nanoscale was observed. The performance of supercapacitors based on the SBS-g-POEM electrolyte was much higher than that of the widely used conventional PVA/H_3PO_4 electrolyte.

Keywords: supercapacitor, mesoporous TiN, Graft Copolymer, solid electrolyte.

[1] D. J. Kim, J. K. Kim, J. H. Lee, H. H. Cho, Y.-S. Bae, J. H. Kim, J. Mater. Chem. A, 2016, 4, 12497.

[2] J. Y. Lim, J. K. Kim, J. M. Lee, D. Y. Ryu, J. H. Kim, J. Mater. Chem. A. 2016, 4, 7848.

Acceptance ID: NRAE-P

Photoelectrochemical Performance of $CuIn_3Se_5$ for Water Splitting System and Surface Defect Site Dependency

Joo Sung Kim,[1] Young Been Kim,[1] Seung Ki Baek,[1] Young Dae Yun[1] and Hyung Koun Cho[1,]*

[1]School of Advanced Materials Science and Engineering, Sungkyunkwan University, 2066, Seobu-ro, Jangan-gu, Suwon, Gyeonggi-do 16419, Republic of Korea
Corresponding author: chohk@skku.edu

Photoelectrochemical (PEC) water splitting system is one of the attractive energy harvesting methods due to the exhaustion of fossil energy problems. Water decomposition is suitable processes for ideally obtaining pure hydrogen for long term storage. For efficient PEC devices, a narrow band gap and chemical stability is one of the important factors. The search of photo-active materials with suitable band gap led us to research chalcopyrite compounds. Recently, many papers are reported about the physical properties of $CuInSe_2$ and the feasibility of photovoltaics has been reported, and Cu-In-Ga-Se compounds show high solar energy conversion efficiency of 20.4 %. However, just fewer papers dealing with the physical properties of $CuIn_3Se_5$ have been reported for photoanode. In extension, our study presents a work relative to $CuIn_3Se_5$ which is n-type semiconductor.

$CuIn_3Se_5$ is a suitable photo-absorption material for PEC water splitting system because of its adequate direct band gap of 1.3 eV, which can absorb a significant part of the solar spectrum. The holes excited into the valence band of $CuIn_3Se_5$ are energetic enough to be transferred to water for oxygen evolution. Nevertheless, $CuIn_3Se_5$ photo-anode has a critical limitation in terms of high PEC performance. The high performance of $CuIn_3Se_5$ based PEC cells has been limited because of secondary phases such as Cu_2Se, and surface defect sites which cause a decline of charge transfer at the interface between electrolyte and surface. In addition, chemically unstable property in aqueous environments reduces the performance, despite their several advantages such as suitable band gap and band position.

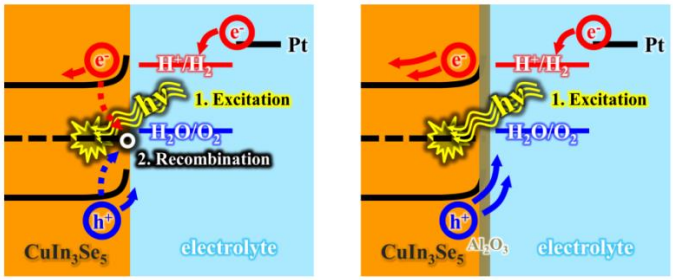

Bare $CuIn_3Se_5$ Al_2O_3 covered $CuIn_3Se_5$

In this work, at first to enhance the photo-absorption and stability performance, we fabricated annealing process to synthesize the $CuIn_3Se_5$ compound. And then, we optimized the Al_2O_3 passivation layer growth process for improving the surface condition. Enhanced surface condition of $CuIn_3Se_5$ with Al_2O_3 passivation layer shows a high photo-absorption performance it because of suppressed the charge recombination on the surface, and good stability. A high photocurrent with only one photo-absorption layer $CuIn_3Se_5$ is highly significant result for PEC water splitting system.

Acceptance ID: NV4F-P

Straining Pd nanoshells: Tuning electrocatalytic properties towards formic acid oxidation and CO_2 reduction.

David J. Fermin

School of Chemistry, University of Bristol, Cantocks Close, Bristol BS8 1TS, UK

Thin metal overlayers on foreign supports can exhibit very distinctive electrocatalytic activity with respect to bulk materials. The activitity of these systems are often linked to the so-called ligand and strain effects, which are rather difficult to dissentangle experimentally. In this contribution, we shall establish quantitative correlations between the electrocatalytic properties of thin Pd shells on Au cores and the effective Pd strain as probed by selected area electron diffraction. The electrocatalytic oxidation of adsorbed CO (CO_{ads}) and HCOOH, as well as CO_2 reduction are investigated employing differential electrochemical mass spectrometry (DEMS), on-line electrochemical mass spectrometry (OLEMS) and in-situ Fourier transform infrared (FTIR) spectroscopy. Increasing Pd shells from 1.3±0.1 (CS1) to 9.9±1.1 nm (CS10) promotes an effective strain relaxation from 3.5 to less than 1%. In situ FTIR studies show that the mean CO_{ads} coverage and oxidation mechanism at the Pd nanoshells is affected by electronic effects introduced by the Au core. In particular, the potential dependence of the CO stretching band (Stark slope) reveals that the orbital coupling of CO to Pd is weaker for thinner (strain) Pd shells. FTIR spectroscopy also reveals the presence of OH_{ads},bands in the case of CS10, but not on CS1. This behaviour has important consequences in the oxidation of HCOOH, which occurs more readily at relaxed Pd shells (CS10). In the case of CO_2 reduction, DEMS and OLEMS show a clear change in product selectivity from primarily CO at CS1 particles to HCOOH, CH_4 and C_2H_6 at CS10 nanostructures. DFT calculations are used to estimate the contributions of the so-called ligand and strain effects on the local density of states of the Pd *d*-band. The calculations confirm that the key parameters contributing to the change in mechanism is the effective lattice strain.

Acceptance ID: PER5-O

Semiconducting eutectic materials for photoelectrochemical water splitting

J. Sar[1], K. Kołodziejak[1], K. Wysmułek[1], P. Osewski[1], A. Trenczek-Zajac[2], M. Radecka[2], D.A. Pawlak[1,3]

[1]Institute of Electronic Materials Technology, Wolczynska 133, 01-919 Warsaw, Poland
[2]AGH University of Science and Technology, Faculty of Materials Science and Ceramics, 30 Mickiewicza Ave., 30-059 Cracow, Poland
[3]Centre of New Technologies, University of Warsaw, Banacha 2C, 02-097 Warsaw, Poland
jarosław.sar@itme.edu.pl

Nowadays one of the most important questions is to find alternative fuel that can supply running out conventional fossil fuels. Hydrogen can be found as alternative source of energy mainly due to high energy conversion efficiency, carbon free emission and ability to be produced from renewable sources. One of the ways to produce clean hydrogen is photoelectrochemical (PEC) water splitting where hydrogen and oxygen are produced directly from water under the solar energy.

The Laboratory of Functional Materials at the Institute of Electronic Materials Technology, proposed the application of semiconducting eutectic materials as ~~a~~ photosensitive electrode materials for hydrogen production [1,2]. The use of eutectic materials is beneficial mainly due to: multiple band gaps, various possible eutectic composites, high crystallinity, sharp interfaces and possibility to adjust properties by: doping, annealing and etching.

This work will show photoelectrochemical and photocatalytic results of two eutectic based materials: $SrTiO_3$-TiO_2 and TiO_2-WO_3. Materials were fabricated by directional solidification using the micro-pulling-down method [3,4]. $SrTiO_3$-TiO_2 composite showed increasing photocurrent response during 30h long test and reaching 8.5 mA/cm^2. The advantage of TiO_2-WO_3 composite is that it enables absorption of ultraviolet and visible light. Results show that eutectic materials can be competitive with analogous heterostructures.

Keywords: Eutectic Materials, Photoelectrochemical Cell, Hydrogen Production, Photoanode.

[1] WYSMULEK, K., SAR, J., OSEWSKI, P., ORLINSKI, K., KOLODZIEJAK, K., TRENCZEK-ZAJAC, A., RADECKA, M. & PAWLAK, D.A. 2017. A SrTiO3-TiO2 eutectic composite as a stable photoanode material for photoelectrochemical hydrogen production, *Appl. Catal. B, Environ.*, 206, 538–546.

[2] KOLODZIEJAK, K., SAR, J., OSEWSKI, P., WARCZAK, M., ORLINSKI, K., WYSMULEK, K., SADKOWSKI, A., RADECKA, M. & PAWLAK, D.A. 2017 When eutectics meet the photoelectrochemistry - UV-VIS hybrid photoanodes. *J. Catal.*, Submitted.

[3] PAWLAK, D. A., TURCZYNSKI, S., GAJC, M., KOLODZIEJAK, K., DIDUSZKO, R., ROZNIATOWSKI, K., SMALC J., VENDIK, I., 2010. How far are we from making metamaterials by self-organization? The microstructure of highly anisotropic particles with an SRR-like geometry, *Adv. Funct. Mat.* 20, 1116-1124.

[4] BIENKOWSKI, K., TURCZYNSKI, S., DIDUSZKO, R., GAJC, M., GORECKA, E. & PAWLAK, D.A. 2011. Growth of a plate-shaped SrTiO3-TiO2 eutectic. *Cryst. Growth Des.*, 11, 3935–3940.

Acceptance ID: Q6TU-O

Hollow Prussian Blue Analogue Nanocrystals on Graphene Nanosheets for Efficient Lithium Storage

*Jinpei Hei, Liwei Su, Lianbang Wang,**

(State Key Laboratory Breeding Base of Green Chemistry-Synthesis Technology, College of Chemical Engineering, Zhejiang University of Technology, Hangzhou, P. R. China, 310014, E-mail: wanglb99@zjut.edu.cn)

Prussian blue analogues (PBAs) possess square opening structures and different redox states, which are beneficial for ions insertion/extraction for energy storage systems, while there are two problems. One is that the existence of mass crystal water (generally containing 1-14 H_2O) in PBAs might damage the organic electrolyte system which is sensitive to the moisture and hence seriously hamper their application.[1] Thus, the PBAs should be promising cathode materials for LIBs if minimizing the negative effect of crystal water. The other problem is the relatively low solubility product of PBAs that makes it difficult to be prepared into nanomaterials with high crystalline and good distribution, whereas nanomaterials can bring shorter the electron/Li^+ transport distance and larger surface area for better capability for lithium storage. Although researchers have been focusing on exploiting facile strategies to obtain PBA nanomterials for many years, few positive results are obtained.[2-5]

In this work, we develop a route to synthesize M-PBA nanocrystals by adopting M/graphene nanocomposites as precursors without the help of any surfactants. Amazingly, the prepared M-PBA nanocrystals have hollow structures, ultra small particle size (< 50 nm), and good spatial distribution on graphene nanosheets (GNS). Naturally, the PBA/GNS nanocomposites presented an excellent electrochemical performance for lithium storage. This work may offer a new avenue to exploit PBAs as promising cathode materials in the organic electrolyte LIB system. More importantly, this simple and green method without any surfactants and etching treatment by acid and alkali solution will be a great breakthrough on preparing hollow PBA nanomaterials, which will be attractive for various application fields including chemical catalysis, photonics, biomedical carriers, gas sensors, molecular magnets, and hydrogen storage media.

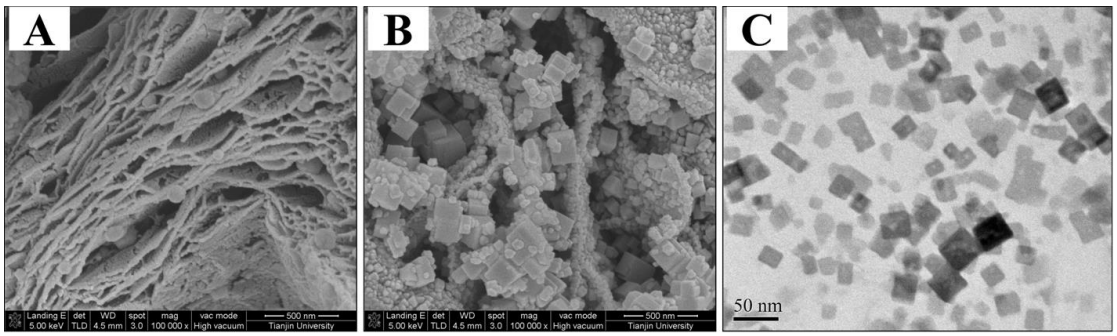

Fig. 1 SEM images of M/GNS (A) and M-PBA/GNS (B). TEM image of M-PBA/GNS

References:

1. C. D. Wessells, R. A. Huggins, Y. Cui, *Nature Commun.* **2011**, *2* 550.
2. L. Su, Y. Jing, Z. Zhou, *Nanoscale* **2011**, *3* 3967.
3. L. Su, J. Jiang, L. Wang, Y. Wang, M. Ren, ChemElectroChem 2015, 2, 789-794.
4. L. Su, Y. Zhong, Z. Zhou, J. Mater. Chem. A 2013, 1, 15158-15166.
5. L. Su, Z. Zhou, X. Qin, Q. Tang, D. Wu, P. Shen, Nano Energy 2013, 2, 276-282.

Acknowledgments: This work was supported by the National Natural Science Foundation of China (21403195 and 21421001) and the Key Research and Development Program (2015C01001 and 2016C01SA500898) of Science and Technology Department of Zhejiang Province.

Acceptance ID: QDU9-P

2D Homologous Organic-Inorganic Hybrids as Light-Absorbers for Planer and Nanorod-based Perovskite Solar Cells

Xiaoyan Gan[a,b], Ou Wang[c], Keyong Liu[c], Xiangjun Du[c], Liling Guo[c]and Hanxing Liu[c]*

a. Hubei Key Laboratory of Advanced Technology for Automotive Components, Wuhan University of Technology, 122 Luoshi Road, Wuhan 430070, China;
b. Hubei Collaborative Innovation Center for Automotive Components Technology, Wuhan University of Technology, 122 Luoshi Road, Wuhan 430070, China;
c. School of Material Science and Engineering, Wuhan University of Technology, 122 Luoshi Road, Wuhan 430070, China

We present the fabrication and characterization of two dimensional (2D) perovskites $(PEA)_2(MA)_{m-1}Pb_mI_{3m+1}$ (PEA=phenylethylammonium, MA=methylammonium, m=1,2,3) for application as light absorbers in solar cells. Films of 2D perovskite series show high stability under humid air, with band gaps decreasing with increasing m values, from 2.36 eV for $(PEA)_2PbI_4$ (m=1) to 1.94 eV for $(PEA)_2(MA)_2Pb_3I_{10}$ (m=3). Owning to the smaller bandgap, favourable vertical growth characteristics, and appropriate energy band structure of $(PEA)_2(MA)_2Pb_3I_{10}$, planer perovskite solar cells based on $(PEA)_2(MA)_2Pb_3I_{10}$ exhibit best cell performance. Incorporation of TiO_2 nanorod arrays into $(PEA)_2(MA)_2Pb_3I_7$ based perovskite solar cells are further found to be useful in improving the cell performance, ascribing to the improved quality and coverage of the perovskite films, as well as the enhanced electronic contact between the perovskites and the electron transporting layer. By optimizing the TiO_2 NR lengths, an efficiency of 3.72% is obtained for $(PEA)_2(MA)_2Pb_3I_{10}$ perovskite cells with 600 nm-long TiO_2NRs as scaffolds, which is more than a time higher than that of the planer analogue device. Our study to design 2D perovskite solar cells demonstrates the importance of material structure and device configuration for efficient solar cells, highlighting the validity of TiO_2 nanorods in functionalizing 2D perovskites for photovoltaic applications.

Acceptance ID: QJ7M-O

Photoelectrocatalytic Production of Something Useful

Prof. Curtis P. Berlinguette

Departments of Chemistry and Chemical & Biological Engineering,
The University of British Columbia, Vancouver BC, Canada
cberling@chem.ubc.ca

The primary mission of our program is to use renewable energy to convert feedstocks into higher value products. One key theme within our laboratories is the development of (photo)electrocatalytic reactions that produce products with economic value. This presentation will outline our proof-of-principle methodologies for mediating interfacial photo-driven redox processes that produce chemicals people will actually pay for while using reaction conditions where breakdown of the active materials is avoided. This effort includes, but is not limited to, the conversion of CO_2 into products at the high current densities needed for commercialization.

Keywords: solar fuels, photochemistry, electrocatalysis.

Acceptance ID: RAJF-O

Defect Engineering of Formamidinium Tin Halide Perovskite for Non-toxic and Efficient Solar Cells

Seon Joo Lee

Advanced Materials Division, Korea Research Institute of Chemical Technology (KRICT), 141 Gajeong-ro, Yuseong-gu, Daejeon 34114, Republic of Korea
(sjlee614@krict.re.kr)

Lead halide perovskite with the general formula of $APbX_3$ where A is a monovalent cation such as Cs, methylammonium (MA), or formamidinium (FA), and X is a halide has attracted a lot of attention due to its superior optical and electrical properties. Also, the development of solar cells containing lead halide perovskite layer as a light absorber has accelerated in a short period, finally achieving the power conversion efficiency (PCE) of 22.1%. However, the toxicity issue for lead still remains unrevealed and limits the further practical commercialization of lead-based perovskite solar cells (PSCs). As an alternative to lead, tin-based perovskite material is considered as the most promising candidate in terms of its device performance as well as its optical and electrical properties. Nevertheless, the instability of Sn^{2+} upon exposure to air is problematic point which causes the unwanted p-type doping in the perovskite film, thereby limiting the device performance and reproducibility. In this presentation, we will introduce strategies for highly efficient formamidinium tin halide PSCs via defect engineering. Our approaches effectively reduced defect concentrations and hence the background carrier density in perovskite film. The reduction of background carrier density suppressed charge recombination in device, which improves charge collection. Consequently, we successfully fabricated a formamidinium tin halide perovskite solar cells with the best PCE of 5.5% and high reproducibility. Surprisingly, the encapsulated devices showed a remarkable light-stability over 1000 hours under the continuous one sun illumination (humidity = ~25%, temperature = ~30 $^{\circ}$ C).

Acceptance ID: SJCU-P

Carbon Counter Electrode based $CH_3NH_3PbI_{3-x}Br_x$ Perovskite Solar Cells and its Controllable Photovoltaic Performance

Zhiyong Liu[a], Bo Sun[a], Youni Wu[a], Tielin Shi[a], Zirong Tang[a] and Guanglan Liao[a,b]*

[a] State Key Laboratory of Digital Manufacturing Equipment and Technology, Huazhong University of Science and Technology, Wuhan 430074, China.
[b] Flexible Electronics Research Center, Huazhong University of Science and Technology, Wuhan 430074, China. E-mail: guanglan.liao@hust.edu.cn.
** Address correspondence to (G. Liao) guanglan.liao@hust.edu.cn. Telephone: 86-13971636606, Fax: 86-27-87793103*

Organometal perovskites have exhibited considerable prospects as next generation photovoltaics due to its unique properties, including low cost, large carrier mobility, bipolar transport, long photo-generated carrier diffusion length and strong absorption in the visible range. With an indepth understanding of working mechanism, judicious design and controllable fabrication, the power conversion efficiency (PCE) of perovskite solar cells (PSCs) has skyrocketed from initial about 3.8% to 22.1% as certified in NREL (the National Renewable Energy Laboratory), exhibiting incredible momentum of development and potential value of application. Considering the cost and the stability of the PSCs, printable carbon counter electrode based hole-conductor-free PSCs have been proven to be one of the most promising photovoltaic devices. $CH_3NH_3PbI_3$ (CH_3NH_3 abbreviated as MA hereafter) is the most commonly used perovskite material. Meanwhile, the mixed halide $MAPb(I_{1-x}Cl_x)_3$ and $MAPb(I_{1-x}Br_x)_3$ analogues by partial substitution with chlorine and bromine, which are supposed to be chemically stable in conjunction with humidity resistance, have also been widely investigated. Until now, benefited from the continuously tunable bandgap from 1.6 eV to 2.3 eV with different incorporation ratio, the mixed-halide perovskite $MAPbI_{3-x}Br_x$ is still one of the most promising candidates as the wide-bandgap light absorber in solar cells. In this study, the fabrication of carbon counter electrode based $MAPbBr_xI_{3-x}$ perovskite solar cells is investigated. The energy band gap can be tuned by controlling the Br content in $MAPbI_{3-x}Br_x(0\leq x\leq 0.5)$. Under standard AM1.5G illumination, the current density (J_{SC}) decreases from 21 mA cm^{-2} to 6.1 mA cm^{-2} with increasing x, whereas open circuit voltage (V_{OC}) increases from 0.74 to 0.92 V. In addition to the significant improvement in V_{OC}, a slight increase in the fill factor (FF) from 0.48 to 0.53 is also observed upon the incorporation of the Br ions. The reduction of J_{SC} with increasing x is directly related with the blue-shift of the absorption onset and the improvement of V_{OC} is attributed to the widening of the band gap with increasing x in $MAPbI_{3-x}Br_x$. A highest PCE of 9.41% is achieved when the Br content (x) is set at 0.1. Our work paves the way for the realization of low-cost and high-performance photovoltaic devices.

Acceptance ID: SJHE-O

Synthesis of Novel structured Fe_3O_4/C composite nanofibers and their application in lithium-ion batteries

Qiaofang Shi, Qianhui Wu, Long Huan, Guowang Diao, Ming Chen*,*

College of Chemistry and Chemical Engineering, Yangzhou University, Yangzhou 225002, P. R. China
qfshi@yzu.edu.cn; chenming@yzu.edu.cn;gwdiao@yzu.edu.cn

Lithium-ion batteries have received significant attention because of its widely applied in electric vehicles and renewable energy storage owing to their high energy density, high rate capability, long cycle life as well as environmental compatibility. However, commercial graphite anodes can not satisfy the enormous demands of energy consumptions. Among all the potential anode materials for lithium-ion batteries, Fe_3O_4 have attracted most attention owing to its high theoretical capacity (926 mA h g^{-1}), low cost, earth abundance and ecological friendliness. In this paper, novel structured Fe_3O_4/C composite nanofibers were successful fabricated by simple electrospinning method followed by a thermal treatment process, which were flexible electrode film without any current collector, binder and additional conductive agent. As a result, the novel structure Fe_3O_4/C composite nanofibers exhibited high specific capacity, rate capability and excellent cycling stability, which could be employed as an excellent flexible anode material for high-performance LIBs.

In summary, The Fe_3O_4/C-N3-600 NFs have been successfully prepared by direct electrospinning and annealing process. FeOOH was incorporated into the PAN-based spinning solution, FeOOH/PAN nanofibers was obtained by electrospinning, and calcined at 600 ℃ in argon to obtained novel structured Fe_3O_4/C composite nanofibers. The composite material exhibits high capacity of 780 mA h g^{-1} is still remained after 150 cycles, stable cycle performance and excellent rate performance.

Keywords: electrospinning, Fe_3O_4/C composite nanofibers, flexible anode material, lithium ion battery

[1] Wang, Y., Yang, L., Hu, R., Sun, W., Liu, J., Ouyang, L., Yuan, B., Wang, H., Zhu, M., 2015. A stable and high-capacity anode for lithium-ion battery: Fe_2O_3 wrapped by few layered graphene. *J. Power Sources* 288, 314-319.

[2] Xia, H., Wan, G., Yuan, G., Fu, Y., Wang, X. 2013. Fe_3O_4/carbon core–shell nanotubes as promising anode materials for lithium-ion batteries. *J. Power Sources* 241, 486-493.

Acceptance ID: SXJ9-P

* Corresponding authors.
E-mail address: chenming@yzu.edu.cn (M. Chen), gwdiao@yzu.edu.cn (G. Diao)

Coordination Engineering and Interface Engineering for High-Performance Perovskite Solar Cells

*Yan Keyou[1,2] * Xu Jian-Bin[1*], Long Mingzhu[1], Zhang Tiankai*

[1]Department of Electronic Engineering & Materials Science and Technology Research Center, The Chinese University of Hong Kong, Shatin, New Territory, Hong Kong SAR
[2]Department of Chemistry, The Hong Kong University of Science and Technology, Clear Water Bay, Kowloon, Hong Kong SAR

Organic-inorganic ABX_3 (A: MA, FA, Cs…; B: Pb, Sn …; X: halide) three-dimensional perovskite (3DP) received worldwide interest due to high extinction coefficient, free-carrier like exciton and long diffusion length up to 100 μm in single crystal, delivering over 22% efficiency in perovskite solar cell (PSC). However, the stability of 3DPs is a big challenging problem for commercialization. So far, the deposition of the highest-performing perovskite is generally based on approximately stoichiometric reaction between MAI/FAI (solid) and PbI_2 (solid) through solution process. The completing coordination of dimethylformamide/dimethylsulfoxide (DMF/DMSO) solvents results in halide deficiency after solvent removal and permits the penetration of moisture to degrade the perovskite. In this report, we will present an alternative reaction route to avoid the halide vacancy and enhance the stability through coordination engineering. Besides, two-dimensional perovskites (2DPs) formulated as $(R\text{-}NH_3)_2(A)_{n-1}B_nI_{3n+1}$ (R, alkyl; n=1,2,…) have much higher stability than 3DPs but its efficiency has only achieved a half due to degraded electronic properties. We will introduce the development of alternative synthetic methodology and interface engineering to reduce the trade-off between efficiency and stability in 2DPs.[1-6]

Acknowledgement

The work is in part supported by the Research Grants Council of Hong Kong, via grant numbers T23-407/13-N and AoE/P-03/08, and the CUHK Group Research Scheme 2013.

1 Yan, K. *et al.* Near-Infrared Photoresponse of One-Sided Abrupt MAPbI3/TiO2 Heterojunction through a Tunneling Process. *Adv. Funct. Mater.* **26**, 8545-8554, doi:10.1002/adfm.201602736 (2016).

2 Long, M. Z. *et al.* Ultrathin efficient perovskite solar cells employing a periodic structure of a composite hole conductor for elevated plasmonic light harvesting and hole collection. *Nanoscale* **8**, 6290-6299, doi:10.1039/c5nr05042a (2016).

3 Long, M. *et al.* Nonstoichiometric acid–base reaction as reliable synthetic route to highly stable CH3NH3PbI3 perovskite film. *Nat. Commun.* **7**, 13503, doi:10.1038/ncomms13503 (2016).

4 Yan, K. Y. *et al.* High-Performance Graphene-Based Hole Conductor-Free Perovskite Solar Cells: Schottky Junction Enhanced Hole Extraction and Electron Blocking. *Small* **11**, 2269-2274, doi:10.1002/smll.201403348 (2015).

5 Yan, K. *et al.* Hybrid Halide Perovskite Solar Cell Precursors: Colloidal Chemistry and Coordination Engineering behind Device Processing for High Efficiency. *J. Am. Chem. Soc.* **137**, 4460-4468, doi:10.1021/jacs.5b00321 (2015).

6 Wei, Z., Chen, H., Yan, K., Zheng, X. & Yang, S. Hysteresis-free multi-walled carbon nanotube-based perovskite solar cells with a high fill factor. *J. Mater. Chem. A* **3**, 24226-24231, doi:10.1039/c5ta07714a (2015).

Acceptance ID: TN69-O

The Design and Synthesis of Photochromic Sensitizers for DSSCs

*Chang Young Jung, Jong Min Park, Jae Yun Jaung**

Department of Organic and Nano engineering, Hanyang University
jjy1004@hanyang.ac.kr

Photochromic compounds have received special attention due to their potential applications for optical switching. Among the photochromic dyes including spiropyrans, diarylethens and azobenzenes, bisthienylethene derivatives are one of the most promising materials due to their high sensitivity, excellent fatigue resistance and thermal stability. Generally, bisthienylethene derivatives form six-membered ring via 6-pi electrocyclic reaction during irradiation with UV light, leading to change of absorption band and color. The ring closed-form returns to open-form under visible light. On the other hands, with increasing interest in alternative energy, especially solar energy, dye-sensitized solar cells (DSSCs) have attracted research due to their high power conversion efficiency, low cost, and high semiconductor stability. In this study, we designed and synthesized bisthienylethene based donor-π-acceptor sensitizer in order to develop optical switching sensitizer for DSSCs. The synthesized compounds were characterized by ^{1}H-NMR and MALDI-TOF mass spectroscopy. Also, photochromic properties of sensitizers were confirmed using UV-visible absorption spectroscopy. Furthermore, they were applied as photochromic sensitizer for DSSCs.

Keywords: Photochromism, bisthienylethene, dye-sensitized solar cells.

[1] S. N. IVANOV, B. V. LICHITSKII, A. A. DUDINOV, A. YU. MARTYNKIN, & M. M. KRAYUSHKIN. 2001. Synthesis of substituted 1,2,4-triazines based on 1,2-bis(2,5-dimethyl-3-thienyl)ethanedione. Chem. Heterocycl. Comp. 37, 85-90.

Acceptance ID: URWB-P

High Performance Electrochemical Capacitors Based on Conductive Two-Dimensional Metal-Organic Frameworks

Maria R. Lukatskaya and Zhenan Bao

Department of Chemical Engineering, Stanford University, CA, 94305, USA

As electronic technology advances, the need in safe and long-lasting energy storage devices that occupy minimum volume arises. Short charging times of several seconds to minutes, with energy densities comparable to those of batteries, can be achieved in electrochemical capacitors (supercapacitors), in particular pseudo-capacitors, which utilize fast redox reactions to store charge and, thus, feature high energy densities. However, metal oxides that are currently used in energy storage technologies have certain limitations. Due to low intrinsic electrical conductivity they might suffer from poor cyclability and deterioration of electrochemical performance for thick electrodes. As an alternative, conductive materials with build-in redox centers pose particular interest.

Herein, we report on the new family of the conductive 2D porous metal organic frameworks and we investigated their potential for electrochemical capacitors. Our evaluation in a range of electrolytes demonstrated impressive gravimetric capacitance up to 400 F/g for scan rates above between 1 to 100 mVs^{-1}. We also studied submillimeter thick pellets of MOFs which showed high volumetric capacitances up to 760 F cm^{-3} and high areal capacitances over 10 F cm^{-2}. Furthermore, prepared MOF electrodes exhibited highly reversible redox behaviors and good cycling stability with a capacitance retention of 90% even after 12,000 cycles. This demonstrates that redox-active conductive MOFs can potentially outperform other traditional materials in energy storage applications..

Acceptance ID: UX54-O

Title: Miscanthus biomass for the sustainable fractionation of ethanol-water mixtures

Leila Dehabadi[1] *and Lee D. Wilson*[1]*

[1]*Department of Chemistry, University of Saskatchewan, 110 Science Place, Saskatoon, SK. Canada S7N 5C9*
**Corresponding and presenting author: lee.wilson@usask.ca, Tel. +1-306-966-2961*

The use of alcohol in the biofuel industry is very important and it requires new sustainable materials to remove water from biofuel mixtures to improve quality. Miscanthus is a rich source of lignocellulosic biomass with a great potential for applications ranging from biofuel production to value-added biomass derived products. The rapid growth and low mineral content of Miscanthus contributes to its utility as an adsorbent biomaterial. In this research, the utility of Miscanthus and its modified forms were used for the fractionation of water (W) and ethanol (E) mixtures using an *in situ* analytical method, referred to as quantitative NMR (qNMR) spectroscopy. Therefore, raw and pretreated Miscanthus with variable biopolymer content (cellulose and lignins) and variable particle size were evaluated as sorbents in binary water-ethanol (W-E) mixtures. The pretreated Miscanthus was prepared by an acid and then an alkaline hydrolysis for the removal of hemicellulose and lignins, leading to cellulose enriched biomass. As a result, the raw and pretreated Miscanthus was characterized using IR spectroscopy, thermogravimetric analysis (TGA) and nitrogen adsorption-desorption isotherms. Isotherm results reveal preferential water uptake properties according to the relative biopolymer content, while the fractionation properties of Miscanthus and its biopolymer constituents display molecular selectivity ($R_{selectivity}$) between water and ethanol. The reusability of Miscanthus was shown to be regenerated over four adsorption-desorption cycles. This research contributes to a greater understanding of biopolymer components and pretreatment strategies for the biomass fractionation of binary W-E solvent systems relevant to beverage, food, and energy production.

Acceptance ID: UYPJ-P

Ultrathin Layered Hydroxide Cobalt Acetate Nanoplates Face-to-Face Anchored to Graphene Nanosheets for High-Efficiency Lithium Storage

*Liwei Su, Jinpei Hei, Lianbang Wang**

(State Key Laboratory Breeding Base of Green Chemistry-Synthesis Technology, College of Chemical Engineering, Zhejiang University of Technology, Hangzhou, P. R. China, 310014, E-mail: wanglb99@zjut.edu.cn)

The dramatically increasing demand of high-energy lithium ion batteries requires advanced substitution for graphite-based anodes urgently. According to the conversion mechanism, the theoretical capacities of transition metal oxides (TMOs) are 700-1000 mAh g^{-1}, while most of them display much higher capacities, i.e., extra capacity phenomenon. Researchers found that the solid electrolyte interphase (SEI) components (such as Li_2CO_3, LiOH, LiAc) could decompose and regenerate reversibly under the catalysis of transition metal, accompanied by the storage and release of more lithium ions and electrons. According to this mechanism, after discharging process layered hydroxide cobalt acetates (LHCA) will transform into Co nanocrystal, LiOH and LiAc which are similar with the SEI components. Concurrent with lithium ions insert, LiOH and LiAc might supply more capacity under the electrocatalyst of Co metal nanocrystals.

Inspired from the extra capacity of SEI films, herein LHCA ($Co(Ac)_{0.48}(OH)_{1.52}\cdot 0.55H_2O$) are introduced as novel and high-efficiency anode materials. Furthermore, ultrathin LHCA nanoplates are face-to-face anchored on the surface of few-layered graphene nanosheets (GNS) through a facile solvothermal method to improve the electronic transport and avoid the agglomeration during repeated cycles. Profiting from the parallel structure, LHCA//GNS nanosheets exhibited ultrahigh long-term reversible capacity and extraordinary high-rate performance. At the current densities of 1000 and 4000 mA g^{-1}, the reversible capacities maintain ~1050 mAh g^{-1} after 200 cycles and ~780 mAh g^{-1} after 300 cycles, respectively, much higher than the theoretical value of LHCA according to conversion mechanism. Fourier transform infrared spectoscopy confirmed the conversion from acetate to acetaldehyde after lithiation. A reasonable mechanism is proposed to elucidate the lithium storage behaviors referring to the electrocatalytic conversion of OH groups with Co^0 metal nanocatalysts. This work can help us further understand the contribution of SEI components (especially LiOH and LiAc) to lithium storage. It is envisaged that layered transition metal hydroxides can be used as advanced materials for energy storage devices.

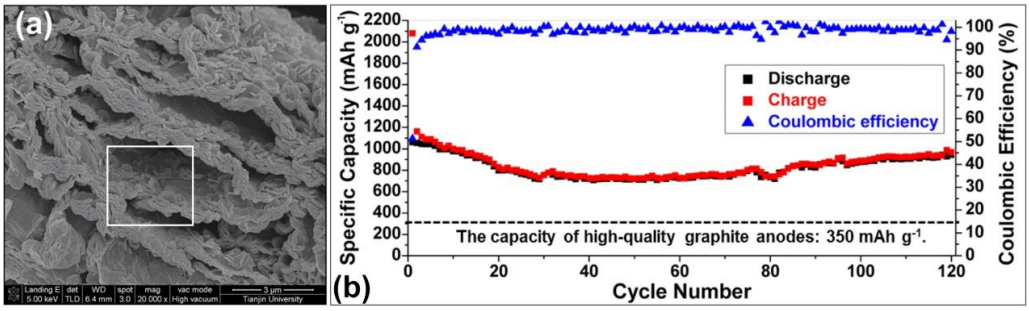

Fig. 1 (a) SEM image and (b) cycling performances at 350 mA g^{-1} of LHCA//GNS hybrid nanosheets

References:

1. P. Zhang, L. Wang, J. Xie, L. Su, C. A. Ma, J. Mater. Chem. A 2014, 2, 3776-3782.
2. L. W. Su, Z. Zhou, M. M. Ren, Chem. Commun. 2010, 46, 2590-2592.
5. L.Wang, W. Tang, Y. Jing, L. Su, Z. Zhou, ACS Appl. Mater. Interfaces 2014, 6, 12346-12352.
3. L. Su, J. Jiang, L. Wang, Y. Wang, M. Ren, ChemElectroChem 2015, 2, 789-794.
4. L. Su, Y. Zhong, Z. Zhou, J. Mater. Chem. A 2013, 1, 15158-15166.
5. L. Su, Z. Zhou, X. Qin, Q. Tang, D. Wu, P. Shen, Nano Energy 2013, 2, 276-282.

Acknowledgments: This work was supported by the National Natural Science Foundation of China (21403195 and 21421001) and the Key Research and Development Program (2015C01001 and 2016C01SA500898) of Science and Technology Department of Zhejiang Province.

Acceptance ID: VCXC-P

Synthesis and Structural Characterization of Cadmium substituted Cobalt advanced nano-functional materials by citrate-gel auto combustion method

Nehru boda[a], Gopal boda[b], G. Aravind[c], D. Ravinder[a], A. Panasa Reddy[b*].*

[a.] *Department of physics, Osmania university, Hyderabad, 500007, Telangana, India.*
[b.] *Department of chemistry, college of Engineering, Osmania university, Hyderabad, 500007, Telangana, India.*
[c] *Methodist college of Engineering and Technology, Abids, Hyderabad, Telangana, India*
[*] ***Correspondence Author;D. Ravinder; email:*** ***ravindergupta28@rediffmail.com***

ABSTRACT: Advanced Nano-functional materials having the chemical formula $Co_{1-x}Cd_xFe_2O_4$ (where x=0.1, 0.2, 0.3, 0.4, 0.5 and 0.6) were synthesized by the citrate-gel auto combustion method. Synthesized powders were sintered at 500^0C for four hours in air and characterized by XRD, SEM, EDS, FTIR. X-ray diffraction (XRD) analysis showed cubic spinel structure of the ferrites and the values of lattice constant (a) and x-ray density (d_x) increased with the increase of Cd content. The surface morphology of the samples was observed by scanning electron microscopy (SEM). An elemental composition of the sample has studied by Energy Dispersive Spectroscopy (EDS). The FTIR spectra shows the two significant absorption bands in the wave numbers range of 370-600 cm^{-1} arising due to the inter-atomic vibrations in the tetrahedral and octahedral coordination compounds. The observed results can be explained on the basis of composition.

KEY WORDS: Co-Cd advanced functional materials, citrate-gel auto combustion Technique, XRD, SEM, EDS, FTIR.

Synthesis flow chart of citrate gel auto combustion technique:

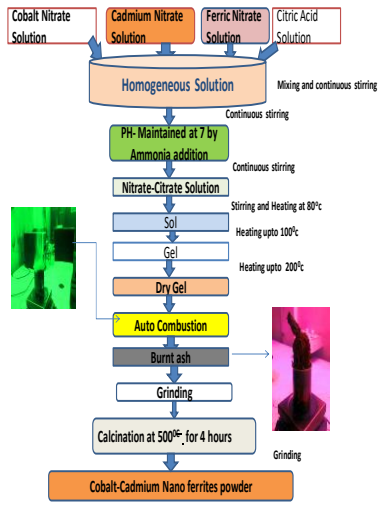

The Effect of Buffer/Window Junction Properties on Cu(In,Ga)Se_2 Thin Film Solar Cells with Window Layers Embedding Silver Nanowires

Jiseong Jang[1], Jun Su Lee[1], Ki-Ha Hong[1], Doh-Kwon Lee[2], Soomin Song[3], Kihwan Kim[3], Young-Joo Eo[3], Jae Ho Yun[,3], and Choong-Heui Chung[*,1]*

[1]Department of Materials Science and Engineering, Hanbat National University, Daejeon 34158, Republic of Korea
[2]Photoelectronic Hybrid Research Center, Korea Institute of Science and Technology, Seoul 02792, Republic of Korea
[3]Photovoltaic Laboratory, Korea Institute of Energy Research, Daejeon 34129, Republic of Korea
E Mail : choong@hanbat.ac.kr

We investigate the effect of buffer/window junction properties on the performance of Cu(In,Ga)Se_2 (CIGS) solar cells with silver nanowire based window layer. Silver nanowire based transparent conductors have been widely employed for thin films solar cells, and the nanowires are necessarily capped or embedded in a window matrix layer to ensure lateral charge-carrier collection [1]. Therefore, various alternative materials, processing methods and stacking structures have been reported for the matrix layer in CIGS thin film solar cells. However, studies of the effects of the buffer/window junction properties on the current-voltage characteristics of the solar cells has seldom been addressed. Here, we quantitatively and analytically investigate the effects of buffer/window junction properties on the energy band alignment and the current-voltage characteristics of CIGS thin film solar cells. Solution processes for the preparation of window layer often induce defect states at the buffer/window interface, which can result in poor energy band alignment, impeding carrier transport in the solar cells. On the basis of our analysis, we suggest an equation relating the interfacial defect density and carrier concentration in the window layer to avoid losses in the power conversion efficiency of the solar cells, even with a substantial number of interfacial defects.

Keywords: CIGS, Silver nanowires, Buffer/window junction, interfacial defects

[1] CHUNG, C. H., SONG, T. B., BOB, B., ZHU, R., DUAN, H. S. & YANG, Y. 2012. Silver nanowire composite window layers for fully solution-deposited thin-film photovoltaic devices. *Adv. Mater.*, 24, 5499–5504.

Acceptance ID: wptv-P

Asymmetric supercapacitor based on reduced graphene oxide and nickel-cobalt double hydroxide nanoneedles deposited on nickel foam

Ni-Co double hydroxide (NCOH) was deposited onto nickel foam (NF) framework using a simple solvent thermal method, which showed unique nanoneedle array morphology. Electrochemical measurements were taken for evaluating the potential application of the thus prepared Ni-Co double hydroxide as an electrode for supercapacitor devices. According to electrochemical tests, the Ni-Co double hydroxide electrode exhibited an excited specific capacitance (1855 $F.g^{-1}$ in the current density of 1.0 $A.g^{-1}$) and good rate performance (53% capacitance retention when current density is increased to 10 $A.g^{-1}$). The specific capacitance retention after 500 charge-discharge cycles is over 90%. An aqueous asymmetric supercapacitor (ASC) device named NCOH/NF // rGO/NF was composed using NCOH deposited on NF skeleton as positive electrode and reduced graphene oxide (rGO) deposited on NF skeleton as the negative electrode. The performance of the ASC device was investigated by cyclic voltammetry, galvanostatic charge-discharge and electrochemical impedance spectroscopy. The ASC exhibited a specific capacitance of 108.7 $F.g^{-1}$ at the current density of 2.5 $A.g^{-1}$ in a potential range from 0 to 1.5 V, and gravimetric energy density of 30.4 $Wh.kg^{-1}$ at power density of 1875 $W.kg^{-1}$ and 14.1 $Wh.kg^{-1}$ at 37.5 $kW.kg^{-1}$. Moreover, the NCOH/NF // rGO/NF had an outstanding cycling stability (almost no capacitance loss after 3000 cycles), which made this device a good candidate for electrochemical energy storage devices.

Acceptance ID: WZ9U-P

Molecular Self-Assembly on Two-Dimensional Atomic Crystals

Organic molecular self-assembly on two-dimensional (2D) materials has wide potential applications, such as passivation layers, organic electronics, photonic devices, solar cells, and graphene-based devices, while understanding the dynamic mechanism of the self-assembly falls far behind its application. Therefore, it is crucial and urgent to understand the physical mechanisms on the self-assembly. Via molecular dynamics simulation, we successfully visualize the nanoscale self-assembly of organic molecules on graphene and boron nitride monolayer from a disordered state to an ordered structure.[1,2] On the basis, we reveal that the intermolecular hydrogen-bonds play a key and positive role in the self-assembly.[3] They can significantly broaden the nucleation area, raise the stability-metastability critical temperature, accelerate the nucleation process, and guide the nucleation direction.[3] Moreover, we propose an effective passivation approach, self-assembly of organic molecules on black phosphorus (BP), to protect BP from the degradation without breaking the original electronic properties of BP.[4]

1. **Zhao, Y.**; Wu, Q.; Chen, Q., Wang, J. Molecular Self-Assembly on Two- Dimensional Atomic Crystals: Insights from Molecular Dynamics Simulations. *J. Phys. Chem. Lett.* **2015**, *6*, 4518-4524.
2. Wu, B.; **Zhao, Y.**; Nan, H.; Yang, Z.; Zhang, Y.; Zhao, H.; He, D.; Jiang, Z.; Liu, X.; Li, Y.; Shi, Y.; Ni, Z.; Wang, J.; Xu, J.-B.; Wang X. Precise, Self-Limited Epitaxy of Ultrathin Organic Semiconductors and Heterojunctions Tailored by van der Waals Interactions. *Nano Lett.* **2016**, *16*, 3754-3759. (Co-first author)
3. **Zhao, Y.**; Wang, J. How to Obtain High-Quality and High-Stability Interfacial Organic Layer: Insights from the PTCDA Self-Assembly. Accepted by *J. Phys. Chem. C* DOI: DOI: 10.1021/acs.jpcc.7b00606.
4. **Zhao, Y.**; Zhou, Q.; Li, Q.; Yao, X.; Wang, J. Passivation of Black Phosphorus via Self-Assembled Organic Monolayers by van der Waals Epitaxy. *Adv. Mater.* **2016**, DOI: 10.1002/adma.201603990.

Acceptance ID: XJAS-O

Remarkable functional behaviour of metal- metal oxide polymer composites in direct ethanol fuel cell: A low Pt and non graphitic approach

Jayati Datta, Abhishek De

Indian Institute of Engineering Science and Technology, Shibpur, Howrah-711103, India
Email : jayati_datta@rediffmail.com / Tel.: +9133 2668 4561.

In the 21st century the quest for clean energy and future sustainability have motivated vigorous research efforts in low temperature fuel cell technology. Among the promising fuels, small organic molecules like alcohols, have received immense importance due to their much simpler peripheral units for fuel delivery and storage infrastructures compared to H_2-O_2 fuel cells. In fact the direct ethanol fuel cell (DEFC) is featured with high volumetric and gravimetric energy densities and reasonable energy efficiency. Further, bio-ethanol can be obtained in large quantities by fermentation of sugar containing agricultural raw materials and has significant advantage of being nearly CO_2 neutral. There is however stringent catalyst requirement for the C-2 molecule which has prompted challenging tasks for developing mixed metallic nano structures, with reduced Pt loading, capable of minimizing activation loses, maximizing exchange current density of the electrode kinetics and providing effective way for exploring the catalyst due to their multiple reaction sites. The carbon as support materials has also several constrains like poor corrosion resistance, insufficient proton conductivity and agglomerated growth of NPs that prevents the electrolyte to be fully accessed, thereby limiting the specific catalytic performance in acid or alkali media. Such critical conditions have triggered various attempts for developing catalyst-support formulation befitting to the ambient environment in a DEFC operating below 100°C. Investigation on support flexibility includes the use of ceramic oxide, transition metal oxide and also polymeric materials. In view of the above, this article presents some of the novel attempts of designing hybrid structure constituting multimetalic catalyst nano-particles(NPs) embedded on transition metal oxide- conducting polymer composite substrate for the study of electro-oxidation of ethanol in acid/alkali environment. As the initial approach chemically prepared MoO_3-polypyrrole composite support was decorated with alloyed PtPd NPs via $NaBH_4$ reduction of the respective precursors. The collective information obtained from the physico-chemical and electrochemical studies in acid media indicates the intervention of molybdenum oxide network in the ethanol oxidation reaction sequence which increases the propensity of the reaction by making the metallites more energy efficient in terms of harnessing sufficient numbers of electrons than with the carbon support. The second attempt involves electro-catalysis in alkaline environment involving WO_3-poly-N-vinyl carbazole, designed with PtPd NPs, which increases the functional behavior of the DEFC in operating condition with good CO tolerance and eventually reduces the cost of the catalyst, at the same time eliminate the typical involvement of graphitic carbon in DEFC.

Keywords: Transition metal oxide, conducting polymer, PtPd nano-particles, electro-catalysis, direct ethanol fuel cell.

[1] AKHAIRI, M. A. F.; KAMARUDIN, S. K. 2016, Catalysts in Direct Ethanol Fuel Cell (DEFC): An Overview. *Int. J. Hydrogen Energy* 41, 4214−4228.

[2] DUTTA, A.; DATTA, J. 2014, Energy efficient role of Ni/NiO in PdNi Nanocatalyst Used in Alkaline DEFC. *J. Mater. Chem. A*, 2, 3237−3250.

[3] DATTA, J.; DUTTA, A.; BISWAS, M. 2012, Enhancement of functional properties of PtPd nano catalyst in Metal-Polymer Composite matrix: Application in Direct Ethanol Fuel Cell. *Electrochem. Commun*. 20, 56−59.

[4] DE, A.; DATTA, J.; HALDAR, I.; BISWAS, M, 2016, Catalytic Intervention of MoO3 toward Ethanol Oxidation on PtPd Nanoparticles Decorated MoO3−Polypyrrole Composite Support, *ACS Appl. Mater. Interfaces*, 8, 28574−28584.

Acceptance ID: XP4S-I

Well-defined 2D Covalent organic polymers for energy conversion

Zhonghua Xiang [1]

[1] *Molecular enegy materials R&D Center; State Key Lab of Organic–Inorganic Composites, Beijing University of Chemical Technology, Beijing 100029 (P.R. China).*
E Mail/ xiangzh@mail.buct.edu.cn

Highly efficient electrocatalysts are vital to meet the energy and environmental challenges. [1]Although numerous nonprecious-metal or metal-free carbon-based catalysts have been demonstrated to entirely or partially replace noble-metal-based electrocatalysis, the absence of precise design and predictable process hindered the development.[2] Well-defined 2D Covalent Organic Polymers (COPs)[3] as a new exciting type of electrocatalyst presented superior potentials with precisely controllable capacities, such as robust tailoring heteroatom incorporation and location of active sites. Here we demonstrate the possibilities and potential of the well-defined 2D COPs used as highly efficient energy electrocatalysts for clean and renewable energy technologies.[4] COP materials as a new family of electrocatalysts offer practical possibilities to study the structure, mechanism and kinetics of energy electrocatalysis and may lead to a possible solution for energy and environmental issues.

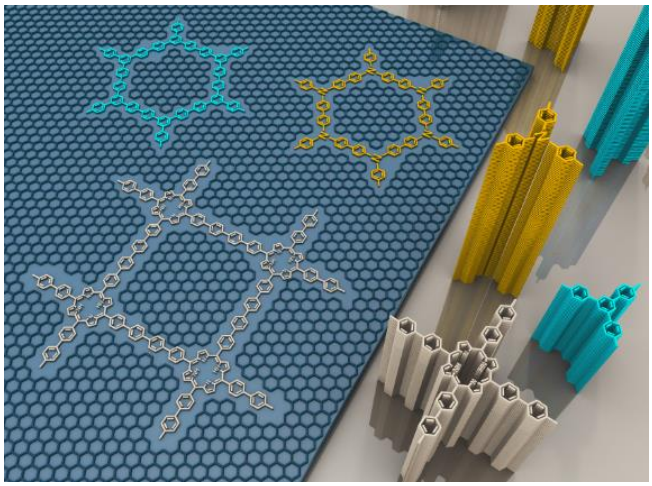

Fig. 1 Hypothetic network fragments for colorful 2D COPs

Keywords: Oxygen reduction reaction, metal organic frameworks, covalent organic framework, hydrogen evolution reaction

[1] GONG, K. P.; DU, F.; XIA, Z. H.; DURSTOCK, M.; DAI, L. M. 2009. Nitrogen-Doped Carbon Nanotube Arrays with High Electrocatalytic Activity for Oxygen Reduction. *Science 323* (5915), 760-764.

[2] DAI, L. M.; XUE, Y. H.; QU, L. T.; CHOI, H. J.; BAEK, J. B. 2015. Metal-Free Catalysts for Oxygen Reduction Reaction. *Chem. Rev. 115*, 4823-4892.

[3] (a) XIANG, Z. H.; DAI, Q. B.; CHEN, J. F.; DAI, L. M. 2016. Edge-functionalization of graphene and two-dimensional covalent organic polymers for energy conversion and storage. *Adv. Mater. 28*, 6253-6261; (b) XIANG, Z. H.; MERCADO, R.; HUCK, J. M.; WANG, H.; GUO, Z. H.; WANG, W. C.; CAO, D. P.; HARANCZYK, M.; SMIT, B. 2015. Systematic tuning and multi-functionalization of covalent organic polymers for enhanced carbon capture. *J. Am. Chem. Soc. 137*, 13301-13307; (c) XIANG, Z. H.; XUE, Y. H.; CAO, D. P.; HUANG, L.; CHEN, J. F.; DAI, L. M. 2014. Highly-Efficient Electrocatalysts for Oxygen Reduction Based On 2D Covalent Organic Polymers Complexed with Non-Precious Metals. *Angew. Chem. Int. Ed. 53*, 2433-2437; (d) XIANG, Z. H.; CAO, D. P.; HUANG, L.; SHUI, J. L.; WANG, M.; DAI, L. M. 2014. Nitrogen-Doped Holey Graphitic Carbon from 2D Covalent Organic Polymers for Oxygen Reduction. *Adv. Mater. 26*, 3315-3320; (e) XIANG, Z. H.;

CAO, D. P.; DAI, L. M. 2015. Well-Defined Two Dimensional Covalent Organic Polymers: Rational Design, Controlled Syntheses, and Potential Applications. *Polym. Chem. 6*, 1896-1911.
[4] CHENG, Y. H.; GUO, J. N.; HUANG, Y.; LIAO, Z. J.; XIANG, Z. H. 2017. Ultrastable hydrogen evolution electrocatalyst derived from phosphide postmodified metal-organic frameworks. *Nano Energy 35*, 115-120.

Acceptance ID: XPDM-O

SYMPOSIUM 5: Advances in Biosensors and Biomaterials

Preparation of amoxicillin/PEG microcapsule by supercritical fluid impinging technology

*Wei WEI, Fengxia LIU, Xiaojuan WANG,Xiaofei XU, Zhiyi LI, Zhijun LIU**

(R&D Institute of Fluid and Powder Engineering, Dalian University of Technology, Dalian 116024, P. R. China)
Presenting author: Wei WEI
Email: hjweiwei@dlut.edu.cn
Corresponding author: Zhijun LIU
Email: liuzj@dlut.edu.cn
Address: No.2 Linggong Road, High-Tech Zone, Dalian City, Liaoning Province, P. R. China

A novel supercritical fluid impinging technology (SFIT) has been developed to coat microparticles. Amoxicillin is chosen as the core particle and polyethylene glycol (PEG) as the coating material. In order to evaluate the microcapsules, the scanning electronic microscopy (SEM) is used to observe the morphologies of the microcapsules, differential scanning calorimetry (DSC) is used to examine the coating integrality, the ultraviolet and visible spectrophotometer (UV-Vis) is used to measure microcapsules release degrees, and laser particle size analyzer (LPSA) is used to measure the microcapsule size and size distribution. During the studies, the effects of operation conditions**,** such as the pressure of the mixing vessel, the temperature of the mixing vessel and the impinging distance on the microcapsule size and distribution in addition the encapsulation efficiency are investigated. Most of microcapsules which range between 7.80 μm and 9.70 μm are spherical and are encapsulated completely. Meanwhile, the microcapsules release slower than raw drug and achieve the purpose of controlled release. Both of the pressure and the impinging distance have significant affection on the encapsulation efficiency, microcapsule size and distribution. Therefore, SFIT is a promising method to produce microcapsules with relatively small microcapsule size and narrow size distribution. In addition, it is particularly suits to coat sensitive pharmaceuticals.

Keywords: Supercritical fluid; Impinging; Microcapsule; Amoxicillin; PEG

Acceptance ID: 253A-O

Drug-conjugated gold nanoparticles and their hybrid liposomes for liver tumor treatment

*Ya Ding[1**], Ying-Ying Zhou[1], Quan-Ying Bao[1], Ning Zhang[1]*

[1]Department of Pharmaceutical Analysis, China Pharmaceutical University, Nanjing, 210009, China
***Corresponding authot. Tel: (+86) 83271326; Fax: (+86) 83271326; E-mail: ayanju@163.com*

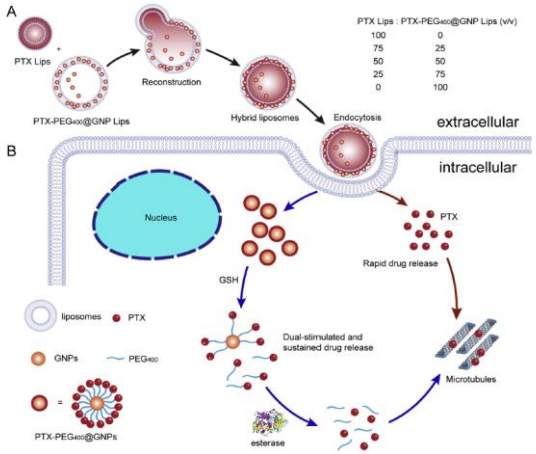

Drug-conjugated gold nanoparticles and their hybrid liposomes.

Gold nanoparticles (GNPs) attract widely attentions in biomedicine, especially for drug delivery and sensing. For the application of drug delivery, their advantages include controllable shape and size, functional diversity via the surface modification, and the cytotoxicity, Biodistribution and in vivo excretion properties modulated by regulating the particle size and surface functionality. Drug-conjugated gold nanoparticles (drug@GNPs), connecting drug molecules such as Tiopronin, Paclitaxel (PTX), and Doxorubicin on the surface of GNPs via covalent bonds, are promising drug delivery systems for the tumor treatment. They can be used as a core-crosslinked prodrug in the scale of nanometer. In these system, many drug molecules (usually more than 100 drug molecules per particle) are connected on gold surface, leading to a high drug concentration in a small volume. The rational design of spacer and covalent linkage between drug molecule and GNP ensures a high stability of systems in the circulation and stimuli-responsive release at the target site. In addition, to avoid the protein adsorption and subsequent opsonization in vivo, drug@GNPs can be encapsulated in other organic carriers, such as liposomes. The enhanced longevity and liver targetability of drug in this system are found. To further improve the antitumor efficacy of drug loaded in this liposome-encapsulating drug@GNP system, gold conjugate-based liposomes with a hybrid cluster bomb structure are developed by simply mixing PTX liposomes and PTX@GNP-loaded liposomes for the liver cancer therapy. Its unique multi-order drug release property provides a more accurate site- and time-release mode for tumor treatment using antitumor drugs.

Acknowledgements
This work was financially supported by the Natural Science Foundation of China (31470916, 31200695, and 31500769), the Program for New Century Excellent Talents in University (NCET-10-0816).

Reference

1. Q.-Y. Bao, D.-D. Geng, J.-W. Xue, G. Zhou, S.-Y. Gu, Y. Ding, C. Zhang, *Inter. J. Pharm.* 446(1-2), 112-118, **2013**.
2. Y. Ding, Y.-Y. Zhou, H. Chen, D.-D. Geng, D.-Y. Wu, J. Hong, W.-B. Shen, T.-J. Hang, C. Zhang, *Biomaterials* 34(38), 10217–10227, **2013**.
3. Q.-Y. Bao, N. Zhang, D.-D. Geng, J.-W. Xue, M. Merritt, C. Zhang, Y. Ding, *Inter. J. Pharm.* 477 (1-2), 408-415, **2014**.
4. Q.-Y. Bao, A.-Y. Liu, Y. Ma, H. Chen, J. Hong, W.-B. Shen, C. Zhang, Y. Ding, *Colloid Surf B* 146, 475-481, **2016**.
5. N. Zhang, H. Chen, A.-Y. Liu, J.-J. Shen, V. Shah, C. Zhang, J. Hong, Y. Ding, *Biomaterials* 74, 280-291, **2016**.

Acceptance ID: 2unu-I
Keywords: Gold nanoparticles; drug conjugates; hybrid liposomes; cluster bomb structure; liver tumor therapy.

Theoretical and Experimental Study on Water Exchange and Emulsion Destabilization in W/O/W Double Emulsion Solvent Evaporation Method to Prepare Polymer Microcapsules

Fengxia LIU, Chao DONG, Xiaofei XU, Zhiyi LI, Zhijun LIU[*]

(R&D Institute of Fluid and Powder Engineering, Dalian University of Technology, Dalian 116024, P. R. China)
Presenting author: Chao DONG
Email: 693653119@qq.com
Corresponding author: Zhijun LIU
Email: liuzj@dlut.edu.cn
Address: No.2 Linggong Road, High-Tech Zone, Dalian City, Liaoning Province, P. R. China

Using double emulsion as template to prepare porous micro-devices is a technique that has been intensively studied over decades. However, there's a lack of attention on the instability of template double emulsion based on organic solvent that can cause significant drug loss and lead to change in the internal structure of the micro-devices .

In this study, both theoretical and experimental approaches have been developed to investigate the destabilization of w/o/w emulsions in the double emulsion solvent evaporation techniques used for drug encapsulation. Since water exchange between different water phases induces double emulsion destabilization, math model based on Fick's law was developed to describe the water exchange rate between internal and external aqueous phases:

$$\frac{dn}{dt} = 4\pi r c(\infty, T) D(c, T) \cdot \left(\frac{r_0^3}{r^3} x_{01} - x_{02}\right) \qquad (1)$$

where $c(\infty, T)$ is the bulk solubility of water in oil phase at temperature T; $D(c, T)$ is the diffusivity of water molecules in oil phase at a polymer concentration of c and temperature of T; x_{01} and x_{02} are the initial molar concentrations of the drug in internal and external aqueous phases; r_0 is the initial radius of internal water droplets and r is radius of the water droplets over time. Equation (1) successfully emphasize the influence of solvent type on double emulsion destabilization, considering that solubility of water in organic solvent can be larger than non-solvent by many orders.

Accordingly, experiments were conducted to investigate the influence of the above mentioned factors on the double emulsion destabilization using the drug initially added in the internal aqueous phase as tracer. Instability was characterized by tracer loss rate after the 2nd emulsification process.

Theoretical and experimental results show that 1) swelling of the oil globules due to water exchange between internal and external water phases and subsequently the rapture of oil film play an determinate role in the destabilization of double emulsion and drug loss; 2) in line with the theoretical analysis, experiments showed that factors such as oil type, original solute molar concentrations in internal and external aqueous phases, initial radius of internal water droplets, polymer concentration in oil phase and temperature all exert considerable influence on drug loss rate.

Further study showed that different internal structures, i.e., single-and multi-compartment (Fig. 1), can be tailored by adjusting water exchange rate from the aforementioned factors.

[*] *Corresponding author: Zhijun LIU, E-mail: liuzj@dlut.edu.cn*

(a) (b) (c)

Fig. 1 Various internal structures of micro-devices prepared from w/o/w emulsion templates : (a) single-compartment; (b) multi-compartment; (c) SEM image of multi- compartiment microcapsule section.

Keywords: Double emulsion, water exchange, destabilization, polymer micro-device, math model

Tubulin-based fusion proteins as multifunctional intracellular tools

Microtubules play a critical role in the cytoskeleton by providing motility and transport alongside integrity to the eukaryotic cell[1]. These polymeric structures exist primarily as heterodimers comprised of α/β-tubulin. β-tubulin (TUBB), in particular, serves as a binding site for all drugs known to disrupt microtubule activity[2]. With the emergence of synthetic biology as a discipline, recent strategies have focused on technologies capable of modulating biological systems in a controlled and precise manner. The MacKay laboratory specifically employs protein polymers known as elastin-like polypeptides (ELPs) for use in intracellular modulation. These fusion proteins effectively undergo a rapid yet reversible self-assembly in response to alterations in temperature. The genetically-encoded nature and recombinant biosynthesis of ELPs further afford precise control over nanoparticle architecture, resulting in nanomedicines suited for the expression of biological moieties as fusion proteins. In addition, our group was the first to discover that these ELP fusions can influence macromolecular targets— intracellular switching— once expressed in living cells[3]. We now report that this platform technology has been further harnessed by exploring bioengineered TUBB-ELP fusions as multifunctional tools which can reversibly regulate the incorporation of β-tubulin into polymerizing microtubules akin to an on/off switch. Our work therefore pioneers a novel strategy allowing researchers to exert spatio-temporal control over microtubule assembly and mitosis via thermoregulation. In summary, ELPs can effectively generate multifunctional, tubulin-based tools that can be employed to elucidate basic microtubule dynamics in addition to serving as nanomedicines for therapeutic applications in the future.

1. Jordan MA, Wilson L (2004) Microtubules as a target for anticancer drugs. Nat Rev Cancer 4(4):253-65

2. Perez EA (2009) Microtubule inhibitors: Differentiating tubulin-inhibiting agents based on mechanisms of action, clinical activity, and resistance. Molecular Cancer Therapeutics 8(8):2086-95

3. Pastuszka MK, Janib SM, Weitzhandler I, Okamoto CT, Hamm-Alvarez S, MacKay JA (2012) A Tunable and Reversible Platform for the Intracellular Formation of Genetically Engineered Protein Microdomains. *Biomacromolecules* 13(11):3439-44

Acceptance ID: 3FTP-P

pH-responsive carbohydrate based molecularcapturer

Yiluo (Hu)[1],*Eunae(Cho)*[2*], *Seunho(Jung)*[1*]

[1]*Department of Bioscience and Biotechnology, Microbial Carbohydrate Resource Bank (MCRB), Center for Biotechnology Research in UBITA (CBRU), Konkuk University, 120 Neungdong-ro, Gwangjin-gu, Seoul 05029, Korea.*

[2]*Center for Biotechnology Research in UBITA (CBRU), Institute for Ubiquitous Information Technology and Applications (UBITA), Konkuk University, 120 Neungdong-ro, Gwangjingu, Seoul 05029, Korea.*

lannyhu0806@hotmail.com,echo@konkuk.ac.krand shjung@konkuk.ac.kr

pH-responsive polymeric materials are important for the controlled drug delivery, sensing, biomedical applications. Here, we synthesized cyclic oligosaccharide derivatives which can accept or release protons depending upon environmental pH. In the first approach, cyclosophoraoses (CyS), β-1,2 linked cyclic glucans with glucopyranose units ranging from 17 to 23, were modified with carboxymethyl(CM) groups, and the pH-dependent complexation of CM CyS with pindolol was investigated. Since CyS have a characteristic flexible conformation, the CM substitution mayinduce structural collapse or stretching on the CyS backbone by the electrostatic attraction or repulsion. Pindolol, a β-adrenoceptor antagonist, has a hydrophobic nature at high pH (pKa = 9.4), and CM CyS can solubilize efficiently pindolol in the high alkaline solution. The formation of the CM-Cys/pindolol complex was analyzed by UV spectroscopy, nuclear magnetic resonance (NMR), Fourier transform infrared (FT-IR) spectroscopy, differential scanning calorimetry (DSC), x-ray diffractometry (XRD), and scanning electron microscopy (SEM) techniques. In the second approach, β-cyclodextrin (β-CD) was derivatized with amino acids and dimerized. The resulting structure is also utilized as a novel pH responsive molecular capturer for target molecules.Based on this study, stimuli responsive carbohydrate based molecular capturer can be developed and improved for the research field of environmental biosensors, functional biomaterials, and drug delivery system.

Keywords: pH responsive, Molecular capturer, Cyclosophoraoses, β-Cyclodextrin,Carboxymethyl group

[1]KAZUNORI NAKANO, KAZUAKI ABURAYA, ICHIRO HISAKI, NORIMITSU TOHNAI, MIKIJI MIYATA. 2008. Flexible Host Frameworks with Diverse Cavities in Inclusion Crystals of Bile Acids and Their Derivatives. The chemical Record, Vol.9, 124-135 (2009).

Interaction of dsDNA with prednisone at poly(glyoxal-bis(2-hydroxyanil)) modified GCE

Gözde (Aydoğdu Tığ)[1], Derya (Koyuncu Zeybek)[2], Bülent (Zeybek)[3], Şule (Pekyardımcı)[1],

[1]Department of Chemistry, Faculty of Science, Ankara University, 06100 Beşevler Ankara/TURKEY
[2]Department of Biochemistry, Faculty of Science and Arts, Dumlupınar University, 43100 Germiyan Campus Kütahya/TURKEY
[3]Department of Chemistry, Faculty of Science and Arts, Dumlupınar University, 43100 Germiyan Campus Kütahya/TURKEY
pekyar@science.ankara.edu.tr/+903122126720/1195

Recently, there have been a growing interest in electrochemical investigation of interaction between drugs and dsDNA [1]. Electrochemical DNA biosensors involve a nucleic acid recognition layer which is immobilized over an electrochemical transducer. The recognition layer detects the changes that occurred in the DNA structure during interaction with DNA-drug molecules [2]. So, the study on the binding mode of drugs and dsDNA plays an important role in understanding of their clinical activities and design of new targeted drugs [3]. Prednisone is a synthetic corticosteroids usually prescribed in the treatment of a wide variety of inflammatory diseases such as asthma, rheumatoid arthritis, various kidney diseases including nephritic syndrome, allergies and cluster headache [4].

In this study, poly(glyoxal-bis(2-hydroxyanil)) (P(GBHA)) modified GCE (GCE/P(GBHA)) was prepared and this electrode was used for the electrochemical monitoring of interaction between the dsDNA and prednisone for the first time. The P(P GBHA film was characterized by scanning electron microscopy (SEM) and X-ray photoelectron spectroscopy (XPS) techniques. The GCE/P(GBHA)/dsDNA electrode was prepared by adsorption of dsDNA upon the P(GBHA) deposited the GCE and the binding of prednisone with dsDNA was investigated via differential pulse voltammetry (DPV) method. The decrease in the guanine oxidation peak current at +0.8 V was used as an indicator for the interaction in 0.5 M acetate buffer (pH 4.8) containing 0.02 M NaCl. The experimental parameters such as dsDNA concentration, drug concentration, adsorption time, interaction time were optimized. Under the optimal conditions, the guanine oxidation peak currents were linearly proportional to the concentrations of prednisone in the range of 1-50 mg/L. The prepared biosensor was applied to validate its capability for the analysis of prednisone in serum samples and pharmaceutical formulations.

Keywords: dsDNA, prednisone, poly(glyoxal-bis(2-hydroxyanil)), biosensor.

References:

[1] G. Xu, J. Fan, K. Jiao, Studies on the Electrochemical Property of Dinuclear Copper(II) Complex Containing Dimethylglyoxime and Its Interaction with DNA, Electroanalysis 20(11) (2008) 1209-1214.
[2] A. Erdem, M. Ozsoz, Electrochemical DNA Biosensors Based on DNA-Drug Interactions, Electroanalysis 14(14) (2002) 965-974.
[3] L. Han, Y. Zhou, X. Huang, M. Xiao, L. Zhou, J. Zhou, A. Wang, J. Shen, A multi-spectroscopic approach to investigate the interaction of prodigiosin with ct-DNA, Spectrochimica Acta Part A: Molecular and Biomolecular Spectroscopy 123 (2014) 497-502.
[4] I. Hafström, M. Rohani, S. Deneberg, M. Wörnert, T. Jogestrand, J. Frostegård, Effects of low-dose prednisolone on endothelial function, atherosclerosis, and traditional risk factors for atherosclerosis in patients with rheumatoid arthritis--a randomized study, The Journal of Rheumatology 34(9) (2007) 1810-1816.
S5:MMA2

Novel Multifunctional Gold Nanoparticles for Early Diagnosis of Inflammatory Diseases

Sun-Mi Lee (Lee)[1], *Chin Hee Mun (Mun)*[2], *Yong-Beom Park (Park)*[2], *Kyung-Hwa Yoo (Yoo)*[1,3]

[1]*Graduated Program for Nanomedical Science and Technology, Yonsei University, Seoul 120-749, Korea.*
[2]*Division of Rheumatology, Department of Internal Medicine, Institute for Immunology and Immunological Disease, College of Medicine, Yonsei University, Seoul 120-752, Korea.*
[3]*Department of Physics, Yonsei University, Seoul 120-749, Korea.*
sunmilee@yonsei.ac.kr

Rheumatoid arthritis (RA), a common chronic systemic autoimmunological disease, is characterized by infiltration of inflammatory cells into the granuloma-like pannus and the joint fluid, cartilage destruction and bone erosion. Recently, the early diagnosis of RA is an important in RA treatment. More recently, new imaging techniques such as nuclear medicine (single photon emission computed tomography and positron emission Tomography) and optical imaging have been proposed with results that can envisage a potential impact in the clinical management of RA. Optical imaging using nonspecific probes provide quick and easy operated multijoint monitoring of hands and feet. We have developed arginine-glycine-aspartic acid (RGD)-attached gold (Au) half-shell nanoparticles containing methotrexate (MTX) for the treatment of RA, where MTX is the most widely used disease modifying anti-rheumatic drug for the treatment of RA, and RGD peptide is a targeting moiety for inflammation. Upon near-infrared (NIR) irradiation, heat is locally generated due to Au half shells, and the drug release rate is enhanced, delivering heat and drug to the inflamed joints simultaneously. RA is a chronic inflammatory disease characterized by synovial inflammation in multiple joints within the penetration depth of NIR light. Furthermore, these multifunctional nanoparticles could be applied to early diagnosis of RA or other inflammatory diseases.

Keywords: Gold nanoparticle, inflammatory disease, near infrared, optical image

Acceptance ID: 4AT3-P

Biomolecule functionalized polydiacetylene -From molecular recognition to the selective visualization

Eunae(Cho)[1],*Jae-pil(Jeong)*,[2]*Seunho(Jung)*[2]

[1]*Center for Biotechnology Research in UBITA (CBRU), Institute for UbiquitousInformation Technology and Applications (UBITA), Konkuk University, 120Neungdong-ro, Gwangjingu, Seoul 05029, Korea.*
[2]*Department of Bioscience and Biotechnology, Microbial Carbohydrate Resource Bank(MCRB), Center for Biotechnology Research in UBITA (CBRU), Konkuk University,120 Neungdong-ro, Gwangjin-gu, Seoul 05029, Korea.*
echo@konkuk.ac.kr and shjung@konkuk.ac.kr

In the present study, we have designed the biomolecule-polydiacetylene (PDA) combinatorial platforms that the molecular recognition can be selectively visualized. Molecular recognition plays a key role in biological systems as a concept of supramolecular chemistry. PDA, the alternating ene-yne molecule, can induce a blue-to-red color transition and an interesting fluorescent response through the distortion of backbone. In the first approach, using polydiacetylenyl β-cyclodextrin (β-CD) based smart vesicles, the selective visualization of arginine and lysine has been explored among twenty amino acids. Secondly, usingsuccinoglycan octasaccharide (SO) serving as a metal coordination ligand, SO functionalized PDA vesicle is fabricated and investigated for color and fluorescence changes targeting nine different metal ions. Furthermore, alginate beads with embedded SO functionalized PDA vesicles are developed and evaluated as the tangible fluorogenic sensor system for barium (II) ions. Lastly, antibody (AB) is functionalized onto PDA for the specific recognition with influenza virus antigen, and the resulting AB PDA is materialized to PVDF strips. These biomolecule-conjugated functional materials will be developed consistently for the field of biomedical applications, functional biomaterials, and biosensors.

Keywords: Biomolecule,Polydiacetylene, Functionalization, Molecular recognition, Visualization

[1]**CHO, E.**, KIM, H., Paik, S. R., JUNG, S*. 2016. Polydiacetyleneyl β-cyclodextrin based smart vesicles for colorimetric assay of arginine and lysine. *Sci. Rep.* 6, 31115-31125.

[2]YUN, D.†**CHO, E.**,†DINDULKAR, S. D., JUNG, S.* 2016. Succinoglycan Octasaccharide Conjugated Polydiacetylene-Doped Alginate Beads for Barium (II) Detection.*Macromol.Mater. Eng*. 301, 805-811. (†These authors contributed equally to thiswork.)

Acceptance ID: 5Z7A-O

Design and synthesis of lipid derivative of Glucosamine for its application in targeting of exigent blood brain barrier

Yadav Nisha[1], *Vavia Pradeep*[1]

[1]*Centre for Novel Drug delivery system, Institute of Chemical Technology, N. P. Marg, Matunga, Mumbai, India.*
nishay.ict@gmail.com / +919773153115

Background: In vertebrates, the blood-brain barrier (BBB) is a dynamic barrier and is universally considered as the most important barrier for maintaining the brain homeostasis and protects the brain from toxic substances and invading organisms. Glucose transporter 1 (Glut1) is highly concentrated in BBB. Glut1 is unique in mediating glucose transfer across the BBB. Such observations led us to hypothesize that Glut1 may have a significant effect in the development of the junctional complexes of the BBB. Hence designing appropriate ligands that can achieve the targeting to BBB can be a promising technology.

Purpose: Glucosamine (GlcN) is structurally homologous to glucose and have been shown to bind to Glut1 transporters. Liposomes exhibit advantage of surface modification and easy uptake by cells however hydrophilicity of glucosamine exhibit hurdle in surface coating of liposomes. Here we synthesized a lipid based GlcN derivative for Glut1 targeting and validated its efficiency in delivery across BBB.

Method: To analyze the receptor binding potential, molecular flexible, *in silico* docking studies were performed by the grid-based ligand docking with energies (Glide). Activation of Glucosamine by N-hydroxy succinimide (NHS) and subsequent coupling with stearic acid by EDC-HCl to yield stearic acid derivative of glucosamine (SAD-GlcN). *In vitro* characterization of SAD-GlcN involved ^{1}HNMR, FTIR, MS, DSC. Afterwards liposome was prepared by ethanol injection technique and SAD-GlcN was incorporated during process. Once *in vitro* haemolysis study was executed, the systematic toxicity of SAD-GLcN was evaluated in healthy Balb/c mice after intravenous injection. Efficiency was validated with cytotoxicity study, cell uptake study and *in vivo* in glioma bearing nude mice models.

Results: The yield of reaction was 90% and *in vitro* uptake was tested in human glioma cell lines, U87MG and SF-268. Cells treated with coumarin-6-labeled and SAD-GlcN coated liposome exhibited higher fluorescence intensity than that of uncoated liposomes, suggesting that glucosylation on particle surface could evidently facilitate the uptake of liposomes.

Figure 1: Docking analysis of D-Glucose and SAD-GlcN respectively.

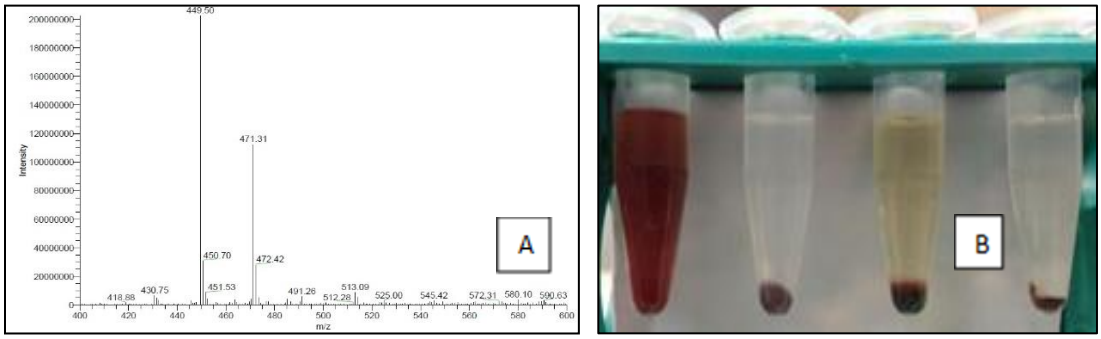

Fig2: (A) Mass spectra of SAD-GlcN, (B) (left to right): *in vitro* haemolysis study of positive control, SAD-GlcN coated, uncoated liposome and negative control respectively.

Conclusion: Successful synthesis of Glucosamine based targeting ligand and validation of its efficiency in delivery across challenging barrier like blood brain barrier. Further studies will be done to evaluate biodistribution.

Keywords: Glucosamine, lipid derivative, targeting, exigent, biological barrier.

References:

[1] GAO, H., QIAN, J., CAO, S., YANG, Z., PANG, Z., PAN, S. 2012. Precise glioma targeting of and penetration by aptamer and peptide dual-functioned nanoparticles. Biomaterials, 33, 5115-23.

[2] TAKATA K, KASAHARA T, KASAHARA M. 1990. Erythrocyte/HepG2-type glucose transporter is concentrated in cells of blood-tissue barriers. Biochem Biophys Res Commun, 173, 67–73.

A Facile, One Step, Microwave Assisted Hydro Thermal Synthesis and Characterization of $NaGdF_4$: Yb, Er, Tm White Upconversion Nanocrystals

$NaGdF_4$ nanocrystals co-doped with Yb, Er, Tm and stabilized with oleic acid are synthesized via microwave assisted hydrothermal method. This synthesis method is simple, one step and takes only 15 minutes to synthesize the nanocrystals. The synthesized nanocrystals give upconversion (UC) emission when excited with 980 nm CW laser. The white UC emission was achieved by fine tuning the ratio of lanthanide ion dopants (Yb, Er and Tm). The CIE co-ordinates (CIE-X = 0.33) and CIE-Y = 0.35) of UC emission are close to standard white light CIE co-ordinates (CIE-X = 0.33) and CIE-Y = 0.33). X-ray diffraction (XRD), field emission – transmission electron microscope (FE-TEM), fourier transform infrared spectroscopy (FT-IR) and photoluminescence (PL) spectroscopy are used characterize the synthesized UC nanocrystals. These UC nanocrystals have emission peaks at different wavelengths, which can be utilized in sensing applications like ratio metric based sensing and multiplexed sensing applications. These UC nanocrystals are also good candidates for bioimaging applications because of 980 nm excitation, which reduces the auto fluorescence from the tissues.

Acceptance ID: 6PF9-O

Graphene-gold nanocomposites for highly sensitive electrochemical detection of *E.coli* and *S. aureus* in less than an hour.

Vedashree Sirdeshmukh[1], Shreeram Joglekar[2], Prashant Alegaonkar[2], Preeti Nigam[3], Anup Kale[*].

[1]Department of Applied Sciences, College of Engineering, Pune – 411005, India,
[2]Department of Biosciences, Defence Institute of Advanced Technology, Pune – 411025, India,
[3]National Chemical Laboratory, Pune-411008, India

The improved diagnostic screening has become essential for detection and prevention of bacterial infections. The selection of an appropriate test or tool depends on the sensitivity, reliability, reproducibility, the time of detection and the specificity of the method involved. The conventional methods like culturing technique, ELISA and PCR based methods are time consuming and do not offer high sensitivity required for the detection at early stage or at very low levels. The electrochemical detection methods are rapid and capable of offering Point-Of-Care diagnosis. Recently, graphene based materials have emerged as most promising nanomaterials for electrochemical analysis. In order to achieve higher sensitivity, we synthesized functionalized reduced Graphene Oxide/gold (rGO-AuNP) nanocomposites and studied their significance over rGO and AuNP alone as detection platform. Electron microscopy revealed the uniform distribution of gold nanoparticles on rGO templates. It was a 3 step detection method: in the first step Screen Printed Electrode (SCE) was modified with rGO-AuNP; the second step was conjugation of specific antibodies on the modified electrode for the pathogenic strains of *E.coli* and *S. aureus* using carbodiimide chemistry, the third step was the detection of pathogens Differential Pulse Voltametry (DPV) method. The results showed that rGO-AuNP nanocomposites offer 2-4 fold higher sensitivity over rGO and AuNP alone. Importantly, the antibody conjugated bioactive SCE were stable for one month leading to carry out only third step at the time of detection. This offered rapid detection of pathogens, in less than an hour. The Limit of detection (LOD) was 2 CFU/mL for both E.coli and S. aureus making it highly sensitive. The physicochemical characterization of nanocomposites suggest that the improved sensitivity and stability was due to reduced band gap in composites and uniform distribution on AuNPs on rGO nanotempletes.

Acceptance ID: 6YN6-P

Double-shelled Hollow Zirconium Dioxide Nanostructure for CT Imaging Guided Tumor Microwave Thermotherapy and Chemotherapy

*Dan Long, Longfei Tan, Tianlong Liu, Changhui Fu, Xianwei Meng**

Laboratory of Controllable Preparation and Application of Nanomaterials, Technical Institute of Physics and Chemistry, CAS, No.29 East Road Zhongguancun, Beijing, China
*E Mail/ Contact Détails (**mengxw@mail.ipc.ac.cn**)*

Microwave (MW) ablation, which transfers the energy of MW to heat and effectively treat tumors, is widely applied to clinical use in China and Japan. However, the high temperature during MW ablation may cause severe normal tissue damage and unbearable pain. It is high desirable to develop new strategy to enhance the tumor specificity for microwave by both increasing ablation area in tumor and decreasing heating effect in normal tissues. This work synthesizes a novel multifunctional drug loading system based on double-shelled hollow ZrO_2 nanoparticles (ionic liquids/doxorubicin/phase change materials, IL/DOX/PCM@D-ZrO_2 NPs). Due to cooperative action of inner self-reflection and spatial confinement effect, the special double-shelled hollow nanostructure can improve the microwave hyperthermia sensitivity property under microwave irradiation. This multifunctional drug loading system could effectively increase the ablation temperature and ablation area to kill tumor cells and inhibit the proliferation of cancer with the help of anti-cancer drug DOX. In vivo experiments indicate that the as-made IL/DOX/PCM@D-ZrO_2 NPs exhibited perfect combined therapy effect of chemo and microwave hyperthermia on superficial tumors using H22 tumor-bearing mice model. Dual source CT is used to monitor the metabolism behavior of the as-made D-ZrO_2 NPs. Frozen section examination and ICP results indicates the temperature rise during microwave will enhance the tumor selectivity of drug delivery and cytotoxicity for chemotherapy.

Keywords: Double shelled, Hollow, ZrO_2, Microwave Thermotherapy, CT imaging

(1) LONG, D., LIU, T.L.; TAN, L.F., & MENG, X.W*, et.al. 2016, Multisynergistic Platform for Tumor Therapy by Mild Microwave Irradiation-Activated Chemotherapy and Enhanced Ablation, *ACS Nano*, 10, 9516–9528.

Acceptance ID: 7JBK-O

Thermosensitive hydrogel loaded with the complex of salmon calcitonin and oxidized calcium alginate for long-term anti-osteopenia therapy

Yanpeng Liu[1], *Xinyuan Xu*[1], *Lin Yu*[2,*], *Jiandong Ding*[2], *Jianshu Li*[1,*]

[1] *College of Polymer Science and Engineering, State Key Laboratory of Polymer Materials Engineering, Sichuan University, Chengdu, 610065, China.*
[2] *Key Laboratory of Molecular Engineering of Polymers of Ministry of Education, Department of Macromolecular Science, Laboratory of Advanced Materials, Fudan University, Shanghai, 200433, China.*
E Mail/ Contact Détails: jianshu_li@scu.edu.cn (J. Li); yu_lin@fudan.edu.cn (L. Yu)

Osteoporosis is an asymptomatic disease that leads to bone fragility and high risk of fracture with the bone mineral density loses and bone microarchitecture disrupts. Among therapies of Osteoporosis and osteodynia, Salmon Calcitonin (sCT) is a highly effective treatment for inhibiting bone resorption and decreasing blood calcium concentration. However, sCT is a functional peptide, which has a short half-life less than 1 h. So frequent injection was used for long-term therapy of osteoporosis in clinic. Here we report oxidized calcium alginate-salmon calcitonin (OCA-sCT) loaded tri-copolymer (PLGA-PEG-PLGA) hydrogel for long-term release. The polymer/water system exhibited a sol-gel transition at about 34 °C. Both the hydrogel degradation and decomposition of OCA-sCT complex play important roles in the process of sCT release. The system prolonged the release of sCT (~30 days) and reconstructed the bone trabecula in glucocorticoid induced model of SD rats. It also confirmed that the conformation of sCT was protected from aggregation during the entire release process. These preliminary results indicate that the injectable and thermoreversible *in situ* gelling systems have substantial potential for controlled peptide/protein drug delivery.

Keywords: Controlled release, peptide drug, salmon calcitonin, thermositive hydrogel, osteoporosis.

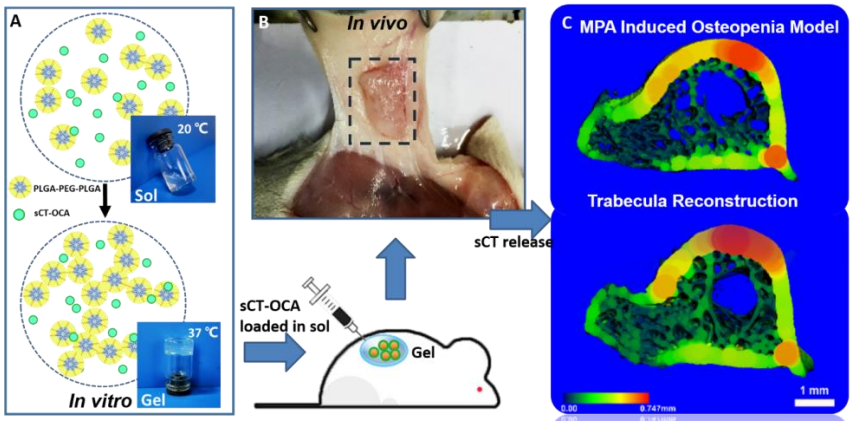

Scheme 1. Illustration of thermosensitive hydrogel for the controlled release of salmon calcitonin for anti-osteopenia treatment. (A) Amphiphilic PLGA-PEG-PLGA triblock copolymers self-assemble into micelles in sCT-OCA mixed solution at 20 ºC and turning into a physical hydrogel at 37 ºC. (B) The polymer formulation subcutaneously injection into the rats of MPA induced osteopenia. (C) After hydrogel degradation, sustained released sCT for osteopenia thearpy evaluated by Micro-CT images of trabecular thickness 3D reconstruction.

[1] MALGOSIA, M. P., SHANE, M., Molly S. S. 2016. Designer protein delivery: From natural to engineered affinity-controlled release systems. *Science*, 351, aac4750.

[2] GUANGTAO, C., TIANYUAN, C., LIN, Y., JIANDONG, D. 2011. Enhancement of the fraction of the active form of an antitumor drug topotecan via an injectable hydrogel. *J. Control. Release*, 156, 21-27.

Acceptance ID: 7T3L-O

Hydroxyapatite Nanoparticles as fluorescent probes for bio-imaging and gene delivery applications

Ketaki Deshmukh, M. Monsoor Shaik, Sutapa Roy Ramanan, ***Meenal Kowshik***[1]

Department of Biological Sciences[1]*, Department of Chemical Engineering*[2]*, Birla Institute of Technology and Sciences Pilani, K K Birla Goa Campus, Zuarinagar, Goa, India*

Bio-imaging has drastically transformed the field of medicine, and made the process of diagnosis easy and fast. Visualization of complete organ to complex biological processes has now become possible. Among the various imaging processes, fluorescence imaging using non-toxic fluorescent nanomaterials is advantageous for several beneficial features including high sensitivity, minimal invasiveness and safe detection limit. In this study, we report synthesis of a new class of non-toxic, self-activated fluorescent hydroxyapatite nanoparticles (fHAp NPs) with various aspect ratios (thin-rods, short-rods, rods), by changing the stabilizing agents (triethyl amine and acetyl acetone) and solvents (water and dimethyl sulfoxide). fHAp NPs exhibit excellent fluorescence with broad emission spectrum ranging from 350-750nm and maximum at 502nm. Presence of fluorescence is attributed to the electronic transition in the asymmetric structure of fHAp NPs as confirmed by ESR spectroscopy and absence of fluorescence in symmetric HAp NPs. In addition to exceptional fluorescence behavior, these NPs were found to be non-toxic in nature and could be easily internalized in both prokaryotic and eukaryotic systems. Results on the development of a one step method for transformation of Gram-positive and Gram-negative bacteria using these functionalized HAp NPs will be discussed. These HAp NPs are proposed as potential biocompatible candidates for bio-imaging and gene delivery applications.

Keywords: hydroxyapatite, nanoparticles, fluorescence, bioimaging, transformation

Acceptance ID: 8BVW-O

Modulation of the Epidermal Growth Factor Receptor using thermo-responsive elastin-like polypeptides

Zhe Li[1], *David Tyrpak*[1], *Mincheol Park*[1], *Curtis Okamoto*[1], *J. Andrew MacKay*[1,2]

[1]*Department of Pharmacology and Pharmaceutical Sciences,*
[2]*Department of Biomedical Engineering,*
University of Southern California, USA.
zli351@usc.edu

The precise manipulation of cell signaling is one of the main challenges for understanding biological systems as well as biomedicine development. Our lab has recently discovered that thermally responsive protein polymers, elastin-like polypeptides (ELPs), are powerful tools to achieve assembly of expressed fusion proteins within living cells,[1,2] Using this method, we generated a rapid and reversible protein switch that controls epidermal growth factor receptor (EGFR) activity in response to temperature changes. In the absence of EGF, fusion of an ELP to the cytosolic domain of EGFR triggers temperature-dependent clustering of EGFR and therefore initiates downstream events including signal activation and receptor internalization. Unlike synthetic ligands[3] or genetic perturbations[4], ELP-mediated receptor clustering can be thermally turned ON and OFF with a resolution of minutes and its reversibility enables dynamic control of downstream activation of ERK1/2. This rational strategy to engineer temperature-sensitive receptors may be a powerful platform to analyze and manipulate cell signals, with potentially broad applicability to other biological processes.

Keywords: environmentally-responsive polypeptide, elastin-like polypeptides, cell signaling, synthetic biology, ERK dynamics

[1] PASTUSZKA, M. K., JANIB, S. M., WEITZHANDLER, I., OKAMOTO, C. T., HAMM-ALVAREZ, S. & MACKAY, J. M. 2012. A Tunable and Reversible Platform for the Intracellular Formation of Genetically Engineered Protein Microdomains. *Biomacromolecules*, 13(11), 3439-3444.

[2] PASTUSZKA, M. K., OKAMOTO, C. T., HAMM-ALVAREZ, S. & MACKAY, J. M. 2014. Flipping the Switch on Clathrin-Mediated Endocytosis using Thermally Responsive Protein Microdomains. *Advanced functional materials*, 24(34), 5340-5347.

[3] SPENCER, D. M., WANDLESS, T. J., SCHREIBER, S. L. & CRABTREE, G. R. 1993. Controlling Signal Transduction with Synthetic Ligands, *Science*, 262, 1019-1019.

[4] DIKIC, I., SCHLESSINGER, J. & LAX, I. 1994. PC12 Cells Overexpressing the Insulin Receptor Undergo Insulin-dependent Neuronal Differentiation, *Current Biology*, 4(8), 702-708.

Acceptance ID: 986L-P

BIOACTIVE MOLECULES INCORPORATED GELATINE SPHEARS AS A MODE OF SUSTAINED DRUG RELEASE FOR THERAPEUTIC APPLICATION

Vitamins, minerals and nutritional supplements are micronutrients that benefit the body to boast up the immune system and repair DNA. Nutritional supplements derived from foods and herbs have shown biologic effects, with some potential in clinical trials for various diseases. Advantage in using these approaches are safe symptom relief and joint remodeling in osteoarthritis. Forty seven percent of adults utilize non prescribed medications for OA including nutritional supplements, such as phytoflavonoids, polyphenols, and bioflavonoids which are natural compound found in trees, spices, wines and vegetables based on their their anti-inflammatory and anti-catabolic actions, and protective effects against oxidative stress. We have used Retinoic acid which is a metabolite of retinol that mediated basic function of growth and development which is well known to have diverse immunomodulatory actions. Role of all trans retinoic acid have been investigated on mice model where retinoic acid have shown their anti-arthritic effect suppressing the clinical signs of arthritis. So here in our work we have tried to encapsulate the retinoic acid molecule inside the gelatin spheres and then further embedded this in the scaffold. Trying to achieve the tissue engineering construct that covers the basic components of tissue engineering i.e. scaffold, chondrocytes, bioactive factors. After synthesis the *invitro* release profile was studied and then further all delivery modes synthesized were studied by MTT, SEM, GAG, Collagen assay. In this study we have shown a steady release of GAG and Collagen matrices which have been proved to be beneficial treating arthritis.

Acceptance ID: 9PQC-O

A Novel Cathepsin L Inhibition Assay using Field Effect Transistor Technology

Tae Wha Seong[1)] *and* *Kwan Hyi Lee*[1), 2)†]

[1]*Center for Biomaterials, Biomedical Research Institute, Korea Institute of Science and Technology (KIST), Seoul 02792 Republic of Korea.*
[2]*Department of Biomedical Engineering, Korea University of Science and Technology (UST), Seoul 02792, Republic of Korea.*
E-mail: kwanhyi@kist.re.kr

Enzymatic inhibition assays are essential in assessing the potency of a novel inhibitor. Along with in vitro cell-line and in vivo animal based experiments, it provides a clue as to which inhibitors may succeed in clinical trials. Inhibitors of cathepsin L have been continuously developed and exhibited suppression of tumor growth, drug resistance, and angiogenesis. Cancers with upregulated cathepsin L including ovarian, breast, prostate, lung, gastric, pancreatic, and colon cancer may benefit from cathepsin L inhibitors. Moreover, there is evidence that cathepsin L inhibition prevents murine autoimmune diabetes via suppression of CD8 T cell activity. The most commonly used method for cathepsin L inhibition assays utilize fluorophores bound to short amino acid sequences. These fluorophores emit fluorescence when cathepsin L cleaves the linkage between the amino acids and the fluorophore. However, fluorometric assays can suffer from wavelength interference caused by impurities and the instability of many fluorescent compounds when exposed to light. Moreover, continuous monitoring of time dependent kinetic studies is hindered by plate reader performance and the low sensitivity of the assay can be an obstacle to high-throughput enzyme activity assays. To overcome these issues, a novel quantitative electrical assay for cathepsin L has been developed utilizing field effect transistors (FET) technology. In this study, the disposable sensing membrane of our FET device has been coated with full length histone H3, which is a known substrate of cathepsin L. Reaction with cathepsin L can be quantitatively measured by the FET device as the full length histone H3 is cleaved by cathepsin L. Furthermore, the efficacy of a cathepsin L inhibitor can also be quantified through quantifying electrical signal changes. Our novel quantitative electrical assay for cathepsin L offers high sensitivity, continuous monitoring of enzyme kinetics, and a circumvention from wavelength interference and fluorophore instability. This clearly signifies the potential of utilizing ISFET for cathepsin L inhibition assays.

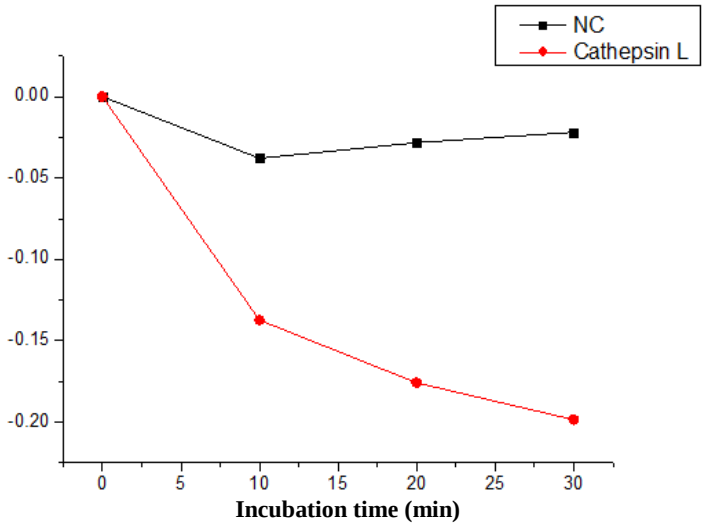

Time dependent voltage shift after cathepsin L & Histone H3 reaction

Keywords: Cathepsin L, Enzyme inhibitor assay, Field effect transistor

Acknowledgements: This research was supported by the Bio & Medical Technology Development Program of the NRF funded by the Korean government MSIP (2015M3A9E2029265).

Acceptance ID: ARZ7-O

Mesoporous Silica-based Nanoparticles for Site-specific Delivery of Small Signaling Molecules

Research during the past three decades has revealed that small molecules like nitric oxide (NO), carbon monoxide (CO) and hydrogen sulfide (H2S) act as important signaling molecules in human physiology and pathology at submicromolar to micromolar levels. Modulations of the levels of these gasotransmitters at specific biological targets lead to various salutary effects. The “toxic” nature of these gaseous molecules however poses as a challenge to deliver them safely in hospital settings. As a consequence, the quest for discrete and biocompatible platforms that can deliver low doses of these gasotransmitters under controlled conditions has gained momentum. We have recently demonstrated that mesoporous silica-based materials and nanoparticles can serve as excellent carriers for pro-drug molecules and aid in site-specific delivery of these unusual “drugs” under the control of light. Recent results of successful delivery of NO and CO to malignant and infection sites will be discussed in this talk.

Acceptance ID: BASZ-O

Detection of Prostate Cancer Specific Biomarkers in Clinical Urine Samples Without a Digital Rectum Exam.

Sungwook Park[1), 2)], Jaewon Choi[1), 2)], Minhong Jeun[1)], Hyunwoo Son[1)], Sang Hoon Song[3)], In Gab Jeong[3)], Choung-Soo Kim[3)] and Kwan Hyi Lee[1), 2)†]

[1]*Center for Biomaterials, Biomedical Research Institute, Korea Institute of Science and Technology (KIST), Seoul 02792 Republic of Korea*

[2]*Department of Biomedical Engineering, Korea University of Science and Technology (UST), Seoul 02792, Republic of Korea*

[3] *Department of Urology, Asan Medical Center, University of Ulsan College of Medicine, Seoul 05505, Republic of Korea*

kwanhyi@kist.re.kr

Initial prostate cancer diagnosis is as important as the actual cancer treatment process, as cancer stage confirmation dictates the treatment type and method. However, conventional methods utilized in the identification of prostate cancer, such as the invasive digital rectum exam (DRE), are a source of great stress to the patient. If the presence of prostate cancer specific biomarker can be detected directly from a physiological urine sample that was not subject to DRE, it will be of great convenience to both the patient and the medical practitioner. Herein lies the problem. Because the solution in which the biomarker is contained is urine, the platform will have to overcome the challenges presented by the urine solution itself. Hardships of urine sample analysis are usually a product the patient's lifestyle and thus, are influenced by the patient's diet and circadian rhythm. This will lead to situations where the chemical composition of different urine samples may differ even though they were obtained from the same patient [1, 2]. This platform is capable of identifying prostate cancer specific biomarkers in a clinical urine sample directly, and without the need to subject the solution to dilution or chemical modification

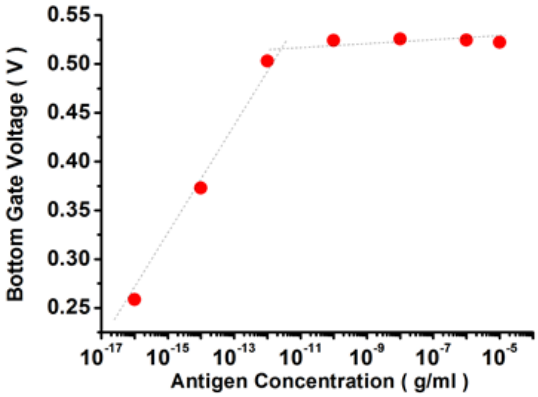

Biomarker Concentration Dependent Voltage Shift

Keywords: Prostate cancer, biomarker, urine, diagnosis

Acknowledgements: This research was supported by the Bio & Medical Technology Development Program of the NRF funded by the Korean government MSIP (2015M3A9E2029265).

[1] J. WILKOSZ, M BRYŚ, AND W. RÓŻAŃSKI, “Urine markers and prostate cancer”, *Cent. European J. Urol*. Vol. 64, pp. 9-14, 2011

[2] M. SCHOSTAK, G.P. SCHWALL, S. POZNANOVIC, K. GROEBE, M. MULLER, D. MESSINGER, K. MILLER, H. KRAUSE, A. PELZER, W. HORNINGER, H. KLOCKER, J. HENNENLOTTER, S. FEYERABEND, A. STENZL, and A. SCHRATTENHOLZ, “Annexin A3 in urine: a highly specific noninvasive marker for prostate cancer early detection”, *J. Urol*. Vol. 181, pp. 343-353, 2009

Acceptance ID: C682-O

Fabrication of laser-induced graphene electrode based flexible and stretchable electrochemical biosensor

*Taeheon Kim, Jeongdae Kim, Saeyoung Kim, James Jungho Pak**

Department of Electrical Engineering, Korea University, 5-ga, Anam-dong, Seongbuk-gu, Seoul 136-713, Republic of Korea
Corresponding author E-mail: pak@korea.ac.kr

Recently, flexible and stretchable bioelectronic systems are notable for its conformability, low-cost manufacturing so that these characteristics can make possible to minimally invasive, implantable, wearable healthcare [1]. However, there are still limitations for the mass production due to the complicated fabrication method and the expensive electrode material [2]. To overcome these limitations, laser-induced graphene (LIG) was employed because of the following advantages [3]: (1) LIG is a chemically inert carbon nanomaterial and the laser photothermal effect makes larger active electrode area with the 3-D network. (2) LIG can be fabricated by a one-step facile laser irradiation process on commercial polyimide films. Specifically, the sp^3-carbon atoms which consist of PI film are photothermally converted to sp^2-carbon atoms by CO_2 infrared laser (3) LIG film can produce a good electrical conductivity, ~25 Scm^{-1}.

In this paper, we describe the fabrication and characteristics of a LIG electrode-based simple flexible/stretchable 3-electrode electrochemical biosensor. In order to realize the LIG electrode-based electrochemical biosensor on any flexible/stretchable polymer substrate, LIG electrode was first made on a polyimide layer and it was transferred onto the flexible/stretchable polymer substrate. Its electrical conductivity can be adjusted by adding the dopant material in a coated material on the polyimide film before laser irradiation process. A simple LIG-based 3-electrode electrochemical sensor was designed, fabricated, and characterized using cyclic voltammetry.

Keywords: laser-induced graphene, stretchable, flexible, electrochemical, biosensor

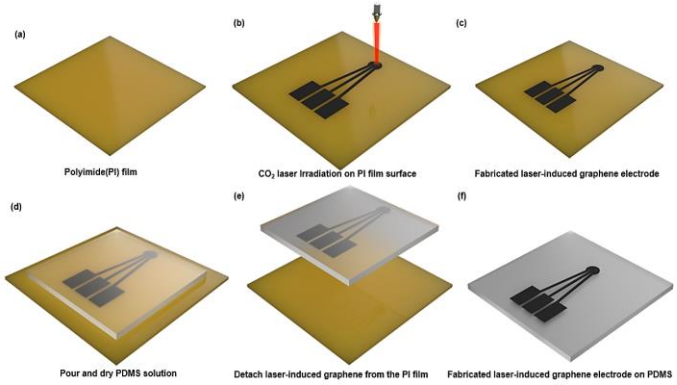

Figure 4 the fabrication method of transferred LIG electrode on flexible/stretchable substrate

References

[1] CHOI, S., LEE, H., GHAFFARI, R., HYEON, T. & KIM, D.-H. 2016. Recent Advances in Flexible and Stretchable Bio-Electronic Devices Integrated with Nanomaterials. Advanced Materials, 28, 4203-4218.

[2] ROGERS, J. A., GHAFFARI, ROOZBEH, KIM, DAE-HYEONG 2016. Stretchable Bioelectronics for Medical Devices and Systems. Springer International Publishing.

[3] LIN, J., PENG, Z., LIU, Y., RUIZ-ZEPEDA, F., YE, R., SAMUEL, E. L. G., YACAMAN, M. J., YAKOBSON, B. I. & TOUR, J. M. 2014. Laser-induced porous graphene films from commercial polymers. Nature Communications, 5, 5714.

Acceptance ID: CBS8-P

Development of phosphorylated pullulans and their application for controlled drug release

Abe[1], *Okajima*[2], *Kamenoue*[2], *Yamamoto*[2], *Nagaoka*[3], *Okihara*[2], *Takashiba*[3], *and Yoshida*[1]

[1]*Graduate School of Dental Medicine, Hokkaido University, Sapporo 060-8586, Japan,* [2]*Graduate School of Natural Science and Technology, Okayama University, Okayama 700-8530, Japan,* [3]*Graduate School of Medicine, Dentistry and Parmaceutical Sciences, Okayama University, Okayama 700-8558, Japan*
*E Mail/ Contact Détails (**sabe@den.hokudai.ac.jp**)*

Polysaccharides such as amylose are well-known to biocompatibility and biodegradability and have been much attention for application in widely fields, especially food, cosmetics, medical, and pharmaceutical applications. Pullulan is a kind of polysaccharide, which is consists of glucose, and the structure is α-1,6-linked maltotriose. This polysaccharide shows excellent low viscosity solution and adhesive properties to hard tissue and then is expected for biological application. In this study, we investigated on a novel preparation of phosphorylated pullulan and their application for effective controlled drug release system. Phosphorylation modification for pullulan based on the microwave heating improved their adhesiveness to hard tissue such as bone and teeth. When the obtained pullulan derivatives (PPL) mixed with cetylpyridinium chloride (CPC), which is a typical antibacterial agent with biphiphilic structure, the mixture indicated turbid depending on the concentration and mixture ratio. It suggests less-soluble complex formation between PPL and CPC. To elucidate their ability of drug carrier, the mixture was adsorbed on the surface of hydroxyapatite and then *S. mutans* were cultured on the apatite plate. When only CPC was treated on the surface even at 100,000 ppm, *S. mutans* grew as same as non-coated ones. However, the plate coated with PPL-CPC complex at 100 ppm, *S. mutans* observed rarely after 12 h cultivation. It suggests that PPL can adhesive to the apatite surface and CPC be released from the PPL-CPC complex effectively. Therefore, PPL-CPC complex can allow to a newly application for controlled drug release system, especially hard tissue.

Keywords: Phosphorylated pullulan, Drug release system

Acceptance ID: F3DJ-P

Control of Molecular Recognition via Nano-Environment Effects for Chemical Sensing

Roman Kostecki[1,], Sabrina Heng[1], Andrew D. Abell[1], Heike Ebendorff-Heidepriem[1], and Tanya M. Monro[1,2]*

[1]*ARC Centre of Excellence for Nanoscale BioPhotonics (CNBP) and Institute for Photonics and Advanced Sensing (IPAS), School of Physical Sciences, The University of Adelaide, Adelaide 5005, Australia.*
[2]*University of South Australia, Adelaide 5000, Australia.*
[*]*roman.kostecki@adelaide.edu.au*

The ability of a sensing molecule to specifically bind an analyte and elicit a response is a central component of any sensing molecule, such as those used to provide functional surfaces to optical fiber based chemical sensors. This binding is driven by molecular recognition as defined by the chemical make-up of both sensing molecule and analyte but also the local molecular nano-environment that they confront. To specifically control the local molecular nano-environment and thus influence binding interactions of a functional surface, without changing chemical structure, is an attractive proposition towards optical fiber based sensing elements with highly selective surfaces for detection of biologically and/or environmentally relevant ions.

Photoswitchable spiropyran-ionophore (SI1) sensing molecule was chosen, as it was found to form both a single-ligand complex with Ca^{2+} and a dual-ligand complex with Al^{3+}, as shown on the left of Fig. 1. We sort to control SI1s selectivity to these ions by subjecting it to a range of significantly different nano-environments, being in solution (Fig. 2A top), chemisorbed onto a fiber core surface (Fig. 2B top), or physisorbed into a thin-film PMMA on the core surface (Fig. 2C top). The fluorescence characteristics of SI1 were used to compare the effect of these three different nano-environments on the ability of SI1 to bind Al^{3+} and Ca^{2+}. Solution-based measurements revealed the MC isomer strongly fluoresced when single-ligand complexed with Ca^{2+} and had modest fluorescence when dual-ligand complexed with Al^{3+}, shown in Fig. 2A. Next, silica

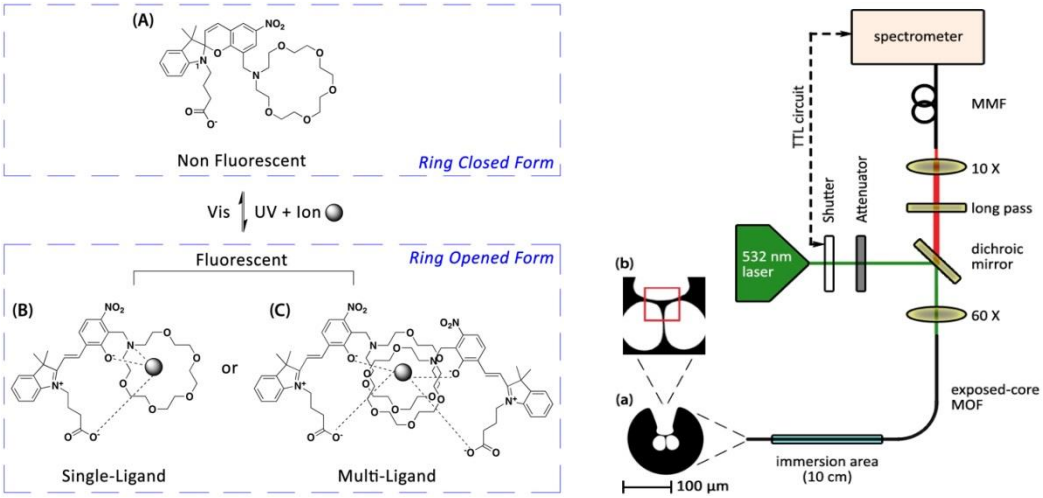

Fig. 1. (Left) Cation interaction with Spiropyran-ionophore molecule (SI1) (Ref. [1] has more details about SI1 type molecules) (a) represents the SP ring-closed, non fluorescent form. (b) and (c) represent the ring-opened, fluorescent forms of MC-cation single- and multi-liganded complexes. (Right) Schematic of the setup used to measure the fluorescence from MC-cation complexes at the surface of silica ECF core, including a cross section of (a) the ECF from a SEM, and enlarged view (b) of the core (7.5 µm effective diameter) indicated by the red square. MMF is multimode fiber.

Fig. 2. Comparison of peak fluorescence intensity from SP isomer without ions, MC isomer without ions, (SI1)MC-Ca^{2+} complex, and

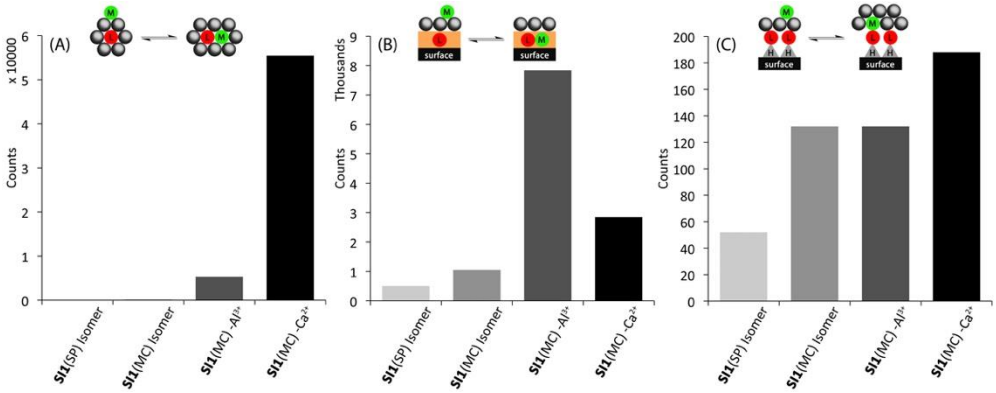

2(SI1)MC-Al^{3+} complex. (A) Shows results of MC isomer and (SI1)MC-cation complexes in solution, (B) shows results from ECF1 (polymer doped (physisorbed) with SI1), and (C) shows results from ECF2 (covalently bound (chemisorbed) SI1.

exposed-core microstructured optical fibers (ECFs)[2] were prepared with SI1 chemisorbed onto the core surface or physisorbed into a thin-film PMMA on the core surface, using methods shown in Refs. [1,3]. The fiber profile, core area and measurement setup is shown on the right side of Fig. 1. The response from the MC isomer of SI1 doped within the thin-film PMMA on the ECF core (Fig. 2B) showed that the fluorescence from the dual-ligand complex with Al^{3+} was twice that of the single-ligand complex with Ca^{2+}. This is in contrast with the solution-based measurements that showed the opposite, i.e. more fluorescence with Ca^{2+} and less with Al^{3+}. The measured response from the chemisorbed MC isomer on the ECF core surface (Fig 2C) showed an increase in the fluorescence intensity when exposed to Ca^{2+}, however in the presence of Al^{3+} did not result in an increase in fluorescence intensity. This result was significantly different from the solution-based experiments (Fig. 2A).

These results demonstrate that defining the associated nano-environment can control the sensitivity and selectivity of a spiropyran-based fluorescent sensing molecule toward a range of metal ions. The different nano-environments had differing affects on the relative affinity for single-ligand and dual-ligand binding to Ca^{2+} and Al^{3+} respectively.

Keywords: Nano-environment effects, Molecular recognition, Sensing and sensors, Chemical analysis, Thin film devices and applications

[1] HENG, S., NGUYEN, M., KOSTECKI, R., MONRO, T. M., & ABELL, A. D. 2013. Nanoliter-scale, regenerable ion sensor: sensing with a surface functionalized microstructured optical fiber. *RSC Adv.* 3, 8308-8317.

[2] KOSTECKI, R., EBENDORFF-HEIDEPRIEM, H., DAVIS, C., MCADAM, G., WARREN-SMITH, S., & MONRO, T. M. 2012. Silica exposed-core microstructured optical fibers. *Opt. Mater. Express* 2, 1538-1547.

[3] KOSTECKI, R., EBENDORFF-HEIDEPRIEM, H., AFSHAR V., S., MCADAM, G., DAVIS, C., & MONRO, T. M. 2014. Novel polymer functionalization method for exposed-core optical fiber. *Opt. Mater. Express* 4, 1515-1525.

Acceptance ID: FYLW-O

Lipid monolayers as gate dielectric in field effect transistors sensors with sub-femtomolar limit of detection Application to the detection of ions in solution

T. Nguyen Duc[1], A. Kenaan[2], R. El Zein[2], H. Dallaporta[2], J.-M. Raimundo[2], A. Charrier[2]

[1]NACENTECH-IMET, Ha Noi, Vietnam
[2]Aix-Marseille Université, CNRS, CINaM UMR 7325, 13288 Marseille, France
charrier@cinam.univ-mrs.fr

The ability to detect ions/molecules at very low concentrations has become a general society requirement. Heavy metals present at low concentrations in natural waters accumulate in plants and animal tissue to reach toxic doses. Endocrine disruptors, such as pesticides or bisphenol are now known to be toxic at femtomolar concentrations. The detection of ions of pathological or physiological interest in the body associated with high sensitivity and specificity offers large opportunities for the early diagnostic and treatment of diseases. For example, the case of the Wilson disease, which is induced by the accumulation of copper in tissues, is one of these typical examples. When the disease is diagnosed early enough it can be efficiently treated while it leads to death when the diagnostic is realized at too advanced stages in the disease. It is therefore crucial to develop a test with unique features such as ease of use, fast and low cost allowing systematic early diagnostic. Our project stands in this framework with the development of ion sensors.

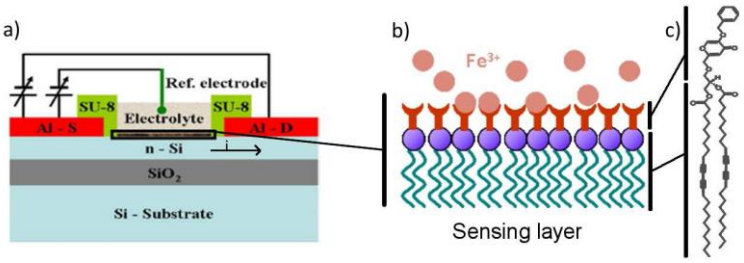

Our device is based on field effect transistor (FET) technology and is constituted of an organic lipid monolayer with a thickness of 2.5 nm used as gate dielectric instead of classical inorganic oxide. Using an ultra-thin dielectric increases the sensitivity of the sensor while allowing using low operating voltage. The specificity of the detection relies on the development of specific chelators that are grafted to the lipids head-groups. Together the lipid monolayer and the chelator constitute the active layer of the device and play a major role in the device performances.

We show how the quality of the monolayer in terms of density and mechanical stability directly impacts its insulating properties and performances [1-4]. Sensing examples regarding iron III and copper II detection are demonstrated with sensitivities down to the sub-femtomolar range and linear quantification over more than 10 decades [5-6]. These are the best results reported so far for small ions detection.

Keywords: Ion-Sensor, ISFET, lipid monolayer, ultra-thin dielectric

[1] A. Charrier, T. Mischki, G.P. Lopinski, *Langmuir* **2010**, 26, 2538-2543.

[2] C. Dumas, R. El Zein, H. Dallaporta, A.M. Charrier, *Langmuir* **2011**, 27, 13643-13647.

[3] R. El Zein, H. Dallaporta, A.M. Charrier, *J. Phys. Chem. B* **2012**, 116, 7190-7195.

[4] A. Kenaan, Ahmad, TD. Nguyen, H. Dallaporta, J.M. Raimundo, **A. Charrier**. *Anal. Chem.* **2016**, 88, 3804-3809

[5] T.D. Nguyen, R El Zein, JM Raimundo, H Dallaporta, A Charrier, *J. Mat. Chem. B* **2013**, 1, 443-446.

[6] T.D. Nguyen., A Labed, R El Zein, S Lavandier, F Bedu, I Ozerov, H Dallaporta, JM Raimundo, A Charrier *Biosens. Bioelectron.* **2014**, 54, 571-577.

Acceptance ID: H69L-O

Fluorescent potassium ion sensors

Yanqing Tian

Materials Science and Engineering, South University of Science and Technology of China, Shenzhen, 518055, e-mail: Tianyq@sustc.edu.cn

Potassium ions which make up about 0.4% of the mass in the human body and are the most abundant intracellular cation, play diverse roles in biological processes including muscle contraction, heartbeat, nerve transmissions, and kidney functions. Abnormal K^+ fluctuations are early indicators of diseases such as alcoholism, anorexia, bulimia, heart disease, diabetes, AIDS, and cancer. Therefore the detection of K^+ in physiological environment is of great significance. One of the earliest and best-known intracellular fluorescent K^+ probes is potassium-binding benzofuran isophthalate (PBFI), which uses a diaz-18-crown-6 as a ligand and a benzofuran derivative as the fluorophore. Unfortunately, PBFI, suffers poor selectivity for potassium ions with respect to sodium ions (Na^+).

Herein, we will describe our results for developing highly selective potassium ion sensors. We used triazacryptand (TAC) as a high selective potassium ion ligand and various fluorophores for preparing highly selective potassium molecular and planar polymeric probes. We constructed a potassium ion sensor using a 2-dicyanomethylene-3-cyano-4,5,5-trimethyl-2,5-dihydrofuran (TCF) as a strong electron withdrawing group and the TAC as the electron donating group for the first intracellular potassium ion sensor. Later we incorporated a triphenylphosphonium (TPP) unit into a BODIPY fluorophore with TAC as the ligand for the first mitochondrial targeting potassium ion probe. These two molecular probes show high selectivity for potassium ions and capable for monitoring intracellular potassium fluxes. Especially the probe with TPP moiety showed high co-localization efficiency for mitochondria. We also prepared a polymerizable potassium ion probe using naphthalimide as the fluorophore for generation of planar thin film-based potassium ion sensors. These polymeric sensors showed potassium ion dynamic response ranges from 1 to 20 mM, indicating its suitableness for extracellular sensing. This sensor also has a minimum influence by pH from 6 to 8, showing its suitableness for biostudies. We tested whether this sensor can be used to monitor extracellular potassium ion concentration changes. We used lysozyme to kill bacteria (E. Coli and B. Subtilis) to release their cellular potassium ions to the media to enable us to monitor potassium concentration changes in real time. Results showed that potassium ion concentration is higher with higher cell densities. We also found the difference among the two species of cells. E coli release potassium ions much slower than that Subtilis did. Thus in this presentation, we will give detailed results about our potassium ion sensors.

[1] Xiangxing Kong, Fengyu Su, Liqiang Zhang, *et al*., A Highly Selective Mitochondria-Targeting Fluorescent K+ Sensor, *Angew Chem Int Ed*, **2015**, *54*, 12053-12057
[2] Xianfeng Zhou, Fengyu Su, Yanqing Tian, *et al*., A New Highly Selective Fluorescent K+ Sensor, *Journal of the American Chemical Society* **2011**, 133, 18530–18533
[3] Xianfeng Zhou, Fengyu Su, Weimin Gao, *et al*., Triazacryptand-Based Fluorescent Sensors for Extracellular and Intracellular K^+ Sensing, *Biomaterials*, **2011**, *32* (33), 8574-8583.
Acceptance ID: J3RC-O

Advanced electrical biosensor for biofluid-based diagnosis

Hye Jin Kim[1, 2], Jinsik Kim[3], YoungSoo Kim[4], Jung Ho Park[2] and Kyo Seon Hwang[1]

[1]Department of Clinical Pharmacology, Kyung Hee University, Seoul 02447, Korea
[2]Department of Electrical Engineering, Korea University, Seoul 02841, Korea
[3]Department of Biomedical Engineering, Dongguk University, Seoul 04620, Korea
[4]Department of Pharmacy, Yonsei University, Incheon 21983, Korea
k.hwang@khu.ac.kr/ Kyo Seon Hwang

A bio-fluid is a representative clinical material used for a diagnosis of disease and composed of various bio-molecules as well as a specific disease marker. In case a disease diagnosis with the bio-fluid, many sensors are suffering from a low sensitivity and accuracy by a random absorption of the bio-molecules [1]. Therefore, a subsidiary processes purifying an unrefined bio-fluid with an analyte without absorbated bio-molecules through a fractionation process such as a centrifuging [2], a microfluidic cell sorting [3] are essential for high sensitive bio-fluid based diagnosis. These fractionation process separated with a detection process lead to a low convenience, hence one-chip based sensing tool which conduct a sensing simultaneously with a fractionation is required for more competitive biosensor.

Here, a novel concept of an interdigitated microelectrodes (IME) based on a dielectrophoresis effects is proposed for high sensitive diagnosis in bio-fluid. By applying the AC voltage to the electrodes, the absorbable molecules are expelled from a reaction region and consequently the deterioration of the sensor`s performance by the molecule's absorption is alleviated without any additional process.

The performance of the IME is verified with an impedance changes (ΔZ) by immune reaction of amyloid beta monomer (Aβ monomer, 4.5 kDa) according to the AC voltage. The IME consisted of a 30 pairs of platinum (Pt) with 5 μm interval and width is fabricated on SiO_2 surface and the antibody is immobilized on the SiO_2. Applied frequency and voltage to fractionate the molecules other than Aβ monomer are fixed at 50 MHz and 0.5 V_{pp} which expel the molecules over 4.5 kDa [4].

To proof the concept, the ΔZ is measured in PBS buffer consist of Aβs with divers structures, Aβ monomer and fibril. The ΔZ is about 4.59% and 1.83% in reaction condition with and without AC voltage respectively by fractionation of the fibril types of Aβ. The improvement of sensor`s performance is also observed using fluorescent image and the intensity by fluorescent is higher about 2-fold in AC condition. Also, the ΔZ is verified in PBS buffer with different types of molecule, HSA and IgG and the ΔZ is enhanced about 3.16% by the AC voltage, which is higher about 1.84-fold than the value verified in reaction condition without AC voltage.

Moreover, the ΔZ is measured in standard plasma according to the concentration of the spiked Aβ monomer. The ΔZ changes about 4.39 to 9.59% in range from 0.01 pg mL^{-1} to 1000 pg mL^{-1} by the AC voltage, whereas it changes in reaction condition without AC voltage about -0.54 to 0.92% according to the Aβ monomer`s concentration range from 0.01 pg mL^{-1} to 100 pg mL^{-1}. As a result, the sensitivity is improved about 1.96-fold and the dynamic range is extended about 2-order by the fractionation of absorbable molecules.

Consequently, we verify that the bio-fluid based diagnosis is able to be occurred in one-chip followed by the enhancement of the sensor`s performance.

Keywords: Enhancement of sensitivity, Lab on a chip, bio-sensor, bio-fluid based diagnosis,

[1] De, M., Rana, S., Akpinar, H., Miranda, O. R., Arvizo, R. R., Bunz, U. H., & Rotello, V. M. (2009). Nature chemistry, 1(6), 461-465.

[2] Boksebeld, M., Blanchard, N. P., Jaffal, A., Chevolot, Y., & Monnier, V. (2017). Gold Bulletin, 50(1), 69-76.

[3] Bose, S., Singh, R., Hanewich-Hollatz, M., Shen, C., Lee, C. H., Dorfman, D. M., ... & Karnik, R. (2013). Scientific reports, 3, 2329.

[4] Kim, H. J., Kim, J., Yoo, Y. K., Lee, J. H., Park, J. H., & Hwang, K. S. (2016). Biosensors and Bioelectronics, 85, 977-985.

Acceptance ID: MQJJ-P

Reconcile rigidity and flexibility for implantable probes

Implantable electrodes have been widely used for biomedical research and therapy. Due to size and mechanical mismatch between electrodes and live cells and tissues, existing probes face many challenges in performance and biocompatibility. Different materials, geometry and strategies have been proposed to solve these challenges, but it is still a difficult task to reconcile the request for scaling down the size of probe, maintaining the mechanical strength for implantation surgery, while having the core structure flexible for bettering interfacing with cells. Here we propose a new strategy to address this challenge by integrating flexible structures on a supporting ultra-small silicon shaft, which features the *in situ* formation of flexible three-dimensional electrodes without any additional etching process by the integration of biodegradable sacrificial layers. Three-dimensional microstructures for tissue-electronics integration can also be realized by engineering the geometry and anchor points. In addition, we will demonstrate precisely controlled positioning and releasing of a whole polymer film probe of sub-10 micrometer thickness which would allow accurate deep implantation of fully flexible probes for the first time.

Acceptance ID: NAW9-O

VISIBLE AND UV CURABLE CHITOSAN DERIVATIVES FOR IMMOBILIZATION OF BIOMOLECULES

*Ga-Dug Han[1]; Eun-Hye Kim[1]; Seung-Hyun Noh[1]; Jae-Won Kim[1]; Yoshihiro Ito[2, 3]; **Tae-il Son**[1*]*

[1]Department of Systems Biotechnology, Chung-Ang University, Anseong-si, Gyeonggi-do 456-756, Republic of Korea
[2]Nano Medical Engineering Laboratory, RIKEN, 2-1 Hirosawa, Wako, Saitama 351-0198, Japan
[3]Department of Computational Intelligence and systems Science, Interdisciplinary Graduate School of Science and Engineering Tokyo Institute of Technology, 4259 nagatsuda-cho, Midori-ku, Yokohama, 226-9501, Japan

** To whom correspondence should be addressed to Son, Tae Il (tisohn@cau.ac.kr)*

Chitosan is a natural polymer with many useful properties and functions for biomedical applications. Of these, the most important properties that make chitosan particularly useful as biomaterials are its excellent biocompatibility and biodegradability. In addition, chitosan possesses an antibacterial activity. Low toxicity, additional function and increased water solubility are often required while maintaining original properties of chitosan when it is used as biomaterial. Growth factors are biomolecules, mainly proteins. They have been known to play crucial roles in many important biological processes. The examples include epidermal growth factor, transforming growth factor-β and bone morphogenetic protein-2, which promote cell growth and proliferation, synthesis of collagen and fibronectin, and osteoblastic differentiation, respectively. Despite of their diverse stimulating activities in many biological processes, their biomedical application has been limited largely. Because they have short-half life in body fluids causing a rapid loss of their stimulating activities once entered into a blood stream. Protein immobilization would provide an effective way to overcome this problem. A variety of immobilization methods have been developed. However, many of these methods use chemical agents that can potentially generate by-products that could cause the denaturation of immobilized proteins. Also, it is difficult to apply equally chemical method to various growth factors because amino acid residues are different from each other. To avoid these problems, we have used a photo-crosslinking method to immobilize growth factors using visible light and UV curable chitosan derivative. The additional advantages of using this method are a relatively simple cross-link procedure, low-cost, easy to scale-up, and low toxicity. We consider that this photo-crosslinking method will be widely used for the immobilization of various biomolecules to apply to medical field. Here, we report the preparation of photo-curable chitosan derivatives that can be used for the immobilization of various biomolecules via photo-crosslinking.

Acknowledgements: This research was supported by Basic Science Research Program through the National Research Foundation of Korea (NRF) funded by the Ministry of Science, ICT and future planning (No. NRF-2014R1A2A1A11052623)

Acceptance ID: NKBV-O

3D Replication of Thermally Responsive Bio-Hydrogel

Samuel Haidong Kim[1], Sangho Lee[1], Jeong Jin Kang[1], Jun Young Hwang[1], and Bumsoo Han[2],

[1]Korea Industrial Institute of Technology, 143 Hanggaul-ro, Sangnok-gu, Ansan-si, 15588, Republic of Korea
[2]Purdue University, 585 Purdue Mall, West Lafayette, IN 47907
jyhwang@kitech.re.kr/ Tel. +82-31-8040-6434, Fax. +82-31-8040-6430

This study targets to develop a patterning system for thermally responsive bio-hydrogel based on drop-on-demand (DOD) printing technology. Recent advances of biotechnology allow numerous innovative and novel biomaterials including polymer scaffolds, engineered cells and tissues. DOD printing of bio-hydrogels has great potential to realize 3D printing of hydrogel-based materials. Especially, thermally responsive, i.e., temperature sensitive, bio-hydrogel is ideal for DOD printing and ultimately will be ideal for additive manufacturing of 3D biomaterials. This study shows the possibility of 3D patterning of thermally responsive bio-hydrogel, poly (n-isopropylacrylamid-co-acrylamide), PNIPAM. We utilized 3D printer to mold high aspect ratio 3D pattern, then printed bio-hydrogel on patterned Polydimethylsiloxane (PDMS). Three dimensional patterning of bio-hydrogel was presented by transferring the hydrogel from PDMS to glass substrate. The results showed the promise of its application to drug delivery, the development of new pharmaceuticals, and bio-mimicry.

Keywords: 3D Printing, Bio Printing, Pattern Transfer, Hydrogel

[1] DRURY, J. L., MOONEY, D. J. 2003. Hydrogels for tissue engineering: scaffold design variables and applications, Biomaterials, 24 (24), 4337-4351.

[2] HOCKADAY, L.A., K.H. KANG, N.W. COLANGELO, P.Y.C. CHEUNG, B. DUAN, E. MALONE, J. WU, L.N. GIRARDI, L.J. BONASSAR, H. LIPSON, C.C. CHU, J.T. BUTCHER, 2012, Rapid 3D printing of anatomically accurate and mechanically heterogeneous aortic valve hydrogel scaffolds, Biofabrication, 4(3)

Acceptance ID: pgvg-P

Regulating dual temperature and pH responsibility constructed from core-shell mesoporous hybrid silica (P@BMMs) via adjusting AA incorporation onto NIPAM

Xiaoqi Jin, Qian Wang, Jihong Sun, Hamida Panezail, Shiyang Bai, Xia Wu*

Beijing Key Laboratory for Green Catalysis and Separation, Beijing University of Technology, Beijing 100124, P. R. China
Email: jhsun@bjut.edu.cn, Tel: 0086-10-67391983, Fax: 0086-10-67391984

Recently, a kind of core-shell hybrid composite (P@BMMs) as ibuprofen (IBU) carrier was successfully prepared in our group [1], in which, bimodal mesoporous silica nanoparticles (BMMs) were used as core and poly[(N-isopropylacrylamide)-co-(methacrylic acid)]) (P(NIPAM-co-AA)) copolymer with dual pH- and temperature-responsive characteristics as shell. The aim of this work is to further explore the influence of the composition of copolymer shell on IBU-release behaviors. The XRD pattern (not shown) of P@BMMs-y (y = 0, 1, 3 , 7, and 10, respectively, presents molar ratio of AA to NIPAM) exhibited the diffraction peaks$_{(100)}$ in the 2θ range of 2º-4º, indicating the presence of mesoporous structure [1], however, its position shifted from 1.94º (P@BMMs-0) to 2.14º (P@BMMs-10). Except that, the intensity of peak$_{(100)}$ of I/P@BMMs-7 become almost undetectable, implying the successful adsorption of IBU molecules in the mesoporous channels. By combination with SEM/TEM, TG-DTG, and C^{13}-NMR analysis, these characterizations suggested that P(NIPAM-co-AA) was successfully coated on the BMMs surface. As illustrated in Fig. 1, it can be found that the pH- and temperature responsive drug release efficiencies were sensitive to additive content of AA of copolymer shell. Obviously, P@BMMs-0 and P@BMMs-1 presented a high temperature-response and poor pH-response, IBU-releasing mechanism followed a Korsmeyer-Peppas model. Comparably, P@BMMs-3 and P@BMMs-10 gradually enhanced the pH-responsive efficiency with increasing AA content.

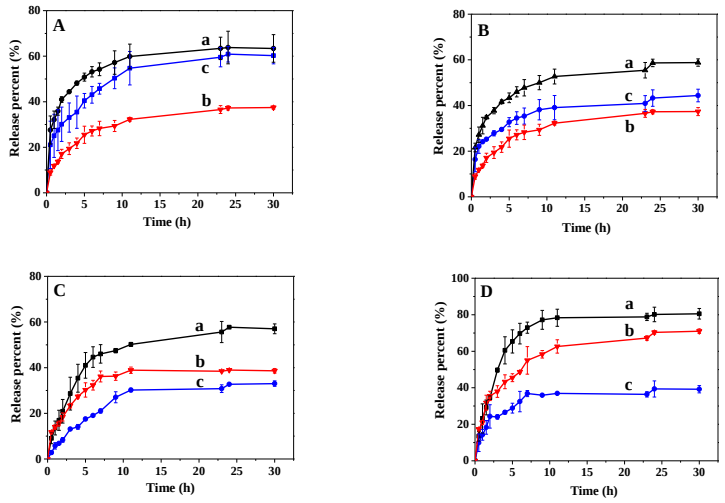

Fig. 1. ***In vitro*** **IBU-release behaviors from (A) P@BMMs-0, (B) P@BMMs-1, (C) P@BMMs-3, and (D) P@BMMs-10 at different conditions (a) pH 2.0 at 37 ºC, (b) pH 2.0 at 25 ºC and (c) pH 7.4 at 37 ºC.**

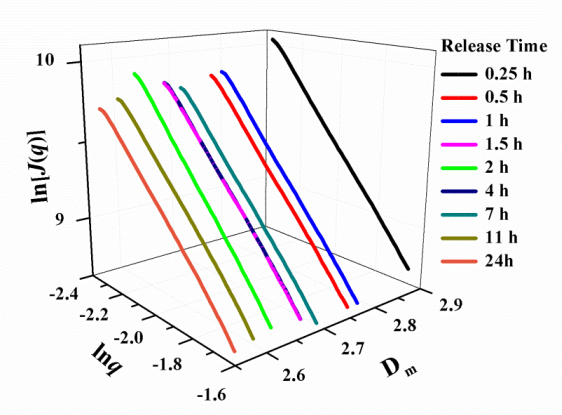

Fig. 2. SAXS patterns of P@BMMs-7 with different release time at pH 2.0 /37 ºC, and corresponding evolution of fractal dimension

As seen in Fig. 2, the SAXS patterns of P@BMMs-7 with different release time from 0.25 h to 24 h indicated the decrease tendencies of mass fractal dimension from 2.89 (t = 0.25 h) to 2.56 (t = 24 h), suggesting that the fractal nature had a close relationship with the evolution of porous structures and surface properties.

Acknowledgments

This project was supported by the National Natural Science Foundation of China (21276005 and 21576005), and the Beijing Municipal Natural Science Foundation (2152005).

Keywords: core-shell structure, P(NIPAM-co-AA) copolymer, bimodal mesopores silica, dual pH- and temperature-response, Ibuprofen, fractal.

References

[1] VALLET-REGI, M., RAMILA, A., DEL REAL, R. P., PÉREZ-PARIENTE, J. 2001. A New Property of MCM-41: Drug Delivery System. *Chem Mater*, 13, 308-311.

[2] GUO, Y. Y., SUN, J.H., BAI, S.Y., JIN, X.Q. 2016. Nanoassemblies Constructed from Bimodal Mesoporous Silica Nanoparticles and Surface-Coated Multilayer pH-Responsive Polymer for Controlled Delivery of Ibuprofen. *J Biomater Appli*, 31, 411-420.

Acceptance ID: PL72-O

Enzymatic Proteolysis Measured using 'Molecular Ruler' of Metal-Insulator-Metal

Amir Syahir[1*], *Kenichi Tajima*[2], *Hiroshi Tsutsumi*[2], *Kotaro Kajikawa*[3], *Hisakazu Mihara*[2]

[1]*Department of Biochemistry, Faculty of Biotechnology and Biomolecular Science, Universiti Putra Malaysia, Serdang 43400, Malaysia.*
[2]*Department of Bioengineering, Graduate School of Bioscience and Biotechnology, Tokyo Institute of Technology, Yokohama 226-8501, Japan.*
[3]*Department of Electronics and Applied Physics Interdisciplinary Graduate School of Science and Engineering, Tokyo Institute of Technology, Yokohama 226-8502, Japan.*

We developed a novel detection platform via optical means using a metal-insulator-metal (MIM) nanosandwich platform to observe protease activity. The technique relies on changes in normal incidence angle reflectivity originated from an optimized dielectric constant of the detection platform that can partially absorb lower wavelength of light in the visible region, particularly at 510 nm. Activities of various proteases such as trypsin, chymotrypsin and prostate-specific antigen (PSA) cleaving two to five amino acid residues from surface-bound substrate peptides were successfully monitored, revealing kinetics parameter that of comparable with other established methods. More importantly, the MIM 'molecular ruler' can simply measure the dimension of one amino acid. Unlike typical plasmon-based methods, the MIM reflectivity does not surface-propagated making it a promising platform to be used in high-density chip format detection.

Acceptance ID: Q6N6-O

Highly Sensitive Quartz Crystal Based Gas Sensor with a Nanofiber-Reinforced Hydrogel Modified Surface

Ju Yeon (Kim)[1], *Joshua (Lee)*[2], *Chan Hee (Park)*[1,2,*], *Cheol Sang (Kim)*[1,2,*]

[1]*Division of Mechanical Design Engineering, Chonbuk National University, Jeonju, Republic of Korea*
[2]*Department of Bionanosystem Engineering, Graduate School, Chonbuk National University, Jeonju, Republic of Korea*
Email : a30603244 @gmail.com, biochan@jbnu.ac.kr, chskim@jbnu.ac.kr

In a life coexisting with an industrialized environment, human beings are exposed to various harmful gases. Recently, the gas sensor industry has been actively working on gas sensors in order to improve quality of life. However, in the case of the conventional semiconductor type and SnO2 type gas sensor, it is difficult to prevent interference by other gases in sensing a desired gas, so applying these sensors where accuracy is required is difficult. Therefore, it is necessary to develop a selective, sensitive, and accurate sensor that can measure only the gas desired by the consumer. In this study, we developed a quartz crystal sensor using self-assembled monolayers (SAMs) that selectively collects gas and developed a high efficiency chemical gas sensing system that can be applied in many industrial fields. We also synthesized an alginate hydrogel membrane with functional groups that react with ethanol to produce a frequency change and placed it on the SAM-coated Au quartz.

Keywords: Quartz crystal gas sensor, self-assembled monolayer (SAMs), nanofibers, hydrogel

[1] YOO, H. Y. & BRUCKENSTEIN, S. 2013. A novel quartz crystal microbalance gas sensor based on porous film coatings. A high sensitivity porous poly(methylmethacrylate) water vapor sensor. *Analytica Chimica Acta*, 785, 98-103.

Acceptance ID: QYVQ-P

Mesoporous silica based stimuli-responsive drug delivery systems

V. Zeleňák[1], E. Beňová[1], M. Almáši[1], A. Zeleňáková[2], V. Hornebecq[3]

[1]Institute of Chemistry, Faculty of Science, P.J. Šafárik University, Košice, Slovakia
[2]Institute of Physics, Faculty of Science, P.J. Šafárik University, Košice, Slovakia
[3]Aix Marseille University, CNRS, MADIREL, Marseille, France
E Mail/ Contact Détails: vladimir.zelenak@upjs.sk

Drugs are essential components in human lives in terms of eliciting a therapeutic outcome in various disease states. However, high doses of the drugs can lead to side effects connected with the drug abuse. Particularly, drug molecules with lack of specificity and water solubility lead patients to take high doses of the drug to achieve sufficient therapeutic effects. The possible solution of these problems is to design biocompatible drug carriers that allow high loadings of drug molecules, including hydrophobic drugs, and their controlled release. Among the nanotechnology systems, recently intensively investigated as drug carriers belong periodic mesoporous silica materials. Mesoporous silica nanoparticles (MSN) represent a biocompatible multifunctional platform with favorable chemical properties. MSNs readily accommodate stimulus-responsive functionalization to enable on-command release of drug cargo in response to a variety of stimuli, including light, pH, temperature, magnetic field. They have shown better properties over free drug both in cell culture, and in animal models [1,2].

In our work we have studied a functionalized nanoporous silica particles responsive to the change of pH or UV radiation. In the first approach we have investigated MSN of MCM and SBA type modified by the photosensitive derivatives of coumarin and p–coumaric acid, which are subject of reversible photodimerization under UV radiation and create a „gate“ on the surface [3]. The obtained results showed the possibility of controlling of the pore accessibility and/or drug release from MSN by physical stimulus. Photodimerisation of p-coumaric acid (closing of pores) was faster then photodimerisation of coumarine.

In the second approach we studied pH-responsive platform consisting of cyclodextrin (CD)-capped MSNs. The pH-responsive nanovalves are composed of an amine-based stalk attached to the walls of silica nanoparticles that can bind beta-cyclodextrin units non-covalently through supramolecular interactions. When the pH is decreased from its initial value (pH=7.4), the amine derivatives become protonated and their binding affinity to the cyclodextrin drastically decreased. The cyclodextrin caps are thus dispersed and pores are un-blocked. In our studies nonsteroidal antiinflammatory drugs naproxen and indomethacin as model drugs were employed or we used an antineoplastic agent for the treatment of gastrointestinal cancers, 5-fluorouracil.

Acknowledgments: This work was supported by the Slovak Research and Development Agency under the contract APVV-15-0520.

Keywords: Mesoporous silica, drug delivery, porous materials, cyclodextrin, cinnamic acid

[1] LU, J., LIONG, M., LI, Z.X., ZINK, J.I. & TAMANOI F. 2010. Biocompatibility, biodistribution, and drug-delivery efficiency of mesoporous silica nanoparticles for cancer therapy in animals. *Small*, 6, 1794-1805.

[2] LI, Z., CLEMENS, D.L., LEE B.Y., DILLON B.J., HORWITZ M.A. & ZINK, J.I. 2015. Mesoporous Silica Nanoparticles with pH-Sensitive Nanovalves for Delivery of Moxifloxacin Provide Improved Treatment of Lethal Pneumonic Tularemia. *ACS Nano*, 9, 10778-10789.

[3] BEŇOVÁ, E., ZELEŇÁK, V., HALAMOVÁ D., ALMÁŠI M., PETRUL'OVÁ, V., PSOTKA, M., ZELEŇÁKOVÁ, A., BAČKOR M. & HORNEBECQ V. 2017. A drug delivery system based on switchable photo-controlled p-coumaric acid derivatives anchored on mesoporous silica. J. Mater. Chem. B, doi: 10.1039/C6TB02040B.

Acceptance ID: RGGG-O

Nano silver ferrite, a better tool of Target drug delivery than other antimicrobial nanoferrites

T. Kondala Rao.,[1] *I. V. Kasi Viswanath.,*[2] *Y. L .N Murthy* [3]

[1]*professor, Sri Sivani College of Engineering, Srikakulam, INDIA*
[2] *professor, K.L.University, Vaddeswaram, ,INDIA*
[3] *professor, Andhra University Visakhapatnam, INDIA*
Email Id: kondalaraotata@gmail.com

Nanosilver ferrite is synthesised through co precipitation method [1] A new silver coated cobalt ferrite nanocomposite [$Ag@CoFe_2O_4$], was prepared by a two-step procedure. In the first step, cobalt ferrite nanoparticles were synthesized by a co precipitation method followed by combustion method using glucose as fuel . This nano cobalt ferrite was then coated with nanosilver via chemical reduction of Ag+ solution using glucose as reducing agent [2]. nanosilver is synthesized by chemical reduction of Ag+ solution. The synthesized nano $CoFe_2O_4$, nano $Ag@CoFe_2O_4$, nanoAg and nano $AgFeO_2$compostes were characterized by X-ray diffraction, Scanning electron microscopy/transmission electron microscopy, and vibrating sample magnetometer. The antibacterial activity of these nanoparticles were investigated against some Gram-positive and Gram-negative bacteria and compared with those of silver nanoparticles and standard antibacterial drugs. it was observed that nano silver ferrite has more antimicrobial action than all other tested nano particles. As the nano silver ferrite has small particle size (4.5nm), good antimicrobial nature,anti fungal nature super paramagnetic and biocompatibility, so it is concluded that nano silver ferrite is better tool for target drug delivery than other tested ferrites. The detailed study is presented.

References

1.Y.L.N.murthy,**T.KondalaRao** I.V.Kasi Viswanath, Rajendrasingh., Journal of Magnetism and Magnetic Materials 322 (2010) 2071–2074

2. **T. Kondala Rao*,** Ch. Jagadeeswara Rao, MagdelonoTravis,I V Kasi Viswanath, Y L N Murthy, **I J NN,** Volume 3, Numbe3(**2012)**, pp. 139-14

Acceptance ID: RMZG-O

PCL (Polycaprolactone) nano encapsulation of Anticancer drugs 5-Fluorouracul (FU), Paclitaxel and HET-0016

Mujibur Khan[1,] Sakib Iqbal[2], Mohammad H. Adeline Wagner[3], Rashid[4], Ali S. Arbab[5]*

[1,2,3] Mechanical Engineering, Georgia Southern University, Statesboro, GA
[4,5] Georgia Cancer Center; Augusta University, Augusta, GA
[*]Corresponding Author: Mujibur Khan, Phone: 912-478-8004 (Office)
915-873-5303 (Cell); Fax: 912-478-1455; Email: mkhan@georgiasouthern.edu

Nano encapsulation of anticancer drugs (5-Fluorouracul (FU),Paclitaxel,HET-0016) with polycaprolactone (PCL) was performed combining electrospraying and emulsion solvent evaporation method. Anticancer drug was electrosprayed to generate its nanocrystal and later nanoencapsulation within PCL using emulsion solvent evap- oration. Different categories of solvent system and manufacturing parameters were used to investigate their effects on morphology,drug release characteristics and cytotoxic effects. Coaxial drug loaded nanofibers were manufactured using high potential electric field of 17-25 kV to draw a compound solution jet from a specialized coaxial spinneret. Emulsion solvent evaporation was performed using sonication and high shear mixing to encapsulate drug within PCL nanoparticles. Morphology of nanostructures were investigated using Scanning Electrosn Microscopy (SEM), Transmission Electron Microscopy (TEM) and Electron Dispersive X-ray Spectrometry (EDS). TEM image of FU loaded PCL NF exhibited continuous drug core within PCL sheath. Thinnest NF was paclitaxel encapsulated fibers which was 22-90 nm and smallest nanoparticles was obtained using electro- spraying whose diameter was 35-80nm. The maximum encapsulation efficiency was 77.5%. In-vitro drug release kinetics of the NFs were performed in Phosphate buffer saline (PBS) using UV-Vis spectroscopy at 265 nm. NFs with drug particles outsides of surface exhibited rapid initial release (52-53%) in 3 days while other sets of NFs released only 13-23% with in the same time period. In-vitro cell viability test with FU encapsulated NFs (category 2) in human prostatic cancer PC3 cells exhibited 38% alive cells at 5 μM concentration while in pristine FU 43% cells were alive. Paclitaxel encapsulated NFs with breast cancer cells also exhibited increased efficacy in com- parison to pristine anticancer drugs and continuous decrease of cell density indicated the slow release of paclitaxel from the NF.

Acceptance ID: S3Z8-O

New Chitosan-Based Thermogels for Biomedical Applications

Kang Moo Huh *

Chungnam National University, Daejeon, Korea
** Email: khuh@cnu.ac.kr*

Over the past few years, thermogelling polymers that undergo sol–gel transition in aqueous media as the temperature increases have been extensively studied for various biomedical applications, especially for drug delivery and injectable tissue engineering [1]. These polymers have been applied to entrap pharmaceutical agents or cells by simple mixing in a solution state, followed by a syringe injection into the target site where they formed hydrogel depots and served as carrier matrices for localized drug delivery or cell growth. Copolymers of poly(ethylene oxide) and poly(propylene oxide) (known as poloxamer), and copolymers of N-isopropylacrylamide have been widely studied as commercially available thermo-sensitive synthetic polymers. They can demonstrate excellent thermo-sensitive properties, but their clinical applications have been limited due to their lack of biodegradability, biocompatibility and physicochemical properties such as gel stability and strength.

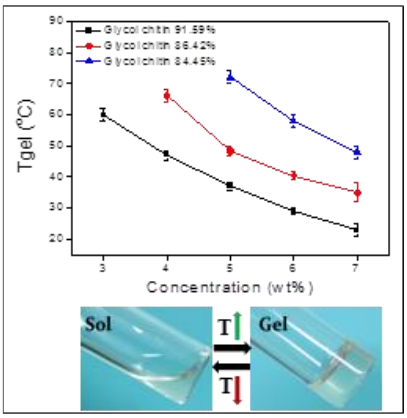

Fig.1 Thermo-reversible sol-gel transition behaviors of acyl glycol chitosans

In this study, new thermo-sensitive polysaccharide derivatives, acyl glycol chitosans, were synthesized by N-acylation of glycol chitosan using a series of acylating agents and evaluated as new thermogelling systems for various biomedical applications. The physico-chemical properties of glycol chitosan derivatives with different types of acyl groups and different degrees of acylation (DA) were investigated in terms of degradation, cytotoxicity, rheological properties, and in vitro and in vivo gel formation. Aqueous solutions of acyl glycol chitosans were observed to demonstrate thermoreversible sol–gel transition properties around the body temperature and their gelation properties could be controlled by various chemical and physical factors. A acetyl glycol chitosan with thermogelling and mucoadhesive properties was used to prepare a new progesterone gel for vaginal application and proposed a promsing alternative to current vaginal progesterone formulation [2]. A thermosensitive hexanoyl glycol chitosan (HGC) was developed as a carrier for topical drug delivery to the eye. The HGC-based formulation showed prolonged retention on the preocular surface and enhanced drug availability and efficacy [3]. The degree of acylation of HGC could be finely tuned to obtain adequate thermo-reversible properties and gel stability. The HGC was also highly effective for forming multi-cellular spheroids when used to coat the surfaces of cell culture dishes. Our findings suggest that acyl glycol chitosans could be useful as a new thermogelling biomaterial for various biomedical applications, including drug delivery, cell and tissue engineering, organ-on-chips, drug screening research, and so on.

[3] [1] B. Jeong, S. W. Kim, Y. H. Bae, *Adv. Drug Del. Rev.* **64**, 154 (2012)
[4] [2] A. Almomen, S. Cho, C.-H. Yang, Z. Li, E. Jarboe, C. M. Peterson, K. M. Huh, M. M. Janát-Amsbury, *Pharm. Res.***32**, 2266 (2015)
[5] [3] I. S. Cho, C. G. Park, B. K. Huh, M. O. Cho, Z. Khatun, Z. Li, S.-W. Kang, Y. B. Choy, K. M. Huh, *Acta Biomaterialia* **39**, 124 (2016)

Acceptance ID: SJ5U-P

Small and Bright:Tailoring Luminescent Nanoparticles in Biology

*Gang Han**

**University of Massachusetts-Medical School*
364 Plantation Street, LRB 806, Worcester, MA USA

Functional luminescent nanoparticles are promising materials for in vitro and in vivo optical imaging and therapy due to their unique optical and chemical properties. In this talk, I will present three new types of biocompatible luminescence nanoparticles. The first type of materials is upconversion nanoparticles (UCNPs). I will present new developments regarding engineering UCNPs towards deep tissue imaging, photodynamic therapy, optogenetic applications in neuroscience and immunotherapy. The second type of nanoparticles is persistent luminescence nanoparticles (PLNPs). They are bioluminescence-like and possess unprecedented in vivo deep tissue energy rechargeability, outstanding signal-to-noise-ratio with no need for an excitation resource (light) during imaging, and they can be directly detected with existing imaging systems. These nanoparticles continue to emit light for minutes or hours and, in some cases, days, after turning off the excitation source. These long-lasting, light-emitting nanocrystals can provide noninvasive imaging technology for evaluating structural and functional biological processes in living animals and patients. The third is a type of organic Biodpy nanoparticles that were tailored with outstanding NIR absorbing ability. Rather than the conventional laser light needed in PDT, I will present their ultralow power lamp operable PDT applications in deep tissue tumor treatment. Finally, I would like also to introduce a nanobug concept towards cancer treatment.

Acceptance ID: u7np-O

Nanopore device with self-aligned nanogap electrodes for DNA characterization

Nanopore sensors, an emerging third-generation DNA sequencing technique with rapid speed, single-base sensitivity and long read lengths, exemplify a new strategy in the characterization of biomolecules that mimic biological membrane pores. In such designs, the dimension of the sensor matches precisely with a single target molecule, so that the presence and/or motion of the molecule inside the sensor can generate measurable time-dependent electrical read-out signals containing significant local structural information. The capability of single-molecule level and label-free detection of sequence and post-transcription modification of DNA and protein molecules promise a new paradigm in both fundamental studies and biomedical applications in personal medicine. However, existing techniques face great challenges such as the scalability and reproducibility of fabrication, lack of control of translocation, and low specificity in read-out signals. Here we propose a new framework of preparing nanopore device arrays with the additional integration of a pair of embedded nanogap electrodes in a self-aligned manner. Specifically, we will introduce our impedance-based feedback control system for the electrochemical deposition of metal on pre-defined nanoscale electrodes within a confined space to construct sub-10 nm nanopores with gate electrodes. We will also present preliminary results of recognition tunneling current readouts as different nucleotides pass through the nanopore devices. Our design can provide a promising platform for the scalable preparation of single-molecule characterization devices with active translocation control and recognition tunneling readout signals.

Acceptance ID: UNDQ-O

Virtual Touch: Smart Polymers for Human-Machine Interaction

Darren J. Lipomi

Associate Professor
Department of NanoEngineering, University of California, San Diego
Affiliate, Department of Chemistry and Biochemistry
dlipomi@ucsd.edu

The sense of touch can trigger our strongest emotions instantly, whether they are positive or negative. While human culture is replete with artifacts that interface with the senses of sight, hearing, taste, and smell, objects designed to convey information or trigger emotion by interfacing with the sense of touch represent an open area for investigation. My research group is developing soft materials that can simulate different tactile sensations: rough or smooth, hot or cold, soft or hard, or even slimy. To accomplish this goal, we are using specially designed and synthesized ionically conductive hydrogels, and electrically conductive polymers. Central to the project is the ability to combine electrical functionality with mechanical softness that is commensurate with that of the skin. The central hypothesis is that there is a minimum number of types of "soft actuators" that can reproduce any tactile sensation a human being is capable of experiencing. An analogy would be to the red, green, and blue (RGB) pixels that are used in display technology to render any color in the gamut of human vision. That is, can there be an "RGB of Touch"? The ultimate goal is to translate these sensations to virtual reality for applications in robotic surgery and surgical training, education, and simulated environments.

Acceptance ID: UYKE-O

Biodegradable Nanoparticles Delivered Genes for Topical Therapy of Cancers

Maling Gou

State Key Laboratory of Biotherapy and Cancer Center, West China Hospital, Sichuan University, and Collaborative Innovation Center for Biotherapy
NO.17 People's South Road Section 3, Chengdu, Sichuan, 610041, P.R. China
goumaling@scu.edu.cn/ +86 13880640692 ***(Maling Gou)***

Gene therapy has promising applications in cancer therapy. Currently, ~64.2% of the 2,143 protocols of gene therapy has been approved for cancer clinical trials worldwide. USA and European countries all have already approved gene drugs in recent years, such as Glybera, Strimvelis and Spinraza. The vesicular stomatitis virus matrix protein (VSVMP) can cause considerable cytopathogenesis of vesicular stomatitis virus (VSV) in the absence of other viral components. Matrix protein induced cytopathic effects through disruption of three types of cytoskeletal elements (actin, vimentin, and tubulin) by interacting with them and through general inhibition of host cell gene expression results in the systemic breakdown of the cell by apoptosis. However, the lack of safe and efficient VSVMP gene delivery systems remains one of the major challenges that restrict the clinical application of gene therapy. Recently, nanoparticle based non-viral gene delivery systems attracted more and more attentions because of its advantages such as low immunogenicity, high gene loading capacity, designable, ease of scale up, and etc. However, conventional nanoparticulate gene delivery systems are cationic which always cause the fast cleansing by RES after intravenous administration. Therefore, topical administration may be a good approach to improve the safety and efficiency of cationic nanoparticle-delivered genes.

Here, we demonstrate a heparin-polyethyleneimine (HPEI) nanoparticle that is prepared by chemical conjugation of low molecular weight PEI by heparin. This degradable and low cytotoxic nanoparticle can interact with VSVMP to form a VSV-inspired nanocomplex. This nanocomplex is demonstrated to efficiently inhibit the growth of orthotopic bladder cancer xenografts and does not cause significant systemic toxicity, showing great potential clinical application in bldder cancer therapy.

Epithelial ovarian carcinoma is the leading cause of gynecologic cancer-related death. We design a DNA delivery nanoparticle composed of 1, 2-dioleoyl-3-trimethylammonium propane (DOTAP) and methoxypoly (ethyleneglycol) (MPEG-PLA), which is low cytotoxic and non-immunogenic. Intraperitoneal administration of DPP/VSVMP complex, consisting of DPP nanoparticle combined with plasmid DNA coding VSVMP (VSVMP), efficiently inhibited the intraperitoneal metastasis of ovarian cancer through apoptosis induction and antiangiogensis, and did not cause significant systemic toxicity.

In summary, the biodegradable HPEI and DPP nanoparticles can efficiently deliver genes into cancer cells. Topical administration of cationic nanoparticles delivered VSVMP gene could effectively inhibit the growth of bladder cancer and intraperitoneal metastasis of ovarian cancer without causing significant systemic toxicity, showing potential clinical application.

Keywords: Non-viral Nanoparticles, Topical, Gene Therapy, HPEI, DPP

[1] L. LUO, T. DU, J. ZHANG, W. ZHAO, H. CHENG, Y. YANG, Y. WU, C. WANG, K. MEN, M. GOU*. 2016. Efficient inhibition of ovarian cancer by degradable nanoparticle-delivered survivin T34A gene. *Int J Nanomed*, 11, 501-513.

[2] M. GOU, K. MEN, J. ZHANG, Y. LI, J. SONG, S. LUO, H. SHI, Y. WEN, G. GUO, M. HUANG, X. ZHAO, Z. QIAN, Y. WEI. 2010. Efficient inhibition of C-26 colon carcinoma by VSVMP gene delivered by biodegradable cationic nanogel derived from polyethyleneimine. *ACS Nano*, 4(10), 5573–5584.

[3] X. DU, J. LANG, J. XU, Y. LU, Y. WEN, J. ZHAO, P. DIAO, Z. YUAN, B. YAO, L. FAN, G. WANG, L. LIU, Z. DING, Y. WANG, T. LI, R. WANG, Y. MAO, B. KAN, H. WU, H. LI, H. YANG, H. WU, Y. WEI, X. ZHAO. 2008. Vesicular stomatitis virus matrix protein gene enhances the antitumor effects of radiation via induction of apoptosis. *Apoptosis*, 13, 1205–1214.

Acceptance ID: VAXK-O

Erythrocyte-Derived Optical Nanoplatforms for Near Infrared Fluorescence Imaging and Phototherapy of Breast Cancer

Joshua M. Burns[1], *Raviraj Vankayala*[1], *Jenny T. Mac*[2], *Bahman Anvari**[1,2]

[1]*Department of Bioengineering, University of California, Riverside, 900 University Ave., Riverside, CA 92521, USA*
[2]*Department of Biochemistry, University of California, Riverside, 900 University Ave., Riverside, CA 92521, USA*
Email: joshua.burns@email.ucr.edu, bahman.anvari@ucr.edu

Our group has engineered nano-sized vesicles derived from erythrocytes that can be loaded with pharmacological agents or optical materials such as the FDA-approved indocyanine green (ICG) (Bahmani et al. 2013). When photo-excited by appropriate near infrared (NIR) wavelengths, these constructs can transduce the photons energy to emit fluorescence, generate heat, or induce chemical reactions. We refer to these constructs as NIR erythrocyte-mimicking transducers (NETs).

The use of erythrocytes as a delivery platform is especially advantageous since natural erythrocytes have a long circulation time (≈ 90-120 days), attributed to the presence of "self-marker" membrane proteins (Oldenborg 2013; Rodriguez, et al. 2013). Therefore, constructs derived from erythrocytes may offer a capability for the availability of their cargo (e.g., ICG) over an extended time. Furthermore, such constructs are expected to be biocompatible.

In this study, we investigated the theranostic capability of NETs in fluorescence imaging and photo-destruction of breast tumors. We fabricated NETs according to our previous protocols, consisting of: (1) isolation of erythrocytes from whole bovine blood; (2) hypotonic treatment of erythrocytes to produce hemoglobin-depleted erythrocyte ghosts (EGs); (3) extrusion of EGs through nano-sized porous membranes to produced nano-sized vesicles; and (4) loading of ICG into the nano-sized vesicles in a hypotonic buffer to produced NETs (Bahmani, et al. 2013; Burns, et al. 2017; Mac, et al. 2016).

We initially carried out a set of *in-vitro* experiments using SKBR3 breast cancer cells to validate the fluorescence imaging and photo-destructive capability of NETs once activated by NIR excitation. NETs exhibited high intracellular uptake and produced reactive oxygen species (ROSs) upon 808 nm photo-excitation, which ultimately led to enhanced cell death.

Next, we explored the theranostic capability of NETs in an *in-vivo* mouse model system consisting of SKBR3 implanted tumors. Following intravenous injection of NETs, we were able to visualize the tumors by whole body fluorescence imaging. We attribute the accumulation of NETs in tumors to the enhanced permeability and retention effect. We irradiated the tumors at 808 nm for 10 minutes at power densities of 340 or 680 W/cm^2. In response to laser irradiation, we observed the destruction of tumors in about 16 days. Haemotoxylin and eosin (H&E) staining and apoptosis assays using caspase 3 immunostaining validated tumor destruction. We attribute the mechanism of tumor destruction to thermal effects and production of ROSs. Our results suggest that NETs as a photo-theranostic agent can offer a great potential in biomedical imaging and phototherapy of cancers.

Keywords: indocyanine green, nanomaterials, photodynamic therapy, photothermal therapy.

[1] BAHMANI, B., BACON, D. & ANVARI, B. 2013. Erythrocyte-Derived Photo-Theranostic Agents: Hybrid Nano-Vesicles Containing Indocyanine Green for Near Infrared Imaging and Therapeutic Applications. *Sci. Rep.*, 3, 2180.

[2] BURNS, J., SAAGER, R., MAJARON, B., JIA, W. & ANVARI, B. 2017. Optical Properties of Biomimetic Probes Engineered from Erythrocytes. *Nanotechnology*, 28, 035101.

[3] MAC, J. T., NUNEZ, V., BURNS, J., GUERRERO, Y. A., VULLEV, V. I. & ANVARI, B. 2016. Erythrocyte-Derived Nano-Probes Functionalized with Antibodies for Targeted Near Infrared Fluorescence Imaging of Cancer Cells. *Biomed. Opt. Express*, 7, 1311-1322.

[4] OLDENBORG, P. A. 2013. CD47: A Cell Surface Glycoprotein Which Regulates Multiple Functions of Hematopoietic Cells in Health and Disease. *ISRN Hematol.*, 2013, 614619.

[5] RODRIGUEZ, P. L., HARADA, T., CHRISTIAN, D. A., PANTANO, D. A., TSAI & R. K., DISCHER, D. E. 2013. Minimal "Self" Peptides That Inhibit Phagocytic Clearance and Enhance Delivery of Nanoparticles. *Science*, 339, 971–975.

Acceptance ID: xxxw-O

Methotrexate-loaded multifunctional nanoparticles with near-infrared irradiation for the treatment of rheumatoid arthritis

The goal of this study was to design photothermally controlled drug release from multifunctional nanoparticles (MNPs) at near-infrared (NIR) irradiated site which could improve therapeutic efficacy and reduce side-effects. The MNPs, methoxtrate (MTX)-loaded poly(ethylene glycol)-poly(lactic-*co*-glycolic acid) (PLGA)-Au half-shell nanoparticles (MTX-loaded NMPs), were fabricated by depositing Au film onto MTX-loaded PLGA nanoparticles. Upon NIR irradiation, heat was locally generated due to NIR resonance of the Au half-shell in MNPs and the release of MTX from PLGA nanoparticles was accelerated. *In vitro* experiments showed a higher therapeutic efficacy for the treatment of MTX-loaded MNPs with NIR irradiation than for chemotherapy or photothermal treatment alone. The *in vivo* NIR images of MTX-loaded MNPs indicated that the MNPs were effectively delivered to the rheumatoid arthritis. Moreover, MTX-loaded MNPs containing a much smaller dosage of MTX (1/1400 of MTX solution: repeated-dose administration) exhibited comparable therapeutic effects to a conventional treatment with MTX solution in collagen-induced arthritis (CIA) mice. These results demonstrate that MTX-loaded MNPs are promising therapeutic agents for rheumatoid arthritis and allow *in vivo* NIR optical imaging.

Acceptance ID: YPRM-P

Sequentially-Activated Quadruple Stimuli-Responsive Polymeric Gene Nanocomplexes for High Gene Expression and Low Cytotoxicity

Hana Cho[1], Sun-Woong Kang[2], Kang Moo Huh[3], Han Chang Kang[1]

[1]Department of Pharmacy, The Catholic University of Korea, Bucheon 14662, Republic of Korea.
[2]Next-generation Pharmaceutical Research Center, Korea Institute of Toxicology, Daejeon, 34114, Republic of Korea.
[3]Department of Polymer Science and Engineering, Chungnam National University, Daejeon 34134, Republic of Korea.
hckang@catholic.ac.kr *(HCK)*

The clinical application of intracellular gene delivery via nanosized carriers is hindered by intracellular multistep barriers that limit high levels of gene expression. To solve these issues, it has been frequently used that many gene delivery systems can be responded to one or two stimuli. However, use of three or more triggers is uncommon. This study efficiently utilized four different intracellular or external stimuli for sequential activation of a polymeric gene carrier, a photosensitizer (pheophorbide A [PhA]), and a genetic therapeutics. PhA-loaded thiol-degradable polycation (PhA@RPC)[1] was mixed with cytomegalovirus (CMV) promoter-equipped pDNA and their electrostatic attraction constructed the designed PhA@RPC/pDNA complexes. After endocytosis of the resulting PhA@RPC/pDNA complexes, their endosomal escape was activated by RPC in PhA@RPC because RPC has endosomal pH-induced endosomolytic activity. Subsequently, RPC was degraded by an intracellular thiol and then the complexes released pDNA and PhA. Late light exposure (LE) (e.g., 12 h post-treatment) activated the released PhA and resulted in the production of reactive oxygen species (ROS). Intracellular ROS successively activated NF-κB, which then reactivated the CMV promoter in the pDNA. These sequential, stimuli-responsive chemical and biological reactions resulted in high gene expression. In particular, early LE induced photochemical internalization but high cytotoxicity, whereas late LE influenced the reactivated pDNA via PhA-generated ROS and activation of NF-κB. In conclusion, the quadruple triggers, such as pH, thiol, light, and ROS, successively influenced RPC, PhA, and pDNA and the tempo-spatial activation of the designed quadruple stimuli-activatable PhA@RPC/pDNA complexes could be potential in gene delivery applications.

Keywords: CMV promoter, gene delivery, photosensitizer, reactive oxygen species, stimuli-responsive

[1] CHO, H., LI, L., BAE, Y. H., HUH, K, M. & KANG, H. C. 2014 Bioreducible branched polyethyleneimine derivatives physically loaded with hydrophobic pheophorbide A: preparation, characterization, and light-induced cytotoxicity. *Macromolecular Bioscience*, 14, 1483-1494.

Acceptance ID: Z5GC-P

Enhanced Luminescence of Ln^{3+} Doped CaF_2 Nanoparticles by Co-doping with Na^+ Ions

Bing Xu (Xu), Ying Ma (Ma)

State Key Laboratory of Materials Processing and Die & Mould Technology, School of Materials Science and Engineering, Huazhong University of Science and Technology (HUST), Wuhan 430074, P. R. China.
E Mail: yingma@hust.edu.cn

Lanthanide ions (Ln^{3+}) doped CaF_2 luminescent nanoparticles exhibit unique optical properties and represent promising candiadates for bio-applications.[1] However, their inherent weak luminescent intensity greatly limits their application. Especially, Nd^{3+} sensitized CaF_2 upconversion nanoparticles (UCNPs) have been rarely reported although UCNPs excited by 800 nm is more favorable for bio-applications than those excited by 980 nm.[2] On the one hand, surface quenching will suppress luminescence greatly especially in ultra-small nanoparticles. On the other hand, non-equivalent substitute Ln^{3+} for Ca^{2+} ions will bring about lots of lattice defects and Ln^{3+} clusters to balance the local charge in the CaF_2 host lattice.[3,4] Consequently, alleviating such lattice defects may improve luminescent intensity of these Ln^{3+} ions doped nanoparticles.

Herein, we have synthesized core-shell (CS) CaF_2:Yb/Er@CaF_2:Nd/Yb nanoparticles with about 10 nm using Nd^{3+} ions as the sensitizer. Na^+ ion has been codoped with Nd^{3+} and Yb^{3+} ions for charge compensation in the CaF_2:Nd/Yb sensitizing layer. The CS structure constructed here could not only isolate the core from the surrounding quenching centres, but also suppress the energy back-transfer from the activators Er^{3+} (in the core) to the sensitizers Nd^{3+} (in the shell) by separating them spatially. Co-doping of Na^+ ion with the Ln^{3+} ions in the shell has improved the crystallinity of the nanoparticles and prolonged the lifetimes of the excited states belonging to both the sensitizer (Nd^{3+} ion) and the activator (Er^{3+} ion) markedly, thus the UCL intensity upon 800 nm irradiation has been enhanced remarkably. Moreover, CaF_2:Nd/Na ultra-small nanoparticles show the strongest infrared emission at a high Nd^{3+} doping lever of 30%. In contrast, both previous reports and our work demonstrate the emission of Na^+-free couterparts would decrease when Nd^{3+} concentration is higher than 6%. This indicates that Ln^{3+} clusters may be effectively reduced since the cross relaxation process of $^4F_{3/2} + {}^4I_{9/2} \rightarrow 2{}^4I_{15/2}$ from adjacent Nd^{3+} ions is greatly supressed in the presence of Na^+ ions.

Similar effects have also been observed in other alkali metal ions co-doped UCNPs, such as Li^+ and K^+ ions, suggesting co-doping with a charge compensator may be an efficient way to enhance the luminescence of Ln^{3+} doped CaF_2 nanoparticles. The as-synthesized ultra-small nanoparticles may be good candidates as excellent imaging nano-probes because of their good biocompatibility and adequate light penetration.

Keywords: Upconversion nanoparticles, CaF_2, lanthanide ions, charge compensator, sodium ion

[1] LIU, T.-M., CONDE, J., LIPIŃSKI, T., BEDNARKIEWICZ, A. & HUANG, C.-C. 2016. Revisiting the Classification of NIR-absorbing/emitting Nanomaterials for In Vivo Bioapplications. *NPG Asia Mater.*, 8, e295.

[2] ZHONG, Y., TIAN, G., GU, Z., YANG, Y., GU, L., ZHAO, Y., MA, Y. & YAO, J. 2014. Elimination of Photon Quenching by a Transition Layer to Fabricate a Quenching-Shield Sandwich Structure for 800 nm Excited Upconversion Luminescence of Nd^{3+}-Sensitized Nanoparticles. *Adv. Mater.*, 26, 2831-2837.

[3] WANG, F. & LIU, X. 2009. Recent Advances in the Chemistry of Lanthanide-doped Upconversion Nanocrystals. *Chem. Soc. Rev.*, 38, 976-989.

[4] LACROIX, B., GENEVOIS, C., DOUALAN, J. L., BRASSE, G., BRAUD, A., RUTERANA, P., CAMY, P., TALBOT, E., MONCORGÉ, R. & MARGERIE, J. 2014. Direct Imaging of Rare-earth Ion Clusters in Yb:CaF_2. *Phys. Rev. B*, 90, 125124.

Acceptance ID: zxjb-P

SYMPOSIUM 6: Advances in Catalysis

On the High Activity Methanol / H_2O_2 Catalyst of Nanoporous Gold from Al-Au Ribbon Precursors with Various Circumferential Speeds

Hui Xu,[a] Kechang Shen,[a] Shuai Liu,[a] Laichang Zhang,[b] Xiaoguang Wang,[c] Jingyu Qin,[a] and Weimin Wang[a]*

[a] *Key Laboratory for Liquid-Solid Structural Evolution and Processing of Materials, Ministry of Education, Shandong University, Jinan 250061, China*
[b] *School of Engineering, Edith Cowan University, 270 Joondalup Drive, Joondalup, Perth, WA6027, Australia*
[c] *Laboratory of Advanced Materials & Energy Electrochemistry, Taiyuan University of Technology, Taiyuan 030024, China*

We have prepared the nano-porous gold (np-Au) with a three dimensional (3D) bicontinuous interpenetrating ligament-channel structure by dealloying the melt spun Al_2Au ribbon precursors with three different circumferential speeds (S_c). With increasing S_c, the lattice constant (a_0) of precursors decreases. After the dealloying procedure, the np-Au samples have an increasing a_0 and a decreasing pore size with increasing S_c. There exists the heredity of the preferred orientation factors (F) between precursors and np-Au samples. The cyclic voltammetry (CV) curves of methanol electro-oxidation reaction (MOR) on np-Au samples are related to their F and show a higher activity with a higher S_c. In addition, np-Au with a lower pore size exhibit a higher sensitivity for the concentration of H_2O_2 in phosphate buffered solutions (PBS), which reaches 73.4 μA $mM^{-1}cm^{-2}$ with S_c = 18.3 m/s. These results suggest that we can change the pore size of the dealloyed np-Au by adjusting the S_c of the precursors, and then enhance the catalytic activity of np-Au.

Acceptance ID: 32S9-O

*Corresponding author.
E-mail address: weiminw@sdu.edu.cn (W. M. Wang)

Photocatalytic degradation of indoor VOCs by nanoporous TiO_2 film with exposed {001} facets

Tongzhou Xu,[a,b] Hong Zheng,[a,] Pengyi Zhang [b,*]*

[a] Beijing Key Laboratory of Materials Utilization of Nonmetallic Minerals and Solid Wastes, School of Materials Science and Technology, China University of Geosciences, Beijing, 100083, China
[b] State Key Joint Laboratory of Environment Simulation and Pollution Control, School of Environment, Tsinghua University, Beijing , 100084, China
[*]Corresponding author: [a]zhengh@cugb.edu.cn; [b]zpy@tsinghua.edu.cn

Volatile organic compounds (VOCs) are common pollutants found in microenvironment. It is a challenge to effectively remove VOCs to improve the indoor air quality[1-3]. Though TiO_2 photocatalysis can degrade most VOCs, the degradation rate is low and the photocatalyst may deactivate in the TiO_2/UV process[4]. 185 nm vacuum ultraviolet (VUV) photocatalysis exhibits better performance to degrade VOCs[5, 6]. In our study, TiO_2 film with exposed {001} facets and uniform nanopores in the crystal facets, a new catalyst with superior photocatalytic activity for degradation of low concentration aqueous pharmaceutical pollutants[7,8], were prepared, and its activity for decomposition of gaseous toluene, a typical indoor VOC, under VUV irradiation were investigated. In dynamic experiments, as shown in Fig.1, the nanoporous TiO_2 film shows good photocatalytic activity for the photocatalytic degradation of gaseous toluene of lower initial concentrations under VUV irradiation. The removal ratios can be further improved with the increase of residence time. When the inlet concentration of toluene and residence time were 100 ppb and 1.1 s, nanoporous TiO_2 film still showed activity under VUV irradiation, about 36% toluene was degraded. Moreover, the effect of the nanoporous TiO_2 film becomes stronger with the decrease of initial toluene concentration.

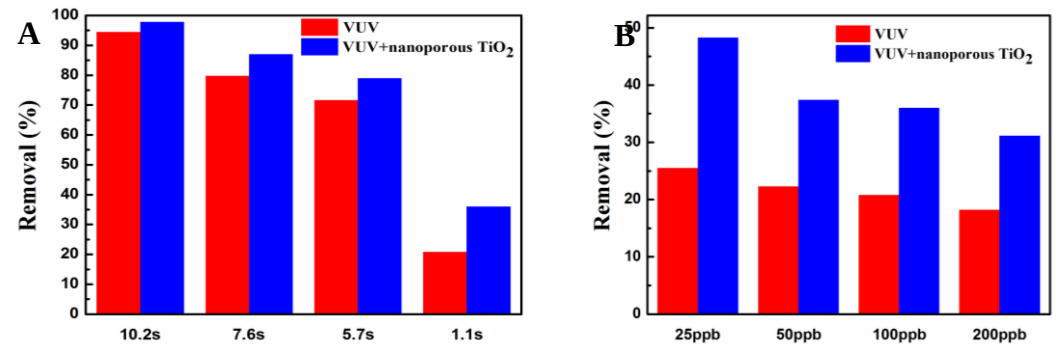

Figure 1. (A) Photocatalytic degradation of gaseous toluene at different residence time under VUV irradiation (inlet concentration is 100 ppb). (B) Photocatalytic degradation of gaseous toluene with different inlet concentrations under VUV irradiation (residence time is 1.1 s).

Furthermore, an air purifier was established to evaluate the performance of nanoporous-TiO_2/VUV and its feasibility for practical use. The photocatalytic unit includes nine VUV lamps (10W) and nanoporous TiO_2/Ti. The ozone removal unit was composed with aluminum sheet coated with Mn-Fe catalyst, heating rods and temperature sensor. The effluent stream was introduced into the ozone removal unit to trap the extra O_3 generated by VUV lamps. Heating rods and temperature sensor can control the temperature at 80 °C for Mn-Fe catalyst regeneration and is beneficial to the degradation of O_3. The system was able to provide up to 96 m^3/h airflow rates and was equipped with a radial fan with speed control mounted at the top of air purifier. The air purifier, composed with nanoporous TiO_2 and VUV lamp, not only has an effect on removal of benzene homologues, aldehyde and ketone pollutants were also removed. After opening the VUV-PCO air purifier, the TVOC of indoor air was significantly reduced (Fig.2).

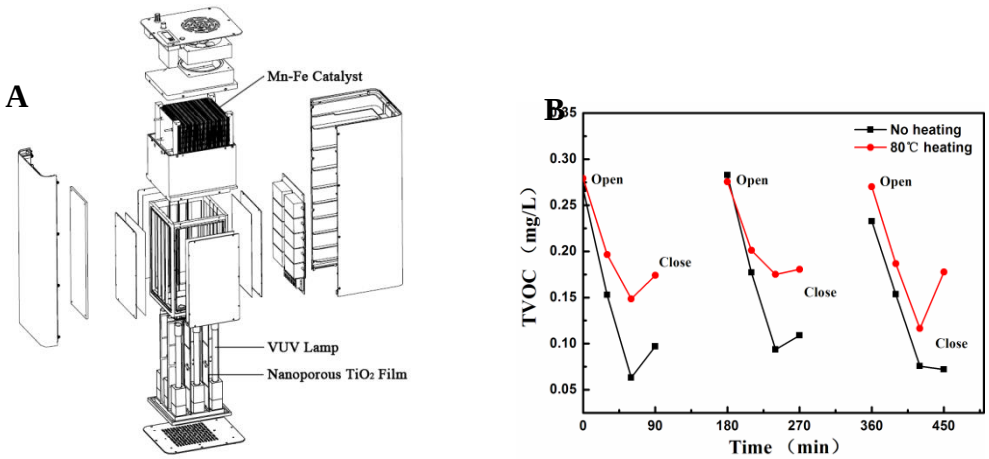

Figure 2. (A) Schematic diagram of the air purifier. (B) Photocatalytic degradation of TVOC in sealed cabinet at RT with a volume of 11.29 m^3.

Keywords: Photocatalytic degradation; indoor VOCs; Nanoporous TiO_2 film; {001} facets

References

[1] J.Y. Jeong, K. Sekiguchi, W.K. Lee, K. Sakamoto, J. Photochem. Photobiol. A: Chem., 169 (2005) 279-287.
[2] J.H. Mo, Y.P. Zhang, Q.J. Xu, Y.F. Zhu, J.J. Lamson, R.Y. Zhao, Appl. Catal. B: Environ., 89 (2009) 570-576.
[3] J.C. Little, A.T. Hodgson, A.J. Gadgil, Atmos. Environ., 28 (1994) 227-234.
[4] K.P. Yu, G.W.M. Lee, Appl. Catal. B: Environ., 75 (2007) 29-38.
[5] P.F. Fu, P.Y. Zhang, J. Li, Int. J. Photoenergy, (2012) 1-8.
[6] P.F. Fu, P.Y. Zhang, J. Li, Appl. Catal. B: Environ., 105 (2011) 220-228.
[7] T.Z.Xu, H. Zheng, P.Y. Zhang, W. Lin, Y. Sekiguchi, J. Mater. Chem. A, 3(2015) 19115-19122.
[8] T.Z.Xu, H. Zheng, P.Y. Zhang, W. Lin, RSC Advances, 6(2016) 95818-95824.

Acceptance ID: 54HB-O

Stability of heterogeneous $Pt/Ti/TiO_2$ catalyst as function of the Pt concentration

J. A. Garcia-Macedo, M. G. Blanco E., A. Gonzalez M.

Departamento de Estado Solido. Instituto de Fisica, Universidad Nacional Autonoma de Mexico. Circuito Exterior Cd. Universitaria, 04510 Mexico D.F.

Automotive three-way catalytic converter uses platinum to oxidize CO to CO2. 100% conversion efficiency is reached at 200C. It is attractive try to diminish this temperature, and then to produce less pollution. In order to obtain this result it is necessary to produce small stable platinum particles. Having this in mind, we prepared $Pt/Ti/TiO_2$ catalyst by sol-gel method, with different metal concentrations. We study the CO to CO2 conversion in a Perkin Elmer Clarus 500 gas chromatograph. We obtain 100% conversion efficiency at 185C in a sample with 2% of Pt. This response was repeated along 45 days with the same sample, stored in a dark draw at room temperature without special care. We reported the efficiency obtained for other Pt concentrations. We also reported the size distribution of Pt particles.

We acknowledge support from SECITI 053/2016, PAPIIT IN113917, CONACyT 179607, and Bilateral Mexico-Italia 174506. And we acknowledge the technical assistance from Diego Quiterio (SEM samples preparation), Roberto Hernandez (SEM) and Antonio Morales (XRD).

*:e-mail gamaj@fisica.unam.mx, phone (5255) 56225103

Waste PET-derived Metal-organic Frameworks (MOF) Materials for Enrichment of Para-Hydrogen

Jianwei (Ren)[1,2], Xoliswa (Dyosiba)[1,2], Nicholas M. (Musyoka)[1], Henrietta W. (Langmi)[1], Mkhulu (Mathe)[1], Marice S. (Onyango)[2]

[1]HySA Infrastructure Centre of Competence, Materials Science and Manufacturing, Council for Scientific and Industrial Research (CSIR), PO Box 395, Pretoria 0001, South Africa
[2]Department of Chemical, Metallurgical and Materials Engineering, Tshwane University of Technology, Private Bag X680, Pretoria, South Africa
E-mail address: jren@csir.co.za;Tel.: +27 12 8412967; fax: +27 12 8412135.

The two forms of hydrogen are transitional in an isolated system but at an extremely slow rate. Hydrogen at room temperature (300 K) is a mixture of 75% ortho-H_2 and 25% para-H_2. Below room temperature the composition of ortho-para fraction varies, and 100% para-H_2 can be achieved when temperature decreases to 20 K. Such conversion can be promoted in the presence of an engineered solid surface, and the catalytic activity of MOF materials have been proved enough to make instantaneous conversion of absorbed H_2 molecules. Ortho-H_2 can be detected using nuclear magnetic resonance (NMR) and quantified by integrating the Fourier transformed Free Induction Decay (FID), while para-H_2 does not produce any NMR signal. In this work, waste PET-derived MOF materials were synthesized as cost-effective catalysts to enrich para-H_2 by flowing ultra-purity H_2 gas at 77 K. NMR was employed to quantify the presence of para-H_2 when an unknown sample was compared to a normal H_2 sample. The achievement from this study will contribute to the building-up of a continuous para-H_2 generation system.

Keywords: Metal-organic frameworks, waste PET, enrichment of para-hydrogen, NMR

[1] BUNTKOWSKY, G., WALASZEK, B., ADAMCZYK, A., XU, Y., LIMBACH, H.H. & CHAUDRET, B. 2006. Mechanism of nuclear spin initiated para-H_2 to ortho-H_2 conversion. Phys. Chem. Chem. Phys. 8, 1929–1935.

[2] FUKUTANI, K. & SUGIMOTO T. 2003. Physisorption and ortho-para conversion of molecular hydrogen on solid surfaces. Prog. Surf. Sci. 88, 379–348.

Synthesis and Modification of MnO_2 Nanomaterials for Mineralization of Airborne Formaldehyde at Room Temperature

*Jinlong Wang, Shaopeng Rong, Lin Zhu, Pengyi Zhang**

State Key Joint Laboratory of Environment Simulation and Pollution Control, School of Environment, Tsinghua University, Beijing, 100084, China
E-mail: zpy@tsinghua.edu.cn

Formaldehyde (HCHO) causes increasing concerns due to its ubiquitously found in the indoor environment and being irritative and carcinogenic to humans. The fast abatement of HCHO at room temperature is of significant practical interest. Recently, we found birnessite-type MnO_2 showed signficant catalytic acitivty for HCHO decompositon at room temperature. The effects of water content and manganese vacancy (V_{Mn}) were investigated. The amount of V_{Mn} showed a dramatic promotion effect on the activity of birnessite for HCHO oxidation. The presence of VMn induced unsaturated oxygen species and K^+ locating nearby V_{Mn} sites for charge balance facilitated the formation of active oxygen species, accordingly the activity for HCHO oxidation was greatly improved. In the meanwhile, cerium modified birnessite-type manganese dioxides (Ce-MnO_2) with different doping ratios were prepared. Upon the doping of cerium, the growth of MnO_2 crystal was inhibited, leading to smaller particle size and higher specific surface. In addition, CeO_2 nanocrystal formed even at low doping ratio (0.1:10), resulting in close contact between CeO_2 and MnO_2 nanocrystals. As a result, the doped material owned higher content of oxygen vacancies and surface adsorbed oxygen species, which contributed to its high activity for HCHO oxidation. Ce-MnO2(1:10) with the nominal Ce/Mn ratio of 1:10 exhibited the best activity and achieved complete HCHO conversion at 100 °C and better activity at room temperature than undoped birnessite. Finanlly, we fabricated a three-dimensional manganese dioxide framework (3D-MnO_2), which owns interconnected network structures, low mass density (~7.3 mg/cm^3), and high absorption capacity for organic liquids. In particular, the 3D-MnO_2 showed excellent activity and stability for HCHO oxidation at room temperature, achieving 45% of 100 ppm HCHO mineralized into CO_2 under high gas hourly space velocity of 180 L/g.h. The excellent performance of 3D-MnO_2 catalysts in decomposing HCHO can be ascribed to their quickly reversible and high water content for replenishing the consumed surface hydroxyl groups during HCHO decomposition, and fully exposed active reaction sites. This is a valuable finding that inexpensive metal oxides such as MnO_2 can transform ppm-level HCHO into harmless CO_2 in as short as sub-second at room temperature.

Keywords: Manganese dioxide, formaldehyde, indoor environment, degradation

1. WANG J., ZHANG P., LI J., JIANG C., YUNUS R., KIM J. 2015. Room-Temperature Oxidation of Formaldehyde by Layered Manganese Oxide: Effect of Water. *Environmental Science & Technology*, 49 (20):12372–12379
2. RONG S., ZHANG P., YANG Y., ZHU L., WANG J., LIU F. 2017. MnO_2 Framework for Instantaneous Mineralization of Carcinogenic Airborne Formaldehyde at Room Temperature. *ACS Catalysis*, 7(2), 1057−1067
3. WANG J., ZHANG P., LI J., SUN Z., HAYAT G., KIM J. 2017. The Effect of Mn Vacancy in Birnessite on Its Activity for Formaldehyde Oxidation at Room Temperature. *Applied Catalysis B*, 204: 147–155

Acceptance ID: 6dj5-O

In-situ (W,N) co-doping of RF-sputtered TiO_2 thin films for use as photoanodes for the electro-photocatalytic degradation of pollutants under sunlight.

N. Delegan,[1] R. Pandiyan,[1] A. Dirany,[2] P. Drogui,[2] S. Johnston,[3] and M. A. El Khakani[,1]*

[1]*Institut National de la Recherche Scientifique, Centre-Énergie, Matériaux et Télécommunications, 1650 Blvd. Lionel-Boulet, Varennes, QC, J3X-1S2, Canada*
[2]*Institut National de la Recherche Scientifique, Centre-Eau, Terre et Environnement, 490 Rue de la Couronne, Quebec, QC, G1K-9A9, Canada*
[3]*National Renewable Energy Laboratory, Golden, CO 80401, USA*
**Corresponding author: elkhakani@emt.inrs.ca*

Monodoping has been widely used to photosensitize TiO_2 in visible light by effectively narrowing its bandgap. This process is however accompanied by the formation of local recombination centers that significantly limit the overall per-photon efficiency of monodoped TiO_2 photoanodes. In order to counteract this limitation, we have developed an *in-situ* codoping process for the RF-magnetron-sputter-deposited TiO_2:W,N films. We were thus able to tune the *in-situ* concomitant incorporation of both W and N dopants into TiO_2 films over a wide concentration range (i.e.; 0-3 at.% for W and 0-9 at.% for N, respectively). X-ray photoelectron spectroscopy and X-ray diffraction analyses revealed that both W and N dopants are mostly of substitutional nature in the TiO_2 films. These energy levels associated with the dopants were found to narrow significantly the optical band-gap from 3.2 eV (for undoped TiO_2) down to a value as low as 2.3 eV (for optimally codoped TiO_2:W,N at the respective contents of 3.8 at.% and 5.8 at.% for W and N), while maintaining the anatase structure. Most importantly, the codoping approach is found to greatly reduce the density of recombination centers in the TiO_2:W,N films, as compared to monodoped TiO_2:N films. Indeed, visible-light flash photolysis time resolved microwave conductivity (FP-TRMC) measurements revealed that the lifetime of generated photocharges increased from 340 ns (for monodoped TiO_2:N) to 890 ns (for codoped TiO_2:W,N). These FP-TRMC results constitute the first direct quantitative demonstration of the beneficial effects of acceptor-donor (W,N) codoping on photocharge lifetimes. Finally, these codoping beneficial effects were exploited by integrating these TiO_2:W,N based photoanodes into an EPC process for the sunlight degradation of atrazine herbicide (a toxic water contaminant) in water at the initial content of 60 ppb. Our results confirmed a significant increase in the pseudo-first order degradation constant values increasing from 0.026 min^{-1} for the undoped-TiO_2 to 0.106 min^{-1} for the optimally doped TiO_2:W,N photoanodes.

Keywords : RF-magnetron sputtering, in-situ doping, TiO_2, sunlight electro-photo-catalysis, bandgap narrowing, electronic passivation.

Acceptance ID: 6LCU-O

Micro/nanostructured Conducting Polymers for Electrochemical Energy Conversion

*Ying Zhu**

Key Laboratory of Bio-Inspired Smart Interfacial Science and Technology of Ministry of Education, School of Chemistry, Beihang University, Beijing 100191, China
Email: zhuying@buaa.edu.cn

The heterocyclic conjugated polymers, including polyaniline (PANI), polypyrrole (PPy) , and poly(3,4-ethylenedioxythiophene) (PEDOT), have recently been investigated as inexpensive electro-catalysts because of their low cost, high electronic conductivity, and distinct redox properties. Generally speaking, these polymers can act as electrochemical catalysts in the following three ways: 1) as catalysts on their own, 2) as precursors for pyrolyzed M-Nx/C catalysts, and 3) as matrix for entrapping non-precious metals, 4) Conducting polymers with its micro/nanostructures over a large surface area can itself be an outstanding intrinsic electrochemical catalyst. We have developed a new class of efficient non-precious-metal ORR catalysts by doping PEDOT with hemin via a one-step self-assembling mothod. It is demonstrated that the hemin-induced synergistic effect results a very high 4-electron oxygen reduction reaction (ORR) activity, a better stability, and free-from methanol crossover effect even in a neutral phosphate buffer solution due to hemin molecular characteristic, in which the iron centre of Fe-N4–C served for ORR, while the carboxyl groups used dopant for conducting PEDOT. Moreover, PANI nanofibers fabricated by electrochemical polymerization of aniline can act as a solid-state polymeric mediator for bacterial extracellular electron transfer (EET), which enables not only the dramatically enhanced EET current at a certain potential but also tunable EET behavior in a controlled manner. Image

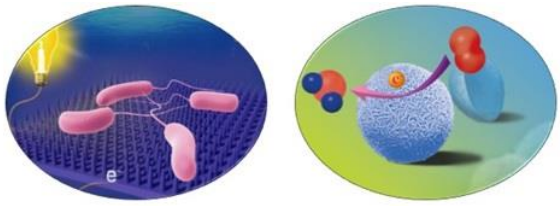

Micro/nanostructured conducting polymers for electrochemical energy conversion

1. Chunmei Ding, Huan Liu, Ying Zhu*, Meixiang Wan, Lei Jiang (2012) Energy Environ. Sci., 5:8517-8522
2. Z. Guo, H. Liu, C. Jiang, Y. Zhu*, M. Wan, L. Dai, L. Jiang (2014) Small, 10:2087-2095.
3. Guangyuan Ren, Yunan Li, Zhaoyan Guo, Guozheng Xiao, Ying Zhu*, Liming Dai, Lei Jiang, (2015)Nano Research, 8: 3461-3471.
4. Chun-mei Ding, Mei-ling Lv, Ying Zhu, Lei Jiang, and Huan (2015) Angew. Chem. Int. Ed. 54:1446-1451.
5. Zhaoyan Guo, Guangyuan Ren, Congcong Jiang, Xianyong Lu, Ying Zhu*, Lei Jiang, Liming Dai (2015) Scientific Reports, 5:17064.
6. Zhaoyan Guo, Zhen Xiao, Guangyuan Ren, Guozheng Xiao, Ying Zhu*, Liming Dai* and Lei Jiang (2016) Nano Research, 9:1244-1255. Acceptance ID: 7LER-O

Hydrogenation of 4-Nitroophenol to 4-Aminophenol at Room Temperature: Boosting Nanocrystals Efficiency by Coupling with Copper via Liquid Phase Pulsed Laser Ablation

Hanbit Park[1], *Rory Ma*[1], *Tae Kyu Kim*[1*]

[1]*Department of Chemistry, Pusan National University, Busan, Republic of Korea.*
Presenting Author's E Mail : qgc0120@gmail.com
Corresponding Author's E Mail : tkkim@pusan.ac.kr

Ultra-dispersed bimetallic nanomaterials have attracted much attention in the hydrogenation of highly toxic aromatic nitro compounds to aromatic amines owing to their high stability, superior activity, reusability, and unique optical and electronic properties, as compared to monometalic nanocrystals. However, the lack of facile and economically controllable strategies of producing highly pure ultra-dispersed bimetallic nanocatalysts limits their practical industrial applications. Considering the above obstacles, we present a simple and effective strategy for the formation of bimetallic (PdCu) nanocrystals by liquid phase pulsed laser ablation using a bulk Pd metal plate submerged in $CuCl_2$ solutions with different concentrations, in contrast to the complex and costly experimental methods used previously. The microstructural and optical properties of the synthesized nanocrystals indicate that the obtained bimetallic nanostructures are highly pure and monodispersed. Moreover, bimetallic PdCu nanostructures show a higher catalytic activity than monometallic Pd nanocrystals for the hydrogenation of 4-nitrophenol to 4-aminophenol at room temperature, also exhibiting high stability for up to four recycles. The mechanism of the enhanced catalytic activity and stability of bimetallic nanocrystals is discussed in detail. Finally, we believe that the presented design strategy and utilization of bimetallic nanocrystals for catalytic applications enables the development of novel bimetallic nanostructures by liquid phase pulsed laser ablation and their catalytic application for environmental remediation.

Keywords: PdCu, liquid phase pulsed laser ablation; catalytic activity; nitrophenol reduction

Acceptance ID: BHNS-P

Rational Design of Bimetallic Nanoparticles as Highly Efficient Catalysts for Various Reactions

Önder Metin

[1] *Department of Chemistry, Faculty of Science, Atatürk University, 25240 Erzurum, TURKEY*
e-mail : ometin@atauni.edu.tr

The interest in the use of bimetallic nanoparticles as catalysts instead of monometallic ones has been increased daily because the bimetallic NPs either in alloy or core@shell form show higher activity, selectivity and stability compared to the monometallic counterparts owing to the "*Synergistic*" effects formed between two distinct metal atoms. In particular, more economical catalysts could be developed by the preparation of bimetallic alloy or core@shell nanoparticles of noble metals with a non-noble metal, which is considered to be very advantageous for the catalytic reactions using noble metals as catalyst.

In this presentation, our very recent studies on the general synthesis of various monodisperse bimetallic NPs (alloy or core/shell), their structural characterization and their several catalytic applications in the organic and inorganic reactions will be presented. Among the bimetallic NPs, monodisperse **M**-Pd (**M:** Ni, Cu, Ag) alloy NPs and **M**@Pd (**M:** Ni and Ag) core@shell NPs as examples would be mentioned. These NPs were supported either on 2D materials including reduced graphene oxide (rGO) or mesoporous graphitic carbon nitride (mpg-C_3N_4) before their catalytic use.

Keywords: Bimetallic nanoparticles; nanocatalysis; reduced graphene oxide; mesoporous graphitic carbon nitride; catalytic applications

[1] MEENAKSHISUNDARAM, S., DIMITRATOS, N., MIEDZIAK, P. J., WELLS, P. P., KIELYE, C. J. & HUTCHINGS, G. J. 2012. Designing bimetallic catalysts for a green and sustainable future. ***Chem. Soc. Rev.*, 41,** 8099-813.

Acceptance ID: BXML-O

Sustainable catalytic oxidation of hydrocarbons with hydrogen peroxide

Mourão[1], Botelho[1], Carneiro[1], Silva[1]

[1]Department of Chemistry, CICECO, University of Aveiro, 3810-193 Aveiro, Portugal.
ana.rosa.silva@ua.pt

Hydrocarbons are relatively abundant and therefore are a low-cost feedstock [1]. The main oxidized products of cyclohexane are of great industrial significance and a large amount of cyclohexanol and cyclohexanone is produced worldwide [1,2]. Phenol is also an important intermediate for the synthesis of petrochemicals, agrochemicals, and plastics. While industrially cyclohexanol and cyclohexanone are obtained with 80% selectivity at 4% conversion using a Co(II) naphthenate catalyst at 160◦C and 15 bar [2], phenol is produced in three reaction steps from benzene [3]. The development of economical catalysts that work under mild reaction conditions in the direct activation of C-H bonds is still a scientific challenge [1].

Transition metal coordination compounds with very versatile non-heme polydentate ligands were applied as selective homogeneous catalysts in the oxidation of cyclohexane and benzene under mild conditions and using environmentally benign hydrogen peroxide. Cyclohexanone and cyclohexanol were the main products of the oxidation of cyclohexane, with higher yields than the industrial process [4]. Phenol was the main product of the direct oxidation of benzene in acetonitrile at 50°C with very high selectivities [5]. The best catalysts for both reactions were the Fe(III/II) complexes with Schiff base ligands in only 1 mol% based on the substrate [4,5]. Cyclooctane and *n*-hexane could also be oxidized to the corresponding ketones and alcohols by the Fe(III) complex with N_2O_2 Schiff base ligand [4]. Commercially available VO(IV), Fe(II) and Fe(III) acetylacetonate acted as well as homogeneous catalysts in the oxidation of cyclohexane [4], *n*-hexane [6] and benzene [5].

The sustainability of the homogeneous catalysts in the catalytic reactions was improved by using economic and environmentally acceptable solid porous supports: hexagonal mesoporous silica and activated carbon. Due to their easy anchoring when compared with the Schiff base complexes, the readily available Fe(II), Fe(III) and VO(IV) acetylacetonate complexes were immobilized onto these porous supports, previously functionalized with amine groups [5,6]. Characterization of the materials showed that both porous materials were conveniently functionalized and that the metal complexes could be effectively anchored onto these materials by Schiff condensation [5,6]. They were active as heterogeneous catalysts in the oxidation of cyclohexane and *n*-hexane at room temperature with hydrogen peroxide, giving the respective alcohols and ketones [6]. And they were also active in the direct oxidation of benzene to phenol with higher yield and selectivity than the original metal complexes in homogeneous phase [5]. All the heterogeneous catalysts prepared could also be recycled by simple filtration and re-used at least in two more consecutive cycles without significant loss of catalytic activity [5,6]. Comparable or higher phenol yields to the best reported in the literature were obtained [5].

Keywords: catalysis, iron, materials, immobilization, hydrogen peroxide

[1] SHILOV, A. E., SHUL'PIN, G. B. 1997. Activation of C-H bonds by metal complexes. *Chem. Rev.* 97, 2879–2932.

[2] RETCHER, B., SÁNCHEZ COSTA, J., TANG, J., HAGE, R., GAMEZ, P., REEDIJK, J. 2008. Unexpected high oxidation of cyclohexane by Fe salts and dihydrogen peroxide in acetonitrile. *J. Mol. Catal.A: Chem.* 286, 1–5.

[3] JIANG, T., WANG, W., HAN, B. 2013. Catalytic hydroxylation of benzene to phenol with hydrogen peroxide using catalysts based on molecular sieves. *New. J. Chem.* 37, 1654-1664.

[4] SILVA, A. R., MOURÃO, T., ROCHA, J. 2013. Oxidation of cyclohexane by transition-metal complexes with biomimetic ligands. *Catal. Today* 203, 81-86.

[5] CARNEIRO, L., SILVA, A. R. 2016. Selective direct hydroxylation of benzene to phenol with hydrogen peroxide by iron and vanadyl based homogeneous and heterogeneous catalysts. *Catal. Sci. Technol.* 6, 8166-8176.

[6] SILVA, A. R., BOTELHO, J. 2014. Peroxidative oxidation of cyclic and linear hexane catalysed by supported iron complexes under mild and sustainable conditions. *J. Mol. Catal. A: Chem.* 381, 171-178.

Acknowledgements: This research was supported by a Marie Curie European Reintegration Grant within the 7th European Community Framework Programme (FP7-PEOPLE-2009-RG-256509). ARS thanks FCT, FSE and POPH for the contract IF/01300/2012. TM thanks FCT for an under-graduate BII fellowship of 2009. This work was developed within the scope of the project CICECO-Aveiro Institute of Materials (Ref. FCT UID /CTM /50011/2013), financed by national funds through the FCT/MEC and when appropriate co-financed by FEDER under the PT2020 Partnership Agreement.

Acceptance ID: J36E-O

Synthesis and Characterization of Nitrogenated $ZnTiO_3$ Nanoparticles with Strongly Enhanced Visible-light Photocatalytic Activity

*Somendra Singh, Shama Perween, and Amit Ranjan**

[*] *Department of Chemical Engineering, Rajiv Gandhi Institute of Petroleum Technology, Jais, Amethi, Utter Pradesh, India-229304*
E Mail/ Contact Détails : aranjan@rgipt.ac.in */ +91-9473672998*

In visible light photocatalysis the catalytic activity of the catalyst is further improved by presence of visible radiation. Photocatalysis aided by visible light is extremely desirable due to an abundance (44-47%) of the visible region in the solar spectrum with UV light accounting for only 3-5% of the total power, and hence attracts active research pursuits. Visible light photocatalysts are promising candidate materials particularly for public health concerns, as they may expedite the degradation of various environmental pollutants in presence of sunlight. In a prior work [1] we have reported a facile approach to produce zinc titanate ($ZnTiO_3$) nano-powders with improved photocatalytic activity under visible light. The method consists of calcining the electrospun mats obtained by spinning a sol that yields a white crystalline nano-powder. The $ZnTiO_3$ nanopowders prepared by calcining the mats obtained after sol-electrospinning showed improved activity towards degradation of phenol (an important environmental pollutant) in presence of visible light as compared to those prepared by conventional sol-gel route [1].

In this work we aim towards improving the visible-light photoactivity of these materials by doping nitrogen. Nitrogen is chosen as the dopant atom as it can, in addition to favorably introducing gap states and narrowing the band gap, suppress the recombination of the photoelectrons and increase the carrier lifetimes, thereby enhancing the efficiency of the photocatalysis process [2]. To achieve nitrogen doping, the precursor sol is mixed with urea, electrospun, and calcined. Photocatalytic activity of these powders is studied by monitoring the photocatalytic degradation of phenol in the presence of visible light provided by the 100 watts incandescent light bulb. It is found that the $ZnTiO_3$ powder obtained from electrospinning the urea mixed precursor sol strongly enhanced the degradation rate of the phenol. The first order rate constant for undoped $ZnTiO_3$ is $k = 0.0033\ s^{-1}$ and for nitrogenated electrospun $ZnTiO_3$, $k = 0.01065\ s^{-1}$. In light of this encouraging result, further characterizations and optimization of the catalyst performance is under way.

Keywords: $ZnTiO_3$, Phenol degradation, Visible light photocatalysis, Nitrogen doping, Sol-electrospinnig.

[1] PERWEEN S., RANJAN A. 2017. Improved visible-light photocatalytic activity in $ZnTiO_3$ nanopowder prepared by sol-electrospinning, 2017. *Solar Energy Materials & Solar Cells*, 163, 148–156.

[2] CONG Y., ZHANG J., CHEN F., ANPO M. 2007. Synthesis and characterization of nitrogen-doped TiO_2 nanophotocatalyst with high visible light activity. *Journal of Physical Chemistry C*, 111(19), 6976-6982.

Acceptance ID: K89C-O

Visible-light TiO_2 photocatalyst doped with silylated porphyrin

*Julien G. Mahy [1] *, Carlos A. Paez [1], Géraldine L.-M. Léonard [1], Michel Wong Chi Man [2], Carole Carcel [2], Andrew Tatton [3], Christian Damblon [3], Benoît Heinrichs [1], Stéphanie D. Lambert [1]*

[1] *Department of Chemical Engineering – Nanomaterials, Catalysis & Electrochemistry, University of Liège, B6a, Quartier Agora, Allée du six Août 11, 4000 Liège, Belgium*
[2] *Institut Charles Gerhardt Montpellier, UMR-5253, ENSCM, Université Montpellier, CNRS, 8 Rue de l'École Normale, 34296 Montpellier, France*

[3] Structural Biological Chemistry Laboratory, University of Liège, Liège, Belgium

**E-mail/Contact details:* julien.mahy@ulg.ac.be

In this work, a silylated porphyrin (Tetrakis(3-(triethoxysilyl)propylamine) (tetrakis(p-aminophenyl) porphyrin) carbamate) is synthesized to dope TiO_2 formed by sol-gel process in order to produce efficient photocatalysts under low energy light. Two TiO_2 synthetic routes are considered: the organic way and the aqueous way depending the solvent used. Samples are characterized by X-Ray diffraction (XRD), Fourrier Transformed Infra-Red spectroscopy (FT-IR), Nuclear Magnetic Resonance measurements (NMR), nitrogen adsorption–desorption measurements and diffuse reflectance spectroscopy measurements. Results show that (i) for the organic way, TiO_2-anatase catalysts with a crystallite size of 23 nm and a low specific surface area are formed, while (ii) for the aqueous way, TiO_2-anatase and brookite catalysts with a crystallite size of 5 nm and a high specific surface area are obtained. For doped samples, the absorption spectrum of TiO_2 presents visible wavelengths absorption, consequence of bonding between the porphyrin and TiO_2. Then, the photocatalytic activity of samples are tested for the degradation of p-nitrophenol under UV/visible light or low energy light showing an increase of the activity for the doped catalysts with porphyrin. Indeed, porphyrin is excited by absorption of visible light causing the transfer of an electron from the HOMO level (Highest Occupied Molecular Orbital) level to the LUMO level (Lowest Unoccupied Molecular Orbital). Photosensitization of TiO_2 resulting from the transfer of the photo-induced electron of the LUMO level of the porphyrin into the conduction band of TiO_2 [1-3].

Keywords: TiO_2-based photocatalysis, Silylated porphyrin, Sol-Gel process, p-nitrophenol degradation

[1] Kathiravan, A., Renganathan, R. and Anandan, S. (2010). Electron transfer dynamics from the singlet and triplet excited states of meso-tetrakis (p -carboxyphenyl) porphyrin into colloidal TiO_2 and $AuTiO_2$ nanoparticles, *Journal of Colloid And Interface Science*, 348(2), 642–648. .
[2] Liu, G., Jaegermann, W., He, J., Sundstro, V. and Sun, L. (2002). XPS and UPS Characterization of the TiO_2/ZnPcGly Heterointerface: Alignment of Energy Levels, *Journal of Physical Chemistry*, 106, 5814–5819.
[3] Tasseroul, L., Lambert, S. D., Eskenazi, D., Amoura, M., Páez, C. A., Hiligsmann, S., Thonart, P. and Heinrichs, B. (2013). Degradation of p -nitrophenol and bacteria with TiO_2 xerogels sensitized in situ with tetra (4-carboxyphenyl)porphyrins, *Journal of Photochemistry & Photobiology, A: Chemistry*, 272, 90–99.

Acceptance ID: LEL4-O

Oxidative Desulfurization Catalyzed by Metal Oxide Subnanoclusters

Jiasheng Wang, Wenpei Wu, Ming Bao

School of Petroleum and Chemical Engineering, Dalian University of Technology, Panjin 124221, China.
*E Mail: jswang@dlut.edu.cn (**Jiasheng Wang**)*

Ultra-deep desulfurization of fuels has recently attracted great attention because of the serious environmental problems and harsh legal requirements. Usually high temperature and high pressure are needed for the traditional hydrodesulfurization. In contrast, the oxidative desulfurization is a promising method which can remove the sulfur under mild conditions without hydrogen. However, improvement of the catalysts' activity is still required. Subnanoclusters are the particles with diameters between 0.1 nm and 1.0 nm (Lu and Chen, 2012). As an intermediate size regime between nanoparticles and molecules, subnanoclusters have exhibited some new properties which are different from their nano-counterparts. In this work, we synthesized subnano-MoO_3 supported on ultrasmall mesoporous silica nanoparticles (UMSN). Then we tested its catalytic activity towards oxidative desulfurization. The subnano-MoO_3/UMSN exhibited enhanced catalytic activity compared to conventional nanoparticles supported on silica. This is the first time for applying metal oxide subnanoclusters to catalyze oxidation desulfurization. Ultra-deep desulfurization of fuels can be realized under mild conditions with this new kind of subnano catalyst.

Keywords: subnanocluster, ultrasmall mesoporous silica, heterogeneous catalysis, oxidation desulfurization (Maximum Five)

[1] LU, Y. & CHEN, W. 2012. Sub-nanometre sized metal clusters: from synthetic challenges to the unique property discoveries. *Chemical Society Reviews,* 41**,** 3594-623.

Acceptance ID: PLVT-O

Design Principles of Efficient Carbon-based Electrocatalysts for Clean Energy Conversion and Storage

Zhenghang Zhao, Zhenhai Xia

Department of Materials Science and Engineering, Department of Chemistry, University of North Texas, Denton, TX 76203, USA

Clean and sustainable energy technologies, such as fuel cells, metal-air batteries, water-splitting and solar cells, are currently under intensive research and development because of their high efficiency, promising large-scale applications, and virtually no pollution or greenhouse gas emission. At the heart of these energy devices, there are three critical chemical reactions: *oxygen reduction reaction* (ORR), *oxygen evolution reaction* (OER) and *hydrogen evolution reaction* (HER) that determine the efficiencies of energy conversion and storage. These reactions, however, are sluggish and require noble metals (*e.g.*, platinum) or their oxides as catalysts. The limited resources and high cost of platinum have hampered the commercialization of these technologies. Therefore, it is necessary to search for alternative materials to replace Pt. Carbon nanomaterials, such as carbon nanotubes (CNTs) and graphene, are appealing as an alternative for metal-free catalytic applications because of their structures and excellent properties. Although the superior catalytic capabilities of heteroatom-doped carbon nanomaterials for ORR have been demonstrated, trial-and-error approaches are still used to date for the development of highly-efficient catalysts. To rationally design a catalyst, it is critical to understand which intrinsic material characteristics, or descriptors that control catalysis. Through first-principles calculations, we have identified a material property that serves as the activity descriptor for predicating ORR and OER activities, and established a volcano relationship between the descriptor and the bifunctional activities of the carbon-based nanomaterials. Such descriptor enables us to design new metal-free catalysts with enhanced ORR and OER activities, even better than those reported for platinum-based metal catalysts. The design principles can be used as a guidance to develop various new carbon-based materials for clean energy conversion and storage.

Acceptance ID: QBJD-O

Preparation and Applications of Peptide Noble Metal Composites

Chang-jun Liu

Tianjin Co-Innovation Center of Chemical Science & Engineering, School of Chemical Engineering and Technology, Tianjin University, Tianjin 300072, China.
E Mail. Ughg_cjl@yahoo.com ; coronacj@tju.edu.cn

Peptide noble metal composites have been extensively applied in medicine, catalysis and others. A controllable preparation of peptide noble metal composites still remains as a significant challenge. To overcome this challenge, we recently developed a room temperature electron reduction for the syntheses of peptide noble composites.[1] The size, shape, facet, structure, and composition of obtained composites could be specifically controlled under the mild synthesis conditions. The obtained peptide composites exhibit enhanced activity and stability. For example, the obtained peptide Pt composites show a significantly high activity for photo-catalytic water splitting and CO_2 conversion.[2] They also show high activity and enhanced stability for oxygen reduction.[3] More applications are be tested and will be reported in our future works.

Keywords: Peptide, noble metal, composite, catalyst, water splitting

[1] YAN, J.M., PAN, Y.X., CHEETHAM, A.G., LIN, Y.-A., WANG, W., CUI, H.G., LIU, C.-J. 2013. One-Step Fabrication of Self-assembled Peptide Thin Films with Highly Dispersed Noble Metal Nanoparticles. *Langmuir*, 29, 16051-16057.

[2] PAN, Y.-X., CONG, H.-P., MEN, Y.-L., XIN, S., SUN, Z.-Q., LIU, C.-J., YU, S.-H. 2015. Peptide Self-Assembled Biofilm with Unique Electron Transfer Flexibility for Highly Efficient Visible-Light-Driven Photocatalysis. *ACS Nano*, 9, 11258–11265.

[3] WANG, W., WANG, Z.Y., YANG, M.M., ZHONG, C.-J., LIU, C.-J. 2016. Highly Active and Stable Pt (111) Catalysts Synthesized by Peptide Assisted Room Temperature Electron Reduction for Oxygen Reduction Reaction, Nano Energy, 25, 26–33.

Acceptance ID: QZAX-I

Preparation and performance of Cu_2O/TiO_2 nanocomposite thin film and photocatalytic degradation of Rhodamine B

Xiaojiao Yu[*,a], *Song Kou*[a], *Xiyan Tang*[a], *Ju Li*[a], *Qian Yang*[a], *Yuchen Wei*[b], *Jinfen Niu*[a]

[a]*Department of Applied Chemistry, Xi'an University of Technology, Xi'an 710048, China*

A constant current electrodeposition approach was employed to prepare Cu_2O/TiO_2 nanocomposite thin film. XRD, XPS, SEM, Raman, UV-Vis and PL were used to characterize and analyze the thin film microstructure, surface morphology and photoelectric properties. Effect of annealing treatment on the thin film properties was discussed. Response surface methodology was employed to optimize the main influences of Rhodamine B photocatalytic degradation by thin film, and the quadratic multinomial mathematical model was established. Photocatalytic degradation process of Rhodamine B was studied. The results indicated that the prepared Cu_2O thin film was of high purity, with (111) crystal plane preferred orientation. The average particle diameter was about 150 nm, and the absorbing boundary was about 600 nm. After annealing treatment, the absorbing boundary and open circuit voltage increased, Cu_2O thin film exhibited obvious absorbance response in visible light range. The R^2 in the established quadratic model is 0.9888, which was of better fitness and higher reliability. Under optimum conditions, the Rhodamine B degradation rate can reached over 99.36% in 3 h. The Rhodamine B molecules can be decomposed completely. Recycling results revealed that Rhodamine B degradation rate can still reached 86.8 % after 8 cycles.

Acceptance ID: RN89-O

Palladia/ceria robust methane oxidation catalyst

Mahmoud M Khader, Mohammed J. Al- Marri, Sardar Ali, Ahmed G. Abdelmoneim*

Gas Processing Center, College of Engineering, Qatar University
Doha, P. O. Box 2713, Qatar

We report on the synthesis and testing of an active and stable catalyst for methane oxidation. The catalyst is a solid state solution of pallida/ceria supported on alumina (PCA). It is prepared via a one-step solution-combustion synthesis (SCS) method in which aqueous solutions of $Pd(NO_3)_2$, $Ce(NO_3)_3$, $Al(NO_3)_3$ and glycine are heated in air till full combustion. Contrary to the catalyst prepared by conventional impregnation method, investigation by x-ray photoelectron spectroscopy (XPS) shows that SCS results in the formation of a solid solution in which the Pd ions are doped into the ceria lattice, and associated with the reduction of Ce^{4+} into Ce^{3+} ions, and presumably, the formation of oxygen vacancies. Pd has three oxidation states corresponding to Pd^0, Pd^{2+} due to PdO and highly ionized Pd ions ($Pd^{(2+X)+}$) which may originated due to insertion of Pd ions into the ceria lattice. Pallida/ceria segregates on the surface of the alumina support and, its intrinsic Ce^{3+}, oxygen vacancies and highly ionized Pd, are believed to play the major role in the catalytic reaction. For higher Pd loading samples, bulk PdO and metallic Pd are detected by XRD.

The light-off curves show that methane oxidation exhibits three distinctive regions: the high temperature region (above 400℃) is characterized by 100% activity. The behavior of the catalyst above 400℃ is independent on the Pd content and on whether the reaction occurs under wet or dry conditions. This region corroborates with the Mar-van Krevlen mechanism. The second region of the light off curves lies between ~ 400 and ~ 300℃. In the second region, the catalytic activity gradually decreases with decreasing the temperature. Increasing the Pd loading as well as reducing the catalyst prior to reaction greatly enhance the activity in the second region. Methane oxidation in this region is suggested to follow the Langmuir-Hinshelwood mechanism. The third region extends from ~300℃ down to ~200℃, it is characterized by exponential decay in activity with decreasing temperature. The activity in the third region decreases significantly in the presence of steam. Catalyst deactivation in the third region is suggested to be due to surface hydroxylation because of the accumulation of H_2O on the surface.

**Presenting author: Email: mmkhader@qu.edu.qa, Phone (+974-55825744)*

Acceptance ID: SLA7-O

Controlling the Catalytic Properties of Thiolate Capped Metal Nanoparticles for Selective Organic Reactions

Young-Seok Shon[*]

Departments of Chemistry and Biochemistry and the Keck Energy Materials Program (KEMP), California State University Long Beach, Long Beach, CA 90840, USA
**Email: ys.shon@csulb.edu*

The systematic evaluation of metal nanoparticle catalysts functionalized with well-defined small organic ligands can provide important fundamental understandings on the influence of chemical environments near active sites. Our group previously reported that the thiosulfate protocol using sodium S-alkylthiosulfates instead of alkanethiols could generate catalytically active Pd nanoparticles (PdNPs) capped with a lower density of alkanethiolate ligands.[1,2] These unsupported PdNP catalysts exhibited an excellent selectivity toward the isomerization of allylic alcohols to carbonyls in organic solvents.[3,4] PdNPs were also found to be selective for the isomerization of terminal alkenes to internal alkenes and the mono-hydrogen-ation of dienes and trienes.[5] Herein, we report an investigation of various PdNPs capped with alkanethiolate ligands with linear alkyl, cyclic, or phenyl terminal groups and also PdNPs capped with constitutional isomers of pentanethiolate ligands (with one or two methyl groups at different locations (α, β, or γ) from the surface-bound sulfur). The catalysis studies show that the non-covalent and steric interactions between surface ligands and incoming substrates in the near-surface environment greatly influence the overall activity and selectivity of PdNP catalysts.

References:

1. Sadeghmoghaddam, E.; Lam, C.; Choi, D.; Shon, Y.-S. *J. Mater. Chem.* **2011**, 21, 307-312.
2. Gavia, D.; Shon, Y.-S. *Langmuir* **2012**, *28*, 14502-14508.
3. Sadeghmoghaddam, E.; Gu, H.; Shon, Y.-S. *ACS Catal.* **2012**, *2*, 1838-1845.
4. Gavia, D. J.; Shon, Y.-S. *ChemCatChem* **2015**, *7*, 892-900.
5. Zhu, J. S.; Shon, Y.-S. *Nanoscale*, **2015**, *7*, 17786-17790.

Acceptance ID: SNB3-O

A novel insitu protocol to design cobalt porphyrin - TiO_2 hybrids for effective photocatalysis

Jinfen Niu, Peixuan Dai, HefengNing, Binghua Yao, Xiaojiao Yu

Xi'an University of Technology, China

TiO_2-based heterogeneous photocatalysis has been widely considered as a useful and rapid technique for wastewater treatment. Photosensitization using metalloporphyrin allows efficient sensitization of TiO_2 in the visible light region as compared to the other methods. Generally, the composites were achieved by physically adsorbing the metalloporphyrins on the TiO_2 surface. However, the interfacial phase existing within this inorganic-organic hybrid materials will become the photoinduced electron transfer potential barrier, hence that would accelerate the combination of electron- hole pair, and lower the photocatalytic efficiency. Herein the hybrid of TiO_2 nanoparticles sensitized by metalloporphyrin was successfully synthesized via a rapid insitu microwave hydrothermal method, derived from butyl titanate as the titanium precursors and metalloporphyrin (CoTCPP) as a sensitizer. The composition and structure of the as-synthesized CoTCPP-TiO_2 hybrids were characterized by XRD,SEM,EDX mapping, TEM, SAED,IR,DRS,et al. The photocatalytic activity was evaluated by the decomposition of methylene blue (MB) under visible-light. The results show that the CoTCPP-TiO_2 nanocomposite exhibits superior photocatalytic performance to the bare TiO_2 and CoTCPP sensitized TiO_2 preparing via traditional route upon MB degradation. The removal of 10 mg/L methylene blue (MB) over CoTCPP-TiO_2 under visible light irradiation can reach about 5 times than that of P25. The enhanced photocatalytic performance could be attributed to more effective and easy photo-excited electrons transportation channels via the chemical bond between the photosensitizer and the surface molecules of TiO_2. A possible photocatalytic mechanism was also proposed.

Acceptance ID: tcdr-P

Homogeneous Catalysis for a Polymerization of Methyl Methacrylate: Synthesis and Characterization of Transition Metal Complex

Hyosun Lee

Department of Chemistry, Kyungpook National University, 80 Daehakro, Buk-gu, Daegu-city, 41566 Republic of Korea
hyosunlee@knu.ac.kr

We have investigated catalytic activity for the methyl methacrylate (MMA) polymerisation in the presence of catalysts transition metal complexes and co-catalyst modified methylaluminoxane (MMAO). Several groups of a series of ligands, namely, *N*,*N'*-bidentate *N*-cycloalkyl 2-iminomethylpyridine, *N*,*N*'-bidentate *N*-(pyridin-2-ylmethyl)aniline, *N*,*N'*,*N*-tridentate *N*,*N*-di(2-picolyl)cycloalkylamine, *N*,*N'*,*X*-tridentate *N*-substituted 2-iminomethylpyridine and 2-iminomethylquinoline and *N*,*N'*-bidentate or *N*,*N'*,*N*-tridentate *N*'-substituted *N*,*N*-bis[(1H-pyrazol-1-yl)methyl]amines have applied to the transition metals such as cobalt, copper, zinc, palladium, and cadmium, to give a series of the corresponding transition metal complexes. All complexes were characterized by spectroscopic methods and X-ray crystallography. Their activity for the MMA polymerization was reached the order of 10^5 (g PMMA)/(mol cat)·h at 60°C and syndiotacticity of poly(methylmethacrylate) (PMMA), characterised by ^{1}H NMR spectroscopy, was *ca.* 0.73.

Keywords: catalysis, polymerization, methyl methacrylate, transition metal complex

[1] SONG, Y., NAYAB, S., JEON, J., PARK, S. H. & LEE, H. 2015. Cadmium(II) complexes containing *N*'-substituted *N*,*N*-di(2-picolyl)amine: The formation of monomeric versus dimeric complexes is affected by the *N*'-substitution group on the amine moiety. *J. Organomet. Chem.*, 783, 55-63.

Acceptance ID: U9LC-O

Heterostructured WS_2-MoS_2 Ultrathin Nanosheets Integrated on CdS Nanorods for Promoting Charge Separation and Migration to Improve Photocatalytic Hydrogen Evolution Performance

*Rory Ma[1], D. Amaranatha Reddy[1], Hanbit Park[1] and Tae Kyu Kim**

[1]Department of Chemistry and Chemical Institute for Functional Materials, Pusan National University, Busan 46241, Republic of Korea.
E-mail: tkkim@pusan.ac.kr

The large consumption and depletion of non-renewable fossil fuels such as coal, petroleum, oil, and gas, and increasing global warming issues have triggered the urgent necessity to develop highly efficient, environmentally friendly, and sustainable energy sources[1,2]. Hydrogen fuel has been long regarded as a promising clean and sustainable alternative to fossil fuels in the future [3, 4]. The solar-driven photocatalytic water splitting process, to produce hydrogen with high product purity with a simple process and little pollution, has been recognized to be one of the most promising ways for energy conversion.[5, 6] However, for efficient solar-driven water splitting and to explicate the photocatalytic water splitting technology towards industrialization, finding active photocatalysts with high stability and efficiency is of paramount importance[7].

In this study, for the first time we designed a highly efficient and stable noble metal-free CdS/WS_2-MoS_2 nanocomposite through a facile hydrothermal approach. When assessed as a photocatalyst for water splitting, the as-synthesized CdS/WS_2-MoS_2 nanostructures exhibited remarkable photocatalytic hydrogen evolution performance and impressive durability. We achieved an excellent hydrogen evolution rate of 209.79 mmol·g^{-1}·h^{-1} under simulated sunlight irradiation, which is higher than those of CdS/MoS_2 (123.31 mmol· g^{-1}·h^{-1}) and CdS/WS_2 (169.82 mmol· g^{-1}·h^{-1}) nanostructures, and the expensive CdS/Pt benchmark catalyst (34.98 mmol· g^{-1}·h^{-1}). The apparent quantum yield reached 51.4% at 425 nm in 5 h. Furthermore, the obtained hydrogen evolution rate is better than those of several noble metal-free catalysts reported earlier. The observed high rate of hydrogen evolution and remarkable stability may be due to the ultrafast separation of photo-charge carriers and transportation between the CdS nanorods and the WS_2-MoS_2 nanosheets, thus increasing the number of electrons involved in hydrogen production. We believe that the proposed designed strategy will may open a new door to design advanced noble metal free photocatalytic materials for efficient solar driven hydrogen production.

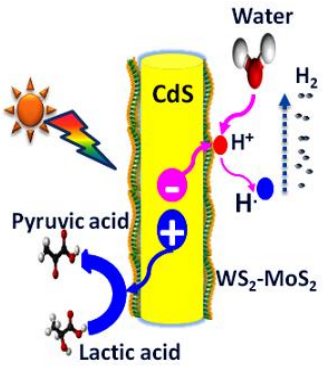

Fig1. Schematic illustration of the formation process of CdS/WS_2-MoS_2 nanocomposites.

1. H. B. Gray, Nat. Chem, 1, 7 (2009).
2. N. S. Lewis, D. G. Nocera, Proc. Natl. Acad. Sci. U. S. A., 103, 15729–15735 (2006).
3. K. Maeda, K. Teramura, D. Lu, T. Takata, N. Saito, Y. Inoue, K. Domen, Nature, 440, 295 (2006).
4. J. A. Turner, Science, 305, 972–974 (2004).
5. M. S. Dresselhaus, I. L. Thomas, Nature, 414, 332–337 (2001).
6. D. Ravelli, D. Dondi, M. Fagnoni, A. Albini, Chem. Soc. Rev, 38, 1999–2011 (2009).
7. K. Maeda, K. Domen, J. Phys. Chem. Lett, 1, 2655–2661 (2010).

Acceptance ID: US9T-P

Development of SiO_2@TiO_2 and SiO_2@TiO_2-Prussian Blue core-shell photoactive nanocomposites for environmental photocatalysis

Ferreira-Neto E.P [1], *Ullah S.*[2], *Rodrigues-Filho U.P.*[1]

[1]*Instituto de Química de São Carlos, Universidade de São Paulo, São Carlos, SP, Brazil*
[2]*Institute of Chemical Sciences, University of Peshawar, Peshawar, Pakistan*
Contact : eliaspaiva@usp.br, uprf@iqsc.usp.br

Heterogeneous photocatalysis using TiO_2 based nanomaterials is regarded as a promising approach for environmental remediation as it can promote both organic pollutants photodegradation and photo-assisted heavy metal ions removal [1]. However, the overall efficiency of photocatalytic processes is still low and there is great interest in the development of highly active photocatalysts for such environmental applications. Preparation of nanocomposites based on TiO_2 nanoparticles and other functional inorganic compounds is a very interesting strategy to improve the performance of these photoactive materials, as it allows tailoring TiO_2 nanostructured materials physical properties, as well as combination with more suitable electronic and catalytic properties [2]. In this study, we report the preparation of enhanced nanostructured photocatalysts by the sol-gel synthesis of SiO_2@TiO_2 core-shell particles and their further modification with Iron Ferrocyanide (Prussian Blue or PB). SiO_2@TiO_2 particles were prepared by the grafting and controlled hydrolysis of titanium isopropoxide on the surface of silica particles in ethanol/isopropanol mixtures [3] and further modified with PB by photodeposition method [4]. Characterization by electron microscopy and XRD analysis evidenced the formation of the core-shell particles by coating of SiO_2 submicron spheres with porous TiO_2 shells constituted of anatase nanocrystals, while modification with PB was confirmed by FTIR, Mossbauer spectroscopy, XRD and XRF elemental composition analysis. SiO_2@TiO_2 particles exhibited superior photocatalytic activity for Crystal Violet dye degradation compared to unsupported TiO_2 nanoparticles of similar size, which is attributed to improved adsorption of dye molecules, efficient light harvesting and better dispersion of the silica-supported anatase nanoparticles [3]. Further improvement of the photocatalytic activity of SiO_2@TiO_2 is observed upon calcination at 800-1000^{0}C due to increase in crystallinity, while a drastic decrease in photoactivity is observed for calcined unsupported titania caused by almost complete conversion of anatase into rutile and significant loss of specific surface area. Additionally, Prussian Blue modified samples showed enhanced photocatalytic activity for Cr(VI) reduction, achieving a 98% removal of hexavalent chromium for a 10mg/L Cr(VI) solution in deionized water (pH =5,6) after 1h exposure to UV radiation. The photoactive behavior of SiO_2@TiO_2-PB material is based on the photo-reduction of PB to Prussian White (PW) triggered by interband photo-excitation of the TiO_2 nanoparticles. By acting as electron receptor and mediator, the PB layer promotes effective charge separation in the titania interface, thus resulting in increased photocatalytic reduction activity.

Keywords: Photocatalysis, SiO_2, TiO_2, Prussian Blue, sol-gel

[1] CHONG, M.N., JIN, B., CHOW, C.W.K., SAINT, C., 2010. Recent developments in photocatalytic water treatment technology: A review. *Water Res.* 44, 2997–3027.

[2] DAHL, M., LIU, Y., YIN, Y., 2014. Composite Titanium Dioxide Nanomaterials. *Chem. Rev.* 114, 9853–9889.

[3] ULLAH, S., FERREIRA-NETO, E.P., PASA, A.A., ALCÂNTARA, C.C.J., ACUÑA, J.J.S., BILMES, S.A., RICCI, M.L.M., LANDERS, R., FERMINO, T.Z., RODRIGUES-FILHO, U.P., 2015. Enhanced photocatalytic properties of core@shell SiO_2@TiO_2 nanoparticles. *Appl. Catal. B Environ*. 179, 333–343.

[4] TADA, H., SAITO, Y., KAWAHARA, H., 1991. Photodeposition of Prussian Blue on TiO_2 Particles. *J. Electrochem. Soc.* 138, 140–144.

Acceptance ID: UZ8J-O

Interface controlled epitaxial growth of ceria nanoparticles on Anatase titania powders

Hyun You Kim[1], Mark S. Hybertsen[2], and Ping Liu[3]

[1]Department of Materials Science and Engineering, Chungnam National University
99 Daehak-ro, Yuseong-gu, Daejeon 34134 Republic of Korea
[2]Center for Functional Nanomaterials, Brookhaven National Laboratory, Upton, New York 11973, USA
[3]Chemistry Department, Brookhaven National Laboratory, Upton, New York 11973, USA

Interfaces of oxides and metal nanoparticles have shown extensive potential for accelerating various catalytic processes, via direct participation[1-3] or the strong metal-support interaction (SMSI).[4] To tune the catalytic activity and selectivity, rational control of interfacial structures has been a long standing goal in catalysis, in particular for powder supports used in practical catalysts. Motivated by a recent experimental study,[5] we demonstrate a "bottom-up" approach to understand the epitaxial growth of the ceria nanoarrays on Anatase (A)-titania powders based on density functional theory (DFT) calculations. According to our results, the delicate balance in the relative rigidity of A-TiO_2 facets, the CeO_2-CeO_2 interaction energy, surface energy of CeO_2 facets, and the TiO_2-CeO_2 interface formation energy controls the growth behavior of ceria nanoarryas on A-TiO_2 powders. We then extend the study to show that added Pt atoms preferentially nucleate at the TiO_2-CeO_2 interface allowing them to potentially participate in the catalysis at the Pt-CeO_2-TiO_2 multi-phase interface. Experimental observation confirms the strong geometric correlation between the CeO_2 architectures and the and deposited Pt clusters. Our results pave the way towards the rational design of practically relevant nanomaterials with enhanced stability and functionality.[6]

1. Cargnello, M.; Doan-Nguyen, V. V. T.; Gordon, T. R.; Diaz, R. E.; Stach, E. A.; Gorte, R. J.; Fornasiero, P.; Murray, C. B., Control of Metal Nanocrystal Size Reveals Metal-Support Interface Role for Ceria Catalysts. *Science* **2013,** *341* (6147), 771-773
2. Green, I. X.; Tang, W.; Neurock, M.; Yates, J. T., Spectroscopic Observation of Dual Catalytic Sites During Oxidation of CO on a Au/TiO_2 Catalyst. *Science* **2011,** *333* (6043), 736-739
3. Rodriguez, J. A.; Ma, S.; Liu, P.; Hrbek, J.; Evans, J.; Pérez, M., Water-gas shift Reaction on inverse CeOx/Au(111) and TiOx/Au(111) catalysts: Active role of oxide nanoparticles. *Science* **2007,** *318*, 1757-1760
4. Campbell, C. T., Catalyst-support interactions: Electronic perturbations. *Nat. Chem*. **2012,** *4* (8), 597-598
5. Johnston-Peck, A. C.; Senanayake, S. D.; Plata, J. J.; Kundu, S.; Xu, W.; Barrio, L.; Graciani, J.; Sanz, J. F.; Navarro, R. M.; Fierro, J. L. G.; Stach, E. A.; Rodriguez, J. A., Nature of the Mixed-Oxide Interface in Ceria–Titania Catalysts: Clusters, Chains, and Nanoparticles. *J. Phys. Chem. C* **2013,** *117* (28), 14463-14471.
6. Kim, H. Y.; Hybertsen, M. S.; Liu, P. Controlled Growth of Ceria Nanoarrays on Anatase Titania Powder: A Bottom-up Physical Picture. *Nano Lett.* **2017**, 17, 348-354.

This work was performed using facilities in the Center for Functional Nanomaterials, which is a U.S. DOE Office of Science User Facility, at Brookhaven National Laboratory under Contract No. DE-SC-00112704. This research used resources of the National Energy Research Scientific Computing Center, a DOE Office of Science User Facility supported by the Office of Science of the U.S. Department of Energy under Contract No. DE-AC02-05CH11231.

Acceptance ID: WQXE-O

Spontaneous hydrolysis of borohydride required before its catalytic activation by metal nanoparticles

*Sungmoon Choi, and Junhua Yu**

Department of Chemistry Education, Seoul National University, 1 Gwanak-Ro, Gwanak-Gu, Seoul 08826, South Korea
** To whom correspondence should be addressed. Email: junhua@edu.ac.kr*

Metal nanoparticles enable pseudohomogeneous catalytic reactions in solution while retaining excellent sustainability and activity. Borohydride and its derivatives are frequently used as a hydrogen source. Meanwhile, the reduction of 4-nitrophenol (4NP) by borohydride has been frequently used to examine the catalytic activity of metal nanoparticles. However, the mechanism of these reactions is not very clear yet. For example, such reactions are mostly accompanied by an induction time. The cause of the delay and the science beneath the delay is still under debate. In addition to screening of potential nanoparticles, researchers have put effort into studying the mechanism that promotes catalytic efficiency. When we screened the catalytic activity of metal nanoparticles, we found that the spontaneous hydrolysis of borohydride anions played a more important role in determining the catalytic reaction than the metal nanoparticles, in which neutral intermediates were formed. The intermediate was able to donate active hydride to nanoparticles instantly upon contact. Activated metal nanoparticles showed a hugely different catalytic tendency towards hydrogen generation and nitrophenol reduction. The existence of induction time implied that a certain part of reducing power was wasted before the reducing agent started to work.[1, 2] Our research indicated that minimizing the charge repulsion between the reactants in designing reducing agents and catalysts was an alternative to increase the reaction efficiency.

1. S. Choi, Y. Jeong and J. Yu, *Catalysis Communications*, 2016, **84**, 80-84.
2. S. Choi, Y. Jeong and J. Yu, *Rsc Advances*, 2016, **6**, 73805-73809.

Acceptance ID: X2R3-O

Synthesis and characterization of Ti-MCM-22, Ti-MCM-41 and Ti-SBA-15 and their activity in oxidation of α-pinene and ethyl oleate

Nguyen Thi Ha, Hanoi University of Science and Technology-1 Dai Co Viet str., Hanoi, Vietnam

Synthesizing microporous materials MCM-22 and mesoporous materials MCM-41 and SBA-15 substituted Ti in the framework. Characterizing obtained samples by many physical chemistry measurements. Investigating their activity of these catalysts on oxidation of α-pinene and ethyl oleate. Study of the effecting conditions on the reaction: nano size of materials, temperature reaction, time reaction...give high selectivity to high valued products such as epoxit, hydroxyls.

Acceptance ID: X3UK-P

Copper Oxide supported on Mesoporous Titania for Catalytic CO Oxidation

Abdallah F. Zedan and ***Siham Y. AlQaradawi***

Department of Chemistry and Earth Sciences, Qatar University, Doha 2713, Qatar
siham@qu.edu.qa

The heterogeneous catalytic oxidation of carbon monoxide to carbon dioxide is an important reaction for CO removal in many environmental and industrial applications such as in purification of hydrogen from CO traces in polymer electrolyte membrane fuel cell systems and removal of toxic CO from flue gas emissions. Precious metals such supported on reducible metal oxides have been known for their high catalytic activity for CO oxidation but they are expensive and their activity is subject to rapid deactivation particularly at high temperatures due to particles sintering. Therefore, there is a great need to develop non-expensive, active and durable catalysts for catalytic CO oxidation at low temperature. Herein, we fabricated a series of efficient CuO nanocatalysts supported on anatase TiO_2 nanotubes and studied their activity and stability toward the catalytic CO oxidation. In order to understand the effect of Cu content on the defects structure of the TiO_2 nanotubes support and on the catalytic activity, a series of CuO/TiO_2 nanotubes catalysts with different Cu loading from 2-65 wt.% were prepared and tested for CO oxidation. We demonstrated the influence of CuO modification in the increased formation of defects in the TiO_2 nanotubes matrix possibly due to the partial reduction of Ti^{4+} into Ti^{3+} in the TiO_2 support which could increase the catalytic activity for CO conversion due to synergy between active sites at Cu and TiO_2 entities. The best catalyst demonstrated CO conversion rate of 36 µmole s^{-1} g^{-1}, apparent activation energy of 81.98±1.64 kJ $mole^{-1}$and a stable performance for 60 h in continuous stream.

Acceptance ID: Y2R9-P

SYMPOSIUM 7: Low Dimensional, Nano and 2D Materials

Ion rectification and metal ion separation effect of graphene nanopore supported by PET membrane

Huijun Yao[1,], Zhan Li[2], Jian Zeng[1], Pengfei Zhai[1], Zongzhen Li[1,3], Jiande Liu[1], Dan Mo[1], Jinglai Duan[1], Youmei Sun[1], Jie Liu[1,*]*

Institute of Modern Physics, Chinese Academy of Sciences, Lanzhou 730000, China
Lanzhou Institute of Chemical Physics, Chinese Academy of Sciences, Lanzhou 730000, China
University of Chinese Academy of Sciences, Beijing 100049, China

Graphene has become an ideal candidate for the development of solid state nanopore due to its atomic thickness, high mechanical strength and strong chemical stability. A facile method was adopted to prepare single- and multi- graphene nanopore supported by PET membrane (G/PET nanopore) within three steps assisting with swift heavy ion irradiation and asymmetric etching technology.

The reversion of ion rectification effect was confirmed in G/PET nanopore while comparing with bare PET nanopore in KCl electrolyte solution. By modifying the wall charge state of PET conical nanopore with hydrochloric acid from negative to positive, the ion rectification effect of G/PET nanopore was extremely enhanced and the giant rectification ratio up to 190 was obtained. By comparing the “on” conductance and “off” conductance of G/PET nanopore while it was immersed in the solution of pH value lower than isoelectric point of etched PET (IEP, pH=3.8), the voltage dependent of “off” conductance was established and it was confirmed that the giant rectification effect was strongly related to the particularly low “off” conductance at higher applied voltage.

The permeation ratio of ions strongly depends on the temperature and H+ concentration in the driving solution. An electric field can increase the permeation ratio of ions through the graphene nanopores, but it inhibits the ion selective separation. Meanwhile, excellent metal separation effect was also confirmed and was attributed to the ion exchange between metal ions and protons on the two sides of graphene nanopores.

Acceptance ID: 2fMP-O

2D/3D heterostructure for Energy harvesting and optoelectronic devices

Shisheng Lin[1]

[1]*Colledge of Microelectronics, Colledge of Information Science and Electronic Engineering, Zhejiang University, Hangzhou 310027, China*

The electrons in graphene behave as Dirac Fermions and have a very high mobility. The linear electronic band structure of graphene and the low density of states near the Dirac points allow that the Fermi level of graphene is highly tunable. The junction formed by graphene and semiconductor is ultrashallow and near the graphene layers. Those merits make graphene/semiconductor heterostructure highly efficient for optoelectronic devices. We have realized plasmon enhanced graphene/GaN light emitting diodes through inserting Ag nanodots into the interface between graphene and GaN[1]. Through introducing the ideas of plasmon enhanced absorption, photo-induced doping and field effect, we have achieved a high efficient graphene/GaAs solar cell with a power conversion efficiency of 18.5%, which can be further improved to 25% according to the simulations[2,3]. As an important family member of 2D materials, MoS_2 based solar cell and photodetector should be optimized for practical implications. By designing the interface between MoS_2 and GaAs, we have achieved nearly 10% efficient solar cells and photodetectors with extremely high-detectivity[4,5]. Graphene is also a monolayer of honeycomb carbon, the interface between graphene and piezoelectronic material can largely influences the electronic properties of graphene. Through understanding the interaction between water, graphene and piezoelectronic substrate, we have achieved the electricity output through flowing DI water over graphene/piezoelectronic material heterestructure[6].

1, Z. Q. Wu, Y. H. Lu, W. L. Xu, Y. J. Zhang, J. F. Li, **S. S. Lin***, Surface plasmon enhanced graphene/p-GaN heterostructure light-emittingdiode by Ag nano-particles, Nano Energy 30, 362 (2016).

2, **S. S. Lin***, Z. Q. Wu, X. Q. Li, Y. J. Zhang, S. J. Zhang, P. Wang, R. Panneerselvam, J. F. Li*, *Stable 16.2% Efficient Surface Plasmon-Enhanced Graphene/GaAs Heterostructure Solar Cell*, Adv Energy Mater, 6, 1600822 (2016).

3, X. Q. Li, W. C. Chao, S. J. Zhang, Z. Q. Wu, P. Wang, Z. J. Xu, H. S. Chen, W. Y. Yin, H. K. Zhong, **S. S. Lin***, *18.5% efficient graphene/GaAs van der Waals heterostructure solar cell*, Nano Energy, 9, 310 (2015).

4, **S. S. Lin***, X. Q. Li, W. P, Z. J. Xu, S. J. Zhang, H. K. Zhong, Z. Q. Wu, W. L. Xu, H. S. Chen, *Interface designed MoS2/GaAs heterostructure solar cell with sandwich stacked hexagonal boron nitride*, Scientific Reports, 5, (2015).

5, Z. J. Xu, **S. S. Lin***, X. Q. Li, S. J. Zhang, Z. Q. Wu, W. L. Xu, Y. H. Lu, S. Xu, *Monolayer MoS2/GaAs heterostructure self-driven photodetector with extremely high detectivity*, Nano Energy, 23, 89, (2016).

6, H. K. Zhong, J. Xia, F. C. Wang, H. S. Chen, H. A. Wu, S. S. Lin*, *Graphene-Piezoelectric Material Heterostructure for Harvesting Energy from Water Flow*, Adv. Functional Mater. 27, 1604226 (2017)

Acceptance ID: 2GDT-O

Periodic Modulation of the Doping Level in Striped MoS_2 Superstructures

Xiebo Zhou[1,2], Zhongfan Liu[2], and Yanfeng Zhang[1,2]

[1]Department of Materials Science and Engineering, College of Engineering, Peking University, Beijing 100871, China
[2] Center for Nanochemistry, Peking University, Beijing 100871, China
E-Mail address (Yanfeng Zhang): yanfengzhang@pku.edu.cn

Although the recently discovered monolayer transition metal dichalcogenides (TMDCs) exhibit novel electronic and optical properties, fundamental physical issues such as the quasiparticle band-gap tunability and substrate effects remain undefined. Herein, we present the first report of a quasi-one-dimensional periodically striped superstructure for monolayer MoS_2 on Au(100). The formation of the unique striped superstructure is found to be mainly modulated by the symmetry difference between MoS_2 and Au(100) and their lattice mismatch. More intriguingly, we find that the monolayer MoS_2 is heavily n-doped on the Au(100) facet with a bandgap of 1.3 eV; the Fermi level is upshifted by ~0.10 eV on the ridges (~0.2 eV below the conduction band) in contrast to the valley regions (~0.3 eV below the conduction band) for the striped patterns. This tunable doping effect is considered to be mediated by the weak/strong coupling effects between MoS_2 and Au(100) with respect to the ridge/valley regions. Additionally, an obvious bandgap reduction is observed in the vicinity of the domain for monolayer MoS_2 on Au(100). This work should therefore inspire intensive explorations of adlayer-substrate interactions and their effects on band-structure engineering of monolayer MoS_2.

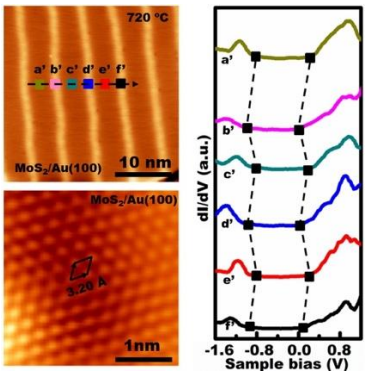

Fig. 1: The Scanning Tunnelling Microscopy/Spectroscopy of the MoS_2 on Au(001)

[1] Xiebo Zhou; Yanfeng Zhang*, *Acs Nano* **10**, 3461-3468 (2016).

Acceptance ID: 2upu-P

Injectable nanoprobes for multimodal imaging of breast cancers: rational design and pharmaceutical development

K. Hervé-Aubert[1], M. Pacaud[1,2], N. Aubrey[3], E. Allard-Vannier[1], A. Ignatova[4,5], I. Dimier-Poisson[3], A. Fahmi[2], A.V. Feofanov[4,5], and I. Chourpa[1]

[1]EA 6295 Nanomédicaments et Nanosondes, Université F. Rabelais de Tours, Tours, France.
[2]Faculty Technology and Bionics, Rhein-Waal University of Applied Sciences, Kleve, Germany.
[3]IPVBAI - UMR 1282 ISP INRA, Université F. Rabelais de Tours, Tours, France.
[4]Laboratory of optical microscopy and spectroscopy of biomolecules, Shemyakin and Ovchinnikov Institute of Bioorganic Chemistry, Russian Academy of Sciences, Moscow, Russia.
[5]Biological Faculty, Lomonosov Moscow State University, Moscow, Russia igor.chourpa@univ-tours.fr, *31 avenue Monge, 37200 Tours, France.*

Recent nanotechnology progress allows one to combine in the same nanosystem several physical properties useful for its use as agent (probe) for multimodal biomedical imaging. The multimodality is intended to improve the diagnosis specificity/efficacy. For instance, there are well-defined benefits of detecting cancer cells by complementary use of magnetic resonance imaging (MRI) and optical imaging in near infrared (NIROI). The NIR light (wavelength from 700 to 1100 nm) is less attenuated by biological tissues than visible light and induces almost no autofluorescence background. The high-resolution 3D MRI data may serve for pre-operative diagnosis without patient exposure to ionising radiation, while the *in situ* cancer cells identification by means of NIROI can be helpful for intra-operative guidance of surgeon. However, this type of applications requires development of injectable nanoprobes, being able not only to provide the dual MRI-NIROI response, but also to selectively accumulate in target cancer cells.

In the present talk, we will present our recent results on development of the injectable cancer-targeting MRI-NIROI nanoprobes based on inorganic core and organic shell. The inorganic cores are made of superparamagnetic iron oxide nanoparticles (SPION), coated or not with a plasmonic gold surface. The SPION are known to provide a negative contrast in MRI, while the plasmonic gold surface is able to enhance the optical response (fluorescence emission, Raman scattering) of organic dyes adsorbed on it[1]. Rational design of the nanoprobes includes engineering of the multifunctional nanocores and coating them with organic shell made of polymers, fluorophores and biological targeting ligands (folic acid[2], scFv antibody fragments[3]). We will also describe our pharmaceutical development strategy which implies a careful control of the nanoprobes quality and optimization of their biological behavior, namely cancer cells targeting, internalization, intracellular interaction/toxicity and multimodal imaging.

This work was partially supported by grants RFBR 16-54-76013, BMBF 01000812D and MENESR project N°321 MINERVA in the frames of European program ERA-NET RUS PLUS.

Keywords: SPION, plasmonic surface, scFv, MRI, optical imaging.

[1] A. CARROUÉE, E. ALLARD-VANNIER, S. MÊME, F. SZEREMETA, J.C. BELOEIL, I. CHOURPA. 2015. Sensitive Trimodal Magnetic Resonance Imaging-Surface-Enhanced Resonance Raman Scattering-Fluorescence Detection of Cancer Cells with Stable Magneto-Plasmonic Nanoprobes. *Anal Chem*, 87, 11233-11241.

[2] E. ALLARD-VANNIER, K. HERVÉ-AUBERT, K. KAAKI, T. BLONDY, A. SHEBANOVA, KV SHAITAN, A.A. IGNATOVA, M.L. SABOUNGI, A.V. FEOFANOV, I. CHOURPA. 2016. Folic acid-capped PEGylated magnetic nanoparticles enter cancer cells mostly via clathrin-dependent endocytosis. *Biochim Biophys Acta*. Dec 2. pii: S0304-4165(16)30485-8. doi: 10.1016/j.bbagen.2016.11.045. [Epub ahead of print]

[3] C. ALRIC, N. AUBREY, E. ALLARD-VANNIER, A. DI TOMMASO, T. BLONDY, I. DIMIER-POISSON, I. CHOURPA, K. HERVÉ-AUBERT. 2016. Covalent conjugation of cysteine-engineered scFv to PEGylated magnetic nanoprobes for immunotargeting of breast cancer cells. *RSCAdv* 6, 37099-37109.

Acceptance ID: 2WML-O

Calcium charge and release of glass ionomer cement containing nano-porous silica particles

Koichi Nakamura[1], *Shigeaki Abe*[2], *Yasutaka Yawaka*[1]

[1]*Department of Dentistry for Children and Disabled Persons, Graduate School of Dental Medicine, Hokkaido University. Kita 13 Nishi 7, Kita-ku, Sapporo 060-8586, Hokkaido, Japan.*
[2]*Department of Biomaterials and Bioengineering, Graduate School of Dental Medicine, Hokkaido University*
E Mail : pika@den.hokudai.ac.jp Corresponding author : Koichi Nakamura, Department of Dentistry for Children and Disabled Persons, Graduate School of Dental Medicine, Hokkaido University. Kita 13 Nishi 7, Kita-ku, Sapporo 060-8586, Hokkaido, Japan.

Nano-porous silica (NPS) has a nano-porous structure uniform in pore size about 1 nanometer and having a large specific surface area. Then NPS is expected as sustained drug release carrier, catalyst support and so on. We investigated whether NPS was effective as a dental material. Specifically, we prepared the NPS contained glass ionomer cement, which is a medical material used as matrix, (denoted as GIC-NPS), and their calcium charge and release behaviors were determined. NPS was synthesized in accordance with the protocol described by Tagaya[1]. The GIC-NPS specimens (1 mm in thickness and 10 mm in diameter) were immersed into the calcium chloride solutions of 5 wt% calcium concentration for 24 h at 37 ºC. After removal from the calcium solutions, they were rinsed with distilled water. Then the obtained specimens containing calcium were immersed into 5 mL of distilled water at 37°C for 7 days. Distilled water was changed every day; the water was analyzed to determine its calcium ion release. Calcium ion release was measured each day using inductively coupled plasma atomic emission spectroscopy (ICP-AES). To understand the distribution of calcium in the specimens, they were analyzed using an energy-dispersive X-ray spectroscope (SEM-EDS). As a result, GIC-NPS showed significantly much calcium ion release compared to control. SEM-EDS observation indicated that calcium was contained inside of the specimens and the distribution decreased from the surface to inside, suggesting calcium penetration and charge into GIC-NPS inside. These results show that GIC-NPS has the ability of calcium charge and release. It may become the materials helping remineralization of bone and tooth.

Keywords: Nano-porous silica, calcium charge and release, glass ionomer cement

[1] TAGAYA, M., IKOMA, T., YOSHIOKA, T., MOTOZUKA, S., XU, Z., MINAMI, F., TANAKA, J. 2011. Synthesis and luminescence properties of Eu (III)-doped nanoporous silica spheres. J. Colloid Interf. Sci. 363,456-464.

Acceptance ID: 39XL-P

A novel route towards consistent-chirality synthesis: *in-situ* entanglement of a monochromatic ultralong carbon nanotube

Zhenxing (Zhu)[1], *Nan (Wei)*[2], *Huanhuan (Xie)*[1], *Lianmao (Peng)*[2], *Fei (Wei)*[1*]

[1] *Beijing Key Laboratory of Green Chemical Reaction Engineering and Technology, Department of Chemical Engineering, Tsinghua University, Beijing 100084, China.*
[2] *Key Laboratory for the Physics & Chemistry of Nanodevices, Peking University, Beijing 100871, China.*
Presenting: zhenxing1013hg@163.com*; Corresponding:* wf-dce@tsinghua.edu.cn

Controllable synthesis of carbon nanotubes (CNTs) with consistent chirality and high areal density remains a challenge. Here, we report a novel route towards consistent-chirality synthesis of CNT aggregates by entangling an individual monochromatic ultralong CNT with an 'acoustic-induced vortices' [1] or 'magnetic-controlled flow' [2] method. Each as-synthesized high-density CNT tangle was made of one self-entangled CNT with the length over 100 mm, tandem with a $1\sim10\times10^4$ μm^2 area range controlled by a minimum consumed energy model. Rayleigh and Raman characterization demonstrated chiral-consistency of these CNT tangles with a consistent color and RBM mode, providing a feasible method of directly separating those with specific chirality according to their colors. Also, electron scattering offset between overlapped CNTs was calculated from a Raman mapping for a CNT tangle [2]. Transistors fabricated with one tangle had an on/off ratio up to $10^3\sim10^6$ at 4 mA on-state current, which is also the highest record so far among single-CNT-based transistors.

Keywords: ultralong carbon nanotubes, chirality, entanglement, CNTFETs

[1] ZHENXING, Z., NAN, W., HUANHUAN, X., RUFAN, Z., YUNXIANG, B., QI, W., CHENXI, Z., SHENG, W., LIANMAO, P., LIMING, D., FEI, W. 2016. Acoustic-assisted assembly of an individual monochromatic ultralong carbon nanotube for high on-current transistors. *Science Advances*, 2, e1601572.

[2] ZHENXING, Z., FEI, W. unpublished results.

Acceptance ID: 45TJ-O

Study of Co-Cu-Zr substitution Barium Hexaferrite nanoparticles on magnetic and microwave absorption properties

Hossein. Nikmanesh [1,2], Reza Shams Alam [2], Arash Dehzangi[3], Yiyun Zhang[3], Farhad Larki[1], Pouya Dianat[3], Mahmood Moradi [2], Gholam Hossein Bordbar [2], Razieh Moayedi [2], Parviz Kameli [1]*

[1] *Physics Department, Isfahan University of Technology, Isfahan 84156, Iran*
[2] *Physics Department, College of Sciences, Shiraz University, Shiraz 71946, Iran*
[3]*Center for Quantum Devices, Department of Electrical Engineering and Computer Science, Northwestern University, Evanston, Illinois, 60208, USA*
** Email corresponding author: (arash.dehzangi@northwestern.edu)*

Recently a demand for development of magnetic material has been remarkably increases owing to their application in new emerging technologies [1]. M-type barium hexaferrites (BaM) with magnetoplumbite structure is an imperative magnetic material with a wide range of usage in several applications due to their chemical stability low-cost and tunable electrical and magnetic properties, e.g. magnetic recording media, telecommunications and microwave devices [1]. Up to now, many studies have been carried on ferrites to investigate dopant variation impact on magnetic and microwave characteristics of in order to find new application for them in new technologies.

In this research study, multi dopant barium hexaferrites nanoparticles with nominal composition of $BaCo_xCu_xZr_{2x}Fe_{12-4x}O_{19}$ (x= 0.0, 0.1, 0.2, 0.3, 0.4, and 0.5) was prepared using sol-gel auto-combustion method. Then, the magnetic and microwave properties of nanoparticles were studied in detail. These characteristics were investigated using various techniques including X-ray diffraction (XRD) by the FULLPROF program, Fourier transform infrared spectroscopy (FTIR), transmission electron microscopy (TEM), vibrating sample magnetometer (VSM) and vector network analyzer (VNA). The XRD, along with FTIR evaluations confirmed successful substitution of Co, Cu and Zr cations in the barium hexaferrite lattice. The VSM analysis proved that by increasing cobalt, copper and zirconium substitutions, the saturation magnetization, coercivity and remanence values are decreased. With an increase in concentration of Co-Cu-Zr ions, a monotonic reduction in coercivity, ranging from 3350 Oe to 420 Oe was also observed. The causes for the changes in magnetic and microwave absorption properties by adding the impurities were also investigated. It was found that the bandwidth and RL of the samples is changed with increasing the concentration of dopants, and the samples with higher concentration showed an effective microwave absorption performance, and as a result, they could be counted as a single layer attenuator materials candidate for microwaves applications. Likewise, the samples with lower concentration of dopants could be used in magnetic recording media.

Keywords : Substituted Barium hexaferrite; Magnetic properties; Microwave absorption.

[1] Pullar, Robert C. "Hexagonal ferrites: a review of the synthesis, properties and applications of hexaferrite ceramics." *Progress in Materials Science* 57.7 (2012): 1191-1334.

[2] Nikmanesh, Hossein, et al. "Positron annihilation lifetime, cation distribution and magnetic features of Ni 1− x Zn x Fe 2− x Co x O 4 ferrite nanoparticles." *RSC Advances* 7.36 (2017): 22320-22328.

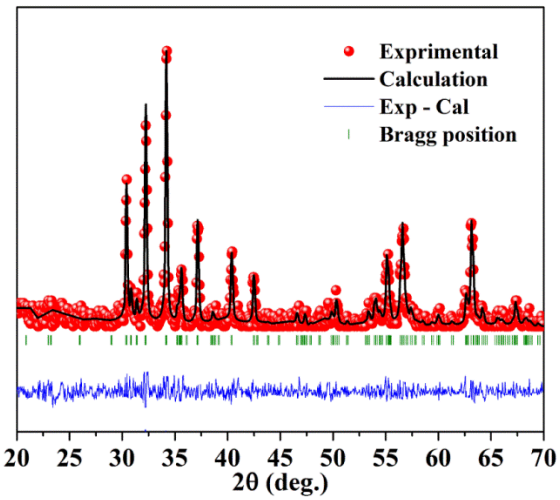

Fig. 1. Typical Rietveld refinements of XRD data (x=0).

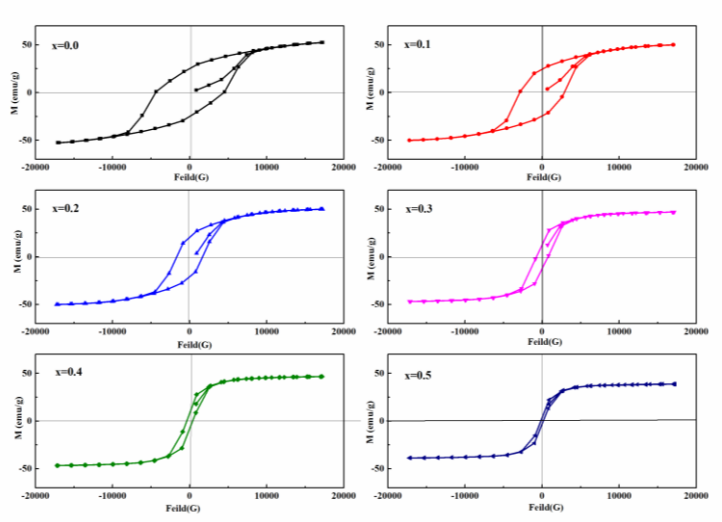

Fig. 2. The VSM curves of $BaCo_xCu_xZr_{2x}Fe_{12-4x}O_{19}$ at various amount of substitution (x).

Acceptance ID: 4CVE-O

Structure and Properties of fluorescent carbon nanoparticles

*S. Khan, N. C. Verma, A. Sharma, S. Jain, C. Rao, C. K. Nandi**
School of Basic Sciences, Indian Institute of Technology, Mandi, India
Syamantak.iitkgp@gmail.com, chayan@iitmandi.ac.in

Fluorescent Carbon nanoparticles, also known as carbon dots, are a new member of the carbon family. These nanoparticles have been proved useful in diverse applications including bio-imaging, drug-delivery, molecular sensing, optoelectronics and photovoltaics. Especially, it has been extensively used as an imaging probe in live cells due to their non-toxic nature. The mechanism of bright photoluminescence is yet not understood clearly due to unavailability of the structural detail. Their excitation dependent emission, which gives rise to multicolor emission, is also remained elusive till date. These are the major challenge for advancement in the field of carbon dots towards their industrial scale applications. We have used time-resolved spectroscopy to discover that the photoluminescence of carbon dots is in-homogeneously broadened. We found spectral migration of fluorescence spectra at nano-second time scale. This excited state dynamics was found to be controlled by excited state protonation process coupled with solvent relaxation. This slow energy relaxation, gives rise to spectral migration of the time resolved emission spectra in nanosecond time scale and excitation dependent fluorescence emission in steady state fluorescence, apparently violating the kasha's rule. We prove that photoluminescence in carbon nanodot originates directly from oxygenated functional groups, which are solvent accessible, and therefore, invariably sensitive to the environment. Due to this, fluorescence of carbon dots can be easily controlled by tuning the pH and the polarity of the solvent. We also solved the structure of carbon nanoparticles, derived from citric acid, using X-ray crystallography of single fluorescent crystals, coupled with Nuclear Magnetic Resonance Spectroscopy (NMR). We discover that the crystalline cores of the nanoparticles are periodic arrangement of small molecular units containing carbonyl groups. Finally we achieved reversible photo-switching of single fluorescent carbon dots using single molecule technique. The single molecule fluorescent fluctuations were tuned with electron transfer reaction by creating a cationic dark state. With a controlled ON-OFF rate of fluorescence blinking, these carbon nanoparticles emerge as a potential probe for localization based super-resolution imaging. We are working on specific labeling of these nanoparticles to particular cellular structures for their full-scale application as a cheap, bright, and non-toxic imaging probe is near future. We are also working on the application of carbon dots in small molecule sensing, in light emitting devices and in solar energy conversion.

Keywords: carbon dot, time resolved fluorescence, cell labeling, single molecule imaging

[1] KHAN, S., GUPTA, A., VERMA, N. C. & NANDI, C. K. 2015. Time-Resolved Emission Reveals Ensemble of Emissive States as the Origin of Multicolor Fluorescence in Carbon Dots. *Nano Lett.*, 15, 8300-8305.

[2] KHAN, S., VERMA, N. C., GUPTA, A. & NANDI, C. K. 2015. Reversible Photoswitching of Carbon Dots. *Sci. Rep.*, 5, 11423.

[3] VERMA, N. C., KHAN, S. & NANDI, C. K. Single-molecule analysis of fluorescent carbon dots towards localization-based super-resolution microscopy. *Methods Appl Fluoresc.* 4, 044006.

[4] GUPTA, A., CHAUDHARY, A., MEHTA, P., DWIVEDI, C., KHAN, S., VERMA, & NANDI, C. K. Nitrogen-doped, thiol-functionalized carbon dots for ultrasensitive Hg(II) detection. *Chem. Commun.* 51, 10750-10753 .

[5] KHAN, S., JAIN, S., GUPTA, P., GHOSH, S. & NANDI, C. K. Direct Evidence of Excited State Dynamics in Carbon Nanodots: Origin of Complex Photoluminescence (Under Review)

[6] KHAN, S., SHARMA, A., VERMA, N. C., HAZRA, M. & NANDI, C. K. Crystal structure of fluorescent carbon dots derived from citric acid (Under Review)

Acceptance ID: 4EYZ-P

Tuning of gold nanoclusters emission peak with bovine serum albumin and bromelain for the trace level detection of Hg^{2+} ion

Jigna R. Bhamore[1] *and K. Suresh Kumar*[1*]

[1]*Applied Chemistry Department, S. V. National Institute of Technology, Surat-395007, Gujarat, India*

A facile and green synthetic approach for gold nanoclusters (Au NCs) was carried using bovine serum albumin (BSA) and bromelain and characterized by UV-visible, fluorescence spectrophotometer, FT-IR and HR-TEM. As synthesized BSA-bromelain–Au NCs illustrate orange-red emission under UV light at 365 nm and exhibit emission peak at 633 nm when excited at 490 nm. The emission peak of Au NCs was selectively and sensitively quenched by Hg^{2+} ion at 633 nm. The quenching mechanism is based on the interaction between Hg^{2+}-Au^{+} interaction[1]. The linear spectra was carried in the range of $1x10^{-5}$ - 100 µM (Fig. 1.) and the calibration graph was carried in the range of $1x10^{-5}$ -5 µM (R^2= 0.9903) with the detection limit of 0.66 $x10^{-5}$ µM.

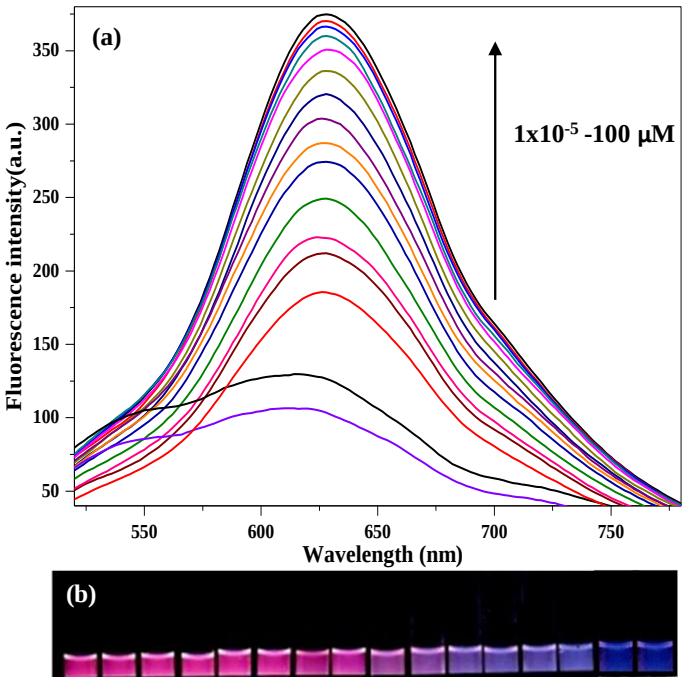

Fig. 1. (a) Fluorescence emission spectra of BSA-bromeain-Au NCs with different concentration of Hg^{2+} ion in the range of $1x10^{-5}$ -10 µM. (b) image of BSA-bromeain-Au NCs with different concentration of Hg^{2+} ion in the range of $1x10^{-5}$-10 µM.

Reference

1. J. Xie, Y. Zheng and Jackie Y. Ying, *Chem. Commun*., **2010**, 46, 961–963

Acceptance ID: 4HKA-O

Advanced Functional Materials and Devices via Plasmonic Coupling

Dong Ha Kim

Department of Chemistry and Nano Science, Ewha Womans University,
52, Ewhayeodae-gil, Seodaemun-gu, Seoul 03760, Korea
E-mail: dhkim@ewha.ac.kr

Plasmonics have been recognized as a promising platform that may premise the performance enhancement of diverse advanced functional materials and devices. Representative examples include the exploitation of plasmonic nanostructures for photovoltaic devices, photodectors, photocatalysis and optical biosensors. It is noted that a universal paradigm to construct high-efficiency plasmonic solar cells with long term stability has not been established. In this presentation, we propose a few strategies to develop viable plasmonic dye-sensitized solar cells and organic photovoltaic devices based on the integration of metal-graphene oxide core-shell nanostructures or lithographically-induced plasmonic nanopatterns. The development of highly sensitive and selective photodectors has been an interesting issue yet to be resolved. We introduce a simple protocol for the fabrication of wavelength-selective polymer and perovskite photodiodes with enhanced detectivity/responsivity based on plasmonic effects. Surface plasmons has also been exploited to develop visible light active photocatalysis for environmental remediation and solar fuel generation via water splitting. We propose a few model photocatalytic systems via plasmonic coupling. Surface plasmon based optical biosensors constitute a well-established model that efficiently realized the activity of plasmonics for viable optoelectronics. We discuss plasmonic-coupling based concepts to develop optical biosensors with enhanced sensitivity.

References

[1] Yoon Hee Jang, Yu Jin Jang, Seokhyoung Kim, Li Na Quan, Kyungwha Chung, Dong Ha Kim,* "Plasmonic Solar Cells: From Rational Design to Mechanism Overview", *Chem. Rev*., in press.

[2] Saji Thomas Kochuveedu, Yoon Hee Jang, Dong Ha Kim,* "A Study on the Mechanism for the Interaction of Light with Noble Metal-Metal Oxide Semiconductor Nanostructures for Various Photophysical Applications", *Chem. Soc. Rev.* **2013**, *42*(21), 8467 – 8493.

[3] Yulin Oh, Ju Won Lim, Byung-Hyun Kang, Young Wook Park, Heejun Kim, Yu Jin Jang, Jihyeon Kim, Dong Ha Kim,* Byeong-Kwon Ju,* "Plasmonic Periodic Nanodot Arrays via Laser Interference Lithography for Organic Photovoltaic Cells with >10% Efficiency", *ACS Na*no, DOI: 10.1021/acsnano.6b05313.

[4] Ji-Eun Lee, Jumi Lee, Kyungwha Chung, Kwanwoo Shin,* Dong Ha Kim,* "In-situ Studies of Surface Plasmon Resonance Coupling Sensor Mediated by Stimuli-sensitive Polymer Linker", *Adv. Funct. Mater*. **2015**, *25*(18), 6716 – 6724.

[5] Jung Eun Kim, Ji Hye Choi, Marion Colas, Dong Ha Kim,* Hyukjin Lee,* "Gold-based Hybrid Nanomaterials for Biosensing and Molecular Diagnostic Applications", *Biosens. Bioelectron*. **2016**, *80*, 543 – 559.

Acceptance ID: 4RZM-O

Decolorization of Textile Dye C.I. Yellow 28 in Water using Environmentally Friendly Bi2-x(Lu, Er)xO3 Photo-nanocatalyst

Abbas Amini

Australian College of Kuwait, Western Sydney University
abbasust@gmail.com

$Bi_{2-x}(Lu, Er)_xO_3$ nanoparticle is proposed as a photocatalyst to decolorize C.I. Basic Yellow 28 (BY28) dye solution from water under visible light irradiation. To achieve a high removal efficiency, the operational parameters, including the amount of Er_2O_3 (Er) and Lu_2O_3 (Lu) dopants, photocatalyst dose, and initial dye concentration are examined. By applying un-doped Bi_2O_3 and 0.1% Lu^{3+}, Er^{3+} co-doped Bi_2O_3, the decolorization efficiency increases from 48.52% to 95.62% after 180 minutes of irradiation, while by using 0.5% Lu^{3+}, Er^{3+} co-doped Bi_2O_3, it decreases from 95.62% to 56.52%. After 180 minutes, the photocatalytic activity improves at the higher dose of Lu^{3+}, Er^{3+} with the following order 0.1% mol>0.5% mol>un-doped Bi_2O_3. Increasing the amount of Lu^{3+} and Er^{3+} up to a specific optimum value of 0.1% mole in the structure of photocatalyst results in an exceeding large space charge layer, through allowing visible light penetration into Bi_2O_3 nanoparticle environment. This makes the recombination of electron-hole pairs easier, and lowers the photocatalytic decolorization efficiency. The best decolorization efficiency of 100% is obtained in 5 mg/l BY28 with 1 g/l photocatalyst concentration after 180 minutes. Moreover, the effect of initial BY28 concentration (5, 10, 15, 20, 35 mg/l) on decolorization efficiency is investigated in the presence of

1 g/l of 0.1% Lu^{3+}, Er^{3+} co-doped Bi_2O_3 nanoparticles. The increase in the initial dye concentration reduces the decolorization efficiency from100% (5 mg/l) to 91.43% (35 mg/l). The highest decolorization efficiency is obtained at 1 g/l photocatalyst concentration (97.62%).

Acceptance ID: 5CS4-O

Novel Methods for Designing 2D (MXene) Particulates

S. Gupta, M. Fuka, F. Al-Anazi, and M. Dey,

Department of Mechanical Engineering
University of North Dakota, ND 58201
Corresponding author: surojit.gupta@engr.und.edu

Recently, it was shown that it is possible to separate each layer of MAX Phases ($M_{n+1}AX_n$ (MAX) phases (over 60+ phases) are thermodynamically stable nanolaminates displaying unusual, and sometimes unique, properties where n is 1, 2, or 3, M is an early transition metal element, A is an A-group element and X is C or N with layered hexagonal (space group D^4_{6h}–$P6_3/mmc$) structure with two formula units per cell) and form 2D solids, MXenes. Different investigators have shown that it is possible to fabricate different types of complex chemistries like Ti_2C, TiNbC Ti_3CN_x Ta_4C_3 Ti_3C_2, Ta_4C_3, TiNbC, $(V_{0.5},Cr_{0.5})_3C_2$, Mo_2TiC_2, $Mo_2Ti_2C_3$, Cr_2TiC_2 and Ti_3CN_x. Recent studies have demonstrated that 2D solids have showed promising properties, for example, clay like properties, intercalation by Li, urea, hydrazine, methyl formamide, dimethyl sulphoxide, among others. These novel 2D solids can be potentially used for different cutting edge applications in different demanding areas like energy storage, electromagnetic interference shielding, reinforcement for composites, water purification, gas- and biosensors, lubrication, and photo-, electro- and chemical catalysis. In this presentation, we will demonstrate some of the recent to further engineer the 2D MXenes, and develop different structures from these solids.

Acceptance ID: 5V4Z-O

The biocompatibility of new developed TiO_2-based photocatalytic nanoparticles on human skin and lung fibroblasts

Anca Dinischiotu, Ionela Cristina Nica, Miruna Stan, Iuliana Dumitrescu, Lucian Diamandescu

TiO_2-based photocatalysis is used in several environmental applications including self-cleaning surfaces, air and water purification systems as well as sterilization. However, obtaining biocompatible photocatalysts is still a key problem, and the mechanism of their toxicity received recently an increased attention. Two types of TiO_2 nanoparticles co-doped with 1% atoms of iron and nitrogen (TiO_2-1% Fe-N) obtained under hydrothermal conditions at two different pH values of 8.5 (HT1) and 5.5 (HT2), and their cytotoxic effects exerted on human pulmonary and dermal fibroblasts were assessed. Our results demonstrated the biocompatibility of TiO_2-1 % Fe-N nanoparticles at low doses on lung and dermal cells, which may initiate oxidative stress through dose accumulation. Although no significant changes were observed between the two tested photocatalysts, the biological response was cell type specific and time- and dose-dependent. The viability of both cell types was not affected by the exposure to the two types of TiO_2 nanoparticles, even if an oxidative stress occurred. This was counteracted by the increased activity of antioxidant enzymes. GSH levels were not significantly changed, suggesting that photocatalysts were well tolerated. However, the lung cells proved to be more sensitive to nanoparticles' exposure. Taken together, these experimental data provide useful information for future photocatalytic applications in the industrial, food, pharmaceutical and medical fields.

Acceptance ID: 6GN6-P

Aligned Growth and Controlled In-Plane Heterojunction Formation of WSe_2

*Bilu Liu, Yuqiang Ma, Liang Chen, Anyi Zhang, Mingyuan Ge, Ahmad N. Abbas, Yihang Liu, Chenfei Shen, Haochuan Wan, and Chongwu Zhou**

Ming Hsieh Department of Electrical Engineering, University of Southern California, Los Angeles, California 90089, United States

Monolayer WSe_2 is a two-dimensional (2D) semiconductor with a direct band gap, and it has been recently explored as a promising material for electronics and optoelectronics. Aligned growth and low field-effect mobility are two of the main constraints preventing WSe_2 from becoming one of the competing channel materials for field-effect transistors (FETs). Here we report a step-edge-guided nucleation and growth approach for the aligned growth of 2D WSe_2 by a chemical vapor deposition method using C-plane sapphire as substrates. We found that at temperatures above 950 ºC the growth is strongly guided by the atomic steps on the sapphire surface, which leads to the aligned growth of WSe_2 along the step edges on the sapphire substrate. In addition, we also found that controlled heating in air significantly improves device performance of WSe_2 FETs in terms of on-state currents and field-effect mobilities. The underlying chemical processes involved during air heating and the formation of in-plane heterojunctions of WSe_2 and WO_{3-x}, which is believed to be the reason for the improved FET performance. Our works introduced an efficient way to achieve the oriented growth and controlled modification of the 2D WSe_2 and potentially other 2D materials.

Acceptance ID: 6HSY-P

Direct observation of the band gap transition in atomically thin ReS_2

L. Plucinski, FZ Jülich PGI-6

ReS_2 is considered as a promising candidate for novel electronic and sensor applications. The low crystal symmetry of the van der Waals compound ReS_2 leads to a highly anisotropic optical, vibrational, and transport behavior. However, the details of the electronic band structure of this fascinating material are still largely unexplored. We present a momentum-resolved study of the electronic structure of monolayer, bilayer, and bulk ReS_2 using k-space photoemission microscopy in combination with first-principles calculations. We demonstrate that the valence electrons in bulk ReS_2 are - contrary to assumptions in recent literature - significantly delocalized across the van der Waals gap. Furthermore, we directly observe the evolution of the valence band dispersion as a function of the number of layers, revealing a significantly increased effective electron mass in single-layer crystals. We also find that only bilayer ReS_2 has a direct band gap. Figure presents the experimental angle-resolved photoemission (ARPES) band dispersions of a monolayer and bilayer ReS_2 which shows the valence band maximum at $\bar{\Gamma}$ only in the case of a bilayer film. Our results establish bilayer ReS_2 as an advantageous building block for two-dimensional devices and van der Waals heterostructures. Further details of this work can be found in Ref. [1].

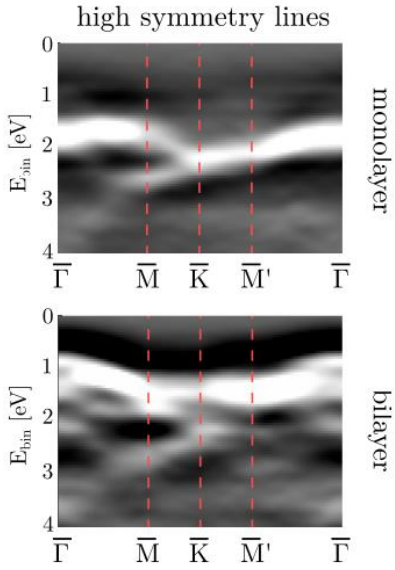

Figure: Experimental band dispersions of monolayer and bilayer ReS_2 showing the renormalization of the bands near the Brillouin zone center.

[1] M. Gehlmann, I. Aguilera, G. Bihlmayer, S. Nemšák, P. Nagler, P. Gospodarič, G. Zamborlini, M. Eschbach, V. Feyer, F. Kronast, E. Młyńczak, T. Korn, L. Plucinski, Ch. Schüller, S. Blügel, and C. M. Schneider, Direct observation of the band gap transition in atomically thin ReS2, arXiv:1702.04176 (2017).

Acceptance ID: 72KQ-O

Nanoparticle decorated Graphene and other 2D metals for air quality control gas sensors

M. Rodner[1], *R. Yakimova*[1,2], *A. Lloyd Spetz*[1], *J. Eriksson*[1]

[1]*Department of Physics, Chemistry and Biology, Linköping University, SE-58183, Sweden.*
[2]*Graphensic AB, SE-58333 Linköping, Sweden.*
E-Mail: marius.rodner@liu.se

Two-dimensional materials, such as graphene, offer a unique platform for sensing where extremely high sensitivity [1] is a priority, since even minimal chemical interactions can cause noticeable changes in electrical conductivity. Using the unique properties of graphene as a transducer and its high sensitivity, these sensor devices can be used for gas detection where even low concentrations of chemicals are necessary to be detected including air quality control for human health. Besides a high sensitivity, also a good selectivity has to be addressed to get a useful sensor device. It was already shown that decoration of the graphene surface with metal/oxide nanoparticles can lead to a higher selectivity towards certain gases e.g. nitrogen dioxide [2], benzene and formaldehyde [3]. Using a "soft" decoration approach, the surface chemistry of the sensing layer could be modified without changing the transducers electronic properties [2].

We have previously found that monolayer graphene is crucial for optimum gas sensitivity [4]. To that end, we have shown that the graphene thickness uniformity can be significantly tuned by careful control of the EG/SiC morphology [5], in turn leading to high reproducibility of sensors [3]. With the reproducibility of high quality epitaxial graphene on silicon carbide (SiC) [6] and a very precise technique for a controlled surface decoration [7], a new route for high quality graphene-nanoparticle hybrid sensors was found. Trying different metal/oxide nanoparticles for the decoration, the selectivity can be tuned towards optimization for certain applications. Furthermore, a smart operation mode like temperature-cycled operation (TCO) [8] can also be used to further enhance sensitivity, selectivity and sensor response times, since the working temperature modifies the amount of chemical reactions taking place on the sensor surface.

A field effect transistor (FET) offers some benefits towards standard resistance graphene sensors but is also a more challenging setup due to its complex structure. It was already shown that by using a suspended gate FET, the sensor response could be optimized not only by controlling the working temperature and the electric field, but also by modulating the gate bias (GBCO).

The technology of epitaxial growth of graphene on SiC [6] offers a possibility to develop novel 2D systems beyond graphene. It has been found that specially reconstructed SiC surfaces offer a unique possibility to arrange catalytic metallic materials (e.g. Pt, Pd) on the surface to form macroscopic, electrically continuous 2D metals. Early stage gas sensor tests using 2D Pt on SiC shows promise in terms of stronger interaction with certain gases and higher temperature stability compared to graphene, while maintaining the extreme sensitivity inherent to 2D materials.

Keywords: graphene, 2D-metal, nanoparticle, gas sensor, benzene

[1] SCHEDIN, F., GEIM, A. K., MOROZOV, S. V., HILL, E. W., BLAKE, P., KATSNELSON, M. I., NOVOSELOV, K. S. 2007. Detection of individual gas molecules adsorbed on graphene. *Nature Materials*, 6, 652-655.

[2] ERIKSSON, J., PUGLISI, D., KANG, Y. H., YAKIMOVA, R., LLOYD SPETZ, A. 2014. Adjusting the electronic properties and gas reactivity of epitaxial graphene by thin surface metallization. *Physica B*, 439, 105-108.

[3] ERIKSSON, J., PUGLISI, D., STRANDQVIST, C., GUNNARSSON, R., EKEROTH, S., IVANOV, I. G., HELMERSSON, U., UVDAL, K., YAKIMOVA, R., LLOYD SPETZ, A. 2015. Modified Epitaxial Graphene on SiC for Extremely Sensitive and Selective Gas Sensors. *Materials Science Forum*, 858, 1145-1148.

[4] PEARCE, R., ERIKSSON, J., IAKIMOV, T., HULTMAN, L., LLOYD SPETZ, A., YAKIMOVA, R. 2013. On the Differing Sensitivity to Chemical Gating of Single and Double Layer Epitaxial Graphene Explored Using Scanning Kelvin Probe Microscopy. *ACS Nano* 7 (5), 4647–4656.

[5] ERIKSSON, J., PEARCE, R., IAKIMOV, T., VIROJANADARA, C., GOGOVA, D., ANDERSSON, M., SYVÄJÄRVI, M., LLOYD SPETZ, A., YAKIMOVA, R. 2012. The influence of substrate morphology on thickness uniformity and unintentional doping of epitaxial graphene on SiC. *Applied Physic Letters*, 100, 241607.

[6] VIROJANADARA, C., SYVÄJÄRVI, M., YAKIMOVA, R., JOHANSSON, L. I., ZAKHAROV, A. A., BALASUBRAMANIAN, T. 2008. Homogeneous large-area graphene layer growth on 6 H -SiC(0001). *Physical Review B*, 78, 245403.

[7] GUNNARSSON, R., PILCH, I., BOYD, R. D., BRENNING, N., HELMERSSON, U. 2016. The influence of pressure and gas flow on size and morphology of titanium oxide nanoparticles synthesized by hollow cathode sputtering. *Journal of Applied Physics*, 120, 044308.

[8] BUR, C., BASTUCK, M., PUGLISI, D., SCHUETZE, A., LLOYD SPETZ, A., ANDERSSON, M. 2015. Discrimination and quantification of volatile organic compounds in the ppb-range with gas sensitive SiC-FETs using multivariate statistics. *Sensors and Actuators B: Chemical*, 214, 225-233.

Acceptance ID: 75ZC-O

A synaptic transistor based on two-dimensional molybdenum oxide

Dashan Shang, Chuansen Yang, Nan Liu, Xi Shen, Gang Shi, Richeng Yu, Yongqing Li, Young Sun*

Beijing National Laboratory for Condensed Matter Physics, Institute of Physics, Chinese Academy of Sciences, Beijing 100190, P. R. China
**E-mail of the Corresponding Author: shangdashan@iphy.ac.cn*

The biological synapses are functional links between neurons, through which 'information' transmitted in the neuron network. The information can be stored and processed simultaneously in the same synapse through tuning synaptic weight, which is defined as the strength of the correlation between two neighboring neurons, and the operation is collective and adaptive. Although silicon-based complementary metal-oxide-semiconductor circuits have been developed to emulate synaptic behaviors, it is still facing significant challenges in large-scale integrations and huge energy consumption. Memristive devices, in which the conductance can be retained according to the history of applied voltage and current, provide a more promising way to emulate synapses by substantial reduction in complexity and energy consumption. Recently, ionic/electronic hybrid three-terminal memristive devices have been introduced. It gives a more flexible operation for the signal processing and learning in synaptic circuits. In this work, we investigated a lateral three terminal memristive device based on α-phase molybdenum oxide (α-MoO_3), a typical two-dimensional (2*D*) transition metal oxides, in ambient atmosphere, and capitalized on the nanoscale device to mimic a biological synapse. Ionic liquid was selected as gate terminal, serving as pre-synaptic neuron to generate neurotransmitters. The ultrathin α-MoO_3 single crystal flake serves as post-synaptic neuron, whose conductance can be modulated. The excitatory post-synaptic current, depression and potentiation of synaptic weight, paired-pulse facilitation, the transition of short-term plasticity to long-term potentiation have been demonstrated in the three terminal devices. These results provide an insight into the potential application of two-dimentional α-MoO_3 for synaptic devices with high scaling ability, low energy consumption, and high processing efficiency.

References

[1]C. S. Yang, D. S. Shang, *et al*., Moisture effects on the electrochemical reaction and resistance switching at Ag/molybdenum oxide interfaces. Phys. Chem. Chem. Phys. 18 (2016) 12466-12475
[2]C. S. Yang, D. S. Shang, *et al*., Electrochemical-reaction-induced synaptic plasticity in MoOx-based solid state electrochemical cells. Phys. Chem. Chem. Phys. (2016) DOI: 10.1039/c6cp06004h
[3]J. Shi, *et al*., A correlated nickelate synaptic transistor. Nat. Commun. 4 (2013) 2676.
[4]L. Q. Zhu, *et al*., Artificial synapse network on inorganic proton conductor for neuromorphic systems. Nat. Commun. 5 (2014) 3158.

Acceptance ID: 7NMS-P

Silicon-Quantum-Dot Materials and Optoelectronic Devices

Xiaodong Pi[*], *Zhenyi Ni, Wei Gu, Xiangkai Liu, Shuangyi Zhao, Deren Yang*

State Key Laboratory of Silicon Materials and School of Materials Science and Engineering, Zhejiang University, Hangzhou 310027, Zhejiang, China
E-Mail : xdpi@zju.edu.cn

Given the abundance and nontoxicity of Si and their compatibility with conventional Si technologies, silicon (Si) quantum dots (QDs) hold great promise to improve existing Si-based technologies and advance the use of Si toward new fields such as wearable and biointegrable electronics. The remarkable electronic and optical properties of Si QDs are intimately related to their tunable size in the nanometer-sized regime. We have recently shown that surface states[1] and impurities[2-7] also matter for Si QDs. The optimum light emission efficiency of Si QDs exists as the QD size varies, resulting from the interplay between the quantum confinement effect and surface effect[1]. We demonstrate that localized surface plasmon resonance (LSPR) occurs to both P- and B-doped Si QDs[2-5]. The LSPR frequency increases with the increase of the dopant concentration and the decrease of the QD size, highlighting the remarkable tunability of LSPR in doped QDs. Regarding the optoelectronic applications of Si QDs, we have made progress on the use of Si QDs in the structures of solar cells[8], light-emitting diodes[9] and photodetectors[10].

Keywords: Silicon quantum dots, doping, light-emitting diodes, photodetectors, solar cells

[1] X. K. Liu, Y. H. Zhang, T. Yu, X. S. Qiao, R. Gresback, X. D. Pi and D. Yang, *Part. Part. Syst. Charact.* 33, 44, **2016**.
[2] X. D. Pi and C. Delerue, *Phys. Rev. Lett.* 111, 177402, **2013**.
[3] S. Zhou, X. D. Pi, Z. Y. Ni, Y. Ding, Y. Y. Jiang, C. H. Jin, C. Delerue, D. Yang and T. Nozaki, *ACS Nano* 9, 378, **2015**.
[4] Z. Y. Ni, X. D. Pi, S. Zhou, T. Nozaki, B. Grandidier and D. Yang, *Adv. Opt. Mater.* 4, 700-707, **2016**.
[5] S. Zhou, Z. Y. Ni, Y. Ding, M. Sugaya, X. D. Pi and T. Nozaki, *ACS Photonics* 3, 415, **2016**.
[6] Z. Y. Ni, X. D. Pi and D. Yang, *Phys. Rev. B* 89, 035312, **2014**.
[7] Z. Y. Ni, X. D. Pi, S. Cottenier and D. Yang, *Phys. Rev. B*, in press, **2017**.
[8] S. Y. Zhao, X. D. Pi, C. Mercier, Z. C. Yuan, B. Q. Sun, D. Yang, *Nano Energy* 26, 305-312, **2016**.
[9] W. Gu, X. K. Liu, X. D. Pi, X. L. Dai, S. Y. Zhao, L. Yao, D. S. Li, Y. Z. Jin, M. S. Xu, D. Yang, and G. G. Qin, *IEEE Photonics J*., in press, **2017**.
[10] T. Yu, F. Wang, Y. Xu, L. L. Ma, X. D. Pi and D. Yang, *Adv. Mater.* 28, 4912-4919, **2016**.

Acceptance ID: 7P98-O

Porous Silicon for Tumor Imaging and Drug Delivery: Peptide-Functionalization and *In Vitro* Studies

J. S. Kanathasan[1], U. D. Palanisamy[2], A. K. Radhakrishnan[3], ***V. Swamy[1]****

[1]School of Engineering, Monash University Malaysia, Bandar Sunway, Selangor, 46150, Malaysia.
[2]Jeffrey Cheah School of Medicine and Health Sciences, Monash University Malaysia, Bandar Sunway, Selangor, 46150, Malaysia.
[3]International Medical University, Bukit Jalil, 57000 Kuala Lumpur, Malaysia.

Intrinsically fluorescent porous silicon (pSi) is being extensively investigated as a functional biomaterial that is noncytotoxic, biodegradable, and biocompatible for cancer theranostics, biolabeling, and drug delivery [1,2]. In addition to biocompatibility, desirable optoelectronic properties (efficient photoluminescence, long light emission wavelength, and large Stokes shifts that can overcome photobleaching under fluorescence imaging) allow pSi to be used for deep tissue imaging. Various surface functionalizations of pSi have been shown to allow its use as an agent for imaging tumor cells and for targeted drug delivery to the affected cells [2,3]. We have recently reported on the surface functionalization, size optimization, and fluorescence response characterizations of conjugated pSi by using Y-shaped and single-chain legumain targeting peptides [4]. Legumain is an intracellular lyosomal cysteine protease expressed both in normal healthy cells as well as in the tumor microenvironments and tumor cell surfaces of breast, colon, and prostate cancers, suggesting its potential as a biomarker for cancer targeting. Here we report our results on the stability studies of the functionalized (peptide-conjugated) pSi under physiological conditions (temperature: 20-50 °C; pH: 6-8; media: serum and PBS) and *in vitro* characterizations of their breast cancer cell targeting specificity and efficiency (using confocal microscopy, flow cytometry, and ELISA). Between the two types of legumain targeting peptides studied, the one with more tumor cell targeting specificity and binding efficiency has been identified.

References

1. H.A. Santos, E. Makila, A.J. Airaksinen, L.B. Bimbo, J. Hirvonen, Porous silicon nanoparticles for nanomedicine: preparation and biomedical applications, Nanomedicine 9 (2014) 535-554.
2. A. Tzur-Balter, G. Shtenberg, E. Segal, Porous silicon for cancer therapy: from fundamental research to the clinic, Rev. Chem. Eng. 31 (2015) 193-207.
3. M. Ferreira, P. Almeida, M.A. Shahbazi, A. Correia, H.A. Santos, Current trends and developments for nanotechnology in cancer, in: N. Vale (Ed.), Biomedical Chemistry: Current Trends and Developments, 1st Edition, De Gruyter Open, 2016, pp.290–342.
4. J. S. Kanathasan, V. Swamy, U. D. Palanisamy, A. G. K. Radhakrishnan, Legumain targeting peptide conjugated fluorescent porous silicon nanoparticles for breast cancer imaging, Advances in Science and Technology, 102 (2016) 45-50.

Acceptance ID: 8JLK-O

Effect of solidification rate on the microstructures and magnetic properties of isotropic (Nd,Pr)-(Fe,B,Co,Ti,C,Ga) melt-spun ribbons

Rahim Sabbaghizadeh,

Physics Department, Faculty of Science and Technology, National University of Malaysia, 43600 Bangi, Selangor, Malaysia

Rapid solidification processing of $Nd_{9.4}Pr_{0.6}Fe_{68.5-x}B_6Co_6Ti_{4.5}C_{4.5}Ga_{0.5}$ alloys was studied in order to obtain better understandings of the ‘‘direct’’ process in which an $Nd_2Fe_{14}B$/ α-Fe type nanocomposite structure is formed during the rapid solidification of a melt. Melt-spun ribbons have been prepared at different quenching wheel speeds (15, 20 and 25 m/s) and investigated for microstructural and magnetic properties. As-spun ribbons were examined by using X-ray diffractometer (XRD) with Cu-kα radiation, differential scanning calorimetry (DSC) and vibrating sample magnetometer (VSM). Based on the results obtained, it was seen that the higher quenching wheel speed leads to a lower grain size and higher amorphous phase amount. Further, it was shown that the Ti and C enhance the glass forming ability and increase the crystallization temperature.

Key words: Nanocomposite, Nd-Fe-B, solidification rate, wheel speed.

Acceptance ID: 9MYD-O

Magnetoplasmonic Particles and Their Multidimensional Assembled Structures

Van Tan Tran, Younseong Song, Sangjin Oh, Jeonghyo Kim, Jaebeom Lee[*]

Department of Cogno-Mechatronics Engineering, Pusan National University, Busan, 609-735, Republic of Korea
**Corresponding author: E-mail: jaebeom@pusan.ac.kr*

Controlling and understanding the assembly of colloidal nanoparticles remain a challenging issue for optimizing magnetic-plasmonic devices for various applications including sensors, displays, bio-imaging and therapy. A magnetic field is successfully utilized to induce the fabrication of multidimensional structures composed of magnetoplasmonic particles, which exhibit intriguing optical properties. An effective and highly controlled dip-coating technique for fabrication of one-dimensional (1D) structure of magnetoplasmonic particles on large-area surface is proposed by combining electrostatic and magnetic dipole interactions. This technique is demonstrated to be a very powerful approach to modulate optical properties of magnetoplasmonic particles. Moreover, a magnetic-field assisted coating technique for fabrication of two-dimensional (2D) amorphous photonic crystal (APC) film of the magnetoplasmonic particles on a filter membrane is proposed. The magnetoplasmonic 2D APC exhibits strong dual reflected colors caused by structural scattering and plasmon resonance scattering. The water absorption ability of the membrane and the high refractive index sensitivity of plasmon resonance scattering are utilized to fabricate a simple colorimetric humidity sensor. Additionally, a mechanical colorimetric sensor that exhibits instantly responses to both bending and stretching forces is fabricated by embedding the 2D APC film into PDMS substrate. Because of unique features including dual-color characteristic, flexibility and high plasmonic sensitivity, these kinds of platform could be highly promising as wearable devices for physical, chemical and biological sensing with naked eye detection.

Acceptance ID: BQ7A-P

Solvent-free mechanochemical preparation of graphene-based composites

Guy Guday[1], *Ievgen Donskyi*[1], *Mohsen Adeli*[1,2] *and Rainer Haag*[1]

[1]*Institut für Chemie und Biochemie, Freie Universität Berlin, Takustr. 3, 14195 Berlin, Germany*
[2]*Faculty of Science, Lorestan University, Khorram Abad, Iran*
gguday@zedat.fu-berlin.de / +49-30-838-55370

Graphene and its derivatives are continuously gaining interest and being applied to new challenges, as they can provide highly adaptable platforms for conjugated systems with complex architectures and unique properties. In this work, we report on a new process for the mechanochemically initiated functionalization of graphene sheets using 2-azido-4,6-dichloro-1,3,5-triazine. With this mechanochemical route, we provide a scalable method for the modification of graphene using low concentrations of monoazidated cyanuric chloride, without the need for additional solvent or reagents.

The use of azide moieties as a means for covalent conjugation to graphene sheets is an established synthetic route. Azide groups can react with double bonds in graphene or other carbon nanomaterials like fullerenes and nanotubes, in a 2+1 cycloaddition reaction.[1-3] Recent work in our group has shown the utility of azidated cyanuric chloride for convenient preparation of graphene. The two significant advantages over other azides are the low temperatures for the reaction, and the stepwise post-modification of the two remaining chlorine groups of cyanuric chloride. This is possible because the reactivity of the two chloride groups is discrete, so that simple temperature control can be used for sequential activation.[1] These multi-functional, two-dimensional nanomaterials could be used for a wide range of applications, especially for biological or medical applications, as the post-modification is carried out under mild conditions. This can allow for the co-localized conjugation of two distinct functionalities, even biomolecules that are too sensitive for many reaction conditions. The benefits of co-localization could be particularly intriguing for biosensing and pathogen interaction and/or destruction.

Mechanochemistry with ball milling has been used to exfoliate graphene and graphene oxide.[4-7] Some methods can even allow for regioselectivity of oxidized groups.[6] Mechanochemistry also has been shown to be useful for the modification or functionalization of nanomaterials, offering unique reaction conditions that can open doors for novel synthetic routes.[6-10] The environment in the milling chamber, combining local temperatures significantly higher than the ambient temperature in the mill, and physical factors like extreme sheer or friction forces and high-energy impacts, is very distinct from solution chemistry.[10,11]

Here, a reaction between prepared graphene sheets and azidated cyanuric chloride (an oily liquid) was conducted in (pseudo) solid state via planetary ball milling, without the need for solvent. By controlling the milling parameters, it is possible to achieve different degrees of functionality and produce desired products. These can then be stepwise post-modified to produce myriad graphene-based composites.

Keywords: Graphene, functional, nanomaterial, ball mill, mechanochemistry

(1) BEIRANVAND, Z., KAKANEJADIFARD, A., DONSKYI, I. S.; FAGHANI, A.; TU, Z., *et al.* 2016. Functionalization of fullerene at room temperature: Toward new carbon vectors with improved physicochemical properties. *RSC Adv.*, 6, 112771–112775.

(2) STROM, T. A., DILLON, E. P., HAMILTON, C. E. & BARRON, A. R. 2009. Nitrene addition to exfoliated graphene: a one-step route to highly functionalized graphene. *Chem. Commun.*, 46, 4097–4099.

(3) GAO, C., HE, H., ZHOU, L., ZHENG, X., ZHANG, Y. 2009. Scalable Functional Group Engineering of Carbon Nanotubes by Improved One-Step Nitrene Chemistry. *Chem. Mater.*, 21, 360–370.(4) YAN, L., LIN, M., ZENG, C., CHEN, Z., ZHANG, S., *et al.* 2012. Electroactive and biocompatible hydroxyl- functionalized graphene by ball milling. *J. Mater. Chem.*, 22, 8367.

(5) PATON, K. R., VARRLA, E., BACKES, C., SMITH, R. J., KHAN, U., *et al.* 2014. Scalable production of large quantities of defect-free few-layer graphene by shear exfoliation in liquids. *Nat. Mater.*, 13, 624–630.
(6) JEON, I.-Y., SHIN, Y.-R., SOHN, G.-J., CHOI, H.-J., BAE, S.-Y., *et al.* 2012. Edge-carboxylated graphene nanosheets via ball milling. *Proceedings of the National Academy of Sciences*, 109, 5588–5593.
(7) LEÓN, V., QUINTANA, M., HERRERO, M. A., FIERRO, J. L. G., LA HOZ, A. DE, *et al.* 2011. *Chem. Commun.*, 47, 10936–10938.
(8) BEYER, M. K. & CLAUSEN-SCHAUMANN, H. 2005. Mechanochemistry: The mechanical activation of covalent bonds. *Chemical Reviews*, 105, 2921–2948.
(9) SEO, J.-M., JEON, I.-Y. & BAEK, J.-B. 2013. Mechanochemically driven solid-state Diels–Alder reaction of graphite into graphene nanoplatelets. *Chem. Sci.*, 4, 4273.
(10) BODYREV, V. V. & TKACOVA, K. 2000. Mechanochemistry of Solids: Past, Present, and Prospects. *J. Mat. Synth. Process.*, 8, 121–132.
(11) VENKATARAMAN, K. S. & NARAYANAN, K. S. 1998. Energetics of collision between grinding media in ball mills and mechanochemical effects. *Powder Technology*, 96, 190–201.

Acceptance ID: CPUA-P

Single-Particle Spectroscopic Studies of Semiconductor Perovskite Nanocrystals

Xiaoyong Wang,[1] Fengrui Hu,[1] Chunyang Yin,[1] Chunfeng Zhang,[1] and Min Xiao[1,2*]*

[1] National Laboratory of Solid State Microstructures, School of Physics, and Collaborative Innovation Center of Advanced Microstructures, Nanjing University, Nanjing 210093, China
[2] Department of Physics, University of Arkansas, Fayetteville, Arkansas 72701, USA
Author e-mail addresses: wxiaoyong@nju.edu.cn, mxiao@uark.edu.

Single photon emission is demonstrated from single perovskite nanocrystals (NCs) synthesized from a facile colloidal approach to confirm their quantum-emitter nature. Moreover, the photoluminescence blinking and spectral diffusion effects are suppressed at the cryogenic temperatures, leading to the observation of bright-exciton fine structure splittings in a single perovskite NC.

References

[1] L. Protesescu, S. Yakunin, M. I. Bodnarchuk, F. Krieg, R. Caputo, C. H. Hendon, R. X. Yang, A. Walsh, and M. V. Kovalenko, "Nanocrystals of cesium lead halide perovskites ($CsPbX_3$, X = Cl, Br, and I): Novel optoelectronic materials showing bright emission with wide color gamut," Nano Lett. **15,** 3692-3696 (2015).

[2] F. Hu, H. Zhang, C. Sun, C. Yin, B. Lv, C. Zhang, W. W. Yu, X. Wang, Y. Zhang, and M. Xiao, "Superior optical properties of perovskite nanocrystals as single photon emitters," ACS Nano **9,** 12410-12416 (2015).

[3] F. Hu, C. Yin, H. Zhang, C. Sun, W. W. Yu, C. Zhang, X. Wang, Y. Zhang, and M. Xiao, "Slow Auger recombination of charged excitons in nonblinking perovskite nanocrystals without spectral diffusion," Nano Lett. **16,** 6425-6430 (2016).

Acceptance ID: D42Z-O

Mobility Boosting in Black Phosphorus Field-Effect Transistors by Interface Engineering of Inserting Atomic-Layer-Deposited High-*k* Dielectrics

H. M. Zheng, Q. Ma, J. Gao, S. M. Sun, W. J. Liu, S. J. Ding*,*
P. Zhou, H. L. Lu, L. Chen, Q. Q. Sun, David W. Zhang
State Key Lab ASIC & Syst., Dept. Microelectronics, Fudan University, Shanghai 201203, China
** Email: wjliu@fudan.edu.cn; sjding@fudan.edu.cn*

Abstract: Recently, black phosphorus (BP) has attracted great attention because of its unique properties, such as high mobility, direct and tunable bandgap. Thus, it has been considered as a promising material for future applications in electronic and optoelectronic devices. However, the interface engineering of BP is challenging to the achievement of high performance BP field-effect transistors (FETs). In this work, atomic-layer-deposited Al_2O_3 and AlN layers were inserted between SiO_2 and BP channel to tune the transfer characteristics of BP FETs. The results indicate that the field-effect mobility of the BP FETs improves dramatically compared to the controlled devices without the inserted Al_2O_3 and AlN layers. The interface properties of the FETs were evaluated by low frequency noise measurements. Moreover, the capping effects of the dielectric layer on the BP channel were also investigated.

Keywords: Black Phosphorus, Al_2O_3, AlN, Atomic Layer Deposition, Field-Effect Transistors

Acceptance ID: DB24-P

Multifunctional Nanomaterials: Synthesis, Properties and Applications

*Tokeer Ahmad**

Nanochemistry Laboratory, Department of Chemistry, Jamia Millia Islamia, New Delhi 110025, INDIA
E-mail: tahmad3@jmi.ac.in

Nanomaterials are among the most challenging areas of current scientific and technological research because of the variety of interesting changes in their properties at nano-dimension. The preparation of nanoparticles with well defined size and morphology is an important challenge for various industrial applications. Multiferroic materials exhibit ferromagnetic and ferroelectric properties which may lead to number of applications for future computer memory concepts, multiple state memory devices, sensors, spin valves, actuators and transducers etc and play an important role in solid oxide fuel cells, catalysts materials for electrodes and chemical sensors. Multiferroic YMO_3 (M = Fe, Mn & Cr) nanoparticles have been prepared successfully by using polymeric citrate precursor method. XRD studies revealed the monophasic orthorhombic structure of $YFeO_3$, $YCrO_3$ and hexagonal structure of $YMnO_3$ nanopowder. The TEM and SEM studies showed that the particles are nearly spherical and hexagonal with an average grain size of 22-77 nm. Highest specific surface areas of nano-sized $YFeO_3$, $YCrO_3$ and $YMnO_3$ were found by using multipoint BET surface area studies. UV−visible reflectance studies of YMO_3 (M = Fe, Mn & Cr) and photoluminescent properties of $YMnO_3$ were studied. The temperature and frequency dependences of electrical properties including dielectric constant, dielectric loss and conductivity properties of YMO_3 (M = Fe, Mn & Cr) were investigated. The room temperature ferroelectric properties of nanocrystalline YMO_3 (M = Fe, Mn & Cr) compounds were also reported. Magnetic results of YMO_3 (M = Fe, Mn & Cr) possesses wasp-waisted, wedge shaped, and normal ferromagnetic loop of $YFeO_3$, $YCrO_3$ and $YMnO_3$ respectively with well saturation magnetization (M_s), remanent magnetization (M_r) and coercive field. The characteristics of the humidity sensing properties of $YFeO_3$ and $YCrO_3$ and the performances of $YFeO_3$ nanoparticles on power conversion efficiency of the dye sensitized solar cell (DSSC) as well as photocatalysis for hydrogen evoloution have been also explored. The chemistry of $GdFeO_3$ and $GDCrO_3$ will also be discussed.

References:

1. T. Ahmad, I. H. Lone and M. Ubaidullah, *RSC Advances*, **5**, 58065–58071, 2015.
2. T. Ahmad and I. H. Lone, *New Journal of Chemistry*, **40**, 3216-3224, 2016.
3. T. Ahmad, I. H. Lone and S. G. Ansari, *Materials& Design* (Under Review) 2017.

Acceptance ID: E75S-O

Synthesis of dimension controlled copper nanomaterials for conducting ink applications

Jin-Won Lee[1], *Jiyoon Han*[1], *Sukang Bae*[1], *Dong Su Lee*[1], *Sang Hyun Lee*[1], *Gunuk Wang*[2], *and Tae-Wook Kim*[1*]

[1] *Applied Quantum Composites Research Center, Korea Institute of Science and Technology, Jeollabuk-do 565-905, Republic of Korea*
[2] *KU-KIST Graduate School of Converging Science and Technology,* Korea University, *Seoul 136-701, Republic of* Korea

**E-mail : twkim@kist.re.kr*

Abstract: Indium tin oxide (ITO) has been used as one of the representative transparent conducting electrode (TCE) due to its high transparency and low sheet resistance. However, it has several problems such as high processing temperature, limited indium resources and high preparation costs. [1] Most of all, efficient ITO still have trouble to apply to flexible electronic devices because it is mechanically brittle. Therefore it is necessary to develop cost efficient, flexible and solution-processible electrodes for flexible optoelectronic devices. Hence many groups have been studied conductive polymer (e.g. PEDOT:PSS), graphene, carbon nanotube, and metal nanowires (e.g. AgNWs, CuNWs) as an alternative ITO for flexible electrodes. [2, 3] Among them, metal nanowires have attracted considerable attention due to their potentials such as excellent opto-electrical property, solution processability and mechanical flexibility. [4] Especially, the property of flexibility is an important factor of metal nanowire electrodes because it suited well for flexible device applications.

Here, we synthesize copper nanowires (CuNWs) nanostructure using a hydrothermal process at low temperature (~ 100 °C), as shown in Figure 1. The shape of copper nanowires was carefully controlled by changing several variables such as reaction time, temperature, and amount of reductant. We studied dimension controlled copper nanomaterials for conducting ink applications. We will discuss detailed structural, electrical, and optical characteristics of the dimension controlled copper nanomaterials.

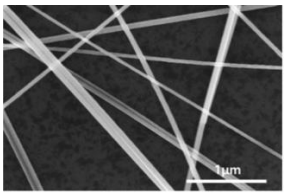

Figure 1 SEM images of copper nanowire

Keywords: Copper nanomaterials, Cu Nanowire, Conducting ink, Dimension control,

[1] AHN, Y., JEONG, Y., LEE. D., LEE. Y. 2015. Copper Nanowire–Graphene Core–Shell Nanostructure for Highly Stable Transparent Conducting Electrodes. *ACS Nano*, 9, 3125-3133.

[2] JUNG. S. M., JUNG. H. Y., DRESSELHAUS. M. S., JUNG. Y. J., KONG. J. 2012. A facile route for 3D aerogels from nanostructured 1D and 2D materials. *Sci. Rep*., 2, 849.

[3] LEE. M. -S., LEE. K., KIM. W. -Y., LEE. H., PARK. J., CHOI. K. -H., KIM. H. -K., KIM. D. -G., LEE. D. -Y., NAM. S. W., PARK. J. -U. 2013. High-Performance, Transparent, and Stretchable Electrodes Using Graphene–Metal Nanowire Hybrid Structures. *Nano lett*., 13, 2814-2821.

[4] IM. H. -G., JUNG, S. -H., JIN. J., LEE. D., LEE. J., LEE. D., LEE. J. -Y., KIM. I. -D., BAE. B. -S. 2014. Flexible Transparent Conducting Hybrid Film Using a Surface-Embedded Copper Nanowire Network: A Highly Oxidation-Resistant Copper Nanowire Electrode for Flexible Optoelectronics. *ACS Nano*, 8, 10973-10979.

Acceptance ID: EML4-P

Ion track-based plasmonic nanopillar-nanogroove hierarchical architectures for quantitative and ultrasensitive SERS detection

*Yibo Zhou,[a,b,‡] Chen Xu,[a,b,‡] Shuangbao Lyu,[a,‡] Huijun Yao,[a] Dan Mo,[a] Khan Maaz,[a] Yonghui Chen,[a] Yongliang Zhang,[*c] Jinglai Duan,[*a,d]*

[a] *Materials Research Center, Institute of Modern Physics, Chinese Academy of Sciences, Lanzhou 730000, China.*
[b] *School of Physical Science and Technology, Lanzhou University, China.*
[c] *Department of Applied Physics, The Hong Kong Polytechnic University, Hong Kong, China.*
[d] *University of Chinese Academy of Sciences*
[‡] *These authors contributed equally.*
E-mail address: j.duan@impcas.ac.cn (JLD); ylzhang@mail.ipc.ac.cn (YLZ)

Diverse fields which are close to our daily life, including biochemical sensing, human health care, food safety, pollution monitoring, homeland security, appeal for developing detection techniques that possess ultrahigh sensitivity. One such technique is surface-enhanced Raman spectroscopy (SERS) which can realize an ultrasensitive detection even down to single-molecule level. In this work, we theoretically propose a first-ever plasmonic hierarchical nanoarchitectures for improved cascaded optical field enhancement (CFE) boosted by sharp nanoridges. Theoretical simulations reveal that the magnitude of EM field of the sharp nanoridge enriched hierarchical nanoarchitecture is significantly improved in comparison with the similar nanoarchitectures of same nominal structural parameters with moderately sharp ridges and no ridges, unveiling that sharp nanoridges are efficient and effective boosters for improved CFE. We further show that such state-of-the-art plasmonic hierarchical nanoarchitectures with sharp nanoridges was experimentally accomplished by "top-down" etching of dense ion tracks in polymer and self-assembly of nanogrooves through physical vapor deposition (CVD). Additionally, we also demonstrate that the sharp nanoridge enriched hierarchical nanoarchitectures possess combined advantages in cost-effective and large-area fabrication, signal uniformity and reproducibility, mechanical flexibility, and multidirectional responsivity. We expect that such intriguing hierarchical nanoarchitectures open up possibilities for real-world SERS applications, especially those at complex working conditions.

Acceptance ID: F9JG-P

A tactile sensor using single-layer graphene for surface texture recognition

*Sungwoo Chun[1], Wonkyeong Son[1], Soa Bang[1], and Wanjun Park[1]**

[1]Department of Electronics and Computer Engineering, Hanyang University,
Wangsimni-ro 04763, Seoul 133-791 South Korea
Fax: +82(31)-2220-4319 E-mail address: wanjun@hanyang.ac.kr

Texture recognition is essential to emulate the tactile sensation of human skin [1] that is obtained from spatial encoding with complex process including detection of both pressure and vibration [2]. Emulation of this feature has been difficult to attain because spatial resolution at the level of human perception requires integrated matrix architecture with the miniaturized sensor elements. Matrix architecture, however, suffers from many practical difficulties including wiring, sneaker paths, complex driving circuit, and addressing. Moreover, materials used for the sensor element are critically limited for the integration process involving soft materials that are applicable to the artificial skin forms.

In this paper, we describe a flexible force sensor that can detect surface texture based on single sensor architecture. We developed this sensor by taking advantage of the unique electromechanical characteristics of single layer graphene (SLG), which is a continuous film with single atomic thickness, and exhibits a piezo-resistive response to local deformation. The sensitivity was enhanced by 57% by the introduction of a pressure-amplifying structure (PAS), which was a uniform array of micro-structured square pillars. Furthermore, the sensors were able to detect a vertical pressure as low as 24 Pa with a fast response of ~ 2 ms for deformation and ~ 3 ms for restoration. Introduction of an APFS structure inspired by a human finger print allowed perception of surface texture using a single sensor through FFT analysis of the resistance changes due to vibrations induced by the slip motion between the sensor and roughness of the interacting surface. Because the spatial resolution of the proposed tactile sensor can be improved by adjusting the size and periodicity of the AFPS patterns, the proposed work provides a simple method for surface texture recognition at the level of human sensation without the requirement for matrix architecture, which requires high density integration technology with force and vibration sensors.

Keywords: Graphene composite, Graphene absorbent, Hydrophobic coating

[1] Maheshwari, V. & Saraf, R. 2008. Tactile devices to sense touch on a par with a human finger. Angew. Chem. Int. Ed., 47, 7808-7826.

[2] Hollins, M. & Risner, S. R. 2000. Evidence for the duplex theory of tactile texture perception. Percept. Psychophys., 62, 695-705.

Acceptance ID: FEMW-O

Vertical field-effect transistor using ZnO nanotube arrays grown on graphene films

*Hongseok Oh[1], Jong-woo Park[1], Jun Beom Park[1], Youngbin Tchoe[1] and Gyu-Chul Yi[1]**

[1]Department of Physics and Astronomy, Institute of Applied Physics, and Research Institute of Advanced Materials, Seoul National University, Seoul 08826, Korea
Presenting author E-mail: hoh331@snu.ac.kr
Corresponding author E-mail: gcyi@snu.ac.kr

Flexible electronics have recently attracted much attention for use in wearable devices and biomedical applications. For the bendable, stretchable and wearable devices, organic materials have widely been employed as carrier channels due to their excellent scalability and flexibility.[1] However, the organic materials exhibit low carrier mobility, easy degradation and low device density. To resolve this problem, we propose to use hybrid-dimensional material composed of one-dimensional (1-d) inorganic nanostructures vertically grown on two-dimensional (2-d) nanomaterials such as graphene films for flexible electronic devices. When the 1-d inorganic nanostructures are used as carrier channels of the devices, high carrier mobility and device density as well as excellent stability and reliability can be shown. Furthermore, the layered structure of graphene films ensures easy transfer of the materials onto foreign substrates such as plastics and excellent flexibility. Nevertheless, poor electrical characteristics and lack of precise position control of 1-D nanostructures on graphene hindered to their flexible electronic device applications. Here we report position-controlled growth of ZnO nanotube arrays on graphene and fabrication of vertical field-effect transistor (FET) arrays for flexible electronics.

Position-controlled ZnO nanotubes were grown on few-layered graphene films with a submicron hole-patterned SiO_2 growth mask which selectively suppresses nucleation of ZnO. The typical diameters and pitches of the holes were 100–500 nm and 1–8 micrometers, respectively. Then, ZnO nanotube arrays were selectively grown on SiO_2-mask-patterned graphene films by catalyst-free metal-organic vapor phase epitaxy. The ZnO nanotubes exhibited well-controlled dimension and position. Furthermore, we fabricated vertical FET arrays using the nanotube arrays. For fabrications of metal-semiconductor field-effect transistor (MESFET), a 100-nm-thin Au layer as a Schottky gate was coated directly on the outside walls of ZnO nanotube arrays. Then polyimide spacer layer was filled. Finally, the device fabricated depositing a thin Ti/Au layer as ohmic contact on the nanotube tips. The device characteristics and flexible operation of the vertical MESFET devices will be shown and discussed.

Keywords: vertical field-effect transistor, flexible, electronics, ZnO, graphene

[1] Jie Xu et al, "Highly stretchable polymer semiconductor films through the nanoconfinement effect" Science 2017 355, aah4496 (2017)

Acceptance ID: FQUT-O

Empowering Seed-Mediated Growth Method for Synthesizing High-Index Faceted Noble Metal Nanocrystals

Ranguwar Rajendra (presenter) and Nirmalya Ballav

Development of synthetic protocols for noble metal nanocrystals with the high-index facet (HIF) is of significant interest to the nanomaterial's scientific community. Such nanocrystals exhibit high density of insufficiently coordinated atoms at steps, kinks and ledges on their surfaces which enhanced catalytic activity in comparison with low-index faceted NCs (spherical, octahedral and cubic). However, due to the synthetic challenges, to date, limited reports are available on the aqueous-phase synthesis of HIF Au NCs where ascorbic acid (AA) is the only reagent that was used as a reducing agent. Recently, we reported the dimension-controllable synthesis of elongated tetrahexahedra (ETHH) Au nanocrystals (Au NCs) via state-of-the-art seeded-growth method in which tannic acid (TA) was used as a mild reducing agent for the first time and those Au NCs were enclosed with high-index {730} facets. [1] Out study on the evolution of ETHH Au NCs has shown that these NCs were evolved via cylindrical nanorods as intermediates. Remarkably, electrocatalytic oxidation of formic acid revealed a linear dependency between average particle dimensions and catalytic activities. Finally, we demonstrate that under similar experimental conditions, simply by changing the pH of the growth solution, it is possible to synthesize morphologically identical Au NCs with reducing agents intrinsically differed in reduction activities. We anticipate our results to stimulate the use of various other organic molecules as mild reducing agents in the seed-mediated growth of HIF noble metal NCs with controllable size-property relationship.

[1] R, Rajendra et al. *Nanoscale*, 2016, **8**, 19224-19228.

Acceptance ID: FVWZ-O

Influence of cycle index to CuO nanoparticle characteristics synthesized by reduction-oxidation cycle

*Bo Gong, Tielin Shi, Siyi Cheng, Chen Chen, Zirong Tang**

State Key Laboratory of Digital Manufacturing Equipment and Technology, Huazhong University of Science and Technology, Wuhan 430074, China
**corresponding author, 1037 Luoyu Road, Wuhan 430074, China. Tel.: +86 27 87792241; fax: +86 27 87792413; E-mail address: zirong@hust.edu.cn.*

In this work, the influence of reduction-oxidation cycle to CuO nanoparticles was studied. CuO nanoparticles were synthesized by reduction-oxidation cycles with different cycle indexes. The grain size of CuO nanoparticles decreased with the increasing of cycle index. The intensity of a characteristic peak (1 1 1) enhanced after three reduction-oxidation cycles, which indicated that the cyclic process improved the ctystallization property of CuO nanoparticles. CuO nanoparticales exhibited higher practical specific charge due to the complete oxidation/reduction of Cu^{+} during the cycles [1-4]. The results of the gas sensing test to ethanol shows the gas sensitivity of CuO nanoparticles was also promoted due to the increase of reduction-oxidation cycle. The reduction-oxidation cycle is an effective approach to improve the morphology, composition and crystallization property of CuO nanoparticles. We would like oral presentation and the abstract to be considered for presentation in the topic “Advances in the Synthesis and Characterization of low dimensional, nano and 2D materials”.

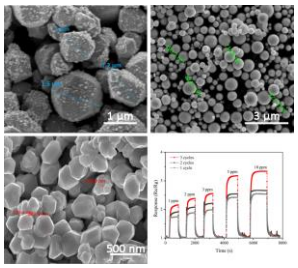

Keyword: Reduction-oxidation cycle, CuO mamoparticle, gas sensing

[1] GRUGEON S., LARUELLE S., HERRERA-URBINA R., DUPONT L., POIZOT P., TARASCON J-M. 2001. Particle Size Effects on the Electrochemical Performance of Copper Oxides toward Lithium. J. Electrochem. Soc., 148, A285-A292.

[2] GAO X., BAO J., PAN G., ZHU H., HUANG P., WU F., SONG D. 2004. Preparation and Electrochemical Performance of Polycrystalline and Single Crystalline CuO Nanorods as Anode Materials for Li Ion Battery. J. Phys. Chem. B, 108, 5547-5551.

[3] ZHANG D., YI T., CHEN C. 2005. Cu nanoparticles derived from CuO electrodes in lithium cells. Nanotechnology, 16, 2338-2341.

[4] OLIVER W., MICHEAL H., ANDREAS G., PETR N., SONTIRIS E. 2013. Size controlled CuO nanoparticles for Li-ion batteries. J. Power Sources, 241, 415-422.

Acceptance ID: FX24-O

Method of preparing a polar based magnetic ink suitable for inkjet printing and characterization of Ni and Mn ferrite thin film

Evarestus Enuka[1], Mahmuda Akter Monne[1], Xing Lan[2], Vincent Gambin[2], Rachel Koltun[2], Jesse Tice[2], Maggie Yihong Chen[1]

[1]Electrical Engineering, Texas State University, San Marcos, TX 78666 USA
[2]NG Next, Northrop Grumman, One Space Park, Redondo Beach, CA 90278 USA
E Mail: cee44@txstate.edu, yc12@txstate.edu

The objective of this paper is to present a novel method of preparing magnetic ink belonging to the class of ferrofluids which contains magnetic particles with a polar surface active agent known as surfactants, adsorbed on the particle surface and thereafter dispersed in an aqueous medium. The magnetic material belongs to the group known as magnetite (Fe_3O_4), typically to those with γ-Fe_2O_3 and their likes. They exhibit strong ferromagnetism with properties that are nearly isotropic, they often show low coercivity, low hysteresis loss, high permeability, and high electrical resistivity. A Ni-Zn ferrite and Mn-ferrite ink were prepared using this method. The ink has a Ph value and total dissolved solute (TDS) of about 6.3, 3.78 mS and 5.9, 4.2 mS respectively, measured using OAKTON Ph meter and a viscosity of about 7 cPa, 7.4 cPa respectively, measured using Rheosense m-Vroc. The magnetic properties of the inks were measured using a microstrip transmission line resonator method. The saturation magnetization of Mn-ferrite ink at 300K was 4.2 emu/cm^3. This lower value of the saturation magnetization Mn-ferrite compared to the bulk is because of the shell-core structure of the surfactant coated ferrite particles. The inks were used to prepare various thicknesses ranging from 0.5um to 20um of both Nickle-Zinc ferrite and Manganese ferrite thin films. The surface morphology of the thin film was observed using Atomic Force Microscopy (AFM). The AFM image shows a dense and relatively smooth film. The microstrip transmission line permeameter approach were used to extract the permittivity and permeability of the thin film samples within the frequency range of 50MHz-5GHz. A relative permeability of 2.62 was measured of Manganese ferrite thin films on Kapton substrate.

Index Terms: Inkjet printing, magnetic ink, Ferrites, thin film, permittivity, permeability.

Acceptance ID: GBWK-P

Growth and Electronic, Optical and Spin-related Phenomena in SiGe Quantum Dot Heterostructures

Name: A.V.Dvurechenskii[1,2], A.I.Yakimov[1,3], A.V.Nenashev[1,2], A.F.Zinovieva[1], V.A.Zinovyev[1]

[1]Rzhanov Institute of Semiconductor Physics, Siberian Branch of the Russian Academy of Sciences, prospekt Lavrent'eva 13, 630090 Novosibirsk, Russia
[2]Novosibirsk State University, 630090 Novosibirsk, Russia
[3]Tomsk State University, 634050 Tomsk, Russia

The major challenges for semiconductor fundamental research and technological development are confined to a variety of silicon-based nanostructured systems, thin films, and heteroepitaxy on patterned silicon substrates. The hot topics are selective epitaxy for advanced electronic applications, strain engineering in strained layer epitaxy, study of spin relaxation, decoherence and dephasing, spin-orbit interaction, development of light emitters, amplifiers and detectors, also their coupling with plasmonic materials to manipulate light at the nanoscale on the Si platform, which are efficient CMOS-compatible readout schemes.

The present talk aimed to show results and technology development in Si with Ge quantum dots (QDs). The most highly developed technology for fabrication of Ge/Si QDs utilizes strain-driven epitaxy of Ge on a Si(100) surface. Ge/Si(100) QDs formed by strain epitaxy exhibit a type-II band lineup. The large (≈0.7 eV) valence band offset leads to an effective localization of holes in Ge regions, which represent potential barriers for electrons. Tensile strain due to the 4% lattice mismatch between Ge and Si causes splitting in the nearby Si of the sixfold-degenerate Δ valleys into the fourfold-degenerate in-plane Δ_{xy} valleys and twofold-degenerate Δ_z valleys along the [001] growth direction. The lowest conduction band edge is formed by the Δ_z valleys yielding the triangle potential well for electrons in Si near the apex of pyramidal shape Ge nanocrystal.

The electron localization in Si is selective advantage of materials on spin relaxation values. The weak spin orbit coupling in Si and existence of developed technology to reduce none zero magnetic moment isotopes make provision for long decoherence time of electron spin in Si. Even in natural abundance Si the electron coupling to nuclear spins is orders of magnitude weaker than in A3B5 materials. The long spin coherence time is the main requirements to select materials for spintronic, quantum computation on quantum dot qubits. For selective access to individual qubits needed for implementation of one-qubit and two-qubit operations there are many ideas based on magnetic field, coherent light, and electric field. One of the ability is to distinguish electrons by g-factor value.

The main items of the talk are following:

1. Strain-induced nucleation and epitaxial growth of nanocrystals (quantum dots) with surface modification by *a)* low energy ion-beam action at epitaxy; *b)* ion-beam-assisted nanoimprint lithography; *c)* heterophase substrate.
2. Strain-induced tuning of electron localization, optical and spin properties. Luminescence enhancement, strong increasing of photoelectric gain and responsivity.
3. Spin relaxation in array of tunnel-coupled quantum dots. A few (multi) electron spin localization on one quantum dot. g-factor engineering.
4. Quantum dot photodetectors for near and mid-infrared operation.
5. Challenges facing fundamental research and technological development.

The work was funded by Russian Scientific Foundation (grant 14-12-00931).

Acceptance ID: GHKB-O

Cu_2ZnSnS_4 Nanocrystals with Rapid Clearance for Dual Model Imaging Guided Cancer Thermal Therapy

*Longfei Tan, Tianlong Liu, Changhui Fu, Xianwei Meng**

Laboratory of Controllable Preparation and Application of Nanomaterials, Technical Institute of Physics and Chemistry, CAS, No.29 East Road Zhongguancun, Beijing, China
*E Mail/ Contact Détails (**longfeitan@mail.ipc.ac.cn**)*

Theranostics based on nanoagents is becoming one of the prospective directions of nanomedicine. However, the nanoagents with large sizes are easily recognized and taken up by mononuclear phagocyte system cells exist in vital organs such as liver and spleen. The development of ultrasmall nanoagents simultaneously have therapeutic and imaging capability as well as rapid renal clearance properties remains an important goal to achieve more efficient theranostic platform. By choosing suitable source materials and tuning the molar ratio of the elements, quaternary nanocrystals could be endowed with multiple functions without increasing sizes. In our work, ultrasmall Cu_2ZnSnS_4 (CZTS) nanocrystals are synthesized as rapid clearance multifunctional theranostic platform for photoacoustic (PA) / magnetic resonance (MR) imaging-guided tumor PTT therapy. The obtained CZTS@BSA exhibits excellent in vivo photothermal therapy effects due to their efficient NIR absorption and photothermal conversion abilities. The high photothermal conversion abilities also make CZTS@BSA an ideal PA imaging contrast agent. Meanwhile, for the first time, the prepared CZTS@BSA are reported as an efficient T1 contrast agent for in vivo MR imaging, which contributed to the improved longitudinal relaxivity by intrinsic substitutional defects of CZTS. The rapid renal clearance in vivo is tracked by PA/MR imaging and confirmed by ICP-MS measurement in organs. In vivo evaluation of systematic acute toxicity indicates CZTS@BSA have good biocompatibility to normal tissues and blood, showing great promise for the future application.

Keywords: Cu_2ZnSnS_4, Theranostic, Photothermal Therapy, Magnetic Resonance Imaging

(1) TAN, L.F., WANG, S.P., XU K. & MENG, X.W*, et.al. 2016, Layered MoS_2 Hollow Spheres for Highly-Efficient Photothermal Therapy of Rabbit Liver Orthotopic Transplantation Tumors, *Small*, 12, 2046-2055.

Acceptance ID: H6FG-O

Study of Graphene-Metal Contact by using Raman Spectroscopy

Hejun Xu[1], Guohui Su[1], Chaolun Wang[1], Fei Qiao[2], Jian Zhang[1], Xing Wu[1], Junhao Chu[1]*

[1]Shanghai Key Laboratory of Multidimensional Information Processing, Department of Electrical Engineering, East China Normal University, Shanghai 200241, China
[2]Department of Electronic Engineering, Tsinghua University, BeiJing, China
[*]corresponding author: xwu@ee.ecnu.edu.cn

Graphene with various record properties as a candidate for post-silicon electronics has attracted enormous interests in the field of two dimensional (2D) materials since it was discovered by Andre Geim in 2004.[1,2] Contacts between graphene and metals play a significant role in the electrical performance of nanoscale devices and flexible devices made of 2D materials.[3] The contact resistance is one of the most protuberant problems that hinder applications of graphene in electronics. Raman spectroscopy technique as a nondestructive, rapid methodology provides a direct, unambiguous identification of the electrical structural changing induced by interactions between various metals and graphene. Graphene samples with the same thickness were prepared by mechanical cleavage and identified by optical microscopy and Raman spectroscopy.[4] Interactions between electrode metals such as Ni (Nickel), Ti (Titanium), Cr (Chromium) and Ag (silver) and graphene introduce shifts in G peak and G' peak. Wetting metals like Ni and Ti form metal carbide with graphene, which leads to a red shifts of G peak. This result is not coinciding with the previous reports[5,6,7] that doping makes blue shift of G peak, and blue shift and split G' peak by more than 10 cm^{-1}. Cr and Ag as non-wetting metals merely blue shift both G peak and G' peak by 2 cm^{-1}. Our works provide a different understanding of the adhesion and the properties between graphene and evaporated metals, which may be benefit to reduce contact resistance existed in graphene and other layered materials.

Reference:

1. *science* **306**, 666-669 (2004).
2. *Nanoscale* **7**, 4598-4810 (2015).
3. *ACS Nano* **10**, 4895-4919 (2016).
4. *Nat Nanotechnol* **8**, 235-246 (2013).
5. *Nature materials* **6**, 198-201 (2007).
6. *Nature nanotechnology* **3**, 210-215 (2008).
7. *Journal of Physics D: Applied Physics* **49**, 105301 (2016).

Acceptance ID: H6N9-P

Investigating the growth of Sn on the Ag(111) surface

Dah-An Luh[1,2], Chia-Hsin Wang[2], and Yaw-Wen Yang[2]

[1]Department of Physics, National Central University, Taoyuan, Taiwan
[2]National Synchrotron Radiation Research Center, Hsinchu, Taiwan

Stanene, the Sn version of graphene, has attracted interests because it is predicted to be a 2D topological insulator. In this study, we characterized systematically the growth of thin Sn layer on Ag(111) with the varied Sn coverage and substrate temperature with LEED, XPS, and STM. Our results showed that the surface alloying of the Sn atoms on Ag(111) can occur at a temperature as low as 100 K. The surface alloying results in a disordered surface; the surface will not become ordered until the substrate temperature is higher than 400 K. In addition, after the Sn film on Ag(111) is annealed at a temperature higher than 400 K, the Sn coverage of the annealed film will not be more than 1/3 ML; the excessive Sn diffuses into the Ag substrate. According to our results, the √3 reconstruction may be the only ordered phase existing on the Sn/Ag(111) film.

Acceptance ID: HKAY-P

Orientation-Induced Enhancement in Microwave Absorption Properties of Core/Shell/Shell-Structured Ni/SiO_2/PANI Nanoplates

Jiaheng Wang[1,2], *Siu Wing Or*[1]*

[1]*Department of Electrical Engineering, The Hong Kong Polytechnic University, Hung Hom, Kowloon, Hong Kong*

[2]*Department of Mechanical Engineering, Xuancheng Campus, Hefei University of Technology, Xuancheng 242000, Anhui, China*

**E Mail: eeswor@polyu.edu.hk (S. W. Or; Corresponding Author)*

Microwave absorbers based on magnetic/dielectric core/shell nanostructures have been a main research focus to alleviate electromagnetic (EM) interference and pollution problems in recent years. The deficiency in the generally weak absorption, caused by the intrinsically small permeability close to unity and the inadequate EM impedance match with the relatively large permittivity, in the L–Ku microwave bands of 1–18 GHz has greatly impeded them from commercial uses [1],[2]. These include global positioning systems (GPSs), weather and ship radars, mobile communications and satellites, etc.

In this paper, core/shell/shell-structured Ni/SiO_2/PANI (NSP) nanoplates having a plate-shaped anisotropic Ni magnetic core coated by a 1st amorphous SiO_2 insulating dielectric shell and a 2nd amorphous PANI conducting dielectric shell are prepared and their phase, morphology, microstructure, etc. are studied (Figs. 1(a)–(d)). The NSP nanoplates are fabricated into three characteristic types of paraffin-bonded NSP nanocomposite rings with vertical, horizontal, and random orientations of the easy magnetization planes of the NSP nanoplates in the paraffin binder under the presence and absence of a dc magnetic orientation field (Figs. 1(e) & (f)) in order to reveal the effect of directional orientation of the easy magnetization planes on their microwave absorption properties. The complex relative permeability ($\mu_r = \mu_r' - j\mu_r''$) and permittivity ($\varepsilon_r = \varepsilon_r' - j\varepsilon_r''$) of the NSP nanocomposite rings are evaluated experimentally and theoretically in the 1–18 GHz range (Figs. 1(e) & (f)). It is found that the easy magnetization planes induced by shape anisotropy and oriented by the dc magnetic orientation field in the vertically oriented ring result in a general enhancement in permeability of 5–10% in the low-frequency L, S, and C (1–8 GHz) microwave bands, while those in the horizontally oriented ring lead to a significant enhancement of 253–3100% in the high-frequency X and Ku (9–18 GHz) bands, both in comparison with the randomly oriented ring. The observed permeability agrees with the theoretical prediction based on the Landau–Lifshitz–Gilbert equation and the Bruggeman's effective medium theory (Fig. 1(e)) [3]. The horizontal and vertical arrangements of dipolar polarizations in the vertically and horizontally oriented rings give rise to 25 and 15% enhancement and weakening in permittivity, respectively, in comparison with the randomly oriented ring. The enhancement in permeability also improve and broaden the microwave absorption in both the vertically and horizontally oriented rings, especially in the Ku bands for the horizontally oriented one with ~4 GHz absorbing bandwidth at 7.9 mm thickness and the maximum reflection loss (*RL*) value of -41.8 dB at 17.2 GHz at 8.7 mm thickness (Fig. 2).

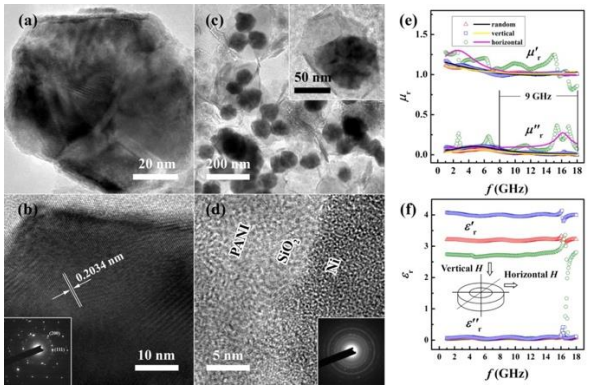

Fig. 1. (a) TEM and (b) HRTEM images of a typical Ni nanoplate; (c) TEM image typical NSP nanoplates; (d) HRTEM image of the Ni/SiO_2/PANI interfaces of the NSP nanoplate in (c); the insets in (b) and (d) are the SAED patterns; (e) Measured (symbols) and

calculated (lines) frequency (f) dependence of μ_r' and μ_r'' for randomly, vertically, and horizontally oriented NSP nanocomposite rings. (f) Measured f dependence of ε_r' and ε_r'' for randomly, vertically, and horizontally oriented NSP nanocomposite rings.

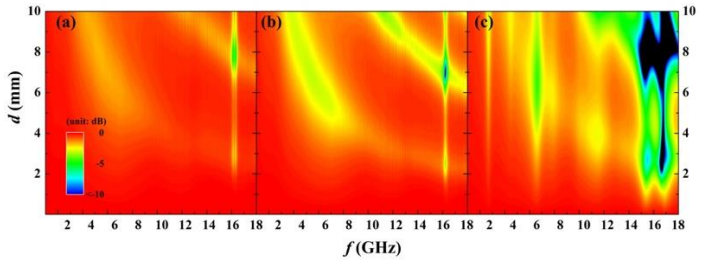

Fig. 2 2*D*-contour plots of frequency (*f*) and thickness (*d*) dependences of reflection loss (*RL*) for (a) randomly, (b) vertically, and (c) horizontally oriented NSP nanocomposite rings.

This work was supported by The Hong Kong Polytechnic University under Grant Nos. G-YBPP and G-YBLL.

Keywords: Core/shell/shell nanoplates; Microwave absorption properties; Magnetic field-induced directional orientation; Microwave absorbers.

[1] ZHANG X. F., DONG X. L., HUANG H., LIU Y. Y., WANG W. N., ZHU X. G., LV B., LEI J. P., & LEE C. G. 2006. Microwave absorption properties of the carbon-coated nickel nanocapsules. *Applied Physics Letter*, 89, 053115.

[2] LIU X. G., FENG C., OR S. W., SUN Y. P., JIN C. G., & Li W. H. 2013. Investigation on microwave absorption properties of CuO/Cu_2O-coated Ni nanocapsules as wide-band microwave absorbers. *RSC Advances*, 3, 14590-14594.

[3] YOUSSEF J. & BROSSEAU C 2006, Magnetization damping in two-component metal oxide micropowder and nanopowder compacts by broadband ferromagnetic resonance measurements. *Physics Review B*, 74, 214413.

Acceptance ID: HS9X-P

Design and full wave analysis of compact ultra-wide-band graphene based tunable band-pass filter

Neetu Joshi[1, a], *Nagendra P. Pathak*[2, b]

[1, 2]*Department of Electronics & Comm. Engg.*
Indian Institue of technology, Roorkee
Roorkee, India
[a]*neetu_sec@rediffmail.com*
[b]*nagppfec@iitr.ac.in*

This paper presents the design and simulation of a simple tunable band-pass filter based on graphene in the terahertz frequency regime. The tunability properties can be achieved with the help of change in the material properties like chemical potential, relaxation time, etc. which can be varied with the external bias voltage. The characteristic impedance values are high in the range of k**Ω** as compared to non-graphene plasmonic waveguides.

Keywords: graphene; terahertz; filter; tuning.

Acceptance ID: JGG3-O

AlGaN-based DUV microdisk lasers on Si

Y. Zhang[1a], P. Li[2], A. Dehzangi[1], L. Wang[2], H. Li[3], X. Yi[2], G. Wang[2]

[1] Department of Electrical Engineering and Computer Science, Northwestern University, Evanston, Illinois 60208, USA

[2] Institute of Semiconductors, Chinese Academy of Sciences, Beijing 10083, China

[3] Materials Department, University of California, Santa Barbara, California 93106, USA

[a]yiyun.zhang@northwestern.edu

We demonstrate optically-pumped single-mode deep-ultraviolet lasing operating at room temperature from ~1-μm 150nm-thick undercut microdisk resonators with AlN/$Al_{0.35}Ga_{0.65}N$ (5.5nm/2.5nm) MQWs on Si platform. The lasing mode centers at ~300.1nm with a linewidth of ~1.0nm as the excitation exceeds the lasing threshold as low as ~24.2 mJ/cm^2. The quality factor is about ~300. An emission coupling factor (β) of ~0.92×10^{-2} is estimated based on the light output characteristics of the AlN/AlGaN microdisks with increasing the pumping densities. The lasing peaks are attributed to fundamental-order TE whispering-gallery modes (WGMs), confirmed by 3D FDTD simulations.

The process flow of fabricating the undercut microdisk cavities can be found in the **Fig. 1**. Similar processing techniques can be referred in our previous studies. [1] **Fig. 2** shows the 1-μm undercut AlN/AlGaN-based microdisks supported on Si from a tilted angle of 75 degree. By zoom-in SEM image, we can observe a very smooth sidewall of the fabricated microdisk cavities, which plays a critical role in achieving excellent optical confinement of the microdisk cavities for whispering-gallery modes (WGMs) with lower light-scattering loss at the disk edge. **Fig. 3** demonstrates room-temperature PL spectra from AlGaN microdisk with excitation energy densities below and above the lasing threshold. When the excitation densities are low, it can be clearly identified the emission from AlGaN MQWs centers at 305.3nm, with a bandwidth about 28.4nm. Above the E_{th} of 24.2mJ/cm^2, the spectral peak at a center wavelength of ~300.1 nm becomes sharp and dominant throughout the PL spectra, with a linewidth of ~1.0nm. Inset shows the xy-plane electric-field energy intensity patterns of first-order WGM (TE) at ~301nm from the 3D-FDTD simulations. This work presents a significant step forwards to achieve single-mode operating microdisk lasers on Si with emitting wavelengths reaching UVB range by using the AlGaN MQWs as the gain mediums. It is also promising to serve as efficient deep UV coherent light sources for the photonic integration of the nitride-based semiconductor devices on Si platform.

Keywords: AlGaN-based microdisk resonators; Whispering-gallery modes; Deep-ultraviolet lasing;

References

[1] Y. Zhang, Z. Ma, X. Zhang, T. Wang, and H. W. Choi, Appl. Phys. Lett. Vol. 104 (2014), p. 221106.

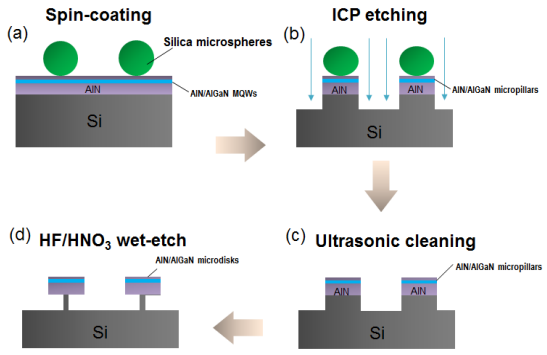

Fig. 1 Fabrication process flow of AlGaN-based microdisk lasers on Si.

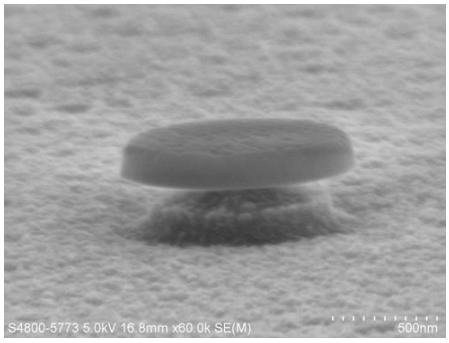

Fig. 2 A single AlGaN-based undercut microdisk resonator on Si.

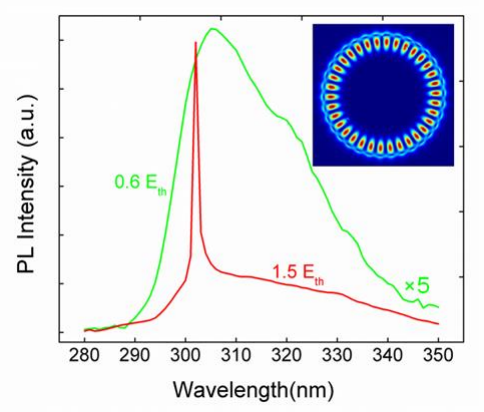

Fig. 3 PL spectra from the AlGaN microdisk below and above the lasing threshold.

Acceptance ID: KU7M-P

Earthicle: A Conceptually New Type of Composite Particle

Vuk Uskoković[1,2]

[1] *Department of Biomedical and Pharmaceutical Sciences, Center for Targeted Drug Delivery, Chapman University, Irvine, CA 92618-1908, USA*
[2] *Department of Bioengineering, University of Illinois, Chicago, IL 60607-7052, USA*

**Corresponding author: uskokovi@chapman.edu; uskok@uic.edu.*

Composite, multifunctional fine particles are bound to be at the frontier of materials science for any foreseeable length of time. We have recently pioneered a conceptually new type of submicron composite particle also known as earthicle. Earthicle roughly mimics the stratified structure of the Earth, having a zero-valent iron core, silicate/silicide mantle and an atomically thin carbon crust resembling the biosphere and its geological remnants. It is synthesized using precipitation from aqueous solutions and pyrolysis of citric acid. The ratio between the thicknesses of the metallic core, the silicate mantle and the carbon crust is similar to that between the core, the mantle and the crust of the Earth. The size of the earthicles ranged from 60 to 500 nm depending on the ionic concentration of the precursors and additives. Particles were formulated in a stable colloidal form and made to interact with various types of healthy and cancer cells in 2D and 3D *in vitro* models to observe the uptake, the subcellular localization and the effects on viability and morphology. Silica layer typically increased the biocompatibility of the metallic core, but the further addition of the carbonic layer reduced it compared to silica-coated iron. Results of cell culture assays carried out in an alternate magnetic field (312.75 A/m, 1 MHz) suggested that earthicles could be used for hyperthermia treatments, although their properties should be optimized for a more intense effect. A single-cell immunofluorescent analysis of the interaction of earthicles with primary fibroblasts and cancer cells demonstrated that the cell uptake and perinuclear localization are responsible for the necrotic effect. This analysis also showed that composite $Fe/SiO_2/C$ particles may have the ability to cause the rupture of the cancer cell nucleus while having a harmless effect on the primary cells. Such a selective anticancer activity is promising from the point of view of the intended use of earthicles for tumor targeting across the blood-brain barrier.

Acceptance ID: LJ6C-O

Direct Chemical Vapor Deposition Growth and Band Gap Characterization of MoS_2/*h*-BN van der Waals Heterostructures on Au Foils

Zhepeng Zhang,[1] *Zhongfan Liu,* [1] *Yanfeng Zhang,*[*,1,2]

[1] *Center for Nanochemistry (CNC), Beijing Science and Engineering Center for Nanocarbons, Beijing National Laboratory for Molecular Sciences, College of Chemistry and Molecular Engineering, Academy for Advanced Interdisciplinary Studies, and* [2] *Department of Materials Science and Engineering, College of Engineering, Peking University, Beijing 100871, P. R. China*

[*] *Address correspondence to Yanfeng Zhang (yanfengzhang@pku.edu.cn)*

Stacked transition-metal dichalcogenides on hexagonal boron nitride (*h*-BN) are platforms for high-performance electronic devices. However, such vertical stacks are usually constructed by the layer-by-layer polymer-assisted transfer of mechanically exfoliated layers. This inevitably causes interfacial contamination and device performance degradation. Herein, we develop a two-step, low-pressure chemical vapor deposition synthetic strategy incorporating the direct growth of monolayer *h*-BN on Au foil with the subsequent growth of MoS_2. In such vertical stacks, the interactions between MoS_2 and Au are diminished by the intervening *h*-BN layer, as evidenced by the appearance of photoluminescence in MoS_2. The weakened interfacial interactions facilitate the transfer of the MoS_2/*h*-BN stacks from Au to arbitrary substrates by an electrochemical bubbling method. Scanning tunneling microscope/spectroscopy characterization shows that the central *h*-BN layer partially blocks the metal-induced gap states in MoS_2/*h*-BN/Au foils. The work offers insight into the synthesis, transfer, and device performance optimization of such vertically stacked heterostructures.

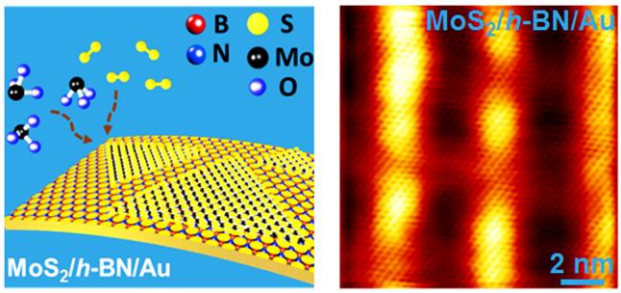

Acceptance ID: MLG4-P

Hybrid polariton bands in organic-dye-doped nanostructures

Ru-Wen Peng, Kun Zhang, Yue Xu, Wen-Bo Shi, and Mu Wang*

National Laboratory of Solid State Microstructures, School of Physics, and Collaborative Innovation Center of Advanced Microstructures, Nanjing University, Nanjing 210093, China

Recently controlling light-matter interactions by nanostructures has attracted much attention, due to both fundamental interests and practical applications. In this work, we present the possibilities to realize hybrid light-matter interactions, which can effectively achieve hybrid polariton bands in organic-dye-doped nanostructures. We demonstrate experimentally the hybrid coupling among molecular excitons, surface plasmon polaritons (SPPs), and Fabry-Perot (FP) mode in a nanostructured cavity, where a J-aggregates doped PVA (polyvinyl alcohol) layer is inserted between a silver grating and a thick silver film. By tuning the thickness of the doped PVA layer, the FP cavity mode efficiently couples with the molecular excitons, forming two nearly dispersion-free modes. The dispersive SPPs interact with these two modes while increasing the incident angle, leading to the formation of three hybrid polariton bands. By retrieving the mixing fractions of the polariton band components from the measured angular reflection spectra, we find all these three bands result from the strong coupling among SPPs, FP mode, and excitons. Besides, we have also experimentally explored multimode photon-exciton coupling in an organic-dye-attached photonic quasicrystal. We show hybrid strong coupling between multiple photonic modes and excitons in an organic-dyeattached photonic quasicrystal. The excitons effectively interact with the photonic modes offered by the photonic quasicrystal, and multiple hybrid polariton bands are verified in both experiments and calculations. Our investigations may inspire related studies on hybrid light-matter interactions, and achieve potential applications on multimode polariton lasers and optical spectroscopy.

References:

1) Kun Zhang, Wen-Bo Shi, Di Wang, Yue Xu, Ru-Wen Peng, Ren-Hao Fan,

Qian-Jin Wang, and Mu Wang,

Appl. Phys. Lett. (2016) **108**, 193111.

2) Kun Zhang, Yue Xu, T. Y. Chen, Hao Jing, W. B. Shi, Bo Xiong, Ru-Wen Peng, and Mu Wang,

Optics Letters (2016) **41**, 5740.

*Email: rwpeng@nju.edu.cn

Acceptance ID: MTNX-O

Negative resistive characteristics of low dimension thin film transistors

Teresa Oh[1]

[1]*Department of Semiconductor Engineering, Cheongju University, Cheongju, Chungbukdo, South Korea*
E Mail : teresa@cju.ac.kr

This reports the high stability and mobility in amorphous oxide semiconductors due to the high Schottky barriers (SB) with the deep depletion region. An effect of Schotty barriers and electrical behaviors in a depletion layer of indium-gallium-zinc-oxide (IGZO) thin film deposited on SiOC gate insulators was investigated. The Schottky potential barrier as a depletion region was in inverse proportion to the drain potential. The tunneling phenomenon in IGZO/SiOC transistors was showed the ambipolar characteristics with decreasing the drain potential, but the trapping conduction was observed the n-type characteristics owing to the majority carriers with increasing the drain potential. The unipolar performance of n-type characteristics improved with increasing the drain voltage, in spite of the ambipolar properties had good performance in the lower drain voltage. The current at the common Ohmic contact increased with increasing the annealing temperature but the Ohmic contact by diffusion currents showed the current decreased with increasing the annealing temperature owing to the SB.

Keywords: XPS, Oxygen vacancy, Depletion region, Ohmic contact, Schottky contact.

[1] T. Oh, EML, 11. 853-86 (2015).

Acceptance ID: MWUU-P

Correlated 2-dimensional fermionic materials for attojoule-per-bit computation

Pouya Dianat[1] and Bahram Nabet[2]

[1]Center for Quantum Devices, Northwestern University, 633 Clark St, Evanston, IL 60208 USA
pouya.dianat@northwestern.edu
[2]Department of Electrical and Computer Engineering, Drexel University, 3141 Chestnut St, Philadelphia PA 19104 USA
nabet@ece.drexel.edu

A quantum capacitor is described for low-power logic operations with ~9aJ/bit energy and fast photodetection based on "plasmorons," unbounded by transport limitations. These are achieved by optoelectrical exploitation of quantum-exclusive energies of interacting 2D hole plasma.

OCIS Codes: (250.0250) Optoelectronics; (040.5570) Quantum Detectors; (200.0200) Optics in Computing

References

[1] D. A. B. Miller, "Sorting out light," Science 347, 1423-1424 (2015)
[2] D. A. B. Miller, " Attojoule Optoelectronics for Low-Energy Information Processing and Communications: a Tutorial Review," ArXiv e-prints 1609.05510, (2016)
[3] P. Dianat, A. Persano, F. Quaranta, A. Cola, B. Nabet, "Anomalous Capacitance Enhancement Triggered by Light," IEEE JST Quantum Electronics 21, 228-232 (2015)
[4] P. Dianat, R. W. Prusak, A. Persano, F. Quaranta, A. Cola, B. Nabet, "An Unconventional Hybrid Variable Capacitor with a 2-D Electron Gas," IEEE Trans. Electron Device 61 (2), 445-451 (2014)
[5] R. Kuttappa, L. Khuhn, B. Nabet,, B. Taskin, "Reconfigurable Threshold Logic Gates using Optoelectronic Capacitors" Design, Automation and Test in Europe (DATE), Lausanne, Switzerland, March 27-31, 2017.
[6] B.I. Lundqvist, "Single-particle Spectrum of Degenerate Electron Gas," Phys. Kondens. Materie 6, 193-205 (1967)
[7] O. E. Dial, R. C. Ashoori, L. N. Pfeiffer, K. W. West, "Observation of Plasmarons in a 2-dimensional system: Tunneling Measurement Using Time Domain Capacitance Spectroscopy," Phys. Rev. B 85, 081306(R) (2012)
[8] R. Jalabert and S. Das Sarma, "Many-polaron interaction effects in two-dimensions," Phys. Rev. B 39, 5542(R), (1989)

Acceptance ID: N2LB-O

Investigation of Radiation Effects in Silicon Carbide

Chaohui He, Hang Zang, Daxi Guo, Jianqi Xi

School of Nuclear Science and Technology, Xi'an Jiaotong University, Xi'an, 710049, China

Silicon carbide(SiC) is a promising material for nuclear application and microelectronic devices, facing neutron and heavy ion irradiation. Irradiation inevitably introduces defects into the SiC, which leads to degradation in performance. The primary damage states and the production of He and H by neutrons with the spectra of fusion reactor (ITER first wall under DT and DD operation), the high temperature gas-cooled reactor (HTGR) and high flux isotope reactor (HFIR) were computed and compared. With the same neutron fluence, the DD and DT spectra lead to similar displacement damage which is higher than those of the HTGR and the HFIR spectra. The production of He and H in the HTGR and the HFIR are comparable, while much higher gas production is obtained in the case of fusion spectra. A new method to compare the neutron and heavy ion irradiations was introduced to study the feasibility to emulate the 14MeV neutrons irradiation by low energy ions. To best fit the 14MeV neutron irradiation, a scheme of mixed-ion irradiation was proposed and the weighted primary recoil spectra at the Bragg peak region of the mixed-ion irradiation was calculated. The impact of different kinds of point defects on the volumetric swelling and elastic modulus of 3C-SiC were studied and results show that there are two different mechanisms for the swelling and Young's modulus. A framework of multi-scale modeling is developed to investigate the long-term evolution of displacement damage induced by heavy-ion irradiation in SiC. The annealing behavior of isolated point defects and cascade damage is found to be similar, which indicates that the influence of spatial correlation in primary damage is insignificant for SiC, when the damage dose is high enough. 6H-SiC were irradiated by 4 MeV Kr-ions, with irradiation fluences from 1.0×10^{16} to 5.0×10^{16} cm^{-2} at room temperature, 300℃ and 500℃ respectively (5.0×10^{16} cm^{-2} at 550℃). The irradiation-induced swelling was strictly measured by X-ray Diffraction (XRD) and 3D surface profile. The swelling strongly depends on the irradiation temperature and the ion fluence. The surface of RT-irradiated samples became rough as a result of crystallizing to amorphous state and no significant modification of surface is observed at 300℃ and 550℃ irradiation. He and Kr cavities with a wide range of size distributions are observed in He^{2+}, Kr^{15+} and He^{2+} + Kr^{15+} ion-implanted polycrystalline 3C-SiC around their depth profiles following thermal annealing at 1600˚C. Processes involving He-vacancy interactions, He trapping and He aggregation at vacancy sites are responsible for nucleation and growth of He cavities in SiC at 1600˚C.

Key words: Silicon carbide, radiation effects, long-term defect evolution
Acceptance ID: N3AP-O

Self-assembly of adenine-silver nanoparticles forms rings resembling the size of cells

*Sungmoon Choi, Soonyoung Park, and Junhua Yu**

Department of Chemistry Education, Seoul National University, 1 Gwanak-Ro, Gwanak-Gu, Seoul 08826, South Korea

** To whom correspondence should be addressed. Tel: +82-2-889-9159; Fax: +82-2-889-0749; Email: junhua@edu.ac.kr*

Supramolecular chemistry may have played critical roles in the origin of life. Mineral surface adsorption and catalysis of molecules leads to their evolution and the accumulation of prebiotic materials. While researchers focus on the contribution from light metal derivatives to prebiotic chemistry, heavy metals are rarely considered. The heavy metals have been existed on primitive Earth and we cannot exclude the possible contribution of heavy metals to the origin of life on primitive Earth. But why are they not reflected in modern life? Here we show that, with the interactions between silver and nucleobases as a model, ssDNA oligomer-stabilized silver nanoparticles and adenine self-assemble to form ring-like compartments similar to the size of modern cells, especially when the aqueous solution of such a mixture undergoes drying on a glass surface. However, the silver ions only dismantle the self-assembly of adenine. The membrane-like edge of the ring is composed of adenine filaments glued together by silver nanoparticles. Interestingly, chemicals are confined and accumulated inside the ring, suggesting that this might be an alternative to the compartmentalization of bioactive molecules by the lipid bilayer in the origin of life.

Acceptance ID: N469-O

Photovoltage Enhancement in Twisted-Bilayer Graphene using Surface Plasmon Resonance

Wei Xin, Zhi-Bo Liu, Xiao-Qing Yan, Xu-Dong Chen, Jian-Guo Tian*

The Key Laboratory of Weak Light Nonlinear Photonics Ministry of Education
Teda Applied Physics Institute and School of Physics, Nankai University, Tianjin 300071, China
E-mail: rainingstar@nankai.edu.cn

The development of novel two-dimensional materials however has revealed graphene-based photodetectors as potential alternatives, with competitive ultra-fast operating speeds (10^2 GHz) and an ultra-wide spectral response (300 nm-6 μm). However, a low external quantum efficiency and the mere 2.3% absorption of monolayer graphene, remain a limiting challenge to practical applications of graphene photodetectors. To solve this problem, graphene has been combined with other two-dimensional materials or nanomaterials to increase the optical absorption, such as in graphene-MoS_2, graphene-ZnO nanorods, and graphene-quantum dots. For a pure graphene photodetector, enhancement of the graphene-light interaction has been realized by two methods: localized field enhancement (surface plasmon resonance-based graphene photodetector) and interaction-distance increase (graphene-Bragg-mirror-microcavity type photodetector, graphene-silicon waveguide photodetector). Here, using a traditional Kretschmann configuration, we integrate two gold thin films with different graphene samples (monolayer, bilayer, trilayer, 10.0° TBG and 12.0° TBG) and place them on a quartz rectangular-prism to form typical MGM architecture photodetectors. Analyzing the photoresponse as a function of graphene layer number or twist angle, we find that photovoltage is a more useful parameter than photocurrent as a more reasonable physical parameter for characterizing the photoelectric response of graphene in MGM architectures. More importantly, we combine an optimization of layer number, twist angle, and SPR enhancement to produce a 700% increase in the photovoltage of TBG over normal-incidence-type MLG.

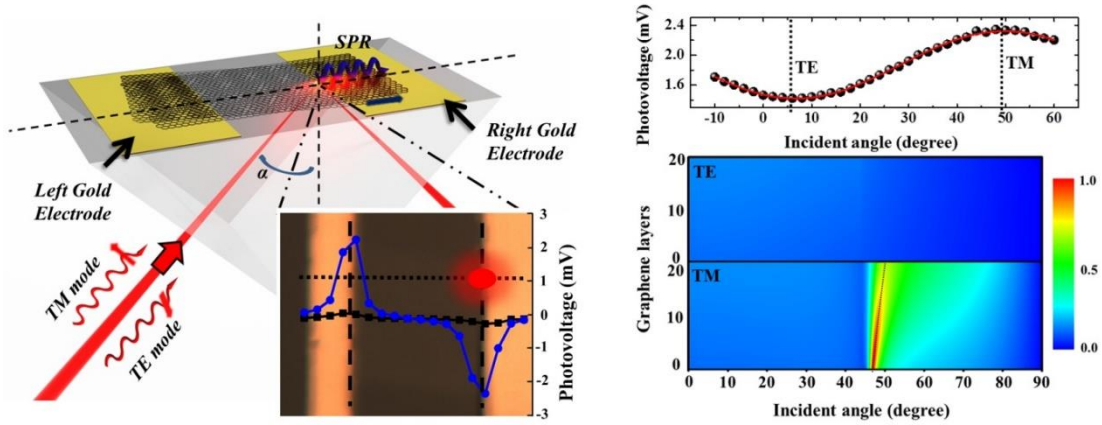

Acceptance ID: NFZQ-P

Calculation of the enhanced thermoelectric Seebeck coefficient of two-dimensional electron gas at the $SrTiO_3$ (001) surface

C. Jaisuk[1], *P. Moontragoon*[2], *T. Eknapakul*[1], *S.-K. Mo*[3], *S. Pinitsoontorn*[2], *P.D.C. King*[4], *and W. Meevasana*[1]

[1] *School of Physics, Institute of Science, Suranaree University of Technology, Nakhon Ratchasima, 30000, Thailand*
[2] *Department of Physics, Faculty of Science, Khon kaen University, Khon kaen, 40002, Thailand*
[3] *Advanced Light Source, Lawrence Berkeley National Laboratory, Berkeley, CA 94720, USA*
[4] *School of Physics and Astronomy, University of St. Andrews, St. Andrews, Fife KY16 9SS, United Kingdom*
E Mail: chut.jaisuk@gmail.com

Two-dimensional electron gas (2DEG) at the interface between the insulating oxides $LaAlO_3$ and $SrTiO_3$ has displayed many interesting properties such as superconductivity and magnetic effect. Relating to these 2DEGs at the interface between two oxides, many studies have also focused on the enhanced thermoelectric effect at superlattices (crystalline layers of modulated dopings) after the suggestion by Hicks, et al. [1]. It was found that a high-density 2DEG confined within a unit cell of $SrTiO_3$ shows large thermoelectric Seebeck coefficient, S [2]. This S value could be 5-fold larger than the value in bulk while high conductivity was maintained at this performance. In this work, by using Boltzmann transport equations, we have performed realistic calculation of Seebeck coefficient based on the experimentally-extracted band structure. We have used the electronic structure of the two dimensional electron gas (2DEG) at the (001) surface of $SrTiO_3$ measured by angle-resolved photoemission spectroscopy (ARPES) (from our previous study [3]) and then calculate the tight binding parameters correspondingly to the experimental data. In general, we have found that the Seebeck coefficient can increase upon decreasing of the confined length. We will also discuss about how to estimate the renormalization effect (e.g. electron-phonon coupling) and how this renormalization factor enhances the Seebeck further (where the test calculation in bulk form can be shown to be in agreement with previous studies).

Keywords: thermoelectric Seebeck coefficient, two-dimensional electron gas, $SrTiO_3$

[1] HICKS, L. D. & DRESSELHAUS, M. S. 1993. Effect of Quantum-Well Structures on the Thermoelectric Figure of Merit. Physical Review B, 47(19), 12727.

[2] OHTA, H., KIM, S., MUNE, Y., MIZOGUCHI, T., NOMURA, K., OHTA, S., NOMURA, T., NAKANISHI, Y., IKUHARA, Y., HIRANO, M., HOSONO, H. & KOUMOTO, K. 2007. Giant Thermoelectric Seebeck Coefficient of a Two-Dimensional Electron Gas in $SrTiO_3$. Nature Materials, 6(2), 129-134.

[3] MEEVASANA, W., KING, P. D. C., HE, R. H., MO, S. K., HASHIMOTO, M., TAMAI, A., SONGSIRIRITTHIGUL, P., BAUMBERGER, F. & SHEN, Z. X. 2011. Creation and Control of a Two-Dimensional Electron Liquid at the Bare $SrTiO_3$ Surface. Nature Materials, 10(2), 114-118.

Acceptance ID: P6VA-O

Thermally-induced Strain on graphene/MoS_2 and graphene/h-BN hybrid structures

*Seunghwan Kim[1], Sooho Choi[1], Moon-Deock Kim[2], Tae Geun Kim[3], and Woochul Yang[1]**

[1]Deparment of Physics, Dongguk University, Seoul 04620, Korea
[2]Department of Physics, Chungnam National University, Daejeon 305-764, Korea
[3]School of of Electrical engineering, Korea University, 02841, Korea
** E-mail address: wyang@dongguk.edu*

Two-dimensional (2D) materials are attractive because they have excellent carrier mobility, flexibility, and transparency for novel device applications. Among the 2D materials, the graphene is the most well-known material due to outstanding electrical, mechanical and optical properties [1]. In order to utilize these properties for various device applications, the fabrication of graphene-based hybrid structures was suggested by many groups. For instance, molybdenum disulfide (MoS_2) is one candidate for 2D material hybrid structures. Graphene/MoS_2 hybrid structure was proposed to use for high performance photo-devices [2, 3]. The transfer and annealing processes are required to obtain a high quality-hybrid structure. However, the annealing process can give rise to damaging to graphene-based hybrid structures owing to thermal expansion coefficient mismatch between hybrid materials.

In this study, we investigate strain effect of thermal process on the graphene/MoS_2 and graphene/hBN hybrid structures during annealing from 100 °C to 250 °C under H_2/Ar mixture gas atmosphere and ambient pressure. Graphene, MoS_2, and h-BN flakes were grown by using chemical vapor deposition (CVD) and hybridized by conventional transfer method. After annealing of the hybrid structures, AFM and Raman measurements were performed to characterize the morphology and structure. Raman measurements showed that G and 2D peaks of the graphene in graphene/MoS_2 were red-shifted. The Raman shifts indicates that a graphene was received tensile strain in the hybrid structure. However, a graphene was given compressive strain after annealing at 200 °C. Furthermore, the morphology of graphene in graphene/MoS_2 hybrid structure was changed rapidly. On the other hand, Raman peak positions of graphene in graphene/hBN hybrid indicated compressive strained graphene after annealing process at various temperatures. The strain information of the 2D materials' hybrid structures during synthesized process will be fruitful to fabricate hybrid structure-based novel devices.

References

1. A. H. Castro Neto, F. Guinea, N. M. R. Peres, K. S. Novoselov and A. K. Geim, *Rev. Mod. Phys.* 81, 109 (2009)
2. C. H. Liu, Y. C. Chang, T. B. Norris and Z. Zhong, *Nat. Nanotechnol.* 9, 273 (2014)
3. W. Zhang, C. P. Chuu, J. K. Huang, C. H. Chen, M. L. Tsai, Y. H. Chang, C. T. Liang, Y. Z. Chen, Y. L. Chueh, J. H. He, M. Y. Chou and L. J. Li, *Sci. Rep.* 4, 03826 (2014)

Acceptance ID: P83V-P

Enhancing the magnetocaloric effect of Ni-Mn-Ga alloys through size effect

Mingfang Qian[a], Xuexi Zhang[a,], Xinhao Wan[a], Hehe Zhang[a], Huan Wang[b], Faxiang Qin[b], Lin Geng[a], Hua-Xin Peng[b]*

[a] *School of Materials Science and Engineering, Harbin Institute of Technology, Harbin 150001, China*
[b] *Institute for Composites Science Innovation (InCSI), School of Materials Science and Engineering, Zhejiang University, Hangzhou, 310027, PR China*
[*] *Corresponding author. Tel: 86-451-86415894, Fax: 86-451-86413921, E-mail: xxzhang@hit.edu.cn*

The microstructure, magentostructural transition behavior, hysteresis loss and the magnetocaloric effect (MCE) of the Ni-Mn-Ga single crystalline powders were demonstrated in the present work. Powders with size ~38.5-45 μm were prepared and normally annealed. Different from our previous work in the Ni-Mn-Ga microwires, the effect of chemical ordering annealing at 998 K on the magnetization of the powders showed not much improvement than that of the stress relief annealing at 773 K, implying less defects and atomic disorder in the as-ground powders. The hysteresis losses of both bulk and powder alloy were examined. A much smaller thermal hysteresis of ~1.3 K and negligible average magnetic hysteresis loss of ~ 1.9 J/kg were obtained compared to that of the bulk alloys of ~4.6 K and ~9.7 J/kg, respectively. The reduction of neighboring grain constraints on volume change during martensitic transformation was considered to be the main reason to understand the observed phenomena. A magnetic entropy change (ΔS_m) peak of ~6.8 J/kgK with full width at half maximum (δ_{FWHM}) of ~21K was attained at ~315K, yield a high refrigerate capacity (*RC*) value of ~115 J/kg. The broad peak was shown to appear mainly due to the partly overlapped magnetostructrual transition state in the powders. The increased surface area of the Ni-Mn-Ga favored the composition variation during vacuum annealing that enlarged the martensitic transformation (MT) range also enhanced the δ_{FWHM}. These experiments clearly show that there are two essential ingredients to observe the high broad peak and low hysteresis loss: partly overlapped magnetostructural transition and the surface effect of the small-sized single crystalline powder. Based on these results a possible approach for the high magnetic refrigeration efficiency is expected and discussed.

Acceptance ID: pJJY-O

High-index GaAs substrates for nanoscale Y-junctions self-assembling

Esteban Cruz-Hernandez

CIACYT-UASLP
echzeroth@gmail.com

Self-assembling of complex nanostructures such as Y-junctions is a significant issue hindering potential technological applications and one-dimensional (1D) Physics exploration. In this contribution we report on the observation of high-order and two-dimensional mechanisms in the Molecular Beam Epitaxy faceting on high-index GaAs substrates. These mechanisms allow the formation of a regular alternating pattern of bifurcated structures, the Y-junctions. Our findings indicate that a subjacent long-range elastic interaction (of lateral period 695 nm) is behind the formation of the Y-structures of lateral period 60 nm and up to 35 μm long. Finally, we discuss the potential use of the bifurcated structures to study one-dimensional electronic transport and as a viable alternative to carbon nanotubes Y-junctions for nanoelectronics applications such as ballistic switching and rectification.

Acceptance ID: PUYG-O

Transfer Printing Gold Nanoparticle Arrays by Tuning the Surface Hydrophilicity of Thermo-Responsive pNIPAAm

Sirous (Khabbaz Abkenar)[1], *Ali (Tufani)*[1], *G. (Ozaydin Ince)* [1,2], *Hasan (Kurt)*[1], *Ayse (Turak)*[3], *and Cleva W. (Ow-Yang)*[1,2]

[1] *Materials Science and Nano-Engineering Program, Sabanci University, Orhanli, Tuzla, 34956 Istanbul, Turkey.*
[2] *Nanotechnology Application Center, Sabanci University, Orhanli, Tuzla, 34956 Istanbul, Turkey.*
[3] *Department of Engineering Physics, McMaster University, Hamilton, Ontario L8S 4L8, Canada.*
cleva@sabanciuniv.edu

Processes for integrating precise 2-D arrangements of colloidal nanoparticles into organic electronic devices tend not to be universally suitable across the broad spectrum of substrates of choice, rendering it necessary to first deposit the array onto a sacrificial substrate and then transfer it to a target one. Although many approaches have been developed to address the transfer by chemical and mechanical means [1], we sought a solution to transfer a deterministically assembled array of gold nanoparticles formed by polymeric templating, while retaining the geometry-dependent plasmonic properties arising from cooperative behavior [2] in a monolayer of ordered nanoparticles. Thus, we have developed a new method for transferring 2-D gold nanoparticle (NP) arrays based on a thermo-responsive polymer, poly-N-isopropylacrylamide (pNIPAAm), coating on a polydimethylsiloxane stamp [3]. We demonstrate the transfer of NP arrays between silicon wafer substrates with the preservation of array characteristics to within 15%, spanning areas of several microns. Through wetting contact angle analysis, atomic force microscopy, and spectroscopic ellipsometry, we show that adhesion between the NP array and the pNIPAAm surface is tuned via the temperature-dependent hydrophilicity of the pNIPAAm surface—*i.e.*, from a more hydrophilic surface for pick up at 5 °C to a less hydrophilic character for release at 50 °C. For validating the utility of this transfer process, we demonstrate integration of the transferred gold NP arrays into demonstrator bulk heterojunction organic solar cells, showing efficiency enhancement from the transferred plasmonic interlayer superior to similar cells containing anodes modified by directly templated gold NP arrays [4].

Keywords: transfer printing, nanoparticle array, poly-N-isopropylacrylamide (pNIPAAm), plasmonic solar cell

[1] CARLSON, A., BOWEN, A.M., HUANG, Y., NUZZO, R.G. & ROGERS, J.A. 2012. Transfer Printing Techniques for Materials Assembly and Micro/Nanodevice Fabrication, *Adv. Mater.*, 24, 5284–5318.

[2] TOK, U., OW-YANG, C.W. & SENDUR, K. 2011. Unidirectional broadband radiation of honeycomb plasmonic antenna array with broken symmetry, *Optics Express*, 19, 22731-22742.

[3] KHABBAZ ABKENAR, S., TUFANI, A., OZAYDIN INCE, G., KURT, H., TURAK, A. & OW-YANG, C.W. *under review*, Transfer Printing Gold Nanoparticle Arrays by Tuning the Surface Hydrophilicity of Thermo-Responsive Poly N-isopropylacrylamide (pNIPAAm).

[4] KURT, H., OW-YANG, C.W. 2016. Impedance Spectroscopy Analysis of the Photophysical Dynamics due to the Nanostructuring of Anode Interlayers in Organic Photovoltaics, *Phys. Status Solidi A*, 213, 3165-3177.

Acceptance ID: PVER-O

Fluorescent Carbon nanoparticles for Single Molecule Imaging

*N. C. Verma, S. Khan, C. Rao, A. Gupta, C. K. Nandi**

Indian Institute of Technology Mandi, Kamand, Himachal Pradesh, India.
*E Mail :navneetcverma@gmail.com, chayan@iitmandi.ac.in**

The single molecule fluorescence-based optical nanoimaging involves sequential localization of photoswitchable fluorophores to achieve the resolution beyond the optical limit of diffraction. A bright, photoswitchiable fluorescence probe is a primary requirement for this process. The fluorescent carbon nanoparticles or nano-dots (CNDs) are easy to synthesis, non-toxic and cell penetrable nano-materials. These carbon based nanomaterials provide us new alternatives among the existing fluorophores due to their superior optical properties such as excitation dependent multicolor fluorescence emission. Very few reports are available regarding the single moleculer properties of CNDs, among them single molecule blinking based super resolution imaging is rare in literature. We achieved revrsiable photoswitching in CNDs with red emission using an electron transfer mechanism. The CNDs can be switched between dark and bright state under exposure of red and blue light respectively by formation of cationic dark state. The natural fluorescence switching of the CNDs can be tuned using an electron acceptor or donor molecule. We characterized the single molecule fluorescence of three CNDs and observed that all of them showed a long lived dark state in presence of an electron acceptor. The average on-off rate in between fluorescent bright and dark state, which is one of the important parameter for single molecule localization based super resolution microscopy, were measured by changing the laser power. We observed that the photon budget and on-off rate of these CNDs are good enough to get single molecule localization with a precision of ~35nm. On the other hand, the CNDs assembled in CTAB-DAO artificial templates exhibit stochastic fluorescence on−off switching, due to the excited state electron transfer reaction, under single laser excitation in the visible range. The distribution of CNDs in the periphery of these templates enables optical nanoimaging of these templets at an average resolution of 80-nm. The CNDs can be used for optical nanoimaging of the self-assembly of such artificial nanostructures with sub-diffraction resolution. These CNDs can be surface modified by different functional groups for specific binding and our group is working to develop it further for the advance bioimaging applications.

Keywords: Carbon dots, nano imaging, photoswitch, stochastic blinking, electron transfer mechanis.

[1] VERMA, N. C., KHAN, S., NANDI, C. K. 2016. Single Molecule Analysis Of Fluorescent Carbon Dots Towards Localization Based Super-Resolution Microscopy. Methods and Applications in Fluorescence 4,4, 044006.

[2] KHAN, S., VERMA, N. C., GUPTA, A., NANDI, C. K. 2015. Revearsiable Photoswitching of Carbon Dots. *Scientific reports*, 5, 11423.

[3] KHAN, S., GUPTA A, VERMA N. C, NANDI, C. K. 2015. Time-Resolved Emission Reveals Ensemble of Emissive States as the Origin of Multicolor Fluorescence in Carbon Dots. *Nano letters* 15 , 12, 8300-8305.

[4] GUPTA, A., VERMA, N. C., KHAN, S., NANDI, C. K. 2016. Carbon Dots for Naked Eye Colorimetric Ultrasensitive Arsenic and Glutathione Detection. *Biosensors and Bioelectronics*. 81, 465-472.

[5] GUPTA, A., VERMA, N. C., KHAN, S., TIWARI, S., CHAUDHARY, A., NANDI, C. K. 2016. Paper Strip Based and Live Cell Ultrasensitive Lead Sensor Using Carbon Dots Synthesized from Biological Media. *Sensors and Actuators B: Chemical*. 232, 107-114.

[6] GUPTA, A., CHAUDHARY, A., MEHTA, P., DWIVEDI, C., VERMA, N. C., KHAN, S., AND NANDI, C. K. 2016. Nitrogen-Doped, Thiol-Functionalized Carbon Dots for Ultrasensitive Hg (II) Detection. *Chemical Communications* 51, 53, 10750-10753.

Acceptance ID: QN5J-P

Molecular dynamics simulations of carbon nanotubes and their interactions with polymers and lipids

Hwankyu Lee (Lee)[1]

[1]*Department of Chemical Engineering, Dankook University, Yongin, 16890, South Korea.*
leeh@dankook.ac.kr

We performed coarse-grained molecular dynamics (MD) simulations of the self-assembly of the mixture of single-walled carbon nanotubes (SWNTs) and different types of lipids, and the interactions between SWNTs and other molecules such as lipids, polyethylene glycols (PEGs), and lipid bilayers. The following topics will be presented: (1) effects of lipid structure and PEGylation on the self-assembly of lipids and SWNTs ; (2) interparticle dispersion, membrane curvature and penetration induced by SWNTs wrapped with lipids and PEGylated lipids ; (3) membrane penetration and curvature induced by SWNTs: the effect of diameter, length, and concentration ; (4) the effect of PEG size and grafting density on the conformational transition of PEGylated SWNTs between brush and mushroom. This work aids in the rational design of the size and grafting density of PEG chains to increase the drug-delivery efficiency for applications in nanomedicine.

Keywords: Molecular dynamics simulation, carbon nanotube, PEGylation, drug delivery

Acceptance ID: QU5M-P

Molecular Dynamics Simulation on Crossroad-Type Graphene-Resonator Accelerometer

Oh Kuen Kwon[1], Jeong Won Kang[2]

[1]Department of Electronic Engineering, Semyung University, Jecheon 390-711, Republic of Korea.
[2]Graduate School of Transportation, Korea National University of Transportation, Uiwang-si 437-763, and Department of IT Convergence, Korea National University of Transportation, Chungju 380-702, Republic of Korea.
jwkang@ut.ac.kr

Highly sensitive accelerometers have multiple applications in industry and science, and can be used as sensors in a wide variety of devices. Here, we investigate the application of crossroad-type graphene resonators as ultrahigh sensitivity accelerometers by performing classical molecular dynamics simulations. The relationships between the resonance frequencies and acceleration could be divided by two regions. The simulation data showed that when the accelerations were higher than 0.1 nm/ps^2, the resonance frequency increased with increase of the acceleration. In particular, acceleration, as a function of frequency, was regressed by a power function and shown to have a linear relationship on a *log-log* scale. Crossroad-type graphene resonators have multiple applications to nanoscale sensors, filters, switching devices, and quantum computing, as well as ultra-fast response resonators.

Acknowledgement: This research was supported by the Basic Science Research Program through the National Research Foundation of Korea (NRF) funded by the Ministry of Science, ICT and Future planning (2015R1A1A1A05027643).

Keywords: Graphene, Molecular Dynamics, Resonator

Acceptance ID: R2VS-P

Large-Scale 3D Conformal Electrode for Micro/Nano Single-Crystal Field -Effect Device

Qingxin Tang[1], Xiaoli Zhao[1], Yanhong Tong[1], Yichun Liu1[*]

[1]Key Laboratory of UV Light Emitting Materials and Technology under Ministry of Education, Northeast Normal University, Changchun 130024, P. R. China.
E Mail: tangqx@nenu.edu.cn

New generation of electronic equipments, such as flexible/elastic portable bionic electronic skin, wearing smart devices and display products in the future have a huge demand space. Organic field-effect devices have a unique advantage in these applications. Organic semiconductors have excellent physical properties, such as low density, small Young's modulus, and local jump carrier transmission mechanism. Therefore, organic electronic equipment is light weight, flexible, and can be maintained electrical performance under the conditions of deformation. However, for these new practical applications, organic devices integration is one of the major scientific issues, and is urgent to address to achieve the development of functional organic integrated circuits.

We propose a new method combining photolithographic electrode arrays with insulating layers. Large-scale electrode and device array are obtained by peeling and laminating overlap. The electrode has good flexibility and elasticity, and is as light as 4-5 g/m2. Moreover, the electrode is still maintain good electrical performance at the bending radius of 0.25 mm, the relative deformation of 180%, and can intimately fit to irregular three-dimensional objects showing potential application prospects in the stretchable electronic skin, ultra-flexible display. To verify its electrical performance, we attach the rubrene single crystal on the electrode to fabricate field-effect device. Its mobility is up to 20 cm2/Vs whether on the plane or three-dimensional spherical surface. In addition, inverter, NAND gate, and NOR gate circuit can be obtained based on a single crystal.

Keywords: three-dimensional surface, conformal, large-scale electrode, field-effect device, organic micro/nano single crystals

[1] X. L. Zhao , Y. H. Tong , Q. X. Tang*, Y. C. Liu*, “Wafer-Scale Coplanar Electrodes for 3D Conformal Organic Single-Crystal Circuits”, Advanced Electronic Materials 1(2015) 1500239. Cover paper.

Acceptance ID: RXKT-P

Organic microlasers with tunable output

Yongli Yan, Yanhui Wei, Wei Zhang, Yong Sheng Zhao

Institute of Chemistry, Chinese Academy of Sciences, Beijing 100190, China
University of Chinese Academy of Sciences, Beijing 100049, China
Email: yszhao@iccas.ac.cn

Microlasers are essential components for integrated optoelectronic devices. The abundant excited state processes in organic molecules are helpful for the design of novel laser materials and for the construction of high-performance laser devices. In addition, the unique optical properties revealed in the stimulated organic materials provide more effective means for the study of their excited state dynamics. We build the four-level energy structure via various excited state processes for the realization of microscale lasers with different functionalities. Starting from the design and synthesis of organic photofunctional molecules, we constructed microscale resonant cavities with specific structures via the controlled assembly of organic molecules, and then study their excited state processes. We achieved a type of wavelength tunable microlaser based on the encapsulation of organic dye in metal-organic frameworks (MOF), where the polarity controlled population distribution in locally excited state and intramolecular charge transfer states enables to tune the lasing wavelength over a wide range. On this basis, we tried to figure out the relationship among the molecular structures, crystal structures, excited states, and laser performances, for the final realization of multifunctional microlasers.

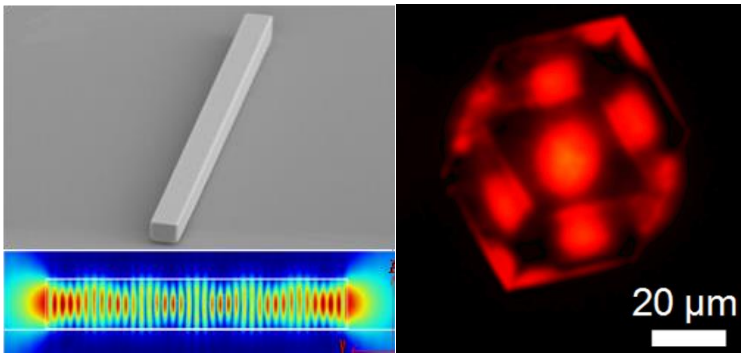

Figure 1. (left) SEM image and electric field distribution of a single organic microwire. (right) Photoluminescence image of a single dye@MOF crystral.

References

1. W. Zhang, Y. Yan, J. Gu, J. Yao, Y. S. Zhao *Angew. Chem. Int. Ed.* **2015**, *54*, 7125-7129.
2. Y. Wei, H. Dong, C. Wei, W. Zhang, Y. Yan, Y. S. Zhao, *Adv. Mater.* **2016**, *28*, 7424-7429.

Acceptance ID: RY5J-O

Room temperature hydrogen sulfide gas sensing properties using mono layer transferred MoS_2/GaN hybrid structure

Maddaka Reddeppa[1], Byung-Guon Park[1], Moon-Deock Kim[1] Woo-Chul Yang[2], Do-Jin Kim[3]*

[a]Department of Physics, Chungnam National University, Daejeon 305-764, Republic of Korea
[b]Division of Physics and Semiconductor Science, Dongguk University, Seoul 04620,Republic of Korea.
[c]Department of Materials Science and Engineering, Chungnam National University, 99 Daehang-no, Yuseong-gu, Daejeon 305-764, Republic of Korea
Corresponding author E-mail: **mdkim@cnu.ac.kr*
Tel.: +82 42 821 5452, Fax: +82 42 822 8011

In this work, room temperature H_2S gas sensing properties of monolayer transferred molybdenum disulfide (MoS_2) /GaN films were demonstrated. Comparative studies were also carried out with MoS_2 on insulating substrate and pristine GaN films. The morphological and structural analyses were measured by using atomic force microscopy and Raman spectroscopy. The gas sensing properties of pristine, MoS_2 on insulating substrate and MoS_2/GaN film were measured at different gas concentration. The MoS_2/GaN film exhibits 6 times higher responses to H_2S compared to pristine GaN film. The MoS_2/GaN film showed remarkably improved response under UV illumination. The gas sensing mechanism was explained in terms of MoS_2/GaN hetero structure band diagram. Our experimental results suggested that MoS_2/GaN hetero structure is effective way to improve the gas sensing properties.

Key words: GaN film, MoS_2 monolayer, Hetero structure, Hydrogen Sulfide, UV illumination

Acceptance ID: RZ7T-P

A Stretchable Patch-type Electrode for Long-term Bio Potential Monitoring

D. H. KWON[1], H. C. JUNG[1], S. H. LEE[1], S. A. LEE[1], A. H. KIM[1], J. H. MOON[1]

[1]Department of Research & Development, OSONG Medical Innovation Foundation, Cheonju, Republic of Korea
E Mail/ dahkwon@gmail.com

In this study, a stretchable patch-type electrode was fabricated by mix a silicon-based elastomer (Ecoflex®) with carbon nanofibers (CNFs) physically for long-term bio potential monitoring. The most commonly used silver / silver chloride (Ag / AgCl) electrode is a wet-type electrode that is dried when used for a long time, resulting in reduction of electrical conductivity and skin trouble and so on. This stretchable patch as a dry electrode was fabricated to solve these problems.

This electrode is divided into two parts as an electrode part and an adhesive part. The electrode part is mainly made from metals or nanomaterials to make stretchable conductors. When using metals, we are faced some problems such as high-cost, reactivity with oxygen, biocompatibility and so on. For these reasons the electrode part used a carbon-based nanomaterial which is excellent in mechanical and electrical characteristics. So, CNFs are selected for conductive nanomaterials because carbon nanotubes (CNTs) has trouble dispersing uniformly in elastomer compare with CNFs. The uniformly dispersed CNFs and a silicon-based elastomer were blended using an ultrasonic and a vortex mixer. Then, the electrode part is fabricated by a drop-casting method of the mixed solution. Secondly, the adhesive part was fabricated using elastomer that can be attached to skin and can be detached from skin. Then, it needs to make a hole in the center of them to insert a conventional snap. After then, the electrode part is attached to adhesive part to fabricate the stretchable patch.

As the concentration of CNFs increased, the electric conductivity improved but cracks were found. Secondly, the thickness of electrode part was important variables to obtain high-quality electrocardiograms (ECGs) signals. To make the optimal sticky patch, we tested the adhesive power by controlling the curing temperature and the thickness of adhesive part. We confirmed the biocompatibility through the cytotoxicity test and observed that skin problems such as erythema, pruritus and dermatitis were not found by long-term attaching test. Based on these results, the stretchable electrode is expected to utilize easily for long-term bio potential monitoring.

Keywords: Stretchable, CNFs, Carbon nanofibers, elastomer, patch

[1] YU, X., MAHAJAN, B. K., SHOU, W. & PAN, H. 2017. Materials, Mechanics, and Patterning Techniques for Elastomer-Based Stretchable Conductors. *Micromachines* ***2017***, 8, 7.

Acceptance ID: SFNN-P

Suppression of two-dimensional electron gases at oxide surfaces across the ferroelectric transition

P. Jaiban,[1] M.-H. Lu,[2] T. Eknapakul,[1] S.-K. Mo, [3], A. Watcharapasorn,[4] Z.-X. Shen,[5] H. Y. Hwang,[5] S. Maensiri,[1] and W. Meevasana[1]

[1]*School of Physics, Suranaree University of Technology, Nakhon Ratchasima, 30000, Thailand*
[2]*College of Engineering and Applied Sciences and National Laboratory of Solid State Microstructures, Nanjing University, Nanjing 210093, China*
[3]*Advanced Light Source, Lawrence Berkeley National Lab, Berkeley, CA 94720, USA*
[4]*Department of Physics and Materials Science, Faculty of Science, Chiang Mai University, Chiang Mai, 50200, Thailand*
[5]*Departments of Physics and Applied Physics, Stanford University, CA 94305, USA*
Email: worawat@g.sut.ac.th

The discovery of a two-dimensional electron gas (2DEG) at the $LaAlO_3/SrTiO_3$ interface has set a new platform for all-oxide electronics which could potentially exhibit the interplay among charge, spin, orbital, superconductivity, ferromagnetism and ferroelectricity. From our previous studies, by using angle-resolved photoemission spectroscopy (ARPES), we have showed that a similar 2DEG could also be formed on the bare paraelectric $SrTiO_3$ and $KTaO_3$ surfaces under exposure to intense ultraviolet irradiation [1,2]. In this work, by using this same methodology and conductivity measurement, we have studied the behavior of photon-induced 2DEGs at the bare surfaces of ferroelectric oxides: $KNb_xTa_{1-x}O_3$ (KTN) (x = 0.02, 0.03 and 0.05), $BaTiO_3$ (BTO), $Ba_{0.85}Ca_{0.15}Zr_{0.1}Ti_{0.9}O_3$ (BCZT)) and $(Ba_{0.7}Ca_{0.3})_{1-1.5x}La_xTiO_3$ (BCLT). We found that the onset of ferroelectric polarization induces a delocalization transition for the quantum well states at the surface. We propose that this suppression could be due to that the ferroelectric polarization makes the quantum well states become spatially delocalized along the direction perpendicular to the surface and hence changes the conductivity nature. This finding suggests an opportunity for controlling the 2DEG at a bare oxide surface (instead of interfacial system) by using both light and ferroelectricity.

Keywords: Electronic structure, two-dimensional electron gas (2DEG), ferroelectricity, angle-resolved photoemission spectroscopy, transition metal oxide

[1] MEEVASANA, W., et al. 2011. Creation and control of a two-dimensional electron liquid at the bare SrTiO3 surface. *Nat. Mater.*, 10, 114-118.

[2] KING, P. D. C., et al. 2012. Subband Structure of a Two-Dimensional Electron Gas Formed at the Polar Surface of the Strong Spin-Orbit Perovskite $KTaO_3$. *Phys. Rev. Lett.* 108, 117602.

Acceptance ID: SMQH-O

Synthesis of Superparamagnetic Fe3O4 Nanocrystal synthesized by Citrate Groups for Magnetically Responsive Photonic Crystals

Qianli Li[1], Xiaolei Li[1], Wei Wang[2], Ang Zheng[2] ,Yue Xu[1],Lin Zhuang[2]

[1] Department of Orthodontics, Guanghua School of Stomatology, Sun Yat-sen University, Guangzhou.
[2] School of physics, Sun Yat-sen University, Guangzhou.
Presenting author :Qianli Li E-mail address :414138508@qq.com
Corresponding authors: Lin Zhuang E-mail address: stszhl@mail.sysu.edu.cn
Corresponding authors : Yue Xu E-mail address: kou9315@hotmail.com

Recently, the fabrication of water-soluble iron oxide nanocrystals with fast magnetic response, satisfactory biocompatible and desirable surface properties has raised a great amount of interest[1]. We reported a kind of magnetically responsive photonic nanocrystals stabilized in water by Citrate Groups. Superparamagnetic Fe3O4 clusters are synthesized by one-step hydrothermal reaction, which shows long-term stable photonic performances. The attachment of citrate groups on the surface of the magnetite nanocrystals increased the negative charge density on the surface and prevents them from aggregating into large single crystals. The high surface charge of Fe3O4 is attributed to the consistent photonic performance. The Fe3O4 is found to be nearly spherical with an average diameter of 80 nm, which indicates the particles are reasonable uniformity in size. The simple synthesis of Fe3O4 is believed to have potential practical applications in photonics, catalysis, biomedicine and other areas.

Keywords: Photonic, Citrate Groups ,

[1] Jia Liu, Zhenkun Sun, Yonghui Deng, Ying Zou, Chunyuan Li, Xiaohui Guo, Liqin Xiong, Yuan Gao, Fuyou Li, Dongyuan Zhao.2009. Highly Water-Dispersible Biocompatible Magnetite Particles with Low Cytotoxicity Stabilized by Citrate Groups. Angewandte Chemie International Edition, 48: 5875–5879

Acceptance ID: ss4f-O

Control and Modulation of Tunneling Charge-Transport with Light and Self-Assembly

Marco Carlotti[1,2], Sumit Kumar[2], Parisa Pourhossein [1,2] and Ryan C. Chiechi[1,2]

[1]Stratingh Institute for Chemistry & [2]Zernike Institute for Advanced Materials, University of Groningen, Groningen, the Netherlands
r.c.chiechi@rug.nl

Self-assembled monolayers (SAMs) that define the smallest dimension of a molecular junction serve as a template for both the physical dimensions and electrical details of the tunneling barrier. They are relatively straightforward to address experimentally because the SAM and bottom electrode can be interrogated *ex situ*, but are quite complex on a single-molecule level; defects, domains, molecular packing, etc. all affect tunneling charge transport. These complexities present a challenge to the exploitation of electron tunneling mediated by molecules to produce functional nano-devices. This talk will focus three recent examples of overcoming these challenges through the exploitation of the collective effects present in tunneling junctions comprising SAMs using two bottom-up approaches; eutectic Ga-In and SAM-templated nano-gap electrodes. (i) We exploited the thermodynamics of self-assembly to eliminate fatigue in spyropyran-based optical switches.[1] (ii) We found destructive quantum interference effects governed by through-space pathways that are defined by the self-assembly process and that are sensitive to sub-Angstrom differences in conformation.[2] (iii) We modulated the conductance of nano-devices in real time with light by incorporating dyes that affect different tunneling probabilities in the ground and excited states.[3]

Keywords: Self-assembly, tunneling junctions, mixed-monolayers, optical switching

(1) Kumar, S.; van Herpt, J. T.; Gengler, R. Y. N.; Feringa, B. L.; Rudolf, P.; Chiechi, R. C. "Mixed Monolayers of Spiropyrans Maximize Tunneling Conductance Switching by Photoisomerization at the Molecule-Electrode Interface in EGaIn Junctions." *J. Am. Chem. Soc.* **2016**, *138* (38), 12519.
(2) Carlotti, M.; Kovalchuk, A.; Wächter, T.; Qiu, X.; Zharnikov, M.; Chiechi, R. C. "Conformation-driven quantum interference effects mediated by through-space conjugation in self-assembled monolayers." *Nat Commun* **2016**, *7*, 13904.
(3) Pourhossein, P.; Vijayaraghavan, R. K.; Meskers, S. C. J.; Chiechi, R. C. "Optical modulation of nano-gap tunnelling junctions comprising self-assembled monolayers of hemicyanine dyes." *Nat Commun* **2016**, *7*, 11749.
Acceptance ID: TRHH-O

Tuning the electronic bands and orbitals of $HfSe_2$ by doping alkali metal

T. Eknapakul[1], I. Fongkaew[1], S. Chaiyachad[1], S.-K. Mo[2], H. Takagi[3,4], P. D. C. King[5], S. Limpijumnong[1,6], W. Meevasana[1,6]

[1]School of Physics, Institute of Science, Suranaree University of Technology, Nakhon Ratchasima 30000, Thailand
[2]Advanced Light Source, Lawrence Berkeley National Laboratory, Berkeley, CA 94720, USA
[3]Department of Physics, University of Tokyo, Hongo, Tokyo 113-0033, Japan
[4]Magnetic Materials Laboratory, RIKEN Advanced Science Institute, Wako, Saitama 351-0198, Japan
[5]SUPA, School of Physics and Astronomy, University of St. Andrews, St. Andrews, Fife KY16 9SS, United Kingdom
[6]NANOTEC-SUT Center of Excellence on Advanced Functional Nanomaterials, Suranaree University of Technology, Nakhon Ratchasima 30000, Thailand
[*]E Mail: sujinda.chaiyachad@gmail.com

Layered-transition metal dichalcoginides (LTMDs) (or so-called materials beyond graphene) exhibit various interesting physical and electrical properties[1][2] with potential applications in spintronics, optoelectronics, and valleytronics. In this work, we study 1T-$HfSe_2$ with band gap of around 1.1 eV, which may be suitable for photovoltaic and optoelectronic application. By using angle resolved photoemission spectroscopy (ARPES), we measured the electronic structure of 1T-$HfSe_2$ as a function of various alkali metal doping. By varying the 2D carrier density between ~0 (i.e. nearly insulating) and $5x10^{14}$ cm^{-2} (i.e. around 0.2 electrons per unit cell in 2D), we have observed that the valence band maximum became split in energy as large as 350 meV and its band gap became reduced by 250 meV. We also observed the counter-intuitive effect called negative electronic compressibility (NEC)[2] where the chemical potential became lowered by 60 meV upon electron doping in this same range of carrier density. To have a better understanding of these changes, we have further varied the polarization of the ARPES light source to identify the orbital character of each band and also performed density-functional-theory calculation (DFT). From our calculation, the top of $HfSe_2$ valence band consists of Se p-orbital degenerating at Γ-point. Upon doping of 25% (close to the experimental value), the DFT results suggest that the atomic structure became noticeably distorted; the out-of-plane lattice constant (lattice constant c) increases around 11% and the in-plane lattice constant reduces around 3% in direction (lattice constant a). In the new set of calculation, when we manually apply this 3% uniaxial compressive and tensile strain, the DFT calculation shows a good agreement with our experimental ARPES data mentioned above (e.g. both of valence band splitting and band gap shrinkage). The p_y and p_z-orbital bands were also studied and compared with the polarization-dependent data. Interestingly, by changing the compressive strain, the order of p_x-orbital band and p_y-orbital band in energy can be reversed. Our findings here suggest the possibility in using strain or doping for engineering the orbital characters, band gap and NEC effect in $HfSe_2$, prompting some application in optoelectronics and valleytronics.

Keywords: $HfSe_2$, Angle-resolved photoemission spectroscopy, electronic structure, alkali metal doping, density function theory calculations

[1] EKNAPAKUL, T., KING, P. D. C., ASAKAWA, M., BUAPHET, P., HE, R. H., MO, S. K., TAKAGI, H., SHEN, K. M., BAUMBERGER, F., SASAGAWA, T., JUNGTHAWAN, S., & MEEVASANA, W. 2014. Electronic Structure of a Quasi-Freestanding MoS_2 Monolayer. *Nano letters*, *14*(3), 1312-1316.

[2] RILEY, J. M., MEEVASANA, W., BAWDEN, L., ASAKAWA, M., TAKAYAMA, T., EKNAPAKUL, T., KIM, T. K., HOESCH, M., MO, S.-K., TAKAGI, H., SASAGAWA, T., BAHRAMY, M. S. & KING, P. D. C. 2015. Negative Electronic Compressibility and Tunable Spin Splitting in WSe_2. Nature nanotechnology, 10(12), 1043-1047.

Acceptance ID: TRXM-O

Enhanced Formaldehyde Sensing Performance of Co-Doped In_2O_3 Nanostructures

Changliang (Hou), Fubo (Gu), Dongmei (Han), Zhihua (Wang) *

State Key Laboratory of Chemical Resource Engineering, Beijing University of Chemical Technology, Beijing 100029, China.
Corresponding author E Mail: zhwang@mail.buct.edu.cn
Presenting author E Mail: gufb@mail.buct.edu.cn

The development of sensors with high sensitivity, selectivity and stability has emerged as a hot research topic[1, 2]. There are many reports discussing the gas sensing properties of In_2O_3 nanomaterial due to its applications in hazardous gas detection[3, 4]. In our manuscript, a novel formaldehyde (HCHO) sensor was fabricated based on the synthesized rod-like Co-doped In_2O_3 nanomaterial with enhanced sensitivity and selectivity (Figure 1). The response of Co-doped In_2O_3 to 100 ppm formaldehyde was 220 at 230 °C, approximately 3 times higher than that of pure In_2O_3. Compared with other gas sensors reported in the literature[5, 6], our Co-doped In_2O_3 sensor exhibits much higher gas sensitivity for HCHO detection. The synthetic method of this Co-doped In_2O_3 nanomaterial is not only efficient, but also atom-economical and environmentally friendly.

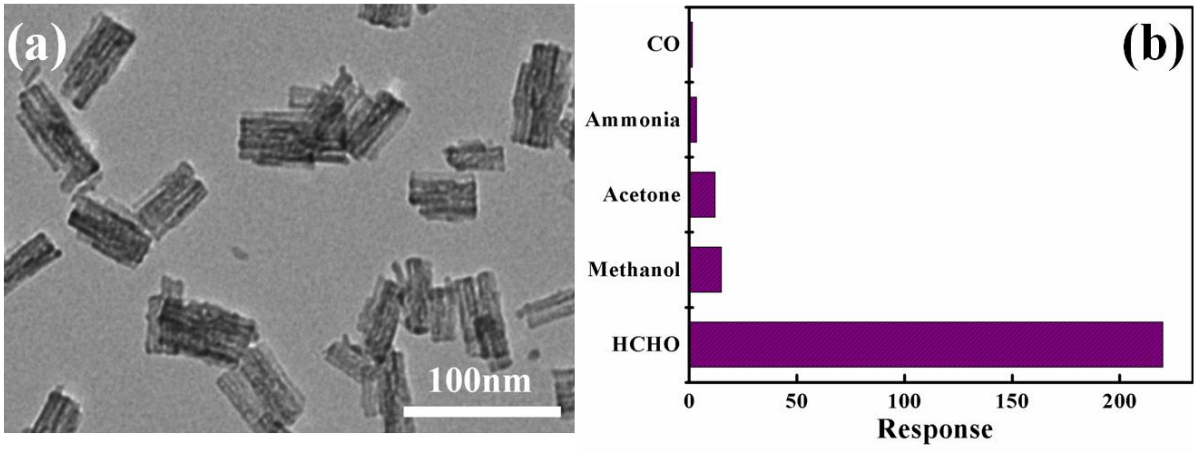

Figure 1: TEM image (a) and the selectivity to 100 ppm different toxic gases at 230°C (b) of rod-like Co-doped In_2O_3

Keywords: Co doping, In_2O_3, nanomaterial, HCHO, gas sensor

This work was supported by the National Natural Science Foundation of China (No. 21575011, 21275016).

[1] CHO, S. Y., YOO, H. W., KIM, J. Y., JUNG, W. B., JIN, M. L., KIM, J. S., JEON, H. J. & JUNG, H. T. 2016. High-Resolution p-Type Metal Oxide Semiconductor Nanowire Array as an Ultrasensitive Sensor for Volatile Organic Compounds. *Nano Letters*, 16, 4508-4515.

[2] WANG, Z., FAN, X., HAN, D. & GU, F. 2016. Structural and Electronic Engineering of 3DOM WO_3 by Alkali Metal Doping for Improved NO_2 Sensing Performance. *Nanoscale*, 8, 10622-10631.

[3] PARK, S., KIM, S., SUN, G. J. & LEE, C. 2015. Synthesis, Structure, and Ethanol Gas Sensing Properties of In_2O_3 Nanorods Decorated with Bi_2O_3 Nanoparticles. *ACS Applied Materials Interfaces*, 7, 8138-8146.

[4] SHANMUGASUNDARAM, A., RAMIREDDY, B., BASAK, P., MANORAMA, S. V. & SRINATH, S. 2014. Hierarchical $In(OH)_3$ as a Precursor to Mesoporous In_2O_3 Nanocubes: A Facile Synthesis Route, Mechanism of Self-Assembly, and Enhanced Sensing Response toward Hydrogen. *The Journal of Physical Chemistry C,* 118, 6909-6921.

[5] WANG, S., XIAO, B., YANG, T., WANG, P., XIAO, C., LI, Z., ZHAO, R. & ZHANG, M. 2014. Enhanced HCHO Gas Sensing Properties by Ag-Loaded Sunflower-Like In_2O_3 Hierarchical Nanostructures. *Journal of Materials Chemistry A,* 2, 6598-6604.

[6] LAI, X., SHEN, G., XUE, P., YAN, B., WANG, H., LI, P., XIA, W. & FANG, J. 2015. Ordered Mesoporous NiO with Thin Pore Walls and Its Enhanced Sensing Performance for Formaldehyde. *Nanoscale,* 7, 4005-4012.

Acceptance ID: U9J9-O

Stability of graphitic structure in BAlN and BGaN alloy semiconductors

Toru Akiyama, Yuma Tsuboi, Kohji Nakamura, Tomonori Ito

Department of Physics Engineering, Mie University, Tsu 514-8507, Japan.
E-Mail : akiyama@phen.mie-u.ac.jp/Tel: +81-59-232-1211

Two-dimensional (2D) nanostructures in the honeycomb lattice have currently been paid much attentions for applications in nanoelectronic devices. Among various 2D materials, hexagonal BN has received considerable attentions as a dielectric template for electronic devices [1]. However, this material is available mainly in the form of small flakes, and successful fabrications of thin films with large area are limited. On the other hand, it has recently been reported that ultrathin AlN nanosheets with graphite-like hexagonal lattice have been successfully grown by molecular beam epitaxy on Ag(111) substrate [2]. Besides, computational study using hybrid density-functional and G_0W_0 methods has recently identified dynamically stabilized 2D structures in III-V materials and their electronic properties [3]. These experimental and theoretical findings inspire us to investigate structural stability of group-III nitrides with graphite-like hexagonal lattice. Here, we expect that this structure is stabilized in boron incorporated AlN and GaN within a certain boron composition range due to the presence of stable hexagonal BN, and examine the stability of 2D BAlN and BGaN alloy monolayers using density functional calculations. Our calculations demonstrate that both AlN and GaN with wurtzite structure whose lattice constants are smaller than those with hexagonal structure are stabilized, consistent with the experimental results [2]. In contrast, hexagonal BN with smaller lattice constant is favorable and hexagonal graphitic structure is found to be stabilized for $B_xAl_{1-x}N$ and $B_xGa_{1-x}N$ with boron composition x lager than 0.75. These results provide a valuable guidance for synthesis and potential applications of 2D group-III nitrides.

Keywords: Graphitic structure, BN, AlN, GaN, Density functional calculations

[1] KIM, K. K., et al. 2012. Synthesis of Monolayer Hexagonal Boron Nitride on Cu Foil Using Chemical Vapor Deposition. *Nano Letters*, 12, 161-166. [2] TSIPAS, P., et al. 2013. Evidence for Graphite-Like Hexagonal AlN Nanosheets Epitaxially Grown on Single Crystal Ag(111). *Appl. Phys. Lett.*, 103, 251605. [3] ZHUANG, H. L., SINGH, A. K., and HENNIG, R. G. 2013. Computational Discovery of Single-Layer III-V Materials. *Phys. Rev. B*, 87, 165415.

Acceptance ID: V7D6-P

Electrical property improvement in Cu@graphitic-carbon nanocables

*Danmin Liu[1, 2, *], Tian Tian[1], Bo Zhang[1], Dandan Zhang[1], Ruiwen Shao[1], Kun Zheng[1], Yongzhe Zhang[2]*

[1]*Institute of Microstructure and Property of Advanced Materials, Beijing University of Technology, Beijing, 100124, China.*
[2]*College of Materials Science & Engineering, Beijing University of Technology, Beijing, 100124, China.*

Nanocables of metallic copper nanowire cores coated with amorphous carbon (Cu@C NCs) and graphitic carbon (Cu@G NCs) were mass synthesized via a hydrothermal approach and a further carbonization process. TEM and other techniques revealed that ≈15nm thickness graphitic carbons uniformly encapsulated the well crystallized copper nanowires along the [110] direction. The electrical resistivity measurement indicated that the Cu@C NCs are insulating while the Cu@G NCs are conductive. In addition, the electrical resistivity of a single Cu@G NC was ≈ $1.6158\times10^{-5}\,\Omega\cdot$cm at room temperature, lower than that of Cu nanowires. We predict that the electrical conductivity and air stability of many other metal nanowires will be enhanced by graphitic carbon encapsulation. This will have broad applications in nanoelectronics.

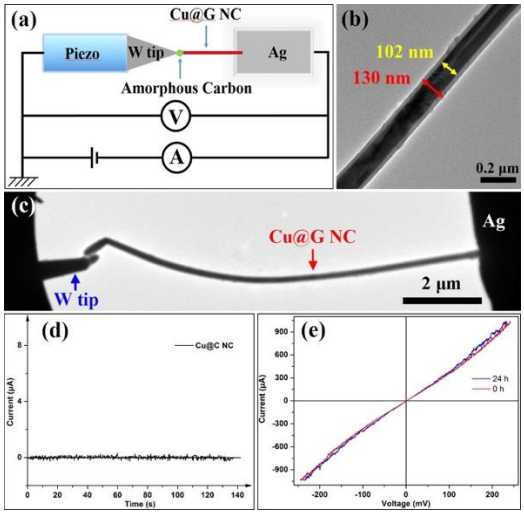

Fig. 1. (a) A schematic drawing of the experimental setup in the Nanofactory Instrument. (b) TEM image of the Cu@G NC measured in this paper. (c) TEM image of W tip, Ag electrode, and a bonded Cu@G NC. (d) I–V curve of the Cu@C NC. (e)The corresponding I–V curves of the Cu@G NC in (b) and (c).

Acceptance ID: VYS7-O

Large-Area Flexible Photodetector Based on Vertically Stacked Atomically Thin MoS_2/Graphene Film

Bo Sun[1,2], Tielin Shi[1], Zhiyong Liu[1], Youni Wu[1], Jianxin Zhou[2], Guanglan Liao[1]*

[1] State Key Laboratory of Digital Manufacturing Equipment and Technology, Huazhong University of Science and Technology, Wuhan 430074, China.
[2] State Key Laboratory of Materials Processing and Die & Mould Technology, Huazhong University of Science and Technology, Wuhan 430074, China.
**Corresponding author: Prof. Liao, E-mail: guanglan.liao@hust.edu.cn, Tel: +86-27-87793103. Presenting author: Dr. Sun, E-mail: bosun@hust.edu.cn.*

Vertical van der Waals junctions formed by stacking selected 2D materials, such as graphene, MoS_2 and WSe_2, etc. have attracted tremendous attentions for their tunable photonic, electronic and mechanical properties [1, 2]. However, the growth of high-quality large-area atomically thin transition metal dichalcogenides (TMDs) is still a big challenge. As a result, most of the relevant works are based on mechanical exfoliated flakes, which strictly limit its application in large-area flexible optoelectronics [1, 3, 4].

Here, we present a large-area flexible photodetector based on vertically stacked atomically thin MoS_2/graphene film with high spectral responsivity. To fabricate the device, large-area graphene grown on copper foil was transferred on the PET substrate by PMMA-assisted wet chemical etching method. Then the film was patterned via photolithography and reactive ion etching. High quality single layer MoS_2 islands about 20 μm in size were grown on SiO_2/Si substrates using CVD method. The islands film typically possesses an area about 1 mm^2, which then was transferred and stacked on the center of the graphene. Ag/Ti electrode was deposited with the channel length range from 50 μm to 1 mm. Electrical measurements reveal that the photodetector possesses high sensitivity and fast response speed for visible light due to the efficient injection of photoexcited electrons from MoS_2 islands to graphene. Top gate is also introduced to further improve the performance of the photodetector. Besides, the flexible photodetector exhibits an excellent mechanical bending endurance.

We attempt to combine large-area graphene with the MoS_2 islands instead of mechanical exfoliated flakes. Despite of the slightly reduced charge carriers transfer efficiency due to film defects, such configuration paves the way for large-scale flexible optoelectronics based on TMDs films. Meanwhile, our results directly demonstrate the great potential of atomically thin MoS_2/graphene film for high sensitive flexible optoelectronic.

Keywords: Graphene, MoS_2, Atomically thin film, Flexible photodetector.

[1] LIU, Y., WEISS, N.O., DUAN, X., CHENG, H. C., HUANG, Y., DUAN, X. 2016. Van der Waals Heterostructures and Devices. *Nature Reviews Materials*, 1:16042.

[2] LEE, C. H., LEE, G. H., VAN DER ZANDE, A. M., CHEN, W., LI, Y., HAN, M., CUI, X., AREFE, G., NUCKOLLS, C., HEINZ, T. F., GUO, J., HONE, J., KIM, P. 2014. Atomically Thin P-N Junctions with van der Waals Heterointerfaces. *Nature Nanotechnology*, 9, 676-681.

[3] FURCHI, M. M., POSPISCHIL, A., LIBISCH, F., BURGDÖRFER, J., MUELLER, T. 2014. Photovoltaic Effect in an Electrically Tunable van der Waals Heterojunction. *Nano Letters*, 14, 4785-4791.

[4] LONG, M., LIU, E., WANG, P., GAO, A., XIA, H., LUO, WEI., WANG, B., ZENG, J., FU, Y., XU, K., ZHOU, W., LV, Y., YAO, S., LU, M., CHEN, Y., NI, Z., YOU, Y., ZHANG, X., QIN, S., SHI, Y., HU, W., XING, D., MIAO, F. 2016. Broadband Photovoltaic Detectors Based on an Atomically Thin Heterostructure. *Nano Letters*, 16, 2254-2259.

Acceptance ID: WW6B-O

Metal alloy nanoparticles: synthesis, characterization, and size-dependent phase diagram calculations

Jiri Pinkas,[1,2,] Vit Vykoukal,[1,2] Ales Kroupa[3]*

jpinkas@chemi.muni.cz
[1] *Masaryk University, Department of Chemistry, Kotlarska 2, 611 37 Brno, Czech Republic.*
[2] *Masaryk University, CEITEC MU, Kamenice 5, 625 00 Brno, Czech Republic.*
[3] *Institute of Physics of Materials, ASCR, Zizkova 22, 616 62 Brno, Czech Republic.*

Nanoparticles of metal alloys have attracted considerable attention from the theoretical and practical point of view. They display many interesting properties, such as depression of melting point,[1] plasmon resonance,[2] catalytic activity,[3] and phase separation.[4] Nanoalloys could be synthesized by many different routes. The solvothermal synthesis by the hot-injection technique in oleylamine[1,3–5] ensures homogeneous conditions for nanoparticle nucleation and growth. Binary metal alloy nanoparticles (AgNi, CuNi, AgCu, NiSn, NiSb) were prepared by injection of an oleylamine solution of metal precursors to a mixture of oleylamine and octadecene at 230 °C. After 10 min, the reaction mixture was cooled down to room temperature and resulting nanoparticles were washed, isolated, and redispersed in hexane for characterization. Dynamic Light Scattering (DLS), Transmission Electron Microscopy (TEM), Elemental analyses (ICP OES), and Small-Angle X-ray Scattering (SAXS) analyses were performed for determination of the chemical composition, average size, size distribution, and shape of the prepared nanoparticles. Plasmon resonances were also observed. Phase separation was followed by High Temperature X-Ray Diffraction (HT-XRD) technique and was confirmed by Scanning Electron Microscope (SEM) and by measuring of magnetic properties during heating. The CALPHAD method was used for modelling of size-dependent phase diagrams of binary systems. Temperatures of invariant reactions were obtained by DSC measurements and experimental results were compared to calculated values.

This research has been financially supported by the MEYS CR under the project CEITEC 2020 (LQ1601) and by the Czech Science Foundation (GA 17-15405S). CIISB research infrastructure project LM2015043 is gratefully acknowledged for the financial support of the measurements at the X-ray diffraction and BioSAXS Core Facility.

(1) Sopousek, J.; Vrestal, J.; Pinkas, J.; Broz, P.; Bursik, J.; Styskalik, A.; Skoda, D.; Zobac, O.; Lee, J. *Calphad* **2014**, *45*, 33–39.

(2) Link, S.; El-Sayed, M. A. *Annu. Rev. Phys. Chem.* **2003**, *54*, 331–366.

(3) Zhang, Y.; Huang, W.; Habas, S. E.; Kuhn, J. N.; Grass, M. E.; Yamada, Y.; Yang, P.; Somorjai, G. A. *J. Phys. Chem. C* **2008**, *112* (32), 12092–12095.

(4) Sopousek, J.; Zobac, O.; Bursik, J.; Roupcova, P.; Vykoukal, V.; Broz, P.; Pinkas, J.; Vrestal, J. *Phys. Chem. Chem. Phys.* **2015**, *17*, 28277–28285.

(5) Sopousek, J.; Pinkas, J.; Broz, P.; Bursik, J.; Vykoukal, V.; Skoda, D.; Styskalik, A.; Zobac, O.; Vrestal, J.; Hrdlicka, A.; Simbera, J. *J. Nanomater.* **2014**, *2014*, 1–13.

Acceptance ID: XDC5-P

Design of Band-pass Filter Based on the Concept of Plasmonic Metamaterial

Rahul Kumar (Jaiswal)[1], Nagendra Prasad (Pathak)[2]

[1,2]Radio Frequency Integrated Circuits and System Lab, Department of Electronics and Communication Engineering,
Indian Institute of Technology, Roorkee, Uttarakhand, India, 247667

rahul120391@gmail.com, nagppfec@iitr.ac.in

In this paper, we report the design of band-pass filter based on the concept of plasmonic metamaterial i.e. spoof or designer surface plasmon polaritons (SSPP's) at microwave frequency. Surface plasmon polaritons are unique electro-magnetic surface waves at optical frequecny which are propagating at the interface of metal-dielectric and decaying exponentially at surface. The interaction of free electron in metal and surrounding EM fields bring about to special properties of SPPs i.e. extraordinary ability to manipulate and confine the light with high intensity at sub-wavelength scale and thus attracted much attention during the past decades for developing new types of photonics devices and overcome the diffraction limit. Natural SPPs do not exist naturally in THz or Microwave regime, but can be assisted by plasmonic meta-materials, which are the corrugated periodical grooves at metal surfaces i.e. by drilling holes and cutting the grooves on metallic surfaces. This is termed as spoof or designer SPP and have inherited exotic features of optical SPPs, such as field confinement and non-diffraction limit. The most important feature of this spoof SPP is that the cutoff frequency and dispersion property can be engineered at will by changing the geometrical parameters. SRR are used in periodic configurations to design metamaterial structures and also used to design slow wave transmission line and different type of microstrip filters. The circuit model of SRR elements is similar to parallel L and C components that are placed in series form in a transmission line hence, used in the design of band-stop filters. Using duality theorem and Babinet's principles, CSRR can be used to design band-pass filters. In present work, we have proposed a structure which consist of a stepped stub like corrugation on top of the dielectric substrate as shown in Fig 1, is a transition structure from QTEM mode of microstrip to SSPP mode and two U-shape CSRR on the bottom part of the substrate and analysed two cases: first case, two U-shape CSRR's inserted in ground plane are symmetrical and second case, two CSRR's are asymmetrical. Dimensions of one strip in transition structure are *h=4, d= 4, e= 1, w=2, a= 0.5, b= 1.5, r=1, s= 0.5 (all in mm).* Neltec Substrate has been used with thickness: 1.52 mm, relative permittivity ε_r: 3.38, loss tangent: 0.0016 and copper thickness: 0.035 mm. CSRR dimensions are w_g*= 1,* $\lambda = \lambda_1$*=6 and* λ_2*= 8 (in mm).* The fabricated prototype for both cases has been shown in Fig. 2 and 3 along with their simulated and measured results. The proposed devices are designed and fabricated and shows the excellent band-pass filtering characteristics. Simulated and measured results of reflection and transmission coefficient are in good agreement at microwave frequency. The numerical simulation is performed using CST Microwave studio. The characterization of all aforementioned devices has been performed using vector network analyzer (VNA) (R & S ZVM 1127-8500).

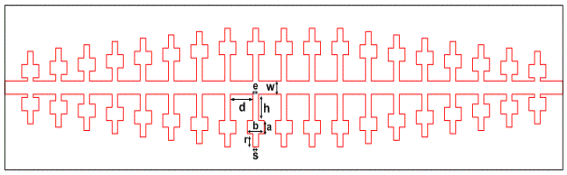

Fig.1 Schematic of top of the substrate

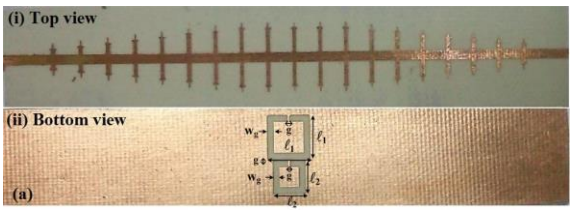

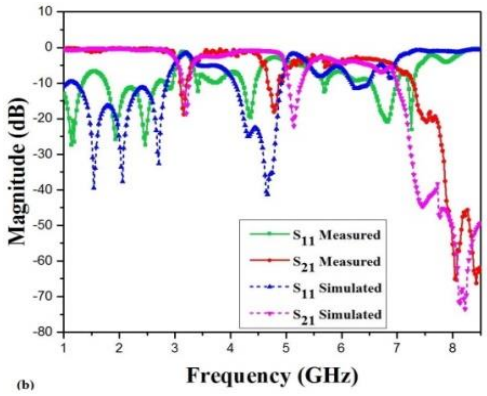

Fig 2. (a) Prototype of BPF with asymmetric U shape CSRR in the ground plane (b) Simulated and measured characteristics of BPF with asymmetric U shape CSRR in the ground plane

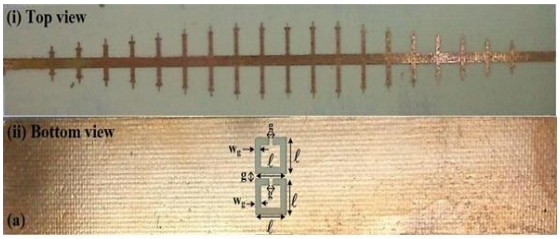

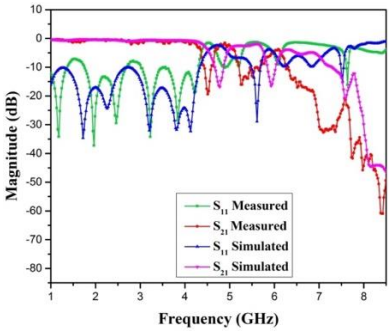

Fig 3. (a) BPF with symmetric U shape CSRR in the ground plane (b) Simulated and measured characteristics of BPF with symmetric U shape CSRR in the ground plane

Keywords: Band-pass, filter, Complementary split ring resonator (CSRR), Designer (spoof) surface plasmon polaritons (SPP)

[1] PENDRY, J. B., MARTIN-MORENO L., & GARCIA-VIDAL, F. J. 2004. Mimicking Surface Plasmons with Structured Surfaces. *Science* 305, 847-848.

[2] HIBBINS, ALASTAIR P., BENJAMIN R. EVANS, & SAMBLES J ROY. 2005. Experimental Verification of Designer Surface Plasmons. *Science Mag*., 308.

[3] ZHANG W., ZHU G., LIGUO SUN, & FUJIANNG LIN. 2015. Trapping of Surface Plasmon Wave Through Gradient Corrugated Strip with Underlayer Ground and Manipulating its Propagation. *J. App. Phys*., 106.

[4] GAO XI, ZHOU L., LIAO Z., HUI FENG MA, & CUI T. J. 2014. An Ultra-Wideband Surface Plasmonic Filter in Microwave Frequency. *J. App. Phys.*, 104.

Acceptance ID: XE6Z-O

Multifunctional graphene nano-electromechanical (GNEM) devices for Extreme Sensing

M. Muruganathan[1], D. Kato[1], F. Seto[1], J. Sun[1], M. E. Schmidt[1], and H. Mizuta[1]

[1]School of Material Science, Japan Advanced Institute of Science and Technology, Japan.
E Mail : mano@jaist.ac.jp

Graphene has an ultra-high Young's modulus of 1 TPa, which makes it a promising candidate for future nanoelectromechanical (NEM) applications. The graphene NEM (GNEM) switches have potential to realize minimized electrical leakage, sharp switching response, low actuation voltage and high on/off ratio [1]. Despite these applications, GNEM devices give a unique platform to realize high sensitivity gas molecules detection. It is due to the graphene exceptional low electronic noise characteristics and suspended nature of graphene channel in GNEM devices. Substrate induced noises to the graphene channel is avoided by the physical isolation of the GNEM channel from the substrate. GNEM switches are fabricated using the bottom-up procedure to get suspended graphene with a polymer sacrificial spacer. The advantage of this fabrication method is that it does not need any acid etching to get suspended graphene. In these GNEM switches, low pull-in voltage of less than 2V is achieved [2]. This pull-in voltage is compatible with the conventional, complementary metal-oxide-semiconductor circuit requirements.

To realize the extreme resolution of different gas molecules sensing, *ie*., detection of single molecule, detailed understanding of vdW interaction in graphene-molecule complex is needed. van der Waals (vdW) interaction plays a central role in molecules adsorption on to a surface. The charge fluctuations associated with the molecules adsorption is electro-dynamically correlated with the charge fluctuations in the adsorbed surface, which can be modified by the external electric field. The charge transfer between the graphene and the gas molecules can be accurately traced from the Dirac point monitoring under a range of electric field. Hence, to verify the theory, we measure doping concentrations in graphene with adsorptions formed at different tuning voltages. For the tuning voltage range of -20 V to 40 V, increased hole doping concentrations uncover the role of adsorbed CO_2 molecules as an acceptor. Moreover, higher doping is observed at larger tuning voltage. These externally controlled doping concentrations clearly demonstrate the evidence of the tuned charge transfers [3].

In order to realize the extreme sensing capability, the suspended bilayer graphene GNEM switches are exploited. Using the electrostatic force, the central part of the suspended beam is pulled-down to the bottom metal electrode. This novel design of suspended graphene beam architecture avoids any further mechanical deflection of pulled-down beams on to the substrate when the electric field is applied from the substrate. The step-like changes in the graphene beam resistance with a quantized value of ~62 Ω are measured when exposed to low concentration CO_2 molecules. These discrete responses are clear evidence to individual CO_2 molecule adsorption onto the slanted graphene beam. In order to enhance the molecular adsorption rate, the electrical field is introduced around the suspended graphene region by applying the back-gate voltage. The first-principles calculations and molecular dynamics simulations elucidate the role of van der Waals interaction between molecules and graphene during detection and the back gate effects on accelerating the molecules adsorption [4]. Furthermore, we have carried out the extreme sensing by 1/f noise measurement and mass detection methods as well.

Acknowledgement: This work is supported by Grant-in-Aid for Scientific Research (S) No. 25220904, and Grant-in-Aid for Young Scientists (B) 16K18090 from Japan Society for the Promotion of Science.

Keywords: Graphene nanoelectromechanical system (GNEMS), van der Waals (vdW) interaction, Single molecule detection, Electrically tuned vdW interaction

References:

[1] Loh, O.Y. and Espinosa, H.D., 2012. Nanoelectromechanical contact switches. *Nature nanotechnology*, *7*(5), pp.283-295.

[2] Sun, J., Wang, W., Muruganathan, M. and Mizuta, H., 2014. Low pull-in voltage graphene electromechanical switch fabricated with a polymer sacrificial spacer. *Applied Physics Letters*, *105*(3), p.033103.

[3] Muruganathan, M., Sun, J., Imamura, T. and Mizuta, H., 2015. Electrically Tunable van der Waals Interaction in Graphene–Molecule Complex. *Nano letters*, *15*(12), pp.8176-8180.

[4] Sun, J., Muruganathan, M. and Mizuta, H., 2016. Room temperature detection of individual molecular physisorption using suspended bilayer graphene. *Science advances*, *2*(4), p.e1501518.

Acceptance ID: Y48B-I

Graphene Synthesis using Plasma Based Ion Implantation

*Tyousyun Yoneyama, Kento Ishimuro, Junho Choi**

The University of Tokyo, 7-3-1 Hongo, Bunkyo-ku, Tokyo 113-8656, Japan
**E-Mail/ Contact Détails (choi@mech.t.u-tokyo.ac.jp)*

Graphene is a 2-dimensional hexagonal lattice of carbon atoms, and it has received much attention in the scientific community because of its distinct properties and potentials in nano-electronic and tribological applications. Many reports have been made on graphene's very high electrical conductivity at room temperature, transparent electrodes and tribological properties. *Graphene* has been *synthesized* in various ways; thermal chemical vapor deposition (CVD) on catalytic metal surfaces, graphitization of hexagonal SiC crystals during annealing at high temperatures *in vacuum*, and carbon ion implantation. Wide applications of graphene require structurally coherent graphene on a wafer-scale. However, coherent graphene synthesis on a wafer-scale substrate still remains challenging. In this study, we report a new method for graphene synthesis by using plasma based ion implantation (PBII) technique, which allows highly uniform ion implantation on a large-scale substrate even the sample has a three-dimensional shape. Ni films were deposited on silicon oxide substrates by sputter. Methane ions are implanted using PBII on the Ni films and annealed at 800 – 1000 ºC in a high vacuum. We observed Raman 2D peaks, representing existence of graphene, for the samples annealed at 800 and 900 ºC. The sample annealed at 900 ºC shows a smaller D peak, indicating fewer defects in the graphene film.

Keywords: Graphene, ion implantation, PBII, Ni

Acceptance ID: Y58F-P

Calculation of Magnetization and Magneto-crystalline Anisotropy for Carbon-doped Fe-Pt Ferromagnet

Minyeong Choi[1], Yang-Ki Hong[1], Woncheol Lee[1], Hoyun Won[1], Chang-Dong Yeo[2]

David S. Kuo[3], and Gary J. Mankey[4]

[1] Department of Electrical & Computer Engineering and MINT Center, the University of Alabama, Tuscaloosa, AL 35487 USA

[2]Department of Mechanical Engineering, Texas Tech University, Lubbock, TX 79409 USA

[3] Seagate Technology LLC, Fremont, CA 94538 USA

[4]Department of Physics & Astronomy and MINT Center, the University of Alabama, Tuscaloosa, AL 35487 USA

ykhong@eng.ua.edu / University of Alabama

$L1_0$-ordered FePt ferromagnetic film has been intensively studied to achieve 4 Tbits/in^2 of areal density for heat-assisted magnetic recording (HAMR) media [1, 2]. In order to meet this areal density, grain size and film thickness need to be smaller than 5 nm and thinner than10 nm, respectively [3]. Therefore, carbon (C) is used to isolate the FePt grains from each other, thereby, magnetic and thermal isolations between adjacent FePt grains [4]. However, the addition of C to FePt decreased both magneto-crystalline anisotropy constant (K_u), *i.e.* coercivity (H_{ci}), and saturation magnetization (M_s) [5]. The atomic radius of C (0.077 nm) is much smaller than those of Pt (0.138 nm) and Fe (0.126 nm). Therefore, it is very likely that C atoms can diffuse through interstitial sites [6]. There is no report on theoretical interpretation of magnetic properties of C-doped FePt thin films. We have performed first principles calculation on $(FePt)_{0.8}C_{0.2}$ crystal to investigate magnetic properties. Prior to performing, we have calculated electron density for pure FePt if there are sites available for C atoms. Fig. 1 shows 2D electron density of pure FePt and interstitial sites (red regions) available for C doping. After interstitially doping FePt with C atoms, we performed first principle calculations. Densities of state (DOS) for FePt and $(FePt)_{0.8}C_{0.2}$ are shown in Fig. 2. It was found that the M_s and K_u decreased to 832 emu/cc from 1,117 emu/cc and to 2.31 MJ/m^3 from 16.8 MJ/m^3 of pure FePt, respectively. On the other hand, the Curie temperature (T_c) of $(FePt)_{0.8}C_{0.2}$ slightly increased to 729 K from 719 K of pure FePt. In this paper, we will present detailed calculations and calculated results to give an insight into the magnetic properties of C-doped FePt ferromagnetic thin film for HAMR applications.

ACKNOWLEDGMENT: This work was supported in part by the NSF-CMMI under Awards 1463301 and 1463078.

Keywords: First principles calculation, electronic structure, magnetic properties

[1] D. WEllER, G. PARKER. O. MOSENDZ, A. LYBERATOS, D. MITIN, N. Y. SAFONOVA, and M. ALBRECHT. *J. Vac. Sci. Technol*. B **34**, 060801 (2016).

[2] J. PARK, YANG-KI HONG, CHANG-DONG YEO, SEONG-GON KIM, DAVID S. KUO, LI GAO, and JAN-ULRICH THIELE. *IEEE Transactions on Magnetics*. **52**, 3201904 (2016).

[3] H. PANDEY, J. WANG, T. SHIROYAMA, B. S. D. Ch. S. VARAPRASAD, H. SEPEHRI-AMIN, Y. K. TAKAHASHI, A. PERUMAL, and K. HONO. *IEEE Trans. Magn*. **52**, 3200108 (2016).

[4] B. S. D. Ch. S. VARAPRASAD, B. ZHOU, T. MO, D.E. LAUGHLIN, and J. G. ZHU. *AIP Advances*. **7**, 056503 (2017).

[5] A. PERUMAL, Y. K. TAKAHASHI, and K. HONO. *J. of Applied Physics*. **105**, 07B732 (2009).

[6] Y.F. DING, J.S. CHEN, E. LIU, B.C. LIM, J.F. HU, and B. LIU. *Thin Solid Films.* **517**, 2638 (2009).

Acceptance ID: YWQM-O

Perfluoropolyether Nanomedicines as Controllable Immunomodulators in Inflammatory Diseases

Jelena M. Janjic

Duquesne University
janjicj@duq.edu

Immunomodulation is underappreciated approach for treatment of inflammatory diseases. As cancer immunotherapy continues to make impressive impact on cancer therapy, immunomodulation as the means for treatment of other diseases is not fully explored to its potential. In this talk I will discuss the promise of nanomedicine approach to immunomodulation with the goal effective, safe and individualized approach to treatment of injury associated inflammation leading to better control of pain and improved healing. Perfluoropolyethers (PFPEs) are polymeric materials with a broad range of applications, from lubricants, surfactants, and antifouling agents, to cosmetics, drug delivery, and imaging. Over the past several years we have explored their use in the synthesis of bimodal imaging agents (NIR/^{19}F MR) and in drug delivery formulations, from nanoemulsions to hydrogels. PFPE can be used for the synthesis of multimodal nanomedicine formulations that can be produced with scalable processes and with a high level of quality control. For example, PFPEs can be formulated into hydrogels with a shelf life beyond 6 months. Further, PFPEs are formulated as stable (>350 days shelf life) nanoemulsions that can incorporate varied payloads, from anti-inflammatory drugs to natural products and optical probes. PFPE fluorous behavior in organic media makes them easily chemically modified to support the introduction of targeting agents and additional imaging probes, as well as promote self-assembly for increased colloidal stabilization. PFPEs are chemically modified to carry either fluorescent or PET imaging moieties and formulated into nanoemulsions, nanoemulgels and crosslinked hydrogels for parenteral and oral delivery. Here we present preclinical results that support the future advancement of PFPE based nanomedicine for immunomodulation in several injury and inflammation models. Specifically we were able to demonstrate that drug loaded PFPE nanoemulsions can selectively modulate monocyte behavior in live animals leading to reduced inflammation and pain behavior following injury. Detailed discussion of the PFPE nanomedicines effects on key immune cells in vitro and in vivo will be presented. We hope that this work serves as a model for others to consider immunomodulation with nanosystems as an effective approach to treatment and imaging of inflammatory diseases.

Acceptance ID: YWWN-O

Wrinkling behaviors of graphene films adhered to a polymer substrate

Seyoung Im and Moon Hong Kim

Department of Mechanical Engineering, KAIST
291 DaeHak-Ro, YuSeong-Gu, DaeJeon, S. Korea

Structural theory is developed for graphene films, and combined with a plate theory for a polymer substrate in order to construct a structural deformation theory for composite plates wherein graphene sheets are adhered to a polymer substrate. We next seek finite element implementation of this composite plate theory to explore various wrinkling deformation modes of graphene sheets bonded to the polymer substrate, which have diverse applications in flexible electronic devices and micro/nano channels. Numerical simulation predicts various wrinkling behaviors of the graphene sheets adhered to the polymer substrate, depending upon the parameters related to the deformation, the material properties and geometry of the system.

Acceptance ID: Z4YJ-O

Defect level engineering in transition metal dichalcogenides

Hyesung Park

Department of Energy Engineering, School of Energy and Chemical Engineering, Low Dimensional Carbon Materials Center, Perovtronics Research Center, Ulsan National Institute of Science and Technology (UNIST), 50 UNIST-gil, Ulju-gun, Ulsan 44919, Republic of Korea
Corresponding e-mail: hspark@unist.ac.kr

Graphene, representative of 2-dimensional materials, has been demonstrated in diverse field of applications such as transparent electrode, touch screen, flexible optoelectronics, thin-film transistor, and catalysis. However, direct applications of graphene in digital electronic devices are challenging due to its zero-band gap and low on-off ratio. Another family of 2D materials, three-atom-thick transition metal dichalcogenides (TMDs) has been proposed as the complementary material to graphene due to their semiconducting properties, where the associated band gap can be tuned between direct and indirect values depending on the layer number of TMD sheets. In TMD materials, the relative degree of defects in TMDs can play an important role in its applications. For example, low-defect (low active sites) TMDs are applicable to electronic devices, whereas TMDs with high-defect (high active sites) are more appropriate in catalytic reactions. Therefore, controlling the degree of defect levels in TMDs can be a useful means to diversify the application of TMD-based materials. In this study, we show that the defect levels in molybdenum diselenide ($MoSe_2$) can be modified by adjusting the H_2 concentration during the synthesis stage from the chemical vapor deposition (CVD) process. We propose that the reactivity of transition metal and chalcogen atoms vary with the concentration of H_2 gas, which leads to the change in the defect level from the as-synthesized $MoSe_2$ film. Our study suggests a viable strategy to modify the defect level in TMDs, which could contribute to the performance enhancement in TMD-based device applications.

Acceptance ID: Z5PB-P

Two-Dimension Nanosheets and Their Excellent Removal of Pb(II) Ions

Wei Zhou, Qiuya Zhang, Wei Cao

School of Chemistry and Environment, Beihang University, Beijing, 100191
*E Mail/ Contact Détails (**zhouwei@buaa.edu.cn**)*

Ultrathin two-dimension (2D) nanomaterials have aroused much attention as their outstanding electronic and electrochemical property, considerable surface area, and flexible support [1-3]. Through the interaction between heavy metal ions and abundant surface oxygen-containing groups of the adsorbent, high-efficient removal of heavy metal ions from polluted water has been achieved [4, 5]. Herein, the polyethylene oxide functionalized graphene oxide nanosheets (PEO-*f*-GO) were synthesized via a simple wet-chemical process, which exhibited a superior adsorbent in removing metal ions. Effects of composition, preparation temperature, amount of adsorbent, pH, contact time for removal of Pb (II) were systematically investigated. The maximum adsorption capacity of Pb (II) on GO-*f*-PEO (70:10, w: w) at pH=6.0 was 148.51 $mg \cdot g^{-1}$. Results also suggested the prepared adsorbent showed quite higher removal efficiency and adsorption capacity toward multiple metal ions within 20s. The ultrafast adsorption could be ascribed to intense binding force from the functional groups of PEO and Pb(II) ions. Besides, another kind of ultrathin nanosheets, cobalt hydroxide with an average thickness of 7 nm have been synthesized and used as adsorbent for removal of Pb(II) ions. The exposed rich hydroxyls made these sheets good adsorption towards heavy metal ions. With the assisting of CO_2, the adsorption equilibrium of the cobalt hydroxide nanosheets could be balanced within 2 mins with removal capacity of ~1860 mg/g and the removal efficiency of ~93 %. The unpublished two examples confirmed the advantage of 2D nanomaterials after modifying in heavy metal ions degradation from polluted water.

Keywords: Two-Dimension nanomaterial, Adsorption, Pb(II) ions, Modification

[1] SCHOLES, G. D. 2011. Semiconductor Nanostructures: Two Dimensions Are Brighter. *Nature Mater.*, 10, 906-907.

[2] ZHANG, F.; XIA, C.; ZHU, J. J.; AHMED, B.; LIANG, H. F.; VELUSAMY, D. B.; SCHWINGENSCHLOGL, U. & ALSHAREEF, H. N. 2016. $SnSe_2$ 2D Anodes for Advanced Sodium Ion Batteries. *Adv. Energy Mater.*, 6, 1601188.

[3] YANG, G. Z.; SONG, H. W.; WU, M. M. & WANG, C. X. 2016. SnO_2 Nanoparticles Anchored on 2D V_2O_5 Nanosheets with Enhanced Lithium-Storage Performances. *Electrochim. Acta*, 205, 153-160.

[4] MA, L. J.; WANG, Q.; ISLAM, S. M.; LIU, Y. C.; MA, S. L. & KANATZIDIS, M. G. 2016. Highly Selective and Efficient Removal of Heavy Metals by Layered Double Hydroxide Intercalated with the MoS_4^{2-} Ion. *J. Am. Chem. Soc.*, 138, 2858-2866.

[5] LING, L. L.; LIU, W. J.; ZHANG, S. & JIANG, H. 2016. Achieving high-efficiency and ultrafast removal of Pb(II) by one-pot incorporation of a N-doped carbon hydrogel into FeMg layered double hydroxides. *J. Mater. Chem. A*, 4, 10336-10344.

Acceptance ID: ZED5-O

WS_2 nanotubes, 2D nanomeshes, and 2D in-plane films through one single CVD route

Zichen (Liu)[1,2], *Adelina (Ilie)*[1,2]

[1]*Department of Physics, University of Bath, Bath, BA2 7AY, United Kingdom*
[2] *Centre for Graphene Science, University of Bath, Bath, BA2 7AY, United Kingdom*
Z.Liu2@bath.ac.uk/ a.ilie@bath.ac.uk

A variety of bottom-up growth processes for two dimensional (2D) layers of transition metal dichalcogenides (TMDs) have been proposed and demonstrated in recent years. For WS_2, one such growth process uses chemical vapor deposition (CVD) in conjunction with tungsten oxide and sulfur as precursors. Here we demonstrate a CVD route capable of producing *in a single process stream*, at successive stages, a variety of WS_2 morphologies, encompassing nanotubes, a new type of 2D nanomesh, and 2D in-plane mono- and few layer films, on insulating substrates. As a result of stage decoupling, which is not revealed in conventional CVD of 2D TMDs, we also gain insight into the growth mechanism of 2D in-plane layers. 2D mono- and few-layer WS_2 can be grown in a self-seeding process where the nucleation sites and the source of precursor material are provided by the same phase.

A variety of techniques (i.e. high resolution transmission electron microscopy and associated analytical techniques, Raman spectroscopy, EDX, XRD, and atomic force microscopy) were used to assess the nature, composition and crystallinity of the resulting WS_2 morphologies. We also investigate functional properties (e.g. magnetic order and conductance) of the WS_2 2D nanomesh phase synthesized.

Keywords: transition metal dichalcogenides, growth, in-plane 2D layers, 2D nanomeshes, functional properties.

Acceptance ID: ZL54-O

Terahertz wavefront manipulation with tunable fermi levels in graphene ribbon array

Yongyuan Jiang[1, 2], *Ruiuan Tian*[1, 2]

[1] *Department of Physics, Harbin Institute of Technology, Harbin, 150001, China*
[2] *Key Lab of Micro-Optics and Photonic Technology of Heilongjiang Province, Harbin 150001, China*
jiangyy@hit.edu.cn

Conventional metasurfaces based on engineered metallic nanostructures for wavefront manipulation usually cannot be tuned effectively and seldom work at mid-infrared or lower frequencies. Graphene is a perfect candidate due to its peculiar plasmon resonance properties, which can be tuned over a broad terahertz frequency range via changing graphene's size or electrostatic doping, exhibiting remarkably large oscillator strengths and leading to stable and reliable performance at room-temperature[1]. The metasurface composed of graphene ribbons array-dielectric-metallic film structure has been utilized to manipulate the terahertz wavefront[2]. The phase of the reflected light could vary from almost $-\pi$ to π with the appropriate graphene ribbons width and the dielectric spacing layer thickness, while the reflection amplitude could remain at high values. Through changing the width of graphene ribbons indeed can modulate the plasmonic resonances in graphene, and realize various reflective planar graphene photonic devices. However, for a given device, it can only achieve a certain kind of fixed function, which is not flexible enough.

To overcome the lack of modulation flexibility of the aforementioned work, we engineer the local phase shifts on metasurface through tuning the Fermi levels of each graphene ribbon, inspired by the study of Takumi Yatooshi et al[3]. Fermi level of graphene can be changed via electrical gating [1], which is usually reversible, so that one can perform various kinds of photonic devices based on one certain graphene metasurface with given structure parameters. The metasurface composed of graphene ribbons array-dielectric-metallic film structure is utilized to manipulate the terahertz wavefront dynamically and efficiently. Each ribbon, with different Fermi levels, has the same width that is far less than the wavelength of incident light. By changing the Fermi levels of graphene ribbons, the phase can almost cover the necessary 2π range and the reflectivity maintains higher than 54.2%, so it is able to engineer novel planar optical devices and control reflected THz waves efficiently.

With this electric tunable graphene metasurface, anomalous reflection, focusing mirrors, non-diffracting Airy beam generation and Bessel beam generation have been realized successfully only by changing the Fermi levels of the graphene ribbons. This paper proves the excellent dynamic tuning performance of graphene metasurface and provides multiple functions of a graphene metasurface with given structural parameters, which may greatly facilitate the fabrication and integration of multifunctional photonic devices.

Keywords: Metamaterials, Plasmonics, Terahertz wavefront manipulation, Phase modulation

[1] JU, L., GENG, B., HORNG, J., GIRIT, C., MARTIN, M., HAO, Z., BECHTEL, H. A., LIANG, X., ZETTL, A. SHEN, Y. R. & WANG, F. 2011. Graphene plasmonics for tunable terahertz metamaterials. *Nat. Nanotechnol.* 6(10), 630-634.

[2] LI, Z., YAO, K., XIA, F., SHEN, S., TIAN, J., & LIU, Y. 2015. Graphene plasmonic metasurfaces to steer infrared light. *Sci. Rep*. 5, 12423.

[3] YATOOSHI,T., ISHIKAWA, A. & TSURUTA, K. 2015. Terahertz wavefront control by tunable metasurface made of graphene ribbons, *Appl. Phys. Lett.* 107(5), 053105.

Acceptance ID: ZZTK-O